Paris-proof power

Exploring the impacts of different decarbonisation strategies in the European electricity sector

William Zappa

Paris-proof power

Exploring the consequences of different decarbonisation strategies in the European electricity sector

William George Zappa

ISBN: 978-90-8672-090-3
Printing: Ridderprint | www.ridderprint.nl
Cover: W. Zappa & M. van Tulder
This thesis has been printed on 100% recycled paper
© W. Zappa 2020

Paris-proof power

Exploring the consequences of different decarbonisation strategies in the European electricity sector

Paris-proof power

Verkenning van de gevolgen van verschillende decarbonisatie strategieën in de Europese elektriciteitsector

(met een samenvatting in het Nederlands)

Proefschrift

ter verkrijging van de graad van doctor aan de
Universiteit Utrecht
op gezag van de
rector magnificus, prof.dr. H.R.B.M. Kummeling,
ingevolge het besluit van het college voor promoties
in het openbaar te verdedigen op

vrijdag 8 mei 2020 des ochtends te 10.30 uur

door

William George Zappa

geboren op 4 april 1986

te Perth, Australië

Promotor:

Prof. dr. M. Junginger

Copromotor:

Dr. ir. M. van den Broek

This thesis was accomplished with financial support from the European Union's Horizon 2020 projects Flexifuel SOFC (Grant agreement 641229) and Flexifuel CHX (Grant agreement 654446); the CATO-2 research project, funded by the Dutch Ministry of Economic Affairs, TKI-Gas, and the CATO-2 consortium parties; and Topsector Energy funding from the Dutch Ministry of Economic Affairs and Climate Policy.

Contents

Abbreviations

AC	Autocorrelation
ACF	Autocorrelation function
AD	Anaerobic digestion
AFOLU	Agriculture, forestry, and other land use
AR	Autoregressive
ARIMA	Autoregressive integrated moving average
BECCS	Bioenergy with carbon capture and storage
BIOAD	Biogas from anaerobic digestion
BIOSOL(-CCS)	Solid biomass (with CCS) i.e. BECCS
bn	Billion (10^9)
BRP	Balance responsible party
BSP	Balancing service provider
CAES	Compressed air energy storage
CAPEX	Capital expenditure
CCGT(-CCS)	Combined cycle gas turbine (with CCS)
CCS	Carbon capture and storage
CDDA	Common Database on Designated Areas
CDR	Carbon dioxide removal
CHP	Combined heat and power
CIGRE	Council on Large Electric Systems
CLC	Corine Land Cover
CM	Capacity market
COP	Coefficient of performance
CRM	Capacity remuneration mechanism
CSP	Concentrating solar power
CV	Coefficient of variation
CWE	Central Western Europe
DA	Day-ahead
DAC	Direct air capture
DNI	Direct normal irradiance
DSM	Demand-side management
EC	European Commission
ECF	European Climate Foundation
ECMWF	European Centre for Medium-Range Weather Forecasts
EEA	European Environment Agency
EEZ	Exclusive Economic Zone
ENTSO-E	European Network of Transmission System Operators for Electricity
EOM	Energy-only market
ERA-Interim	European Reanalysis Interim Dataset
ETRI	Energy Technology Reference Indicators
ETS	Emissions Trading Scheme
EU	European Union
EV	Electric vehicle
FCR	Frequency containment reserve
FLH	Full load operating hours
FOM	Fixed operating and maintenance
FRR	Frequency restoration reserve; automatic (aFRR) or manually (mFRR) activated
GARCH	Generalised autoregressive conditional heteroscedasticity
GDP	Gross domestic product
GHG	Greenhouse gas
GT	Open-cycle gas turbine
HDH	Heating degree hour
HP	Heat pump
HVAC	High-voltage alternating current
HVDC	High-voltage direct current
IAM	Integrated assessment model
IDC	Interest during construction
IEA	International Energy Agency
IEC	International Electrotechnical Commission
IPCC	Intergovernmental Panel on Climate Change
ISP	Imbalance settlement period
JRC	European Union Joint Research Centre
LCOE	Levelized cost of electricity
LLSQ	Linear least squares
LoLE	Loss of load expectation
LoLP	Loss of load probability
LRMC	Long-run marginal cost

LT	Long term
MA	Moving average
MAAPE	Mean arctangent absolute percentage error
MAF	Mid-term adequacy forecast
MBE	Mean bias error
MENA	Middle East and North Africa
MILP	Mixed-integer linear programming
NAO	North-Atlantic oscillation
NET	Negative emission technology
NDC	Nationally determined contribution
NIMBY	'Not in my backyard'
NPV	Net present value
NTC	Net transfer capacity
OCC	Overnight capital cost
OCGT	Open-cycle gas turbine
OECD	Organisation for Economic Co-operation and Development
OPF	Optimal power flow
PACF	Partial autocorrelation function
PEM	Proton exchange membrane
PHS	Pumped hydro storage
PR	Performance ratio
PSM	Power system modelling
PV	Photovoltaic
RED	Renewable energy directive
RES	Renewable energy source(s)
RMSE	Root mean square error
RoR	Run-of-river hydro
RR	Replacement reserve
SMR	Steam methane reforming
SR	Strategic reserve
SRMC	Short-run marginal cost
SSRD	Downwards surface solar radiation
ST	Short term
STO	Storage hydro
TCR	Total capital requirement
TSO	Transmission system operator
TYNDP	Ten-year Network Development Plan
UCED	Unit commitment and economic dispatch
UNFCCC	United Nations Framework Convention on Climate Change
VoLL	Value of lost load
VOM	Variable operating and maintenance
vRES	Variable renewable energy source(s)
WACC	Weighted average cost of capital

Country abbreviations

AT	Austria
BE	Belgium
BG	Bulgaria
CH	Switzerland
CY	Cyprus
CZ	Czech Republic
DE	Germany
DK	Denmark
EE	Estonia
EL	Greece
ES	Spain
FI	Finland
FR	France
GB	Great Britain
HR	Croatia
HU	Hungary
IE	Ireland
IT	Italy
LT	Lithuania
LV	Latvia
LU	Luxembourg
NI	Northern Ireland
NL	the Netherlands
NO	Norway
PL	Poland
PT	Portugal
RO	Romania
SE	Sweden
SI	Slovenia
SK	Slovakia
UK	United Kingdom

Introduction

1

1.1 The climate emergency

The potential for greenhouses gases (GHG) such as carbon dioxide (CO_2) to warm the planet has been known to science since the late 19th century (Arrhenius, 1896). However, despite the expected catastrophic consequences of global warming or – as it more commonly called nowadays – climate change, it has taken decades to build the political will and momentum to address the issue. In 1992, the United Nations Framework Convention on Climate Change (UNFCCC) treaty was adopted with the objective to "*stabilise greenhouse gas concentration in the atmosphere at a level that would prevent dangerous anthropogenic interference with the climate system*"(UNFCCC, 2019), but no specific targets on GHG reductions were set. This was followed in 1997 with the ratification of the Kyoto Agreement which set binding GHG targets on a group of 37 mostly developed countries. More recently in 2016, the Paris Agreement was signed with the aim of keeping global warming "*well below 2 °C above pre-industrial levels and pursue efforts to limit the temperature increase to 1.5 °C above pre-industrial levels*". This will come into force after the Kyoto Protocol lapses in 2020 (Climate Analytics, 2016; UNFCCC, 2017b). In response to the more ambitious target of 1.5 °C warming set by the Paris Agreement and concerns from many countries that the consequences of 2 °C warming would be too disastrous, the Intergovernmental Panel on Climate Change (IPCC) released its *Global Warming of 1.5 ºC* report in 2018, which assessed the impacts of global warming of 1.5°C above pre-industrial levels (IPCC, 2018)[1]. This report showed that despite the commitments made by countries to reduce their emissions indicated by their nationally determined contributions (NDCs) as part of the Paris Agreement, projected global emissions were too high to limit warming to even 2°C, highlighting that more ambitious action would be necessary.

Based on integrated assessment models (IAMs), which integrate computer models describing human activities (e.g. energy systems and land use) with models describing natural systems (e.g. the climate and vegetation), the IPCC identified how much more GHG could be emitted in total to limit global warming to specific levels, also known as carbon budgets (Table 1-1) (van Vuuren et al., 2015)[2]. The budgets show that in order to have a 50% chance of limiting global warming to 2 ºC compared with pre-historical levels, mankind can emit no more than 1500 Gt CO_2 from 2018 onwards, falling to 580 Gt CO_2 for the more ambitious target of 1.5 ºC (Rogelj et al., 2018). At 2018 emission levels of approximately 37 Gt CO_2 y^{-1}, this leads to the sobering conclusion that the budget giving a better chance (67%) of meeting the 1.5 ºC warming target will be exceeded within 11 years. This has motivated a growing number of organisations and governments to declare a 'climate emergency' (Aidt, 2019).

While carbon budgets give the total net amount of CO_2 which can be emitted over a given period, the IAM results show that there are many different emission trajectories or pathways consistent with a given budget. This is because higher emissions in the short term (i.e. before mid-century) can be offset by delivering net-negative emissions in the long term. To achieve

Table 1-1 | Estimated remaining global carbon budgets from 1/1/2018 for limiting global warming to 1.5 and 2 ºC with varying levels of certainty. Based on Table 2.2 from (Rogelj et al., 2018). The values given in regular typeface are the total remaining carbon budgets in Gt CO_2. The italicised values in brackets indicate the number of years remaining (from 1/1/2018) until the budget is exceeded, assuming global emissions remain at 2018 levels of approximately 37 Gt CO_2 y^{-1}.

Approximate warming since period between 1850-1900 (ºC)	Likelihood of limiting warming to specified level (%) [a]		
	33%	50%	67%
~1.5 ºC	840 *(23)*	580 *(16)*	420 *(11)*
~2.0 ºC	2030 *(55)*	1500 *(41)*	1170 *(32)*

[a] The budgets above are not directly equivalent with those from the IPCC 5th Assessment Report where the likelihood of limiting warming to a specified level is based on the fraction of model simulations which do not exceed the specified warming limit. Rather, the likelihood reported here is the percentile of the transient climate response to cumulative emissions of carbon, assessed by the IPCC 5th Assessment Report to fall likely between 0.8–2.5°C/1000 PgC considering a normal probability distribution. Note that these budgets do not include potential earth system feedbacks (-100 Gt CO_2), and should be seen in the context of several uncertainties and their potential impact on the budget including (i) non-CO_2 GHG emissions (±250 Gt CO_2) and (ii) the climate response to these emissions (-400 to +200 Gt CO_2), (iii) the distribution of the climate response (+100 to +200 Gt CO_2), (iv) uncertainty in historical temperatures (±250 Gt CO_2), and uncertainties in recent emissions (±20 Gt CO_2).

these net-negative emissions, techniques which remove CO_2 from the atmosphere – often referred to as carbon dioxide removal (CDR) or negative emission technologies (NETs) – will be required. Major advantages of NETs are that they can offset higher GHG emissions in the short term, allowing for a more gradual (and potentially less costly) transition, and that they can offset emissions from sectors where emissions reductions are more difficult or costly to achieve (van Vuuren et al., 2017). Some NETs mimic natural processes to store carbon such as afforestation (growing more trees), soil carbon sequestration (locking up CO_2 as organic matter in soils), enhanced weathering (locking up CO_2 chemically in the ground using alkaline minerals), and ocean carbon storage (locking up CO_2 in the oceans chemically or biologically) (Fuss et al., 2018). Two other NETs rely on carbon capture and storage (CCS) technology to store CO_2 under the ground: bioenergy with carbon capture and storage (BECCS), and direct air carbon capture (DAC). BECCS typically involves growing biomass to capture CO_2 from the air, releasing the CO_2 from the biomass (typically by burning), then capturing and storing it underground. In contrast, DAC shortcuts this process by removing CO_2 directly from air using physical or chemical means and storing it underground.

When aiming to limit warming to a certain level by the end of the century, different emission pathways can lead to global temperature rise overshooting the target, as long as the temperature ultimately returns to the target level. However, this overshoot poses large risks both for human society and the environment as some impacts, such as ecosystem loss, may be irreversible (Hoegh-Guldberg et al., 2018). Figure 1-1 depicts four different illustrative model pathways (global net emission trajectories) in which the target of limiting warming to 1.5 ºC can be achieved but varying in the underlying assumptions on factors like future energy demand, land use, available technology options and population growth. As a result of these factors, the technologies deployed, GHG emission profiles and temperature overshoot vary between the different pathways. Almost all pathways that limit global warming to 1.5 °C with limited or no temperature overshoot will require CDR to some extent (Allen et al., 2018).

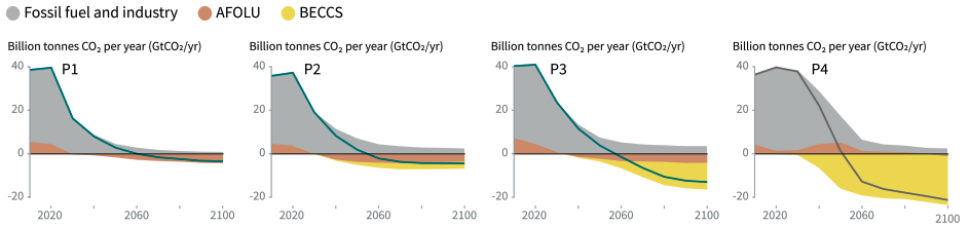

P1: A scenario in which social, business, and technological innovations result in lower energy demand up to 2050 while living standards rise, especially in the global South. A down-sized energy system enables rapid decarbonisation of energy supply. Afforestation is the only CDR option considered; neither fossil fuels with CCS nor BECCS are used.

P2: A scenario with a broad focus on sustainability including energy intensity, human development, economic convergence and international cooperation, as well as shifts towards sustainable and healthy consumption patterns, low-carbon technology innovation, and well-managed land systems with limited societal acceptability for BECCS.

P3: A middle-of-the-road scenario in which societal as well as technological development follows historical patterns. Emissions reductions are mainly achieved by changing the way in which energy and products are produced, and to a lesser degree by reductions in demand.

P4: A resource and energy-intensive scenario in which economic growth and globalization lead to widespread adoption of greenhouse-gas intensive lifestyles, including high demand for transportation fuels and livestock products. Emissions reductions are mainly achieved through technological means, making strong use of CDR through the deployment of BECCS.

Global indicators	P1	P2	P3	P4	**Interquartile range**
Pathway classification	No or low overshoot	No or low overshoot	No or low overshoot	High overshoot	No or low overshoot
CO_2 emission change in 2030 (% rel to 2010)	-58	-47	-41	4	(-59,-40)
└ in 2050 (% rel to 2010)	-93	-95	-91	-97	(-104,-91)
Kyoto-GHG emissions in 2030 (% rel to 2010)*	-50	-49	-35	-2	(-55,-38)
└ in 2050 (% rel to 2010)	-82	-89	-78	-80	(-93,-81)
*Final energy demand** in 2030 (% rel to 2010)*	-15	-5	17	39	(-12, 7)
└ in 2050 (% rel to 2010)	-32	2	21	44	(-11, 22)
Renewable share in electricity in 2030 (%)	60	58	48	25	(47, 65)
└ in 2050 (%)	77	81	63	70	(69, 87)
Primary energy from coal in 2030 (% rel to 2010)	-78	-61	-75	-59	(-78, -59)
└ in 2050 (% rel to 2010)	-97	-77	-73	-97	(-95, -74)
from oil in 2030 (% rel to 2010)	-37	-13	-3	86	(-34,3)
└ in 2050 (% rel to 2010)	-87	-50	-81	-32	(-78,-31)
from gas in 2030 (% rel to 2010)	-25	-20	33	37	(-26,21)
└ in 2050 (% rel to 2010)	-74	-53	21	-48	(-56,6)
from nuclear in 2030 (% rel to 2010)	59	83	98	106	(44,102)
└ in 2050 (% rel to 2010)	150	98	501	468	(91,190)
from biomass in 2030 (% rel to 2010)	-11	0	36	-1	(29,80)
└ in 2050 (% rel to 2010)	-16	49	121	418	(123,261)
from non-biomass renewables in 2030 (% rel to 2010)	430	470	315	110	(243,438)
└ in 2050 (% rel to 2010)	832	1327	878	1137	(575,1300)
Cumulative CCS until 2100 ($GtCO_2$)	0	348	687	1218	(550, 1017)
└ of which BECCS ($GtCO_2$)	0	151	414	1191	(364, 662)
Land area of bioenergy crops in 2050 (million hectare)	22	93	283	724	(151, 320)
Agricultural CH_4 emissions in 2030 (% rel to 2010)	-24	-48	1	14	(-30,-11)
in 2050 (% rel to 2010)	-33	-69	-23	2	(-46,-23)
Agricultural N_2O emissions in 2030 (% rel to 2010)	5	-26	15	3	(-21,4)
in 2050 (% rel to 2010)	6	-26	0	39	(-26,1)

NOTE: National and sectoral characteristics can differ substantially from the global trends shown above.
** Kyoto-gas emissions are based on SAR GWP-100*
*** Changes in energy demand are associated with improvements in energy efficiency and behaviour change*

Figure 1-1 | Characteristics of four illustrative model pathways in relation to global warming of 1.5°C from the IPCC. Source: (Allen et al., 2018, p. 19)**.** These pathways show a range of potential mitigation approaches and vary widely in their projected energy and land use, as well as their assumptions about future socioeconomic developments, including economic and population growth, equity and sustainability. A breakdown of the global net anthropogenic CO_2 emissions into the contributions in terms of CO_2 emissions from fossil fuel and industry, agriculture, forestry and other land use (AFOLU), and bioenergy with carbon capture and storage (BECCS) is shown. Further characteristics for each of these pathways are listed below each pathway. These pathways illustrate relative global differences in mitigation strategies, but do not represent central estimates, national strategies, and do not indicate requirements.

In pathways relying less on CDR, such as P1, emissions fall more quickly than in pathways which use CDR, implying more urgent actions would be necessary to increase energy efficiency, reduce the use of fossil fuels, and deploy more low-carbon energy sources. For example, in P1, GHG emissions fall by nearly 60% (relative to 2010) and the share of electricity coming from RES reaches 60% by 2030. In pathways relying more heavily on CDR, such as P4, deployment of efficiency measures and renewable energy could be slower, but significant negative emissions must be achieved from 2030 onwards. Thus, limiting warming to 1.5 °C in line with the ambition of the Paris Agreement will mean either urgent decarbonisation[3] of our energy and agricultural systems, urgent deployment of NETs, or – more likely – both.

1.2 The role of the electricity sector in meeting climate targets

In 2018, global carbon emissions from power generation were approximately 13 Gt, or 38% of total energy-related CO_2 emissions (IEA, 2019). This makes electricity production the largest CO_2-emitting sector globally (Bruckner et al., 2014). Given its contribution to global emissions electricity plays a major role in mitigation scenarios aiming for deep cuts in GHG emissions, with most scenarios showing that the power sector must fully decarbonise or even deliver net-negative emissions by 2050 (Bruckner et al., 2014; Rogelj et al., 2018). Apart from its significant contribution, there are three other reasons why decarbonising the electricity sector should be a key priority.

The first is that many mature low-carbon technologies are already available to decarbonise the electricity sector (Bruckner et al., 2014). For example, hydropower is a renewable energy source (RES) which has been providing low-carbon electricity for more than a century and, with a share of 16%, continues to be the largest source of low-carbon electricity globally (Olivier & Peters, 2018). Thanks to subsidies and significant cost reductions, more modern RES technologies such as solar photovoltaic (PV) and wind power have also seen significant growth, which in 2017 supplied 1.7% and 4.4% of electricity respectively (Olivier & Peters, 2018). While costlier than PV and wind, concentrating solar power (CSP) and bioelectricity are two other low-carbon RES technologies which have been deployed at commercial scale, with 5 GW and 115 GW respectively installed globally by the end of 2018 (IRENA, 2019). Aside from RES, nuclear power is another generation technology that has been providing low-carbon electricity for more than half a century, and currently supplies 10% of electricity globally (Olivier & Peters, 2018). Lastly, CCS is a technology that can be applied to power plants using coal, natural gas or biomass to reduce their CO_2 emissions by around 90%. At the end of 2018 there were 18 large-scale commercial CCS facilities in operation across the globe with a further five under construction, and 20 in various stages of development (Global CCS Institute, 2018). Most of these CCS facilities are in industries such as natural gas processing where CO_2 capture is an integral part of the process; however, there are two cases where CCS is applied to power

plants[4]. Thus, while future innovation and upscaling will reduce the costs of RES and other low-carbon technologies, no technical hurdles exist for their deployment.

The second reason is that by increasing the share of electricity in total energy consumption, low-carbon electricity can help to decarbonise the heating, industry, and transport sectors (Eurelectric, 2018; Sugiyama, 2012). For example, in 2015 the share of electricity within total final energy consumption in the European Union (EU) was 22%, and studies show this could rise to between 30% and 60% by 2050 (Eurelectric, 2018; Sugiyama, 2012). With global demand for electricity rising by 4% annually driven by growth in developing countries (IEA, 2019), coupled with additional electrification of heating and transport, electricity will play an increasingly important role in the global energy system.

The third reason is that BECCS and DAC, two of the NETs that may be needed to limit global warming to 1.5 °C, are strongly linked with the electricity sector. This is because a biomass power plant equipped with CCS can be expected to generate about 1.25 MWh of electricity for every tonne of negative CO_2 emissions it delivers, whereas a DAC plant consumes about 0.5 MWh of electricity for every tonne of negative CO_2 emissions delivered (Daggash et al., 2019). While there are a variety of other NETs available such as afforestation and biochar production, and BECCS can be deployed in other sectors, deploying DAC and BECCS in the electricity sector may offer advantages[5]. For example, compared with afforestation, the underground may be a safer long-term store for carbon as forests are vulnerable to wildfires, the risk of which increases as the climate warms (Settele et al., 2014).

1.3 Europe's electricity sector

In the EU, the transition to low-carbon energy sources is already underway, especially in terms of RES (Figure 1-2). Between 2008 and 2018, the installed wind capacity in the EU tripled from 60 to 180 GW, and solar PV capacity increased from 10 to 115 GW (EurObserv'ER, 2018, 2019; Eurostat, 2017b; SolarPower Europe, 2019). Thanks to this growth, since 2015 solar PV and wind together have generated more electricity annually than hydro, historically the largest provider of RES electricity in the EU. This growth has largely been the result of policies aimed at increasing the share of RES in energy supply, a central tenet of EU climate policy since the first *EU Directive on Electricity Production from Renewable Energy Sources (2001/77/EC)* came into force in 2001 (European Parliament, 2001). The role of RES was strengthened with the *Renewable Energy Directive (RED) (2009/28/EC)* mandating for 20% of gross final energy consumption in the EU to come from RES by 2020 (European Parliament, 2009), and again in 2018 with the recast RED mandating at least 32% by 2030 (European Parliament, 2018a).

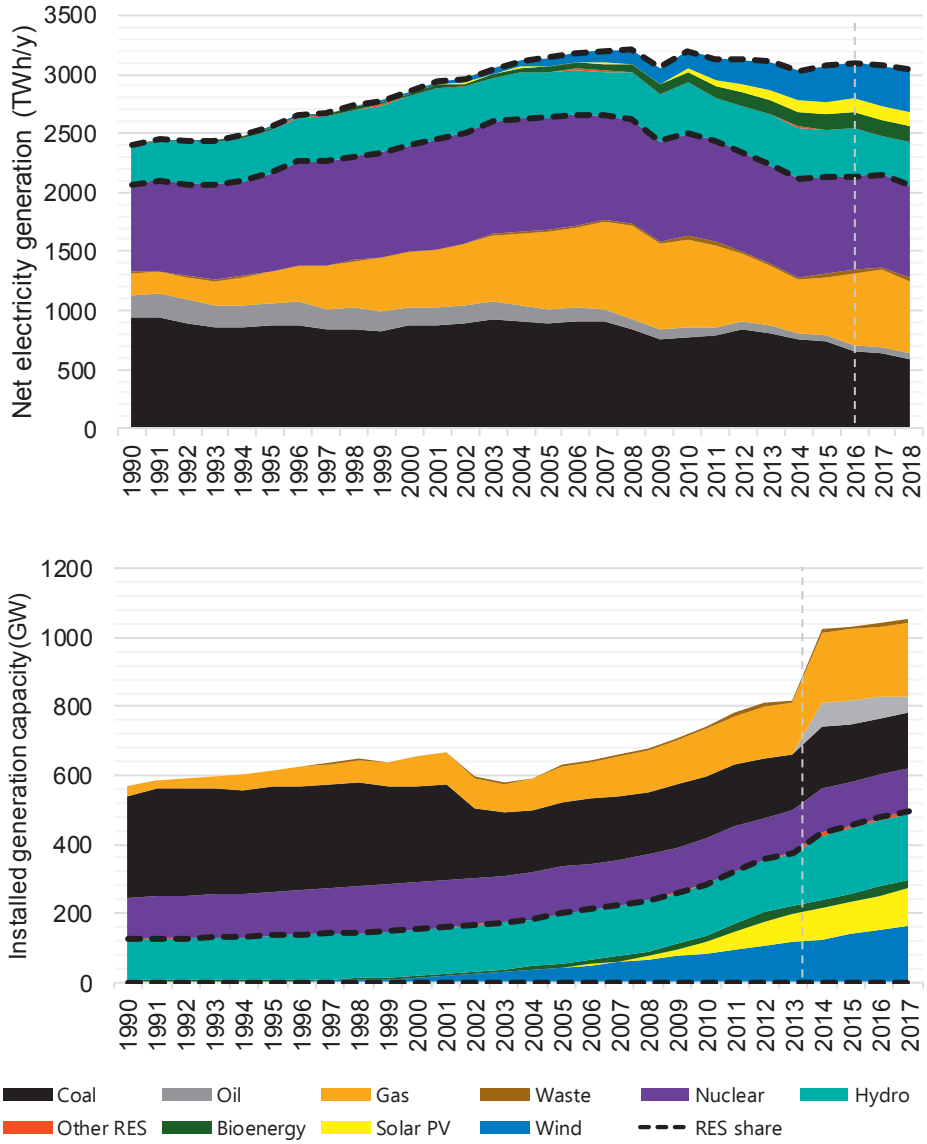

Figure 1-2 | Historical development of total electricity generation (above) and installed generation capacity (below) in the EU28 countries since 1990. Based on data from Eurostat for earlier years and ENTSO-E for more recent years, with the changeover year indicated by the dashed vertical lines (ENTSO-E, 2019b; Eurostat, 2019b, 2019c). The use of different data sources leads to jumpy behaviour in the changeover years, and different generation categories reported. The graph regions between the two dashed black lines indicate the approximate RES share (excluding RES waste). Eurostat reports only gross generation from fossil fuels, which was converted to net generation based on the ratios between net and gross generation from the ENTSO-E data. Other RES includes CSP, geothermal and tidal/ocean energy. Waste includes both RES and non-RES. Hydro includes pumped storage. Note that the technologies are ordered differently in the lower graph to minimise the effect of using different data sources.

In addition to RES support, another key element of EU climate policy is the EU Emission Trading Scheme (ETS). Launched in 2005, the ETS was the world's first international emissions trading system and covers around 40% of total EU GHG emissions (EEA, 2019). Each year, all large emitters operating in one of the covered sectors must surrender enough emission certificates in order to cover their total carbon emissions. As a cap and trade system, the total volume of carbon emissions from installations covered by the ETS is set annually, which decreases gradually to ensure that total emissions fall over time (Healy et al., 2019). As emitters can trade allowances with one another, the price of CO_2 is set by the market, and emissions are reduced in the economy where it is cheapest to do so. As a result of an overallocation of allowances and weaker than expected industrial demand following the 2008 financial crisis, the allowance price fell from a level of 20 € t^{-1} in 2008 at the start of the second trading period to 5 € t^{-1} in 2013, where it largely remained for the period 2013 to 2017 (Healy et al., 2019) (Figure 1-3).

While the EU ETS has reduced the competitiveness of fossil-fuel installations, some evaluations (e.g. Healy et al. (2019) and Marcu et al. (2019)) are somewhat critical of the results obtained by the EU ETS, arguing that the effective carbon price has been insufficient to drive a major fuel shift from coal- to gas-fired electricity generation or encourage development of low-carbon technologies. Meanwhile, others (e.g. Delbeke (2019)) defend the EU ETS as a system that successfully established an explicit price on carbon, and reduced CO_2 emissions in the covered sectors by 26% between 2005 and 2017. In any case, thanks to reforms aimed at reducing the oversupply of allowances, such as the market stability reserve introduced in January 2019 (EC, 2020), the EU ETS is expected to become more resilient to market shocks, and allowance prices are expected to increase in the future. Indeed, allowance prices increased by more than 200% from 7 € t^{-1} in 2018 to 25 € t^{-1} in 2020.

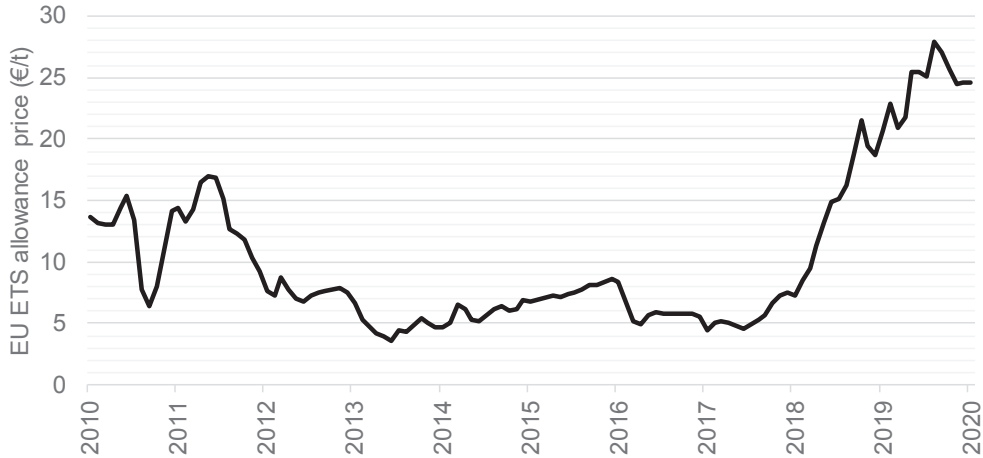

Figure 1-3 | Development of the monthly average EU ETS allowance price between 2010 and 2020. Source: (Markets Insider, 2020).

While wind and PV have seen significant deployment, growth in other RES technologies has been slower. For example, the installed capacity of all other RES technologies (not including renewable waste) merely doubled from 17 GW in 2008 to 35 GW in 2018, mostly thanks to solid biomass and biogas plants (Figure 1-2). In contrast to RES, growth in other low-carbon technologies like CCS and nuclear has been lacklustre. After several setbacks and project cancellations, no commercial-scale power plants equipped with CCS plants have been built in Europe[6]. Eight large-scale CCS facilities are currently in development; however, the majority of these are intended for industry or the production of hydrogen and not for the power sector (Global CCS Institute, 2018). Meanwhile, nuclear power, which has provided around 30% of electricity in Europe for decades, appears to be in decline. For example, Germany and Belgium have committed to phasing out nuclear power by 2022 and 2025 respectively (Schneider & Froggatt, 2018). Even France, which for many years has been a global leader in nuclear power and the largest electricity exporter in Europe, plans to reduce its share of nuclear from 75% to 50% by 2035 (World Nuclear Association, 2018). If carried through, these policies will mean that at least 17 GW of the 120 GW of nuclear capacity installed in Europe will be decommissioned by 2025, rising to a total of around 32 GW by 2035. At the same time, only 4 GW of new capacity is under construction (Schneider & Froggatt, 2018).

The EU has long been a global leader in combatting climate change and deploying RES technologies. With the resolution of the European Parliament in November 2019 to join the growing number of governments in declaring a climate emergency, to call for increasing the EU's GHG reduction target to 55% by 2030, and to encourage member states to increase funding for climate action in developing countries, the EU is set to maintain its leadership role in the future (European Parliament, 2019). However, this means that the EU will have to confront the challenges of the energy transition sooner than other regions. Therefore, studying how to deal with the challenges of the energy transition in the EU is not only timely, but may yield valuable insights for other regions looking to develop their own decarbonisation strategies.

1.4 Challenges facing the European electricity sector

Thanks largely to the growth in RES, GHG emissions from public electricity (and heat) generation in the EU fell by 24% between 2008 and 2017 to approximately 1 Gt y^{-1} (Eurostat, 2019a). However, this still represents 31% of total EU CO_2 emissions, or 25% of total EU GHG emissions[7]. While Europe's electricity sector must decarbonise, it is not clear how this should be done as there are three broad strategies which could be followed. Firstly, studies have shown that cost-effective low-carbon generation portfolios can be constructed from a mix of RES, nuclear and fossil generation with CCS (Jenkins et al., 2018; Sepulveda et al., 2018). By committing to a target of net-zero emissions by 2050 and deploying a mix of RES, nuclear and

potentially CCS, the United Kingdom (UK) is following such as a *technology-diverse approach* (UK Government, 2019). A second strategy, followed by countries such as Denmark and Sweden, is to aim for a power system based almost *exclusively on RES* (KEFM, 2018; Swedish Ministry of the Environment and Energy, 2019). Germany, which has set a minimum target of 80% RES electricity by 2050, is following a similar high-RES strategy (BMWi, 2018). A third strategy would be large-scale *deployment of NETs* to offset emissions from continued fossil fuel use in the electricity or in other sectors, though this strategy is not currently being followed by any country. Whichever strategy is implemented, the European electricity sector is likely to face three major challenges over the coming decades.

Firstly, the **growing penetration of variable renewable energy sources** like solar PV and wind is raising concerns about the reliability of the power system. For decarbonisation strategies targeting high levels of RES, this will be a challenge. However, given the falling cost of wind and PV (IRENA, 2018), many technology-diverse portfolios are also likely to rely heavily on solar and wind. Secondly, decarbonisation ambitions are becoming increasingly stringent over time, and even net-zero power sector emissions by 2050 may not be enough to meet a 1.5 °C warming limit**.** Thus, deployment of NETs may become unavoidable, and it is unclear what the **impacts of large-scale deployment of NETs** on the European electricity sector could be. Lastly, there are concerns whether Europe's current liberalised **electricity market design** will be able to incentivise investment in enough low-carbon generation capacity to ensure security of supply. These three challenges are explained in more detail in the following sections.

1.4.1 Integration of variable renewable energy sources

In 2017, solar PV and wind represented 15% of total EU28 electricity generation (Eurostat, 2019d). If total generation from PV and wind continues to grow at around 8% annually, these two technologies together could generate some 2500 TWh y^{-1} by 2040, or approximately 80% of current EU electricity demand[8]. While 80% in 2040 represents a large increase compared with today, such levels are under consideration by policymakers. For example, the *Energy Roadmap 2050* study published by the European Commission (EC) in 2011 considers 32% to 65% PV and wind by 2050 (EC, 2011d), while a more recent EC study considers between 65% and 72% by 2050 (EC, 2018a). In their long-term planning scenarios, the European Network of Transmission System Operators for Electricity (ENTSO-E) consider PV and wind shares between 48% and 58% by 2030 for the EU28 (including Norway and Switzerland), and between 65% and 81% by 2040 (ENTSO-E & ENTSO-G, 2018). In the academic literature the shares can be even higher. For example, Child et al. (2019) consider 75% to 78% by 2050 (including Turkey, Iceland, Ukraine and the Balkan states), while Plessman et al. (2017) consider 83% (including the Balkans). Accommodating these high levels of wind and solar PV in the power system will be challenging as unlike traditional centralised, synchronous, dispatchable power plants (e.g. natural gas, nuclear, hydropower), generation from solar PV and wind is asynchronous,

distributed, and varies depending on the prevailing weather conditions (Hirth & Ziegenhagen, 2015). For this reason, they are often termed intermittent or variable renewable energy sources (vRES)[9]. The variability introduced by vRES can be both short term, caused by sub-hourly fluctuations in wind speed and cloud movements; and long term, as a result of as interannual weather variability (IRENA, 2017). Another challenge of vRES is that their dependence on the weather makes their generation uncertain, and their generation schedules must be based on forecasts. As these forecasts are imperfect, transmission system operators (TSOs) must activate operating reserves when vRES forecast errors (together with load forecast errors and unplanned outages) cause electricity supply and demand to become unbalanced. As a result, higher vRES penetrations are likely to increase the need for operating reserves (Brouwer et al., 2014; Ortner & Totschnig, 2019).

Several European countries have already integrated large amounts of vRES into their power systems including Germany and Denmark, where vRES penetration reached 28% and 44% respectively in 2018 (ENTSO-E, 2019b). The transmission networks in these countries are well-interconnected with those of their neighbours, allowing them to rely to a large extent on cross-border transmission to integrate vRES by importing electricity during periods of low domestic vRES generation, and exporting electricity during periods of surplus generation (Wynn, 2018). This is possible as weather conditions vary in different locations, allowing for wind and solar generation across geographical areas to balance out (Widén et al., 2015). However, as more EU countries plan to increase their shares of vRES, it is unclear whether this strategy will continue to be effective as with higher vRES penetrations, neighbouring countries may both find themselves in periods of simultaneous electricity surplus/deficit, limiting the potential for cross-border transmission. Apart from transmission, previous studies have shown that other sources of flexibility can help accommodate the variability of vRES in power systems, including fast-ramping generators, electricity storage, and demand-side response (Brijs et al., 2017; Brouwer, Van den Broek, et al., 2016). The capacity mix of solar PV and wind technologies can also affect their integration due to complementarity in their seasonal generation patterns (Heide et al., 2010). Studies have also investigated optimal spatial distributions of vRES in single countries (Zeyringer et al., 2018) and small regions (Jerez, Trigo, Sarsa, et al., 2013). However, the potential of optimising both the mix and spatial deployment of solar PV and wind capacity to better match electricity demand patterns across the entire European continent has not been explored.

Integrating large shares of vRES will be particularly challenging for 100% RES power systems, which have received increasing attention as a strategy for decarbonising the power sector (Brown et al., 2018; Heard et al., 2017; Jacobson & Delucchi, 2018). Several scenarios for a 100% RES European power system have been published by non-governmental organisations including the European Climate Foundation's *Energy Roadmap 2050* (ECF, 2010a) and Greenpeace's *Energy Revolution* (GWEC et al., 2015). These scenarios are typically developed using energy system models to assess whether projected demand could be met by RES supply.

However, sufficient RES supply does not indicate that a 100% RES power system is feasible as, due to the variable and stochastic nature of vRES, keeping electricity demand and supply balanced is likely to become more difficult in power systems with large shares of vRES generation (Hirth & Ziegenhagen, 2015). Moreover, most of the existing studies on 100% RES power systems do not model the spatial distribution of vRES in detail, which can have complex effects on total system cost due to trade-offs between transmission costs, exploiting (and depleting) solar and wind resources at favourable locations, geographical balancing of vRES generation between different locations, and proximity to load centres (Gernaat, 2019; Zeyringer, 2017). As a result, apart from a handful of countries with significant endowment of dispatchable renewable sources such as hydro and geothermal (e.g. Iceland, Costa Rica, Norway), it is unclear whether 100% RES power systems relying on large shares of vRES are feasible in practice, and can deliver cost-effective, reliable electricity for society while meeting climate goals. Thus, if EU policymakers choose to follow a decarbonisation strategy aiming for 100% RES in Europe (or close to it), it is important to gain a better understanding of what the consequences may be for system reliability and cost.

1.4.2 Shifting climate ambition levels, Paris-compliance and the impact of NETs

As a result of delayed climate action, scientists warning that the earth is warming faster than predicted, and public opinion coalescing behind stronger climate action, each successive analysis produced by governments outlining pathways to a decarbonised energy system tends to be more ambitious than the last. In other words, the more we come to understand about the energy transition, the more urgent and challenging it becomes. For example, the EC's *Roadmap 2050* long-term decarbonisation scenarios for the EU published in 2011 aimed for a reduction of power sector emissions between 96 and 99% by 2050 (EC, 2011a). To achieve this level of decarbonisation, the scenarios employed diverse portfolios with varying shares of fossil fuels (9.6% to 33.3%) mostly equipped with CCS, nuclear (2.5% to 26.4%) and RES (40.3% to 80.1%) (EC, 2011b). In new scenarios released as part of the *Clean Planet for All* package in 2018, the share of RES increased (81% to 85%), while the shares of fossil (2% to 6%) and nuclear (12% to 15%) decreased compared with the 2011 scenarios (EC, 2018a). Additionally, in the scenarios consistent with the Paris Agreement, between 280 and 600 Mt CO_2 y^{-1} is captured from the air in 2050 using a combination of biomass (84 to 276 Mt CO_2 y^{-1}) and DAC (123 to 210 Mt CO_2 y^{-1}), reflecting the need for NETs (EC, 2018a). This shows that the ambition levels for the power sector are becoming more stringent over time and, if decarbonisation is further delayed, may tighten again and increase the need for NETs. Moreover, some have concluded that by eliminating the use of fossil fuels, 100% RES power and other net-zero emission power systems are consistent with the ambitious goals set out in the Paris Agreement (Child et al., 2019). However, as shown by the most recent IPCC scenarios (see Figure 1-1), negative emissions may already be necessary in the 2030s to be consistent with a 1.5 ºC

warming target. Currently, BECCS and DAC are only demonstration-scale technologies and while studies have looked at their impact on individual countries (e.g. (Daggash et al., 2019; Pour et al., 2018), little is known about their potential impact on the power sector and electricity markets when deployed at scale across Europe. Thus, more insights are needed into the potential consequences for the European power sector of large-scale deployment of BECCS and DAC in the event that (i) more aggressive climate action is needed, (ii) decarbonisation in other sectors (e.g. aviation, agriculture) is more challenging than expected and the power sector must also offset emissions from these sectors, or (iii) deployment of other CDR technologies proves unsuccessful.

1.4.3 Electricity market design and generator business cases

Designing an efficient electricity industry involves identifying all the tasks that must be performed, assigning these tasks to different groups, and designing the necessary structures, rules and incentives to encourage these groups to perform their tasks effectively and efficiently (Biggar & Hesamzadeh, 2014, p. 73). Some of these tasks concern actions with a short-term horizon, such as efficient scheduling of the available generation, demand, and transmission resources, and ensuring supply and demand are kept in balance to maintain system frequency at the target level (e.g. 50 Hz in Europe). Other tasks have a long-term horizon, such as ensuring efficient investment in supply-side, demand-side and network resources. Historically, many of these tasks were in the hands of state-owned vertically integrated monopolies. However, since the privatisation and unbundling reforms implemented in the 1990s and 2000s, independent TSOs have been given the role of maintaining system frequency, and most other tasks have been given to liberalised electricity markets. In this context, designing the structures, rules and incentives which govern how the power sector operates is essentially a question of market design. While there are many objectives of electricity market design, the overarching objective historically has been to provide electricity reliably to consumers at the lowest possible cost (Munasinghe, 1979, p. 29). However, as society has evolved over recent decades, so have its expectations for the electricity sector, and the objectives of market design have been extended to include environmental and wider sustainability considerations. Satisfying these three objectives – *reliability*, *affordability* and *sustainability* – involves trade-offs, and is sometimes referred to as the energy trilemma (Poudineh & Jamasb, 2012) (Figure 1-4). Achieving these objectives is a stated goal of the EU's Internal Energy Market (EC, 2014d).

Across Europe, approximately half of all electricity is traded via power exchanges on day-ahead electricity markets[10]. In these markets, electricity suppliers (i.e. generators) make offers to supply a certain quantity of electricity at a given price for each market period (e.g. hourly), while electricity consumers (e.g. large industries, and electricity retailers representing households) make bids to purchase enough electricity to meet their expected demand. The market price in each period is set by the marginal bid (the price of the last MWh of generation

required to meet demand) and generation companies receive revenues based on the amount of energy they produce.

Until now, these markets have served reasonably well to ensure efficient short-term market operation and long-term investment[11]. However, there are concerns that the current energy-only market design may not be adequate to cope with the challenges facing the European power system, in particular the increasing penetration of vRES which, due to its almost zero marginal cost, tends to put downward pressure on electricity prices (Figure 1-5) (Clò et al., 2015). In particular, studies have pointed to the increasing penetration of vRES as being an important (but not the only) driver behind the fall in electricity prices across Europe between 2011 and 2015 (Figure 1-6) (Hirth, 2018). There is concern amongst some EU countries, policymakers and academics that if prices continue to fall due to increasing vRES deployment, the market may provide insufficient incentives for investment in new generation capacity, threatening security of supply (EC, 2016c). In response to these concerns, 15 European countries have implemented (or are planning to implement) capacity remuneration mechanisms (CRMs), which reward generators a fixed amount for their capacity irrespective of how much electricity they supply (ACER & CEER, 2019). However, according to ENTSO-E's 2018 Mid-term Adequacy Forecast (MAF), seven of these countries do not appear to be facing a security of supply problem in the near future (i.e. before 2025) (ACER & CEER, 2019) and 13 European countries continue to operate energy-only markets, with all but one facing no security of supply problems (ENTSO-E, 2018c). Moreover, electricity prices have recovered in recent years from the low levels seen in 2015[12]. Thus, it is not clear whether CRMs, which cost EU consumers €2.5 billion in 2018 (ACER & CEER, 2019), are a necessary element of market designs in the long term.

Figure 1-4 | The energy trilemma for the electricity sector is to find the optimal balance between sustainability, reliability and affordability.

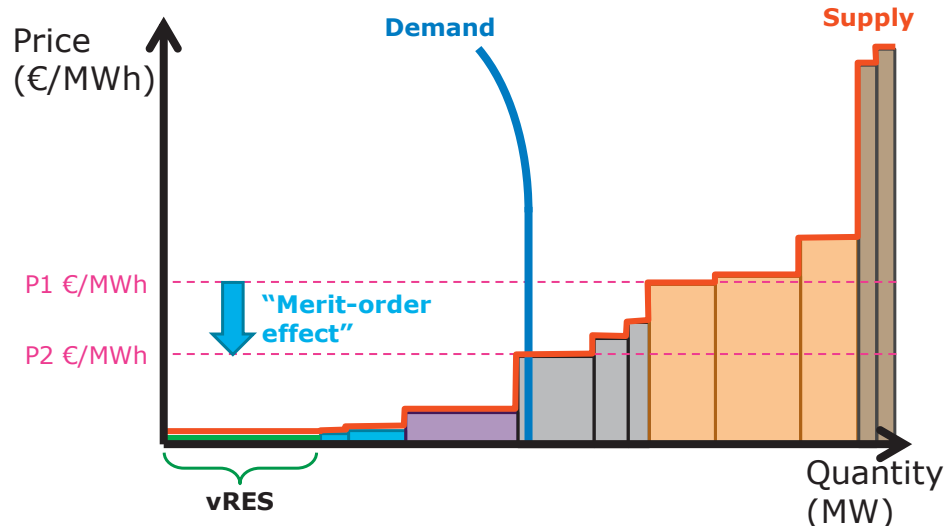

Figure 1-5 | The impact of vRES on electricity prices. The horizontal axis contains all the generator price-volume bids sorted according to increasing price (i.e. in merit order), which together make up the supply curve (in red). The price at which the demand curve (blue) intersects the supply curve determines the market price, P1, and the capacity dispatched. With nearly zero marginal costs, vRES technologies like PV and wind shift the supply curve to the right. Thus, for the same level of demand, the addition of vRES to the market causes the price to drop from P1 to P2. This is known as the merit-order effect.

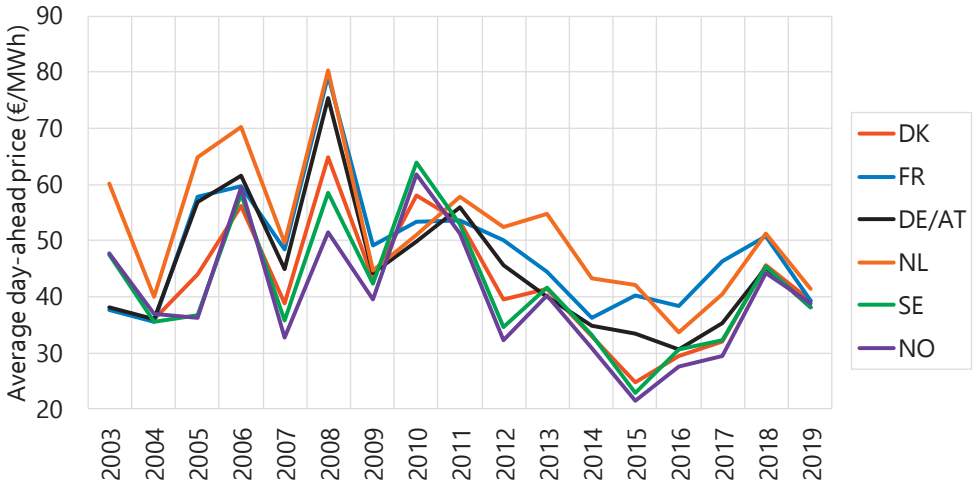

Figure 1-6 | Development of day-ahead wholesale electricity prices in €2019/MWh over time in selected European countries, adjusted for inflation. Germany (DE) and Austria (AT) (and Luxembourg) constituted a single bidding zone for most of the considered period. Some countries including Denmark (DK), Sweden (SE) and Norway (NO) are made up of several bidding zones, the average price is shown here. The prices for 2019 only include data up to November 2019. Data taken from ENTSO-E, EPEX, Nord Pool, and a number of literature sources (Hirth, 2018; Huisman & Kiliç, 2013; Khoshrou et al., 2019)

Despite the recovery in day-ahead prices since 2015, it is uncertain how increasing vRES penetration will affect market prices in the long term, and what the flow-on consequences for generator revenues may be. Apart from day-ahead markets, increasing vRES penetration is likely to have impacts on other markets, such as the intraday and balancing markets. For example, studies show that requirements for balancing capacity and energy are likely to increase over time with increasing vRES penetration (Borne et al., 2018). Intraday trading and imbalance netting, which have played an important role in reducing German balancing requirements (Koch & Hirth, 2019), could also have a significant role at the European level. Some studies have explored these potential developments, but only for rather limited vRES penetrations of up to 27% (Ortner & Totschnig, 2019). Thus, further insights are needed about how these various markets may develop as a result of different decarbonisation strategies, and what elements of market design are more likely to support the overall objective of delivering low-carbon electricity reliably to consumers at the lowest possible cost.

1.5 Thesis aims and outline

This thesis aims to provide insights into the consequences of following different decarbonisation strategies in the European electricity sector until the year 2050[13], and how these strategies address the three challenges outlined in the previous section. Thus, the main research question driving this thesis is:

What are the consequences of pursuing different strategies in the European power sector for reliability, achievement of climate objectives, and economic viability?

In addressing this broader question, this thesis focusses in more detail on the following sub-questions (SQ):

1. To what extent can the mix and spatial distribution of solar PV and wind be used to help integrate them into the power system?

2. What are the potential consequences of aiming for a 100% renewable power system?

3. What are the potential consequences of relying on BECCS and DAC in the power sector to meet a 1.5 ^{o}C warming target?

4. What elements should be present in future market designs to address the energy trilemma?

These sub-questions are addressed in four core chapters (Table 1-2), which are outlined briefly below .

Table 1-2 | Correspondence between the chapters and research questions of this thesis

Chapter	Topic	Research question			
		SQ1	SQ2	SQ3	SQ4
2	Consequences of the mix and spatial distribution of wind and solar PV for residual demand	X	X		
3	Consequences of high vRES penetration in European electricity sector for intraday and balancing markets		X		X
4	Consequences of a 100% renewable power system	X	X		
5	Consequences of aiming for a 1.5 ºC target with BECCS and DAC under different market designs			X	X

Chapter 2, titled '*Can the mix and spatial distribution of wind and solar PV facilitate their integration in the power* system?', examines to what extent the spatial deployment of wind and solar PV capacity across Europe could be used to facilitate its integration into the power system by matching vRES generation patterns with electricity demand. This is done by developing and applying an algorithm to optimise the amount of solar PV and wind installed across Europe using a high-resolution spatial grid, so that the aggregated vRES generation profile across Europe matches the aggregated electricity demand profile as closely as possible. The algorithm is run using 36 years of weather data to account for interannual weather variability. The method includes constraints on vRES deployment to ensure they are only installed in appropriate areas.

Chapter 3, titled *'How might intraday and balancing markets develop in a future highly renewable power system?',* explores what role intraday and balancing markets could play in a highly renewable European power system with increasing vRES capacity. This is achieved by developing a new method for creating synthetic day-ahead forecasts for electricity demand and vRES generation, with error distributions which are consistent with historical forecasts. This method is then demonstrated by performing simulations for the European power system in which the penetration of vRES increases from 15% in 2017 to 50% in 2040.

Chapter 4, titled *'Is a 100% renewable European power system feasible by 2050?'* explores this very question by considering scenarios for a fully renewable European power system. This chapter tests whether these 100% RES systems could be as reliable as today's power system, how they perform in terms of total costs, and whether the necessary deployment of RES technologies could be achieved by the year 2050. This analysis is based on detailed power system simulations performed using the PLEXOS power market modelling framework.

Chapter 5, titled '*Can liberalised electricity markets support decarbonised portfolios in line with the Paris Agreement? A case study of Central Western Europe*' considers two scenarios for a future decarbonised power system in Central Western Europe: one targeting net-zero

emissions by 2040 consistent with a 2 ºC warming limit, and the other targeting significant net-negative emissions, consistent with a more ambitious 1.5 ºC warming limit. Using the PLEXOS modelling framework, this chapter explores how electricity generation portfolios should develop to supply electricity reliably to consumers at the lowest cost, to what extent these least-cost portfolios can be supported by market revenues under different archetypal market designs, and how the deployment of negative emission technologies could affect the electricity market.

Based on the insights provided in the core chapters, Chapter 6 summarises the key findings of this thesis, discusses these findings in the context of the wider energy and climate debate, and proffers some key recommendations for policymakers and for further research.

Each core chapter begins with a short abstract and a listing of any mathematical nomenclature. Abbreviations are redefined in every chapter so that they can be read independently, with a full list of abbreviations provided after the contents page. Footnotes are numbered separately per chapter and can be found at the end of each chapter. An extensive appendix is included at the end of this thesis providing additional explanations on the assumptions, methods, and results for each core chapter, as well as a description of the PLEXOS modelling framework used in Chapters 4 and 5.

Footnotes to Chapter 1

[1] While the 0.5 ºC difference between a 1.5 ºC and 2 ºC target seems relatively small, it has large consequences. For example, coral reefs are expected to decline by 70–90% at 1.5°C warming, but will all but disappear (>99% loss) at 2ºC (Allen et al., 2018). Also, the number of insect, plant and vertebrate species expected to lose over half their habitat is likely to double for 2°C warming than for 1.5°C warming.

[2] More precisely, a carbon budget is the estimated cumulative amount of net global anthropogenic CO_2 emissions from a given start date to the time that these emissions reach net zero that should limit warming to a specified level, with a certain degree of confidence (Rogelj et al., 2018)

[3] The term *decarbonisation* is used in this thesis to mean reducing net emissions of CO_2 to the atmosphere to zero or even negative values, mostly in reference to the electric power system. It does not preclude the use of carbon (in all its forms) in the energy system and fossil fuels and biomass are still considered, providing total net emissions are reduced to target levels.

[4] The two examples of commercial-scale CCS applied in the electricity sector are the Boundary Dam coal power station in Canada, and the Petra Nova project at the WA Parish Generating Station in the US. However, these two plants use the captured CO_2 for enhanced oil recovery, rather than permanent storage. In fact, almost 90% of the 35 Mt CO_2 y^{-1} CCS capture capacity installed globally in 2018 was used for enhanced oil recovery.

[5] The most common conception of BECCS is a biomass power plant equipped with CCS; however, BECCS can be deployed in several ways in different sectors at potentially lower cost than in the electricity sector. For example, in the transport sector, the fermentation of sugars to produce ethanol for road transport produces a stream of nearly pure CO_2 which can be captured and stored, thereby also generating negative CO_2 emissions (Moreira et al., 2016). In the pulp and paper industry, CO_2 can be captured from the flue gas of a black liquor recovery boiler in Kraft pulp mills (Möllersten et al., 2003). However, BECCS deployment in these sectors is limited to those countries where these industries are present, and the global potential is limited.

[6] Some examples of high-profile CCS setbacks were the cancellation of the ROAD project by Engie and Uniper in 2017, which aimed to capture CO_2 from a coal plant located in Rotterdam (Port of Rotterdam, 2017; van Cappellen et al., 2018); and the UK government's withdrawal of £1 bn of funding for CCS in 2015, which halted both the Peterhead and White Rose projects (Carrington, 2015).

[7] CO_2 represents around 80% of total GHG emissions in the EU and globally. The remaining GHG emissions come mostly from methane, nitrogen oxides, and various hydrofluorocarbons.

[8] This is the compound annual growth rate over the five years between 2013-2018 based on the generation data from Eurostat and ENTSO-E shown in Figure 1-2.

[9] Different definitions of intermittent and variable renewable energy sources can be found in the literature. However, the most usual definition is generation sources which are: (i) weather-dependent, and thus have *limited dispatchability*, (ii) *uncertain* in their output, (iii) *location constrained*/specific, (iv) *asynchronous* (i.e. they are interfaced with the grid via power electronics, not directly connected and synchronised with the grid via a rotor spinning at the same frequency as the alternating current waveform), and (v) *not necessarily connected to the transmission grid*, but also to the distribution grid (IRENA, 2017). Solar PV and wind, while the most discussed, are not the only vRES technologies. For example, wave energy also depends on the weather and could be considered a vRES technology; however, its deployment prospects are currently so low that it is not considered in this thesis. Also, run-of-river hydropower plants could be considered a vRES technology, depending on the amount of storage they have available. Concentrating solar power is typically equipped with several hours of thermal storage, and thus not considered a vRES technology in this thesis.

[10] Own calculation based on day-ahead trading volumes in 2017 on the EPEX (EPEX, 2018b), Elspot (Nord Pool, 2017), MIBEL (Omie, 2017) and MGP (GME, 2017) exchanges, compared with 2017 demand (ENTSO-E, 2018e).

[11] This is inferred based on a Web of Science search for publications containing the words "electricity", and either "capacity market" or "capacity remuneration mechanism", and either "Europe", "Germany", or "United Kingdom". Before 2005 there were fewer than 3 such publications per year, rising to an average of 12 per year between 2005 and 2015. Publications peaked at 51 in 2016 (after the low electricity prices in 2015) and have since fallen to 36 per year. However, it is important to consider that many of Europe's power plants (especially hydropower, nuclear and coal plants) are over 30 years old (Kanellopoulos, 2018; Schneider & Froggatt, 2018) and were built by state-owned utilities before market liberalisation in the 1990s.

[12] Assuming a loss of load expectation (LoLE) threshold of 1 hour per year.

[13] The time horizon varies between the different chapters. For example, Chapters 2 and 4 consider snapshots of the year 2050, while Chapters 3 and 5 consider developments between 2017 and 2040 (actually up to 2100 in Chapter 5 as the carbon budgets are based on emission profiles for the whole 21st century). In any case, the time horizon is only indicative as the focus is on the long-term consequences of different decarbonisation strategies, rather than developments in individual years.

Can the mix and spatial distribution of wind and solar PV facilitate their integration in the power system?

William Zappa

Machteld van den Broek

Published as: Zappa, W & van den Broek, M (2018). Analysing the potential of integrating wind and solar power in Europe using spatial optimisation under various scenarios. Renewable and Sustainable Energy Reviews 94. 1192-1216.

2

Abstract

The integration of more variable renewable energy sources (vRES) like wind and solar photovoltaics (PV) is expected to play a significant role in reducing carbon dioxide emissions from the power sector. However, unlike conventional thermal generators, the generation patterns of vRES are spatially dependent, and the spatial distributions of wind and PV capacity can help or hinder their integration into the power system. After reviewing existing approaches for spatially distributing vRES, we present a new method to optimise the mix and spatial distribution of wind and PV capacity in Europe based on minimising residual demand. We test the potential of this method by modelling several scenarios exploring the effects of vRES penetration, alternative demand profiles, access to wind sites located far offshore, and alternative PV configurations. Assuming a copper-plate Europe without storage, we find an optimum vRES penetration rate of 82% from minimising residual demand, with an optimum capacity mix of 74% wind and 26% PV. We find that expanding offshore wind capacity in the North Sea is a 'no regret' option, though correlated generation patterns with onshore wind farms in neighbouring countries at high vRES penetration rates may lead to significant surplus generation. The presented method can be used to build detailed vRES spatial distributions and generation profiles for power system modelling studies, incorporating different optimisation objectives, spatial and technological constraints. However, even under the ideal case of a copper-plate Europe, we find that neither peak residual demand nor total residual demand can be significantly reduced through the spatial optimisation of vRES.

Nomenclature

Symbols

A	Left-hand-side constraint coefficient matrix
B	Right-hand-side constraint value matrix
c	Installed generation capacity (MW)
C	Vector containing values of c
CC	Capacity credit (%)
d	Electricity demand (MW, MWh h^{-1})
f	Capacity factor (-)
F	Matrix containing values of f (-)
g	Generation (MW, MWh h^{-1})
r	Residual demand (MW, MWh h^{-1})
R	Total residual demand (MWh)
T	number of generation technologies

Subscripts

c	country
eq	equality
i	vRES generation technology
ieq	inequality
LT	long-term
ST	short-term
t	time step
x	grid cell
y	year

2.1 Introduction

Decarbonisation of the electric power sector is one of the key transitions which must take place as part of Europe's commitment to reducing CO_2 emissions in order to avoid dangerous climate change (ECF, 2010b; Jägemann et al., 2013). This will be achieved mainly through the integration of more renewable energy sources (RES) such as onshore wind, offshore wind, solar photovoltaics (PV), hydro and biomass into the power system. Many studies have presented scenarios of what such a low-carbon European power system could look like in the long term, typically by 2050 (Connolly et al., 2016; Eurelectric, 2009; GWEC et al., 2015; Steinke et al., 2013; van de Putte & Short, 2011). These scenarios must employ nearly 100% RES, or a combination of RES and other low-carbon technologies such as nuclear power, bioenergy, or fossil fuels with carbon capture and storage (CCS). However, with several countries aiming to reduce nuclear power capacity and slow development of the European CCS industry (Bassi et al., 2015), a heavier dependence on RES may be more likely[1]. This will pose a challenge as, without significant development in nuclear or CCS capacity, comparing the current installed wind and PV capacities with those in several high-RES scenarios (Table 2-1) suggests that an additional 300 GW to 700 GW of wind capacity and 720 GW to 870 GW of PV capacity would need to be installed by 2050 (ECF, 2010b; ENTSO-E, 2015a; EREC, 2010; EWEA, 2016; GWEC et al., 2015). The question then arises, where should all this capacity be built?

As generation from variable renewable energy sources (vRES) such as PV and wind is intermittent, the challenge is even greater as any residual demand[2] – the difference between the total demand and vRES generation – must be provided by dispatchable fossil (e.g. coal, oil, gas), renewable (e.g. hydro, biomass, concentrating solar power (CSP)) or nuclear backup generation capacity (Brouwer et al., 2014). Given that vRES generation profiles depend on both the type of technology and weather regime where they are installed, optimizing the mix and spatial distribution of vRES has been suggested as one way of helping to integrate vRES into the power system (Becker et al., 2014; Budischak et al., 2013). Steps have been taken in this direction in the literature; however, most existing studies have shortcomings in that they: (i) *consider complementarity between vRES generation profiles but do not consider demand* (Alliss et al., 2011; Cassola et al., 2008; Hoicka & Rowlands, 2011; Kougias et al., 2016; Mills & Wiser, 2010; Monforti et al., 2014; Santos-Alamillos et al., 2014, 2015; Thomaidis et al., 2015; Widén, 2011); (ii) *allocate, rather than optimise the spatial distribution of vRES*[3] (Bruninx et al., 2015; DNV GL, 2014; Heide et al., 2011, 2010; Jerez, Thais, et al., 2015; Rodríguez et al., 2014; Steinke et al., 2013); (iii) *consider only a limited number of vRES technologies* (Grossmann et al., 2013, 2014; Lassonde et al., 2015, 2016), (iv) *are limited in geographical scale* (Abdelhaq, 2012; Cassola et al., 2008; Jerez, Trigo, Sarsa, et al., 2013; Kost et al., 2015; Monforti et al., 2014; Pereira et al., 2014; Rauner et al., 2016; Santos-Alamillos et al., 2014; Thomaidis et al., 2015; Widén, 2011); or (v) *optimise capacity, but do not examine the robustness of the resulting*

distributions to different weather years (Clack et al., 2014; Kost et al., 2015; MacDonald et al., 2016; Short & Diakov, 2014).

For example, the first group of studies investigate how different vRES generation patterns can be used to complement or balance each other, in order to achieve more constant overall generation. This has typically been done from: a technology perspective, by using combinations of different technologies (e.g. PV and hydro (Kougias et al., 2016), wind and CSP (Santos-Alamillos et al., 2015; Thomaidis et al., 2015), wind and PV (Hoicka & Rowlands, 2011)); from a spatial perspective, using combinations of different sites (Cassola et al., 2008; Santos-Alamillos et al., 2014); or considering both different technologies as well as site diversity (Alliss

Table 2-1 | Comparison of the installed power generation capacity in Europe in 2015 with the installed capacity from several (nearly) 100% RES scenarios for Europe in 2050. The values in percentages indicate the share of the total portfolio.

Generation Type	Installed capacity in 2015 (GW)		Installed capacity in high-RES scenarios (GW)		
	(EWEA, 2016)	(ENTSO-E, 2015a) (EU28+CH+NO)	Roadmap 2050 (ECF, 2010b) [a]	Energy Revolution (GWEC et al., 2015) [b]	Re-thinking 2050 (EREC, 2010) [c]
Onshore wind	130.6 (14%)	136.0 (13%)	245 (12%)	594 (23%)	462 (24%)
Offshore wind	11.0 (1%)		190 (9%)	237 (9%)	
PV	95.4 (10%)	94.6 (9%)	815 (41%)	926 (36%)	962 (49%)
Ocean	0.3 (0.03%)	-	-	53 (2%)	65 (3%)
CSP	5.0 (0.6%)	-	203 (10%)	208 (8%) [g]	96 (5%)
Biomass	16.7 (1.8%)	25.4 (3%)	85 (4%)	108 (4%)	100 (5%)
Geothermal	0.82 (0.1%)	-	47 (2%)	52 (2%)	77 (4%)
Hydro	141.1 (16%)	193.9 (19%) [d]	205 (10%)	223 (9%)	194 (10%)
Natural Gas	192 (21%)	216.8 (21%)	215 (11%)	-	-
Coal	161 (18%)	187.0 (18%) [e]	-	-	-
Oil	33.7 (4%)	31.8 (3%)	-	-	-
Nuclear	120.2 (13%)	124.6 (12%)	-	-	-
Other	-	2.3 (0.2%)	-	181 (7%) [h]	-
Total RES	401.0 (44%)	403.9 (40%)	1790 (89%)	2401(93%)	1956 (100%)
of which vRES [f]	*237.3 (26%)*	*230.6 (23%)*	*1250 (62%)*	*1810 (70%)*	*1489 (76%)*
Total Non-RES	506.9 (56%)	608.4 (60%)	215 (11%)	181 (7%)	-
Total	908	1012	2005	2582 [g]	1956

[a] *100% RES, 20% demand side management scenario, included EU27 + NO + CH*

[b] *5th edition, Advanced Scenario, included OECD Europe (EU27 – Baltic Countries + Turkey)*

[c] *Included EU27*

[d] *ENTSO-E report 'renewable' (145.6 GW) and 'other' (48.3 GW) hydro, with the former including run-of-river and hydro plants with storage, 'other' being pumped storage plants with no natural inflow. Only renewable counted in renewable total.*

[e] *Including anthracite, peat and other non-RES fuels*

[f] *Excluding run-of-river hydro*

[g] *Total installed capacity (2460 GW) and generation (5764 TWh) reported in original study for OECD Europe did not include assumed import of 620 TWh y^{-1} from North African CSP, thus CSP capacity increased to compensate for this by assuming the same capacity factor for North African CSP as for European CSP in the study (55%).*

[h] *Hydrogen*

et al., 2011; Mills & Wiser, 2010; Monforti et al., 2014; Widén, 2011). However, these studies only focus on generation, without considering electricity demand. Others have gone further and matched vRES generation with demand, but generally only considering single countries (Nagata et al., 2017; Rauner et al., 2016) without performing any spatial optimisation. Another group of studies allocate vRES capacity based on different factors such as government targets, land suitability, proximity to load or the potential resource (Bruninx et al., 2015; DNV GL, 2014; Jerez, Thais, et al., 2015; Rodríguez et al., 2014; Steinke et al., 2013), but make no attempt to optimise the actual spatial vRES distribution. Others have combined aspects of complementarity, demand matching and allocation studies by spatially optimizing vRES capacity for minimum residual demand (or a similar metric), but only for single vRES technologies in one (Lassonde et al., 2015, 2016) or more (Grossmann et al., 2013; Reichenberg et al., 2014) countries, or multiple technologies in a single country (Abdelhaq, 2012; Jerez, Trigo, Sarsa, et al., 2013; Killinger et al., 2015; Pereira et al., 2014). Others which have included a larger geographic scale and more technologies have done so only in a very aggregated way, typically by assuming a spatial vRES distribution, and varying the shares of wind and PV (Becker et al., 2014; Heide et al., 2011, 2010). Only a few studies have attempted to optimise the spatial distribution of vRES in a power system model (PSM) for a single country (Clack et al., 2014; Kost et al., 2015; MacDonald et al., 2016; Short & Diakov, 2014), including two specifically seeking to minimise residual load (Clack et al., 2014; Short & Diakov, 2014), but the optimisation was only performed for a single year and not checked for long-term performance. To our knowledge, no studies have examined how robust their optimised spatial distributions are in the long term, nor has the potential of a residual-demand-based capacity optimisation been assessed for Europe as a whole.

In this study, we present a method to optimise the detailed spatial distribution of wind and PV by minimising residual demand and apply it to the case of a future European power system. Given uncertainties in weather patterns, vRES uptake, electricity demand and technology parameters, we apply this method for several scenarios to see the full potential and robustness of approach. Firstly, we spatially optimise vRES capacity using long-term weather data and test how robust the resulting optimised distributions are with respect to interannual weather variability. Secondly, we determine if the penetration of vRES affects the optimal mix and spatial distribution for minimising residual demand. Thirdly, we investigate how future changes in electricity demand, due to an expected increase in the penetration of e.g. heat pumps (HPs) and electric vehicles (EVs), could affect the optimum distribution of vRES for minimising residual demand (Barton et al., 2013; ECF, 2010b; Veldman et al., 2013). Fourthly, we examine the potential of floating offshore wind technology to give access to stronger and steadier winds located in deeper offshore waters. Fifthly, we consider the effect of alternative PV orientations, since several studies have shown that the tilt and azimuth (orientation) angle of PV panels can be used to match solar PV generation with demand (Hartner et al., 2015; Killinger et al., 2015)[4]. Lastly, we compare the minimum-residual-demand-based vRES capacity

optimisation with a more traditional approach of preferentially selecting vRES sites with the highest capacity factors. Through these contributions, we seek to answer the following research question:

To what extent can optimising the mix and spatial distribution of vRES capacity minimise residual demand in a future European power system, and how does this depend on different factors?

Our study is focussed on the EU28[5] countries, Switzerland and Norway. The temporal scope is 2050, by which time we assume that high penetrations of vRES will be required. We consider four vRES generation technologies[6]: onshore wind, offshore wind, rooftop PV and ground-based utility PV. After an explanation of the methods used (Section 2.2), the results of the study are presented (Section 0), followed by a discussion (Section 2.4) and conclusion (Section 2.5). Further details on the method and results from this chapter are provided in Appendix A.

2.2 Method

An overview of the steps followed in this study is shown in Figure 2-1. First, we formulate an optimisation algorithm in which the objective function is to minimise residual demand (Section 2.1). The decision variables are the installed capacities of each generation technology per grid cell, using an irregular spatial grid constructed across Europe (Section 2.2). Inputs to the optimisation are capacity factor profiles for each generation technology (Section 2.3), constraints on the maximum installed capacity per technology (Section 2.4), and electricity demand profiles (Section 2.5). This optimisation is then performed for 36 years of weather data for a number of scenarios examining the effects of different assumptions on vRES penetration rate, electricity demand, PV panel orientation, and the extent of the spatial grid (Section 2.6). For each scenario, the mean and coefficient of variation (CV[7]) of the optimised installed capacity per technology are calculated for each grid cell to examine how consistently the method distributes vRES capacity given interannual weather uncertainty. The mean optimised capacity distribution is then simulated for all weather years to check how it perfoms in the long term.

2.2.1 Formulate optimisation algorithm

Treating the whole of Europe as a copper plate, we assume no losses or constraints on the transmission of electricity between or within countries[8]. In this way, Europe is treated as a single integrated power system and total electricity demand d_t is simply the sum of the demand across all countries c in hourly time step t.

$$d_t = \sum_c d_{c,t} \tag{2.1}$$

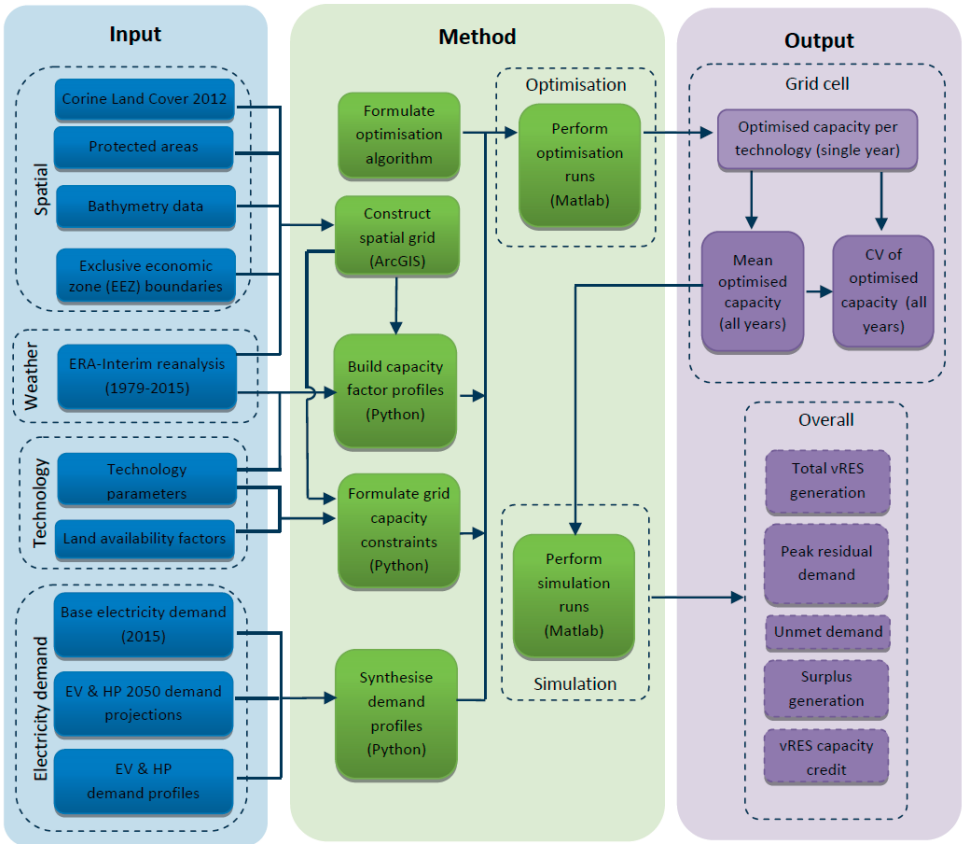

Figure 2-1 | Overview of study method.

Within each grid cell, different vRES generation technologies can be built. The generation from technology i in grid cell x is calculated as the product of its capacity factor $f_{i,x,t}$ and installed capacity, $c_{i,x}$.

$$g_{i,x,t} = c_{i,x} f_{i,x,t} \tag{2.2}$$

The values of $c_{i,x}$ are the decision variables in the optimisation. As we want to explore the full potential of spatially optimising vRES capacity without being restricted by the current system, we treat Europe as a clean slate and do not consider any existing or planned PV or wind capacity[9]. Under this assumption, the lower bound of $c_{i,x}$ is zero and the upper bound is the maximum installed capacity for that technology $c_{i,x}^{max}$. The capacity factor profiles $f_{i,x,t}$ take a value between zero and one and are calculated from weather data (see Section 2.2.3). Both $c_{i,x}^{max}$ and $f_{i,x,t}$ are determined exogenously. The total vRES generation g_t is then simply the sum of generation from all technologies across all grid cells.

$$g_t = \sum_i \sum_x g_{i,x,t} \tag{2.3}$$

As we treat the whole of Europe as a copper plate, the residual demand r_t is the difference between total demand and total generation of vRES (Figure 2-2).

$$r_t = d_t - g_t \tag{2.4}$$

When demand exceeds generation r_t is positive. Conversely, when vRES generation exceeds demand then r_t is negative. Positive residual demand is not desirable in a power system as this represents costs in the form of dispatchable backup capacity and backup energy. Negative residual demand (or surplus generation) is also not desirable as it represents costs in the form of storage requirements, or economic losses due to curtailment of electricity which has no market value[10]. Thus, the objective is to minimise both negative and positive residual demand simultaneously. However, with 36 years of weather data, 8760 time steps per year, four technologies and more than 2000 grid cells, the problem quickly becomes intractable and difficult to solve. To avoid non-linearities associated with taking the absolute value of the residual demand, we formulate the optimisation as a linear least squares (LLSQ) problem, constrained by linear equality and bound constraints, where C is a stacked column vector containing the values of $c_{i,x}$ to be optimised, F is a matrix containing the hourly capacity factors $f_{i,x,t}$ for each technology, D is a column vector containing the hourly aggregated

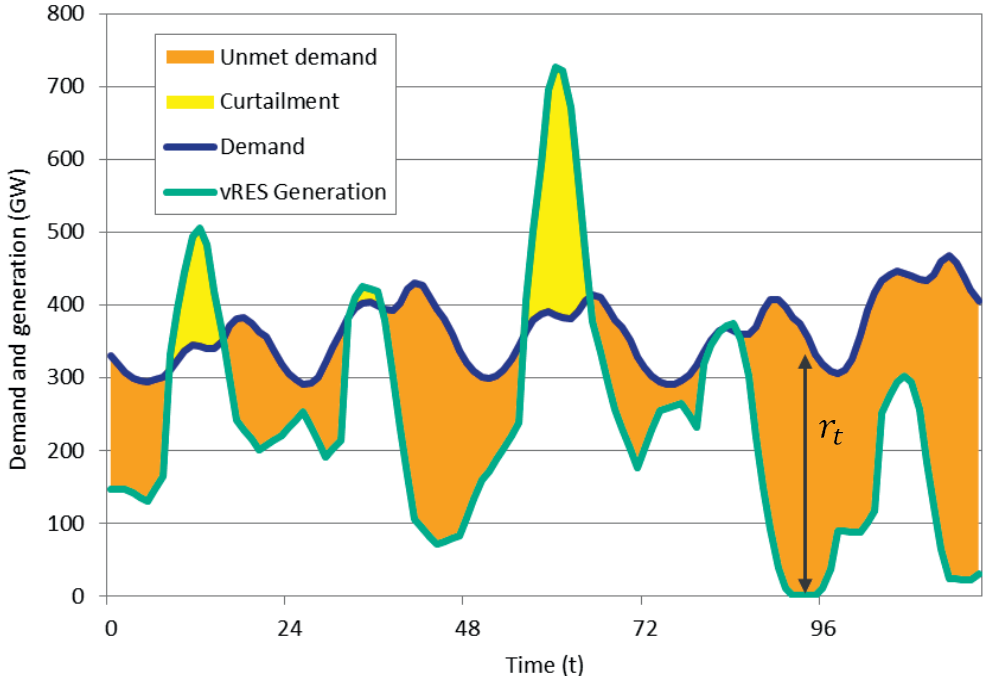

Figure 2-2 | Example of curtailment and residual demand in a power system.

demand values d_t, and C^{max} is a matrix containing the maximum capacities per technology per grid cell $c_{i,x}^{max}$ (i.e. upper bound constraints).

$$\min_{C} \frac{1}{2}\|F \cdot C - D\|_2^2 \quad \text{such that} \begin{cases} 0 \leq C \leq C^{max} \\ A_{eq} \cdot C = B_{eq} \\ A_{ieq} \cdot C \leq B_{ieq} \end{cases} \tag{2.5}$$

The matrices A_{eq} and B_{eq} can be used to supply additional equality constraints to the optimisation, such as constraints on total annual generation, or the total installed capacity per technology. A_{eq} is a coefficient matrix for the elements of C specifying the left-hand side of the equality constraints[11], with the right-hand side specified in B_{eq}. Similarly, the coefficient matrices A_{ieq} and B_{ieq} can be used to add inequality constraints to the optimisation if desired, such as minimum installed vRES capacities for a particular country in order to take into account government policies on vRES deployment.

2.2.2 Construct spatial grid

The spatial grid is built using the software ArcGIS Pro[12] by incorporating a number of spatial datasets. These include European country borders (Eurostat, 2014), Exclusive Economic Zone (EEZ) marine boundaries (Claus et al., 2016), bathymetry data (British Oceanographic Data Centre, 2015), and the 2012 Corine Land Cover Inventory (CLC2012) (EEA, 2016a; Kosztra & Arnold, 2014). The starting point is a regular grid of 0.75° x 0.75° constructed across Europe, corresponding to the resolution of the weather dataset (Section 2.2.3). These regular grid cells are cut by the land and marine borders of each country so that the resulting irregular grid respects all national borders and the installed vRES capacity can be easily calculated or constrained per country in the optimisation. Each cell retains information about the latitude and longitude of its parent grid cell so that it can be associated with the correct wind and PV capacity factor profiles (Section 2.2.3). This irregular grid is merged with the high resolution (100 m x 100 m) CLC2012 raster dataset so that the area of each Corine Land Cover (CLC) class per grid cell can be deduced and used to set capacity constraints for each technology. Grid cells are classified as onshore, offshore, or coastal.

Water depth and distance to shore are two major factors limiting the expansion of offshore wind technology. Due to the high cost and technical limitations of current foundation types such as monopiles, gravity based foundations, jackets, and tripods (Rodrigues et al., 2015), offshore wind farms are typically located up to a distance of 100 km offshore in water depths of up to 50 m (EWEA, 2013; Rodrigues et al., 2015). In this study, we assume that water depth is a greater challenge for the development of offshore wind than distance from shore and limit offshore grid cells to a water depth of 50 m (EWEA, 2013)[13]. However, in the long term Europe is expected to turn to more distant offshore locations in deeper waters to increase offshore wind capacity as many of the most favourable offshore wind sites close to the shore become exploited (EWEA, 2013; Zountouridou et al., 2015). To examine the potential of floating

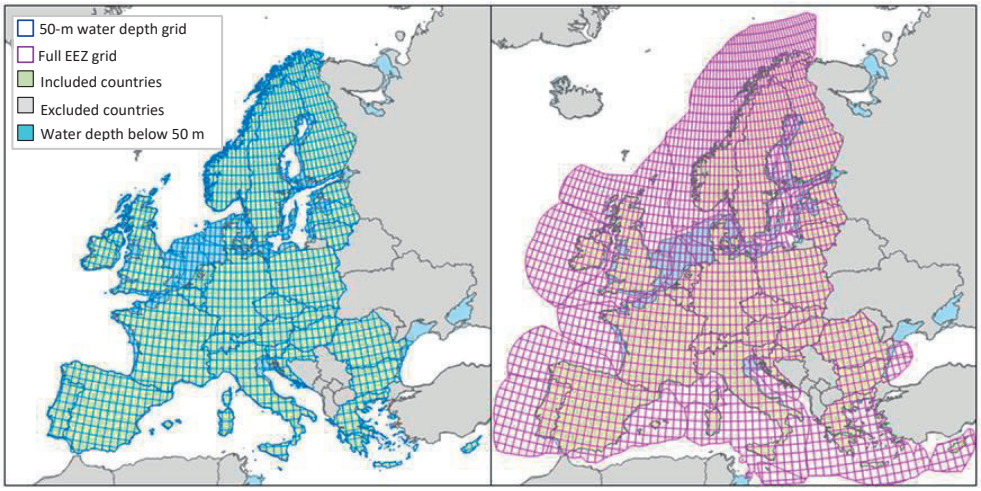

Figure 2-3 | Extents of the 50-m water depth (left) and full EEZ (right) spatial grids

offshore wind technology in the future and the role it could play in minimising residual demand, a second grid variant is built including all offshore locations within the EEZ of each country, irrespective of water depth[14]. The resulting two spatial grid variants are shown in Figure 2-3.

2.2.3 Build hourly capacity factor profiles

The capacity factor profiles are based on the European Reanalysis Interim (ERA-Interim) weather dataset produced by the European Centre for Medium-Range Weather Forecasts (ECMFW) (ECMWF, n.d.). This is a global atmospheric reanalysis covering 36 years from 1979 to the present (2016). Comprising 3-hourly data on various meteorological parameters including wind speed, solar radiation and temperature, it has a spatial resolution of 0.75° x 0.75° or approximately 50 km x 50 km[15] (Dee et al., 2011; ECMWF, n.d.). Reanalyses combine data from a variety of weather observational systems by integrating them with a numerical weather prediction model to produce a temporally and spatially consistent dataset and have been used in a number of vRES integration and power system studies (EWEA, 2009; Gonzalez Aparicio & Zucker, 2015). The ERA-Interim reanalysis is selected due to its extensive geographical coverage (including offshore sites), high spatial and temporal resolution, and inclusion of both wind speed and solar radiation over a long timeframe[16]. As we base our model on historical weather data, any potential impacts of climate change on European weather patterns are beyond the scope of this study and not considered. The 3-hourly ERA-Interim data is downscaled to hourly resolution in order to match the demand data.

Based on recent developments and future expectations, we assume hub heights of 150 m and 100 m for onshore and offshore wind turbines respectively. Extrapolating the 10-m wind speed from the ERA-Interim dataset to hub height and interpolating to hourly values, we assign each grid cell a wind turbine class according to International Electrotechnical

Commission (IEC) 61400 guidelines (International Electrotechnical Commission, 2005)[17]. Based on this wind class (IEC Class S, I, II, III, or IV) we select an appropriate wind turbine and power curve from a major commercial manufacturer, which we subsequently convolute so that aggregated wind generation better reflects generation profiles from real wind farms (Norgaard & Holttinen, 2004). Additional losses of 13% (including wake/array (8%), electrical conversion (2%) and other (3%) losses) are assumed in accordance with values taken from the literature (McKenna et al., 2014; Myhr et al., 2014; Rivas et al., 2009).

PV generation profiles are synthesised by using linear interpolation to first downscale the raw 3-hourly radiation data to hourly irradiance values. Solar position and radiation models from the literature are then used to calculate PV production, assuming a southerly orientation and 35° mounting angle for both PV technologies (Erbs et al., 1982; Reindl et al., 1990). We take high-efficiency (21.5%) monocrystalline silicon and lower-efficiency (16.8%) polycrystalline silicon modules as the basis for the rooftop and utility PV calculations respectively[18]. Finally, a performance ratio (PR) of 90% is assumed in line with reported values for recent PV installations (Fraunhofer ISE, 2016), thus accounting for inverter inefficiency, wiring, cell mismatch, shading and other losses.

2.2.4 Formulate grid cell capacity constraints

Grid cell capacity constraints for each technology are determined following the approach shown in Figure 2-4. First, the *suitable* land (or sea) area for each technology is calculated by assuming that each technology can only be built in specific *suitable* CLC classes. For onshore wind and utility PV these include mainly agricultural and grasslands[19]. We assume rooftop PV can only be built in urban areas, and offshore wind only in open water. Protected areas (land and sea) are excluded using data from the European Environment Agency's (EEA) Common Database on Designated Areas (CDDA) dataset (EEA, 2016b). With the suitable land area determined, we then assume how much of this suitable land is *available* and could be used for vRES, based on values reported in literature. For onshore wind, we assume a land availability factor of 6% in line with (Bruninx et al., 2015; Deng et al., 2015), and for offshore wind we assume a uniform 20% availability irrespective of water depth or distance to shore[20]. For utility PV we consider a land availability of 1%, within the range of values found in the literature. We assume that utility PV and onshore wind can be installed in the same location on the basis that there are examples of such co-located/hybrid parks gaining increasing attention and already being constructed (AECOM Australia, 2016; Cuff, 2016). With shading only affecting the direct component of sunlight, PV losses due to turbine shading are reportedly less than 1% (Mamia & Appelbaum, 2016).

For both wind technologies, we use a representative wind farm capacity density ranging from 4.2 MW km^{-2} to 6 MW km^{-2} (based on the IEC wind turbine class) to calculate the maximum capacity per grid cell from the available area. For the two PV technologies, the panel area is

first required. For utility PV, we assume a panel density of 0.337 m^2 panel m^{-2} land, based on a 35° installation angle and allowing 15° between the top of one panel row and the base of the next to minimise shading. For rooftop PV, we estimate maximum rooftop PV panel area by first calculating the fraction of urban CLC classes covered by buildings using building footprint data from the UK and the Netherlands. Then, assuming 1.22 m^2 roof per m^{-2} building footprint (based on trigonometry), we consider a roof availability factor of 30% based on the literature. The resulting rooftop and utility PV panel areas are multiplied by nominal module specific power densities of 211 and 167 W m^{-2} respectively, based on manufacturer data.

2.2.5 Synthesise demand profiles

An examination of the literature shows that there is no consensus on total expected electricity demand in 2050 with values ranging from 3377 TWh (EC, 2011a) to 6020 TWh[21] (GWEC et al., 2015), depending on the assumed trends in efficiency measures, economic growth, and electrification of other sectors such as transport, heating, and heavy industry (Bruninx et al., 2015; EC, 2011a, 2016b; ECF, 2010b; EREC, 2010; GWEC et al., 2015; PwC et al., 2010). In light of this, we consider different demand levels in this study. As a base case, we take actual hourly 2015 demand data from the European Network of Transmission System Operators for Electricity (ENTSO-E) (ENTSO-E, 2016a)[22] and assume that total annual demand (3111 TWh y^{-1}) remains essentially unchanged, under the assumption that general demand increases due to economic and population growth until 2050 will be largely offset by energy efficiency measures[23].

Then, in order to investigate higher levels of demand and how increased penetration of EVs and HPs may affect the optimal distribution of vRES, we create additional demand profile variants by adding 500 TWh and 800 TWh for HPs and EVs respectively to the base 2015 demand. In addition to the base 2015 demand, this results in three further variants: (1) base with EVs, (2) base with HPs, and (3) base with both EVs and HPs. Annual HP demand is distributed throughout the year based on the number of heating degree hours (HDH), while EV demand is distributed used a charging profile model developed by the European Commission Joint Research Centre (JRC)[24](Pasaoglu et al., 2013). Table 2-2 shows the total annual demand, peak demand and minimum demand for all four demand profile variants.

Even though our study uses only one year of demand data (2015), electricity demand follows quite consistent and predictable patterns (e.g. daily fluctuations, weekly fluctuations, seasonal differences) and we consider including additional years of demand data less important than additional years of weather data. A justification for this, as well as further details about the demand profile formulations, is provided in the appendix.

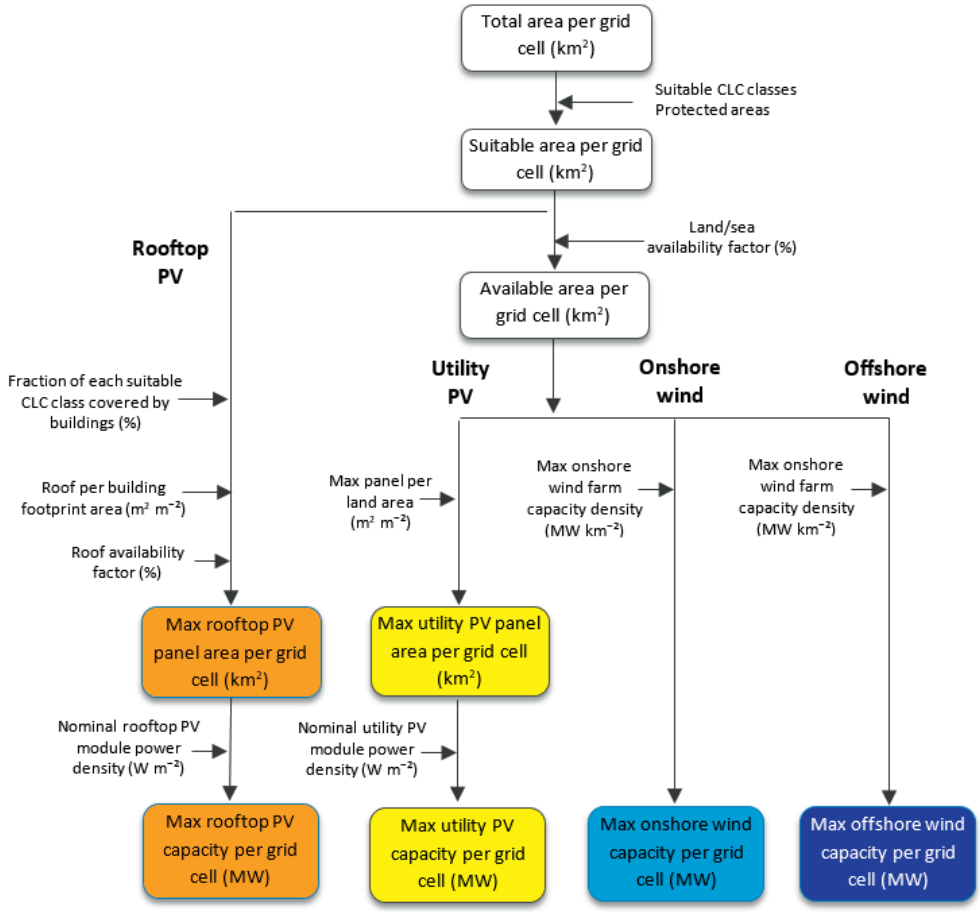

Figure 2-4 | Overview of method used to calculate installed capacity constraints by technology.

Table 2-2 | Total, maximum and minimum demand of the base profile and three variants (including grid losses)

Parameter	Base (2015)	Base + HPs	Base + EVs	Base + HPs +EVs
Total demand (TWh y^{-1})	3111	3611	3911	4411
Maximum demand (GW)	504	640	745	882
Minimum demand (GW)	230	236	236	241

2.2.6 Perform scenario optimisation runs

The minimum residual load optimisation algorithm is implemented and solved using the software Matlab[25]. The optimisation is performed for a number of different scenarios in order to investigate the effects of different factors and uncertainties, as shown in .

- Scenario 1 is the base case ***minimum residual demand optimisation*** using the 50-m water depth grid.
- Scenarios 2a-d investigate how minimising residual demand is affected by ***vRES penetration rate*** by constraining vRES generation to 25%, 50%, 75% and 100% of total demand respectively.
- Scenarios 3a-c examine the impact of uncertainty in ***future electricity demand patterns*** by adding additional demand from HPs and EVs to the base demand.
- Scenario 4 considers the potential of utilising the full EEZ grid with ***floating offshore wind farms***.
- Scenarios 5a-c assess the impact of using ***alternative PV panel orientations*** for rooftop PV and full two-axis tracking for utility PV.
- Scenario 6 compares the minimum-residual-load-based vRES capacity optimisation with the more common approach of selecting sites with the ***highest capacity factors***[26] by modifying the objective function to maximisation of vRES generation, while setting constraints on the capacity per technology to be equal to the mean optimised capacities from Scenario 1.

Each scenario is optimised for all 36 years of weather data seperately[27], from which the mean and CV of installed capacity per grid cell is calculated for each technology in order to test how sensitive the capacity distributions produced by the optimisation algorithm are to individual weather years. Then, the mean optimised distribution is simulated for the full 36 years of weather data to see how it performs in the long term. For each scenario, the mean installed capacity per technology, maximum, minimum and residual demand, surplus generation, net vRES penetration[28], and vRES capacity credit are calculated. Note that in all scenarios except Scenarios 2a-d, we impose no constraint on total annual vRES generation; hence the solver is free to determine the optimum level of vRES penetration. The vRES capacity credit represents the reduction in dispatchable generation capacity that would be possible due to vRES, considering demand and generation from all vRES technologies together at a European level. We calculate the short-term annual capacity credit (CC_{ST}) for a given year, y, following the method of (IEA, 2011) as the difference between the maximum demand and maximum residual demand in that year, divided by the total installed vRES capacity as shown in Eq. (2.6).

$$CC_{ST,y} = \frac{\max\left(d_{t,y}\right) - \max\left(r_{t,y}\right)}{\sum_{ix} c_{i,x}} \tag{2.6}$$

Table 2-3 | Overview of optimisation scenarios performed. The italicised text highlights the differences between each scenario and the Base scenario (Scenario 1).

Scenario		Objective Function	Grid Type	Demand Profile	Additional Constraints/Other	
1		Minimum residual demand	50 m depth	Base	-	
2	a	Minimum residual demand	50 m depth	Base	*Constraint on total vRES generation* [a]	*= 778 TWh y^{-1} (25% penetration)*
	b					*= 1556 TWh y^{-1} (50% penetration)*
	c					*= 2333 TWh y^{-1} (75% penetration)*
	d					*= 3111 TWh y^{-1} (100% penetration)*
3	a	Minimum residual demand	50 m depth	*Base + HP*	-	
	b			*Base + EV*	-	
	c			*Base + HP + EV*	-	
4		Minimum residual demand	*EEZ*	Base	-	
5	a	Minimum residual demand	50 m depth	Base	*West-facing rooftop PV*	
	b				*East-facing rooftop PV*	
	c				*Two-axis tracking utility PV*	
6		Maximum generation	50 m depth	Base	*Total installed capacity per technology based on mean result from Scenario 1*	

[a] *Based on total vRES generation, including any surplus generation.*

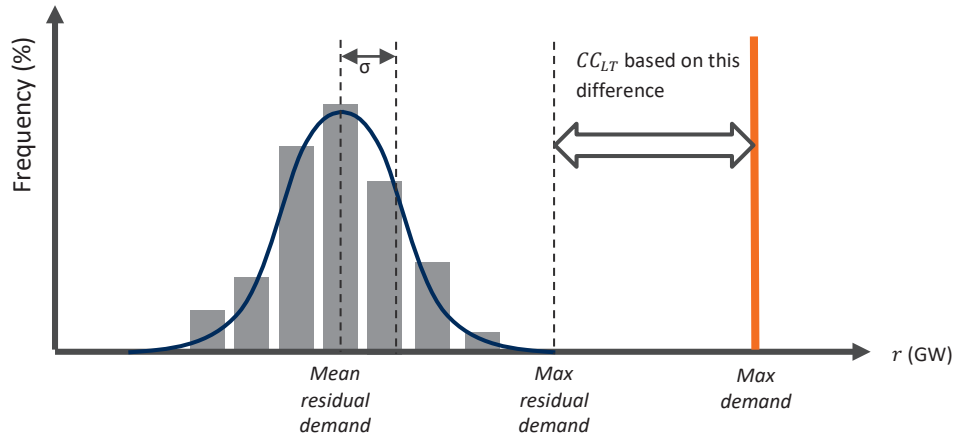

Figure 2-5 | Approach to calculating long-term capacity credit. Figure based on (IEA, 2011).

However, as long-term investment decisions regarding backup capacity are not made annually, it is the long-term capacity credit (CC_{LT}) which is more relevant for system planning. While there are many methods of determining capacity credit in the literature (Amelin, 2009; Dent et al., 2010; Ensslin et al., 2008), in this study we again follow the appoach of (IEA, 2011) but instead of assuming maximum residual demand is normally distributed from one year to the next, we base CC_{LT} on the worst-case year when maximum residual demand is highest (Figure 2-5). In this way, the long-term capacity credit is equal to the minimum short-term capacity credit (i.e. $CC_{LT} = \min(CC_{ST,y})$).

2.3 Results

The overall results for the optimisation runs are shown in Table 2-4, while Table 2-5 presents the overall results from the simulation runs. In addition to the mean and CV, the minimum and maximum values are also shown. As the mean results from the optimised and simulated runs differ only slightly (typically less than 3%), using the mean optimised capacity across a number of weather years – as an alternative to simultaneously optimising all years at once – can generate a single optimised capacity distribution that performs in line with long-term expectations.

The overall results, as well as the detailed vRES distributions, are discussed in the following sections with Scenario 1 – the base minimum residual demand optimisation – serving as a reference with which the other scenarios are compared. Note that in the optimised runs, the capacity distribution may change for each year of the optimisation and the interannual results represent the 'ideal' case, while in the simulation runs, the capacity distribution is the same each year. Thus, unless otherwise stated, overall results are discussed on the basis of the simulation runs as these give a better indication of the interannual variability. However, comparing the results for residual demand across all scenarios, Table 2-4 and Table 2-5 show that neither peak residual demand nor total residual demand can be significantly reduced through spatial optimisation of vRES, even for the ideal case of a copper-plate Europe.

2.3.1 Base minimum residual demand optimisation

When spatially optimised, vRES can satisfy 82% of annual European electricity demand with an installed capacity of 1144 GW. The optimum capacity mix is 74% wind (of which 65% is offshore) and 26% solar PV (of which 67% is rooftop). Figure 2-6 shows the mean installed capacity per grid cell for each technology based on all weather years. Onshore wind is mostly installed at the periphery of southern[29], northern, western and eastern Europe, while very little capacity is installed in countries surrounding the North Sea, which instead host considerable offshore wind capacity. Rooftop PV is mainly installed in a band extending from Portugal to the Nordic countries. Utility PV follows a similar pattern except that total installed capacity is lower, and the capacity shares in Ireland and Norway are higher than for rooftop PV.

Table 2-4 | Overall results from optimisation runs (mean values for weather years 1979-2015). The upper value in each cell is the mean result for all 36 weather years, while the lower value in parentheses is the CV, expressed as a percentage.

Scenario		Installed Capacity (GW)					Demand (TWh y^{-1})	Max Demand (GW)	Min Demand (GW)	Peak residual Demand (GW)	ST vRES capacity credit (%) [a]	Total Generation (TWh y^{-1}) [b]	Net Generation (TWh y^{-1}) [c]	Unmet Demand (TWh y^{-1})	Surplus Generation (TWh y^{-1})	Total residual (TWh y^{-1})
		Onshore wind	Offshore wind	Rooftop PV	Utility PV	Total										
1		300 (11.1%)	549 (2.3%)	197 (9.9%)	98 (18.6%)	1144 (3%)	3111	504	230	336 (7.6%)	14.7% (2.3%)	2771 (1.1%)	2555 (1.2%)	557 (5.7%)	217 (2.2%)	774 (4.5%)
2	a	113 (15%)	134 (8%)	50 (9.9%)	24 (16.5%)	321 (4.2%)	3111	504	230	429 (2.2%)	23.5% (3.5%)	778	778 (0%)	2333 (0%)	0	2333 (0%)
	b	176 (12.2%)	292 (4.2%)	96 (11.8%)	48 (19.2%)	613 (3.8%)	3111	504	230	376 (4.4%)	21% (3.1%)	1556	1556 (0%)	1556 (0%)	0	1556 (0%)
	c	252 (11.4%)	461 (3.2%)	159 (11.1%)	79 (19.5%)	951 (3.6%)	3111	504	230	346 (6.6%)	16.6% (2.5%)	2333	2278 (0.4%)	834 (1.1%)	55 (16.4%)	889 (2%)
	d	340 (10.6%)	615 (2.6%)	228 (10.2%)	114 (16.8%)	1298 (3.5%)	3111	504	230	330 (8.2%)	13.4% (2.1%)	3111	2691 (0.8%)	421 (5%)	420 (5%)	841 (5%)
3	a	385 (8.7%)	641 (2.1%)	176 (11.3%)	92 (16.7%)	1294 (3.1%)	3611	648	235	434 (8%)	16.5% (2.8%)	3187 (1.3%)	2933 (1.5%)	678 (6.6%)	253 (3.3%)	931 (5.4%)
	b	375 (9.5%)	652 (2.2%)	265 (8.2%)	139 (11.3%)	1431 (2.8%)	3912	745	236	545 (5.9%)	14% (2.2%)	3409 (1.2%)	3082 (1.3%)	830 (4.7%)	327 (1.6%)	1157 (3.3%)
	c	480 (5.8%)	704 (1.5%)	257 (9.6%)	137 (11.2%)	1578 (2.6%)	4412	889	241	646 (6.1%)	15.4% (2.5%)	3746 (1.6%)	3419 (1.6%)	993 (5.6%)	327 (3.5%)	1320 (4.1%)
4		54 (18.9%)	675 (2.6%)	124 (9.3%)	73 (14.7%)	927 (2.2%)	3111	504	230	237 (9.1%)	28.8% (2.4%)	3026 (0.3%)	2829 (0.4%)	282 (4.2%)	197 (2%)	479 (3.2%)
5	a	288 (11.4%)	546 (2.3%)	210 (10%)	136 (9.4%)	1180 (2.8%)	3111	504	230	337 (7.6%)	14.2% (2.2%)	2785 (1%)	2569 (1.2%)	542 (5.7%)	216 (2.1%)	758 (4.5%)
	b	303 (10.8%)	545 (2.4%)	143 (10.7%)	184 (8.2%)	1176 (2.9%)	3111	504	230	337 (7.6%)	14.2% (2.2%)	2780 (1%)	2563 (1.2%)	549 (5.8%)	217 (2.2%)	766 (4.5%)
	c	289 (11.2%)	544 (2.4%)	3 (129.6%)	251 (7.6%)	1086 (3.1%)	3111	504	230	337 (7.7%)	15.4% (2.4%)	2795 (1%)	2580 (1.2%)	532 (5.9%)	215 (2.3%)	747 (4.6%)
6		300	550	197	98	1145	3111	504	230	346 (7.3%)	13.8% (2.2%)	3412 (3.5%)	2705 (1.6%)	406 (10.8%)	707 (11.7%)	1113 (4.9%)

[a] Value in parenthesis is standard deviation (in absolute percentage) for capacity credit not CV; [b] Including surplus generation; [c] Excluding surplus generation

Table 2-5 | Overall results from simulations runs based on the mean optimised capacity distributions from 1979-2015.

Scenario		Total Generation [a] (TWh y^{-1})			Net Generation [b] (TWh y^{-1})			Unmet Demand (TWh y^{-1})			Surplus Generation (TWh y^{-1})			Total Residual (TWh y^{-1})			Peak Residual Demand (GW)			Short-term vRES capacity credit (%) [c]		
		Min	Mean	Max	Min	Mean	Max	Min	Mean	Max	Min	Mean	Max	Min	Mean	Max	Min	Mean	Max	Min (CC_{LT})	Mean	Max
1		2605	2770 (2.6%)	2896	2454	2545 (1.9%)	2651	460	566 (8.8%)	658	145	224 (13%)	300	705	790 (4.4%)	858	287	337 (7.5%)	377	11.1%	14.6% (2.2%)	19%
2	a	737	773 (2%)	800	737	773 (2%)	800	2312	2338 (0.7%)	2375	0	0	0	2312	2338 (0.7%)	2375	416	432 (2.4%)	456	15%	22.3% (3.2%)	27.5%
	b	1472	1552 (2.2%)	1612	1472	1552 (2.2%)	1612	1500	1560 (2.2%)	1640	0	0	0	1501	1560 (2.2%)	1640	340	378 (4.6%)	412	15%	20.5% (2.8%)	26.7%
	c	2197	2331 (2.5%)	2431	2163	2271 (2.3%)	2369	743	841 (6.1%)	949	34	60 (18.1%)	91	804	901 (5.1%)	988	297	348 (6.6%)	387	12.3%	16.4% (2.4%)	21.8%
	d	2923	3112 (2.7%)	3260	2600	2684 (1.7%)	2785	326	428 (10.4%)	511	301	428 (10.9%)	541	790	856 (3.8%)	946	272	331 (8.1%)	373	10.1%	13.4% (2.1%)	17.8%
3	a	2984	3186 (2.9%)	3354	2802	2925 (2.3%)	3047	564	686 (9.6%)	809	182	261 (12.8%)	335	870	947 (5.2%)	1047	371	435 (8.1%)	506	11%	16.5% (2.7%)	21.4%
	b	3205	3409 (2.8%)	3575	2963	3076 (2%)	3205	707	836 (7.2%)	949	231	333 (11.6%)	432	1077	1169 (3.3%)	1240	481	545 (5.8%)	603	9.9%	14% (2.2%)	18.5%
	c	3507	3746 (3%)	3948	3270	3413 (2.3%)	3562	850	998 (7.8%)	1141	234	333 (12.1%)	427	1236	1331 (4%)	1439	568	647 (6%)	738	9.6%	15.4% (2.5%)	20.4%
4		2923	3009 (1.4%)	3072	2740	2801 (0.9%)	2842	270	311 (8.3%)	372	168	208 (9.4%)	240	479	519 (3.4%)	555	215	251 (9.8%)	323	19.5%	27.3% (2.7%)	31.2%
5	a	2618	2783 (2.6%)	2909	2470	2561 (1.9%)	2663	449	551 (9%)	642	143	222 (13%)	294	695	773 (4.4%)	840	287	338 (7.5%)	377	10.8%	14.1% (2.1%)	18.4%
	b	2615	2778 (2.6%)	2902	2462	2554 (1.9%)	2657	454	557 (8.8%)	650	145	224 (13%)	298	699	781 (4.5%)	848	287	338 (7.5%)	379	10.7%	14.2% (2.1%)	18.5%
	c	2627	2792 (2.6%)	2911	2473	2570 (1.9%)	2667	444	542 (9%)	638	143	222 (12.9%)	296	687	764 (4.5%)	836	287	338 (7.5%)	379	11.5%	15.3% (2.3%)	20%
6		3138	3404 (3.6%)	3630	2613	2703 (1.7%)	2807	305	409 (11.2%)	498	493	701 (11.5%)	865	959	1110 (4.5%)	1245	286	346 (7.4%)	383	10.6%	13.8% (2.2%)	19%

[a] Including surplus generation; [b] Excluding surplus generation; [c] Value in parenthesis is standard deviation (in absolute percentage) for capacity credit, not CV

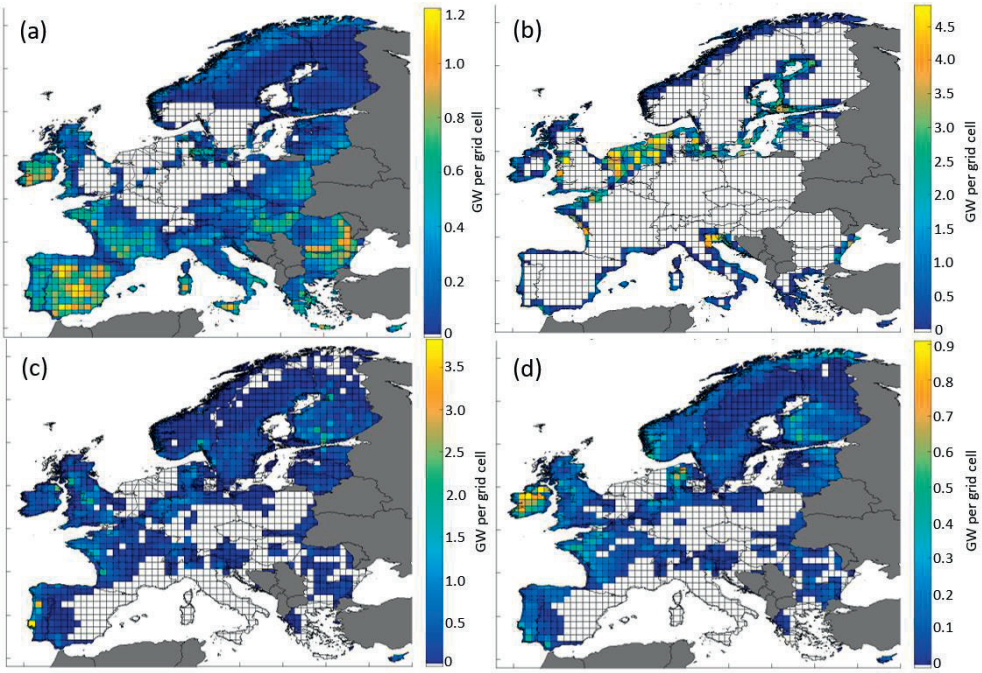

Figure 2-6 | Mean optimised capacity per technology in GW per grid cell for Scenario 1 for (a) onshore wind **(b)** offshore wind **(c)** rooftop PV and **(d)** utility PV. Sites in which no capacity is ever installed are left blank. Note that the axis scale varies per technology.

Notably, only 17% of total PV capacity is installed in the southern European countries of Spain, France and Italy which typically host the largest shares of PV capacity in high-RES studies. Figure 2-7 depicts the calculated CV of optimised installed capacity in each grid cell based on all weather years, showing that capacity is installed more consistently in certain regions than in others. For example, the same onshore wind capacity is almost always built in the Iberian Peninsula, Ireland and the west coast of Britain, southern France, northern Scandinavia, and far-eastern Europe; but varies considerably in central France and Italy. Comparing Figure 2-6 and Figure 2-7 shows that not only does the robustness of the capacity distributions vary between the four technologies, but also that the cells with low CVs are often those cells in which the most capacity is installed. This is demonstrated clearly by Figure 2-8, which gives the share of cumulative installed capacity for each technology as a function of the CV of installed capacity. Offshore wind capacity is distributed most robustly by the optimisation with 66% of capacity installed in the same location each year. The distribution of onshore wind is more variable with only 38% of capacity installed in the same location. By contrast, no locations receive the same rooftop and utility PV capacity each year.

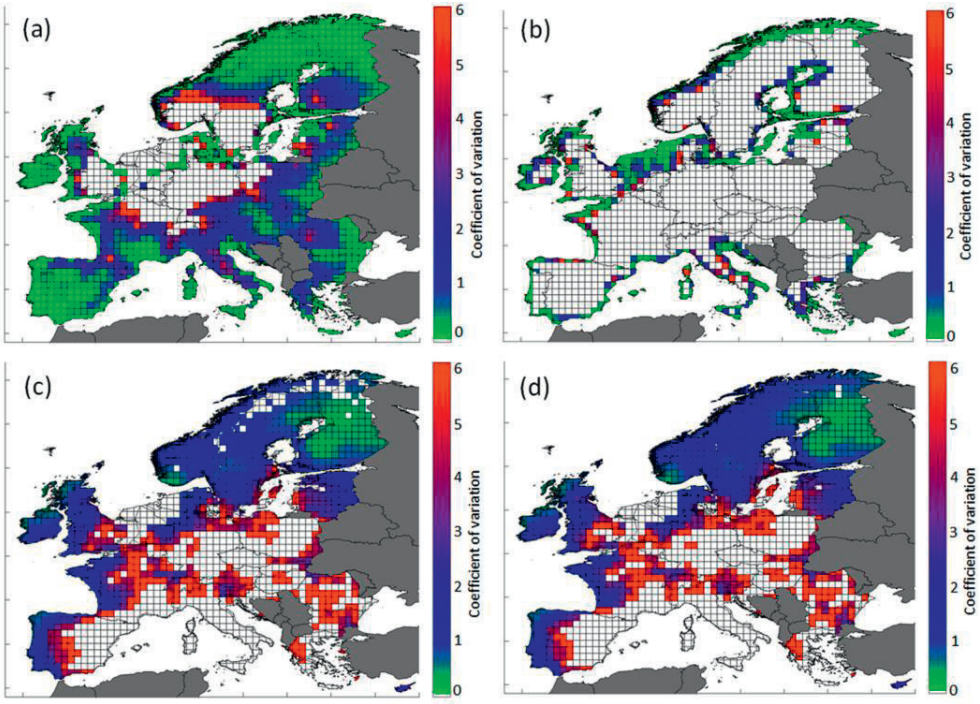

Figure 2-7 | CV of installed capacity per technology for Scenario 1 for (a) onshore wind **(b)** offshore wind **(c)** rooftop PV and **(d)** utility PV. Cells in which the variability in installed capacity from year to year is very low (e.g. CV < 0.1) are coloured green, while cells with high CV are coloured red. Cells in which no capacity is ever built are shown as white.

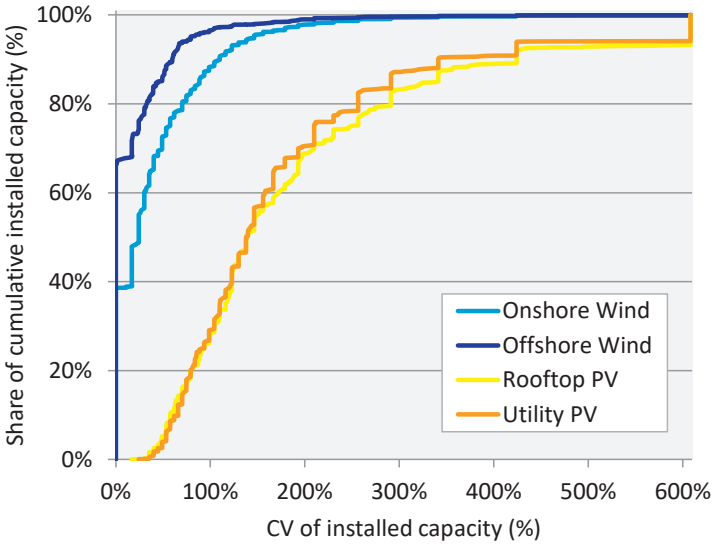

Figure 2-8 | Share of cumulative installed capacity as a function of CV of installed capacity for each grid cell in Scenario 1.

To examine the temporal aspects of how the algorithm optimises residual demand, Figure 2-9 shows hourly box plots of total demand, generation and residual demand for weather year 2015 (as an example), averaged across a representative winter month (January), a representative summer month (July), and the full year. Figure 2-10 shows similar plots for the hourly generation of each technology. In winter, demand increases sharply from 4:00 before peaking at 11:00. It peaks again at 18:00 before falling steeply until the minimum at 4:00. In contrast, total vRES generation is quite steady throughout the day at approximately 400 GW, mainly supplied by offshore wind, with a slight rise at midday due to PV. This combination of demand and vRES generation profiles tends to result in surplus electricity early in the morning and late at night, generation largely matching demand between 7:00 and 16:00, and unmet demand during the evening peak between 17:00 and 20:00. In summer, the demand profile is similar to that in winter, except that the double-peak and sharp evening decline are replaced by a gradual fall in demand, extending from noon until 4:00.

Again, offshore wind provides steady generation of approximately 200 GW (nearly 50% lower than in the winter). This combination of patterns results in unmet demand in both the morning and late evening hours. In contrast to offshore wind, onshore wind generation increases

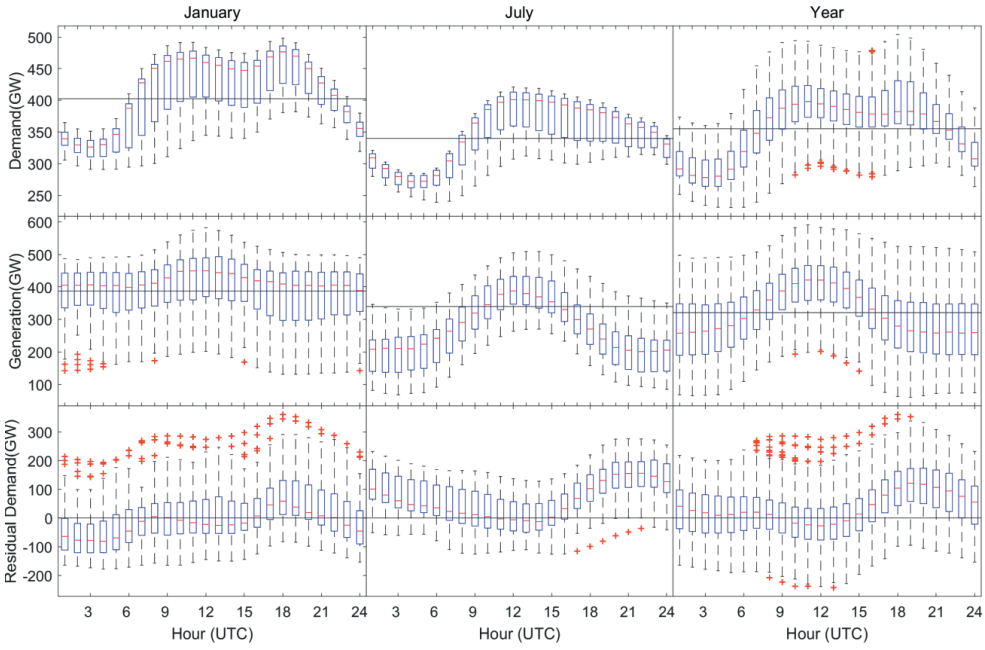

Figure 2-9 | Box plots of hourly demand, vRES generation and residual demand in Scenario 1 for 2015 averaged for all days in January, July and the full year. Box plots are based on the 25th (Q1) and 75th (Q3) percentile values. The central line in each box indicates the 50th percentile (Q2) or median. The '+' signs indicate outliers with values larger than [Q3 + 1.5(Q3 – Q1)] or smaller than [Q1 - 1.5(Q3 – Q1)], or approximately ±2.7σ from the mean. Reference lines are drawn for the mean demand, generation, and zero residual demand for each time period.

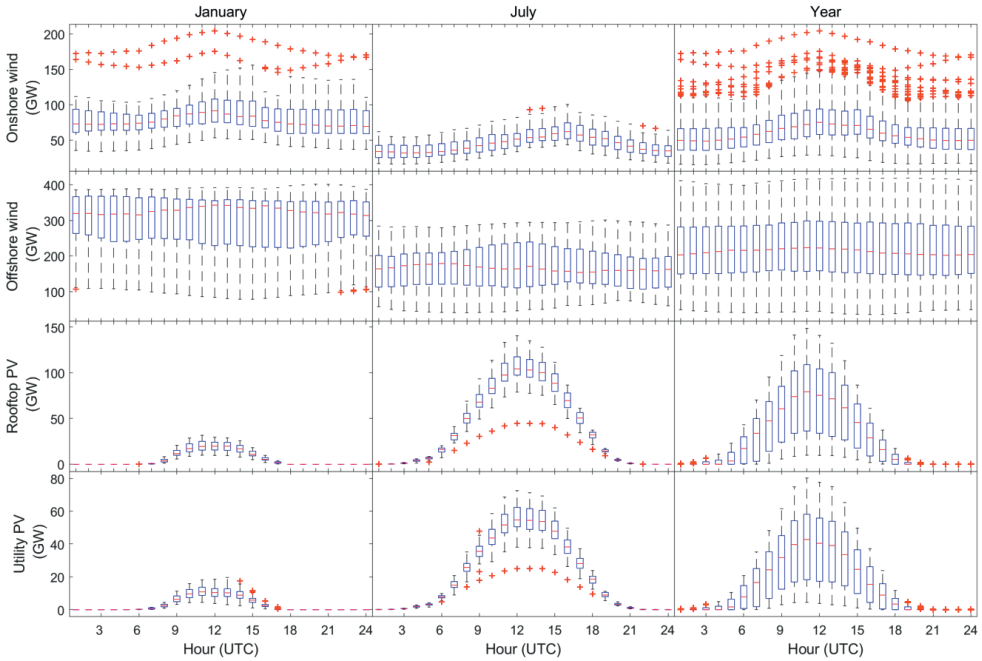

Figure 2-10 | Hourly vRES generation by technology in Scenario 1 for 2015 averaged for January, July and the full year. Box plots are based on the 25th (Q1) and 75th (Q3) percentile values. The central line in each box indicates the 50th percentile (Q2) or median. The '+' signs indicate outliers with values larger than [Q3 + 1.5(Q3 – Q1)] or smaller than [Q1 - 1.5(Q3 – Q1)], or approximately ±2.7σ from the mean. Reference lines are drawn for the mean demand, generation, and zero residual demand for each time period.

notably during the day and peaks in the afternoon before falling off during the night[30]. The net effect of these seasonal differences is that demand can be largely matched by vRES generation between 3:00 and 15:00 across the full year of the optimisation. However, the evening peak demand cannot be covered by installing more wind or PV without increasing surplus electricity production during other periods. As could be expected, PV plays a greater role in summer than in winter in meeting peak daytime demand. However, the algorithm installs far less PV capacity than it could with only 9% and 11% of total rooftop and utility PV potential installed, compared with 55% and 73% for onshore and offshore wind. An explanation for this can be found in Figure 2-9 which reveals that, with demand and generation largely balanced between 8:00 and 15:00, any further midday generation in either winter or summer would lead to negative residual demand and surplus electricity.

Looking in more detail at long term residual demand, Figure 2-11 presents a probability plot of the hourly residual demand for Scenario 1 calculated for all weather years, showing that residual demand is normally distributed with a mean of 39 GW and standard deviation of 104 GW[31]. Based on the maximum observed residual demand of 378 GW, the long-term vRES capacity credit of 11% (see Table 2-5) highlights that even when the mix and distribution of

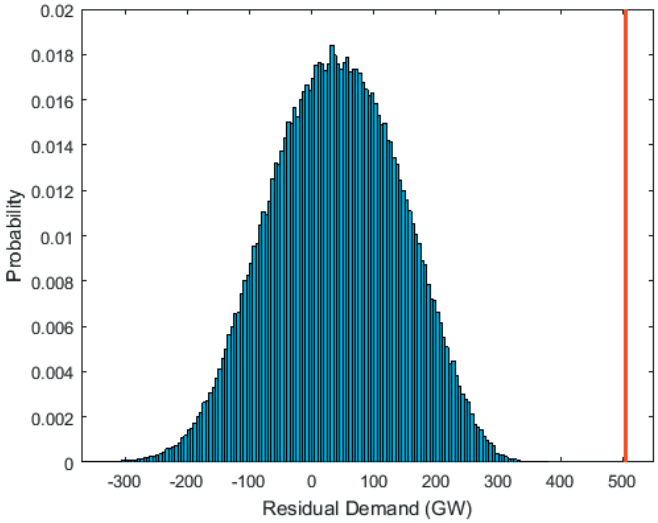

Figure 2-11 | Probability plot of hourly residual demand for Scenario 1 based on all 36 years of weather data from 1979-2015. Hourly residual demand is binned into 5 GW increments. The red line shows the peak demand of 504 GW.

vRES are fully optimised, dispatchable backup capacity of at least 75% of peak demand would still be required to ensure demand could be met in the most challenging year.

2.3.2 Effect of vRES penetration

We find that the penetration of vRES affects not only surplus generation and capacity credit, but also the spatial distribution of vRES capacity. In the first instance, Scenarios 2a and 2b show that by optimising the shares and spatial distribution of vRES capacity, it is possible to supply at least 50% of electricity demand in a copper-plate Europe without any curtailment (Figure 2-12). Attempting to reach a gross penetration rate of 75% (Scenario 2c), results in 2.6% of surplus generation, giving an effective net penetration rate of 73%[32]. The results from Scenario 1 show that the optimum gross vRES penetration is approximately 89% (82% net penetration) as attempting to achieve higher penetration of vRES in Scenario 2d results in an increase in surplus generation, and an increase in total residual.

The long-term vRES capacity credit falls with increasing vRES penetration rate as once the available capacity in the optimum locations is fully exploited at low penetration rates, additional capacity is deployed at less optimal sites. In terms of the mix of vRES technologies, Figure 2-12 also shows that despite a small increase in the share of offshore wind at low penetration rates, the optimum mix of wind and PV is largely independent of vRES penetration.

The effect of vRES penetration on its spatial distribution is best explained with Figure 2-13, which depicts the percentage of the maximum possible capacity built in each grid cell for 25%

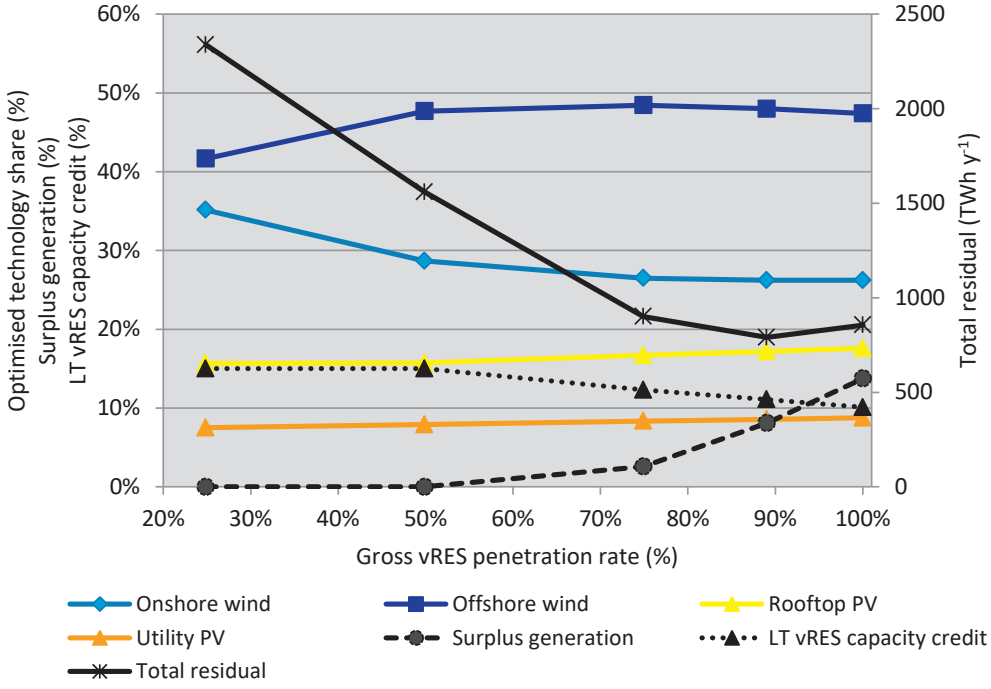

Figure 2-12 | Effect of gross vRES penetration rate on surplus generation, capacity credit, optimum technology shares and total residual when minimum residual demand is optimised. Based on results from Scenarios 2a-d and Scenario 1. The long-term (LT) vRES capacity credit is based on the year with the maximum peak residual demand.

and 75% vRES penetration for onshore wind (Figure 2-13a-b) and rooftop PV (Figure 2-13 c-d). At 25% penetration, onshore wind is almost completely deployed in grid cells located in northern Norway, Ireland, the Iberian Peninsula, and far eastern Europe (Figure 2-13a). As vRES penetration increases to 75% in Scenario 2c (Figure 2-13) (and even 89% in Scenario 1, see Figure 2-6a), these regions of saturated capacity extend further inland. The reason for this is that while the optimisation would prefer to continue installing capacity in locations like Portugal, Ireland and northern Scandinavia, the available capacity in these regions is exhausted and the optimisation must install capacity at sites with similar – but less optimal – wind patterns. However, the most preferable underlying locations for onshore wind are independent of the penetration of vRES.

Rather than filling outwards from specific locations as with onshore wind, the distribution of PV capacity shifts with increasing vRES penetration. At 25% vRES penetration, rooftop PV capacity is built almost entirely in southern Portugal and Spain (Figure 2-13c). However, at 50% vRES penetration this capacity shifts to the west, and at 75% penetration additional capacity is added in northern Europe (Figure 2-13d). The reason for this is that at low penetration rates when demand significantly exceeds vRES generation, residual demand is

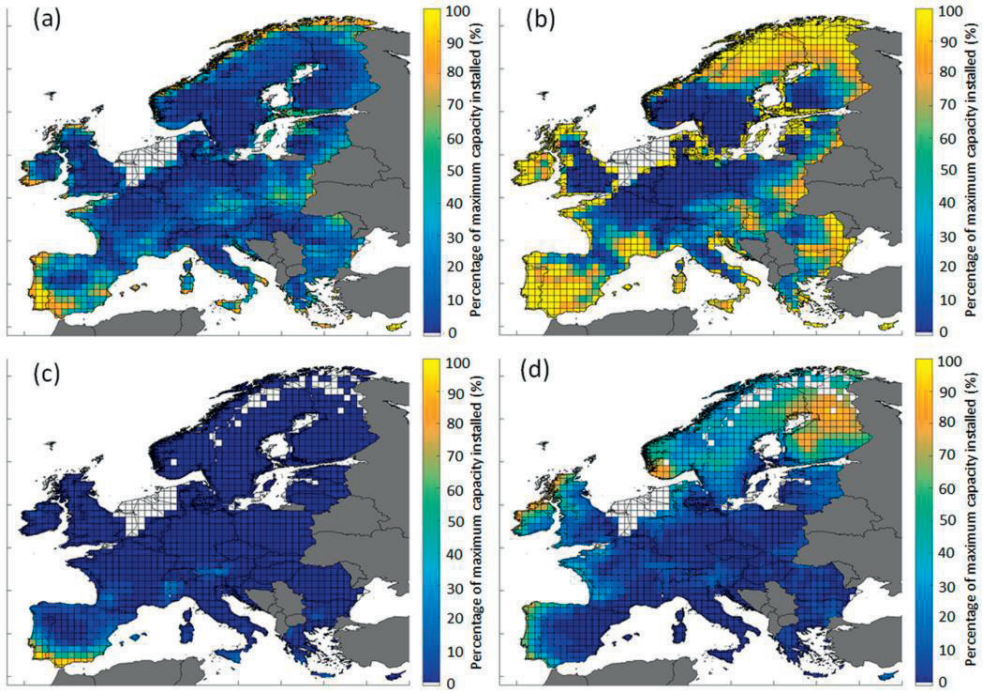

Figure 2-13 | Percentage of maximum installed capacity per grid cell for onshore wind at **(a)** 25% vRES penetration (Scenario 2a) and **(b)** 75% vRES penetration (Scenario 2c); and rooftop PV at **(c)** 25% vRES penetration (Scenario 2a), **(d)** 75% vRES penetration (Scenario 2c).

minimised by maximising generation, and hence sites with high capacity factors in southern Europe can be selected without resulting in significant surplus generation. At higher penetrations however, peaks in summer PV production – coupled with increasing wind generation – mean that this is no longer the case, and the model builds capacity in the west and north. In these locations, PV generation can better match demand without resulting in excessive surplus generation during summer.

2.3.3 Effect of demand profile

The results from Scenario 3a show that adding 500 TWh of demand from HPs increases total net installed vRES capacity by 150 GW (13%) compared with Scenario 1. This additional capacity results from increases in onshore (+85 GW) and offshore (+92 GW) wind, which are partly offset by a fall in PV capacity (-27 GW). Mean ST vRES capacity credit increases by 1.9% (in absolute terms) to 16.5%, showing that the demand profile of HPs matches better with wind generation patterns than it does with PV. However, the LT capacity credit remains unchanged. In Scenario 3b, adding 800 TWh of demand from EVs results in similar increases in onshore (+75 GW) and offshore (+103 GW) wind capacity, as well as increases in rooftop

(+68 GW) and utility (+41 GW) PV capacity in western Europe. The decrease in LT capacity credit in Scenario 3b compared with Scenario 1 shows that vRES generation profiles correlate less well with demand from EVs than with base demand.

These impacts can be explained by the different demand, generation and residual demand profiles for each scenario (Figure 2-14). Demand from HPs is largely seasonal, occurring mainly during winter and remaining largely constant throughout the day. For this reason, an increase in wind capacity is to be expected, given these periods are also associated with higher wind generation (see Figure 2-10). Additional PV capacity is not installed as this would increase surplus electricity during daylight hours in the summer (Figure 2-14b), and contribute only marginally to covering daytime winter HP demand. As a result, the residual demand for Scenario 3a is higher than Scenario 1 in winter, but lower in summer.

Unlike HPs, demand from EVs occurs all year round and exhibits more diurnal variation with peaks during the day and in the late evening when EV batteries start charging as people arrive home. This demand profile is more conducive to PV, which can help meet additional daytime demand in both winter and summer. Additional wind capacity is also useful in covering EV demand in the early morning and late evening once PV generation falls off, particularly in winter. In terms of residual demand, Figure 2-14c shows that the seasonal impact of HPs is largely balanced when the full year is considered. However, the morning and evening demand peaks produced by EVs cannot be covered by vRES, resulting in much higher residual demand in these periods.

Adding demand from HPs and EVs changes not only the total amount of vRES installed, but also the distribution of PV capacity. When HP demand is added (Scenario 3a), the net 26 GW fall in total PV capacity is actually the result of 94 GW being removed from cells in western, central and northern Europe and 68 GW being added in southern Europe. The reason for this is that higher capacity factor sites at lower latitudes allow more daytime demand from HPs to be covered during winter. When EV demand is added (Scenario 3b), the net 109 GW increase in PV capacity is the result of 76 GW being removed from eastern Europe and 185 GW being added to western Europe (Figure 2-15) as, with more PV located in western Europe, PV generation can be extended later into the day as the sun sets helping to cover evening demand from EV charging.

When demand from both HP and EVs is added (Scenario 3c), onshore and offshore wind capacities increase by 180 GW and 155 GW respectively compared to Scenario 1, showing that wind requirements are essentially additive for meeting HP and EV demand as these loads largely coincide.

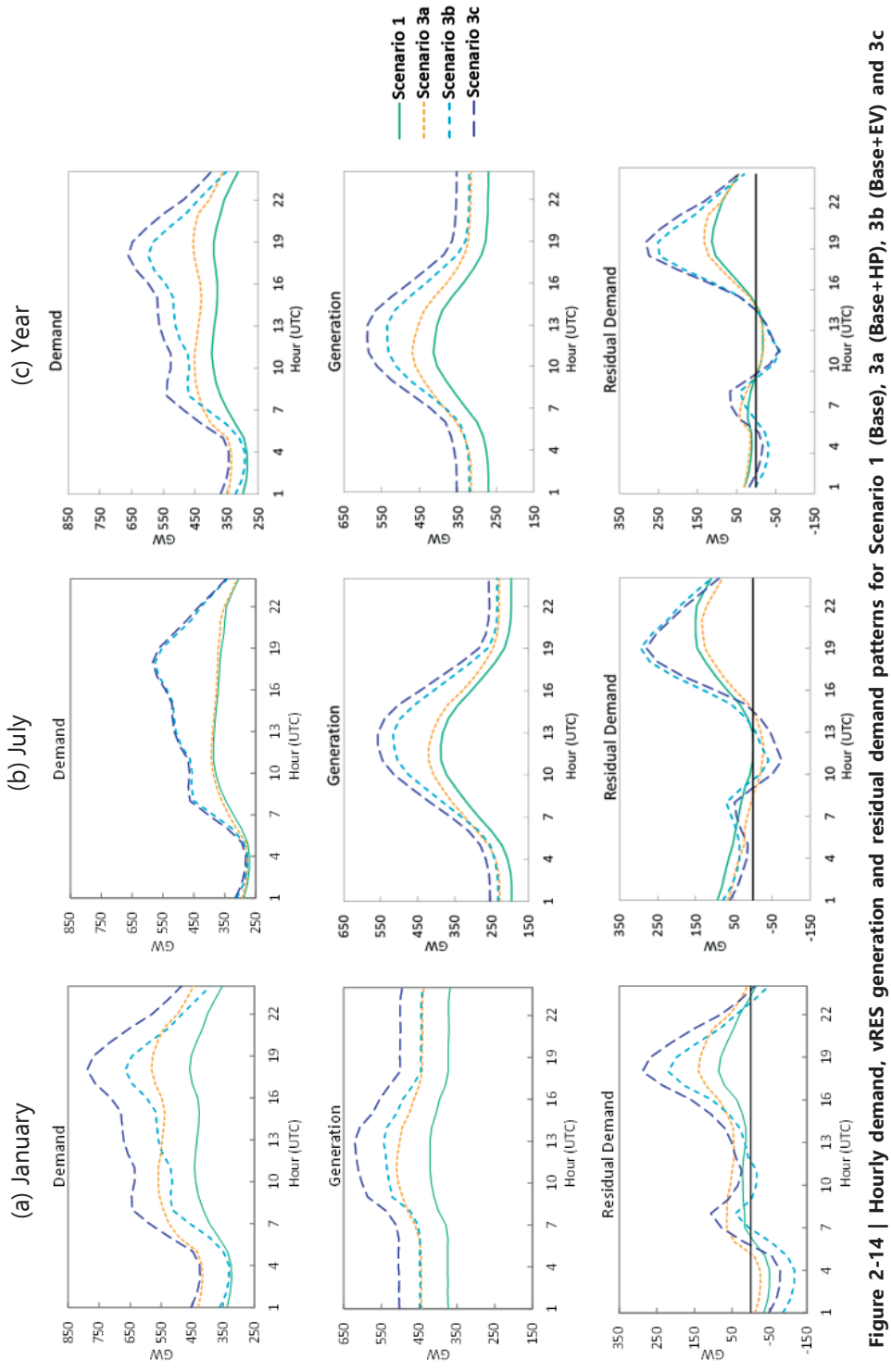

Figure 2-14 | Hourly demand, vRES generation and residual demand patterns for Scenario 1 (Base), 3a (Base+HP), 3b (Base+EV) and 3c (Base+HP+EV) for 2015 averaged for (a) January **(b)** July, and **(c)** Full year.

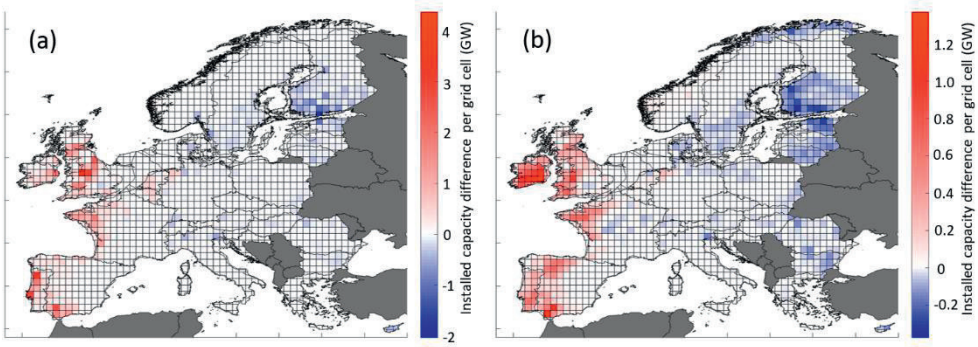

Figure 2-15 | Installed capacity difference maps for Scenario 3b with respect to Scenario 1 for (a) rooftop PV and **(b)** utility PV.

2.3.4 Effect of deep offshore waters

Extending the spatial grid to include the entire European EEZ (Scenario 4) reduces total vRES installed capacity by 19% and increases long-term capacity credit to nearly 20%. This is mainly due to a shift towards higher capacity factor wind sites at the extremes of the EEZ in the Atlantic, North and Norwegian seas. As a result, the maximum peak and total residual demands of 323 GW and 555 TWh in Scenario 4 are the lowest observed in all scenarios, being 14% and 35% lower respectively than in Scenario 1, and 16% and 55% lower respectively than in the maximum capacity factor distribution (Scenario 6). Onshore wind capacity decreases by 82% compared to Scenario 1 while offshore wind capacity increases by only 23%, showing that the development of higher capacity factor sites located far offshore allows less wind capacity to be installed overall. Total PV capacity is reduced by 33% compared with Scenario 1 though the spatial distribution remains largely unchanged. This shows that even with access to the most favourable wind sites, some PV is still beneficial for minimising residual demand.

2.3.5 Effect of PV configurations

When all rooftop PV panels are set to face west (Scenario 5a), the bulk of rooftop PV capacity is installed in the western extremes of Europe (e.g. Portugal, Ireland, UK, France). This extends rooftop PV generation further into the day helping to cover peak evening demand, especially during the summer. As a consequence, however, morning rooftop PV generation falls which would result in unmet demand if the optimisation did not compensate for this by redistributing utility PV capacity to eastern Europe, thus providing additional generation in the morning. This shows that while west-facing PV can be advantageous for meeting peak European evening demand, some morning PV generation is still required. When rooftop PV panels are instead set to face East (Scenario 5b), most rooftop PV capacity is built in north-eastern Europe and again the optimisation compensates by shifting utility PV west. Implementing two-axis tracking for utility PV (Scenario 5c) results in rooftop PV capacity being completely replaced by utility PV, which now generates electricity over a longer period

extending from about 5:00 until 19:00. As a result, total residual falls by 3% compared to Scenario 1 and long-term vRES capacity credit increases slightly to 11.5%.

2.3.6 Comparison with max capacity factors

When the optimised capacities per technology from Scenario 1 are redistributed to maximise capacity factor (Scenario 6), onshore wind capacity shifts to the central European locations previously devoid of capacity such as northern France, Belgium, the Netherlands, Germany and Poland. PV capacity moves to southern Europe as expected due to the higher irradiance. With these higher capacity factor sites, total generation increases by 640 TWh (23%). However, only a fraction (23%) of this can be used to meet demand, leading to far higher surplus generation (707 TWh, 21%) than in Scenario 1.

As peak residual demand remains largely unchanged between Scenarios 1 and 6, backup requirements would be the same irrespective of whether a minimum-residual-demand or maximum-capacity-factor approach was taken. The net effect is that long-term capacity credit falls slightly to 10.6%.

Mean capacity factors for onshore and offshore wind, rooftop and utility PV rise from 22%, 38%, 14% and 13% in Scenario 1 to 31%, 43%, 21% and 22% respectively in Scenario 6. This shows that the minimum residual demand optimisation installs significant capacity in locations with rather low capacity factors. Figure 2-16 depicts cumulative installed capacity against capacity factor, showing that for onshore wind and both PV technologies, the bottom 50% of installed capacity in Scenario 1 has a capacity factor approximately 10% (absolute) lower than in Scenario 6. The difference is less for offshore wind as there are fewer sites available for this technology, and capacity factors are typically higher than onshore.

2.3.7 Seasonal effects of minimising residual demand

Figure 2-9 showed that spatially optimising residual demand does not result in generation matching demand every hour of the day. Instead, the optimisation (on average) results in largely steady generation throughout the day, with a small daytime peak from PV. This can be explained by the seasonal variability of wind and PV generation depicted in Figure 2-17, which gives the monthly generation by technology for Scenario 1. This shows that while wind generation is approximately 50% lower in summer than in winter, PV generation is six-times higher in summer than in winter. Additional PV capacity could be installed to cover the summer shortfall but this would result in winter surpluses, thus the optimisation must make trade-offs between seasonal surpluses and deficits. As a result, the optimisation installs enough wind capacity to largely cover winter demand, while leaving some unserved demand during summer.

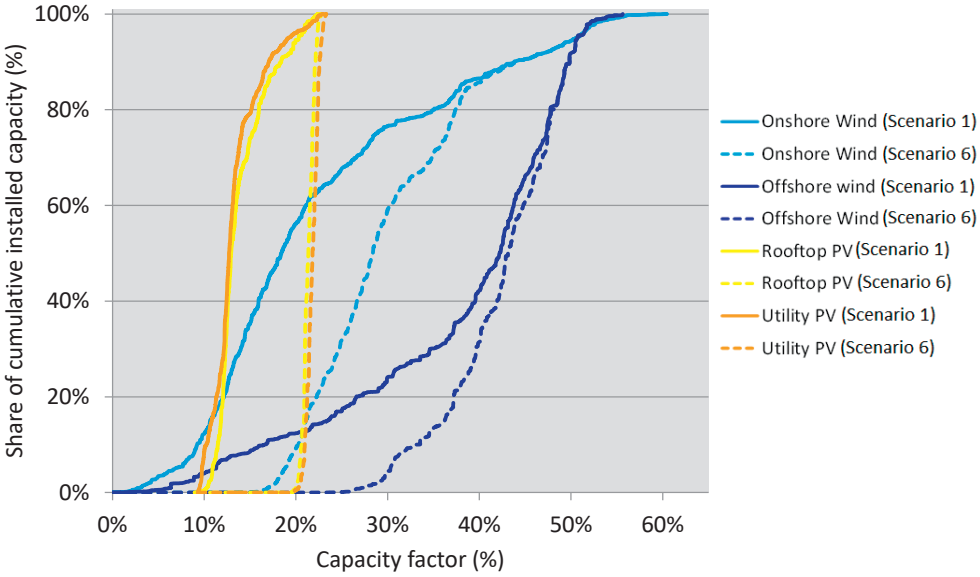

Figure 2-16 | Share of cumulative installed capacity as a function of mean grid cell capacity factor for Scenarios 1 and 6.

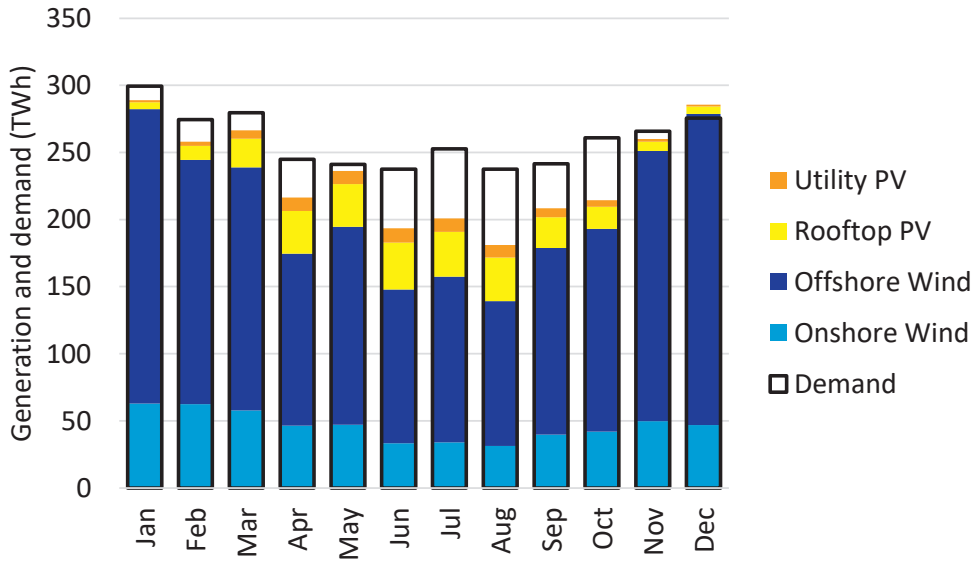

Figure 2-17 | Monthly generation by technology for Scenario 1 in 2015.

This seasonal pattern is somewhat contrary to those in other studies which typically exhibit significant (or even surplus) PV generation and minimal backup requirements during the summer, with unmet demand and significant backup required during the winter. However, these studies do not achieve such high vRES penetration as we do in our study (89% gross energy penetration for Scenario 1, compared with 48% in (ECF, 2010b), 56% in (GWEC et al., 2015), 61% in (EREC, 2010) and 78% in (Haller et al., 2012)) and typically include storage ((ECF, 2010b; Haller et al., 2012)).

Although we do not include storage, we can look at its possible implications by examining how residual demand is distributed throughout the year. Figure 2-18 shows the range of accumulated hourly residual demand for Scenario 1 across all weather years. A flat gradient in this figure indicates that short- to medium-term imbalances largely cancel out, and daily or weekly storage could be used to cover mismatch; while a sustained positive or negative gradient indicates that short- to medium-term imbalances accumulate, and long-term seasonal storage would be beneficial. Thus, Figure 2-18 shows that short-term storage in the order of 100 TWh would be sufficient in most years to ensure that demand could be met from September until late January with wind and PV alone without generation from additional sources[33]. From February until September the accumulated residual follows a negative trend, showing that short- to medium-term imbalances do not balance out, and additional generation capacity or seasonal storage would be required. However, as most years exhibit no

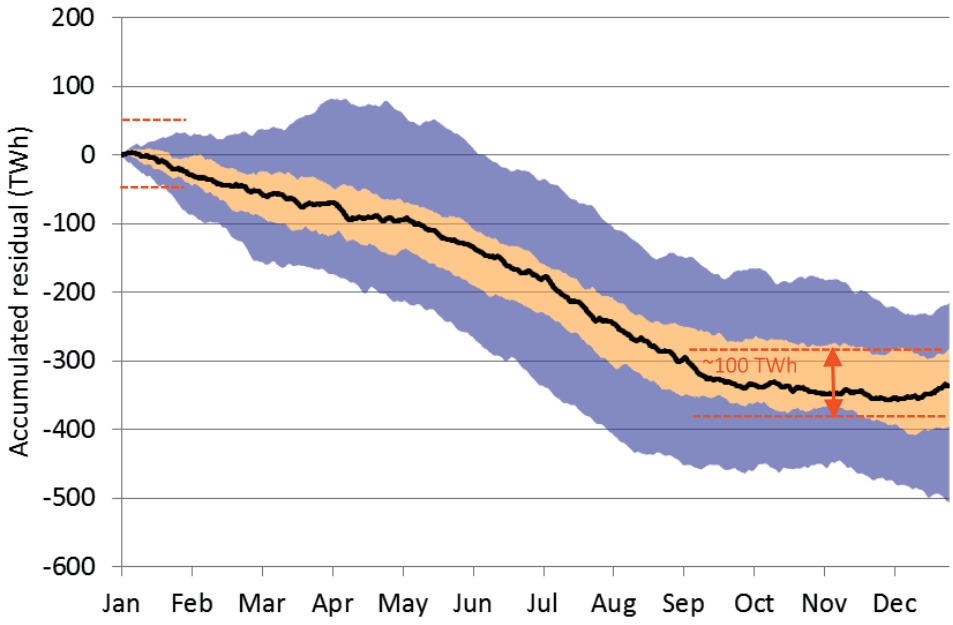

Figure 2-18 | Accumulated hourly residual demand for Scenario 1 based on simulated years 1979-2015. The starting point is 1:00 on January 1st. The black line indicates the median value. The orange and purple regions indicate the interquartile and full range of values respectively.

sustained periods with a positive gradient, no opportunities for charging long-term storage exist and Scenario 1 results in a net annual deficit of 200 TWh to 500 TWh. If seasonal storage were added to the model so that curtailment could be reduced, it is likely that additional capacity would be built to cover this shortfall.

2.3.8 Understanding the spatial distribution

One might expect that the residual demand minimisation would install wind and PV capacity evenly across Europe in order to maximise site diversity. However, the results in Figure 2-6 show that this does not occur. Instead, we find that onshore wind capacity is installed mainly at the periphery of Europe, offshore wind is quite evenly distributed (though concentrated in the North and Baltic seas), and rooftop and utility PV are mostly installed in a band extending from Portugal to Finland.

To understand the reason behind these phenomena, it is necessary to consider the different wind and solar radiation patterns across Europe. Figure 2-19 shows the correlation coefficient between time series as a function of distance between sites for both wind speed and solar

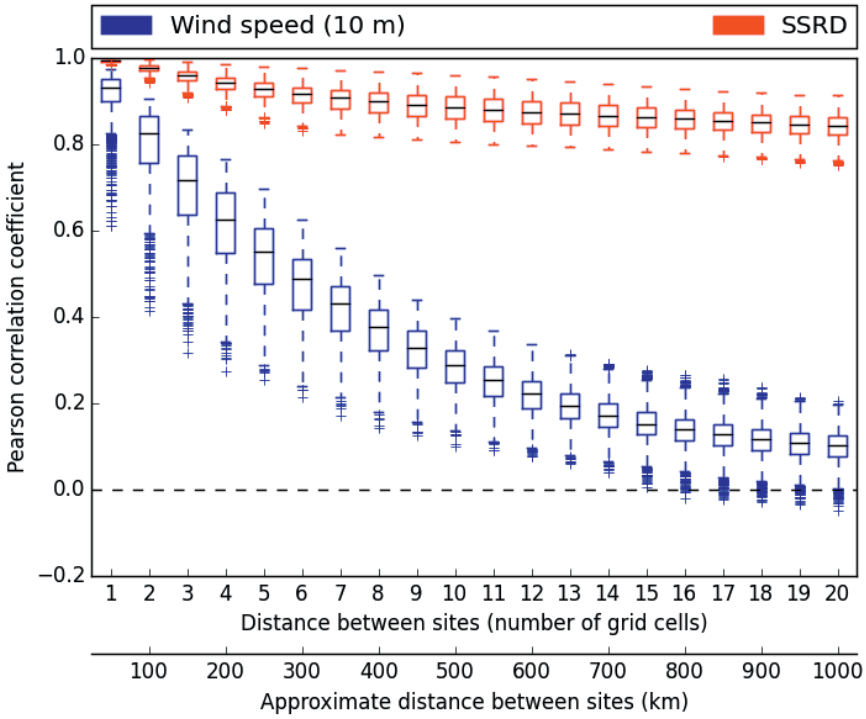

Figure 2-19 | Pearson correlation coefficient between time series as a function of distance for 10 m-wind speed and downwards surface solar radiation (SSRD). Correlations based on 3-hourly values from ERA-Interim. The box plots are based on all grid cells in the 50-m water depth grid for weather year 2015. With a regular grid spacing of 0.75°, the distance in kilometres is approximated by assuming an average grid cell spacing of 50 km.

radiation. This figure highlights that wind generation patterns are strongly spatially correlated, with sites within a radius of five grid cells (approximately 250 km) having correlation coefficients above 0.5. Only at distances in excess of 800 km does the correlation between sites start to turn negative, and generation patterns become complementary. As a result, the optimisation attempts to maximise the distance between wind sites by pushing wind capacity to the geographical extremes of Europe, leading to significant offshore wind capacity in shallow waters around Europe's coastline. The same effect occurs on land, with onshore wind pushed to Europe's land borders. However, the total wind potential at these geographically extreme locations is limited, and restricting capacity only to these sites would result in significant unserved energy at night when PV is not generating. Thus, additional offshore wind capacity is placed in the North Sea due to its favourable generation patterns, which – to avoid excess correlated generation in this region - results in less onshore wind in countries surrounding the North sea (Figure 2-6a). From Figure 2-19, solar radiation is even more strongly correlated than wind with correlation coefficients above 0.8 even at distances of up to 1000 km, thus spatial complementarity does not explain the observed distributions.

To understand the placement of PV, it is necessary to look in more detail at the spatial differences in hourly generation. These are shown in Figure 2-20, which depicts hourly generation by region for (a) the first week of January and (b) the first week of July. Figure 2-20 shows that by installing PV capacity in the Nordic countries, PV generation in the summer can be increased while avoiding surplus PV generation in winter when wind production is highest (Figure 2-20a). Furthermore, the summer generation profile (Figure 2-20b) shows that not only is PV generation increased in the morning due to the easterly latitude[34], but it also generates for longer due to the extended daylight hours at northern latitudes. PV capacity in western locations like Iberia and the British Isles also extends PV generation later into the day, helping to cover evening demand. Although we do not explicitly quantify transmission flows in our study, an examination of aggregated hourly net surplus generation (vRES generation minus demand) from each region (Figure 2-21) shows that with vRES capacity distributed to minimise residual demand, the British Isles and Nordic countries would typically be net exporters of vRES electricity, while the Iberia, Eastern and Central regions would typically be net importers. Thus, in order to bring vRES generation from where it is generated to where it is consumed, significant expansion in transmission infrastructure would be required.

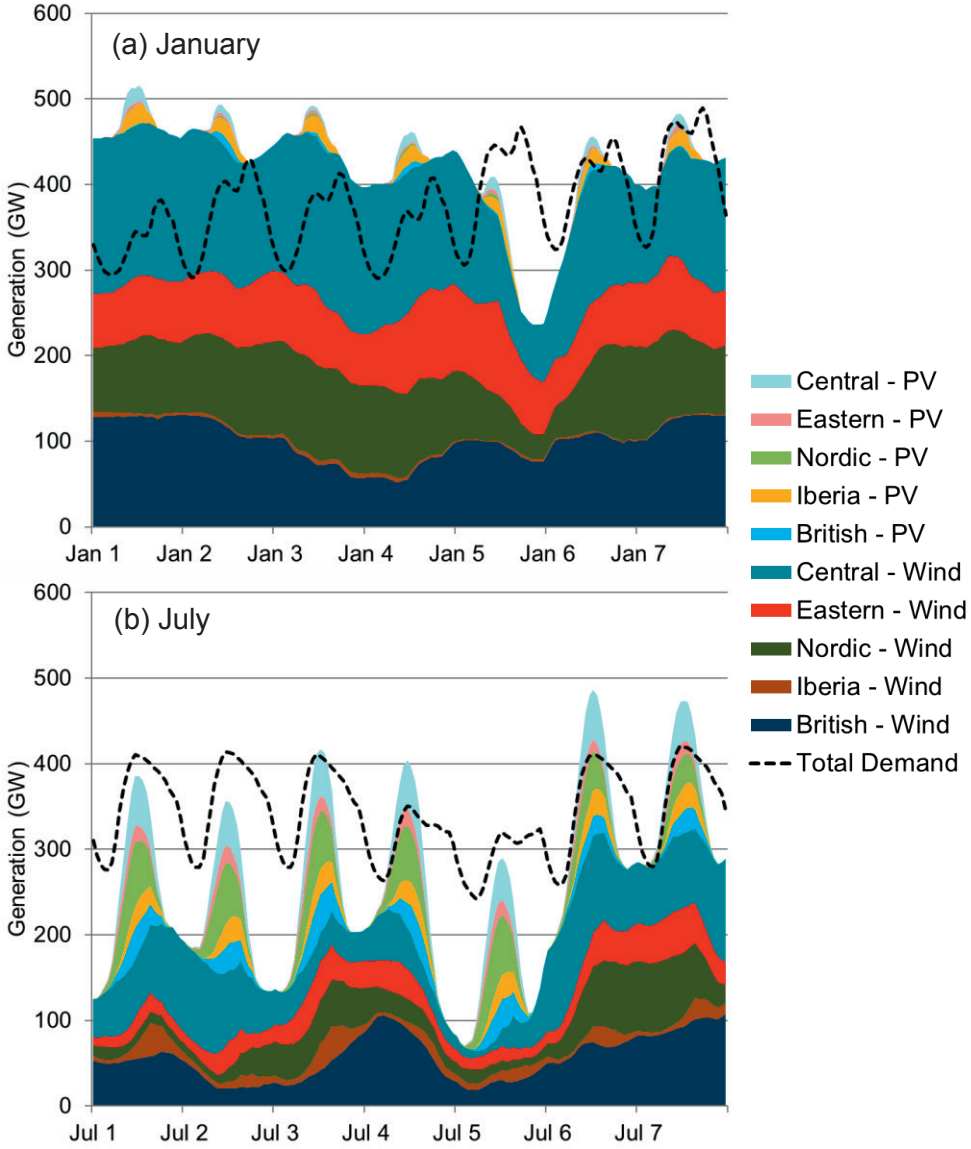

Figure 2-20 | Generation by technology in Scenario 1 for (a) the first week of January and **(b)** the first week of July 2015. Generation from the two wind and PV technologies is aggregated into regions based on the following groups: British Isles - IE, UK; Iberia – PT, ES; Nordic – NO, SE, FI; Eastern – EE, LT, LV, PL, SK, HU, RO, BG, EL, CY; Central: all others.

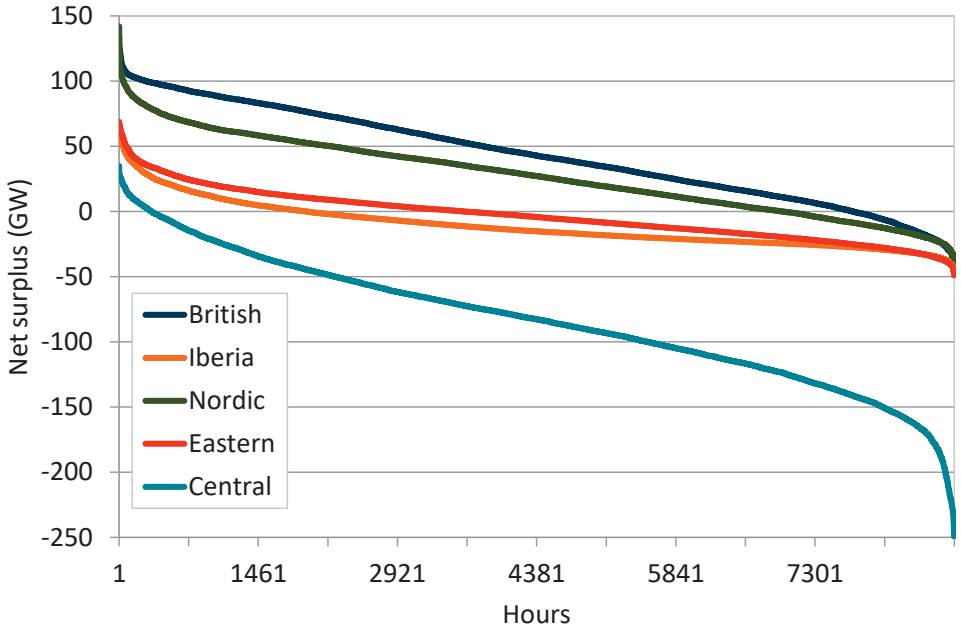

Figure 2-21 | Duration curve of net surplus by region for Scenario 1 for weather year 2015. Regions included: British Isles - IE, UK; Iberia – PT, ES; Nordic – NO, SE, FI; Eastern – EE, LT, LV, PL, SK, HU, RO, BG, EL, CY; Central: all others.

2.4 Discussion

2.4.1 Limitations of study

This study considers explores how optimising the mix and spatial distribution of PV and wind generation capacity can minimise residual demand depending on different factors. Nevertheless, **scope limitations** mean that some aspects are not considered:

- while the ERA-Interim dataset limits the *spatial resolution* to 0.75°, higher spatial resolution is unlikely to make a large impact given the strong spatial correlations identified (Figure 2-19). Extending the *geographic scope* to include other regions could also add further potential for minimising residual demand, however, it remains to be seen whether long-term cooperation and integration of electricity markets, even at the EU level, is achievable.

- a result of the *LLSQ formulation* is that the optimisation weights hours with higher residual demand more heavily. This represents an intermediate approach between a residual energy-based minimisation (minimising backup/storage energy requirements i.e. TWh), and a residual capacity-based minimisation (minimising backup/storage capacity i.e. GW) which are likely to yield different results[35].

- A further consequence of the LLSQ formulation is that it was not possible to include *transmission and distribution*, nor *flexibility-improving* technologies such as demand response and storage. By assuming a copper-plate Europe, congestion limitations and line losses, which would erode the benefits of spatial optimisation by increasing curtailment and other losses, are not considered[36]. This would likely result in vRES capacity being built closer to load centres, rather than more remote locations observed in this study. Furthermore, there are many hurdles to constructing long-distance transmission lines (e.g. social acceptance, environmental impacts, high cost (Doukas et al., 2011)) we do not consider which, if taken into account, would impose additional constraints on transmission and reduce the potential benefits of spatial vRES optimisation. However, despite these transmission simplifications, we show that even in the idealised case of a copper-plate Europe, neither peak residual demand nor total residual demand can be significantly reduced through spatial optimisation of vRES.

- The exclusion of transmission and flexibility technologies means that this study could not directly consider total system *costs*. Only by considering the total costs of vRES investment capacity, dispatchable backup capacity, distribution and transmission infrastructure, and the provision of reserves could the overall cost-effectiveness of a minimum-residual-demand based optimisation be assessed and compared with other methods[37]. However, by minimising residual demand the costs of vRES curtailment and backup capacity have been considered indirectly. Any *flexibility limitations* on the implied portfolio of dispatchable backup technologies (e.g. ramp up/down rates, minimum start-up and shut-down times) are not considered. However, some ex post analysis of hourly changes in residual demand (see Appendix A) suggests that dispatchable ramping requirements for Scenario 1 would be approximately 70-80% higher than today[38], but 50% lower than if vRES were distributed to maximise capacity factor (Scenario 6).

- Government policies, and incentive schemes in particular, can have a significant impact on where renewable technologies are deployed, which were also not considered. Their impact can be clearly seen from Germany's *Energiewende* which, in the period between 2006 and 2016, resulted in higher wind (+30 GW) and PV (+38 GW) deployment in Germany than in any other European country (Eurostat, 2017b; Pegels & Lütkenhorst, 2014), despite the fact that Germany's wind and solar resources are relatively less competitive than other countries (EEA, 2009; Perpiña Castillo et al., 2016), and (from this study) do not coincide particularly well with demand. Alternatively, subsidies could be used to encourage wind and PV deployment in locations which would be more advantageous for the power system by better matching generation with demand.

- As we consider only the power sector, we neglect any *potential synergies with other sectors of the economy* (e.g. transport, industry). Including technologies which could convert

surplus generation to other energy carriers (e.g. power-to-gas) for use in other sectors would reduce the 'penalty' associated with surplus generation, likely leading to a higher share of PV and increased utilisation of high capacity wind and PV sites.

- Any large-scale decarbonisation of the European power sector should not consider only the technical transformation required, but also broader environmental, social and economic aspects of *sustainability* (Steurer & Hametner, 2013). Thus, other factors such as the full lifecycle impacts of the generation technologies, employment, social acceptance, and potential impacts on natural flora and fauna due to large-scale investments would need to be taken into account. However, these aspects were beyond the scope of this paper.

Uncertainty in the underlying data and assumptions made in this study also introduce several potential sources of error:

- variations in *demand profiles* would have a large impact on the results. By using only one year of base demand data and a fixed HP demand, neither the base nor HP demand profiles take into account increased demand in colder years. Furthermore, our HP demand profiles do not consider the effects of temperature on HP efficiency[39], thermal energy storage, or different end-user preferences; while the EV charging profiles assume charging station availabilities, driving patterns and charging preferences which may change in the future. A preference for night-time charging, for example, would likely lead to a higher share of wind capacity. Increased demand for air conditioning may also change the optimal mix and placement of vRES, potentially favouring solar PV due to its correlation with cooling demand[40].

- Estimating *vRES generation profiles* from the underlying weather data requires several steps which each entail uncertainties. For example, due to their poor treatment of aerosols, reanalyses like ERA-Interim can predict clear sky conditions when they may in fact be cloudy, leading to an overestimation of solar generation (Boilley & Wald, 2015). However, this overestimation is reportedly less for ERA-Interim compared with other reanalysis datasets, and is partly offset by periods when clear sky conditions are reported as cloudy (Rienecker et al., 2011). Using more advanced weather models or satellite-derived radiation data which include the effects of aerosols would allow for more accurate estimates of PV production, however this was not possible in our study. Also, assuming a logarithmic vertical wind speed profile does not account for reduced wind speed variability at higher altitudes due to lower turbulence, and may underestimate wind potential (Becker et al., 2014).

- Aside from systemic uncertainties and biases in the weather dataset, the *spatial and temporal resolution* of the dataset also affects the accuracy of our results. For example, the

need to interpolate from the 3-hourly data in ERA-Interim to hourly can introduce errors for PV during sunrise and sunset hours, but as these are periods of low radiation the impact is likely to be small. The main effect of linear interpolation is that the wind and PV generation profiles may be smoother than they would be in reality. However, it has been shown that significant spatial smoothing of wind and PV profiles occurs across large areas due to geographical diversity. For PV for example, one study found that the relative aggregate output variability of PV plants sited 20 km apart was six times less than the output variability of a single site, even at time scales less than 15 minutes (Mills & Wiser, 2010). For wind, significant smoothing effects are observed when wind farms are placed over a wider geographical area due to i) the mitigating effect of many turbines in a wind farm which absorb short-term (sub-hourly) wind gusts, and ii) greater geographical diversity reducing the impact of (multi-hour) diurnal and synoptic wind variations (Albadi & El-Saadany, 2010; Drake & Hubacek, 2007)[41]. Furthermore, the spatial coarseness of the reanalysis dataset means that local terrain features such as hills, trees, and buildings which could affect wind speeds are not considered (Staffell & Pfenninger, 2016). However, given that the focus of our study is balancing vRES output at the continental scale and not trying to accurately reproduce the output of individual wind or PV farms, we consider the 0.75° and hourly resolution sufficiently accurate for this purpose. As in the current power system, sub-hourly power imbalances would need to be managed by balancing power flows using the transmission network, operational reserves, and flexible dispatchable generators which are beyond the scope of this study.

- We assume grid cell *independence* in that kinetic energy harvested from the wind in one cell does not affect wind speeds in neighbouring cells. In reality, this is not strictly true with one study finding competition among turbines reducing peak wind speeds averaged over a 400 km radius reducing by 1 m s^{-1} (Jacobson, Delucchi, Cameron, et al., 2015), however including these effects was not possible with the current model.

- Future changes in European weather patterns due to *climate change* are not considered. However, recent studies on the PV (Jerez, Tobin, et al., 2015) and wind (Tobin et al., 2015) suggest that these impacts are likely to be small.

- Together, the assumed *capacity densities* and *land availabilities* dictate vRES capacity constraints. If technologies improve[42] and capacity densities increase, then more capacity could be installed in optimum locations. Conversely if fewer land classes are suitable or less land is available, the potential for spatial optimisation would reduce. As neither total PV nor wind potential is fully exploited in any optimisation run, the impact on the results is likely to be minor.

2.4.2 Practical implications

It is important to reflect on what residual demand minimisation could mean in practice:

- Although optimising the mix and distribution of different vRES technologies has the potential to smooth generation or minimise residual demand, there is little evidence of this being done in practice (Thomaidis et al., 2015).

- Wind and PV capacity factors at some sites may be too low to be economically viable (e.g. northern Europe, from Figure 2-16). However, if wind and PV costs continue to fall and these sites produce electricity when residual demand and market prices are high (e.g. early morning or late evening), the market value of the electricity generated at these sites may be sufficient to make them economically attractive (IEA, 2016b)[43].

- While they may be potential benefits for Europe as a whole from distributing capacity on a European-wide scale and integrating energy markets in line with current EU policy objectives (EC, n.d.; Schmid & Knopf, 2015), the geopolitics of energy cannot be ignored and individual governments may resist an increasing reliance on supranational generation and interconnectors (Scholten & Bosman, 2016). Thus, a European 'supergrid' – upon which this and many similar studies rely – may never materialise (Macilwain, 2010; van Hertem & Ghandhari, 2010).

2.4.3 Comparison with existing literature

Considering the **mix of wind and PV capacity,** minimising residual demand calls for a higher share of wind (74% in Scenario 1) compared with several studies (e.g. 32% (EREC, 2010), 47% (GWEC et al., 2015), 50% (Tröster et al., 2011), 54% (Bruninx et al., 2015)[44], 56% (EC, 2016b)), though in a similar range to others (e.g. 71% (Pfluger et al., 2011), 75% (Bruninx et al., 2015)[45], 82% (Rodríguez et al., 2014), 60-90% (Heide et al., 2011)). Aside from the fact that many studies assign capacity exogenously, the main reason for these differences is that we do not include storage. If short-term (daily) storage were included then the diurnal variability of PV would result in less residual demand, and the optimum share of PV would likely increase (Heide et al., 2011). Conversely, including seasonal storage would most likely increase the optimum share of wind.

In terms of how **vRES capacity is spatially distributed**, no study could be found including a grid-level spatial distribution for the whole of Europe for comparison. However, when aggregated at the national level, Figure 2-22 shows that our results are mostly within the range of other studies, though there are several exceptions. Namely, our study shows (i) less wind and PV capacity in Germany, (ii) less PV in southern European countries (e.g. Italy, Spain), and (iii) more PV in northern Europe. The main reasons for this are that many studies allocate capacity based on current deployment and future policy plans rather than optimising it (hence

significant capacity in Germany), and the fact that we did not consider costs, storage, or transmission. Including storage would help to reduce summer PV generation peaks making PV more attractive in southern Europe, while including transmission constraints and losses would most likely reduce capacity in the north of Europe and shift capacity closer to load centres in central Europe, for the reasons already discussed.

In terms of **potential transmission requirements**, distributing vRES capacity to minimise residual demand would require massive expansion of transmission and distribution infrastructure, however this feature is common to many other scenarios of high-vRES European power systems ((Couckuyt et al., 2015; ECF, 2010b; ENTSO-E, 2016c; Grossmann et al., 2013, 2014; Haller et al., 2012; Mileva et al., 2016; Rodríguez et al., 2014)). Furthermore, ENTSO-E's Ten-Year Network Development Plan (TYNDP) includes the connections between central Europe and the British Isles, Nordic countries, Iberian Peninsula, and eastern Europe in their 10 key transmission corridors requiring further expansion (ENTSO-E, 2016c). We find that these corridors would also be important for a power system with vRES capacity optimised to minimise residual demand, though the direction and volume of these flows may differ.

Depending on the demand level assumed, the results for **unmet demand** in our study of 566 TWh (Scenario 1, lowest assumed demand) to 998 TWh (Scenario 3c, highest assumed demand), or 18% to 23% of annual demand, are largely in agreement with (Steinke et al., 2013) who report backup energy requirements of 20% in a 100% RES copper-plate Europe. However, assuming that the 194 GW of hydro capacity (see Table 2-1) remains unchanged until 2050 and providing 460 TWh of generation annually[46], the resulting demand shortfall of 104 TWh y^{-1} (Scenario 1) to 536 TWh y^{-1} (Scenario 3c) could be met by a combination of stored surplus generation and other dispatchable generation technologies.

In terms of required **backup dispatchable capacity**, subtracting the current hydro capacity from the peak long-term residual demand of 377 GW (Scenario 1) or 738 GW (Scenario 3c), suggests that at least 180 GW (Scenario 1) to 544 GW (Scenario 3c) of additional dispatchable capacity would be required to ensure demand could be met in the most challenging year. Compared with existing studies (Table 2-1), these dispatchable requirements – and the resulting total capacity requirements[47] of 1521 GW (Scenario 1) to 2316 GW (Scenario 3c) – are in a similar range. However, it should be kept in mind that we include no demand response or storage capacity, which would further reduce backup requirements. Moreover, we calculate backup requirements based on the maximum observed residual demand in 36 years of weather data, while most studies consider only one year.

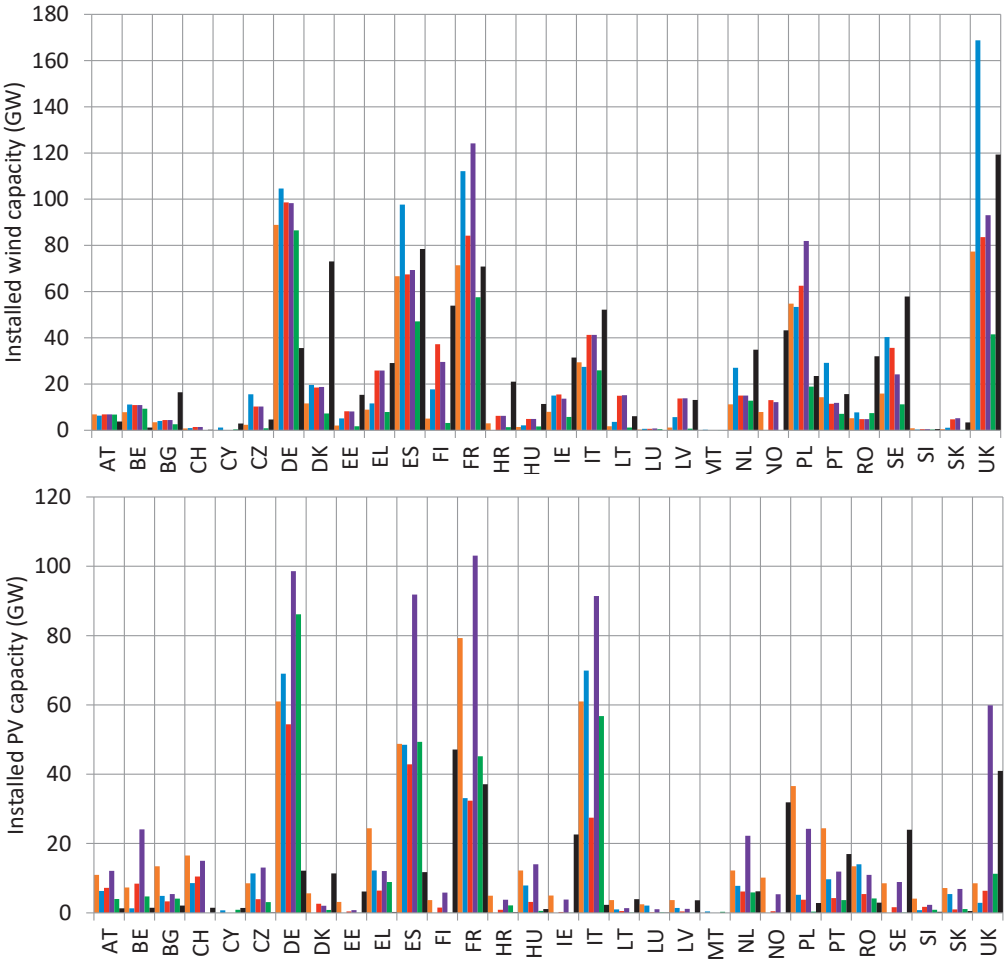

Study	Total (GW)		Share (%)
	Wind	PV	Wind/PV
Energynautics	509	501	50%/50%
Fraunhofer (Scenario B)	790	325	71%/29%
e-Highway 2050 (X-5)	702	238	75%/25%
e-Highway 2050 (X-7)	753	653	54%/46%
EU Ref. Scenario 2016	368	295	56%/44%
This study (Scenario 1)	851	294	74%/26%

Figure 2-22 | Comparison of total installed wind and PV capacity by country in several high-RES scenarios for Europe. (Sources: Energynautics (Tröster et al., 2011), Fraunhofer (Pfluger et al., 2011), e-Highway 2050 (Couckuyt et al., 2015), EU Reference Scenario 2016 (EC, 2016b)). The legend also shows the total installed capacity and capacity share for each technology per scenario.

2.5 Conclusion

In this paper, we have presented a method to optimise the spatial distribution of wind and PV capacity by minimising residual demand, incorporating long-term weather data to ensure the robustness of the optimised capacity distributions to different weather years. Using this approach, we considered the effects of vRES penetration, alternative demand profiles, access to remote offshore sites, and alternative PV configurations. Our method can be used by power system modellers to build detailed vRES spatial distributions and generation profiles for PSM studies, incorporating different optimisation objectives (e.g. minimum residual demand, maximum capacity factor), spatial and technological constraints. From a methodological point of view, we find that using the mean optimised capacity across a number of weather years can generate a single optimised capacity distribution that performs in line with long-term expectations. However, the long-term robustness of the capacity distributions produced by minimising residual demand varies by technology, with wind capacity distributed more consistently than PV.

Our results show that when minimising residual demand under the idealised assumption of a copper-plate Europe and in the absence of storage:

- In the base case optimisation (Scenario 1), wind and PV can provide 82% of annual European electricity demand with a total installed capacity of 1144 GW. The optimum **capacity mix** for minimising residual demand is 74% wind and 26% solar PV, resulting in 8% surplus vRES generation. However, with a long-term vRES capacity credit of only 11%, at least 377 GW (equivalent to 33% total installed vRES capacity, or 75% peak demand) of dispatchable generation capacity would still be required to ensure long-term system adequacy.
- With the maximum peak and total residual demand in Scenario 1 being only 2% and 31% lower respectively than for the traditional capacity-factor-maximisation approach (Scenario 6), optimising the spatial distribution of vRES can play only a **minor role** in reducing residual demand, mainly by reducing curtailment. This is achieved by exploiting lower capacity factor PV sites in northern, western and eastern Europe, and limiting onshore wind capacity in countries surrounding the North Sea where it competes with offshore wind capacity.
- The greatest benefits of spatial vRES optimisation are found when water depth constraints are relaxed and offshore wind capacity can be built anywhere within the EEZ grid. In this case (Scenario 4), the maximum peak and total residual demand are 16% and 55% lower respectively than in the maximum capacity factor distribution (Scenario 6). Thus, **floating offshore wind farms** have the potential to deliver additional benefits to the European power system by granting access to sites with higher wind capacity factors and capacity credits.

- **penetration rate** affects the optimum spatial distribution of vRES, but has little effect on the optimum mix. For example, PV capacity is installed in southern Europe at low vRES penetration rates, but shifts north with increasing vRES penetration in order to avoid surplus summer generation. By contrast, the optimum regions for wind capacity remain the same as vRES penetration increases.
- Changes in future **demand** due to HPs and EVs effect the optimum distribution of vRES. For example, installing PV capacity at the eastern and western extremes of Europe can reduce the midday peak and increase PV generation in the morning and evening, which may be particularly beneficial for meeting future EV demand. Meanwhile, PV in the north of Europe can extend the window of PV generation in summer by taking advantage of longer days at more northerly longitudes.
- Expanding **offshore wind** capacity – especially in the North Sea – is a 'no regret' option due to its favourable correlation with demand, though correlated generation patterns with onshore wind farms in neighbouring countries at high vRES penetrations may lead to significant surplus generation.
- Alternative **PV panel orientations** can play a role in matching generation with demand. For example, installing west-facing PV panels in western Europe can extend generation later into the day to help cover the evening peak, while east-facing PV panels in eastern Europe can increase generation in the morning.

This study has highlighted several areas for further research:

- A comprehensive assessment of the potential benefits of spatially optimising vRES should be performed using a detailed PSM based on total system costs, considering transmission and distribution grid reinforcement, reserves and storage. However, it remains to be seen whether incorporating the spatial distribution of vRES directly in a PSM at the European scale is computationally feasible.
- Rather than being limited to a single PV orientation in a single optimisation run, the formulation should be modified to allow PV panels with different orientations to be installed in each grid cell (e.g. west-facing panels in western Europe, east-facing panels in eastern Europe) to see how the optimum PV orientation varies with location.

Footnotes to Chapter 2

[1] In 2014, Germany, Belgium and Switzerland operated 21 nuclear reactors between them, but plan to phase out nuclear power by 2022, 2025 and 2034 respectively (Strunz et al., 2014). France also aims to reduce its share of nuclear generation from nearly 74% to 50% by 2025 (Legifrance, 2016). Despite these contractions in nuclear capacity, only seven new reactors are currently planned or under construction in Europe.

[2] The terms load and demand are often used synonymously, however this study adopts the ENTSO-E definition of *load* as 'an end-use device or customer that receives power from the electric system' with *demand* defined as 'the measure of power that a load receives or requires' (UCTE, 2004).

[3] We use the term *allocation* to refer to those studies which exogenously assume or weight vRES capacities per region based on parameters such as capacity factor, vRES potential, land suitability or population. This is also the approach taken in most high-level power system modelling studies. We use the term o*ptimisation* to indicate studies which actually formulate the spatial distribution as an optimisation problem with an objective function (e.g. maximum capacity factor, minimum residual demand, minimum cost etc.)

[4] While current wind farms are limited to water depths of 40 m to 50 m (EWEA, 2013; Zountouridou et al., 2015), floating offshore wind turbines have the potential to be installed in much greater water depths. This technology is still in the early stages of development with the world's first pilot 30 MW floating offshore wind farm expected to become operational in 2017 (Statoil, 2015; Zountouridou et al., 2015).

[5] The UK is included despite the June 2016 decision to leave the EU because the UK and continental European power systems are likely to remain heavily integrated.

[6] While wind and solar PV are essentially only two generation technologies, we split them in order to better take into account their spatial constraints and technical differences. Ocean energy and run-of-river hydro can also be considered vRES, however, their contributions to the total installed capacity in most future high-RES scenarios are minor (see Table 1) and so have not been considered.

[7] Calculated as the standard deviation divided by the mean, also known as the relative standard deviation.

[8] This was a necessary simplification in our model in order to reduce the number of variables and make the problem solvable in a reasonable amount of time.

[9] As PV panels and wind turbines typically have a lifetime of 25 to 30 years, all currently existing capacity and new capacity installed before 2020 is likely to be decommissioned by 2050 anyway.

[10] At times of surplus generation, the electricity price in an energy-only market falls to zero.

[11] The coefficients of A_{eq} are either 0 or 1 if the constraint is applied to generation capacity, or full load operating hours (FLH) if the constraint is applied to electricity generation.

[12] ESRI, version 1.2.0, (http://www.esri.com/)

[13] Greater distances to shore usually result in deeper waters (Rodrigues et al., 2015), however there are several remote locations in Baltic the North Sea where the water is not so deep. One example is Dogger Bank where the offshore Teesside A & B wind farms are already planned, located 196 km and 165 km from shore respectively in water depths of up to 40 m (4C Offshore, 2016; Forewind, 2016). Thus, we believe this assumption to be justified.

[14] While expected maximum water depths for floating wind turbines range between 300 m and 900 m (ETI, 2015; Zountouridou et al., 2015) and water depths in the EEZ can exceed 5000 m, floating deep-water oil platforms are already moored at water depths of up to 2900 m (Shell, 2016). Thus, it is possible that with further development, floating wind turbines could also be moored at this or even greater depths.

[15] Distance in kilometres varies with latitude from 65 km in Spain (37°N) to 30 km in northern Norway (70°N).

[16] The accuracy and choice of weather dataset is a complex topic in itself and involves trade-offs between the required temporal and spatial resolution, geographical coverage, meteorological parameters and accuracy. A comprehensive treatment was not possible in this study, however the reader is referred to (Dee et al., 2011) for an explanation of the development and main limitations of ERA-I, and to (Boilley & Wald, 2015; Bojanowski et al., 2014; Mooney et al., 2011) for comparisons with other datasets.

[17] Based on the long term (1979-2015) mean wind speed at hub height

[18] Based on commercially available modules. For rooftop PV we use the Sunpower X21-345 (SunPower, 2014), and for utility PV, the TrinaSolar TSM-PD14 (TrinaSolar, 2016).

[19] These areas are more likely to be flat, accessible, and cause minimal shading for PV panels or turbulence for wind turbines. We exclude wetlands, forests, rocky or alpine areas as these are unlikely to be suitable for large-scale rollout of any technology for reasons of poor soil stability, steep/mountainous terrain or inaccessibility (Dai et al., 2016).

[20] To take into account shipping lanes, fisheries, military zones etc.

[21] This study reported 3889 TWh of base demand, 1924 TWh for hydrogen production, and 207 TWh for synthetic fuel production.

[22] We do not explicitly assume a level of grid losses in this study as the raw demand data from ENTSO-E as well as the HP and EV demand totals from (ECF, 2010b) include grid losses. Losses were on average 6.7% of total net electricity production (excluding own-use) for the EU28+NO from 2006-2015 (Eurostat, 2017c).

[23] A similar assumption was made in (ECF, 2010b).

[24] The model incorporates driving patterns for the six countries in Europe with the highest number of passenger vehicles (DE, UK, FR, IT, ES, PL), for each day of the week.

[25] Matlab R2015b, (www.mathworks.com)

[26] Locations with high capacity factors are generally considered preferable for vRES installations as these result in the lowest generation costs (Huber et al., 2014; Schaber et al., 2012)

[27] Attempting to optimise capacity for all 36 years simultaneously was not feasible with the computing power available.

[28] The share of demand covered by vRES, excluding any surplus/curtailed electricity

[29]In this study the terms northern, southern, western and eastern Europe are used in a general sense to describe geographic regions, not in a geopolitical sense referring to specific countries.

[30] This is likely due to afternoon sea breezes at coastal onshore wind sites. These are caused by cooler, denser air over water advecting towards less dense air over land in the evening that has been warmed during the day (Barthelmie et al., 1996).

[31] Incidentally, this confirms an assumption made by the IEA underpinning their calculation of capacity credit in (IEA, 2011).

[32] Net generation divided by total demand

[33] By comparison, Europe's current (2015) hydro storage capacity is approximately 180 TWh (including Switzerland and the Nordic countries, but excluding Turkey) (Mennel et al., 2015).

[34] Nearly 50% of Nordic PV capacity is in Finland

[35] In any case, it would be unwise to build vRES infrastructure to minimise peak residual capacity as, in reality, these peak hours would be ideal candidates for demand response technologies such as load shedding or load shifting.

[36] Distribution and transmission are particularly relevant for the spatial distribution of vRES as, with capacity spread across Europe and often far from load centres, the amount of grid reinforcement required is likely to be significant (DNV GL, 2014).

[37] To our best knowledge no power system simulation model currently available allows a high-resolution spatial distribution of vRES to be easily incorporated, which provided motivation for this study.

[38] Based on ENTSO-E data for the EU28 + NO + CH, the gross penetration of vRES in 2015 was approximately 13% on an energy basis (ENTSO-E, 2017b).

[39] The performance of HPs falls at lower temperatures, thus electricity consumption would be higher at these times and could lead to a more 'peaky' demand profile.

[40] EU cooling demand in 2010 amounted to 220 TWh (8% of the space heating demand). Space cooling demand is expected to rise to 305 TWh (+38%) in 2020 and 379 TWh in 2030 as the climate warms (Kemna, 2014).

[41] Another study of 17 geographically dispersed wind sites in Ontario showed that aggregated wind power output variability was 60–70% lower compared to the output from one site for both 10-min and hourly data (AWS TrueWind LLC, 2005).

[42] For example higher PV cell efficiencies, larger diameter or taller wind turbines.

[43] IRENA note that the cost of PV fell by 80% from 2009 to 2015, and forecast a further 59% reduction by 2025 (IRENA, 2016).

[44] X-7: 100% RES scenario

[45] X-5: Large-scale RES scenario

[46] Average gross hydro generation (including pumped storage generation) from 1990-2014 was 462 TWh y^{-1} with a standard deviation of 38 TWh y^{-1} (Eurostat, 2017c). It is not clear how much of this is from run of river hydro, thus for these rough estimates we assume full dispatchability.

[47] The total of installed vRES capacity, hydro capacity and additional dispatchable backup capacity required to meet (long-term) peak residual demand

How might intraday and balancing markets develop in a future highly renewable power system?

3

William Zappa

Thomas Walther

Machteld van den Broek

Submitted to Applied Energy (2020)

Abstract

More insights are needed on how large-scale deployment of variable renewable energy sources (vRES) such as solar and wind energy affects intraday and balancing markets. In order to model these markets at different timeframes, it is necessary to have forecasts of load and vRES at different time horizons before real time. In this study, we develop and demonstrate a method for synthesising forecasts which have a strong correlation with the real-time series, but also an error distribution comparable with real-world forecasts. The method incorporates a generalised autoregressive conditional heteroscedasticity (AR-GARCH) model to account for the daily volatility observed in historical forecast errors, and a dependence on real-time generation (or load) level to account for hourly volatility. We demonstrate how this method can be used by performing simulations of a future European power system in which the penetration of vRES rises from 15% in 2017 to 50% in 2040. Using our AR-GARCH method to synthesise day-ahead forecasts, and intraday forecasts based on persistence, we explore how higher vRES forecast errors could affect day-ahead, intraday and balancing market volumes, and to what extent these errors could be resolved by trading between vRES generators in the case of no cross-border trading, and a copper-plate Europe. Other factors which contribute to intraday trading and imbalance volumes such as forced outages, strategic deviations and schedule leaps are not considered. Based on our simulations, we find that potential intraday market volumes increase by 60 TWh y^{-1} (+160%) between 2017 and 2040 as a result of additional day-ahead forecast errors. Intraday trading within countries and between countries could allow between 40% (without cross-border trading) and 75% (copper plate) of day-ahead forecast errors to be resolved by vRES, reducing the need for dispatchable energy. In the absence of intraday trading, these errors would need to be resolved by transmission system operators on balancing markets by procuring additional reserve capacity, highlighting the role liquid intraday markets can play in supporting the integration of vRES in Europe. Regarding balancing markets, we find that full implementation of imbalance netting and a common Europe-wide reserve could reduce balancing energy and capacity requirements for vRES integration by 19% and 32% respectively in 2040 compared with country-specific reserves and no imbalance netting.

Nomenclature

Latin letters

a	Order of the autoregressive component of the daily absolute deviation series
$\mathcal{D}$	Probability density function of an unspecified distribution
F	Forecast (MW)
I	Imbalance (MWh)
N	Normalising factor (MW)
$\mathcal{N}$	Probability density function of a normal distribution
p	Order of the autoregressive GARCH component
P	Percentile
q	Order of the moving average GARCH component
T	Intraday trade (MWh)
Y	Real-time value (MW)
x	Random variable
z	Residuals of AR-GARCH model

Greek letters

α	Moving average GARCH parameter
β	Autoregressive GARCH parameter
γ	Skewness
δ	Total daily absolute error
ε	Forecast error (MW)
ϵ	AR-GARCH model residual
κ	Kurtosis
μ	Mean
ξ	Generation or load-based error
ϕ	AR model parameter
σ	Standard deviation
τ	Length of market period (h)
ψ	Fixed GARCH parameter

Accents and superscripts

$\hat{}$	Normalised
$'$	Synthetic
$\bar{}$	With daily volatility removed
DA	Day ahead
RT	Real time
ID	Intraday

Indices and sets

$c \in \mathcal{C}$	country, includes the set of all EU28 plus Norway and Switzerland
$d \in \mathfrak{D}$	days per year, running from 1 to 365
$g \in \mathcal{G}$	generation technology or load, including onshore wind, offshore wind, solar PV and load
$h \in \mathcal{H}$	hours per day, running from 1 to 24
$m \in \mathcal{M}$	months per year, running from 1 to 12
$t \in \mathcal{T}$	time/market periods per year, running from 1 to $\mathcal{T}$
z	pertaining to the standardised residuals of the AR-GARCH model

3.1 Introduction

The European electricity sector will need to fully decarbonise or even turn net-negative by 2050 if the European Union (EU) is to fulfil its role in international efforts to limit global warming to well below 2 °C (EC, 2011c, 2018a; UNFCCC, 2017b). Thanks to their falling costs and government policies supporting their deployment, variable renewable energy sources (vRES) such as solar photovoltaic (PV) and wind energy are likely to play a significant role in this decarbonisation. Electricity supply and demand must always be kept in balance from one moment to another and, due to their intermittent generation, vRES make balancing electricity demand and supply more difficult (Huber et al., 2014). In Europe's largely liberalised and self-scheduling power systems, the balance between supply and demand is primarily maintained using electricity markets operating at different time scales.

In 2018, around half of the electricity generated in Europe was traded on day-ahead markets via power exchanges (Figure 3-1), with the remainder traded either bilaterally over the counter (i.e. forwards), or as standardised futures products on exchanges[1]. On day-ahead markets, price-volume bids from electricity suppliers (e.g. power plants) and purchasers (e.g. retailers, large industrial consumers) are pooled for each trading period. In this way, forecast supply and demand are matched, and the electricity price during each period is determined by the marginal bid. Most day-ahead markets close at midday the day before delivery (D-1) to allow the scheduling of large thermal power plants (Figure 3-2). Intraday markets, which open shortly after day-ahead markets close, provide an opportunity for balance responsible parties (BRPs) to correct for shifts in their day-ahead nominations due to unexpected outages, or revised demand and generation forecasts (KU Leuven Energy Institute, 2015). This is especially relevant for vRES, as forecast accuracy improves the closer the forecast is made to real time (Foley et al., 2012; J. Zhang et al., 2015). However, despite subsequent corrections on intraday markets, instantaneous imbalances in supply and demand still arise in real time due to a combination of (i) *stochastic* factors such as load and vRES forecast errors, unplanned outages in generators or transmission lines; (ii) *deterministic* factors, such as discrepancies between the duration of different market trading periods (so-called *schedule leaps*) and the discretisation of continuous time into discrete trading periods; and (iii) deliberate *strategic* deviations by BRPs to take advantage of differences in imbalance prices (Brijs et al., 2017; Hirth & Ziegenhagen, 2015; Koch & Hirth, 2019).

Balancing electricity supply and demand is performed by transmission system operators (TSOs) using balancing[2] markets by first estimating how much reserve capacity they need, contracting this capacity from balancing service providers (BSPs), and dispatching balancing energy to deal with imbalances during each imbalance settlement period (ISP) (ENTSO-E, 2018a). Two main types of reserves are procured across Europe: (i) Frequency Containment Reserve (FCR), which is automatically activated within 30 seconds in response to a sudden

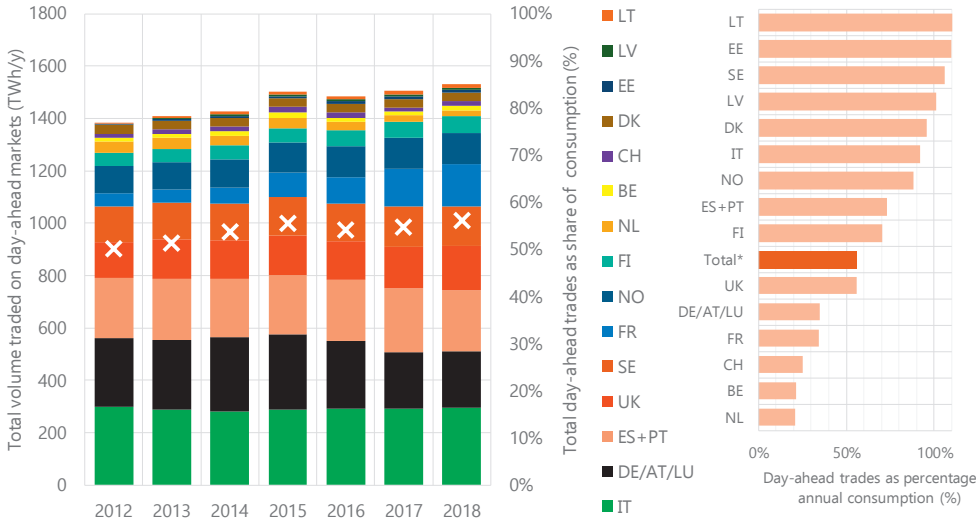

Figure 3-1 | On the left, the development of day-ahead market trading volumes (bars) in selected European countries over time, and as a share of total consumption (X). On the right, the day-ahead market trades in 2018 expressed as a percentage of annual consumption in each country. The total is shown only for the selected countries. Own figure based on day-ahead trade data from EPEX, Nord Pool, OMIE and GME annual reports (EPEX, 2019b; GME, 2019b; Nord Pool, 2019; Omie, 2019b), and electricity consumption data from ENTSO-E statistical reports 2012-2018 (ENTSO-E, 2019c).

major disturbance event (e.g. outage of large power plant or transmission line); and (ii) Frequency Restoration Reserve (FRR), which can be either automatically activated (aFRR) or manually activated (mFRR) within 15 minutes. FRR is used both to free up FCR so that it can be used again, and to mitigate load and vRES forecast errors. A third reserve type known as Replacement Reserve (RR) is used by some countries to free up FRR capacity again. Upward reserves are activated when there is a deficit of energy (i.e. the system is *short*), while downward reserves are activated when there is a surplus of energy (i.e. the system is *long*)[3]. The volume of reserves required by TSOs depends on the magnitude and frequency of the imbalances, and the desired security level (Hirth & Ziegenhagen, 2015). While some recent studies have failed to show strong links between increasing vRES penetration and balancing reserve requirements in Europe (e.g. (Brinkel, 2018; Hirth & Ziegenhagen, 2015)), large-scale vRES deployment is likely to lead to higher reserve requirements in the long term (Borne et al., 2018; Ortner & Totschnig, 2019). With scenarios suggesting that a highly decarbonised EU power system could rely of vRES to supply some 80% of electricity by 2050[4], intraday and balancing markets are receiving increasing attention in the academic literature (Child et al., 2019; EC, 2011d; ENTSO-E & ENTSO-G, 2018; Plessmann & Blechinger, 2017).

Several ex-post empirical studies have examined the impact of increasing vRES penetration on EU balancing markets. A notable example is Hirth & Ziegenhagen (Hirth & Ziegenhagen, 2015), who find that despite German vRES penetration doubling from 7% in 2008 to 15%

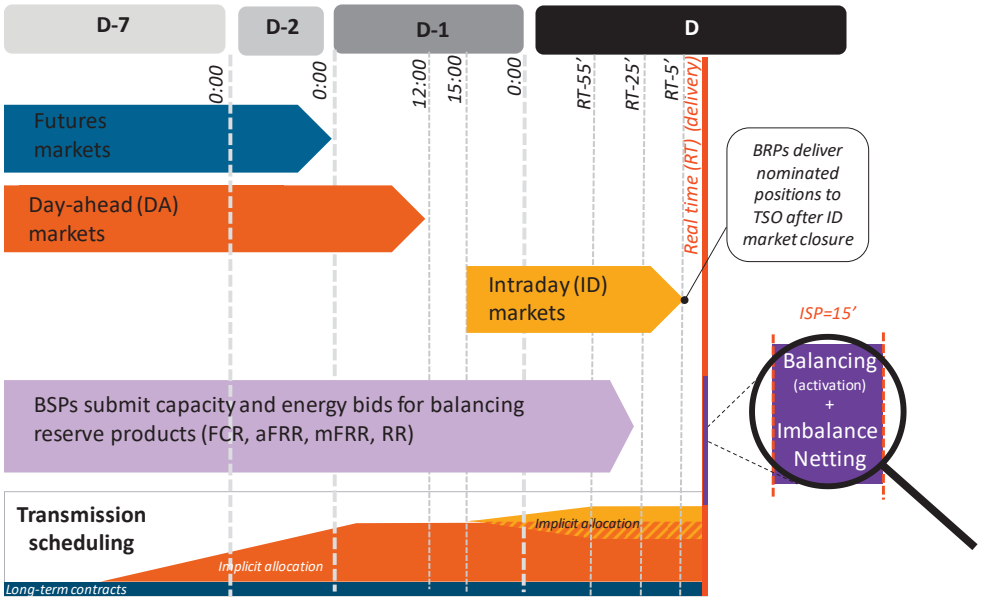

Figure 3-2 | Overview of market timelines, reserve procurement and transmission scheduling processes. As market designs and rules vary across Europe, this figure is only for illustrative purposes. Day-ahead (DA) order books open up to 45 days before delivery. Intraday (ID) markets typically open shortly after day-ahead market closure, and close between one hour and up to five minutes before delivery in real time (RT), depending on the country and market. Balancing markets vary widely between countries and between products. In some countries, BSPs must first bid to supply reserve capacity up to one week in advance. Bids for supplying balancing energy are typically made closer to delivery, but can also be made jointly with capacity. Own figure based on various sources ((ENTSO-E, 2018a; Tennet, 2018)).

in 2015, TSOs were able to reduce the amount of contracted balancing reserves by 15% over the same period. Ocker & Ehrhart (Ocker & Ehrhart, 2017) suggest this was primarily achieved thanks to more intraday trading, and the introduction of imbalance netting, which allows positive imbalances in one control area to be cancelled out against negative imbalances in a neighbouring control area using cross-border transmission, thereby reducing the need for counter activation of reserves in both areas (Doorman & van Der Veen, 2013). Koch & Hirth (Koch & Hirth, 2019) also find that increasing intraday trading has played an important role in reducing German balancing requirements. Since (Hirth & Ziegenhagen, 2015) was published, German intraday trading volumes have continued to increase (Figure 3-3), while the volume of contracted reserves has continued to decrease (Figure 3-4), supporting the findings of (Ocker & Ehrhart, 2017) and (Koch & Hirth, 2019). Gianfreda et al. (Gianfreda et al., 2018) find that balancing requirements have not increased in Italy despite vRES penetration increasing from less than 1% in 2005 to 15% in 2015, mirroring the findings of Hirth & Ziegenhagen for Germany.

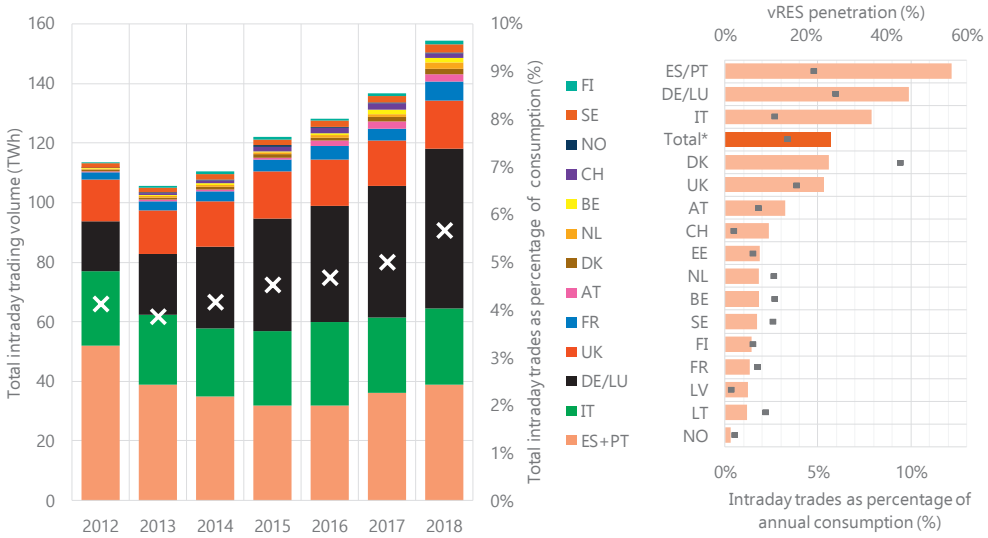

Figure 3-3 | On the left, the development of intraday market trading volumes (bars) in selected European countries over time, and as a share of total consumption (X). On the right, the intraday market trades in 2018 expressed as a percentage of annual consumption in each country (bars), together with the 2018 vRES penetration (•). The total is shown only for the selected countries. Own figure based on intraday data from EPEX, Nord Pool, OMIE, and GME annual reports and trading platforms (EPEX, 2019b; GME, 2019a; Nord Pool, 2019; Omie, 2019a), together with generation and consumption data from ENTSO-E statistical reports 2012-2018 (ENTSO-E, 2019c).

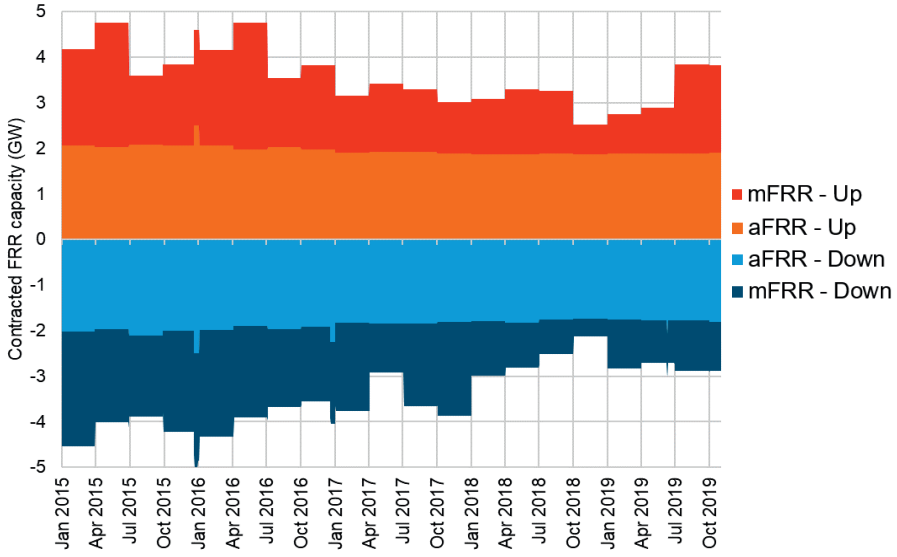

Figure 3-4 | Volume of contracted mFRR and aFRR in Germany over time, averaged per quarter (ENTSO-E, 2018b).

Joos & Staffell (2018) compare balancing market developments in Germany and the UK, and also find no significant increase in balancing requirements in the UK between 2010 and 2016, despite vRES penetration rising from 3% to 14% over the same period.

Aside from ex-post analysis of historical data, some studies use power system modelling to explore how future balancing requirements could increase with rising vRES penetration in individual countries (e.g. Croatia (Vasilj et al., 2016), Germany (Jost et al., 2015; Roos & Bolkesjø, 2018)), or larger regions. For example, Miettinen & Holttinen look at the impact of wind forecast errors on balancing needs in a case study of the Nordic power system up to 30% wind penetration (Miettinen & Holttinen, 2019). Aigner et al. find that a tripling of wind capacity in Northern Europe[5] between 2010 and 2020 would increase gross imbalances by 90% (Aigner et al., 2012). Despite this increase, reserve activation is only 60%–70% of the imbalances thanks to imbalance netting within the Nordic and continental Europe systems, falling to 40%–50% in the case of fully integrated Nordic and continental Europe reserve markets. At the European level, Ortner & Totschnig consider potential developments in European intraday and balancing markets in the year 2030 with a modest vRES penetration of 27%, finding that balancing market volumes are likely to remain only a few percentage points of day-ahead market volumes (Ortner & Totschnig, 2019). Dallinger et al. also analyse EU balancing markets in 2030 under different market design assumptions, finding that shortening the duration of balancing products (e.g. peak/off-peak to 4-hourly), bringing balancing procurement closer to real time (e.g. weekly to daily procurement), allowing non-symmetric procurement of up- and downward reserve capacity, implementing full imbalance netting, and common reserve procurement between countries would lead to significant cost savings (Dallinger et al., 2018).

Analysts wishing to model future power systems can use historical time series, or generate synthetic time series for load and weather parameters using a variety of methods such as autoregressive integrated moving average (ARIMA)[6] models (e.g. (J. Chen & Rabiti, 2017; Greve et al., 2014) for wind), or generalised autoregressive conditional heteroskedastic (GARCH) models, originally proposed by Engle (Engle, 1982) (and developed further by Bollerslev (Bollerslev, 1986)) for economic applications. For example, Lojowska et al. (Lojowska et al., 2010) use an ARMA-GARCH model to model the volatility of wind speed time series. A single time series (historical or synthetic) can be used to model a market in a single timeframe (e.g. day-ahead or real-time). However, in order to model linked markets at different timeframes (e.g. intraday and balancing markets), it is necessary to have not just a single time series, but also forecasts of this series at different time horizons before real time. Synthesising these forecasts poses a challenge, as the forecasts should have a strong correlation with the real-time series, but also an error distribution comparable with real-world forecasts. The simplest approach is a persistence forecast, which assumes that the value of a variable in one time step is the same as in the previous time step (3TIER, 2010). Whilst persistence may deliver acceptable results for short time horizons (e.g. up to 1 hour), it is unsuitable for day-ahead

forecasting. Others use ARIMA based methods such as Weber et al., who use an ARMA model to represent larger wind speed forecast errors with longer forecast horizon in the Wilmar model (Weber et al., 2009). De Mello et al. (de Mello et al., 2011) use an optimisation routine to fit AR(1) models for wind speed and load forecast errors to match statistical behaviour of historical forecast errors to synthesise real-time, day-ahead and hour-ahead forecasts. Meibom et al. (Meibom et al., 2011) generate wind speed (and load) forecast errors using an ARMA(1,1) model and apply them to historical time series. Boone (Boone, 2005) model wind speed forecast errors with an ARMA(1,1) model. Some combine ARIMA with other approaches, like Naimo (Naimo, 2014), who synthesises wind speeds using a Weibull distribution, and forecast errors using an ARMA model. Despite the existing literature, we find that many proposed methods for generating synthetic forecasts are for the underlying weather parameters (e.g. wind speed, solar radiation), which require further processing by modellers to create generation profiles (i.e. MW) and are not convenient for ready implementation in power system models. Furthermore, previous simulation studies on intraday and balancing markets have provided few details about the methods used to generate synthetic forecasts, making it difficult to replicate their approaches, and necessitating significant rework.

In this study, we present a novel method to synthesise time series for day-ahead forecasts for load and vRES generation based on an AR-GARCH model and give a step-by-step example of how to implement it. We then apply our method in simulations of a future scenario of the European power system in which the vRES penetration rises to 50% in 2040, to explore how large-scale vRES deployment could affect day-ahead, intraday and balancing markets. We provide an implementation of our method in Python so that other researchers and analysts can apply it to generate their own synthetic load, wind and PV forecasts.

This study is structured as follows. In Section 3.2, we outline our three-part method which includes (i) an analysis of current day-ahead forecast performance, (ii) an explanation of our approach for synthesising day-ahead forecasts, and (iii) a description of the market simulations. In Section 3.3, we present our results including a step-by-step example of how to apply our day-ahead forecast method, and the findings from the market simulations. In Section 3.4, we discuss the limitations of our method, and round off our study with some concluding remarks in Section 3.5. Further details on the method and results from this chapter are provided in Appendix B.

3.2 Method

Our study is divided into three parts (Figure 3-5). In Part A, we first analyse and determine the accuracy of current day-ahead forecasts for electricity demand and vRES generation based on historical data reported by TSOs. In Part B, we present our method to synthesise time series of normalised day-ahead forecast errors. In Part C, we demonstrate how this method can be used by applying it to the case of a future highly renewable European power system in 2040.

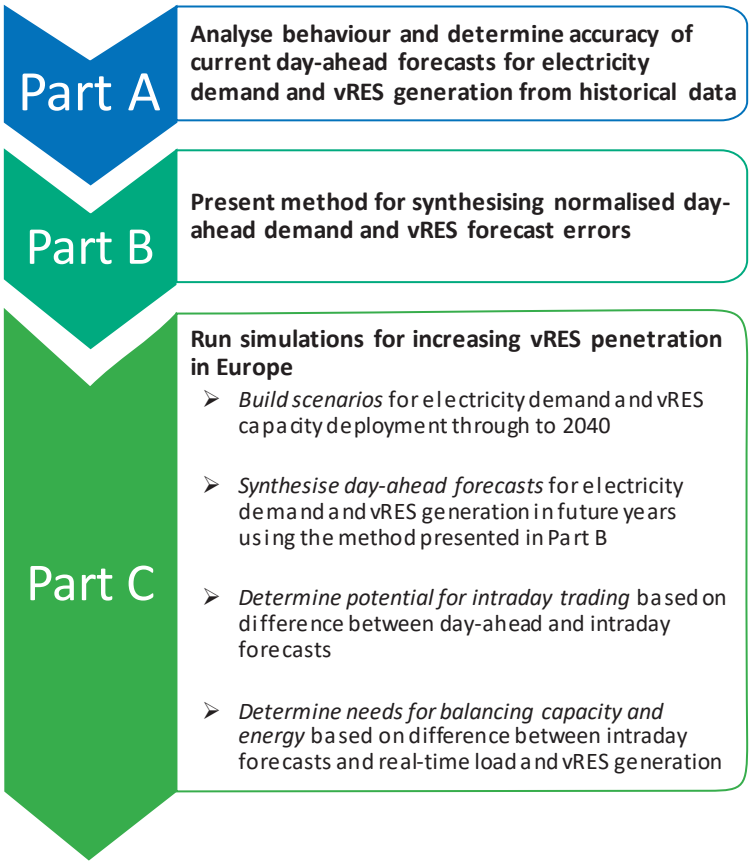

Figure 3-5 | Overview of the approach followed in this study.

3.2.1 Part A – Analyse behaviour and determine performance of current day-ahead forecasts

BRPs use their own forecasting methods to estimate their future production and demand, which inform their day-ahead bids, intraday trades, and ultimately determine their contribution to system imbalance. However, these data from individual BRPs are generally not publicly available, making it difficult to assess their forecast performance. Instead, we use country-level data on day-ahead forecasts and real-time vRES generation and load available from the European Network of Transmission System Operators for Electricity (ENTSO-E) (ENTSO-E, 2018b). We analyse the day-ahead forecasts for eight EU countries with the highest absolute installed vRES capacity (Belgium (BE), Germany (DE), Denmark (DK), Spain (ES), France (FR), Italy (IT), the Netherlands (NL) and the United Kingdom (UK)), assuming that TSOs in these countries are likely to have developed better forecasting methods. The temporal resolution of these data is mostly hourly, though some are 15 minutes, which are upscaled to

hourly for consistency. Forecasts are analysed for the years 2017 and 2018 to see the reliability of the forecasts across multiple years. Before any analysis or model fitting is performed, the raw time series are first checked for clearly erroneous or missing data, which are replaced by data from a nearby time period (i.e. the following hour or day).

Several metrics are used to quantify the behaviour and accuracy of the historical forecasts including the root mean squared error (RMSE) (Eq. (3-1)), the mean bias error (MBE) (Eq. (3-2)), and the mean arctangent absolute percentage error (MAAPE) (Eq. (3-3))[7]. In this study, we adopt a sign convention such that a negative forecast error results in a net deficit of energy (i.e. a short position) to the system, while a positive value results in a net surplus (i.e. a long position)[8]. Thus, when calculating the absolute forecast errors (ε_t) from the day-ahead forecast (F_t) and real-time values (Y_t) in each time step t, for all available periods T, the signs are reversed for load and vRES generation technologies (Eq. (3-4)). Note that the RMSE and MBE are normalised based on a normalisation factor, N, to allow a comparison between the errors for different parameters, for different years, and for different countries. Load errors are normalised to the real-time peak annual load (MW), while vRES generation errors are normalised to the installed capacity (MW).

$$RMSE = \sqrt{\frac{1}{T}\sum_{t=1}^{T}(\varepsilon_t)^2} \Big/ N \tag{3-1}$$

$$MBE = \frac{1}{T}\sum_{t=1}^{T}(\varepsilon_t) \Big/ N \tag{3-2}$$

$$MAAPE = \frac{1}{T}\sum_{t=1}^{T} \arctan\left(\frac{\varepsilon_t}{Y_t}\right) \tag{3-3}$$

$$\text{where } \varepsilon_t = \begin{cases} Y_t - F_t & for\ vRES\ generation \\ F_t - Y_t & for\ load \end{cases} \tag{3-4}$$

On the basis of the calculated metrics, the four best country forecast time series are used to fit models to generate normalised day-ahead forecast errors in Part B (section 3.2.2).

3.2.2 Part B – Method for synthesising normalised day-ahead demand and vRES forecast errors

Based on existing literature and our analysis of the normalised hourly day-ahead forecast errors for load and vRES generation, day-ahead errors typically exhibit certain properties. For example, as they are made one day ahead and are not updated, errors from hourly consecutive forecasts are often autocorrelated, and can exhibit diurnal patterns (Olauson et al., 2016). Moreover, forecast errors can display significant volatility from one day to the next, and hourly

errors distributions are often skewed and heavy-tailed rather than normal (Hodge et al., 2012). Also, forecast errors can depend on the generation (or load) level, with larger errors typically observed during periods with higher generation (or load) (see section 3.3.1)[9].

Our approach accounts for these properties by modelling hourly forecast errors as a function of the real-time generation (or load) level, with forecast errors also exhibiting daily volatility. This daily volatility is modelled as a generalized autoregressive conditional heteroscedasticity (GARCH) process to account for dependence and non-normality in the variance structure of the time series, with an autoregressive (AR) component to account for autocorrelation in the error volatility of consecutive days (Bollerslev, 1986; Engle, 1982). Our method for synthesising day-ahead forecast errors has nine main steps (Figure 3-6).

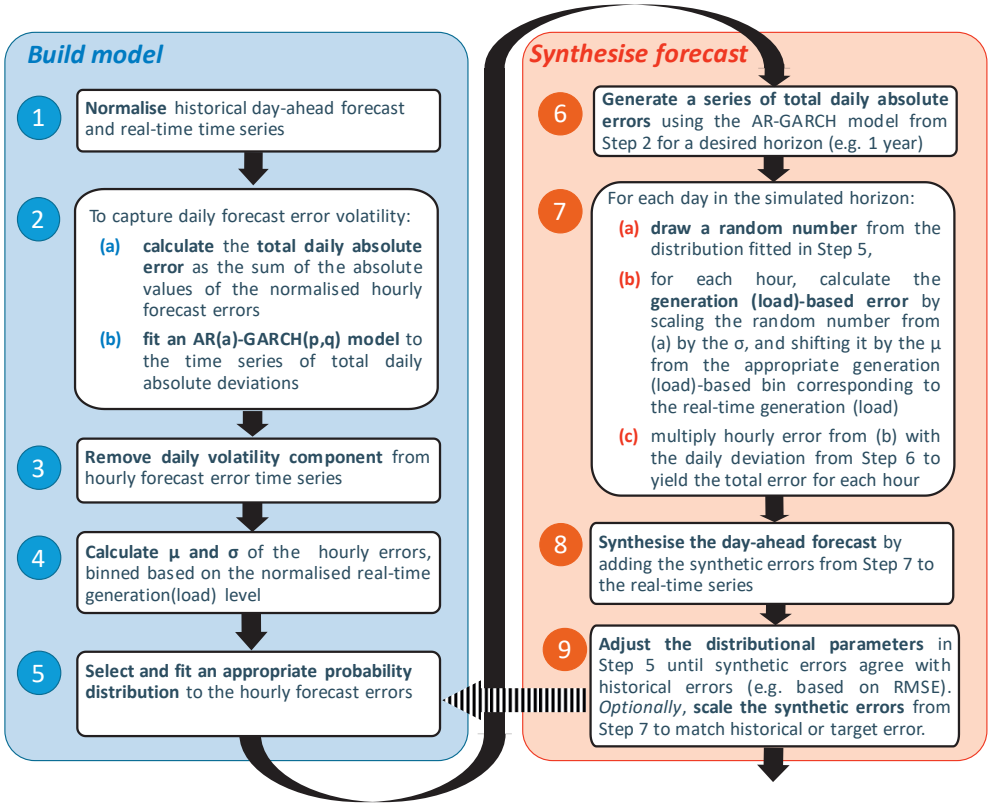

Figure 3-6 | Overview of the proposed method for synthesising normalised day-ahead forecasts

First, Steps 1 to 5 are applied to the historical data to fit the models for each variable (i.e. load, PV, onshore wind, offshore wind).

Step 1. Normalise the historical raw day-ahead forecast and real-time series for vRES generation (or load) by dividing by the installed capacity (or peak load) (Eq. (3-5)).

Using these series, calculate the normalised hourly forecast error $\hat{\varepsilon}_{d,h}$ for each hour h, for each day d (Eq. (3-6))[10].

$$\hat{Y}_t = Y_t/N \qquad \hat{F}_t = F_t/N \tag{3-5}$$

$$\hat{\varepsilon}_{d,h} = \hat{\varepsilon}_t = \begin{cases} \hat{Y}_t - \hat{F}_t & for\ vRES\ generation \\ \hat{F}_t - \hat{Y}_t & for\ load \end{cases} \tag{3-6}$$

Step 2. To capture the volatility of daily forecast errors in the historical data:

a) For each day of the year d (assuming one year of historical data), the total absolute daily error δ_d, is calculated as the sum of the absolute values of the normalised hourly forecast errors for the 24 hours in that day (Eq. (3-7)),

$$\delta_d = \sum_{h=1}^{h=24} \left|\hat{\varepsilon}_{d,h}\right| \qquad \forall d \in \{1 \dots 365\} \tag{3-7}$$

b) Fit an AR(a)-GARCH(p, q) model to the resulting daily time series δ_d, based on an analysis of its autocorrelation function (ACF) and partial autocorrelation functions (PACF)[11]. In this model, δ_d is an autoregressive process with mean μ and residual ϵ_d (Eq. (3-8)), the conditional variance of which, σ_d^2, is a GARCH model (Eq. (3-9) (3-10)) (Lojowska et al., 2010). The standardized residuals z_d are assumed to be independent and identically distributed ($i.i.d.$) with a probability density function $\mathcal{D}$, assumed to follow a Skewed Student t-distribution with zero mean, variance of 1, skewness parameter γ_z and kurtosis parameter κ_z[12]. The AR model parameters ($\mu, \phi_1 \dots \phi_a$) and GARCH parameters ($\psi, \alpha_1 \dots \alpha_p, \beta_1 \dots \beta_q$) are fit using the quasi maximum likelihood method.

$$\delta_d = \mu + \sum_{i=1}^{a} \phi_i \delta_{d-i} + \epsilon_d \tag{3-8}$$

$$\epsilon_d = z_d \sigma_d \quad , \quad z_d \sim \mathcal{D}(0,1,\gamma_z,\kappa_z), i.i.d. \tag{3-9}$$

$$\sigma_d^2 = \psi + \sum_{i=1}^{p} \alpha_i \epsilon_{d-1}^2 + \sum_{j=1}^{q} \beta_j \sigma_{d-j}^2 \tag{3-10}$$

Step 3. Remove the effect of daily error volatility from the hourly normalised forecast errors $\hat{\varepsilon}_{d,h}$ to yield a new series of hourly errors $\overline{\hat{\varepsilon}_{d,h}}$ which does not include the daily volatility. This is done by dividing $\hat{\varepsilon}_{d,h}$ by the hourly conditional volatility $\sigma_{d,h}$ of the

series of total daily deviations (Eq. (3-11)), which itself is calculated from the daily conditional volatility σ_d, assuming a uniform forecast error volatility for each day (Eq. (3-12)).

$$\overline{\hat{\varepsilon}_{d,h}} = \hat{\varepsilon}_{d,h}/\sigma_{d,h} \quad (3\text{-}11)$$

$$\sigma_{d,h} = \frac{\sigma_d}{24} \quad \forall h \in \{1 \dots 24\}, \forall d \in \{1 \dots 365\} \quad (3\text{-}12)$$

Step 4. To capture the dependence of the resulting hourly errors on the real-time generation (or load) level, divide the $\overline{\hat{\varepsilon}_{d,h}}$ series into k bins based on the normalised real-time generation (or load) levels, and calculate the mean μ_k and standard deviation σ_k of the hourly errors in each bin[13].

Step 5. To adjust for the overall common daily error component which is not encapsulated by the generation (or load) level bins, identify an appropriate probability distribution for the hourly forecast errors $\overline{\hat{\varepsilon}_{d,h}}$ (e.g. Normal, Laplace, t), and fit the parameters required to describe this distribution[14].

With all the required model parameters now fitted, Steps 6 to 9 are used to synthesise day-ahead forecasts:

Step 6. Generate a new series of total daily absolute errors, δ'_d, using the fitted AR(a)-GARCH(p, q) model developed in Step 2 for the desired horizon (e.g. one year),

Step 7. For each day d in the horizon:

a) generate a random number, x_d, from the distribution fitted in Step 5,

b) for each hour of the day, h, calculate the raw generation (or load)-based error $\xi'_{d,h}$ by taking the μ_k and σ_k values from the bin corresponding to the real-time generation (or load) in that hour (from Step 4), scaling the random number x_d by σ_k,and shifting it by μ_k (Eq. (3-13)).

$$\xi'_{d,h} = \mu_k + x_d \cdot \sigma_k \quad (3\text{-}13)$$

c) multiply the raw generation (load)-based hourly error from (b) with the simulated total daily errors from Step 6, δ'_d, to yield the total synthetic error for each hour, $\hat{\varepsilon}'_{d,h}$ (Eq. (3-14)).

$$\hat{\varepsilon}'_{d,h} = \delta'_d \xi'_{d,h} = \hat{\varepsilon}'_t \quad (3\text{-}14)$$

Step 8. The final synthetic forecast series $\widehat{F}'_t$ is found by simply adding (or subtracting) the synthetic error from Step 7 to the real-time series $\hat{Y}_t$ (Eq. (3-15)).

$$\widehat{F}'_t = \begin{cases} \hat{Y}_t - \hat{\varepsilon}'_t & for\ vRES\ generation \\ \hat{Y}_t + \hat{\varepsilon}'_t & for\ load \end{cases} \quad (3\text{-}15)$$

Step 9. Calculate a forecast error metric (e.g. RMSE) for the synthetic forecast from Step 8 and compare this with the same metric for the historical forecast. If the difference is unacceptably large, the parameters (especially the scale parameter) of the fitted distribution in Step 5 can be adjusted and a new forecast synthesised, until the error metric matches to an acceptable level. Optionally, the synthetic errors generated from Step 7 can also be scaled up or down to ensure synthetic forecast errors exactly match historical values. Assuming the comparison is based on the RMSE metric, this is done by scaling each synthetic error by the ratio between the target RMSE ($RMSE_{target}$) and the RMSE of the synthetic errors ($RMSE'$) (Eq. (3-16)).

$$\hat{\varepsilon}'_{t,scaled} = \hat{\varepsilon}'_t \left(\frac{RMSE_{target}}{RMSE'} \right) \quad (3\text{-}16)$$

3.2.3 Part C - Simulations for a future highly renewable Europe

In Part C, we demonstrate our method outlined in Part B by performing simulations of European day-ahead, intraday and balancing markets for a future scenario in which the penetration of vRES increases from 15% in 2017 up to 50% by 2040. With these simulations, we explore how day-ahead, intraday and balancing market volumes may grow over time, to what extent load and vRES forecast errors can be smoothed out both within countries and across Europe via intraday trading and imbalance netting, and how much residual demand must be supplied by dispatchable technologies.

An overview of the simulation approach is shown in Figure 3-7. First, we build one scenario for electricity demand and vRES capacity deployment in Europe for the years to 2017 to 2040, based on three scenarios from ENTSO-E's Ten Year Network Development Plan (TYNDP) 2018 (ENTSO-E & ENTSO-G, 2018) (Section 3.2.3.1). The geographical scope includes the EU28 countries, Norway and Switzerland. After collecting historical vRES generation profiles to represent real-time generation in future years, we synthesise day-ahead forecasts of these real-time profiles using our method outlined in Part B (Section 3.2.2). Intraday forecasts are generated based on persistence. Following the approach used by Ortner & Totschnig (Ortner

& Totschnig, 2019), we determine the potential for intraday trading based on the difference between the day-ahead and intraday forecasts. Any deviations remaining between the intraday forecasts and real-time values must then be resolved on balancing markets (section 3.2.3.3). Simulations are run for 24 years from 2017 until 2040, with both electricity demand and the installed capacity of vRES rising over time in accordance with the TYNDP 2018 scenarios. For each year from 2017 to 2040, we simulate the day-ahead, intraday and balancing markets for 32 historical weather years to assess how interannual weather variability impacts market volumes and reserve capacity requirements.

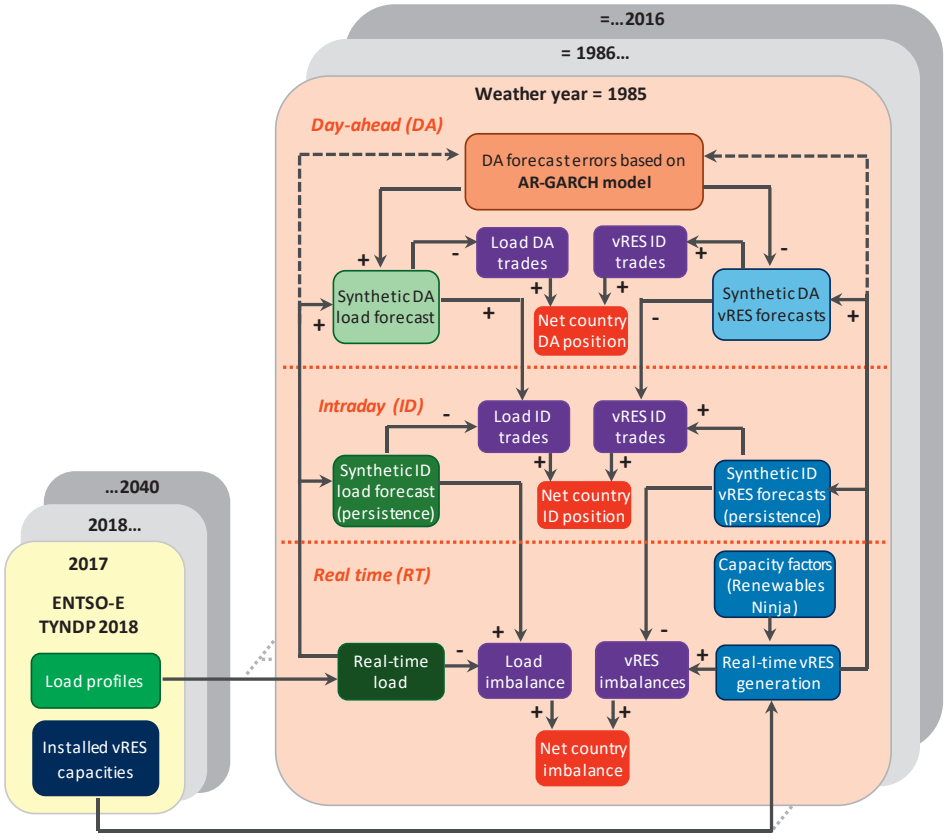

Figure 3-7 | Schematic overview of the simulation procedure per country. For each year from 2017 to 2040, simulations of day-ahead (DA), intraday (ID) trades and balancing volumes are performed using 32 weather years of historical weather data to generate probability density distributions of forecast errors, trade and imbalance volumes. The real-time load and vRES generation are used to calculate the day-ahead forecast errors with the AR-GARCH model. The + and – symbols indicate the sign conventions used in calculating ID trades and imbalances. Potential cross-border trades and imbalance netting are determined based on net country market positions, once all trades and imbalances within each country are resolved.

3.2.3.1 Build future load and vRES capacity scenarios

The scenario assumptions for European vRES deployment and load until 2040 are based on the most ambitious vRES deployment scenarios from ENTSO-E's TYNDP 2018 (ENTSO-E, 2018f)[15]. Starting from 96 GW of solar PV, 148 GW of onshore wind, and 15 GW of offshore wind capacity in 2017 (EurObserv'ER, 2018, 2019), installed capacities in 2040 reach nearly 600 GW, 360 GW and 155 GW respectively, representing a three-fold increase in total vRES capacity (Figure 3-8). Based on these scenarios, average vRES deployment rates are 21 GW y^{-1} between 2017 and 2025, 55 GW y^{-1} between 2025 and 2030, and 40 GW y^{-1} between 2030 and 2040. Starting from a total electricity demand of 3125 TWh in 2017, total demand increases 17% to approximately 3660 TWh in 2040, based on the same TYNDP scenarios.

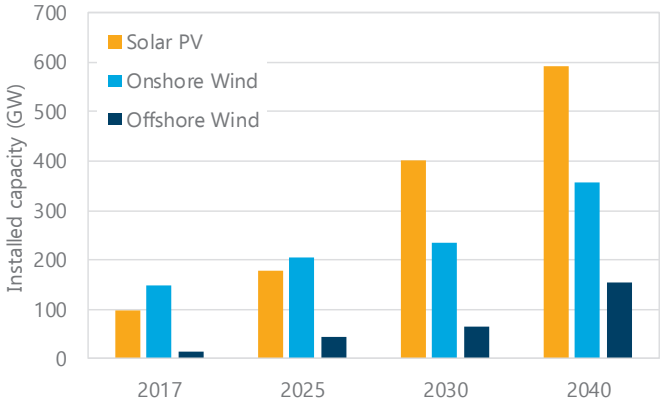

Figure 3-8 | Assumed deployment of vRES capacity in the study region (EU28 plus Norway and Switzerland), based on the ENTSO-E TYNDP 2018 Best Estimate 2020, Best Estimate 2025, Distributed Generation 2030 and Global Climate Action 2040 scenarios (ENTSO-E & ENTSO-G, 2018).

3.2.3.2 Collect 'real-time' data and synthesise day-ahead and intraday forecasts for future load and vRES generation

Country-specific hourly normalised generation profiles for solar PV, onshore and offshore wind are taken from the Renewables Ninja dataset for 32 historical weather years from 1985 to 2016 (Pfenninger & Staffell, 2016; Staffell & Pfenninger, 2016)[16]. These are taken as the *real-time* vRES generation profiles, which are multiplied by the installed capacity per country to yield the real-time generation in MW. Similarly, the demand profiles from TYNDP 2018 are taken as the real-time demand profiles. Day-ahead forecasts for load and vRES generation are synthesised using the AR-GARCH method presented in Part B (Section 3.2.2). The AR-GARCH models are fit based on the best historical forecast series identified from ENTSO-E data for each variable (see Section 3.3.1). Intraday forecasts are based on persistence, which assumes that the value of a variable in the next time period is the same as the previous one (Eq. (3-17)).

$$F_{t+1} = Y_t \quad (3\text{-}17)$$

For wind (onshore and offshore), we assume a simple 15-minute persistence forecast as, at the sub-hourly level, more elaborate methods are reportedly not significantly better than persistence (Widiss & Porter, 2014). For PV, we assume that intraday forecasts are 20% better (i.e. have 20% lower error) than 15-minute persistence forecasts, based on a comparison of methods available in the literature (Kumler et al., 2018)[17]. For load, we also assume a 20% improvement over 15-minute persistence forecasts as, like PV, load tends to follow a more predictable pattern than wind. Given that small BRPs may not have the resources to produce detailed intraday forecasts, while BRPs should have data on their real-time generation and load, we consider this a reasonable approach.

3.2.3.3 Simulate European day-ahead, intraday and balancing markets

To model future day-ahead, intraday and balancing markets, we use a simplified approach in which only the load and vRES generation in each time step is modelled, rather than the full dispatch of all generation technologies in the portfolio. The main assumptions made in these calculations are explained below.

1. We assume four notional BRPs per country: one for load, one for all solar PV capacity, one for all onshore wind capacity, and one for all offshore wind capacity.

2. All day-ahead, intraday and balancing markets operate with 15-minute resolution[18].

3. Each year from 2017 to 2040 is simulated for 32 historical weather years (1985 to 2016), giving a total of 768 simulation years.

4. All electricity is traded on day-ahead markets, based on the day-ahead forecast generation (or load) $F_{g,t}^{DA}$ for each BRP g, per market period, t. A new day-ahead forecast of vRES generation (and load) is synthesised for each weather year simulated. Forecast errors between countries and between technologies are assumed to be uncorrelated[19].

5. Each BRP must nominate a balanced position at the close of the intraday market[20]. To achieve this, each BRP makes intraday trades per market period $T_{g,t}^{ID}$, based on the difference between their day-ahead and intraday $F_{g,t}^{ID}$ forecasts for that period, and the length of the period, τ (Eq. (3-18)). Thus, we assume intraday trading volumes and imbalances are driven only by load and vRES forecast errors. Other factors such as forced outages, schedule leaps, and strategic behaviour are not considered.

$$T_{g,t}^{ID} = \begin{cases} \left(F_{g,t}^{ID} - F_{g,t}^{DA}\right)\tau & for\ vRES\ generation \\ \left(F_{g,t}^{DA} - F_{g,t}^{ID}\right)\tau & for\ load \end{cases} \quad (3\text{-}18)$$

6. Transmission limitations within and between countries are not explicitly considered. Instead, simulations are performed for two extreme cases: (i) assuming *no* cross-border trading/imbalance netting, and (ii) treating Europe as a *copper plate*, with unlimited potential for cross-border trading/imbalance netting:

   - In the case of **no cross-border** trading, we assume that all possible intraday trades are made between vRES and load BRPs within each country first. Then, any *residual* demand (open buy offers) based on the intraday forecast which cannot be met by vRES is assumed to be supplied by some other dispatchable technology(s) in the system e.g. gas power plants, batteries, hydro. Surplus vRES generation is curtailed.
   - In the **copper-plate** case, trades can take place across country borders, and the requirement for residual demand/curtailment is calculated on the net residual demand across all countries.

7. After all intraday trades are made, any remaining deviations between the intraday forecasts and real-time values are resolved on balancing markets. The imbalance for each vRES technology and load, $I_{g,t}$, is calculated as the difference between the real-time value $Y_{g,t}$ and the intraday forecast $F_{g,t}^{ID}$, multiplied by the market period length τ (Eq. (3-19))[21]. Then, the net imbalance $I_{c,t}$ per country c, is calculated as the sum of all the real-time vRES generation and load imbalances within each country (Eq. (3-20)).

$$I_{g,t} = \begin{cases} \left(Y_{g,t} - F_{g,t}^{ID}\right)\tau & for\ vRES\ generation \\ \left(F_{g,t}^{ID} - Y_{g,t}\right)\tau & for\ load \end{cases} \quad (3\text{-}19)$$

$$I_{c,t} = \sum_{g}^{\mathcal{G}} I_{g,t} \qquad \forall c \in \mathcal{C}, \forall g \in \mathcal{G} \quad (3\text{-}20)$$

8. FRR requirements for balancing are calculated using a static method for each year between 2017 and 2040, assuming that 99.5% of imbalances must be covered, considering all 32 historical weather years[22].

   - In the case of **no cross-border** trading (i.e. no imbalance netting)**,** any remaining country imbalance must be met by a separate reserve per country, sized individually based on $I_{c,t}$. The total reserve capacity across Europe is then the sum of the individual country reserve requirements.
   - In the **copper-plate** case (i.e. with imbalance netting) with fully integrated balancing markets, all country imbalances are netted across Europe (Eq. (3-21)), and the common reserve is sized based on the remaining imbalances, I_t[23].

$$I_t = \sum_{c}^{\mathcal{C}} I_{c,t} \quad (3\text{-}21)$$

3.3 Results

This section presents our results. First, we analyse the country-level day-ahead load and vRES generation forecasts for the years 2017 and 2018 (Section 3.3.1). Then, we show step-by-step how to apply our AR-GARCH method to synthesise day-ahead forecast errors, using the selected historical data from Part A (Section 3.3.2). Lastly, we show the results of using the synthetic day-ahead forecasts (together with intraday persistence forecasts) in long-term simulations of European day-ahead, intraday and balancing markets (Section 3.3.3).

3.3.1 Part A – Results of analysis of current day-ahead forecasts

Metrics describing the accuracy of the day-ahead forecast load and vRES generation for the selected countries are shown in Table 3-1. For a given country, load and solar PV forecasts are typically the most accurate, while offshore wind forecasts are typically the least accurate[24]. For example, in Germany, the RMSE ranges from 1.5% for solar PV up to 8.6% for offshore wind. While most country forecasts have bias errors close to zero, some show quite significant errors (e.g. 26% for offshore wind in the Netherlands in 2017), suggesting there may be erroneous data reported by some TSOs to ENTSO-E. Overall, the accuracy of vRES forecasts appears to be highest in Germany, possibly because the higher penetration of vRES has led to better forecasting methods being developed, or the higher locational diversity that comes with higher vRES penetration leads to a greater degree of error 'smoothing' within the country. Excluding the suspect data, we find that the most accurate country forecast series for load, solar PV, onshore wind and offshore wind are those for Spain, Germany, France, and Denmark respectively. The accuracy of these forecasts is somewhat better than historical day-ahead forecast reported in the literature. For example, the RMSE for onshore wind for France and Germany is found to be around 3%, compared with a RMSE of 4.6% for wind for the whole of Germany reported in 2008 (Ernst et al., 2010). However, since 2008, forecast accuracy appears to have increased[25].

To demonstrate the behaviour of the forecasts, Figure 3-9 shows the normalised historical day-ahead forecast and real-time values in the first week of 2018 for the selected country forecasts, while Figure 3-10 shows the forecast errors for the same series. These figures show that the day-ahead forecasts indeed tend to under- or overestimate for several hours, or even a whole day. This is most likely because day-ahead forecasts are generally made only once per day, and any errors in the underlying model predictors (e.g. temperature, weather conditions) made at the time of the prediction are carried through until the next forecast[26].

Table 3-1 | Calculated normalised mean bias error (MBE), normalised root mean square error (RMSE), mean arctangent absolute percentage error (MAAPE) and standard deviation (σ) of day-ahead forecasts for electricity demand, solar PV, and wind generation for selected EU countries for the years 2017 and 2018 based on data reported by ENTSO-E (ENTSO-E, 2018b) and ELIA (Elia, 2019b)**.** Forecast errors are normalised to the peak load in the case of demand, and installed capacity for vRES from (EurObserv'ER, 2018, 2019). Results in bold indicate the country with the lowest overall error metrics.

Country	Metric	Parameter							
		Load		Solar PV		Onshore Wind		Offshore Wind	
		2017	2018	2017	2018	2017	2018	2017	2018
BE	MBE	0.8%	0.3%	0.1%	-0.1%	-2.0%	-1.9%	-0.8%	-0.6%
	RMSE	2.4%	2.1%	3.1%	3.0%	5.7%	5.6%	11.1%	10.0%
	MAAPE	2.6%	2.2%	17.1%	15.8%	30.2%	29.6%	43.3%	47.6%
	σ	2.3%	2.1%	4.0%	3.2%	6.5%	5.3%	11.7%	11.7%
DE	MBE	0.7%	2.0%	**-0.3%**	**0.0%**	-1.2%	0.2%	0.5%	-0.3%
	RMSE	2.4%	3.3%	**1.6%**	**1.5%**	2.9%	2.7%	6.7%	8.6%
	MAAPE	2.6%	3.5%	**15.8%**	**10.1%**	19.6%	13.6%	20.4%	25.6%
	σ	2.3%	2.6%	**1.6%**	**1.5%**	2.6%	2.7%	6.6%	8.6%
DK	MBE	0.0%	0.0%	0.0%	-0.2%	0.6%	0.2%	**1.9%**	**1.0%**
	RMSE	1.0%	1.1%	2.9%	3.2%	4.3%	3.8%	**6.3%**	**4.5%**
	MAAPE	1.0%	1.1%	13.2%	13.7%	13.0%	15.3%	**16.1%**	**16.9%**
	σ	1.0%	1.1%	2.9%	3.2%	4.3%	3.8%	**6.0%**	**4.4%**
ES	MBE	**0.0%**	**0.0%**	*0.0%* [d]	*-0.5%* [d]	*0.0%* [d]	*-0.1%* [d]	-	-
	RMSE	**1.0%**	**0.9%**	*3.3%* [d]	*4.7%* [d]	*0.6%* [d]	*2.6%* [d]	-	-
	MAAPE	**1.1%**	**0.9%**	23.8% [d]	32.5% [d]	*2.2%* [d]	*11.1%* [d]	-	-
	σ	**1.0%**	**0.9%**	3.3% [d]	4.7% [d]	0.6% [d]	*2.6%* [d]		
FR	MBE	-0.1%	-0.1%	0.2%	0.3%	**0.4%**	**0.6%**	-	-
	RMSE	1.3%	1.2%	3.2%	3.4%	**2.8%**	**3.5%**	-	-
	MAAPE	1.7%	1.7%	17.4%	20.3%	**12.3%**	**13.4%**	-	-
	σ	1.3%	1.2%	3.2%	3.4%	**2.8%**	**3.0%**		
IT	MBE	-0.2%	-0.2%	0.5%	0.4%	*2.6%* [b]	1.9%	-	-
	RMSE	1.7%	1.7%	1.9%	2.2%	*4.7%* [b]	4.1%	-	-
	MAAPE	1.9%	1.9%	13.9%	14.1%	*17.1%* [b]	16.8%	-	-
	σ	1.7%	1.7%	1.8%	2.2%	*4.0%* [b]	3.6%		
NL	MBE	*-4.1%* [b]	*-2.9%* [b]	*0.0%* [a]	*0.0%* [a]	*-3.5%* [b]	*-8.7%* [b]	*26.0%* [b]	*12.5%* [b]
	RMSE	*6.2%* [b]	*5.9%* [b]	*0.9%* [a]	*0.7%* [a]	*10.3%* [b]	*14.0%* [b]	*34.9%* [b]	*24.1%* [b]
	MAAPE	*7.3%* [b]	*6.5%* [b]	*0.6%* [a]	*1.9%* [a]	*34.8%* [b]	*45.1%* [b]	*58.2%* [b]	*48.3%* [b]
	σ	4.6%	*5.1%*	0.9%	*0.7%*	*9.7%* [b]	*11.0%* [b]	*23.3%* [b]	*20.6%* [b]
UK	MBE	*3.0%* [b]	*3.4%* [b]	0.1%	-0.3%	*-2.9%* [b]	*-7.3%* [b]	*-5.6%* [b]	*-7.0%* [b]
	RMSE	*5.2%* [b]	*4.7%* [b]	3.4%	3.0%	*10.1%* [b]	*9.6%* [b]	*9.0%* [b]	*10.7%* [b]
	MAAPE	*6.1%* [b]	*6.3%* [b]	29.1%	31.1%	*29.6%* [b]	*31.6%* [b]	*33.2%* [b]	*36.0%* [b]
	σ	4.2%	*3.3%*	3.4%	3.0%	*9.7%*	*6.2%*	*7.0%* [b]	*8.0%* [b]

Note: values in italics indicate problems with the raw data due to (a) extended periods with forecasts equal to the real-time values (b) significant bias errors (>±2%), (c) the inclusion of other generation types (e.g. concentrating solar power (CSP) is included in PV in Spain), or (d) large differences in forecast accuracy between 2017 and 2018. As a result, these values are not considered in the evaluation of the best forecasts.

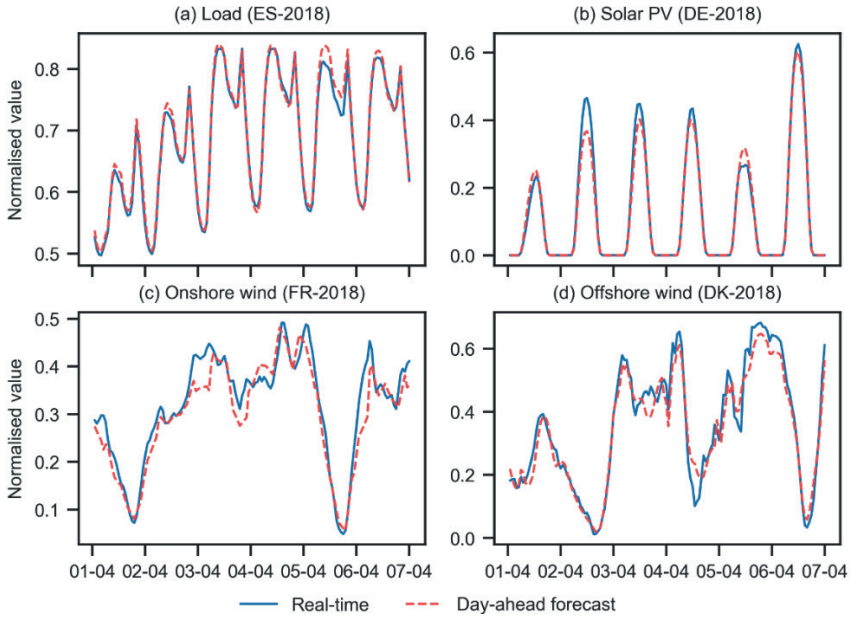

Figure 3-9 | Normalised time series of historical real-time values and day-ahead forecasts from ENTSO-E (ENTSO-E, 2018b) **for the first week of April 2018 for the countries with the most accurate forecasts: (a)** load in Spain **(b)** solar PV in Germany, **(c)** onshore wind in France, and **(d)** offshore wind in Denmark. Load is normalised to peak load, while vRES generation is normalised to the installed capacity.

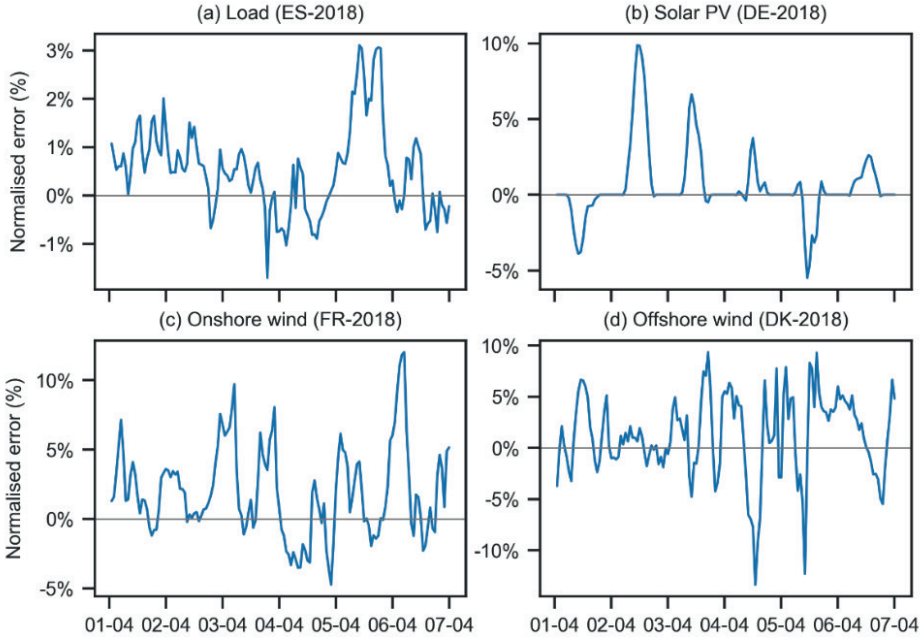

Figure 3-10 | Hourly forecast errors for the time series shown in Figure 3-9 for (a) load **(b)** solar PV, **(c)** onshore wind and **(d)** offshore wind.

3.3.2 Part B – Results of model fits for day-ahead forecast errors

In this section, we show step-by-step the result of applying the method outlined in Part B for synthesising normalised day-ahead forecasts. Given space limitations, we focus on the model fit for onshore wind based on two years of French data from 2017 and 2018. The fitted parameters for the load, offshore wind and solar PV forecasts are provided in Appendix B.

After first normalising the historical real-time values and day-ahead forecast series (Step 1), the total daily absolute errors are calculated (Step 2a) for each parameter as shown in Figure 3-11. The daily errors show volatility throughout the year, but do not display any strong underlying seasonality, except perhaps in the case of solar PV[27]. To determine the appropriate AR(α)-GARCH(p, q) model to fit (Step 2b), we plot the ACF and PACF of the total daily absolute error, shown in Figure 3-12 for onshore wind. Rapid decay of both the ACF and PACF after the first lag suggests that an AR(1)-GARCH(1,1) model would be appropriate to model the daily forecast volatility for this parameter. Fitting the AR-GARCH parameters (using the Python package *arch* (Sheppard et al., 2019)) leads to the following model coefficients: $\mu = 0.4265, \phi_1 = 0.1569, \psi = 0.0156, \alpha_1 = 0.00355, \beta_1 = 0.995$.

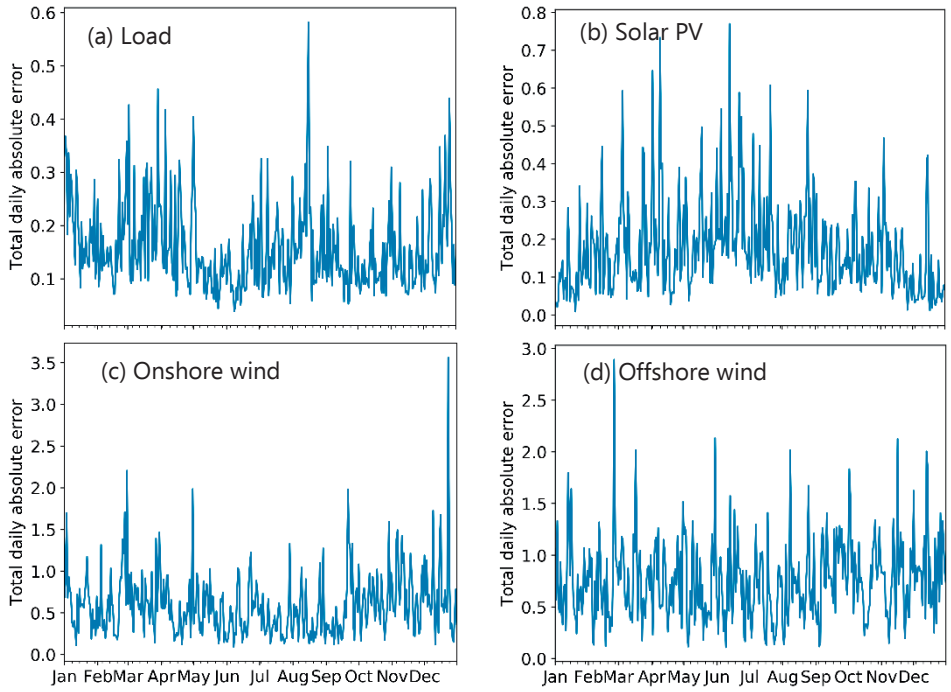

Figure 3-11 | Total daily absolute error based on historical time series for the year 2018 for (a) load in Spain, **(b)** PV in Germany**, (c)** onshore wind in France, and **(d)** offshore wind in Denmark.

After removing the daily volatility component from the hourly errors (Step 3), the hourly errors are binned based on the normalised real-time generation level into 20 bins (i.e. from 0 to 1 with bin size 0.05), and the mean and standard deviation of the errors in each bin are calculated (Step 4). The results are shown in Figure 3-14, highlighting that error volatility generally increases with the generation level[28]. Making a probability density plot of the remaining hourly errors and fitting the data to several distributions shows that a Laplace distribution provides a good fit (Step 5) (Figure 3-13). With all the required model parameters fitted, new day-ahead forecasts can be synthesised for 2017 and 2018 (Steps 6,7,8). The Laplace distribution scale parameter is adjusted iteratively until the RMSE of the synthetic forecast matches the RMSE of the historical forecast, yielding a value of 1.7 (Step 9).

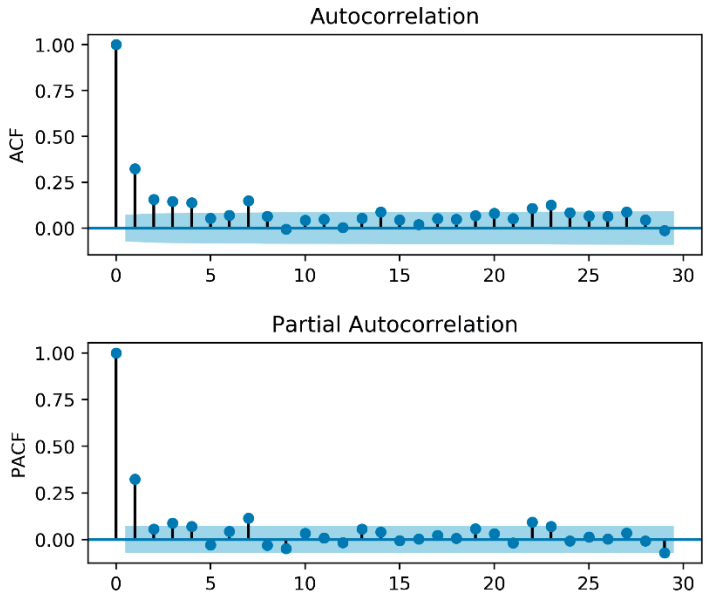

Figure 3-12 | Autocorrelation function (ACF) and partial autocorrelation function (PACF) for the total daily absolute error for onshore wind (France, 2017-2018). Calculated for 30 one-hour time lags.

The performance of the historical and synthetic day-ahead onshore wind forecasts is given in Table 3-2, as well as for load, solar PV, and offshore wind when the same method is applied. Given that the method is stochastic, each synthetic forecast will be slightly different; thus, the error metrics for the synthetic forecasts are calculated for 200 one-year forecasts to yield representative values[29]. Along with these overall metrics, the performance of the synthetic onshore wind forecast on an hourly basis is also shown in Figure 3-15, which depicts the historical real-time onshore wind normalised generation, historical day-ahead onshore wind forecast, and span of the synthetic day-ahead onshore wind forecasts for the first week of April 2018. The span is calculated as the difference between the 95th percentile (P_{95}) and 5th percentile (P_5) values. Table 3-2 and Figure 3-15 show that our method is able to generate synthetic forecasts that agree well with the historical data based on high-level error metrics,

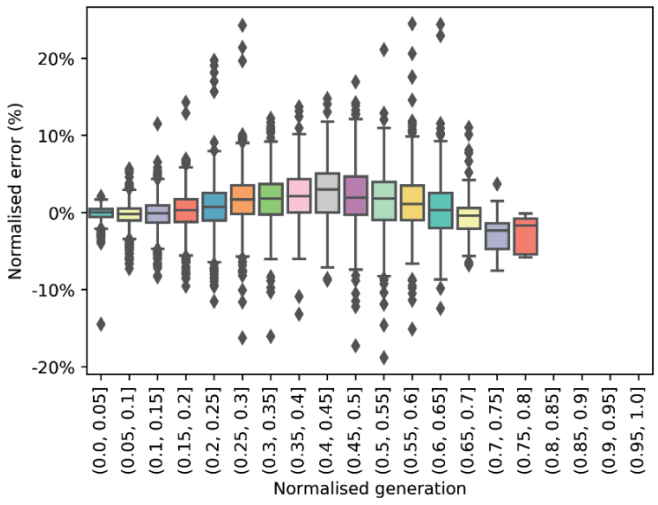

Bin (k)	μ_k	σ_k
[0.0,0.05]	-0.1%	1.0%
(0.05,0.1]	-0.3%	1.3%
(0.1,0.15]	-0.2%	1.8%
(0.15,0.2]	0.2%	2.2%
(0.2,0.25]	0.7%	2.9%
(0.25,0.3]	1.6%	3.2%
(0.3,0.35]	1.8%	3.3%
(0.35,0.4]	2.1%	3.3%
(0.4,0.45]	2.6%	3.6%
(0.45,0.5]	2.1%	4.1%
(0.5,0.55]	1.5%	4.4%
(0.55,0.6]	1.5%	4.7%
(0.6,0.65]	0.6%	4.4%
(0.65,0.7]	-0.5%	3.2%
(0.7,0.75]	-2.6%	2.5%
(0.75,0.8]	-2.8%	2.6%

Figure 3-14 | Box plots of the hourly onshore wind errors with daily volatility removed, binned based on the normalised real-time generation level. The table on the right shows the mean $\boldsymbol{\mu_k}$ and standard deviation $\boldsymbol{\sigma_k}$ of the error in each bin. The bins above 0.8 are empty.

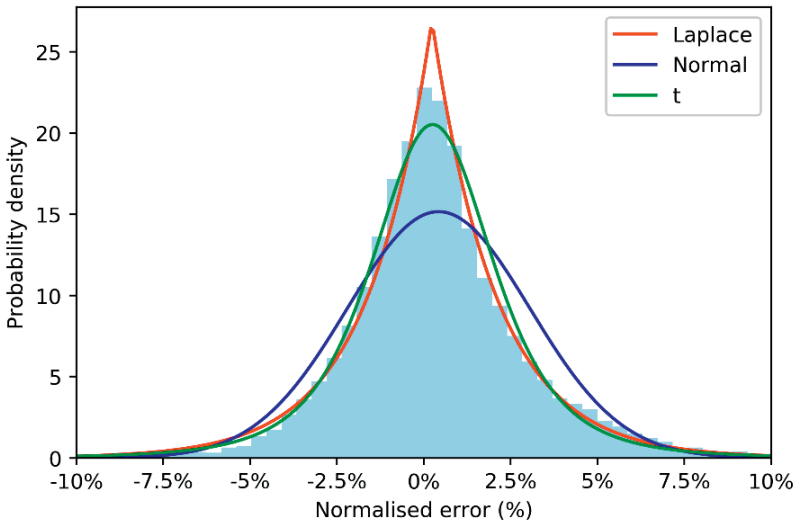

Figure 3-13 | Probability density plot of devolatilitsed hourly onshore wind errors for France (2017-2018), fitted to several distributions.

and generally mimic the behaviour of historical forecasts on an hourly basis. It is not possible to achieve complete agreement on all metrics, as adjusting the distribution parameters to match the historical metrics based on one parameter (i.e. RMSE) in Step 9 can cause the synthetic forecasts to deviate on another.

Table 3-2 | Comparison of error metrics between the historical (2017-2018) forecast errors and synthetic day-ahead forecasts for load (from Spain), solar PV (from Germany), onshore wind (from France) and offshore wind (from Denmark). Error metrics are calculated with respect to the real-time series. The synthetic errors are reported as the mean value based on 200 one-year synthetic forecast simulations, with the 5th and 95th percentile vales (P_5, P_{95}) given alongside in brackets.

	Load		Solar PV	
	Historical	Synthetic	Historical	Synthetic
MAAPE	0.92%	0.85% (0.76%,0.96%)	10.1%	11.6% (10.9%,12.2%)
MBE	0.0%	-0.00% (-0.08%,0.07%)	-0.04%	-0.01% (-0.09%,0.06%)
RMSE	0.98%	0.97% (0.83%,1.18%)	1.5%	1.44% (1.16%,1.76%)
σ	0.11	0.11 (0.11,0.11)	0.16	0.16 (0.16,0.16)
Skew	0.02	0.04 (0.03,0.05)	1.43	1.46 (1.45,1.47)
Kurtosis	-1.01	-0.98 (-0.99,-0.96)	0.81	0.92 (0.87,0.97)
	Onshore wind		Offshore wind	
	Historical	Synthetic	Historical	Synthetic
MAAPE	13.5%	11.6% (10.4%,12.8%)	16.0%	14.7% (13.2%,16.2%)
MBE	0.6%	0.24% (-0.06%,0.53%)	-1.1%	-0.19% (-0.60%,0.22%)
RMSE	3.6%	3.59% (2.99%,4.25%)	4.5%	4.61% (3.95%,5.35%)
σ	0.14	0.15 (0.15,0.15)	0.20	0.20 (0.19,0.20)
Skew	1.5	1.37 (1.29,1.48)	0.23	0.28 (0.24,0.34)
Kurtosis	2.2	1.61 (1.27,2.13)	-1.23	-1.13 (-1.22,-1.00)

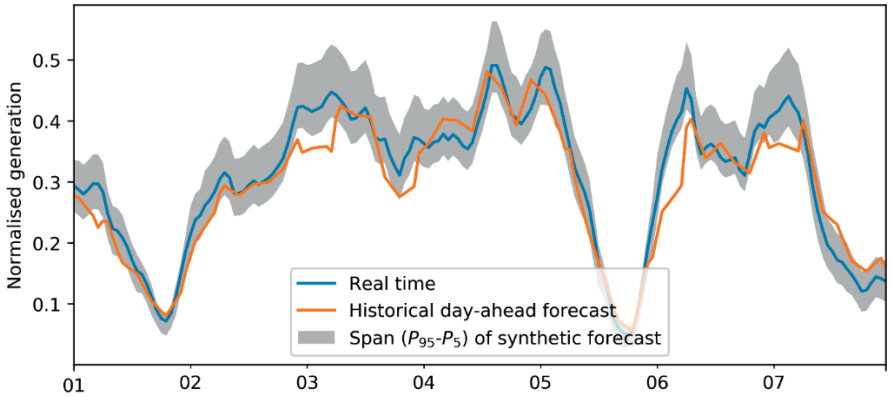

Figure 3-15 | Historical real-time onshore wind generation, historical day-ahead onshore wind forecast, and span (P_{95}-P_5) of synthetic day-ahead onshore wind forecast for France for the first week of April 2018. The span is based on 200 one-year synthetic forecasts.

3.3.3 Part C – Results of European day-ahead, intraday and balancing market simulations

This section presents the results of the day-ahead, intraday and balancing market simulations. To put the volume of each of these markets in perspective, Figure 3-16 shows the average total volume across all weather years of the day-ahead, intraday and balancing markets between 2017 and 2040 for both the no transmission and copper-plate cases. We first discuss the day-ahead results in more detail, followed by the intraday and balancing markets.

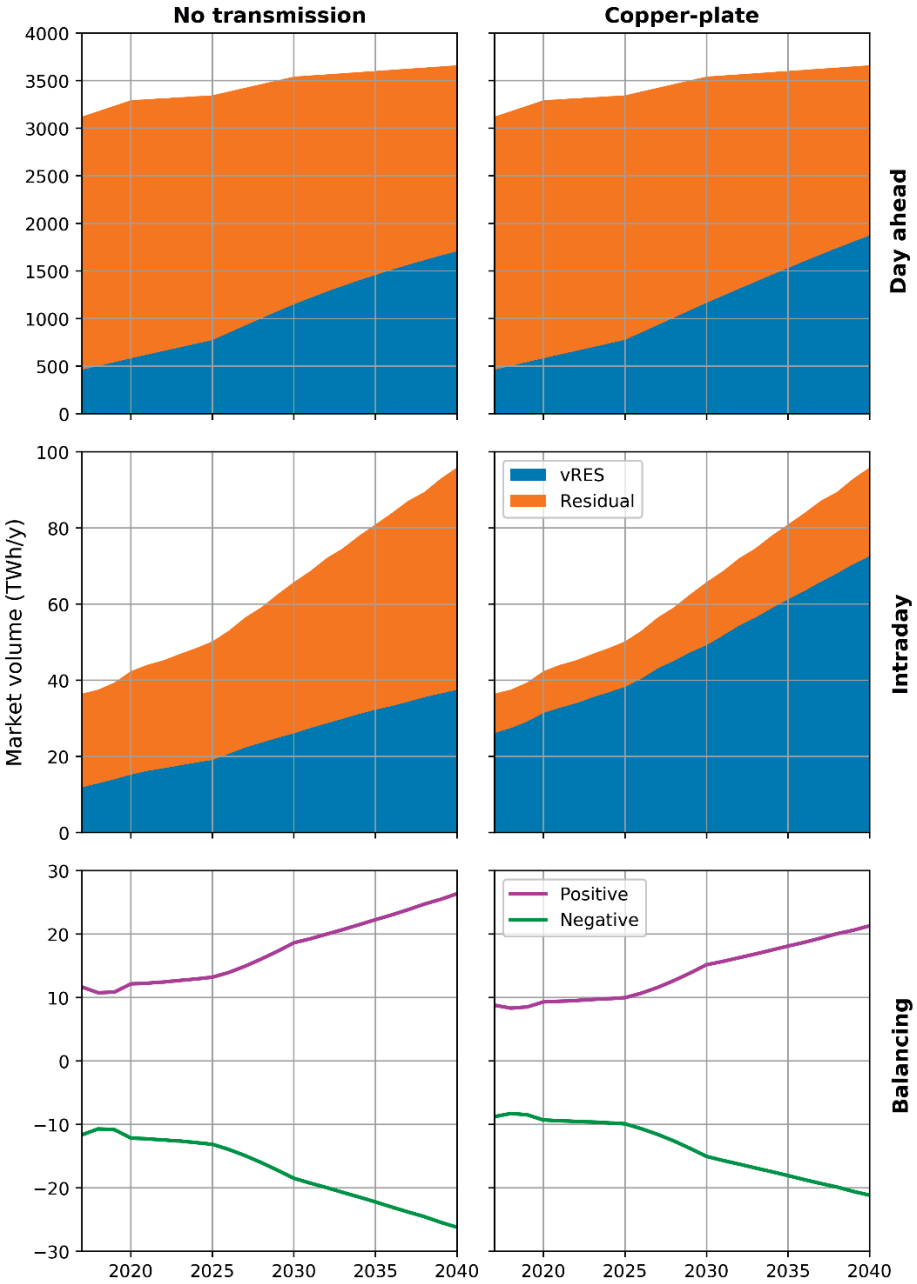

Figure 3-16 | Total annual volumes traded on European day-ahead (top row), intraday (middle row) and balancing (bottom row) markets over time for the case of no transmission (left column) and unlimited transmission (right column). The values shown are the average volumes based on simulations for 32 weather years. For the day-ahead and intraday markets, the share which could be covered by vRES is shown, as well as the residual energy that would need to be provided by residual technologies in the portfolio. For the balancing market, the average positive and negative balancing energy are shown.

3.3.3.1 Day-ahead market

Between 2017 and 2040, total day-ahead trades increase by 17% to an average of 3660 TWh y^{-1}, in line with the assumed increase in electricity demand (Figure 3-16). As a result of the large-scale vRES deployment assumptions, total vRES day-ahead traded volumes increase from an average of just 500 TWh y^{-1} in 2017 to between 1700 (no transmission) and 1870 TWh y^{-1} (copper-plate) in 2040, depending on the level of vRES curtailment. Curtailment ranges between 23 and 46 TWh y^{-1} in 2040 in the copper-plate case, and 171 and 225 TWh y^{-1} in the case of no transmission (Figure 3-17). The net vRES penetration averages 46% in 2040 in the case of no transmission, increasing to 51% in the copper-plate case due to the lower curtailment. As a result of increasing supply from vRES, total residual demand is 870 TWh (33%) and 700 TWh (27%) lower in 2040 than in 2017 in the copper-plate and no transmission cases respectively (Figure 3-18), showing that vRES significantly reduces the need for dispatchable energy in the day-ahead market.

3.3.3.2 Intraday market

Compared with 2017, the total volume of the intraday market increases by 60 TWh y^{-1} (~160%) to nearly 100 TWh y^{-1} by 2040, largely as a result of the additional day-ahead forecast error caused by increasing vRES deployment (Figure 3-16). Without these trades, the additional 60 TWh y^{-1} of day-ahead forecast error would have to be resolved on balancing markets.

In 2017, excluding cross-border transmission, trading between vRES and load BRPs could resolve some 33% (12 TWh y^{-1}) of the 36 TWh y^{-1} of day-ahead forecast errors, leaving an average residual of 24 TWh y^{-1} which would need to be resolved by dispatchable technologies (Figure 3-19). In the copper-plate case, cross-border trading allows for more trades between vRES and load BRPs in different countries, allowing them to resolve on average 72% (26 TWh y^{-1}) of day-ahead forecast errors, leaving only 10 TWh y^{-1} for dispatchable technologies. At the same time as the total intraday market increases, so does the potential for vRES and load trading. By 2040, intraday trading between vRES and load BRPs can resolve 75% (73 TWh y^{-1}) of their day-ahead forecast errors in a copper-plate Europe, falling to 40% (37 TWh y^{-1}) in the case of no cross-border trading. As a result, the requirement for dispatchable energy on intraday markets depends significantly on transmission: in the copper-plate case, residual intraday volumes increase from 10 TWh y^{-1} in 2017 to 23 TWh y^{-1} in 2040, while for the no-transmission case they rise from 24 TWh y^{-1} to 58 TWh y^{-1}. Thus, the need for dispatchable energy grows on the intraday market with increasing vRES penetration, but this is far outweighed by the decline in day-ahead dispatchable market volumes.

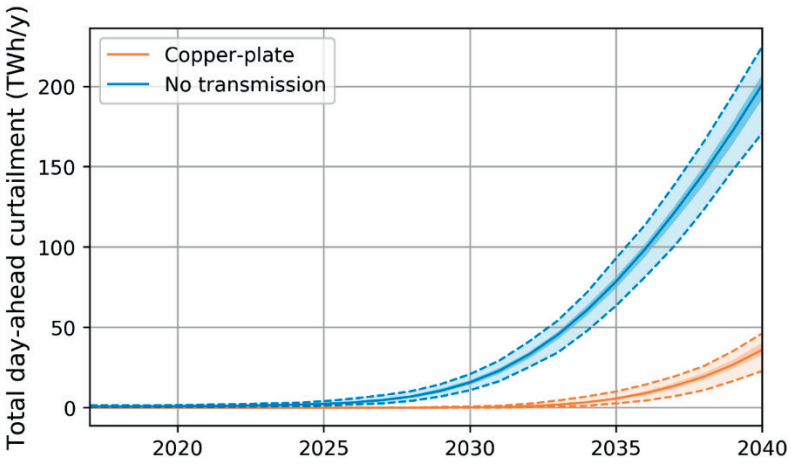

Figure 3-17 | Total annual day-ahead vRES curtailment over time in Europe in the case of unlimited transmission (copper-plate assumption) and no transmission, based on 32 simulated weather years. The area between the dashed lines indicates the range of values across all weather years, while the darker shaded area indicates the interquartile range (P_{75}-P_{25}). The solid lines show the mean value across all weather years.

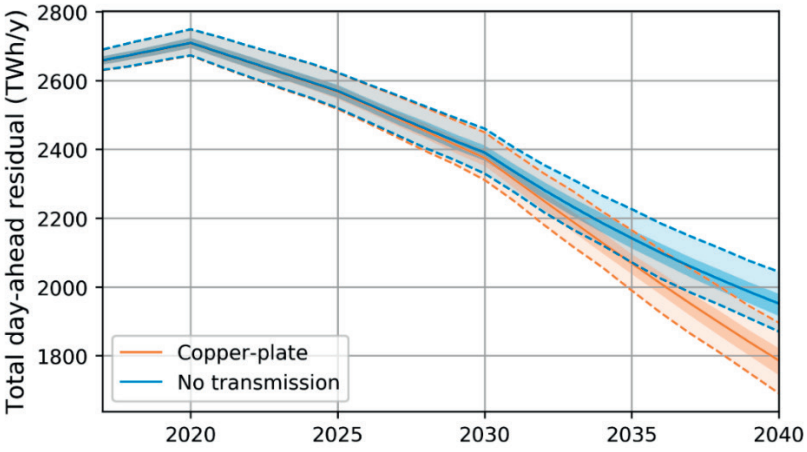

Figure 3-18 | Total annual residual demand in Europe based on day-ahead market trades for the copper-plate and no transmission cases, based on 32 simulated weather years. The shaded area between the dashed lines indicates the range of values across all weather years, while the darker shaded area indicates the interquartile range (P_{75}-P_{25}). The solid lines show the mean across all weather years.

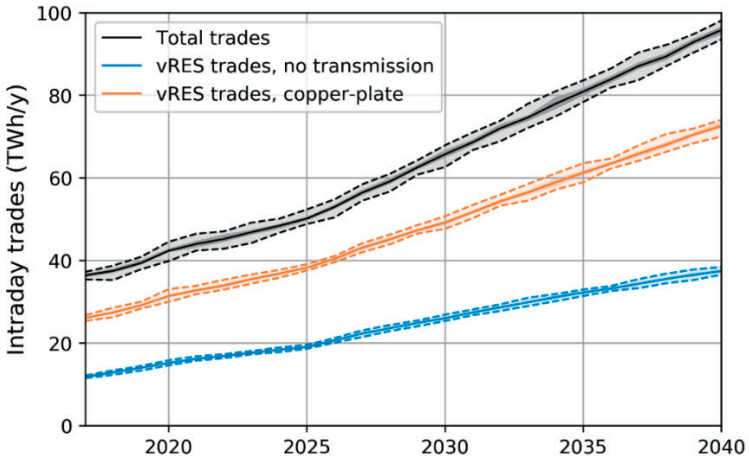

Figure 3-19 | Intraday trading volumes over time. The black trend shows the total intraday trades, the blue trend shows the potential intraday trades between vRES and load BRPs excluding cross-border transmission, while the orange trend shows the potential intraday trades between vRES and load BRPs assuming copper-plate transmission. The light shaded area between the dashed lines indicates the range of values across all weather years, while the darker shaded area indicates the interquartile range (P_{75}-P_{25}). The solid line shows the mean.

3.3.3.3 Balancing market and reserves

Figure 3-20 shows the distribution of imbalance volumes per ISP for selected countries over time, without any contribution from imbalance netting. Due to the increasing penetration of vRES, the imbalance distributions in all countries become flatter, with significantly wider tails. For example, in Germany, 99.5% of imbalances lie in the range of -0.49 GWh to +0.42 GWh in 2017, corresponding to upward and downward reserve requirements of 1.9 GW and 1.7 GW respectively. However, by 2040, 99.5% of imbalances lie in the range of -1.17 GWh and +1.16 GWh, corresponding to a required upward reserve of 4.7 GW and downward reserve of 4.6 GW. At the European level, total requirements for positive balancing energy from dispatchable sources grow from an average of 11.6 TWh y^{-1} in 2017 to 26.4 TWh y^{-1} in 2040 (+127%) assuming no transmission, and from 8.8 TWh y^{-1} to 21.3 TWh y^{-1} (+142%) assuming full imbalance netting across a copper-plate Europe (Figure 3-16). The requirements for negative balancing energy are comparable with those for positive balancing energy. In terms of balancing capacity, Figure 3-21 shows how Europe-wide reserve requirements change over time with increasing vRES penetration, if 99.5% of imbalances must be covered. The plot shows both the total reserve requirement with no imbalance netting between countries, and with maximum imbalance netting (copper plate) and common Europe-wide reserve procurement. Between 2017 and 2040, the requirements for upward balancing capacity increase from 11.4 GW to 23.7 GW (+108%) in the case of no cross-border transmission or reserve sharing, and from 8.8 GW to 16.2 GW (+84%) in the case of full imbalance netting and reserve sharing. Thus, implementing imbalance netting and a common reserve across Europe

could lead to 19% lower balancing energy requirements and 32% balancing capacity requirements in 2040. Reserve requirements remain relatively constant between 2017 and 2025 before increasing until 2040. This is partly due to the slower assumed vRES deployment rate before 2025, but may also be a result of the difference in magnitude between load and vRES forecast errors. At relatively low vRES penetrations (<25%), the imbalances caused by load forecast errors are larger than the imbalances caused by vRES forecast errors, and are the main factor determining reserve requirements. However, at higher penetrations, vRES-induced imbalances become the dominanting factor in determining reserve requirements. The reserve capacities in Figure 3-20 and Figure 3-21 represent the maximum required reserve for a given year while, in practice, applying dynamic reserve sizing (e.g. weekly, daily, hourly) would mean that a lower volume of reserves could be contracted during many periods (de Vos et al., 2019).

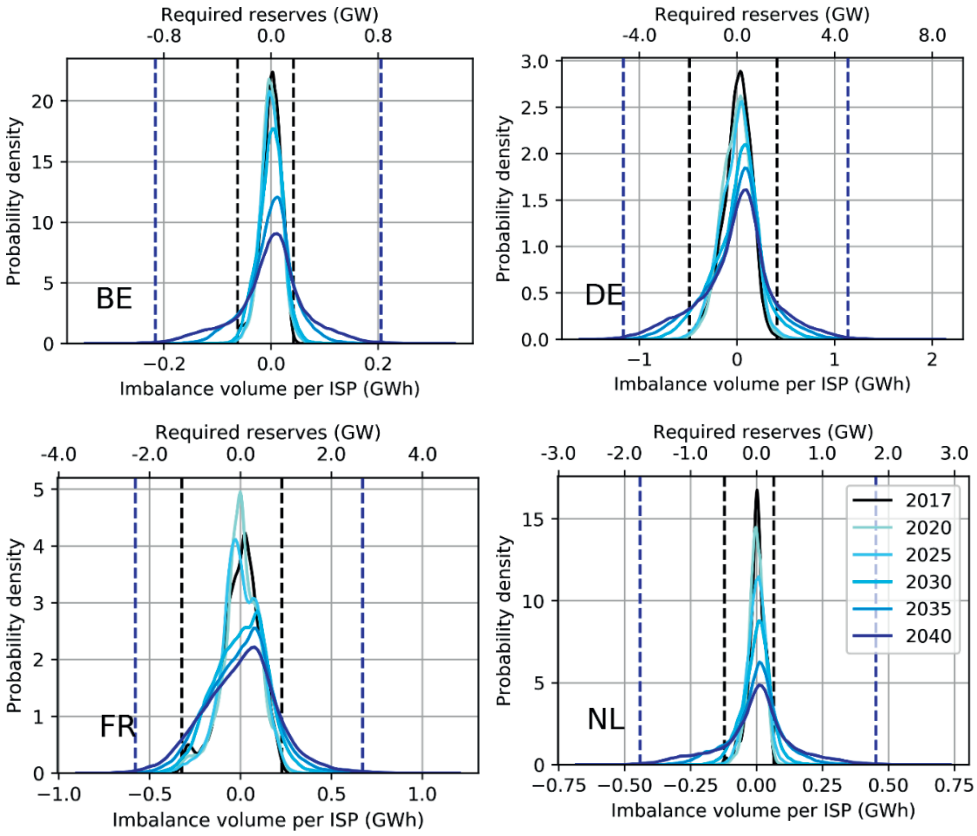

Figure 3-20 | Probability distribution of average imbalance volumes (GWh) and required reserve (GW) per 15-minute imbalance settlement period (ISP) for Belgium (BE), Germany (DE), France (FR) and the Netherlands (NL) for selected years, excluding any contribution from imbalance netting. The dashed vertical lines indicate the required reserve capacity (GW) for the years 2017 and 2040, assuming reserves are sized to cover 99.5% of imbalances. Values are based on simulations of 32 weather years (1985-2016).

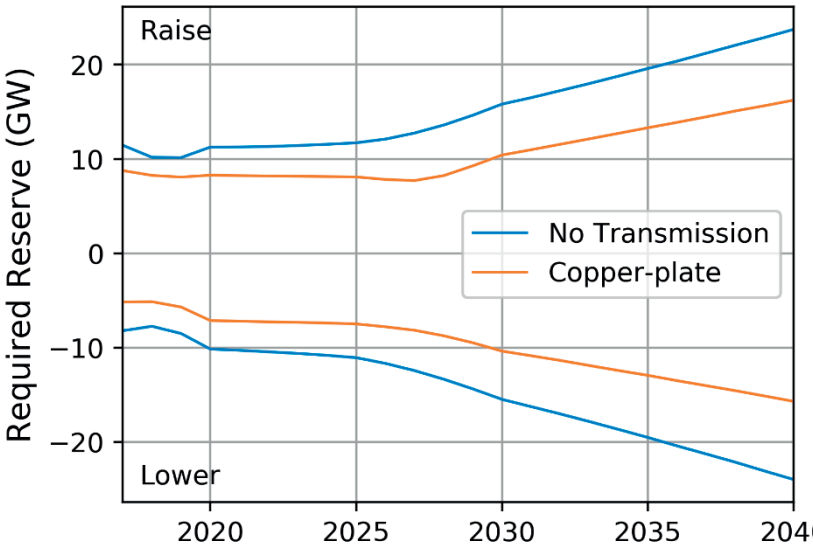

Figure 3-21 | Required reserve capacity over time across Europe, assuming either no transmission and a separate reserve per country, or full imbalance netting (copper-plate transmission) and full reserve sharing between countries. Upward (raise) reserve capacity is shown as positive, while downward (lower) reserve capacity is shown as negative. The reserve requirement is sized to cover 99.5% of imbalances experienced based on 32 years of weather data for each year between 2017 and 2040.

3.4 Discussion

When applying our method for synthesising day-ahead forecast errors and using them for market simulations, attention should be paid to several aspects. These are outlined below.

3.4.1 Limitations of AR-GARCH method for synthetic day-ahead forecasts

In this study, we demonstrate that the AR-GARCH method is a reliable way to synthesise day-ahead forecast errors. However, in certain cases, the method may need to be adjusted for correlations between countries and seasonality, and could be improved with additional historical data:

- Forecast errors for the same parameter (i.e. load, onshore wind, offshore wind, PV) between countries, as well as forecast errors for different parameters within the same country, are assumed to be uncorrelated. This is supported by an analysis of historical forecast errors in several European countries (see Appendix B). However, in other regions, or if significant vRES deployment occurs near national borders, forecast errors may become more strongly correlated (Herre et al., 2019). In this case, the method

needs to be extended to account for correlations between the forecast errors in different countries.

- The method as outlined assumes no seasonality in daily forecast error volatility. As shown in Figure 3-11, this assumption seems valid for load, onshore and offshore wind. Only solar PV displays somewhat more volatile forecasts in summer. The AR-GARCH model can be adjusted to account for this seasonality (e.g. using a Markov-switching model (Haas, 2004)).

- Due to limited good-quality data, we use only two years of historical data to fit the AR-GARCH models, although more historical data would improve the fit.

- We assume day-ahead and intraday forecast accuracy remains the same until 2040. However, country-level forecasts are likely to improve over time due to better forecasting methods, and greater spatial diversity over a wider area (Ernst et al., 2010). Our method can easily account for improved forecast accuracy (see Step 9). Improved day-ahead forecasts would reduce intraday trading volumes, while better intraday forecasts would simultaneously increase intraday trading volumes and reduce balancing volumes.

3.4.2 Interpretation of market simulations

Our market simulations provide insights into the development of day-ahead, intraday, and balancing markets and their interactions under different levels of vRES penetration. However, the results cannot be compared directly with historical data. For example, total European day-ahead trades for the year 2017 from the model (~3100 TWh) are more than double the total amount of historical day-ahead trades in 2017 (~1400 TWh, see Figure 3-1), while the total modelled intraday trades in 2017 (~40 TWh) are less than half of the actual intraday trades in 2017 (~80 TWh, see Figure 3-3). Moreover, the modelled reserve requirements for Germany in 2040 (~4.7 GW, see Figure 3-20) are similar to the requirements contracted today when far less vRES capacity is installed (see Figure 3-4). Thus, when interpreting the market simulation results, the following points should be considered:

- The day-ahead results should be interpreted as indicative of the potential volume of all day-ahead and forwards trades concluded on longer time horizons. This assumption does not affect the intraday and balancing market results, as deviations from contracted volumes on day-ahead and longer-term markets still need to be resolved on these short-term markets.

- Our intraday and balancing market simulations exclude factors such as forced outages, strategic deviations and schedule leaps. Including these factors would increase the

intraday and balancing trading volumes as well as balancing capacities required, bringing them closer to historical values.

- Transmission limitations between and within countries are ignored. This may overestimate the potential of cross-border trading and imbalance netting, and underestimate the amount of intraday trading and imbalances. For comparison, in 2017 approximately of 75% of intraday trades in Europe were made within the same price zone, while 25% were made between price zones (ACER & CEER, 2018). However, by simulating both for the case of no transmission and unlimited transmission (copper-plate), our results provide insights on how the relative sizes of the day-ahead, intraday and balancing markets could change with increasing vRES penetration, depending on the potential of large-scale transmission to facilitate cross-border intraday trading and balancing. The effect of limited transmission capacity could be included by incorporating the synthetic day-ahead and intraday forecasts in a unit commitment and dispatch model and modelling transmission explicitly.

- We assume that load and vRES BRPs trade away all their day-ahead forecast errors on the intraday market based on revised intraday forecasts. However, vRES generators – especially smaller ones – currently face barriers to trading on intraday markets such as high transaction costs and, in some countries (e.g. Spain, Italy), gate closure times which are far from real time (EPEX, 2019a; Hu et al., 2018; Scharff & Amelin, 2016). Moreover, as shown by the relatively low trading volumes (see Figure 3-3), many of Europe's intraday markets are currently rather illiquid (Hu et al., 2018). In the absence of well-functioning intraday markets, day-ahead forecast errors would instead need to be resolved on balancing markets, which could mean an additional 60 TWh y^{-1} by 2040 on top of the requirements shown in Figure 3-19. While there are signs that market liquidity is increasing (see Figure 3-3), reforms such as shifting from continuous to discrete intraday auctions (Chaves-Ávila & Fernandes, 2015), and reforming balancing markets so that vRES receive sufficient price signals to trade on intraday markets would help to facilitate the integration of vRES (ACER & CEER, 2018; Hu et al., 2018).

- Our AR-GARCH models for load, PV and wind day-ahead forecast errors are fit using data from the countries with the most accurate forecasts. Fitting separate AR-GARCH models to each country's day-ahead forecasts may yield higher day-ahead forecast errors, resulting in higher intraday trading volumes. However, given the erroneous data reported for some countries on the ENTSO-E Transparency Platform, and the likely improvement of forecast accuracy in the worst countries, we consider our approach reasonable.

- We model only the single trades required to trade electricity on the day-ahead market, resolve day-ahead forecast errors, and resolve imbalances. However, electricity can be bought and sold more than once across markets in different time frames (e.g. forwards, day-ahead, intraday), and some markets are more liquid than others. For example, market churn rates in Germany are currently 3 to 7 times higher than in most other European markets (EC, 2019b)[30]. This makes it difficult to compare our simulation results directly with historical trading volumes.

- We use historical vRES profiles as a proxy for weather in future years. However, climate change may affect weather patterns, which would impact our results. For example, (Wohland et al., 2017) find that wind conditions over Europe could become more homogenised as Europe's climate warms. This would reduce the potential of geographical smoothing of vRES generation via cross-border intraday trading and imbalance netting, leading to higher reserve requirements.

3.5 Conclusion

In this study, we outline a new method for synthesising day-ahead forecast errors for load, and generation from variable renewable energy sources (vRES) such as solar and wind energy. The method incorporates a generalised autoregressive conditional heteroscedasticity (AR-GARCH) model to account for the daily volatility observed in historical forecast errors, and a dependence on real-time generation (or load) level to account for hourly volatility. By applying our method to country-level data available from transmission system operators (TSOs), we show that it can produce day-ahead forecasts that match well with historical forecasts. Where previous studies have used ad-hoc or non-transparent methods, our study fills a gap by outlining a step-by-step approach for synthesising day-ahead forecasts of a given time series, requiring relatively few parameters.

Our method can be used by power system modellers and TSOs for power system planning studies, based on different projections of load and vRES deployment. We demonstrate how this method can be used by performing simulations of a future European power system in which the penetration of vRES rises from 15% in 2017 to 50% in 2040. Using our AR-GARCH method to synthesise day-ahead forecasts, and intraday forecasts based on persistence, we explore how higher vRES forecast errors could affect day-ahead, intraday and balancing market volumes, and to what extent these errors could be resolved by trading between vRES generators in the case of no cross-border trading, and a copper-plate Europe. Other factors which contribute to intraday trading and imbalance volumes such as forced outages, strategic deviations and schedule leaps are not considered.

Based on our simulations, we find that potential intraday market volumes increase by 60 TWh y^{-1} (+160%) between 2017 and 2040 as a result of additional day-ahead forecast errors. Intraday trading within countries and between countries could allow between 40% (without cross-border trading) and 75% (copper plate) of day-ahead forecast errors to be resolved by vRES, reducing the need for dispatchable energy. In the absence of intraday trading, these errors would need to be resolved by TSOs on balancing markets by procuring additional reserve capacity, highlighting the role liquid intraday markets can play in supporting the integration of vRES in Europe. Regarding balancing markets, we find that full implementation of imbalance netting and a common Europe-wide reserve could reduce balancing energy and capacity requirements for vRES integration by 19% and 32% respectively in 2040 compared with country-specific reserves and no imbalance netting.

Further research could focus on extending our AR-GARCH method to account for cross-correlations in forecast errors between different parameters and countries, and applying it with higher spatial resolution. Further research could also apply the method in unit commitment and economic dispatch simulations of sequential markets (e.g. day-ahead, intraday, balancing) to see the effect of forced outages and transmission limitations on intraday and balancing volumes, and higher temporal resolution to see the impact of schedule leaps.

Footnotes to Chapter 3

[1] Both futures and forwards are contracts to deliver or consume a certain volume of electricity in the future, for a price agreed upon in the present. However, *futures* are standardized products traded on exchanges, while *forwards* are tailored bilateral agreements made over the counter (Economic Consulting Associates, 2015).

[2] Some studies (e.g. (Graabak & Korpås, 2016; Graabak et al., 2017; Grams et al., 2017; Mileva et al., 2016)) use the term *balancing* to refer to supplying residual demand (i.e. hourly demand minus vRES generation) principally on day-ahead markets. However, the European Commission defines balancing as *"…all actions and processes, on all timelines, through which TSOs ensure, in a continuous way, the maintenance of system frequency within a predefined stability range"* (EC, 2017b). Thus, in this study, we use the term balancing to refer to TSOs maintaining supply and demand in balance using real-time balancing markets.

[3] *Balancing capacity* is the volume of capacity (in MW) that a BSP has agreed to hold in reserve (i.e. not offer on day-ahead or other markets) for which they agree to submit bids for corresponding volumes of *balancing energy* (in MWh) to the TSO (EC, 2017b).

[4] For comparison, vRES represented 15% of total EU28 generation in 2017 (Eurostat, 2019d). The *Energy Roadmap 2050* study published by the European Commission (EC) in 2011 considers between 32%-65% vRES by 2050 (EC, 2011d), while a more recent (2018) EC study looking at scenarios consistent with the Paris Agreement considers between 65%-72% vRES by 2050 (EC, 2018a). Meanwhile, ENTSO-E scenarios consider vRES shares between 48%-58% by 2030, and between 65%-81% by 2040 (ENTSO-E & ENTSO-G, 2018). In the academic literature on nearly 100% European renewable power systems, the shares can be higher. For example, Child et al. consider 75% to 78% vRES by 2050 (Child et al., 2019), while Plessmann & Blechinger consider 83% (Plessmann & Blechinger, 2017).

[5] The geographic scope of this study included Norway, Sweden, Denmark, Belgium, the Netherlands and Germany,

[6] ARIMA models model a time series as a combination of autoregressive (AR) and moving average (MA) processes (Hyndman & Athanasopoulos, 2018). If the time series is non-stationary it must first be differenced or integrated (I). The order of the autoregressive p, moving average q, and level of differencing d included in the model define it as an $ARIMA(p,d,q)$ model.

[7] We use the MAAPE as an alternative metric to the more well-known *mean absolute percentage error* (MAPE), as the latter can yield large and undefined values for values of Y_t approaching zero (Kim & Kim, 2016). Essentially, MAAPE is a slope as an angle, while MAPE is a slope as a ratio.

[8] This convention is purely for convenience so that intraday trade and balancing requirements can be simply calculated as the sum of all component forecast errors in section 3.2.3.

[9] In the case of wind, this is at least partly due to the fact that the wind power curve is non-linear with respect to wind speed (Olauson et al., 2016).

[10] We change indices here from time periods (t) to days (d) and hours (h) to clearly show how the daily and hourly-based parameters are calculated; however, the series $\hat{\varepsilon}_t$ and $\hat{\varepsilon}_{d,h}$ are identical. Similarly, when we change back to period-based indices in Step 7, the series $\hat{\varepsilon}'_t$ and $\hat{\varepsilon}'_{d,h}$ are also identical.

[11] The series δ_d should be checked for stationarity before fitting the AR-GARCH model. This can be done using standard statistical tests (e.g. Augmented Dickey Fuller) and, if necessary, transformations applied to make the series stationary. Possible sources of non-stationary are seasonality or, in the case of vRES, increasing deployment of vRES capacity during the period considered.

[12] Engle (Engle, 1982) originally proposed using a normal distribution to model disturbances. However, this sometimes fails to capture the higher kurtosis (i.e. "fat-tailedness") and skewness observed in some processes. Based on our data, we find a Skewed Student t-distribution provides the best results. See Hansen (B. Hansen, 1994).

[13] In our approach we use bins of load or generation. Another approach would be to use bins according to the hour of the day, similar to hourly price forward curves employed in the literature for electricity prices (Kiesel et al., 2019).

[14] The number of parameters required will vary depending on the chosen distribution.

[15] ENTSO-E's TYNDP 2018 presents several scenarios for the years 2020, 2025, 2030 and 2040 with varying levels of vRES deployment and electricity demand. In this study, we assume a vRES deployment trajectory for these years following the *Best Estimate 2020, Best Estimate 2025*, *Distributed Generation 2030* and *Global Climate Action 2040* scenarios respectively (ENTSO-E, 2018f). These scenarios are chosen for the specific time horizons as the *Global Climate Action 2040* scenario has the most ambitious vRES deployment by 2040, while the other scenarios give the most realistic deployment trajectory for 2020, 2025, and 2030. Demand profiles for 2017 are taken from historical data (ENTSO-E, 2018b), and demand profiles for the key years 2020, 2025, 2030 and 2040 are taken from the respective scenarios chosen for the vRES deployment trajectory for consistency. The installed vRES capacity and demand in intervening years are based on linear interpolation between the starting year (2017) and the key scenario years (2020, 2025, 2030 and 2040).

[16] The raw dataset contains 32 years (1985 to 2016) of weather data for solar PV, and 37 years for wind. However, it is important that simulations maintain temporal consistency to preserve correlations between real-time vRES profiles in

neighbouring countries, thus we only use data for the 32 weather years for which both wind and solar PV data are available (1985 to 2016).

[17] Relatively simple methods can be used to improve on persistence forecasts for solar PV, such as accounting for real-time cloudiness, and the path of the sun across the sky. These 'smart persistence' methods can be up to 20% better than persistence for a 30-minute forecast horizon (Kumler et al., 2018). Some studies suggest 15-minute ahead PV forecasts made with advanced neural network techniques could be 40% to 70% better than persistence (Li et al., 2019). However, not all market players may have the resources to develop such advanced methods, which is why we assume lower values.

[18] For simplicity, we model day-ahead, intraday and balancing markets all with a time resolution of 15-minutes. However, most day-ahead markets are hourly, while intraday markets can be based on hourly, 30-min or 15-min products. Commission regulation 2017/2195 establishing a guideline on electricity balancing requires all TSOs to harmonise to an ISP of 15 minutes by 2021 (ENTSO-E, 2018a). As the vRES profiles from Renewables Ninja and load profile scenarios from ENTSO-E are at hourly resolution, we first synthesise hourly forecasts for load and vRES generation, then downscale them (as well as the real-time values) to 15-minute resolution for the simulations. This allows us to account for the impact of vRES on intraday and balancing markets, without the impact of schedule leaps.

[19] This assumption was checked by calculating correlation coefficients for historical forecast errors in neighbouring countries for the years 2017 and 2018, which showed no strong correlations (see Appendix B).

[20] It is a legal requirement in Germany that BRPs nominate a balanced position at the closure of the intraday market. However, in the Netherlands this is not the case, as so-called 'passive balancing' is allowed (Brijs et al., 2017).

[21] Note that Eq. (3-18) and Eq. (3-19) follow the same sign convention as Eq. (3-6). For generators, if the intraday forecast generation is lower than the day-ahead forecast, the BRP will have a *negative* position, thus the BRP must *buy* energy on the intraday market to meet their day-ahead commitments. Conversely, a *positive* value for the intraday trades the BRP has a surplus of generation and can *sell* this on the intraday market. The opposite is true for load BRPs.

[22] FCR requirements are not considered as these are driven mostly by the largest generators or transmission lines in the system. With the possible exception of very large (offshore) wind farms, the loss of power resulting from an outage of a large (e.g. nuclear) power plant is likely to be much larger than the loss of power from an outage of a vRES generator (Brouwer et al., 2014).

[23] Many studies have been performed showing the benefits of integrating European balancing markets (e.g. (Doorman & van Der Veen, 2013; Farahmand et al., 2012; Farahmand & Doorman, 2012; Gebrekiros et al., 2015; van den Bergh et al., 2018)).

[24] Note that caution is necessary when comparing error metrics between solar PV and other parameters, as solar PV forecast error is zero at night, reducing the overall annual error.

[25] For example, the mean absolute error (calculated similar to MBE in Eq. (3-2) but instead taking the absolute value of ε_t) of German wind and solar forecasts has increased over time; however, the relative increase in installed capacity has been far greater. Thus, the mean absolute error of German day-ahead wind and solar forecasts reduced by 25% and 44% (relatively) respectively between 2010 and 2016 (Gürtler & Paulsen, 2018).

[26] Given that European day-ahead markets close at 12:00 (D-1), we checked whether day-ahead forecast error increased throughout the day, suspecting that errors might increase for periods later in the day from when the original day-ahead forecasts are made. However, this did not appear to be the case.

[27] Using the Augmented Dickey Fuller test, the total daily error series for all four parameters were found to be stationary at a 95% significance level ($p < 0.05$) except for solar PV, which yielded a slightly higher p-value of 0.07. This is most likely due to the mild seasonality observed.

[28] The choice of 20 bins is arbitrary. However, the bins should cover all possible values of the real-time generation (or load) if the method is to be applied to other weather years or countries. Depending on the spread of the data, this may mean that some bins are completely empty or contain fewer data points than others, which affects the reliability of the μ_k and σ_k values. This problem can be addressed by including more historical data when fitting the AR-GARCH model, or by replacing the μ_k and $\sigma_k$values in less populated (or empty bins) with more representative values.

[29] Enough simulations were performed for the mean, P_5 and P_{95} values to converge at repeatable values.

[30] The churn rate is an estimate of how many times one MWh of electricity is traded before it is consumed, and is calculated as the total volume of electricity traded (including exchange executed and over-the-counter markets on the spot and the curve) and electricity consumption (EC, 2019b).

Is a 100% renewable European power system feasible by 2050?

William Zappa

Martin Junginger

Machteld van den Broek

4

Published as Zappa,W Junginger, M. & van den Broek, M (2019). Is a 100% renewable power system feasible by 2050?. Applied Energy 233-234. 1027-1050.

Abstract

In this study, we model seven scenarios for the European power system in 2050 based on 100% renewable energy sources (RES), assuming different levels of future demand and technology availability, and compare them with a scenario which includes low-carbon non-RES technologies. We find that a 100% RES European power system could operate with the same level of system adequacy as today when relying on European resources alone, even in the most challenging weather year observed in the period from 1979 to 2015 (2010). However, based on our scenario results, realising such a system by 2050 would require: (i) an 80% increase in generation capacity to at least 1.8 TW (compared with 1 TW installed today), (ii) reliable cross-border transmission capacity at least 140 GW higher than current levels (60 GW), (iii) the well-managed integration of heat pumps and electric vehicles into the power system to reduce demand peaks and biogas requirements, (iv) the implementation of energy efficiency measures to avoid even larger increases in required biomass demand, generation and transmission capacity, (v) wind deployment levels of 7.5 GW y^{-1} (currently 10.6 GW y^{-1}) to be maintained, while PV deployment to increase to at least 15 GW y^{-1} (currently 10.5 GW y^{-1}), (vi) large-scale mobilisation of Europe's biomass resources, with power sector biomass consumption reaching at least 8.5 EJ in the most challenging year (compared with 1.9 EJ today), and (vii) increasing solid biomass and biogas capacity deployment to at least 4 GW y^{-1} and 6 GW y^{-1} respectively. We find that even when wind and solar photovoltaic (PV) capacity is installed in optimum locations, the total cost of a 100% RES power system (~530 €bn y^{-1}) would be approximately 30% higher than a power system which includes other low-carbon technologies such as nuclear, or carbon capture and storage (~410 €bn y^{-1}). Furthermore, a 100% RES system may not deliver the level of emission reductions necessary to achieve Europe's climate goals by 2050, as negative emissions from biomass with carbon capture and storage may still be required to offset an increase in indirect emissions, or to realise more ambitious decarbonisation pathways.

4.1 Introduction

In 2011, the European Union (EU) reaffirmed its objective to reduce greenhouse gas (GHG) emissions by 80-95% by 2050 compared to 1990 levels, this being seen as a necessary step to keep global warming below 2 ºC in line with the projections of the Intergovernmental Panel on Climate Change (IPCC) (EC, 2011a). This was followed in 2016 by the Paris Agreement to keep warming "*well below 2 °C above pre-industrial levels and pursue efforts to limit the temperature increase to 1.5 °C above pre-industrial levels*" (Climate Analytics, 2016; UNFCCC, 2017b). In order to achieve either of these goals, emissions from the power sector must fall essentially to zero, or even turn negative by 2050 (Anderson & Broderick, 2017; EC, 2011c). This will require large-scale implementation of low-carbon technologies such as renewable energy sources (RES), nuclear power, and carbon capture and storage (CCS).

For one reason or another, a number of studies have excluded nuclear and CCS technologies and investigated whether national power systems could rely on 100% RES, such as those for Denmark (H. Lund & Mathiesen, 2009; Mathiesen et al., 2011), the Netherlands (Urgenda, 2014), Germany (Knorr et al., 2014; Wagner, 2014), France (ADEME, 2015), Ireland (Connolly et al., 2011), Australia (Elliston et al., 2014), New Zealand (Mason et al., 2010, 2013) and the United States (Jacobson, Delucchi, Bazouin, et al., 2015). Fully renewable scenarios have also been proposed for the whole of Europe in 2050, of which the most notable are summarised in Table 4-1[1]. These scenarios are usually developed using energy system models to assess whether projected demand could be met by potential RES supply; however, sufficient RES supply does not indicate that a 100% RES power system is feasible as, due to their intermittent generation, variable renewable energy sources (vRES) such as wind and photovoltaics (PV) make balancing electricity demand and supply more difficult than in power systems without vRES (Huber et al., 2014; P. D. Lund et al., 2015; Papaefthymiou & Dragoon, 2016; Papaefthymiou et al., 2014). In a 100% RES power system, any residual demand not supplied by vRES must be provided by one of the dispatchable RES generation technologies (hydro, bioelectricity, concentrating solar thermal power (CSP), and geothermal), or storage. However, in the short term, technical limitations mean that it may not be possible for these plants to ramp up and down quickly enough to keep supply and demand in balance from one moment to the next, leading to over-voltages or unserved energy in the network. In the long-term, some years can be less sunny or windy then others, meaning that wind and PV installations cannot be relied upon to produce the same amount of electricity each year. Therefore, we consider that any assessment of the feasibility of a 100% RES power system should include some analysis of both its long- and short- term reliability.

Table 4-1 | Total electricity generation and installed capacity in several studies featuring high-RES European power systems. For comparison, data for the current (2015) power system are also shown.

Study	Current (2015) (ENTSO-E, 2015a; Eurostat, 2017c)		JRC EU Reference Scenario (EC, 2016b)		High-RES Scenarios									
					EU Energy Roadmap 2050 (EC, 2011c)		Roadmap 2050 (ECF, 2010b)		Energy Revolution (5th Edition) (GWEC et al., 2015)		Re-thinking 2050 (EREC, 2010)		e-Highway 2050 (Bruninx et al., 2015)	
Scenario (year)	-		2050		High RES (2050)		100% RES (2050)		Advanced (2050)		2050		100% RES X-7 (2050)	
Geographical scope	EU28 + NO + CH		EU28		EU28		EU27 + NO + CH (+North Africa for CSP)		OECD Europe (+North Africa for CSP)		EU27		EU28 + NO + CH + Balkans + North Africa	
Demand (TWh y^{-1}) [a]	2912 [h]		3574		3377		4385 [g]		3889 (6020) [e]		-		4385	
Model(s) used [l]	-		PRIMES		PRIMES		Undisclosed		MESAP/Planet		Undisclosed		Antares	
PSM performed?	-		-		No		Yes		Partly [k]		No		Yes	
Generation portfolio	Generation (TWh/y)	Capacity (GW)	Generation (TWh/y)	Capacity (GW)	Generation (TWh/y)	Capacity (GW)	Generation (TWh/y)	Capacity (GW)	Generation (TWh/y)	Capacity (GW)	Generation (TWh/y)	Capacity (GW)	Generation (TWh/y)	Capacity (GW)
Onshore wind	310 (10%)	136 (13%)	980 (24%)	368 (29%)	2504 (49%)	612 (28%)	758 (15%)	245 (12%)	1450 (23%)	594 (23%)	1552 (31%) [b]	462 (24%) [b]	2238 (48%) [b]	875 (40%) [b]
Offshore wind						373 (17%)	758 (15%)	190 (9%)	901 (14%)	237 (9%)				
PV	102 (3%)	95 (9%)	429 (11%)	295 (23%)	843 (16%)	603 (27%)	900 (18%)	815 (41%)	1080 (17%)	926 (36%)	1347 (27%)	962 (49%)	743 (16%) [i]	675 (31%)
CSP	*6 [m]*	*2.3 [m]*	0 (0%)	0 (0%)	0 (0%)	0 (0%)	980 (19%) [b]	203 (10%) [b]	1050 (16%) [f]	208 (8%) [f]	385 (8%)	96 (5%)	278 (6%) [i]	58 (3%)
Ocean [c]	*0.5 [m]*	*0.2 [m]*	0 (0%)	0 (0%)	0 (0%)	30 (1%)	0 (0%)	0 (0%)	160 (3%)	53 (2%)	158 (3%)	65 (3%)	0 (0%)	0 (0%)
Biomass	119 (4%)	25 (3%)	391 (10%)	57 (4%)	494 (10%)	163 (7%)	587 (12%)	85 (4%)	467 (7%)	108 (4%)	496 (10%)	100 (5%)	454 (10%)	184 (9%)
Geothermal	*6 [m]*	*0.8 [m]*	14 (0%)	4 (0%)	31 (1%)	4 (0%)	343 (7%) [b]	47 (2%) [b]	390 (6%)	52 (2%)	601 (12%)	77 (4%)	0 (0%)	0 (0%)
Hydro	536 (17%)	194 (19%)	421 (10%)	142 (11%)	396 (8%)	131 (6%)	591 (12%)	205 (10%)	620 (10%)	223 (9%)	448 (9%)	194 (10%)	890 (19%)	297 (14%)
Natural gas	409 (13%)	217 (21%)	836 (21%)	269 (21%)	386 (8%)	182 (8%)	144 (3%)	215 (11%)	0 (0%)	0 (0%)	0 (0%)	0 (0%)	13 (0%)	73 (3%)
Coal	888 (27%)	187 (18%)	252 (6%)	52 (4%)	108 (2%)	62 (3%)	0 (0%)	0 (0%)	0 (0%)	0 (0%)	0 (0%)	0 (0%)	0 (0%)	0 (0%)
Oil	32 (1%)	32 (3%)	5 (0%)	4 (0%)	0 (0%)	19 (1%)	0 (0%)	0 (0%)	0 (0%)	0 (0%)	0 (0%)	0 (0%)	0 (0%)	0 (0%)
Nuclear	836 (26%)	125 (12%)	737 (18%)	93 (7%)	180 (4%)	41 (2%)	0 (0%)	0 (0%)	0 (0%)	0 (0%)	0 (0%)	0 (0%)	0 (0%)	0 (0%)
Hydrogen [d]	-	-	0 (0%)	0 (0%)	200 (4%)	0 (0%)	0 (0%)	0 (0%)	267 (4%)	181 (7%)	0 (0%)	0 (0%)	0 (0%)	0 (0%)
Total RES	1008 (31%)	404 (40%)	2235 (55%)	866 (67%)	4267 (83%)	1916 (86%)	4917 (97%)	1790 (89%)	6118 (96%)	2401 (93%)	4987 (100%)	1956 (100%)	4603 (100%)	2088 (97%)
of which vRES [j]	412 (13%)	231 (23%)	1409 (35%)	662 (52%)	3347 (65%)	1618 (73%)	2416 (48%)	1250 (62%)	3591 (56%)	1810 (70%)	3057 (61%)	1489 (76%)	2981 (65%)	1549 (72%)
Total Non-RES	2241 (69%)	608 (60%)	1828 (45%)	418 (33%)	874 (17%)	304 (14%)	144 (3%)	215 (11%)	267 (4%)	181 (7%)	0 (0%)	0 (0%)	13 (0%)	73 (3%)
Total	3249	1012	4064	1283	5141	2220	5061	2005	6385 [f]	2582 [f]	4987	1956	4616	2162

Abbreviations: CSP – Concentrating solar power, EU – European Union, PSM – Power system modelling, PV – Photovoltaic, RES – Renewable energy source, vRES – variable renewable energy source.

Footnotes for Table 4-1

[a] *Excluding grid losses and own consumption in electricity generation sector*

[b] *ECF's 100% RES scenario was based on an 80% RES scenario, increased to 100% RES by adding 15% CSP generation from North Africa and 5% from Enhanced Geothermal technologies.*

[c] *Includes wave, tidal and all other forms of marine energy.*

[d] *Hydrogen is reported as non-renewable in this table for clarity as even though some studies assume hydrogen is 100% renewable (e.g. (GWEC et al., 2015)), it is not always clear.*

[e] *Final consumption (3889 TWh) reported does not include 1924 TWh of demand for hydrogen production, or 207 TWh for synfuel production. Once included, total final consumption is 6020 TWh.*

[f] *Total installed capacity (2460 GW) and generation (5764 TWh) reported in original study for OECD Europe do not include assumed import of 620 TWh y^{-1} from north African CSP. Thus, CSP capacity is increased to compensate for this by assuming the same capacity factor for North Africa CSP as for European CSP in the study (55%).*

[g] *Calculated from total reported demand of 4900 TWh y^{-1}, including 10.5% grid losses as assumed in original study.*

[h] *Based on Eurostat data for EU28 and NO, Swiss final consumption (58.2 TWh) from the Swiss Federal Office of Energy (Bundesamt für Energie, 2017).*

[i] *Only aggregated generation from PV and CSP of 1021 TWh was reported in this study. Disaggregated by assuming a 55% capacity factor for CSP.*

[j] *Considering wind, PV and ocean power as variable renewable energy sources (vRES). Run-of-river (RoR) hydro capacity could also be considered vRES, however not all studies indicate the share of RoR capacity.*

[k] *Modelling studies were performed by Energynautics on an earlier (2009) edition of the Energy Revolution report (EREC & Greenpeace, 2009; Tröster et al., 2011). This included transmission but, judging from published information, did not model detailed generator flexibility constraints. No detailed modelling of the most recent version of the Energy Revolution report could be found.*

[l] *PRIMES is an energy system model developed by the E3MLab at the National Technical University of Athens (E3MLab, 2016), it is not a detailed power system model. MESAP and PlaNet are energy system and network planning models originally developed by the University of Stuttgart but now maintained by Seven2one (Aalborg University, 2017). Antares is a sequential Monte-Carlo power system simulator developed by RTE (Doquet et al., 2011).*

[m] *Current contribution is so small that it is not reported specifically by ENTSO-E, thus the value is taken from Eurostat instead but not included in the total (Eurostat, 2017c).In their assessment of the feasibility of 100% RES power systems based on a review of 24 studies, Heard et al. (Heard et al., 2017) found no consistent definition for feasibility, and instead based their assessment on whether studies: (i) performed simulations using PSM to ensure that supply could meet demand reliably, (ii) assumed demand levels consistent with mainstream forecasts, (iii) identified the necessary transmission and distribution requirements, and (iv) considered the provision of ancillary services. Meanwhile, in their critique of Heard et al., Brown et al. (Brown et al., 2018) refuted several of their feasibility criteria as being surmountable at minimal cost, arguing instead that "how to reach a high share of renewables in the most cost-effective manner while respecting environmental, social and political constraints" - is the key issue[2]. Thus, while there is no agreement in the literature on the definition of power system feasibility, achieving a reliable and cost-effective system seems a fundamental requirement.*

Although there is no standard definition, the Council on Large Electric Systems (CIGRE) and the European Network of Transmission System Operators for Electricity (ENTSO-E) define **reliability** as *"the ability of the [power] system to deliver electrical energy to all points of utilization within acceptable standards and in the amounts desired"* (EC, 2014c; UCTE, 2004)[3]. This definition of reliability incorporates two other terms: system **adequacy,** the ability of the power system to supply the required power and energy requirements, subject to outages and operational constraints; and system **security,** the extent to which a power system can withstand sudden disturbances *(ibid.)*. Assessing the reliability of power systems is one of the objectives of power system modelling (PSM).

Surprisingly, only two of the studies presented in Table 4-1 were supported by detailed PSM simulations, which revealed additional portfolio requirements (Bruninx et al., 2015; ECF, 2010a)[4]. Several other studies have also investigated a high-RES European power system using

PSM (Brouwer, Van den Broek, et al., 2016; Bruninx et al., 2015; Bussar et al., 2016; Connolly et al., 2016; ECF, 2010a, 2010b; Gils et al., 2017; GWEC et al., 2015; Haller et al., 2012; Horsch & Brown, 2017; Plessmann & Blechinger, 2017; PwC et al., 2010; Tröster et al., 2011). However, even including these studies, we identify several common limitations – in addition to those raised by Heard et al. (2017) and Brown et al. (2018) – which leave doubts about the feasibility of a 100% RES European power system:

- Generator flexibility limitations are not included, meaning backup and balancing requirements may be underestimated (e.g. (Brouwer, Van den Broek, et al., 2016; Bruninx et al., 2015; Connolly et al., 2016; ECF, 2010a, 2010b; Haller et al., 2012)).
- Bioelectricity is treated crudely using one fuel or generation technology, or without considering regional differences in supply potentials and costs (e.g. (Brouwer, Van den Broek, et al., 2016; ECF, 2010a; Haller et al., 2012; Tröster et al., 2011)).
- Simulations are run for only a single arbitrary (e.g. (Brouwer, Van den Broek, et al., 2016; Horsch & Brown, 2017)) or several weather years (Tröster et al., 2011), which does not guarantee system adequacy.
- Studies rely on significant capacities from technologies such as CSP, geothermal, and biomass which currently show minimal signs of growth (e.g. (Bruninx et al., 2015; ECF, 2010a; EREC, 2010; GWEC et al., 2015)).
- Studies allocate vRES capacity exogenously to countries with the highest capacity factors (e.g. (ECF, 2010a; Plessmann & Blechinger, 2017; Tröster et al., 2011)), or using a single generation profile (e.g. (Brouwer, Van den Broek, et al., 2016; Bussar et al., 2016)). However, insufficient area may be available to support the assumed level vRES deployment, leading to optimistic aggregated generation profiles. Furthermore, simply allocating capacity ignores the potential to reduce costs by optimising the spatial distribution of vRES along with transmission (ECF, 2010a).
- A fixed capacity credit is assumed for vRES technologies, whereas in reality this varies with both location and time (e.g. (Brouwer, Van den Broek, et al., 2016)).
- Significant electricity is imported from the Middle East and North Africa (MENA) countries (e.g. (Bruninx et al., 2015; ECF, 2010a; GWEC et al., 2015; Haller et al., 2012; PwC et al., 2010; Tröster et al., 2011)). While still renewable, it could be considered misleading to label a European power system 100% renewable if it relies on significant imports of RES electricity from outside Europe.
- The power system is modelled at some point in the future (e.g. 2050), without considering whether the transition from the current system and expansion of renewable capacity is practically achievable (e.g. (Brouwer, Van den Broek, et al., 2016)).

In this study, we aim to get insights into the feasibility of a 100% RES European power system in 2050 without these shortcomings by building a model of the power system in which dispatchable generators and their flexibility limitations are modelled in detail. By including the spatial deployment of vRES directly in the optimisation, land availability is accounted for

explicitly, and vRES generation profiles are consistent with their spatial deployment. We model seven scenarios for a 100% RES European power system and explore the impact of uncertainties in future demand and technology development, and compare the costs with one scenario for a non-RES power system. Lastly, we use long-term weather data and detailed hourly simulations to assess system adequacy. Given the lack of consensus on the definitions of power system feasibility, we instead attempt answer the following concrete questions, leaving the final verdict of feasibility to the reader:

- Could a future 100% RES European power system be supplied using European resources alone, and have the same level of system adequacy as today's power system?
- What is the most cost-effective portfolio of RES generation and transmission network capacity?
- How do the costs of a 100% RES European power system compare with a power system which includes non-RES technologies?
- Could the transition to a 100% RES power system be made by 2050?

Our study is structured as follows. First, we outline our overall approach in Section 4.2, which is underpinned by significant input data (Section 4.2.2). Based on the results presented in Section 4.3, we discuss the implications of our study in Section 4.4. Finally, we offer some concluding remarks in Section 4.5. Further details on the method and results from this chapter are provided in Appendix C.

4.2 Method

Our model of a 100% RES power system is built using the PLEXOS[5] software (Section 4.2.1). After supplying the necessary input data and assumptions (section 4.2.2) and defining several scenarios (section 4.2.3), we run a long-term (LT) capacity expansion optimisation to determine the least-cost portfolio of generation technologies and transmission infrastructure investments which can meet demand reliably (Section 4.2.4.1). The optimised portfolio is then simulated at hourly resolution using detailed unit commitment and economic dispatch (UCED) calculations, to ensure that demand can be met in the short term (ST) (section 4.2.4.2). An overview of our method is given in Figure 4-1.

4.2.1 Build model

PLEXOS is a mixed-integer linear programming (MILP) model which has been used in several studies on RES integration and system adequacy (e.g. (Brouwer, Van den Broek, et al., 2016; Deane et al., 2014, 2015; Welsch et al., 2014)). By coupling its LT Plan and ST Schedule modules, PLEXOS can be used to perform both capacity expansion (i.e. building new generation and transmission infrastructure) and UCED calculations, while considering power plant flexibility limitations, and flexible loads. The objective function of the LT Plan is to minimise the total net

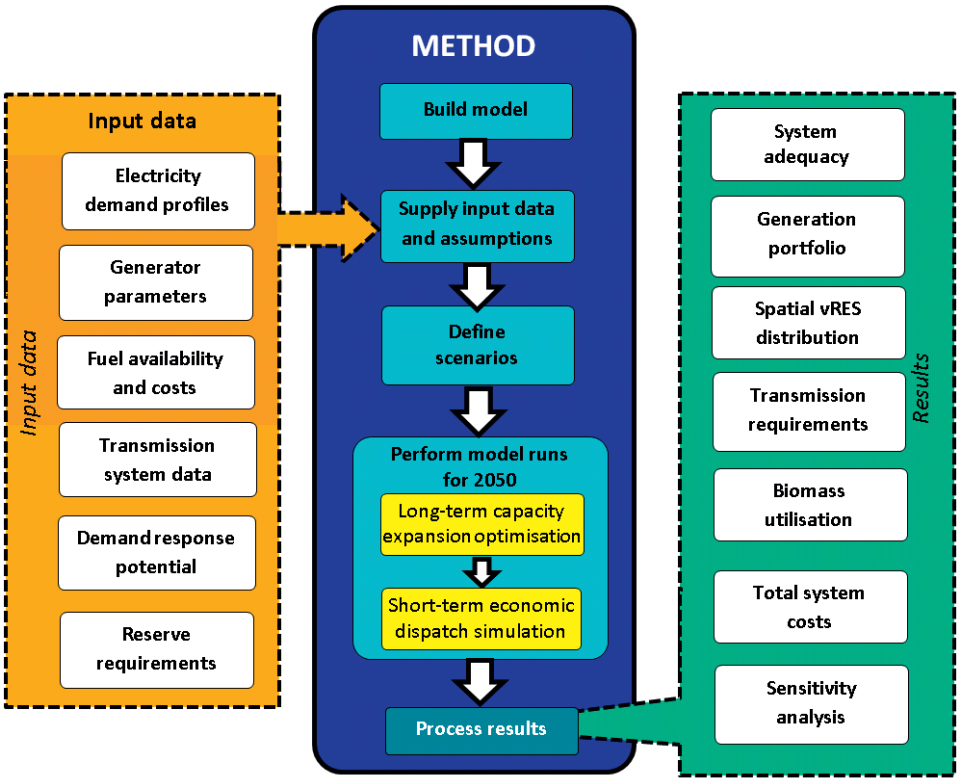

Figure 4-1 | Overview of the method used in this study.

present value (NPV) of build costs, fixed operation and maintenance (FOM) costs and variable operating and maintenance (VOM) costs (Energy Exemplar, 2015), while the objective function of the ST Schedule is to minimise generation costs. A detailed description of the PLEXOS model is provided in Appendix E. We take the geographical scope of Europe in our study as the EU28 countries as well as Switzerland and Norway, as shown in Figure 4-2[6].

Unlike traditional thermal generators, spatial considerations play a vital role in modelling vRES generators as their location determines not only the available, but also how much capacity can be deployed in a given area. To account for this, we introduce the spatial distribution of vRES capacity directly into the optimisation by coupling the PLEXOS model with a high-resolution spatial grid[7]. This grid, indicated in blue in Figure 4-2, is based on a regular 0.75° x 0.75° grid, modified to respect national boundaries (Eurostat, 2014), exclude protected conservation areas (EEA, 2016b), and restricted to offshore water depths of up to 50 m within the Exclusive Economic Zone (EEZ) of each country (Claus et al., 2016). Lastly, we combine the spatial grid with the Corine Land Cover (CLC2012) dataset (EEA, 2016a; Kosztra & Arnold, 2014) and European Reanalysis Interim (ERA-Interim) weather dataset (ECMWF, n.d.), in order to determine both the amount of suitable land area for vRES deployment, and the weather

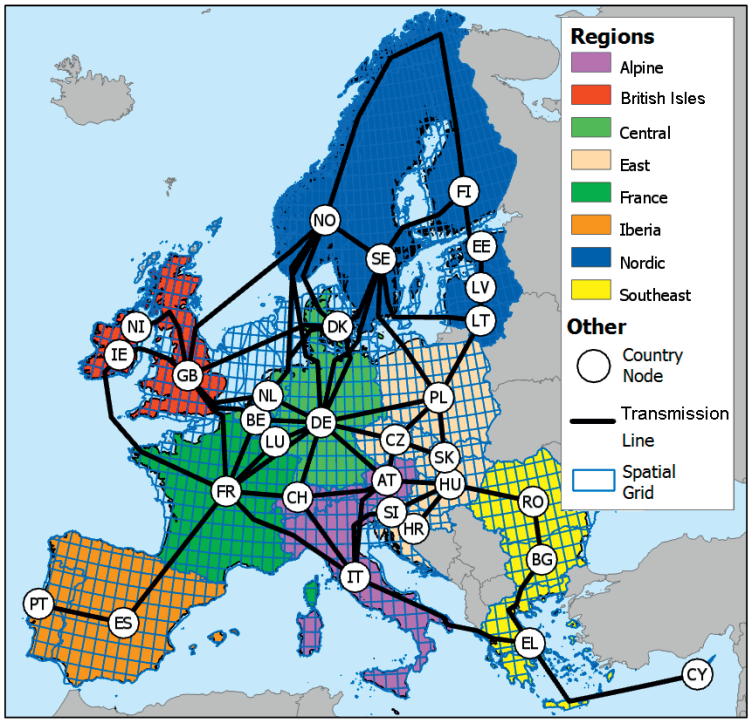

Figure 4-2 | Countries and transmission lines considered. Countries are labelled according to ISO 3166 except for Greece (EL) and the United Kingdom, which is split into Northern Ireland (NI) and Great Britain (GB). Transmission of electricity occurs between the notional load centres of each country using a centre of gravity approach (see section 4.2.2.3). The spatial grid is shown in blue, which includes all land and offshore areas within the exclusive economic zone (EEZ) of each country, up to a maximum water depth of 50 m for offshore wind. Countries not included in the study are shaded grey. The regions are only used to describe results; each country is modelled individually.

conditions at each location[8]. These are used to define the maximum installed capacity and generation profiles for wind and PV per grid cell.

4.2.2 Input data and assumptions

4.2.2.1 Electricity demand

We take the historical electricity demand for each country for the year 2015 as our base demand profile. To account for expected electrification of the heating and transport sectors by 2050, we add additional demand of 500 TWh y^{-1} for heat pumps (HPs), and a further 800 TWh y^{-1} for electric vehicles (EVs), based on the levels assumed in ECF's *Roadmap 2050* study which consider almost complete electrification of passenger vehicles, and significant uptake of HPs (ECF, 2010a).

In addition to the base demand profile, we consider two additional demand profile scenarios to account for uncertainty in future demand. In the *High Demand* profile, we scale up the Base

Table 4-2 | Demand profile parameters

Demand Profile		Source profile	Modifications	Demand		
				Min (GW)	Max (GW)	Annual (TWh)
Underlying source demand profiles	Actual 2015 demand [c]	-	-	230	504	3109
	TYNDP 2016 Vision 4 [d]	-	-	266	563	3616
Modelled demand profiles	Base [a]	Actual 2015 demand	HPs: + 500 TWh y^{-1} EVs: + 800 TWh y^{-1}	241	889	4409
	High Demand	Base	Scaled up to 6020 TWh y^{-1}	329	1214	6020
	Alternative Demand Profile	TYNDP 2016 Vision 4 (for 2030) [b]	Scaled up to 4409 TWh y^{-1}	324	686	4409

[a] *Assuming an average EV efficiency of ~140 Wh km^{-1} (Tesla Model 3) and mileage of 25000 km y^{-1}, 800 TWh y^{-1} would be sufficient to cover approximately 230 million EVs, or more than 90% of the current fleet of 250 million passenger vehicles(Eurostat, 2016). Assuming an average coefficient of performance (COP) of 3, HP demand of 500 TWh y^{-1} would be enough to provide 1500 TWh y^{-1} of useful heat, equivalent to 40% of current residential and service sector heating requirements (Persson & Werner, 2015).*

[b] *Based on published information, the Vision 4 profile assumes increasing total demand, full implementation of smart-grid technology, large-scale adoption of HPs and EVs with flexible charging and generation (~10% vehicle fleet), and large-scale adoption of HPs (~9% heat demand) (ENTSO-E, 2015b).*

[c] *Source: (ENTSO-E, 2017b)*

[d] *Source: (ENTSO-E, 2016d)*

profile to match the Energy [R]evolution scenario annual demand of 6020 TWh y^{-1} (GWEC et al., 2015). In the *Alternative Demand* Profile, we take the 'Vision 4' demand profile from the European Network of Transmission System Operators for Electricity's (ENTSO-E) Ten-Year Network Development Plan (TYNDP) for 2030, and scale it up to 4409 TWh y^{-1} so that total demand matches the Base 2050 demand, but the hourly profile itself is smoother[9].

4.2.2.2 Generation technologies

We consider a broad portfolio of RES generation technologies including wind (onshore and offshore), PV (utility and rooftop), biomass, CSP, geothermal, and hydro power[10]. The main techno-economic assumptions for all generator types are given in Table 4-3. In order to compare the costs of a 100% RES power system with a non-RES power system, Table 4-3 also includes techno-economic parameters for selected natural gas and coal generation technologies (with and without CCS), nuclear, and bioenergy with CCS (BECCS)[11]. For consistency, most costs are taken from the European Commission Joint Research Centre's (JRC) Energy Technology Reference Indicator (ETRI) projections for 2010-2050 (JRC, 2014). As investments for a 100% RES power system by 2050 would need to be made before 2050, we take the costs for 2040. A uniform weighted average cost of capital (WACC) of 8% is used to annualise investment costs in new generation and transmission capacity[12]. A brief explanation of how each technology is modelled is provided in the following subsections.

Table 4-3 | Assumed techno-economic parameters for generation technologies in 2040

Generator type		Nominal size (MW)	Base CAPEX [a] (€ kW^{-1})	FOM [b] (% y^{-1})	VOM [c] (€ MWh^{-1})	Nom. efficiency (%) [d]	Lifetime (y) [c]	Build time (y) [e]
Renewable technologies								
Wind	Onshore	-	1320	1.9%	0	-	25	1
	Offshore	-	2610	2.8%	0	-	25	1
PV [f]	Rooftop	-	950	2%	0	22%	25	<1
	Utility	-	600	1.7%	0	17%	25	1
Hydro [g]	Run-of-river (RoR)	70	5720	1.5%	5.0	87%	60	-
	Storage (STO)	100	2840	1%	4.0	87%	60	-
	Pumped storage (PHS)	400	2840	1.5%	4.0	76%	60	-
Bioenergy	Biomass fluidised bed (Bio-FB)	300	2450	1.8%	3.9	38%	25	3
	Open-cycle biogas turbine (Bio-OCGT)	100 [k]	600	3%	11.2	42%	25	1
	Concentrating solar power (CSP) [h]	50	4930	4%	8.1	40%	30	2
	Geothermal (Geo)	50	4780	2%	0	24%	30	3
Non-renewable, fossil and CCS technologies [i]								
Natural gas	Open-cycle natural gas turbine (Gas-OCGT)	100	600	3%	11.2	42%	30	1
	Natural gas combined cycle (Gas-NGCC)	580	1000	2.5%	2.0	63%	30	3
	NGCC with CCS (Gas-NGCC-CCS)	485	1860	2.5%	4.1	56%	30	4
Coal	Pulverised coal plant (Coal-PC)	750	1980	2.5%	3.7	47%	40	4
	PC plant with CCS (Coal-PC-CCS)	630	3300	2.5%	5.6	41%	40	5
	Bio-FB with CCS (Bio-FB-CCS) [j]	255	4060	1.8%	5.9	28%	25	4
	Nuclear (3rd gen)	1500	5330	1.7%	2.6	33%	60	7

Abbreviations: CAPEX- Capital cost, CCS – Carbon capture and storage, FOM- Fixed operating and maintenance costs, NGCC – Natural gas combined cycle, PV- Photovoltaic, VOM- Variable operating and maintenance costs.
Note: All costs given in $€_{2016}$ using historical Eurozone inflation rates unless otherwise stated (Inflation.eu, 2017).

Footnotes for Table 4-3

[a] *Base CAPEX represents the total capital requirement (TCR), comprising the overnight capital cost (OCC) in 2040 taken from JRC ETRI 2014* (JRC, 2014) *(including grid connection cost), and interest during construction (IDC).*

[b] *FOM costs given as a percentage of OCC taken from the ETRI* (JRC, 2014) *(excluding IDC).*

[c] *JRC ETRI 2014* (JRC, 2014)

[d] *Efficiencies and part-load performance are mostly taken from Brouwer et al.* (Brouwer, Van den Broek, et al., 2016).

[e] *Construction time is used to calculate IDC using an 8% discount rate. Taken from* (Black & Veatch, 2012) *apart from nuclear, which is based on more recent data* (D'haeseleer, 2013). *Plants built within one year have no IDC. IDC is not included for hydro plants as we include no new capacity.*

[f] *Future PV cost estimates vary widely in the literature. For this reason, we include both rooftop (<100 kW) and utility (>2 MW) scale installations to account not only for their different spatial constraints, but also to include a range of investment costs as an implicit sensitivity. Efficiency is based on commercial monocrystalline silicon modules for rooftop PV* (SunPower, 2014)*, and polycrystalline modules for utility PV* (TrinaSolar, 2016).

[g] *For hydro, nominal size is based on average plant size per category from ENTSO-E* (ENTSO-E, 2017b). *For hydro-PHP plants, we assume a reservoir size of 45 GWh per plant (4.5 days) based on the mean calculated specific reservoir size of 113 GWh GW^{-1} for existing hydro-PHP plants from ENTSO-E data. As the cost of Hydro-STO plants depends on capacity, we use an average of the costs for plants between 10-100 MW and >100 MW* (JRC, 2014). *The cost for Hydro-STO is used for Hydro-PHS, as the source does not distinguish between plants equipped with reversible turbines, or plants with dedicated pumping capacity. In any case, hydro capacity is exogenous in all scenarios and the costs do not affect the optimisation. Once-through turbine and pumping efficiency both taken as 87%* (Brouwer, Van den Broek, et al., 2016; Geth et al., 2015).

[h] *CSP plant cost includes 8 hours of molten salt thermal storage per plant* (Mehos et al., 2017). *The peak efficiency of the CSP power block component is 40%, based on electricity generation and total heat input. Overall CSP plant efficiency (output electricity with respect to direct normal irradiance) is approximately 17%* (H. L. Zhang et al., 2013). *Most CSP plants are in the order of 200 MW, consisting of several smaller units of around 50 MW each* (IRENA, 2013).

[i] *Fuel costs of 7 € GJ^{-1}, 2 € GJ^{-1} and 1 € GJ^{-1} are taken for natural gas, coal and nuclear fuel respectively based on the 2-Degree Scenario (2DS) for 2050 from IEA's ETP2016* (IEA, 2016a). *A CO_2 price of 120 € t^{-1} is assumed from the IEA's 2015 World Energy Outlook (WEO) 450 Scenario for 2040* (IEA, 2015). *We assume a uniform CO_2 capture rate for CCS technologies of 90%* (JRC, 2014)*, and CO_2 transport and storage costs of 13.5 € t^{-1} CO_2* (Brouwer, Van den Broek, et al., 2016).

[j] *No data available for Bio-FB-CCS, estimated based on differences between ETRI reported values for Coal-PC with and without CCS: 60% higher CAPEX, 16% lower nominal capacity, 10% (absolute) lower efficiency, and 53% higher VOM than the non-CCS version.*

[k] *Biogas plants are typically small units (< 1 MW), operating on either gas engine or gas turbine technology. However, modelling with such small units can lead to numerical instabilities in the solver, thus we use a higher nominal plant size of 100 MW, the same as Gas-OCGTs.*

Hourly generation from wind farms is estimated by combining wind speed profiles from ERA-Interim with commercial wind turbine power curves. ERA-Interim is also used as the source of solar radiation data to model both PV and CSP. Solar PV is modelled with efficiencies of 21% and 17% for rooftop and utility-scaled systems respectively (SunPower, 2014; TrinaSolar, 2016), while CSP generators are modelled as solar tower plants equipped with two-axis-tracking heliostats, and 8 hours of molten salt storage at nominal load. By calculating the maximum suitable area for wind and PV deployment per grid cell, and limiting how much is available for each technology, we allow PLEXOS to optimise the spatial deployment of wind and PV capacity[13].

We consider two bioelectricity technologies: biomass fluidised bed combustion (Bio-FB) plants and open-cycle gas turbines (Bio-OCGT), which are supplied by three categories of biomass fuels (biogas substrates, solid woody biomass and solid waste biomass), based on country-specific cost-supply curves for 14 different biomass feedstocks (Ruiz et al., 2015) [14]. We assume that solid biomass is combusted in Bio-FBs, while biogas substrates – after conversion

to biogas – are combusted in Bio-OCGTs. Raw biomass fuel costs range from 1.4 € GJ^{-1} to 14.4 € GJ^{-1} depending on the fuel type and country of origin, with a total supply potential of 10 EJ y^{-1} in 2050 (Ruiz et al., 2015)[15]. For biogas substrates, an additional cost of 10.4 € (GJ substrate)$^{-1}$ is included for the conversion by anaerobic digestion (AD) to raw biogas for local use, and a further 3.2 € GJ^{-1} for upgrading to biomethane and injection into the gas grid (Hengeveld et al., 2014). In order to avoid infeasible solutions, biomass supply is modelled as a "soft" constraint by allowing the model to draw on additional biomass supply, at significantly higher cost[16].

Run-of-river (RoR) and storage (STO) hydropower capacity is aggregated in each country using a nominal unit size, with annual capacity factors limited to historical levels (ENTSO-E, 2017b; Eurostat, 2017c). Pumped hydro storage (PHS) capacity is also aggregated for each country but storage is modelled explicitly, assuming an average storage volume of approximately five days at nominal load[17].

While wind turbines and PV panels can be located almost anywhere, hydro and geothermal power plants require sites with specific geological features, and CSP plants must be installed in locations with high direct normal irradiance (DNI). For these reasons, the installed capacity and spatial distribution of hydro, geothermal and CSP are specified exogenously:

- We assume that total hydro capacity in 2050 remains unchanged at approximately 200 GW, with the same geographical distribution and split between RoR (31%), STO (48%) and PHS (21%) capacity as today (Mennel et al., 2015).

- Geothermal capacity is set at 50 GW to reflect deployment levels assumed in previous high-RES studies (ECF, 2010a; GWEC et al., 2015) (see Table 4-1), and allocated to countries in proportion to their economic geothermal potential (van Wees et al., 2013).

- CSP capacity is fixed at 200 GW, reflecting levels found in the most ambitious high-RES scenarios (ECF, 2010a; GWEC et al., 2015) (see Table 4-1). However, many of these studies locate considerable CSP capacity in the MENA countries where higher annual DNI levels are available. In order to fit this capacity into Europe, we allocate CSP capacity to grid cells in order of descending DNI, while adjusting both the minimum cut-off DNI and assumed availabilities of suitable land classes until 200 GW is reached – with a preference for sparsely inhabited areas to minimise impacts on local communities. As a result, CSP is allocated to grid cells with average DNI levels of 1600 kWh m^{-2} y^{-1} or higher, located mostly in Spain (158 GW), Portugal (22 GW), Italy (16 GW), Greece (5 GW) and Cyprus (0.8 GW). Thus, the availability of land for CSP is not taken as a hard constraint (as for PV and wind), but indicates the area which would be required to accommodate 200 GW of CSP in Europe.

The firm capacity for all dispatchable generators (e.g. biomass, hydro, geothermal, CSP) is taken as 90%, assuming 5% unavailability due to unplanned outages, and a further 5% for planned maintenance (ENTSO-E, 2012)[18]. The firm capacity for vRES technologies is estimated per grid cell following the approach of Milligan (Ensslin et al., 2008) as the average capacity factor during the peak 1% of demand hours per year. As a result, PV receives a capacity credit of zero in all grid cells; onshore wind capacity credit has a median of 12%, and offshore wind a median of 10%.

4.2.2.3 Transmission

We use a 'centre-of-gravity' approach to model transmission flows between countries, with the urban area-weighted centres of each country serving as node terminals. Taking the existing capacity in 2016 as a starting point (ENTSO-E, 2017b), new transmission capacity can be built if this lowers total costs, based on the costs given in Table 4-4. Subsea lines are assumed to be high voltage direct current (HVDC), while land-based lines are high voltage alternating current (HVAC). Transmission and distribution within countries is modelled as copper plate.

For the wind and PV technologies, we also estimate the amount of grid reinforcement required to bring this electricity to the main transmission grid by calculating the shortest transmission distance (across either land or sea) to the nominal load centre, and add this amount to the base CAPEX from Table 4-3[19].

Table 4-4 |Techno-economic parameters for HVAC and HVDC transmission infrastructure

Component		CAPEX		FOM [c]	Losses [d]
		Lines (€ MW^{-1} km^{-1})	Substations/ Converters (€ MW^{-1})	(% CAPEX y^{-1})	(% 100 km^{-1})
HVAC [a]	Overhead	330	38,800	3.5%	0.7%
	Underground (Direct buried)	3370			0.45%
HVDC [b]	Subsea	240	121,000	3.5%	0.35%

Note: All costs given in $€_{2016}$ unless otherwise stated. Abbreviations: CAPEX- Capital cost, FOM- Fixed operating and maintenance costs. A lifetime of 40 years is assumed for all transmission system components. A 6% outage rate is assumed for transmission lines, with a mean time to repair of 14 hours (ENTSO-E, 2016b; SKM, 2012).

[a] Based on a study for the UK (Parsons Brinckerhoff, 2012), specific costs range from 333 to 605 € MW^{-1} km^{-1} for overhead HVAC lines and 3370 to 4780 € MW^{-1} km^{-1} for direct-buried lines respectively, depending on the line length and carrying capacity. The quoted values correspond to a double circuit 400 kV 75 km line with 6930 MVA carrying capacity. Given we consider mainly long-distance transmission, we assume a 90%/10% split between onshore overhead lines and underground cables. HVAC converter costs taken from (ACER, 2015)

[b] A complete HVDC line includes the cable length and two converter stations. HVDC line and converter costs taken from (ACER, 2015).

[c] Annual FOM costs equivalent to 3.5% of the base CAPEX (JRC, 2014; Parsons Brinckerhoff, 2012).

[d] HVAC losses taken from (Vaillancourt, 2014), HVDC losses from (Ardelean & Minnebo, 2015). We also include losses of 0.65% per HVDC converter station (average of values from (Guerrero-Lemus & Martínez-Duart, 2013; Vaillancourt, 2014)).

4.2.2.4 Demand response

Demand response, also known as demand side management (DSM), is the willingness of electricity consumers to shift or even curtail their load during times of peak system residual demand (Gils, 2014). In this study, we consider 16 GW of load shedding capacity from heavy industrial processes, and 82 GW of load shifting capacity from various commercial and residential appliances based on the technical potentials reported by Gils (Gils, 2014), and assumed deployment levels (as a percentage of technical potential) from Bertsch et al. (Bertsch et al., 2012). Demand shedding costs vary from 100 € kWh^{-1} to over 2000 € kWh^{-1} depending on the industry, which are activated whenever electricity prices exceed these levels. Limits are imposed on the volume and activation of residential and commercial DSM, depending on the appliance and the season[20].

4.2.2.5 Reserves

Power systems require operating reserves in order to balance out mismatches between demand and generation due to (i) demand forecast errors, (ii) vRES generation forecast errors, and (iii) unplanned generator outages (Ela et al., 2011). In this study we include fast-responding spinning reserves (both up and down regulation) available within five minutes, as well as standing reserves available within one hour. We assume a single Europe-wide reserve market in which all generation technologies are capable of providing reserves, including wind and PV[21].

4.2.3 Define scenarios

In addition to the ***Base*** model run, we consider seven additional scenarios in order to understand the impact of assumptions made in this study and uncertainties involved in modelling a future 100% RES power system (Table 4-5). These scenarios focus on uncertainty in final demand, technological developments and costs:

- In the ***High Demand*** scenario, demand is scaled up by 36% to 6020 TWh y^{-1} keeping the underlying demand profile the same, to see the impact of further growth in demand[22];
- In the ***Alternative Demand Profile*** scenario, we test how sensitive our results are to the base hourly demand profile by using the less peaky 'Vision 4' hourly demand profile from ENTSO-E, scaled to the Base annual demand (4408 TWh y^{-1});
- In the ***No CSP or Geothermal*** scenario, we exclude these two dispatchable technologies to see how critical their future deployment is for a fully renewable European power system;
- In the ***No Biomass*** scenario, we do not allow any power generation from biomass, reflecting possible social opposition to the technology, or complete prioritisation of biomass for other end-use sectors (e.g. heating, industrial processes);
- In the ***Storage*** scenario, we allow the model to build additional grid-scale storage capacity in the form of compressed-air energy storage (CAES)[23];

- In the ***Free RES*** scenario, we specify no exogenous CSP or geothermal capacity and leave the model free to optimise all RES capacity (excluding hydro); and
- In the ***Allow non-RES*** scenario, we allow other low-carbon (but not necessarily renewable) technologies to be built, so that the costs of a fully renewable system can be compared with one which includes non-renewable alternatives.

4.2.4 Perform model runs

With hydro, geothermal, and CSP the only technologies exogenously defined, we first run PLEXOS' LT Plan module in order to find the cost-optimum deployment of the remaining generation capacity and transmission investments which can reliably meet demand (section 4.2.4.1). Then, we test how this system performs at hourly resolution by performing detailed UCED calculations with the ST Schedule module (section 4.2.4.2)[24].

4.2.4.1 Long-term capacity optimisation

One aspect of system adequacy is ensuring that enough generation capacity is available to meet demand reliably. Ideally, this would involve optimising the generation portfolio and transmission network considering all available weather data (i.e. from 1979-2015) simultaneously, to ensure that the risk of short supply is acceptable even in the most challenging weather year, and that the generation portfolio is not sensitive to any individual year. However, optimising the installed capacity of two biomass and four vRES technologies across more than 2000 grid cells – for 37 years of weather data – is not feasible with available computing power. Furthermore, due to the model complexity, it is not amenable to probabilistic methods. Thus, we take the simpler approach of deterministically optimising capacity for the most challenging weather year experienced by Europe in the period 1979-2015. Based on the historical data, we determine 2010 as the year with the overall lowest potential wind and PV generation, and run the capacity expansion optimisation for this year. In performing the capacity expansion optimisation, we make the following assumptions:

- Apart from a reference level of transmission (60 GW) and hydro plant capacity (200 GW), we take Europe as a clean slate and include no legacy generation capacity. Nor do we consider any government policies which may preclude technologies in any given country.
- Transmission is modelled as simple active power transport, rather than a full optimal power flow (OPF) problem[25].
- Generator flexibility parameters and operational reserves are not considered[26].
- To ensure comparability with the 100% RES scenarios, in the *Allow non-RES scenario* we constrain total GHG emissions to 45 Mt y^{-1} in 2050[27]. This represents a reduction of 96% compared with 1990, the level required to ensure that the EU goal of reducing total CO_2 emissions by 80–95% by 2050 can be achieved (EC, 2011c; EEA, 2016c; UNFCCC, 2017a).

Table 4-5 | Scenario runs performed. The text in bold indicates the main differences.

Scenario Group		Scenario	Varied parameters: Demand profile	Varied parameters: Available technologies — Capacity specified	Varied parameters: Available technologies — Capacity optimised
100% RES	Base	*Base*	Base (4408 TWh y^{-1})	▪ Hydro ▪ CSP ▪ Geo ▪ DSM [a]	▪ Wind ▪ PV ▪ Biomass
	Demand uncertainty	*High demand*	Base, **scaled up to 6020 TWh y^{-1}**		
		Alternative demand profile	**ENTSOE 2030 Vision 4 profile, scaled up to 4408 TWh y^{-1}**		
	Technology uncertainty	*No CSP or Geothermal*	Base	▪ Hydro ▪ **CSP = 0** ▪ **Geo = 0** ▪ DSM [a]	
		No Biomass	Base	▪ Hydro ▪ CSP ▪ Geo ▪ **Biomass = 0** ▪ DSM [a]	▪ Wind ▪ PV
		Storage	Base	▪ Hydro ▪ CSP ▪ Geo ▪ DSM [a]	▪ Wind ▪ PV ▪ Biomass ▪ **CAES (storage)**
		Free RES	Base	▪ Hydro ▪ DSM [a]	**All other RES technologies in Table 4-3.**
Non-RES allowed		*Allow non-RES*	Base	▪ Hydro ▪ DSM [a]	**All other RES and non-RES technologies in Table 4-3.**

[a] *Demand shedding (16 GW) is included in both the LT Plan (capacity optimisation) and ST Schedule (hourly UCED) modules for all scenarios, while demand shifting (82 GW) is only included in the ST Schedule runs to minimise computational time.*

In assessing system adequacy, most countries allow for a LoLE between 3 h y^{-1} (e.g. BE, GB, FR) and 8 h y^{-1} (e.g. NI, IE, PT) (EC, 2016a). However, in our study it is not possible to target such a specific LoLE level as we cannot include reserve requirements in the LT Plan, and our vRES firm capacity estimates are not perfect[28]. Assuming that each country must have sufficient capacity reserves to cover its peak demand – either by from its own generators or exchange with neighbouring countries – we increase the capacity margin in each country until no unserved energy is observed in the LT Plan results[29].

4.2.4.2 Short-term hourly dispatch

With the optimum generation portfolios and transmission networks determined from the LT Plan, we then perform detailed UCED simulations for each scenario with PLEXOS' ST Schedule module for the same weather year 2010 - including both generator flexibility constraints and operating reserve requirements. Simulations are run at hourly resolution for one typical week per month, in order to reduce solution time[30]. In assessing system adequacy, we consider a maximum acceptable level of unserved energy of 0.0003% of total annual demand, based on the expected unserved energy for Europe's electricity system in 2020 from ENTSO-E's 2016 Mid-Term Adequacy Forecast (ENTSO-E, 2016b).

4.3 Results

4.3.1 System adequacy

Based on the results of the LT Plan optimisation, feasible solutions are found for all scenarios, with the exception of the *No Biomass* scenario. This shows that with CSP, geothermal, and hydro capacity at their base assumed levels, a 100% RES power system is not feasible without biomass; hence, we do not consider this scenario any further[31]. After simulating the remaining scenarios at hourly resolution, feasible solutions are found with less than 0.0003% unserved energy. From this, we conclude that a 100% RES European power system can achieve the same level of system adequacy as today's power system.

4.3.2 Generation portfolio

The optimised generation portfolio for each scenario is shown in Figure 4-3, while Figure 4-4 shows the annual generation. All 100% RES scenarios show a significant expansion of generation capacity compared to today, with total installed capacity ranging from 1.9 TW in the *Alternative Demand Profile* scenario to 3.1 TW in the *High Demand* scenario. Aside from the higher assumed demand, this increase in capacity is due to the low capacity credit of wind and PV, which must be backed up by dispatchable capacity. With the capacity of geothermal, CSP and hydro set exogenously in most scenarios, the only remaining dispatchable RES technology is biomass, which is installed in significant quantities. Compared to the *Base* scenario, allowing non-RES technologies reduces the size of the total portfolio to 1.4 TW, primarily due to the rollout of some 200 GW of dispatchable zero-carbon nuclear capacity,

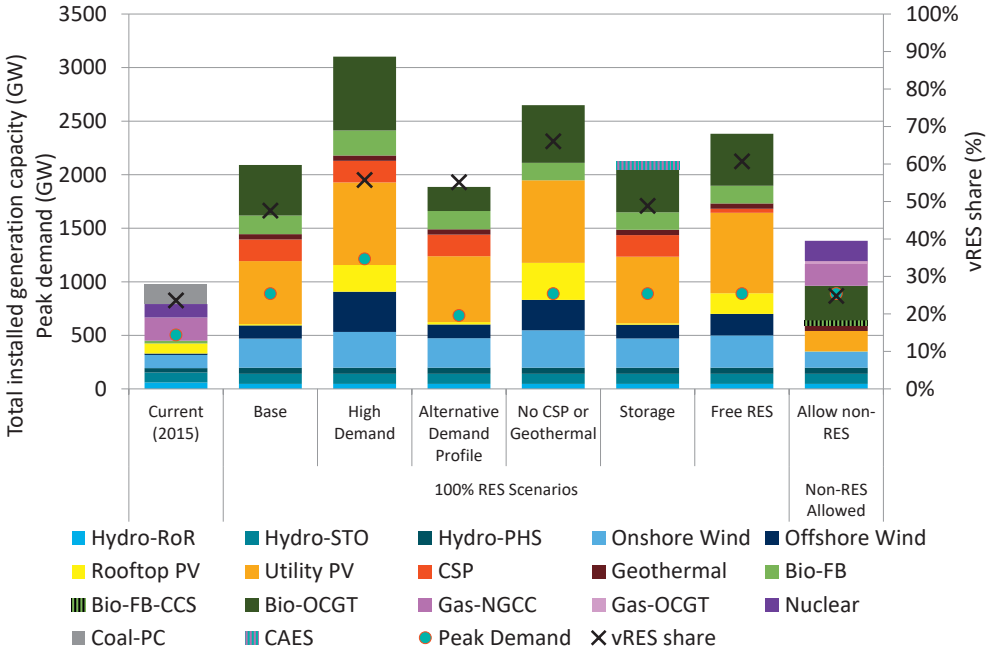

Figure 4-3 | Installed capacity of each technology per scenario in 2050, based on weather year 2010 (the lowest PV and wind supply). For comparison, the current (2015) installed capacity is also shown with coal, natural gas, PV and biomass shown as Coal-PC, Gas-NGCC, Rooftop PV, and Bio-FB respectively, based on ENTSO-E data (ENTSO-E, 2017b). Demand shedding capacity of 16 GW is not shown. The peak total system demand in each scenario is indicated by the '●' symbols (left axis) and the share of vRES capacity indicated by the '×' symbols (right axis).

and 200 GW of Gas-NGCC capacity. Approximately 50 GW of Bio-FB-CCS capacity is also installed as the net-negative emissions it generates allows this lower-cost Gas-NGCC capacity to be included in the portfolio without CCS.

In the 100% RES scenarios, onshore wind deployment ranges between 50% (*Base*) and 64% (*No CSP or Geothermal*) of its maximum potential (543 GW). Due to its higher cost, offshore wind deployment is modest in most RES scenarios at about 17% of its maximum potential (754 GW); however, deployment increases when demand is higher or CSP is excluded from the portfolio. With 65% (*Base*) to 85% (*High Demand*) of its total potential deployed (895 GW), Utility PV represents the largest share of installed capacity in all 100% RES scenarios – despite making no contribution to firm capacity. Due to its higher cost, rooftop PV is only installed in appreciable amounts in the *High Demand* and *No CSP or Geothermal* scenarios, once the best utility PV sites are exploited.

Turning to the dispatchable technologies, biomass plays a critical role in providing peak and load-following capacity in all 100% RES scenarios. This is evidenced by comparing the installed Bio-OCGT capacities in the *Base* (~470 GW) and *Alternative Demand Profile* (~220 GW)

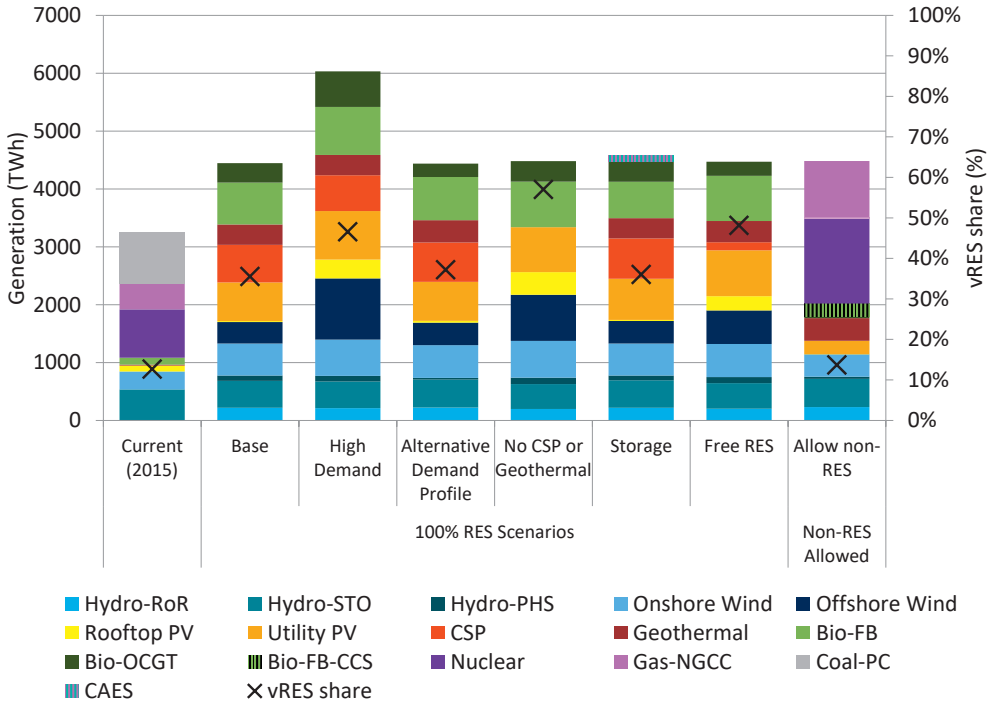

Figure 4-4 | Total generation by technology per scenario in 2050, based on weather year 2010 (the lowest PV and wind supply). For comparison, the current (2015) generation is also given with hydro (total), coal, natural gas, PV (total), wind (total) and biomass shown as Hydro-STO, Coal-PC, Gas-NGCC, Rooftop PV, Onshore Wind and Bio-FB respectively, based on ENTSO-E data (ENTSO-E, 2017b). The share of vRES generation is indicated by the '×' symbols (right axis). Note that the differences in hydro generation are due to the different dispatch results from the ST Schedule runs during the typical weeks,

scenarios, showing that with a lower peak demand and smoother demand profile, Bio-OCGT capacity is approximately 50% lower in the *Alternative Demand Profile* scenario. Meanwhile, Bio-FBs provide between 160 GW and 230 GW of load-following capacity in the 100% RES scenarios. When CSP capacity is optimised, only 38 GW is installed in the *Free RES* scenario and no capacity at all is installed in the *Allow non-RES* scenario. By contrast, geothermal capacity is fully exploited in all scenarios as with lower VOM costs and higher capacity factor, it is more competitive than CSP.

At the assumed cost of 700 € kW^{-1} (88 € kWh^{-1}), just under 80 GW (of CAES is installed in the S*torage* scenario, which displaces an equivalent amount of Bio-OCGT capacity. Total installed generation capacity increases by 30 GW (mostly PV) compared to the *Base* scenario in order to provide additional electricity for charging the storage, as there is no surplus (curtailed) vRES generation in any scenario which can be used to charge the storage[32].

4.3.3 Spatial capacity distribution

Figure 4-5 shows how the optimised generation capacity from the *Base* scenario is deployed across Europe. For the spatially optimised vRES technologies (wind and PV), Figure 4-6 shows how this capacity is distributed within each country at the grid cell level. Onshore wind capacity is mainly installed in countries bordering the North and Baltic seas in a band stretching from the British Isles to the Baltic countries. These locations are preferred due to favourable wind speeds, and their central location in Europe. Offshore wind is mainly installed in the North Sea due to the higher wind speeds (high capacity factors), and central location. PV capacity is spread across most countries. Within countries, capacity is installed either in southerly locations or close to the load centre to reduce costs. Less utility PV capacity is installed in the Iberian Peninsula than might be expected, as much of the suitable land area for vRES is already covered by the exogenous CSP capacity, leaving less room for utility PV. Furthermore, any additional PV capacity in this region would further increase the transmission needs between Spain and France (see section 4.2.2.3).

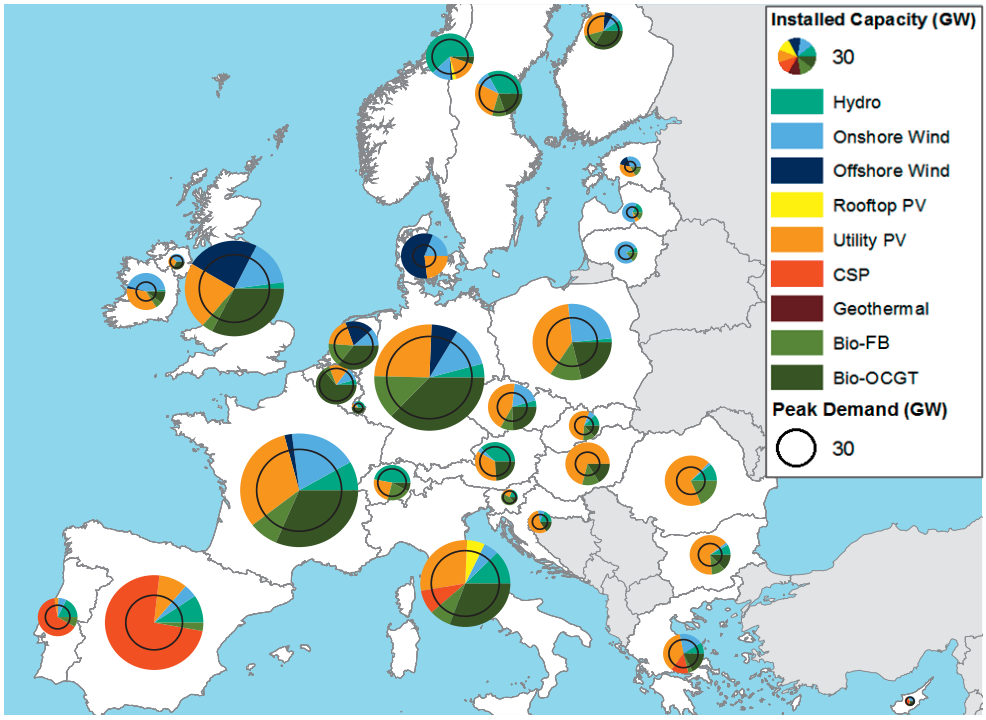

Figure 4-5 | Optimised generation capacity per technology in 2050 per country in the *Base* scenario, based on weather year 2010. The pie charts show the share of capacity per generation technology, while the area of the pie chart is proportional to the total installed capacity. The circles within each pie chart show the peak demand per country. Note that CSP, geothermal and hydro capacity is exogenous.

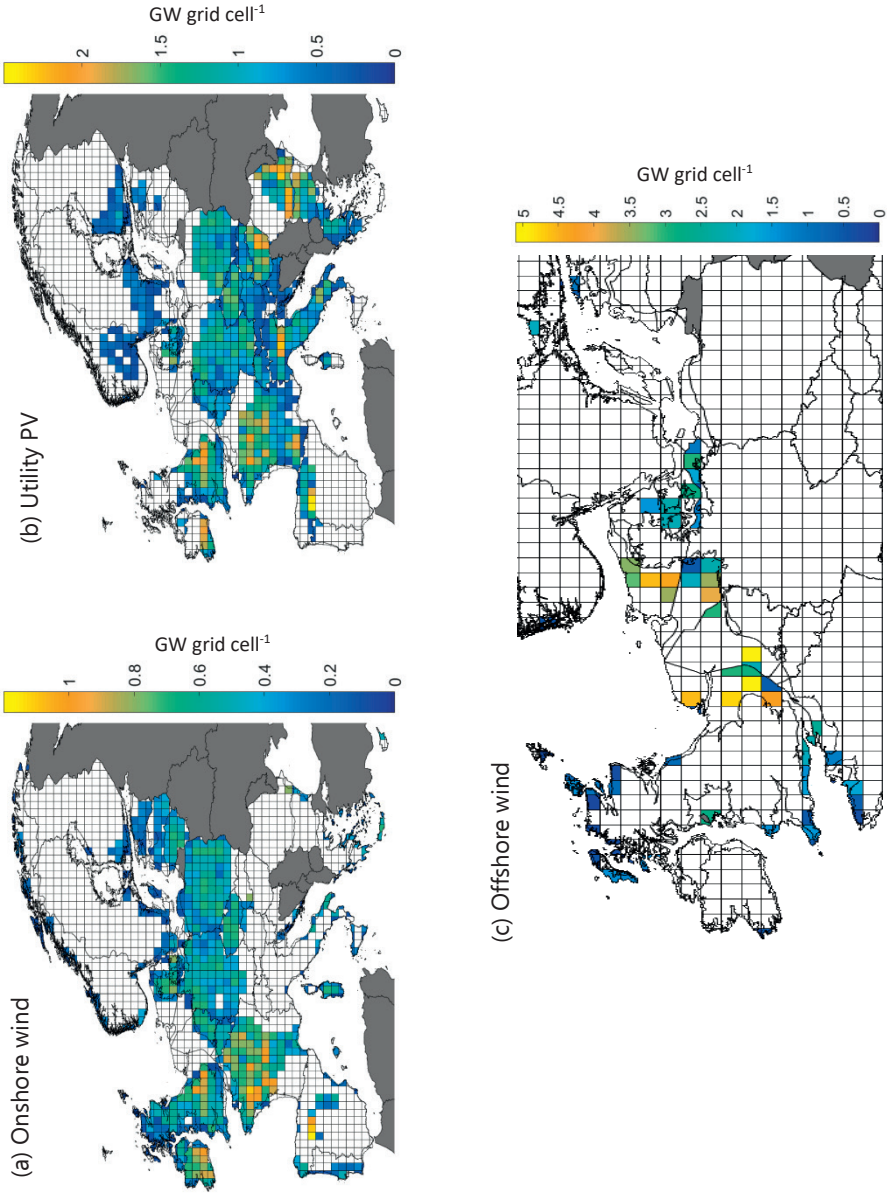

Figure 4-6 | Optimised 2050 spatial deployment of vRES generation capacity in the *Base* scenario in GW (grid cell)$^{-1}$ for **(a)** Onshore wind and **(b)** Utility PV, and **(c)** Offshore wind, based on the most challenging weather year 2010. Only a small amount of rooftop PV is installed in the *Base* scenario, and hence not shown. Note that in almost all cases, if the model installs capacity in a cell, it exploits the full potential per cell. Thus, any cell with capacity installed can be considered fully exploited.

4.3.4 Transmission requirements

The optimised transmission grid reinforcements (on top of the reference capacity of 60 GW) for each scenario are shown in Figure 4-7. In the scenarios including the 200 GW exogenous CSP capacity, reinforcements range from 321 GW and 416 GW, as the transmission corridors FR-ES, FR-DE, FR-BE, and IT-FR must be significantly reinforced to bring CSP generation from Iberia to the rest of Europe. However, when CSP capacity is optimised in the *Free RES* scenario, reinforcements fall to 142 GW due to the more optimal (lower) deployment of CSP. Thus, the exogenously defined CSP capacity has a significant impact on the configuration of the transmission network[33].

Very little additional transmission is built in the *Allow non-RES* scenario due to the lower vRES and no CSP deployment. In the *Storage* scenario, in which 77 GW of CAES are installed, transmission reinforcements only fall by 10 GW (3%) compared to the *Base* scenario. Thus, large-scale transmission expansion appears more cost-effective than utility-scale daily (8 hour) energy storage in balancing supply and demand, even when assuming optimistic reductions in future storage costs. One consequence of a fully interconnected power system is that the reliability of transmission becomes critical for ensuring system adequacy as, with a higher dependence on generators in neighbouring countries, the reliability of generators depends not only on availability, but also on the reliability of the transmission lines which deliver their electricity.

4.3.5 Hourly dispatch

Figure 4-8 shows the results of the ST Schedule hourly dispatch from the *Base* scenario for a typical summer week, while Figure 4-9 shows the hourly dispatch for a typical winter week. Comparing these two figures, we find that:

- Geothermal, Hydro-STO and Hydro-RoR provide baseload capacity throughout the year due to their high investment but relatively low marginal cost.
- Variable PV and wind generation fluctuates hourly, daily, and seasonally. While PV can usually be relied upon for significant daytime generation in summer, wind production is less reliable. While average wind generation tends to be higher in winter, Figure 4-9 shows that there can be periods of low wind generation, even in winter.
- CSP plays a significant role in covering night-time demand during the summer, but cannot provide the same level of coverage in winter due to the lower DNI received.
- Biomass plays quite different roles in summer and winter. In summer, Bio-FB and Bio-OCGT capacity is cycled daily in order to meet peak evening demand, once generation from PV and CSP has ceased. In winter, Bio-FBs are used to provide baseload capacity while day- and night-time peaks – mainly caused by EVs – are met by Bio-OCGTs.

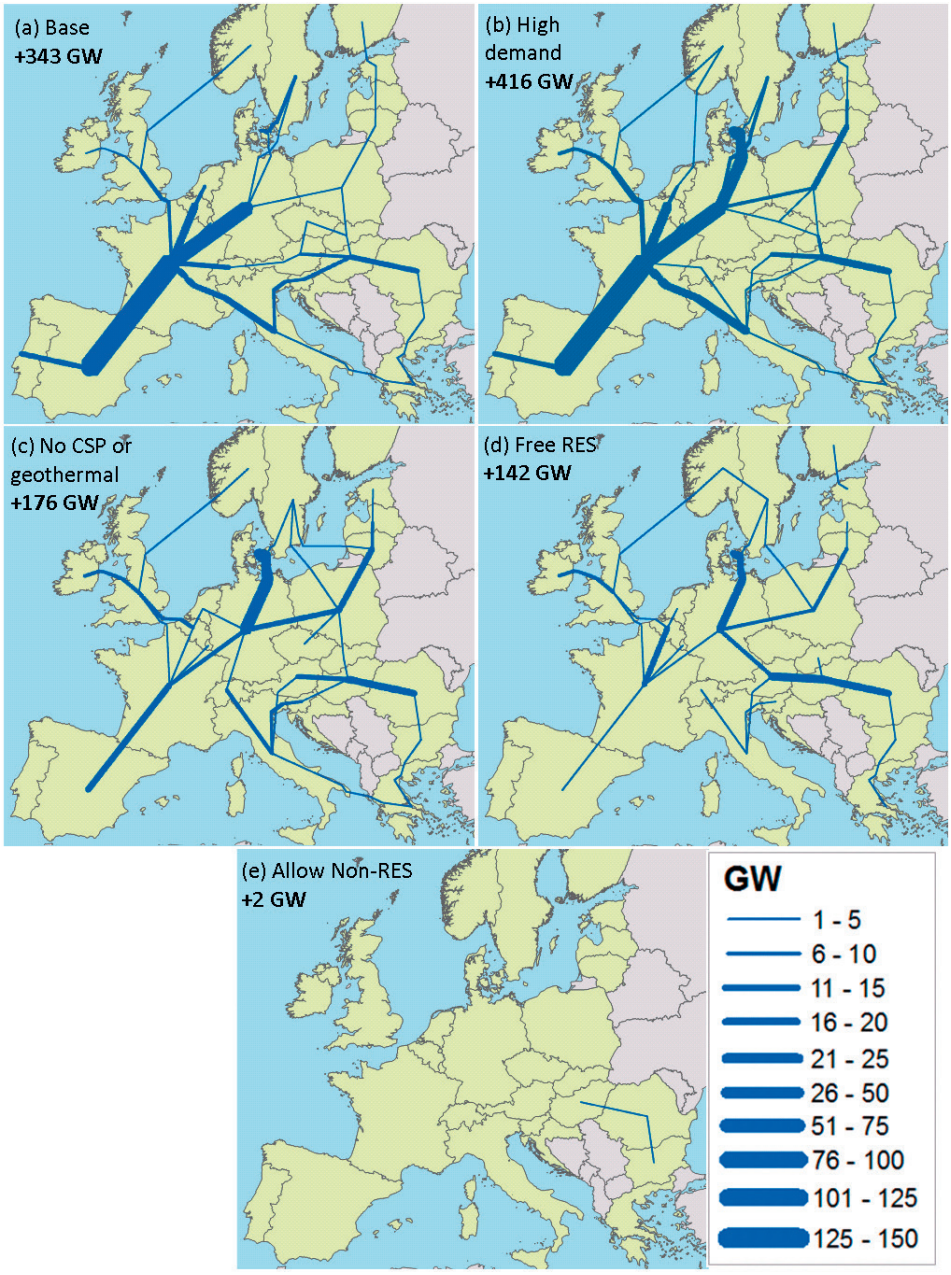

Figure 4-7 | Transmission grid reinforcements (on top of capacity installed in 2016) for the **(a)** *Base*, **(b)** *High demand*, **(c)** *No CSP or Geothermal*, **(d)** *Free RES* and **(e)** *Allow non-RES* scenarios. Although the total installed capacity is lower, the grid topology for the *Storage* (+334 GW) and *Alternative Demand Profile* (+321 GW) scenarios are similar to the *Base* scenario and hence not shown. The reference current transmission capacity (60 GW) is not included in the figures.

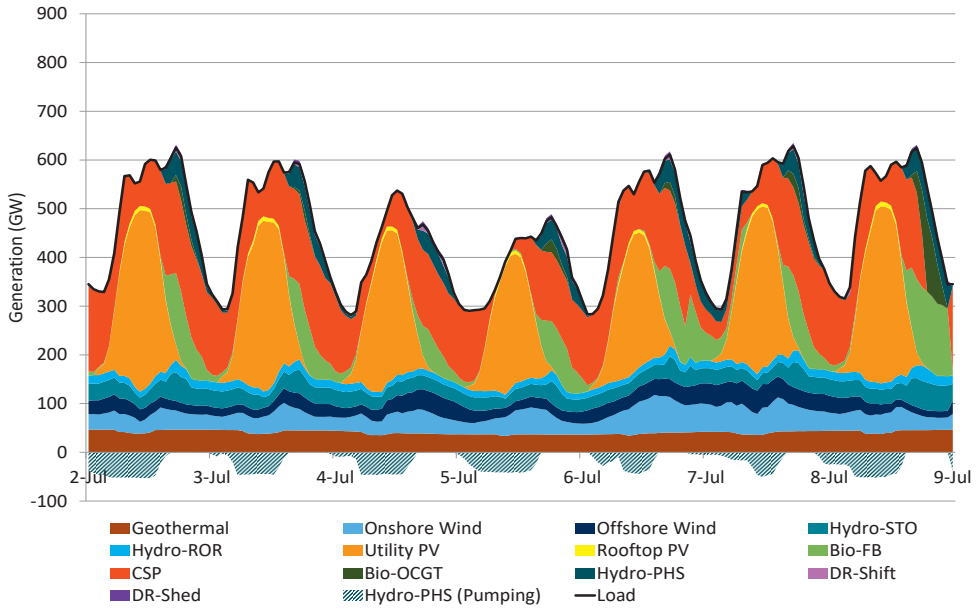

Figure 4-8 | Hourly dispatch for a typical summer week from the *Base* scenario, based on weather year 2010. Electricity demand for hydro pumping is shown as negative below the horizontal axis

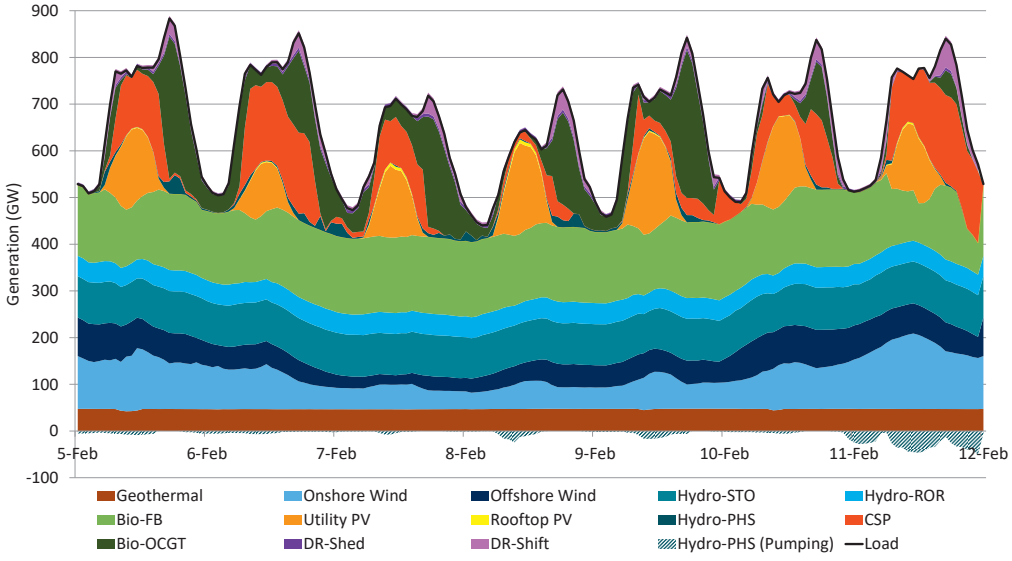

Figure 4-9 | Hourly dispatch for a typical winter week from the *Base* scenario, based on weather year 2010. Electricity demand for hydro pumping is shown as negative below the horizontal axis.

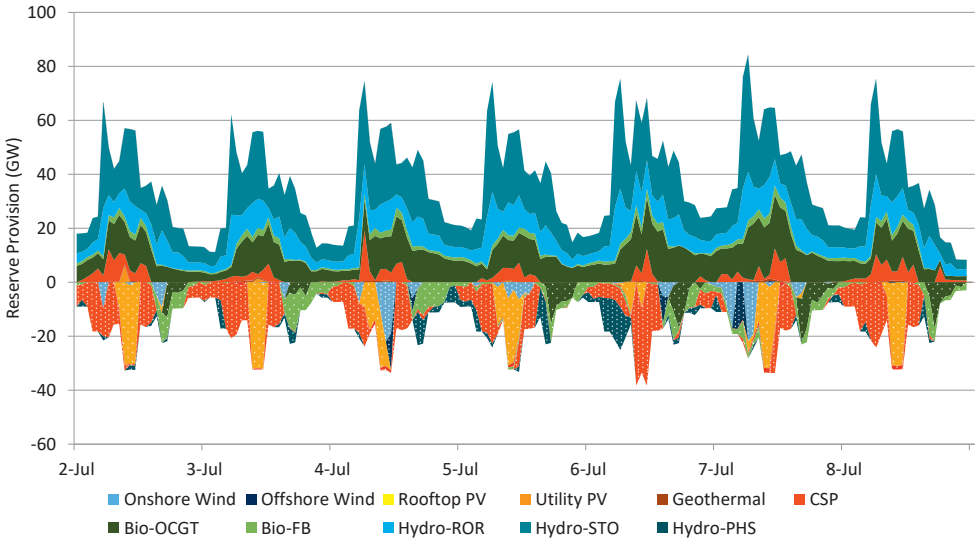

Figure 4-10 | Hourly reserve provision by generator type for a typical summer week from the *Base* scenario, based on weather year 2010. Positive values indicate total up-regulation reserves (spin-up plus stand-up), while negative values indicate down-regulation (spin-down) reserves.

- DSM is used extensively to both shift and curtail demand during peak evening hours, particularly in winter. Hydro-PHS plays a similar role to Bio-OCGTs in providing flexible peak generation during evening hours, especially during summer when electricity from PV can be used for pumping during the day.

Due to the imperfect forecasting of demand and vRES generation, operating reserve requirements in a 100% RES power system with a high vRES share would be higher than today. An example of this is given in Figure 4-10, which shows the provision of operating reserves by each generator type during the same typical summer week shown in Figure 4-8. Spin-up reserves are mainly provided by hydro and CSP, with Bio-OCGTs providing the majority of stand-up reserves. Down-regulation reserves are provided mainly by CSP and vRES, though practically all technologies contribute some down-regulation during the year.

4.3.6 Biomass utilisation

Total demand for biomass in the 100% RES scenarios ranges from 8.5 EJ in the *Base* scenario up to 12.9 EJ in the *High Demand* scenario. In 2015, Europe produced approximately 5 EJ of biomass for energy purposes, of which only 38% or 1.9 EJ was used in the production of electricity (Eurostat, 2017a)[34]. Thus, a 100% RES system would require significant increase in power sector biomass use compared with today. Figure 4-11 gives the consumption of biomass by fuel type for the *Base* and *High Demand* scenarios, showing that it is mainly lower

cost feedstocks (e.g. primary agricultural residues, secondary forestry residues) which are used, with minimal exploitation more costly energy crops (e.g. willow and poplar). By contrast, all available biogas substrates are used, and the model is forced to draw on additional high-cost biogas feedstock – beyond the assumed maximum potential – in order to achieve a feasible solution. The quantity of additional biogas substrate varies from 0.13 EJ in the *Base* scenario, up to 3.4 EJ in the *High Demand* scenario. While the additional 0.13 EJ of substrate used in the *Base* scenario is relatively small and total biogas feedstock use (1.5 EJ) lies within the range of potentials reported in the literature[35], the 4.7 EJ of additional biogas substrate required in the *High Demand* scenario far exceeds reported potentials[36].

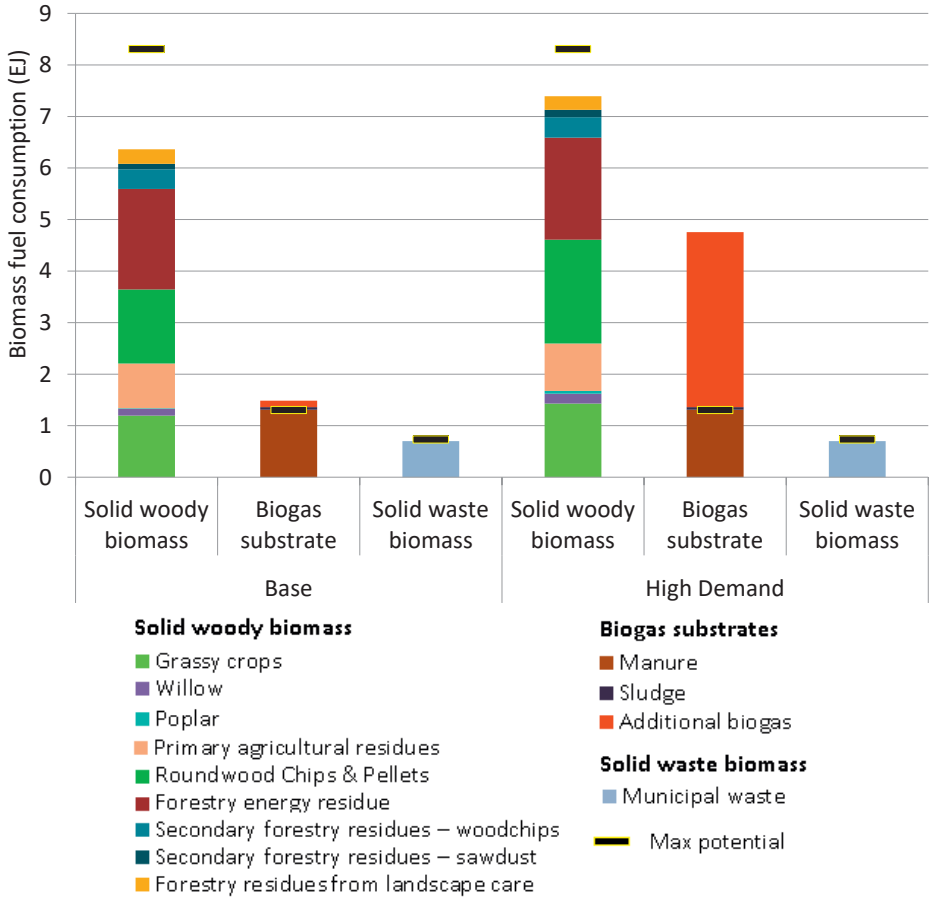

Figure 4-11 | Breakdown of biomass consumption by fuel type for the *Base* and *High Demand* scenarios for weather year 2010. The maximum potential per fuel category is indicated by black horizontal bars. The graph shows that while solid biomass availability is sufficient, 0.13 EJ of additional biogas is required in the *Base* scenario than is available, rising to 3.4 EJ in the *High Demand* scenario

4.3.7 Total cost

In terms of total system costs, Figure 4-12 shows how each scenario performs on an annualised basis, and in terms of the specific cost of electricity[37]. Comparing the costs of all scenarios we draw several conclusions:

- Total system costs in the *Base* scenario, and indeed most of the 100% RES scenarios, are similar at approximately 560 €bn y^{-1}.
- The exogenous CSP capacity of 200 GW is not optimal as it forces up transmission costs, and squeezes lower-cost wind and PV capacity out of the portfolio. As shown by the *Free RES* scenario, a lower capacity (~40 GW) would require far less land area and would be more cost-effective, with costs falling to 530 €bn y^{-1}.
- Allowing non-RES technologies in the portfolio sees costs fall to approximately 410 €bn y^{-1}, or 22% cheaper than the lowest-cost 100% RES scenario.
- The costs of a 100% RES power system increase relatively more (approximately 1.4x) with higher demand, as a 36% increase in demand in the *High Demand* scenario leads to a 50% increase in costs compared with the *Base* scenario. This is due to the higher capacity required, use of more costly biomass sources, a greater need for more costly

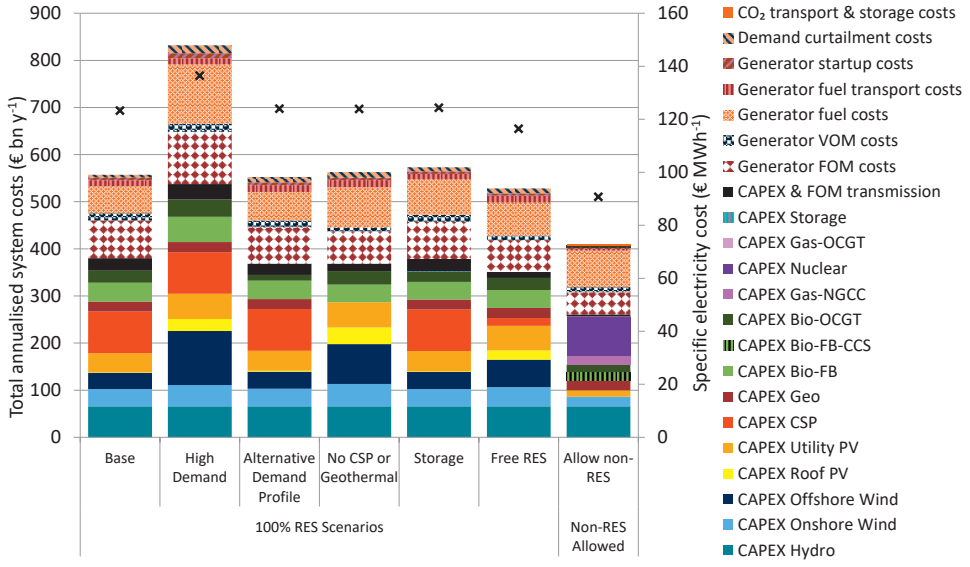

Figure 4-12 | Total annualised power system costs in 2050 for each scenario, based on weather year 2010. The total annualised costs for each scenario are shown on the left axis, while the specific electricity cost is indicated by the '×' symbols on the right axis. Some costs elements such as CAPEX and FOM cost for DSM, reserves, and the cost of unserved energy are relatively small (< 3 €bn y^{-1}) and hence not shown. Transmission costs from vRES to the country node centres are included in the vRES CAPEX costs. While existing hydro is specified exogenously in all scenarios and not built by the model, we include the costs here for completeness.

peaking generators, a shift to offshore wind, and the need to install wind and PV at less optimal sites[38].

- A 100% RES system is possible without CSP and geothermal, but may be more expensive.
- At a cost of 700 € kW^{-1} (88 € kWh^{-1}), daily storage results in negligible cost benefits compared to the *Base* scenario as the savings in Bio-OCGT and transmission costs are offset by the investment costs for the storage and additional generation capacity.
- Given that Europe currently spends in the order of 300 to 400 €bn y^{-1} for an electricity demand of some 3100 TWh y^{-1} (Brown et al., 2018), a 100% RES power system costing 530 €bn y^{-1} and delivering 4400 TWh y^{-1} would be more expensive than the current system, but not unaffordable[39].

4.3.8 Sensitivity analysis

So far, we have shown what different demand levels and technology availability would mean for a 100% RES power system. To provide a cost comparison, we also present one scenario in which non-RES technologies are allowed in the portfolio. However, given uncertainty in future fuel costs, and the fact that based on data from two nuclear plants currently under construction in Europe the cost of nuclear may be significantly higher, comparing the costs of a 100% RES system with this single non-RES scenario may not be realistic[40]. Thus, we perform some additional model runs based on the *Allow non-RES* scenario with:

- 27% higher nuclear CAPEX (6800 € kW^{-1});
- a higher CCS carbon capture rate of 100%, in the event that the assumed 90% CO_2 capture rate may be a limiting factor for CCS deployment at high decarbonisation levels;
- a 50% lower coal price (1 € GJ^{-1});
- a 50% lower natural gas price (3.5 € GJ^{-1}); and
- a 53% higher natural gas price (10.7 € GJ^{-1})[41].

Figure 4-13 shows the optimised generation portfolios for the sensitivity runs, as well as the original *Allow-Non-RES* scenario for comparison. With a higher nuclear CAPEX, nuclear disappears from the portfolio and is replaced by a mix of vRES, natural gas (OCGT, NGCC and NGCC-CCS) and additional Bio-FB-CCS capacity, which offsets the additional emissions from gas. Lower coal and natural gas prices also see nuclear disappear from the portfolio, and replaced by Coal-PC-CCS and Gas-NGCC-CCS capacity respectively. Assuming full CO_2 capture for CCS technologies replaces some nuclear capacity replaced by Gas-NGCCs, and approximately 50% of Bio-OCGTs replaced by Gas-OCGTs. In all sensitivity runs, Bio-FB-CCS plays an important role in offsetting CO_2 emissions from natural gas and coal plants, both with and without CCS.

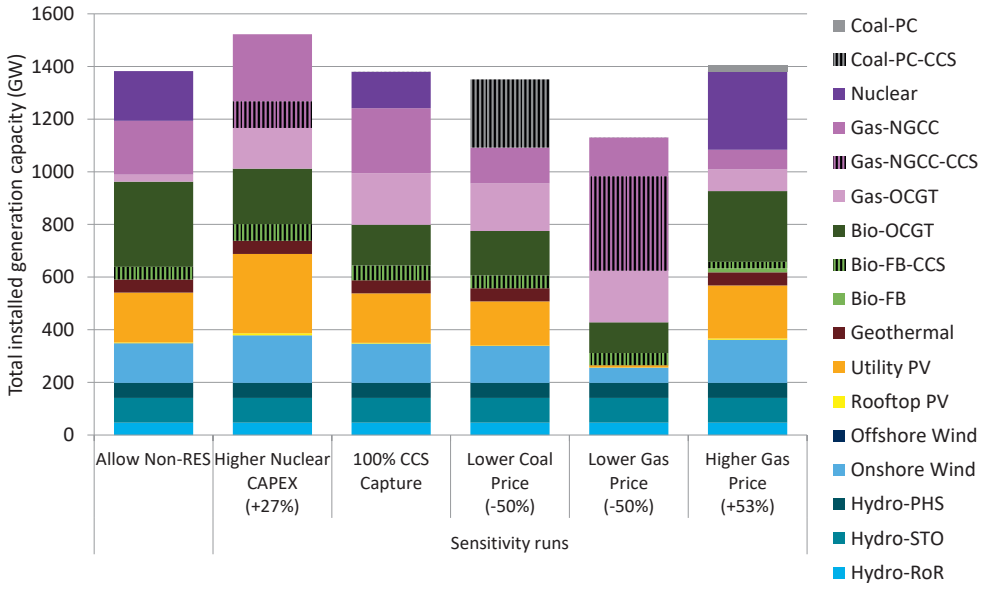

Figure 4-13 | Total installed generation capacity in 2050 in the sensitivity analysis runs based on weather year 2010. The optimised portfolio from the *Allow Non-RES* scenario is shown again for comparison.

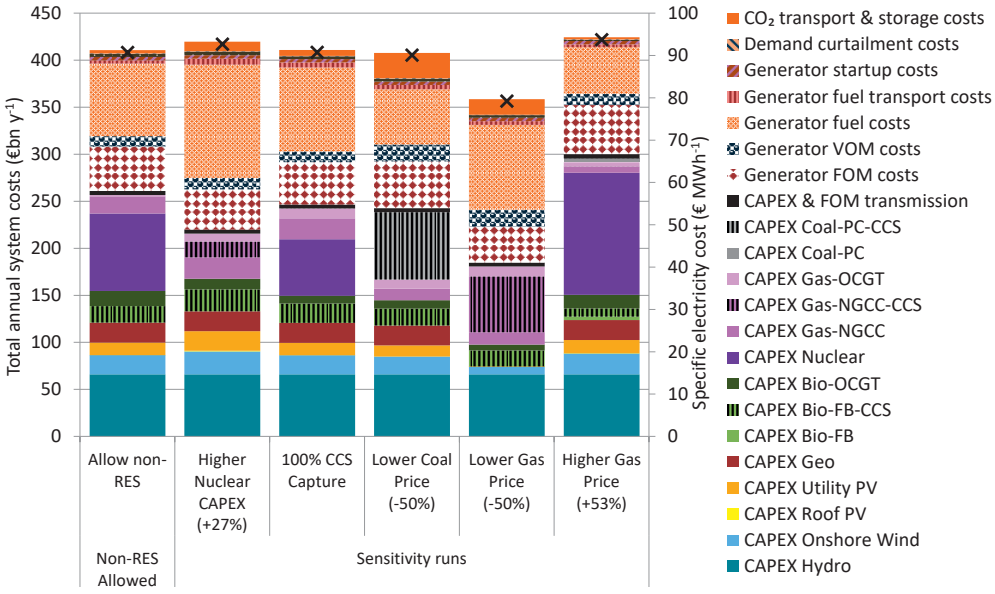

Figure 4-14 | Total annualised power system costs in 2050 for each sensitivity run, based on weather year 2010. The optimised portfolio from the *Allow non-RES* scenario is shown again for comparison. The total annualised costs for each run are shown on the left axis, while the specific electricity cost is indicated by the '×' symbols on the right axis.

In terms of total annualised costs, Figure 4-14 shows that almost all sensitivity runs have similar costs to the *Allow Non-RES* scenario of approximately 410 €bn y^{-1}, despite their different generation portfolios. The reason for this is that under a tight emissions constraint, trying to replace high-cost (but zero-carbon) baseload nuclear capacity from the portfolio with lower-cost Coal-PC-CCS, Gas-NCCC, or Gas-NCCC-CCS is not effective as some high-cost Bio-FB-CCS must also be installed to offset the higher emissions from gas or coal (even with CCS), and any additional CCS capacity (from either fossil fuels or biomass) leads to a concomitant increase in CO_2 transport and storage costs. As a result, total costs are not sensitive to the makeup of the portfolio, and we conclude that 410 €bn y^{-1} is a reasonable figure for benchmarking the cost of a 100% RES power system with a non-RES alternative.

4.4 Discussion

4.4.1 Deployment trajectories to 100% RES

In this study we demonstrate that in 2050, Europe's electricity needs could be met by a 100% RES power system with the same level of system adequacy as today. However, we have not considered whether such a transformation is possible by 2050.

Figure 4-15 shows the historical deployment of wind capacity in the EU28 countries, and linear deployment trajectories required to reach the 2050 installed capacity in each of our 100% RES scenarios[42]. From a starting capacity of 141 GW in 2016, if the current level of net wind deployment continues at approximately 10.5 GW y^{-1} (based on the average annual installations between 2007 and 2016), the installed capacity in 2050 would be sufficient for the majority of the 100% RES scenarios[43]. In fact, the 2050 levels for the *Base*, *Alternative Demand Profile* and *Storage* scenarios could even be achieved with a lower deployment of 7.5 GW y^{-1}. Only in the absence of CSP and Geothermal, or a very large increase in demand, would installations need to rise to 14 GW y^{-1} or 17 GW y^{-1} respectively. Given that nearly 13 GW of wind was installed in 2015, even these higher levels seem achievable. Turning to PV in Figure 4-16, recent deployment levels in the EU have been erratic and in 2016, the 6.1 GW of capacity installed was far below the high of 22 GW achieved in 2011. If the installed capacity from the period 2008-2016 is extrapolated (an average of 10.5 GW y^{-1} net PV installed annually), the installed capacity in 2050 would not be sufficient for any of the 100% RES scenarios. In order to achieve the 2050 capacity in the *Base* (lowest) scenario, average annual PV deployment would need to increase to 15 GW y^{-1} for every year until 2050, rising to 25 GW y^{-1} for the *Free RES* scenario, and 30 GW y^{-1} for the *No CSP or Geothermal* scenario. While ambitious, given that 22 GW of PV was installed in Europe in 2011, these levels could be achievable (GWEC, 2017). Thus, we assert that sufficient wind and PV capacity could be deployed by 2050 to support a 100% RES power system.

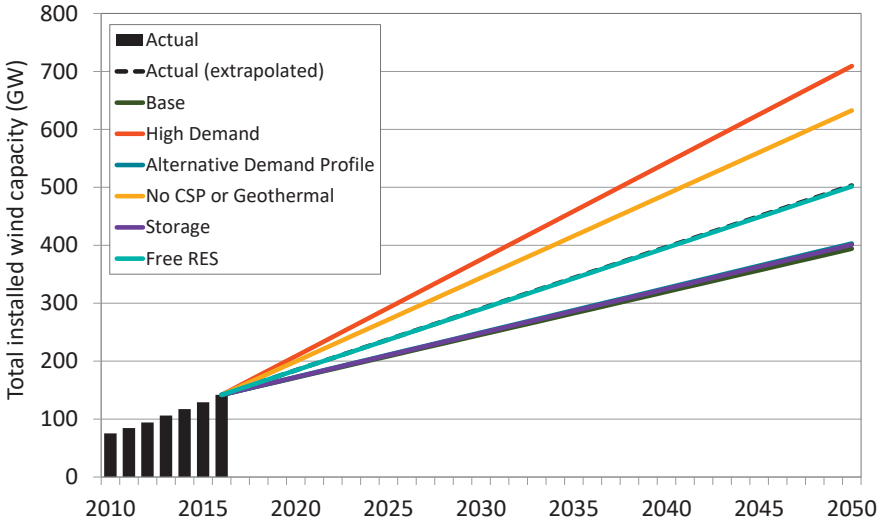

Figure 4-15 | Cumulative deployment of total (onshore + offshore) installed wind capacity in the EU28, showing the linear trend required to reach the installed 2050 capacity in each 100%RES scenario from this study. The dashed line (hidden behind the *Free RES* scenario) shows the linear extrapolation of deployment until 2050, assuming annual installations based on the average for the years 2007 to 2016 (10.6 GW y^{-1}), taken from GWEC (GWEC, 2017). The *Base* and *Alternative Demand Profile* scenario trajectories are hidden behind the *Storage* scenario.

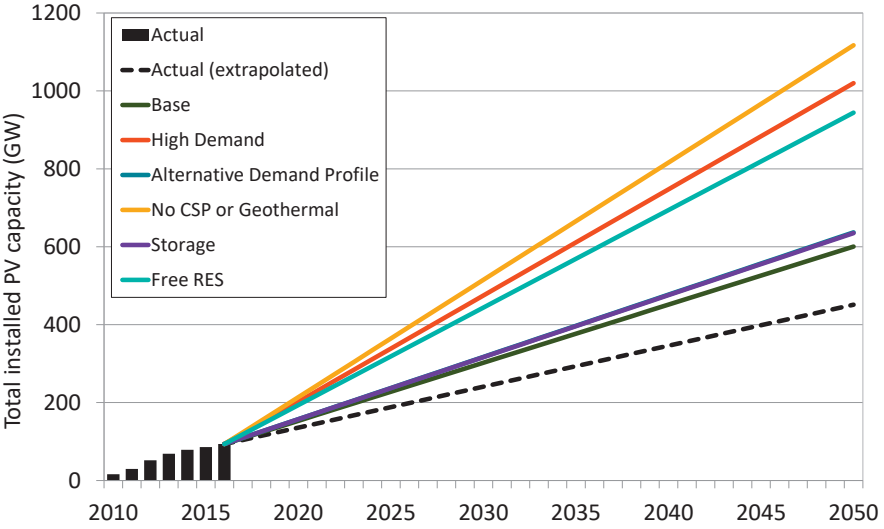

Figure 4-16 | Cumulative deployment of total installed PV capacity in the EU28, showing the linear trend required to reach the installed 2050 capacity in each 100% RES scenario from this study. The dashed line shows the linear extrapolation of deployment until 2050, assuming annual installations based on the average for years 2008 to 2016 (10.5 GW y^{-1}) taken from EurObservER (EurObserv'ER, 2017). The trajectory of the *Alternative Demand Profile* scenario is hidden behind the *Storage* scenario.

However, unlike wind and PV which have significant capacity already installed and are currently experiencing growth, the total installed capacities of solid biomass, biogas, CSP and geothermal in 2015 were only 18 GW, 10 GW, 2.3 GW and 0.8 GW respectively, with recent deployment rates not exceeding 1 GW y^{-1} for any technology (Eurostat, 2017b). In order to reach the installed 2050 capacities in the *Base* scenario, installations of CSP and geothermal capacity would need to average 6 GW y^{-1} and 1.4 GW y^{-1} respectively every year from 2016 to 2050, which has never been demonstrated. Biomass presents an even greater challenge, with annual capacity additions needing to average between 4 GW y^{-1} (*Free RES*) and 6 GW y^{-1} (*High Demand*) for solid biomass, and between 6 GW y^{-1} (*Alternative Demand*) and 19 GW y^{-1} (*High Demand*) for biogas[44]. Even though we show that a 100% RES system is possible without CSP or Geothermal, the infeasibility of the *No Biomass* scenario and large-scale deployment of biomass in the remaining scenarios demonstrate the vital role of bioelectricity in a 100% RES power system as a provider of flexible firm capacity.

In addition to generation capacity, we showed in Section 4.3.4 that cross-border transmission capacity would need to increase by between 142 GW (*Free RES*) and 416 GW (*High Demand*) from the 60 GW installed today, in order to support a 100% RES power system. Given that 58 GW of additional cross-border transmission is currently being planned for commissioning by the 2030s, an additional 84 GW – in line with the *Free RES* scenario – seems achievable by 2050[45]. However, realising the transmission network in the *High Demand* scenario would require 10 GW y^{-1} of new transmission capacity to be installed every year from 2016 until 2050. This seems highly unlikely, given that new interconnectors take several years to plan and build.

4.4.2 Caveats and limitations

By modelling alternative scenarios in our study and performing selected sensitivity analysis, we explore how other assumptions in demand and technology developments would affect our results. Nevertheless, modelling the future is inherently uncertain and our results should be seen in the context of the following uncertainties:

- Different **cost developments** for the different generation technologies would affect both the makeup of the optimised RES portfolios, and their competitiveness with non-RES alternatives. While the costs of vRES have fallen rapidly in recent years, vRES CAPEX costs would need to fall by a further 70% from the base levels (which already assume significant reductions compared to today), in order for the total costs in the *Free RES* scenario to reach parity with the *Allow non-RES* scenario in 2050.

- Our results show that biomass would play a critical role in 100% RES power system in 2050. However, the **future cost and potential supply of biomass** in 2050 are uncertain, and will depend on future rainfall patterns, agricultural practices, and demand from other sectors. Biomass imports from outside Europe, precluded from

this study, would also be possible; however, a 100% RES power system relying on biomass for firm capacity would be vulnerable to what is ultimately a scarce and relatively expensive fuel.

- The quality of our results is underpinned by the quality of the **vRES generation profiles**, which depend first on the accuracy of the underlying weather dataset, and secondly on the methods used to derive generation profiles from the raw meteorological parameters. Both may have resulted in an overestimate of system adequacy:

    - Firstly, the period covered by ERA-Interim (1979-present) is one in which the winter North Atlantic Oscillation (NAO) more often exhibited a positive phase than a negative phase, resulting in above average wind speeds and temperatures in most of Europe (Beranová & Kyselý, 2013; Commin et al., 2017; Jerez, Trigo, Vicente-Serrano, et al., 2013). However, as our study is based on the worst-case year with the NAO in its negative phase, our results are not affected.

    - Secondly, linearly interpolating the 3-hourly temporal resolution of ERA-Interim to hourly values may make wind and PV generation profiles smoother than they would be in reality. However, the impact of this is likely to be small in comparison to the local smoothing which occurs at individual sites (Norgaard & Holttinen, 2004), and large-scale spatial smoothing across Europe (Albadi & El-Saadany, 2010).

- The long-term impact of **climate change** on Europe's weather patterns is also uncertain. However, recent studies suggest that, at the continental scale, these impacts are likely to be small (Jerez, Tobin, et al., 2015; Tobin et al., 2015).

Due to time and research constraints the following aspects could not be considered and remain areas for further research:

- Our assessment of reliability study considers only **system adequacy**, not system security. Thus, without performing transient stability analysis, we do not know how a 100% RES system would perform under transient conditions and what facilities would be required to maintain security (e.g. synthetic inertia, Flexible Alternating Current Transmission Systems (FACTS) (Brown et al., 2018; JRC, 2014; Yan et al., 2015)). However, by modelling reserves we do ensure that sufficient capacity is available to cover forecast errors and sudden generator loss.

- We do not consider the low-voltage **distribution grid** which would need to be upgraded to bring electricity from PV and biogas plants to the wider power system[46]. Enhanced self-consumption with local storage could reduce distribution upgrades for PV (Alam et al., 2013), but biogas must provide peak supply and balancing for the wider system.

- We consider only snapshots of possible 100% RES power systems in 2050, **without considering the transition** from the existing system in detail[47]. Thus, we do not consider whether the cumulative emissions trajectories to reach the 100% RES scenarios in 2050 would fit within Europe's allowable carbon budget to limit global warming to 2°C, nor do we explore more ambitious decarbonisation efforts (beyond 2°C and preferably below 1.5°C) in light of the Paris Agreement. However, any of the 100% RES scenarios could be made net-carbon-negative by equipping some of the Bio-FB capacity with CCS.

- We assume constant **availability of biomass**, while in fact biomass availability fluctuates with the seasons, harvest times, and rainfall[48]. Security of biomass supply could be improved by stockpiling biomass, but this would incur some costs for additional storage and treatment (e.g. torrefaction (W. H. Chen et al., 2015)) to stabilise the biomass, minimise degradation and methane emissions during storage (Alakoski et al., 2016; Röder et al., 2014).

- We model **biogas production and supply** as fully flexible; however, current AD processes have limited flexibility (Hahn, Ganagin, et al., 2014). Flexibility can be improved with storage (either on-site storage, or upgraded gas which is injected and stored in the gas network) or more flexible AD processes (Hahn, Krautkremer, et al., 2014). However, storage can be limited for safety reasons, and not all countries have an extensive gas pipeline network[49].

- We do not account for a potential increase in **indirect GHG emissions**, particularly from biomass. However, rough calculations suggest that indirect emissions from most 100% RES scenarios would be approximately 100 Mt CO_{2eq} y^{-1}: 70% higher than the indirect emissions from the current power system, or approximately 9% of the direct GHG emissions saved by converting to a 100% RES system. These could be offset by equipping approximately 10% of the Bio-FB capacity with CCS.

- **Additional technology options** such as hybrid generators, co-firing, and seasonal storage (e.g. power-to-gas) to reduce costs and/or the reliance on biomass have not been considered[50].

- In power systems with high penetrations of vRES generators, an energy-only market based on marginal-cost pricing may not provide sufficient revenues for generators to cover their costs (Brouwer, Van den Broek, et al., 2016). Thus, any 100% RES power system would need to be supported by an open[51] **electricity market environment** which ensured generators were remunerated adequately. Scarcity pricing and capacity remuneration mechanisms are two possible ways to make up for this revenue shortfall (Hu et al., 2018; Jacobs et al., 2016), but neither have been proven at the European scale.

- Lastly, we do not consider the impacts of **social acceptance on costs**. For example, public opposition to overhead transmission lines and onshore wind could be mitigated by using underground cables, and shifting wind turbines offshore (Batel et al., 2013; Cohen et al., 2014; Mester et al., 2017)[52]. Shifting nuclear and CCS offshore could also make these technologies more palatable for the public (Buongiorno et al., 2016; Lipponen et al., 2017); however, offshore real estate is limited, and the cost and environmental consequences of shifting so much infrastructure offshore are likely to be significant.

4.5 Conclusion

In this study, we model seven scenarios for a fully renewable European power system in 2050 and explore the impact of uncertainties in future demand and technology availability. We find that a 100% RES European power system could operate with the same level of system adequacy as the current power system, even when relying only on domestic European sources in the most challenging weather year. However, based on our scenarios, realising such a system by 2050 would require:

- massively expanding generation capacity to at least 1.8 TW (based on the *Alternative Demand Profile* scenario), compared to the 1 TW installed today;
- expanding cross-border transmission capacity by at least ~140 GW (based on the *Free RES* scenario) from current levels (60 GW), with the consequence that Europe becomes much more dependent on the reliability of its cross-border transmission capacity;
- the well-managed integration of HPs and EVs into the power system (in response to the electrification of heating and transport) through smart charging and other demand-side technologies, in order to reduce peak demand and required OCGT capacity;
- the implementation of energy efficiency measures to prevent a massive increase in electricity demand (on top of that expected from HPs and EVs) in order to reduce demand for biomass, and keep the deployment rate of new transmission and generation capacity manageable by 2050;

- wind deployment levels of at least 7.5 GW y^{-1} to be maintained (currently 10.6 GW y^{-1}) while PV deployment to increase to at least 15 GW y^{-1} (currently 10.6 GW y^{-1}) until 2050 (based on the *Base* scenario);
- the large-scale mobilisation of Europe's biomass resources, with power sector biomass use reaching at least 8.5 EJ (4.5 times higher than today's 1.9 EJ) in the most challenging year (based on the *Base* scenario*)*; and,
- increasing solid biomass and biogas capacity deployment to at least 4 GW y^{-1} and 6 GW y^{-1} respectively every year until 2050 (based on the *Alternative Demand Profile* scenario).

In addition to these requirements, we find that:

- even when wind and PV are placed in the optimum locations, the total annualised costs of a 100% RES power system would be at least 530 €bn y^{-1} (based on the *Free RES* scenario), which are only slightly affected by the makeup of the generation portfolio;
- a 100% RES power system would be approximately 30% more expensive than a power system in which nuclear or CCS technologies are included; and,
- the costs of a 100% RES power system increase relatively more with higher demand, as a 36% increase in demand in the *High Demand* scenario increases costs by 50% compared with the *Base* scenario, as costlier biomass fuels and less optimal vRES sites must be exploited.
- a 100% RES system may not deliver the level of emission reductions necessary to achieve Europe's climate goals by 2050, as negative emissions from biomass with CCS may still be required to offset an increase in indirect GHG emissions, or to realise more ambitious decarbonisation pathways.

Future research should investigate the flexibility of biogas production, system adequacy under different rainfall years, the dispatchability of RoR hydro generators and seasonal availability of water, the potential role of seasonal storage, heat-electricity sector coupling, system security, and the market conditions necessary to support a 100% RES power system.

Footnotes to Chapter 4

[1] Several other scenario studies have also been published for the European power system in 2050 (Eurelectric, 2009; Haller et al., 2012; Heller et al., 2013; McKinsey, 2010; PwC et al., 2010; WWF, 2013), but these are not discussed as they report insufficient technical detail, or do not approach 100% RES.

[2] Brown et al. also propose the two additional criteria that the power system should not rely on fuel sources which will be exhausted within a few decades, or on unproven technologies. Other authors (e.g. Deane et al. (Deane et al., 2015)) have evaluated power systems according to their own feasibility framework.

[3] ENTSO-E uses this definition in the Continental Europe Operation Handbook (2004) (UCTE, 2004), however more recently, ENTSO-E defines another term – s*ecurity of supply* – as "*the ability of a power system to provide an adequate and secure supply of electricity in ordinary conditions*" which is similar to reliability (ENTSO-E, 2016c). The main distinction between system adequacy and security is that security refers to the short-term operation of the power system (e.g. resilience to generator outages, transmission faults), whereas adequacy refers to long-term operation. System adequacy can also be divided into generation adequacy, and transmission adequacy (EC, 2014c).

[4] For example, in (ECF, 2010a), it was found that in addition to the base RES capacity (1790 GW), 215 GW of natural gas turbines were required for back-up and balancing. However, accounting for this gas use reduced the share of RES to 97% and meant the target of 95% decarbonisation was not met. While noting that this natural gas could be replaced by biogas or renewable hydrogen, the consequences and costs of these options were not fully explored. Thus, neglecting analysis with PSM leaves uncertainty as to whether the system would actually work, whether emission reductions can really be achieved, and at what cost.

[5] PLEXOS (version 7.2) is developed by Energy Exemplar (http://www.energyexemplar.com/)

[6] Despite the UK's decision in 2016 to leave the European Union, its power system is likely to remain integrated with that of continental Europe. While part of the Continental European network, we exclude the Balkan states due to a lack of data.

[7] Built using the software ArcGIS Pro from ESRI. (http://www.esri.com/)

[8] ERA-Interim is a global atmospheric reanalysis produced by the European Centre for Medium-Range Weather Forecasts (ECMWF) covering 1979 to the present (2017) and includes 3-hourly data on wind speed, solar radiation, and temperature (Dee et al., 2011; ECMWF, n.d.). The spatial grid in this study is built to match that of ERA-Interim, which has a resolution of 0.75° x 0.75° (approximately 50 km).

[9] The Vision 4 profile was developed for the year 2030 assuming lower penetration of HP and EVs than our Base profile, and includes the effects of smart EV charging and other demand-side technologies which the Base profile does not.

[10] We exclude ocean (tidal and wave) energy (Magagna, 2015; Magagna & Uihlein, 2015) and osmotic power (derived from salinity gradients) (Jia et al., 2014) as their slow growth makes it unlikely for them to produce significant amounts of electricity by 2050.

[11] Even though BECCS uses renewable biomass, we consider any technology using CCS as non-renewable as the potential for CO_2 storage, while significant (~117 Gt CO_2), is finite (EU GeoCapacity Project, 2009).

[12] The cost of capital can vary significantly between countries and between technologies (Noothout et al., 2015). We choose 8% as a common value used in similar energy and PSM studies, assuming that perceived risks for renewable investments are likely to fall in the future (Trutnevyte, 2016). This is higher than the reference financial and social discount rates of 3% - 5% recommended by (EC, 2014b; Trutnevyte, 2016).

[13] Assumed availability is taken from the literature, ranging from 1% for utility PV on arable land to 20% for offshore wind on open water.

[14] Currently, most large-scale bioelectricity plants in Europe are the result of the partial (e.g. co-firing) or complete conversion of existing pulverised coal plants to biomass. However, as many existing coal plants will have been decommissioned by 2050, we do not consider the conversion of existing plants. Instead, we model future large-scale biomass as fluidised bed combustion plants as their projected 2050 costs are similar to coal plants with added costs for biomass co-firing (based on (JRC, 2014)). The alternative would be to assume future biomass plants use more efficient integrated gasification combined cycle (IGCC) technology (as done by (Sanchez et al., 2015)), however these are approximately 40% more expensive, potentially less flexible, and no large-scale units are currently operating.

[15] We do not include sugar, starch and oil crops (which we reserve for liquid biofuel production), roundwood fuel wood (which we reserve for firewood), nor black liquor. We include the transport of solid woody biomass between countries (Hoefnagels et al., 2014), while for practical reasons we assume that solid waste biomass must be used in its country of origin.

[16] As opposed to a 'hard' constraint, a 'soft' constraint can be violated, at the expense of a high penalty cost.

[17] Based on an in-house database of Europe's 120 largest hydro plants and their associated reservoirs incorporating data from various open-source databases (e.g. (Davis et al., 2015; Geth et al., 2015; 'Global Energy Observatory', n.d.)), we calculate average specific reservoir sizes of 60, 1608 and 113 MWh MW^{-1} for RoR, STO and PHP hydro plants respectively. Multiplying these values by the average plant sizes from ENTSO-E (ENTSO-E, 2017b) gives total European

hydro storage capacity of approximately 160 TWh. This total matches quite well with the 180 TWh reported by (Mennel et al., 2015). Also, the value of 60 MWh MW^{-1} for RoR storage shows that most RoR plants also have several hours of storage, and thus capable of some level of dispatchability (Kaunda et al., 2012). The resulting 56 GW of PHS capacity is equipped with 6.4 TWh of storage.

[18] Firm capacity (also known as capacity credit or capacity value) represents the contribution a generator makes to system adequacy. Put simply, it indicates the share of installed capacity which can be relied upon during times of peak demand. For dispatchable generators, a value of 90% is typical and allows for forced and unforced offline periods. While CSP generation depends on intermittent sunlight, the capacity credit of CSP plants can exceed 90% when equipped with at least four hours of storage, thus we assume this value (Madaeni et al., 2011).

[19] These notional 'reinforcement lines' are not modelled explicitly as part of the transmission network, and only serve to include the cost of bringing electricity from more remote vRES sites to load centres.

[20] The potential of DSM from space heating is zero in summer, and vice versa for air-conditioning.

[21] Several countries already require that wind farms connected in Europe must be able to supply primary (and in some cases secondary) reserves, which is possible by operating in de-loaded mode or being equipped with storage capacity (e.g. flywheels) (Díaz-González et al., 2014). PV plants can also provide primary reserves (Dreidy et al., 2017).

[22] This is to match demand in the Energy [R]evolution study (see Table 4-1), which assumed extensive use of electricity for the production of hydrogen for use in other sectors (GWEC et al., 2015).

[23] We assume storage investment costs of 700 € kW^{-1} (including 8 kWh of storage for every kW capacity installed), round trip efficiency of 63%, FOM costs of 35 € kW^{-1} y^{-1}, and lifetime of 35 years, based on (Brouwer, Van den Broek, et al., 2016). Equivalent to 88 € kWh^{-1}, we acknowledge this is rather optimistic given expectations for grid-level storage costs are 340 USD kWh^{-1} (290 € kWh^{-1}) in 2040 (Schmidt et al., 2017). However, with this scenario want to see the potential role of storage in the power system at a given cost, not provide an accurate cost assessment.

[24] The commercial optimization package Gurobi (Gurobi Optimization, 2016) is used to solve the system of MILP equations generated by PLEXOS.

[25] OPF calculations enforce active and reactive power balance constraints at each node, and would provide better estimates for losses and reactive power compensation requirements (e.g. capacitor banks, synchronous condensers) (Dixon et al., 2005; Frank & Rebennack, 2016). However, this is beyond the scope of our paper.

[26] For computational reasons, the LT plan does not simulate each hour. Instead, we slice the year into 12 monthly blocks and optimise based on a simplified 12-step load duration curve (LDC) in each block. As a consequence, chronology is only maintained between the blocks and not within them, thus ramping constraints cannot be considered (Energy Exemplar, 2015). However, both generator flexibility and reserves are included in the ST Schedule.

[27] We assume direct GHG emission factors of 56, 101 and 100 kg CO_2 equivalent GJ^{-1} (NCV) for natural gas, coal and biomass fuels respectively (IPCC, 2010). Note that emissions for biomass are only considered when coupled with CCS in Bio-FB-CCS plants to calculate sequestered CO_2. Otherwise, biomass is considered carbon-neutral as we assume that sufficient new biomass is grown (and CO_2 absorbed) to offset that which is burned.

[28] Reserve requirements depend on vRES generation profiles, which are not known until after the LT Plan is solved. The vRES capacity credit is estimated based on the hours in which total European-wide demand is highest, however these hours do not necessarily coincide with the peak demand hours in each country. For this reason, we must ensure that some over-capacity is included in the LT Plan so that sufficient capacity is available to cover both reserve requirements and vRES firm capacity inaccuracies in the subsequent hourly simulations.

[29] Even if this approach is rather conservative and more capacity is installed by the model than actually required, this capacity will come in the form of OCGTs (the cheapest capacity providers) which ultimately contribute relatively minor amount to total costs (see section 4.3.7).

[30] Performing hourly simulations for one week for one scenario can take more than 4 hours to solve using integer programming with a target MIP gap of 0.1%. Thus, simulating a full year could take more than 200 hours, rising to 60 days for all seven scenarios. Instead, we cap the solver time to two hours and solve only the first week of each month.

[31] We also attempted another scenario excluding biomass but including daily (8 hour) storage; however, this also returned an infeasible solution.

[32] The reason we observe no curtailment in our study is that with both transmission and vRES siting optimised simultaneously, transmission bottlenecks are avoided, and it is more cost-effective to balance the portfolio with firm non-vRES capacity – taking into account the need for peak load and reserve coverage – than install surplus vRES capacity. Furthermore, as we do not model the transmission or distribution grids within countries, any internal bottlenecks requiring vRES curtailment are neglected.

[33] If this CSP capacity was instead located in the Middle East and Northern Africa (MENA) countries, the required network topology would be similar as HVDC connections bringing electricity to central Europe from the MENA must go through Spain, Italy, or Greece. The SAPEI HVDC cable linking Sardinia with mainland Italy is the deepest in the world, with some sections reaching 1650 m (Ardelean & Minnebo, 2015), while significant portions of the Mediterranean Sea (i.e. between Algeria and France) exceed 2500 m depth. Attempting to lay cables at greater depths involves significant technical and cost limitations which are unlikely to be overcome before 2030, leaving only 20 years for a trans-

Mediterranean HVDC network to be developed (Colombo, 2014; SuperGrid Institute, 2017). This leaves Spain, Italy or Greece as the only alternatives.

[34] The total of 5 EJ includes 3.9 EJ of solid biomass, 0.7 EJ of biogas, and 0.4 EJ of renewable municipal waste. The 38% use for electricity includes use in combined heat and power plants. 'Energy purposes' includes both electricity and heat. The remaining biomass not used for electricity production (62%, 3.1 EJ) was used for residential heating or in district heating plants.

[35] Potential biogas production for the EU28 in 2030 is reported to range between 28.8 Mtoe and 40.2 Mtoe (1.2 EJ to 1.7 EJ) (Kampman et al., 2016). Thus, the 2050 potential may be higher than the base levels assumed in our study.

[36] This additional biogas is only required by the model in the hourly ST Schedule runs, not in the LT Plan. This highlights the importance of accounting for generator flexibility limitations and reserve requirements by performing detailed hourly simulations: neglecting them can underestimate the utilisation of peak generators.

[37] Calculated as the total annualised system costs divided by the total annual generation. Note that these are the 'worst case' costs, as generation is based on the most challenging weather year.

[38] From a single data point, it is impossible to determine exactly how costs increase with increasing demand. However, for the reasons given, it is likely to be non-linear.

[39] 300 €bn y^{-1} to 400 €bn y^{-1} is approximately 2% to 3% of Europe's 2015 gross domestic product (GDP) (Brown et al., 2018). Assuming moderate GDP growth (1.5% y^{-1}), 530 €bn y^{-1} would still represent 2% to 3% of GDP in 2050 (EC, 2016b).

[40] Hinkley Point C will have a capacity of 3200 MW at a cost of £19.6 bn (BBC, 2017), while Olkiluoto-3 will have a capacity of 1600 MW at a cost of £8.5 bn (Ward, 2017). On this basis, the investment cost for nuclear could be in the range of ~5300 € kW^{-1} to ~6800 € kW^{-1}. However, it is not clear whether the reported costs include IDC, thus including IDC would increase the costs further.

[41] Higher nuclear CAPEX is based on the calculated cost of Olkiluoto-3 (Ward, 2017). The higher gas price is based on the 4 Degree Scenario (4DS) for 2050 from the IEA's ETP2016 (IEA, 2016a).

[42] While the deployment trend would not necessarily be linear, this demonstrates that exponential growth would not be required to reach the 2050 installed wind and PV capacities for most scenarios.

[43] Net deployment includes the replacement of retired capacity.

[44] Rather than new biomass installations, existing coal and natural gas plants could also be converted to run on 100% biomass or upgraded biogas.

[45] Based on all cross-border lines currently included in ENTSO-E's TYNDP 2016 (ENTSO-E, 2016d).

[46] While large wind farms and centralised power plants (e.g. CSP, biomass) would be connected to the high voltage transmission grid, biogas plants are usually small decentralised facilities located in agricultural areas, more likely to be connected to the LV grid. For example, the most economical size of a biomethane plant ranges between 1 and 2 million Nm^3 biomethane per year (approximately 500 kWe to 1 MWe), depending on availability of feedstock and transport costs (AEBIOM, 2009).

[47] This would require detailed data on Europe's fleet of existing power plants which was not available.

[48] For example, the annual European supply of agricultural residues can vary by as much as +23% and -28% from the long-term average (Scarlat et al., 2010).

[49] For example, in the Nordic countries gas is only available in a few major cities, not in rural areas.

[50] For example, biomass-CSP hybrid generators which can burn biomass during winter and on cloudy days when DNI is low (Soria et al., 2015). Also, co-firing of solid biomass in coal plants (possibly retrofitted CCS) could allow existing coal plants to remain in operation up to (or even beyond) 2050, reducing costs by avoiding stranded assets.

[51] In Germany for example, tertiary balancing power can only be provided by plants above 5 MW (Hahn, Krautkremer, et al., 2014). This would be a major limitation for biogas plants which are typically small. However, aggregators could be used to pool generation capacity for provision of ancillary services.

[52] As shown in Table 4-3 and Table 4-4, the cost of offshore wind is twice that of onshore wind, while underground cables are up to 10 times more expensive than overhead transmission lines.

Can liberalised electricity markets support decarbonised portfolios in line with the Paris Agreement? A case study of Central Western Europe

5

William Zappa

Martin Junginger

Machteld van den Broek

Submitted to Energy Policy (2019)

Abstract

We model the evolution of the Central Western Europe power system until 2040 with an increasing carbon price and strong growth of variable renewable energy sources (vRES) for four electricity market designs: the current energy-only market, a reformed energy-only market, both also with the addition of a capacity market. Each design is modelled for two decarbonisation pathways: one targeting net-zero emissions by 2040 for a 2 ºC warming limit, and the other targeting -850 Mt CO_2 y^{-1} for a 1.5 ºC warming limit. Our key policy findings are: (i) no market design guarantees long-term cost recovery for all technologies, (ii) bioelectricity with carbon capture and storage plays an important role in decarbonised portfolios, but may put downward pressure on electricity prices, (iii) significant direct air carbon capture is deployed in the 1.5 ºC scenarios, increasing electricity demand by 200 TWh y^{-1}, (iv) decarbonisation policies relying primarily on vRES to meet a 1.5 ºC target may increase the cost of the transition by 10-25% compared with more diversified portfolios, and (v) policymakers should consider adding a mechanism in the European emissions trading scheme to remunerate negative emission technologies (NETs) for the emissions they sequester, but this alone is unlikely to see sufficient investment in NETs.

5.1 Introduction

In order to achieve the European Union's (EU) long-term goal of reducing greenhouse gas (GHG) emissions by 80-95% by 2050 compared to 1990 levels, the power sector will need to fully decarbonise by 2050, or even deliver net-negative GHG emissions if the objective of the Paris Agreement to limit global warming to well below 2 °C is to be met (EC, 2011c, 2018a; UNFCCC, 2017b). As a result, policies have been implemented to increase the share of renewable energy sources (RES) in electricity supply. These have been largely successful, with installed wind capacity in the EU tripling from 60 to 180 GW between 2008 to 2018, and solar photovoltaic (PV) capacity increasing tenfold from 10 to 115 GW over the same period (EurObserv'ER, 2018, 2019; Eurostat, 2017b; SolarPower Europe, 2019). As wind and PV are variable renewable energy sources (vRES) with nearly zero short-run marginal costs (SRMC), this additional capacity has displaced more costly thermal generators in the merit order, reduced electricity prices, and the operating hours of thermal plants (Hirth, 2018)[1]. Also known as the "merit-order" effect, this makes it more difficult for thermal plants in energy-only electricity markets (EOMs) to recover their fixed costs, negatively affects the business case for new investments, and threatens security of supply (Clò et al., 2015; EC, 2016a; Hu et al., 2018; Joskow, 2008; Paraschiv et al., 2014).

In response to concerns about security of supply, and scenarios showing that up to 60% of electricity generated in the EU by 2040 could be provided by vRES[2], several countries have implemented capacity remuneration mechanisms (CRMs) of various designs to supplement generator revenues from the EOM[3]. However, there is little empirical evidence of the need for CRMs. For example, many EU countries continue to operate EOMs with no significant reliability problems[4]. Moreover, the fall in market prices observed between 2010 and 2015 – which triggered much of the debate in the EU on the need for CRMs – may have been a sign of EOMs reacting as intended in response to an oversupply of generation capacity (Hirth & Ueckerdt, 2014). In recent years, prices have also shown signs of recovery[5]. Turning to the literature, whether EOMs alone can provide sufficient incentives for investment in thermal generation or if CRMs are necessary has long been a subject of debate, with no clear resolution (Pollitt & Chyong, 2018). Some argue that CRMs are undesirable as they distort EOMs, instead suggesting that if so-called 'market failures' hindering the formation of scarcity prices are resolved, EOMs should be capable of ensuring security of supply (Bucksteeg et al., 2017; Cramton & Ockenfels, 2012; EC, 2016c; Henriot & Glachant, 2013; Hirth & Ueckerdt, 2014)[6]. Others posit that CRMs are necessary due to uncertain scarcity prices, and the risk-averse nature of investors (Petitet et al., 2017). Less attention has been given to the future profitability of vRES generators, whose investments to date have largely been driven by government subsidies (Ecorys, 2017). While there are signs that subsidy-free vRES investments are now possible, with continued vRES deployment the merit-order effect may become so great that

vRES cannibalise even their own revenues (Brouwer, Van den Broek, et al., 2016; Netherlands Enterprise Agency, 2019; Zipp, 2017).

Previous studies have investigated market designs to support both thermal and high levels of vRES capacity in a qualitative way (e.g. (Billimoria & Poudineh, 2018; Ecorys, 2017; Finon & Roques, 2013; Henriot & Glachant, 2013; Keay, 2016; Newbery et al., 2018; Philipsen et al., 2019; Poudineh & Peng, 2017)), but relatively few quantitative studies have been performed. Brouwer et al. (Brouwer, van den Broek, et al., 2016; Brouwer, Van den Broek, et al., 2016) find that the current EOM would not provide sufficient revenues for most thermal, vRES or other low-carbon technologies from 2030 onwards, while Pollitt & Chyong (Pollitt & Chyong, 2018) find that mid-merit plants could be profitable with more vRES if fuel and carbon prices were to rise; while vRES would still need subsidies or further cost reductions. Levin & Botterund (Levin & Botterud, 2015) compare various CRMs, finding that market prices collapse under all designs and reduce the profitability of baseload and wind plants, while mid-merit and peak generators are less affected. Market designs have been evaluated based on a wide variety of criteria, usually based on the author's (often implicit) definition on the objectives of electricity market design. For example, Poudineh and Peng (Poudineh & Peng, 2017) give the purpose of market design as *"[to provide] signals for efficient operation and investment in the power sector"*. Some evaluation criteria that have been used in the literature are reliability (Ecorys, 2017; Kraan et al., 2019; Newbery et al., 2018), adequacy (Petitet et al., 2017), market-based (Ecorys, 2017), efficiency (Poudineh & Peng, 2017), flexibility (Ecorys, 2017), complexity (Ecorys, 2017), affordability (Ecorys, 2017; Newbery et al., 2018), clean (Newbery et al., 2018), renewable (Kraan et al., 2019), sustainability (Kraan et al., 2019), and social efficiency (Petitet et al., 2017).

Despite the existing literature, we find several areas where research is lacking. Firstly, previous studies look mainly at snapshots of the market after the transition to a low-carbon future has taken place (e.g. (Brouwer, Van den Broek, et al., 2016; Ecorys, 2017; Zappa et al., 2019)), without considering the transition period and the impact of market design on the generation portfolios. Secondly, studies focus on integrating vRES as the primary means of achieving decarbonisation, with net-zero carbon emissions from the power sector seen as the final goal (e.g. (Gerbaulet et al., 2019; Kraan et al., 2019)). However, even a fully renewable net-zero emission system may not be consistent with the decarbonisation ambitions of the Paris Agreement, in which negative emission technologies (NETs) such as bioelectricity with carbon capture and storage (BECCS) and direct air carbon capture (DAC) may be needed (van Vuuren et al., 2017). Thirdly, no studies were found which investigate the economic viability of NETs and their potential impacts on the CWE electricity market.

We seek to address these knowledge gaps with a case study of the electricity markets of France (FR), Belgium (BE), the Netherlands (NL), and Germany (DE) – collectively referred to as Central Western Europe (CWE). We model the CWE power system from 2017 until 2040 and address three main questions: *(i)* how should electricity portfolios develop to supply electricity reliably

to consumers at the lowest cost while being consistent with the Paris Agreement?, (ii) what effects do different market designs have on the resulting portfolios and the business cases of different technologies? and (iii) how could the deployment of NETs affect the electricity market?

With the aims of our study thus established, in section 5.2 we outline our method. In section 5.3 we present our results, and discuss their implications in section 5.4. We conclude in section 5.5 with some key findings. Further details on the method and results from this chapter are provided in Appendix D.

5.2 Method

Our approach consists of four main steps (Figure 5-1). First, a power system model of the CWE region and neighbouring countries is built using the PLEXOS modelling framework (section 5.2.1) (Figure 5-2). We model a total of eight scenarios by combining four different market designs with two different decarbonisation trajectories (section 5.2.2). Assuming that the overarching objective of market design is to supply low-carbon electricity reliably to consumers at the lowest possible cost, we first run a long-term (LT) capacity expansion optimisation to find the least-cost pathway of investment decisions in non-vRES generation capacity from the base year 2017 until 2040, taking the decarbonisation trajectories as a hard constraint (section 5.2.3). We assume vRES capacity increases exogenously as current policies are pushing the market in this direction, and it is the increasing penetration of vRES which drives current concerns with the existing EOM market design. Based on the resulting portfolios, short-term (ST) hourly unit commitment and economic dispatch (UCED) simulations of the day-ahead market are performed for selected years to yield more detailed results on market prices and system reliability; two indicators used to evaluate the different market designs.

5.2.1 Build power system model

Our model is built using PLEXOS, a power system modelling framework based on mixed-integer linear programming[7]. By coupling its LT Plan and ST Schedule modules, PLEXOS can be used to perform both capacity expansion and UCED calculations, considering power plant flexibility limitations and flexible loads. The model has perfect foresight over the entire 24-year period from 2017 until 2040. A detailed description of the PLEXOS model is provided in Appendix E. Transmission between countries is modelled based on net transfer capacities (NTCs), while transmission within countries is treated as copper plate. The main inputs for the model are: (i) the installed capacity of existing generators in the base year (2017), (ii) assumed developments in demand, vRES and transmission capacity, (iii) techno-economic parameters for generation, storage and NETs, and (iv) assumed fuel and carbon prices. These inputs are briefly outlined in the following sections.

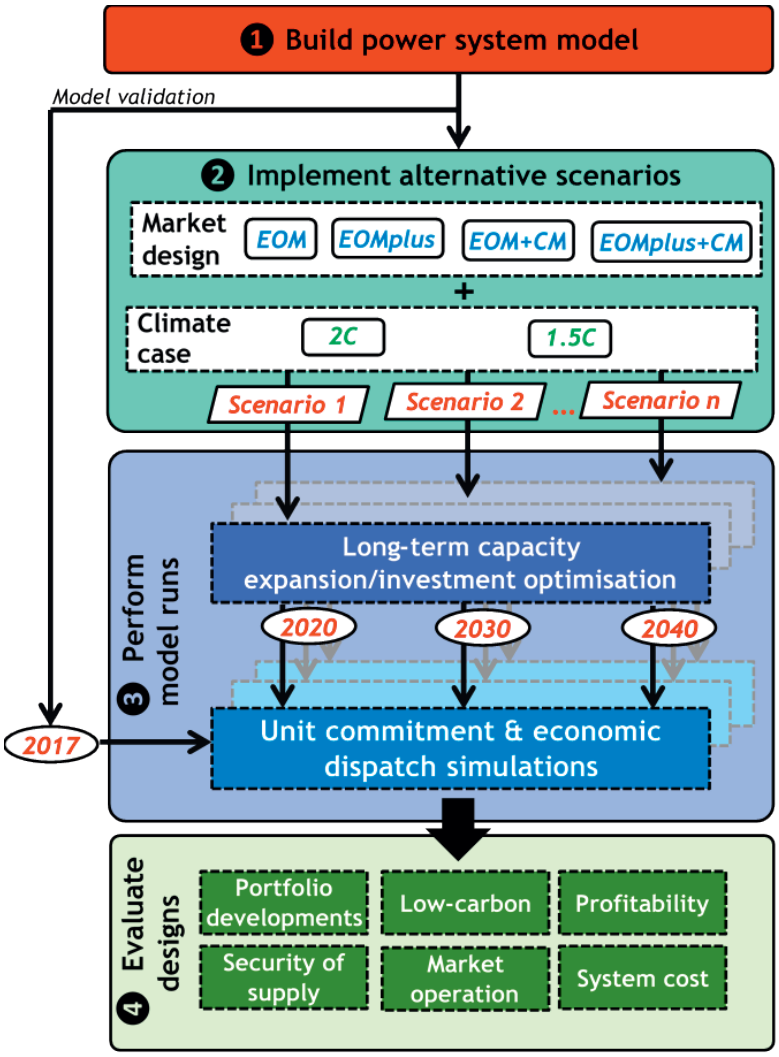

Figure 5-1 | Overview of study method. The scenario designs are explained in section 5.2.2.

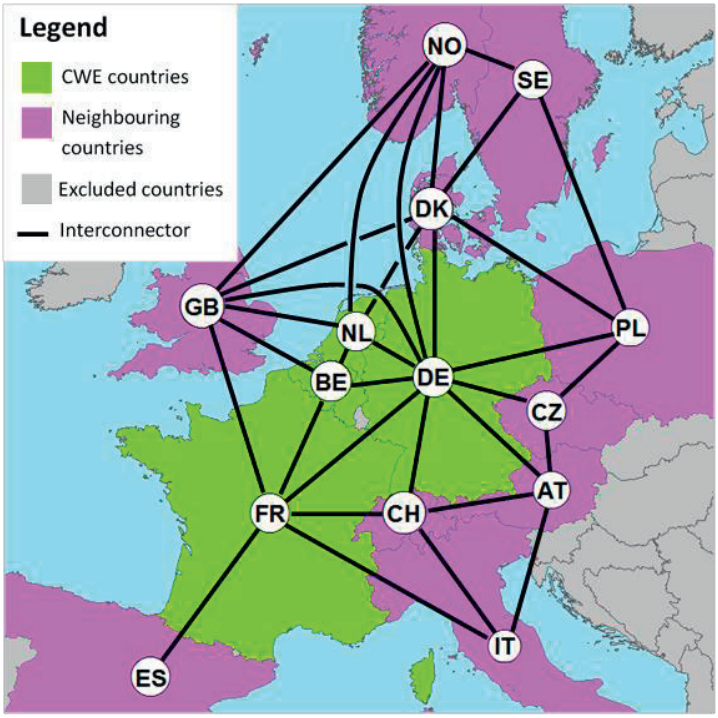

Figure 5-2 | Overview of the Central Western Europe focus study area (green), directly neighbouring countries (purple), and excluded countries (grey).

5.2.1.1 Legacy generation fleet

Data on the fleet of power plants operating in the CWE countries in 2017 are taken from a database of more than 700 power plants (T. Mulder, 2015), validated against the capacity reported by the European Network of Transmission System Operators for Electricity (ENTSO-E) and national statistics (ENTSO-E, 2018b) (Table 5-1). Plants are aggregated based on their type (e.g. coal, combined cycle gas turbines (CCGT), open cycle gas turbine (GT), nuclear), and decade of commissioning. Generators in neighbouring non-CWE countries are modelled more simply[8]. Several assumptions are made regarding the starting portfolio:

- National phase-outs for coal (FR: 2022, NL: 2030, BE: 2017, DE: 2038) and nuclear power (BE: 2025, DE: 2022) are enforced (Bundesamt für kerntechnische Entsorgungssicherheit, 2018; Clean Energy Wire, 2019; Europe Beyond Coal, 2017; World Nuclear News, 2018)[9]. After the coal phase-out year, coal plants must either retire, be retrofitted with carbon capture and storage (CCS), and/or be converted to run on 100% biomass.
- The efficiency of legacy power plants depends on their age (EPA, 2018).
- If not retrofitted, plants must retire within five years of their nominal decommissioning year.

Table 5-1 | Installed generation capacity, demand, and capacity margin per country in 2017

Parameter	Country				Total CWE
	BE	DE	FR	NL	
Net generation capacity (GW) [a]	*20.9*	*210.5*	*128.7*	*34.0*	*394.1*
Combined-cycle gas turbine (CCGT)	4.0	9.1	3.4	10.9	*27.4*
Open-cycle gas turbine (GT)	0.1	9.5	0.0	4.6	*14.2*
Coal	0.0	38.7	3.1	5.8	*47.6*
Oil [h]	0.5	7.9	10.2	0.7	*19.3*
Combined heat and power (CHP)	1.4	15.2	3.3	4.0	*23.9*
Nuclear	6.1	10.7	63.1	0.5	*80.5*
Run-of-river and storage hydro (HYDRO) [b]	0.0	4.7	18.6	0.0	*23.2*
Pumped hydro storage (HYDRO-PHS)	1.3	8.7	5.0	0.0	*15.0*
Solid biomass (BIOSOL) [g]	0.7	8.0	0.4	0.5	*9.6*
Onshore wind (ONWIND)	2.0	50.2	13.6	3.3	*69.0*
Offshore wind (OFFWIND)	0.9	5.4	0.0	1.0	*7.3*
Solar photovoltaic (PV)	3.9	42.4	8.0	2.8	*57.0*
Firm generation capacity (GW) [c]	13.6	105.0	96.8	25.3	240.8
Curtailable load (GW) [d]	0	0	2.4	0.75	3.1
Peak load (GW)	13.6	79.1	93.7	19.0	-
Import capacity (GW)	8.0	23.6	10.0	6.9	-
Export capacity (GW)	2.5	18.1	14.7	6.9	-
Net import capacity (GW) [e]	3.8	17.5	7.5	-3.5	-
Capacity margin (%) [f]	28%	55%	14%	19%	-

[a] *Sources: ENTSO-E, Elia, Bundesnetzagentur, RTE (Bundesnetzagentur, 2018; Elia, 2018; ENTSO-E, 2018b; RTE, 2018)*

[b] *Due to poor data availability we aggregate run-of-river (RoR) and storage hydro capacity in this study. Pumped storage is modelled separately.*

[c] *Firm generation capacity is estimated assuming 90% firm capacity for all dispatchable thermal plants, 50% for hydro plants (based on historical availability during peak hours), 7% for wind, and 0% for PV.*

[d] *Source: (ENTSO-E, 2018b)*

[e] *The Net Import Capacity for a country is calculated as the firm capacity of all importing lines, minus the firm capacity of all exporting lines. These values are determined from a calibration run using PLEXOS for the base year 2017, accounting for the fact that the peak load hours in each country may not coincide.*

[f] *Capacity Margin is reported at the time of the region peak load, and includes any potential contribution from transmission with neighbouring countries. It is calculated as:* $Capacity\ Margin\ (\%) = (Firm\ Generation\ Capacity + Curtailable\ Load + Net\ Import\ Capacity - Peak\ Load)/(Peak\ Load)$

[g] *Includes anaerobic digestion (BIOAD)*

[h] *Includes all other non-renewable fuels*

5.2.1.2 Assumptions for electricity demand, vRES and transmission capacity

Future electricity demand, vRES deployment and transmission capacity in CWE are based on the *Global Climate Action* scenario from ENTSO-E's Ten Year Network Development Plan (TYNDP) 2018 (ENTSO-E, 2018f). Starting from the actual 2017 demand of 1170 TWh, demand increases to 1256 TWh (+7% vs. 2017) in 2040, and the installed capacities of PV, onshore wind and offshore wind reach 269, 146 and 85 GW respectively (Figure 5-3)[10]. Country- and technology-specific hourly capacity factors for wind and PV are taken from the Renewables Ninja dataset (Pfenninger & Staffell, 2016; Staffell & Pfenninger, 2016). Cross-border transmission capacity within CWE rises from 9 GW in 2017 to 21 GW in 2040, while transmission between CWE and neighbouring countries rises from 23 to 60 GW.

5.2.1.3 Techno-economic assumptions

In addition to vRES, a range of dispatchable thermal, storage and NETs is considered (Table 5-3). Exogenous technological learning is assumed for vRES, CCS, storage and NETs. For example, the overnight capital costs (OCC) of PV, onshore and offshore wind fall 60%, 14% and 34% respectively between 2017 and 2040, based on the most optimistic deployment scenarios from (Tsiropoulos et al., 2018). Battery, electrolyser and DAC costs fall by 80%, 53% and 40% over the same period (Child et al., 2019; Keith et al., 2018; Siemens AG, n.d.).

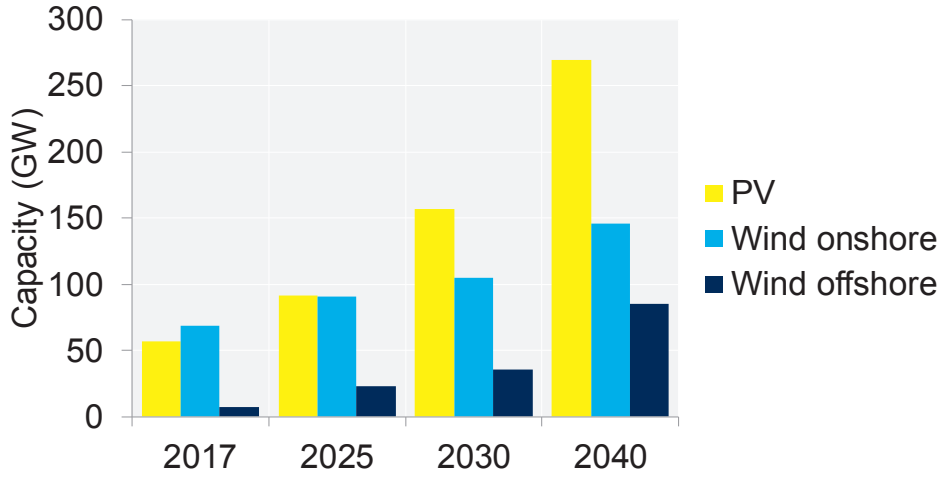

Figure 5-3 | Assumed deployment of PV and wind capacity in CWE. The 2017 capacity is based on historical data. The installed capacity in 2040 is taken from the Global Climate Action scenario in ENTSO-E's Ten Year Network Development Plan 2018 (ENTSO-E & ENTSO-G, 2018). The installed capacity in 2025 is taken from the Best Estimate scenario, while the 2030 capacity is taken from the Distributed Generation scenario.

A uniform weighted average cost of capital (WACC) of 8% is assumed to annualise investment costs[11]. Generator ramping constraints, start-up costs, and part-load efficiencies are based on (Brouwer et al., 2015). Deployment of batteries, electrolysers and DAC is limited to 1 GW y^{-1} per country[12]. In addition to completely new investments, two retrofit options are included for existing generators built between 1990 and 2016, and generators built after 2017: (i) retrofitting with CCS (coal, CCGT and solid biomass plants only), and (ii) full biomass conversion (coal plants only)[13]. The cost of retrofitting with CCS is assumed to be 60% of the cost of a new-build CCS plant (Gibbins et al., 2011), while the cost of biomass conversion is taken as 700 € kW^{-1} (Drax, 2018; JRC, 2014).

5.2.1.4 Fuel and carbon prices

We assume fuel prices remain constant at 2017 levels (Table 5-2). As we consider different climate scenarios by applying annual emission constraints (Section 5.2.2.2), we do not assume a carbon price in the capacity expansion algorithm. However, in the UCED runs for the years 2020, 2030 and 2040, we assume EU Emission Trading Scheme (ETS) certificate prices of 17, 85 and 120 € t^{-1} respectively, following the *450* scenario from the IEA's World Energy Outlook 2016 (IEA, 2016d)[14]. Another key assumption we make is that NETs are remunerated for the negative emissions they generate at the same level as the carbon price.

Table 5-2 | Assumed fuel prices in 2017

Commodity	Price (€ GJ^{-1})	Source
Natural gas	5.3	(EC, 2018b)
Coal	2.5	(EC, 2018b)
Oil	8.5	(EC, 2018b)
Nuclear	0.9	(Bles et al., 2011; Polish Ministry of Economy, 2011)
Biomass [a]	8	(Argus, 2018; Thrän et al., 2019)

[a] *Prices for biomass vary per region and biomass type. In 2017, the spot price of pellets imported to CWE were approximately 9 € GJ^{-1} (Thrän et al., 2019), while wood chips were 7 € GJ^{-1} (Argus, 2018). The value assumed in this study is an average of wood pellets and chips.*

Table 5-3 | Techno-economic parameters for technologies in the year 2030. The costs for vRES, CCS, storage and NETs are assumed to fall over time due to technological learning.

Generator Type [a]	OCC [k] (€ kW^{-1})	Build time (y)	Economic. life (y)	TCR [k] (€ kW^{-1})	Efficiency [l] (%LHV)	VOM (€ MWh^{-1})	FOM (€ kW^{-1} y^{-1})	Refs.
Thermal technologies [m]								
COAL	1600	4	40	1950	48%	3.6	40	[o]
COAL-CCS* [b]	2740	4	40	3300	35%	5.5	69	[o,p]
GT*	550	2	30	620	43%	11	17	[o]
CCGT*	850	3	30	990	62%	2	21	[o]
CCGT- CCS* [b]	1390	3	30	1620	55%	4	35	[o,p]
NUCLEAR*	4100	6	60	5410	38%	2.5-16 [n]	86	[o]
BIOAD*	2750	2	20	3090	40%	3.1	113	[o,p]
BIOSOL* [c]	2330	2	25	2620	37%	3.5	42	[o,p]
Variable renewable energy sources (vRES)								
PV [d]	530	-	25	530	-	0	13	[o,p]
ONWIND [e]	1190	2	25	1340	-	0	26	[o,p]
OFFWIND [f]	2310	3	30	2700	-	0	69	[o,p]
Storage technologies								
BATTERY* [g]	900	-	15	900	90%	0.2	27	[q]
HYDROGEN* [h]	310	-	25	310	75%	1.2	13	[q,r]
Negative emission technologies (NETs)								
BIOSOL-CCS*[b,c,i]	-	-	25	3800	25%	5.4	61	-
DAC*[j]	17400	-	25	17400	-	138.3	-	[s]

Abbreviations: BIOAD – Biogas from anaerobic digestion, BIOSOL – Solid biomass, CCS – Carbon capture and storage, CCGT – Combined cycle gas turbine, DAC – Direct air (carbon) capture, FOM – Fixed operating and maintenance costs, OCC – Overnight capital cost, GT – Open cycle gas turbine, TCR – Total capital requirement, VOM – Variable operating and maintenance costs

Footnotes for Table 5-3

[a] *Technologies indicated with a '*' can be built endogenously by the model in any country, except for nuclear which can only be built in France due to announced nuclear phase-outs in Germany, Belgium, and a low appetite for nuclear in the Netherlands. Solar PV and wind capacity increases exogenously as explained in Section 5.2.1.2.*

[b] *We assume a uniform CO_2 capture rate for CCS technologies of 90% (JRC, 2014), and fixed CO_2 transport and storage costs of 15 € t^{-1} CO_2 (Zero Emissions Platform, 2011) which are added on top of the other generator VOM costs.*

[c] *The total sustainable technical lignocellulosic biomass potential in the CWE region is approximately 3.9 EJ y^{-1} (2030), which excludes biomass from protected areas, and considers sustainability standards for agricultural farming and land management (e.g. maintaining soil organic carbon), as well as forestry management practices (Dees et al., 2017). From this value, we further exclude all stem wood, stumps, and post-consumer waste and assume a maximum potential solid biomass use in the power sector of 2.9 EJ y^{-1} for CWE.*

[d] *Assuming an average of utility-scale (without tracking) and residential-scale (inclined) PV systems.*

[e] *Assuming a medium specific capacity (0.3 kW m^{-2}), moderate (100 m) hub height.*

[f] *Assuming monopole foundations, moderate (30 to 60 km) distance from shore.*

[g] *Assumes 6 hours of storage. Efficiency given as round-trip.*

[h] *Hydrogen cost given on the basis of electrolyser electric (input) capacity, including 90 days of storage capacity. We assume that hydrogen can be used in both new and existing natural gas plants with negligible investment cost. The conversion of electricity to hydrogen by electrolysis is assumed to have 75% efficiency (Siemens AG, 2014), while the conversion from hydrogen back to electricity is the same as for the gas plant. The assumed OCC reductions for electrolysis and storage taken from (Child et al., 2019) are on the optimistic side, with costs falling by 55% and 75% respectively between 2015 and 2030.*

[i] *Limited consistent data is available for Biomass-CCS (BECCS) in the literature. Instead, the OCC is set at a level which makes a new BECCS plant slightly cheaper than retrofitting a new BIOSOL plant with CCS, or converting a new COAL-CCS plant to biomass. VOM costs, FOM costs and efficiency are based on the difference between COAL and COAL-CCS plants. While low, the resulting efficiency is comparable with other literature estimates (e.g. (Bui et al., 2017; Fajardy & Mac Dowell, 2018)). Higher efficiencies are possible with process improvements (e.g. flue gas heat recovery), but would increase costs (Bui et al., 2017).*

[j] *Direct air capture (DAC) consumes electricity, thus the capacity is shown as negative, and the OCC given per kW electricity input. DAC is still in pilot phase and cost estimates are uncertain, ranging from 50 to 800 € tCO_2^{-1} (Fuss et al., 2018). The values assumed in this study (150 to 200 € tCO_2^{-1}) are at lower end of these estimates based on Keith et al. (Keith et al., 2018), for a plant capturing 1 Mt CO_2 y^{-1} (net) from the air assuming a 90% capacity factor, and a DAC process that requires 0.37 MWh electricity and 5.25 GJ heat per (net) tonne of CO_2 sequestered. We assume this heat is provided by natural gas and include the gas costs in the VOM. Carbon emissions from the natural gas combustion are accounted for in the above capture values, which are reported per net tonne CO_2 sequestered.*

[k] *The overnight capital costs (OCC) are taken from (JRC, 2014) for conventional technologies, or from (Tsiropoulos et al., 2018) for most low-carbon technologies. The cost values shown here are indicative for the year 2030, however the costs for most low-carbon technologies fall over time as explained in Appendix E. The total capital requirement (TCR) includes the OCC plus interest during construction (IDC), calculated based on the assumed build time (Black & Veatch, 2012) , economic life (JRC, 2014) , and discount rate (8%). For some technologies with more uncertain costs, only the OCC is used.*

[l] *Efficiency given at nominal load. Generator, ramping constraints, start-up costs, and part-load efficiencies are based on (Brouwer et al., 2015).*

[m] *Approximately 10% of conventional thermal capacity are combined heat and power (CHP) plants. We assume these receive additional revenues of 24 € GJ^{-1} for their heat based on average district heating prices (Orita, 2013; Vattenfall, 2017; Werner, 2016). Seasonal thermal demand profiles are based on (Heat Roadmap Europe, 2019).*

[n] *The VOM of nuclear plants is assumed to range from 2.5 € MWh^{-1} for relatively modern plants (<20 years old) based on (JRC, 2014), and 16 € MWh^{-1} for old (>20 years old) plants to account for higher costs for maintenance and life extensions based on (Schneider & Froggatt, 2018).*

[o] *Source: (JRC, 2014)*

[p] *Source: (Tsiropoulos et al., 2018)*

[q] *Source: (Child et al., 2019)*

[r] *Source: (Siemens AG, n.d.)*

[s] *Source: (Keith et al., 2018)*

5.2.2 Implement market scenarios

Eight different market scenarios are modelled by combining four electricity market design scenarios with two decarbonisation scenarios.

5.2.2.1 Market design scenarios

Four different market designs considered:

- **EOM**: a reference EOM reflecting the 'imperfect' EOM currently operating in most CWE countries. Prices are capped at 3000 € MWh^{-1}, and essentially inelastic to demand (EPEX, 2018a).
- **EOMplus**: a reformed EOM in which two deficiencies in the current EOM are resolved by (i) removing spot market price caps, and (ii) making price more elastic to demand by allowing significant participation of voluntary load shedding.
- **EOM+CM**: a market in which a capacity market (CM) operates alongside the current 'imperfect' EOM.
- **EOMplus+CM**: the combination of a reformed EOM together with a CM.

We make the following assumptions for all scenarios:

- All electricity is traded on the day-ahead market.
- For the base year 2017, we assume the current 'imperfect' EOM market design remains unchanged, and prevent the model from making any new generation investments or retirements in this year so that the model can be validated with historical data[15].
- The same market design is applied in all countries with marginal pricing applying in all markets, and each country constituting its own bidding and price zone[16].
- We account for approximately 1.6 GW of primary control reserves for CWE, in line with the current 3 GW requirement for Continental Europe as a whole (EC, 2017a).
- All generators are price-taking profit-maximisers, and base their offers on their SRMC.
- So that we can examine system costs without the effect of subsidies, we do not consider existing or future support schemes for vRES (e.g. feed-in tariffs) or their impact on bidding behaviour (e.g. negative bids). Moreover, we assume there is no priority dispatch for vRES generators, which must bid into the market like other generators at their SRMC (zero).
- A value of lost load (VoLL) of 10,600 € MWh^{-1} is assumed in the UCED simulations, based on a load-weighted average of VoLL estimates for CWE residential consumers from (Heather et al., 2018)[17].

In the *EOMplus* scenarios we assume all market price caps are removed, and the electricity price can rise to the VoLL if the market is unable to clear. We also make demand more elastic to price by including 25 GW (11% of peak CWE demand) of industrial load shedding, with activation prices varying from 220 € MWh^{-1} up to 6000 € MWh^{-1} based on industry-specific VoLL values from (Heather et al., 2018).

The CM is modelled by applying constraints on the minimum capacity margin in each country, with the capacity price taken as the shadow price of this constraint. Thus, capacity is offered at its marginal cost to the system. The minimum capacity margins are set to remain at 2017 levels, which can be met by firm generation capacity, transmission, or load-shedding capacity[18]. No constraints are placed on the minimum amount of firm generation capacity per country which must be provided by domestic sources. Thus, we assume countries pursue policies promoting further integration of European electricity markets, rather than nationalistic policies aiming at energy independence.

5.2.2.2 Decarbonisation scenarios

Two different decarbonisation scenarios are considered. These are derived from global carbon budgets until 2100 published in the Intergovernmental Panel on Climate Change's (IPCC) Fifth Assessment report (IPCC, 2014), following an approach used in a previous work (van Zuijlen et al., 2018) (Figure 5-4).The first is a **2C** scenario, designed to be consistent with a 66% chance of limiting global warming to 2 ºC by the end of the century. In this scenario, CWE power sector emissions fall from 400 Mt CO_2 in 2017 to essentially net-zero by 2040. In the second **1.5C** scenario, CWE power sector emissions are consistent with a 66% chance of limiting global warming to 1.5 ºC, reaching net -850 Mt CO_2 in 2040[19]. These trajectories are enforced using annual emission caps.

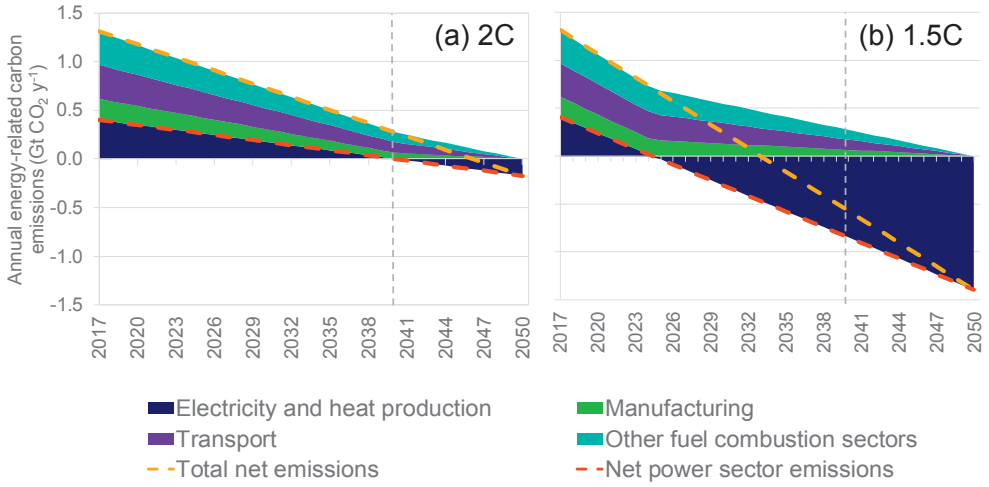

Figure 5-4 | Assumed decarbonisation trajectories for energy-related emissions in the CWE countries consistent with (a) a 66% chance of limiting global warming to 2 ºC and **(b)** a 66% chance of limiting global warming to 1.5 ºC**.** The dashed orange lines show the total net energy-related carbon emissions. The dashed red lines indicate the net power sector emissions, which are enforced as constraints in the model. The dashed grey lines show the model horizon considered in this study (2040), by which time net power sector emissions reach net zero and -0.85 Gt CO_2 in the 2 ºC and 1.5 ºC climate scenarios respectively.

5.2.3 Perform model runs

5.2.3.1 Long-term capacity expansion

The objective function of PLEXOS' investment module is to minimise the net present value (NPV) of the total sum of investment costs, fixed operating and maintenance (FOM) costs, and variable generation costs. Thus, in the absence of any constraints on the capacity margin, the resulting portfolio will be one in which the cost of unmet demand is equal to the marginal cost of an additional unit of generation capacity. It is important to note that the model does not make investments beyond those which achieve minimum system cost, even if those generators may be profitable based on market prices. We solve the capacity expansion module for the whole 34-year horizon in a single step to avoid suboptimal investments which can result in myopic models (Gerbaulet et al., 2019)[20].

5.2.3.2 Short-term hourly dispatch

Using the portfolios from the capacity expansion module, hourly UCED simulations are performed for the day-ahead market for the years 2020, 2030 and 2040 for each scenario. The UCED module ensures that start costs, fuel costs, and variable operating and maintenance (VOM) costs are minimised, subject to generator ramping constraints[21]. Assuming ideal competitive markets and SRMC-based bidding, the UCED simulations approximate the real-world market clearing process. An additional hourly simulation for the year 2017 is performed to validate the PLEXOS model with historical data.

5.2.3.3 Evaluate market designs

We consider that the central objectives of electricity market design are to provide low-carbon electricity reliably to consumers, at the lowest possible cost. By *low-carbon*, we mean in a way that is consistent with the assumed global decarbonisation objective[22]. These objectives are interdependent and involve trade-offs. For example, in liberalised electricity markets, system reliability relies on the market providing sufficient signals for investment in new generation capacity, while excess capacity increases total costs to society. A number of quantitative indicators are used to evaluate the different market design scenarios (Table 5-4). As the three objectives described above are rather high-level, the indicators are classified under the more specific headings of general portfolio development, low-carbon, reliability, market operation, generator profitability, and total cost.

Table 5-4 | Main indicators used to compare scenario results

Indicator group	Indicator	Description
Portfolio development	Generator builds & retirements	Newly built and retired generation capacity (GW)
	Total installed capacity	Installed capacity (GW)
	Generation	Annual generation (GWh)
Low-carbon	Net carbon emissions	Total net carbon emissions (Mt CO_2)
	Shadow carbon price	Shadow price of the annual carbon constraint in the capacity expansion module (€ t CO_2^{-1})
Reliability	Unserved energy	Total demand unmet (GWh)
	Capacity margin	Capacity reserve margin (%)
Market operation	Electricity prices	Day-ahead electricity prices per country, and the load-weighted annual average CWE day-ahead price (€ MWh^{-1})[a]
	Capacity price	Shadow price of the capacity margin constraint (€ MW^{-1}) (*EOM+CM* and *EOMplus+CM* scenarios only)
Generator profitability	Specific net profit	Calculated as the total annual generator revenues (including spot market, reserves, capacity market and negative emissions), minus the variable costs (including fuel, emission, VOM, FOM, reserves, start-up, and pumping/charging costs) and annualised investment costs, divided by installed capacity (€ MW^{-1} y^{-1})
Total cost	Total cumulative costs	The total sum of generation investments (including exogenous vRES), generation costs (fixed + variable), unserved energy, load shedding and capacity payments over the period 2018 to 2040.[b]

[a] *The load-weighted annual average CWE price is calculated from the individual country hourly prices, weighted by the hourly demand per country. This gives a better indication of the average price paid by loads and consumers in the CWE than a simple arithmetical average, which is more strongly affected by hours with very high and low prices.*

[b] *Transmission and carbon-related costs are not included.*

5.3 Results

Sections 5.3.1 to 5.3.6 outline the key modelling results in terms of the defined indicators. In order to analyse the impact of some of our key assumptions, we also perform a selected sensitivity analysis by varying assumptions on model inputs such as fuel prices and technology costs, as well as the (un)availability of certain technologies given uncertainties around technology developments and social acceptance.

5.3.1 Portfolio developments

In the period from 2018 to 2022, the investment and retirement decisions in non-vRES technologies for both climate cases under a given market design are quite similar (Figure 5-6) In the *EOM* scenarios, approximately 70 GW of generation capacity – mostly old coal, oil and natural gas plants – is retired at the earliest opportunity in 2018[23]. Retirements are higher in the *EOMplus* scenarios as the additional load-shedding capacity offsets the need for generation capacity. By contrast, the presence of a CM sees much of this capacity remaining online in the *EOM+CM* and *EOMplus+CM* scenarios until the early 2020s, when the vast majority retires anyway due to age or phase-out[24]. Significant new GT capacity is built to maintain capacity margins at 2017 levels.

From 2023 onwards, the portfolio developments for the two climate cases diverge. In the *2C* climate case, old fossil and nuclear capacity continues to retire as it reaches the end of its useful life. The CM sees most of this capacity replaced by GTs until the early 2030s, by which time batteries have become sufficiently cost-effective to enter the portfolio. While the majority of emission reductions necessary to reach the 2˚C target are delivered by the exogenously increasing vRES capacity, emissions are brought to net zero by the year 2040 by retrofitting approximately 2 GW of coal capacity for BECCS in the late 2030s. In the *1.5C* climate case however, the rate of emission reductions delivered by vRES is insufficient to meet the emissions constraint. As a result, the model converts coal plants to BECCS much earlier and, by 2030, nearly 25 GW of BECCS capacity is installed in CWE[25]. At this point, BECCS has exploited the available biomass potential and between 2028 and 2040, the model deploys 25 GW (input electricity) of DAC to meet the -850 Mt CO_2 y^{-1} target. Additional electricity demand for DAC reaches nearly 200 TWh y^{-1} in 2040, largely provided by generation from BECCS and nuclear.

Ultimately, a CM results in approximately 100 GW more capacity in 2040 than in the EOM-only scenarios; mainly from new GTs, higher battery deployment, and a larger fraction of existing nuclear capacity which is kept online (Figure 5-6). In fact, despite the nuclear phase-outs in Belgium and Germany, the majority of France's existing nuclear fleet remains online until 2040 in all scenarios, which keeps French electricity prices lower than in the rest of CWE.

Batteries reach a maximum deployment of 17 GW in the *EOM+CM 2C* scenario, which help to deal with daily vRES fluctuations. Total battery deployment is higher in scenarios with a CM as batteries can reduce curtailment while substituting GTs as providers of firm capacity. However, for a given market design, battery deployment is lower in the *1.5C* cases as the emission benefits from reduced curtailment are small compared to the deep reductions needed and, with significant BECCS capacity in the *1.5C* portfolios, there is less GT capacity to replace. No electrolyser capacity is built in any scenario, despite the significant cost reductions assumed.

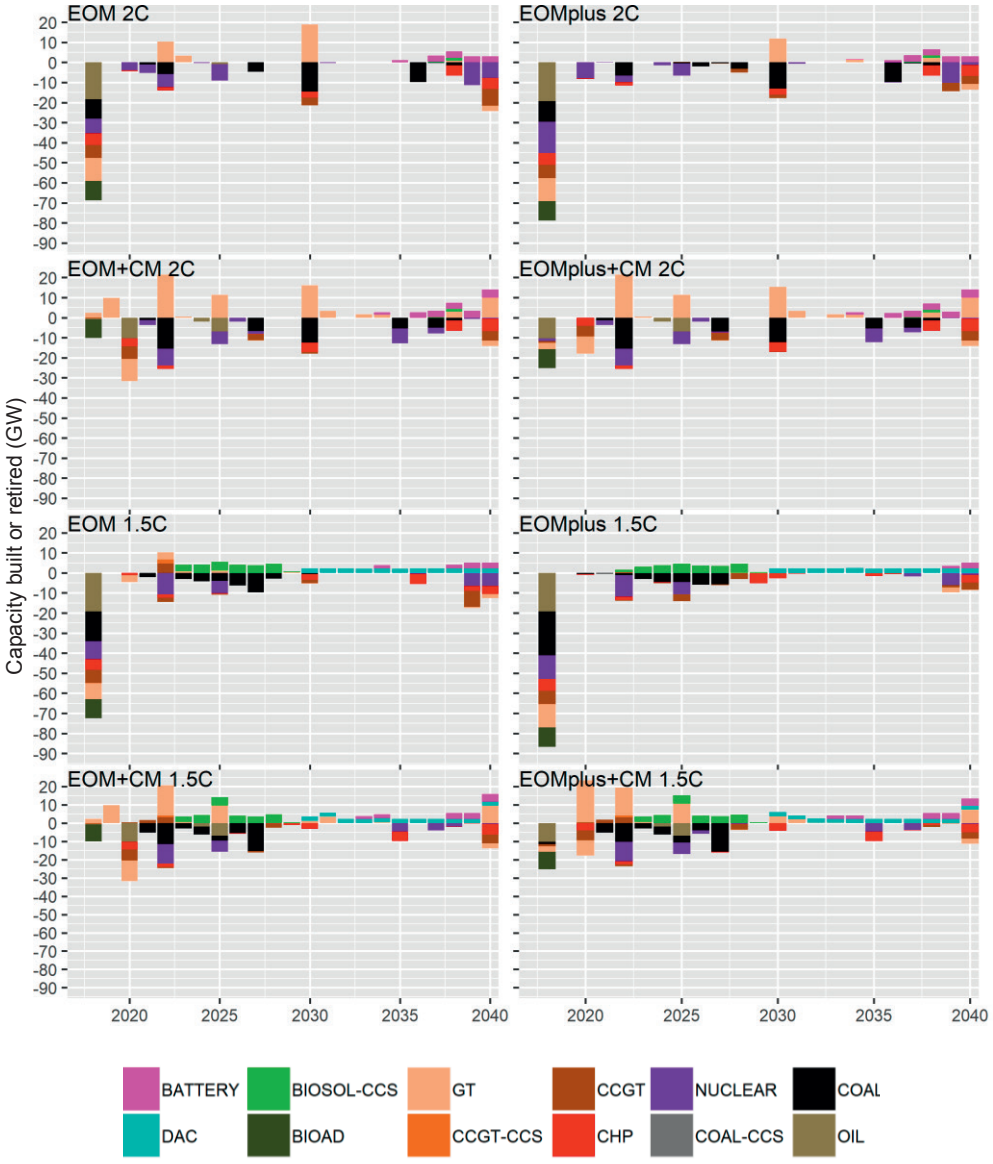

Figure 5-5 | New investments (positive) and retirements (negative) in non-vRES generation capacity for each market design scenario. Retrofits are shown with the quantity of original plant type retiring type below the axis (e.g. CCGT), and the same amount of the new type (e.g. CCGT-CCS) above the axis. Note that DAC capacity represents additional load on the system, not generation capacity.

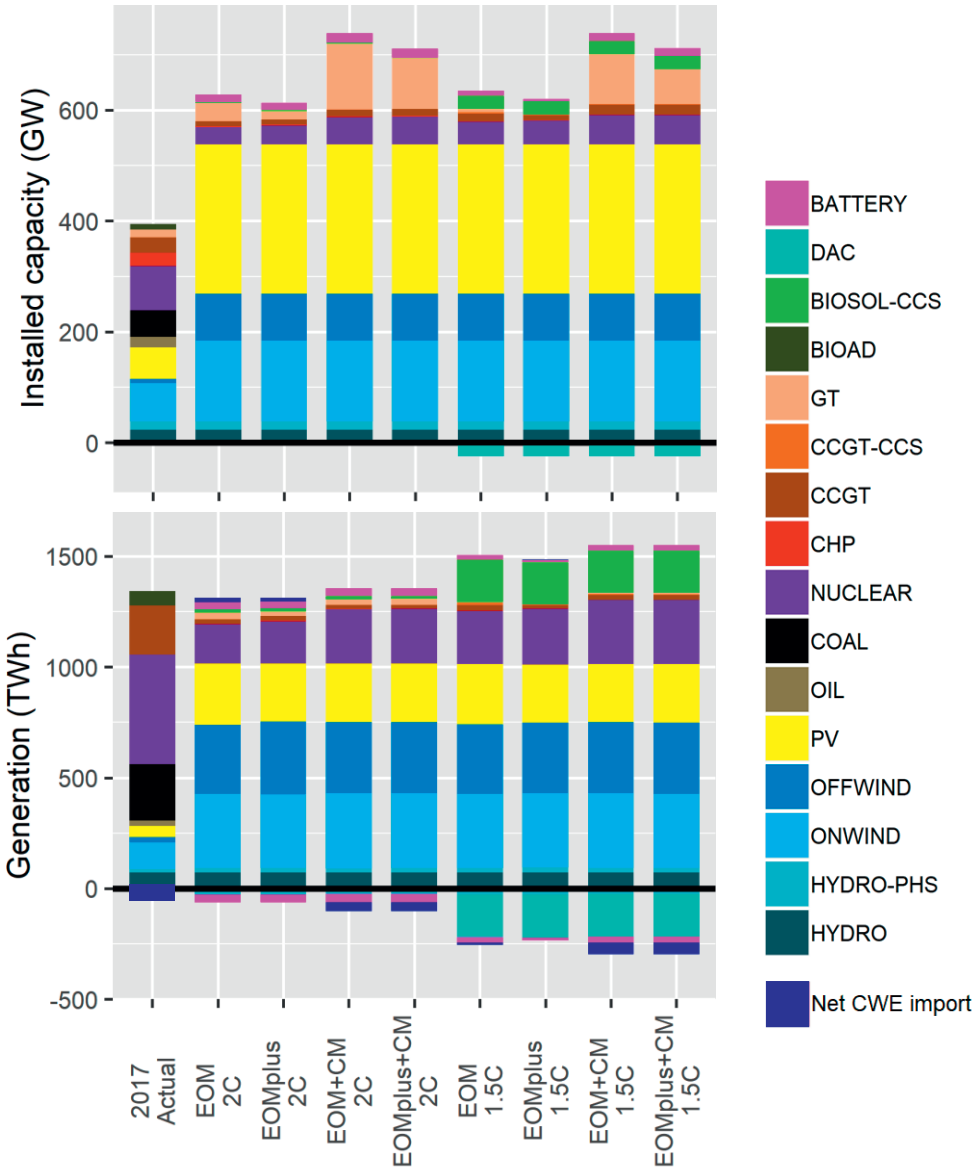

Figure 5-6 | Installed capacity and generation per technology in 2040 for each market scenario based on the UCED runs. The actual capacity and generation in 2017 from ENTSO-E are also given for comparison (ENTSO-E, 2018b). For 2017, biomass generation is aggregated as BIOAD, and gas generation is shown as CCGT. Additional loads on the system from HYDRO-PHS, BATTERY and DAC, as well as net exports from CWE are shown as negative. Net imports to CWE are shown as positive, thus a negative value indicates CWE is a net exporter.

5.3.2 Low-carbon

Thanks to the increasing vRES capacity and carbon constraints, emissions fall as intended in both climate cases (Figure 5-7a). The carbon shadow price in the *2C* scenarios remains far below the *450* scenario price trajectory until the first BECCS capacity is deployed in 2037, when it rises sharply to 100 € t^{-1} (Figure 5-7b). This suggests that if vRES capacity increases at the exogenous rate due to government subsidies rather than strong carbon pricing, it will exert significant downward pressure on the carbon price. In contrast to the *2C* case, the carbon shadow price in the *1.5C* case surpasses the *450* scenario already in 2022, reaching 90 € t^{-1} in 2023 and 250 € t^{-1} in 2030. These dynamics can be explained by the carbon avoidance costs for BECCS and DAC. With an avoidance cost of around 90 € t^{-1}, deploying BECCS is the cheapest way of meeting the carbon budget from 2037 onwards in the *2C* scenarios, and from 2023 in the *1.5C* scenarios. However, once the allowed biomass potential in the *1.5C* scenarios is used for BECCS (achieving -250 Mt CO_2 y^{-1} net carbon emissions), the model must resort to costlier DAC. The choice of market design has no appreciable effect on the carbon shadow price as the marginal cost of the carbon abatement is higher than the marginal cost of capacity.

5.3.3 Security of supply

Due to the significant retirements in 2018, capacity margins fall sharply in the absense of a CM. A small amount of unserved energy is observed in the EOM-based scenarios, mostly in Belgium (Figure 5-8), while no unserved energy is observed in the scenarios with a CM. Transmission plays an important role in maintaining security of supply and reducing system costs in all scenarios, with transmission flows within CWE and with neighbouring countries rising from 160 TWh y^{-1} in 2017 to nearly 250 TWh y^{-1} in 2040 (ENTSO-E, 2018b). Thus, a reliable transmission network would play a pivotal role in maintaining security of supply in a high vRES power system[26].

5.3.4 Market operation

Starting from an average CWE price of around 35 € MWh^{-1} in 2017, day-ahead prices rise in all scenarios before peaking between 2025 and 2030 in the range of 55 to 80 € MWh^{-1}(Figure 5-9)[27]. From 2030 onwards in the *2C* scenarios (2025 in the *1.5C* scenarios), prices begin to trend down and converge in the range of 45 to 55 € MWh^{-1}. The *EOMplus* design results in the highest prices for both climate cases, while the *EOM+CM* design results in the lowest prices. These dynamics are driven by several effects. Firstly, as the carbon price increases over time, the SRMC of carbon-intensive mid-merit and peaking generators also increases which bid higher into the market to cover their costs, leading to higher market prices in the medium term. Secondly, increasing vRES penetration puts downward pressure on electricity prices due to the merit order effect, offsetting the impact of the higher carbon price.

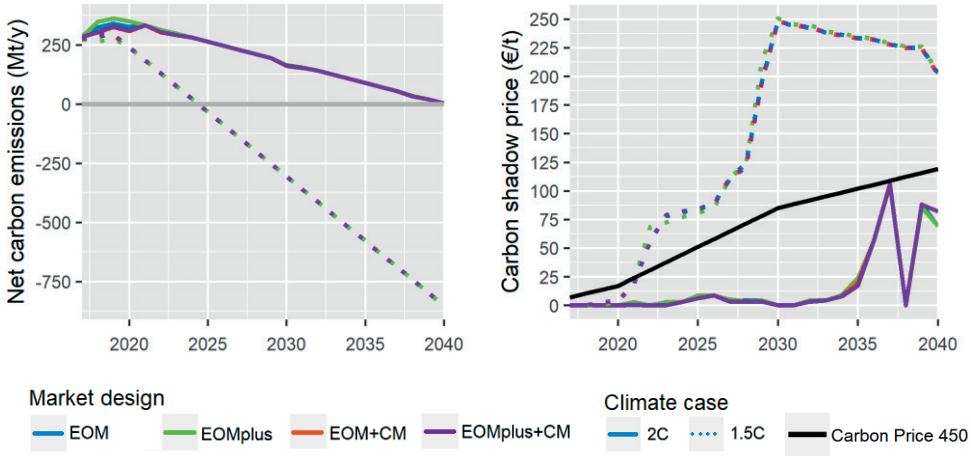

Figure 5-7 | Net carbon emissions and carbon shadow price for each scenario based on the long-term simulations. The solid black line in the shadow price figure indicates the reference IEA 450 scenario accounting carbon price.

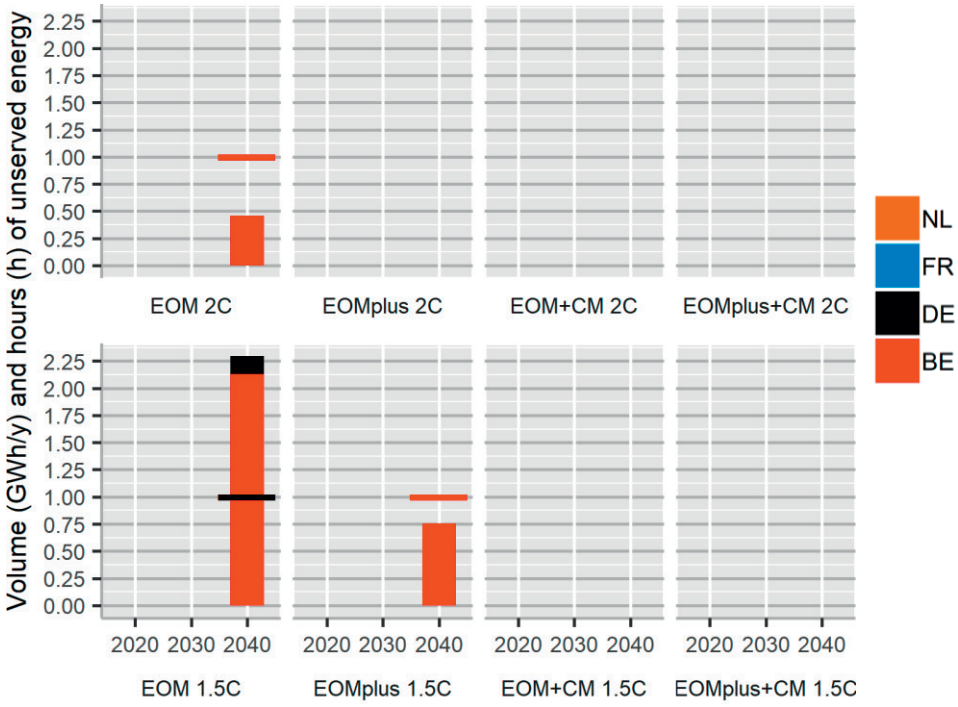

Figure 5-8 | Volume and hours of unserved energy based on UCED simulations for the years 2020, 2030 and 2040 for each market design scenario. Volumes of unserved energy are shown by the vertical bars, while the number of hours with unserved energy are shown with horizontal lines.

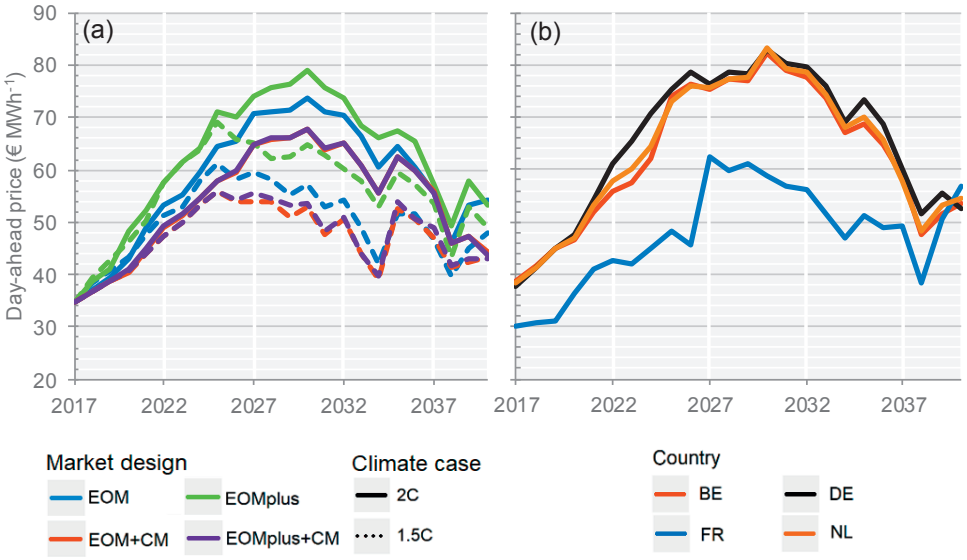

Figure 5-9 | Development of electricity prices over time from long-term simulations. Plot **(a)** shows the load-weighted annual average day-ahead price for the whole CWE region in each scenario, while **(b)** shows the load-weighted annual average price per country for the *EOM 2C* scenario only.

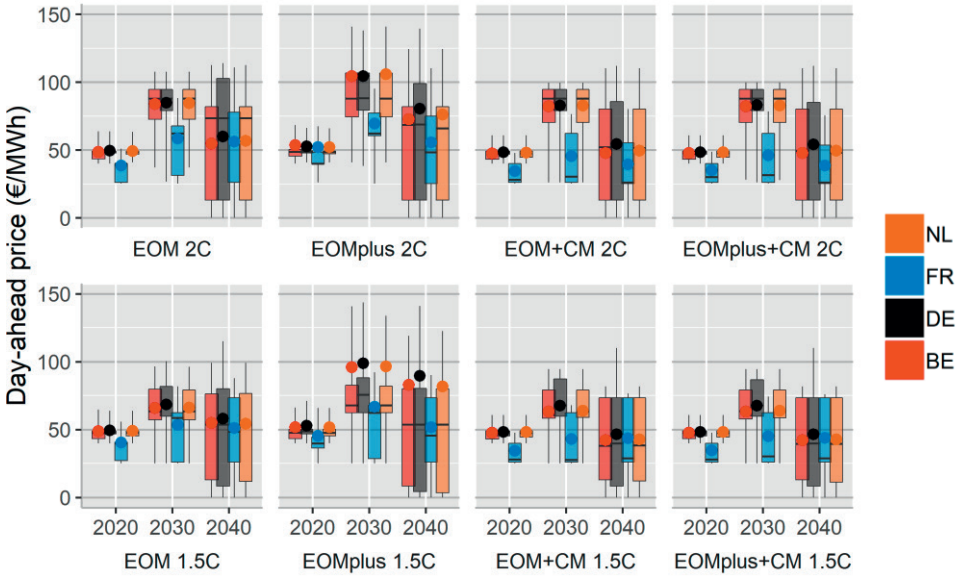

Figure 5-10 | Boxplots of hourly day-ahead electricity prices for the years 2020, 2030 and 2040 based on hourly UCED simulations. The boxes indicate the 25th, 50th and 75th percentile values, while the whiskers indicate the 5th and 95th percentiles. The coloured circles indicate the load-weighted average prices.

Thirdly, thanks to carbon revenues from net-negative emissions, at a carbon price of 120 € t^{-1} BECCS has a SRMC of approximately -20 € MWh^{-1}. At this level, BECCS can underbid mid-merit and even vRES generators; exacerbating the merit order effect, leading to even lower prices in the *1.5C* scenarios. As France maintains its nuclear dominated portfolio which is unaffected by the rising carbon price, and transmission levels are not enough to fully harmonise prices, French electricity prices are the lowest in CWE.

Price volatility increases over time in all countries due to a higher frequency of both low and high prices (Figure 5-10). Mainly as a result of the increasing vRES penetration, the electricity price is zero for approximately 1500 hours in 2040 in the *2C* scenarios. However, these low prices are partly offset by up to 2200 hours with prices above 100 € MWh^{-1} when fossil plants without CCS (in CWE or in neighbouring countries) become price-setting. In the *1.5C* scenarios, the number of hours with zero price increases, while the number of high price hours is lower due to the price-depressing impact of BECCS, leading to lower prices overall.

The presence of a CM also puts downward pressure on electricity prices, as higher supply leads to fewer hours with scarcity and higher prices (Figure 5-11). Setting the CM to maintain capacity margins at 2017 levels may thus be keeping overcapacity in the system[28]. A reformed EOM results in higher prices than in the EOM as load-shedding sets the market price up to 250 hours a year in the *EOMplus 2C* case, and up to 170 hours a year in the *EOMplus 1.5C* case. The presence of a CM not only reduces the frequency of high prices in the *EOM+CM* scenario, but also prevents the activation of demand-side resources in the *EOMplus+CM* scenario, leading to lower prices than in the *EOM* and *EOMplus* scenarios. This suggests that introducing a CM may undermine efforts to develop efficient demand-side response. Overall, however, the climate case has a stronger impact on prices than the market design.

Capacity prices also display considerable volatility, varying mostly in the range of 0 to 100 € kW^{-1} with peaks up to 300 € kW^{-1} (Figure 5-12). Total cumulative capacity payments between 2018 and 2040 range from 325 €bn in the *EOMplus+CM 1.5C* scenario up to 425 €bn in the *EOM+CM 2C* scenario. Total capacity payments are lower in the *EOMplus+CM* scenarios as capacity prices are slightly lower, and there is less capacity receiving payments. GTs and nuclear plants are the largest beneficiaries of a CM in all scenarios, with each receiving approximately one third of total payments, with the remainder going mostly to hydro, CCGT, coal and BECCS plants.

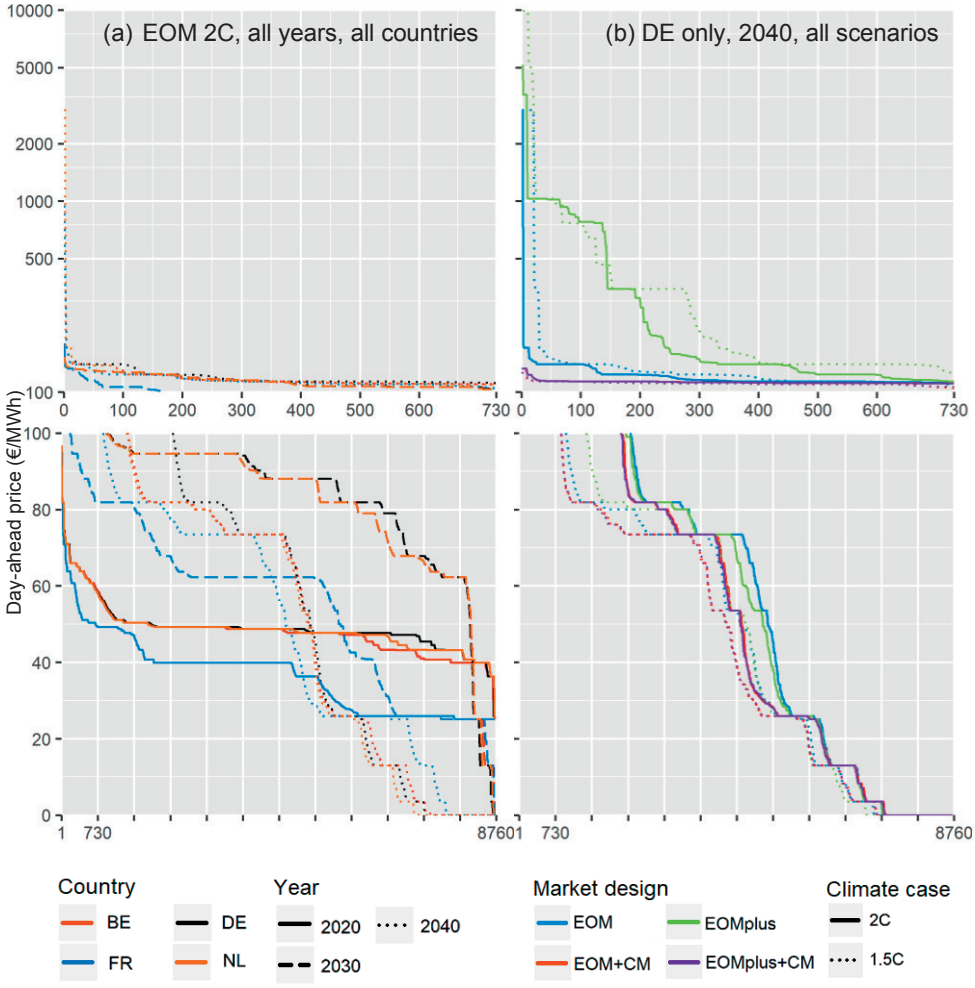

Figure 5-11 | Price duration curves for (a) the EOM 2C scenario, all countries, 2020, 2030, 2040, and **(b)** Germany only, 2040 only, all market designs. The lower plots show the curves for the whole year up to a price of 100 € MWh^{-1}, while the upper plots zoom in on the top 730 hours with the highest prices.

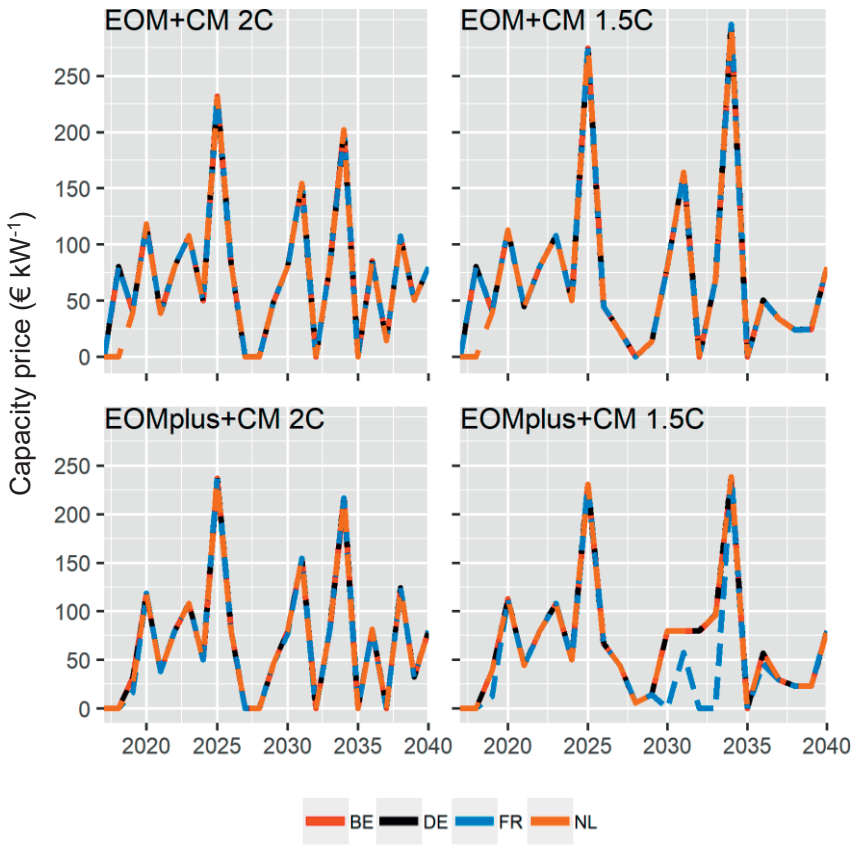

Figure 5-12 | Capacity market prices per scenario.

5.3.5 Generator profitability

On the basis of calculated specific net profits, all conventional thermal technologies fail to recover their long-run marginal cost (LRMC[29]) in most years in the *EOM* and *EOMplus* scenarios (Figure 5-13)[30]. However, if annualised capital expenditure (CAPEX) is excluded (e.g. for existing plants whose investments have already been paid off), nuclear and CCGTs would be profitable in most years (Figure 5-14). The profitability of CCGTs and GTs improves in scenarios with a CM thanks to capacity payments, while the profitability of nuclear falls as the additional revenues from the CM are offset by lower energy market revenues. However, even with a CM, volatile capacity prices mean profitability in any given year is not guaranteed, and may not provide sufficient incentive for new investments. The profitability of baseload nuclear and mid-merit CCGTs increases in the medium term (2030) thanks to higher infra-marginal rents induced by the effect of a higher carbon price on the SRMC of peak gas generators. By 2040 however, this effect is largely dwarfed by the downward pressure of vRES on market prices.

At an aggregated level, most vRES technologies also fail to recover their CAPEX with day-ahead market revenues alone, apart from a short period around 2030 when the impact of the higher carbon price on market prices is not yet offset by the increasing penetration of vRES. Profitability is lower in the *1.5C* than in the *2C* scenarios due to the lower market prices, principally due to BECCS. The market design scenario has less of an impact on the profitability of vRES than on dispatchable technologies as the former are less dependent on scarcity prices and, with low firm capacities, receive only a fraction of the capacity price. Country-specific differences also exist. For example, vRES are less profitable in France than in the other CWE countries due to the lower electricity prices; while in the Netherlands, onshore and offshore wind are more profitable than in the other CWE countries due to higher capacity factors, and are able to recover their CAPEX between 2025 and 2035 in the *2C* scenarios.

Turning to the NETs, BECCS is unable to recover its LRMC until the mid-2030s, once the carbon price has reached around 120 € t^{-1}. When BECCS is deployed in 2037 in the *2C* scenarios however, it is one of the few profitable technologies as it receives not only day-ahead and CM revenues, but also carbon revenues. DAC, on the other hand, is not profitable in any scenario for the time period considered due to its high operating and capital costs, even at a carbon price of 120 € t^{-1}.

5.3.6 Total Cost

Comparing the total costs incurred between 2017 and 2040 per cost type and technology shows that, for a given climate scenario, the *EOM+CM* design results in the highest costs, mostly due to capacity payments (Figure 5-15). In the absence of a CM, load shedding in the reformed EOM in both the *1.5C* and *2C* climate cases has only a marginal impact on total costs (less than 1%), as lower generation costs are mostly offset by the cost of load-shedding. In the *EOMplus+CM* scenarios however, load shedding reduces total costs by up to 5%, mainly by reducing investments in GTs. The exogenous vRES deployment also has a major cost impact, representing around 50% of total costs in the *EOM 2C* scenario, and 28% in the *EOM 1.5C* scenario. Comparing the climate cases, costs in the *1.5C* scenarios range from ~2800 €bn *(EOM 1.5C)* to ~3300 €bn *(EOM+CM 1.5C),* more than double the costs in the *2C* scenarios. This is due to the additional CAPEX and operating costs required for NETs and in particular, DAC. If DAC were not used, and deployment of NETs was limited to the 25 GW of BECCS, total costs in the *EOM 1.5C* scenario would fall to ~1800 €bn, or just 33% more than in the *EOM 2C* scenario. Thus, when biomass supply is limited, the cost of DAC will largely determine the cost-effectiveness of relying on the power sector to offset more than 250 Mt CO_2 y^{-1} emissions from other sectors.

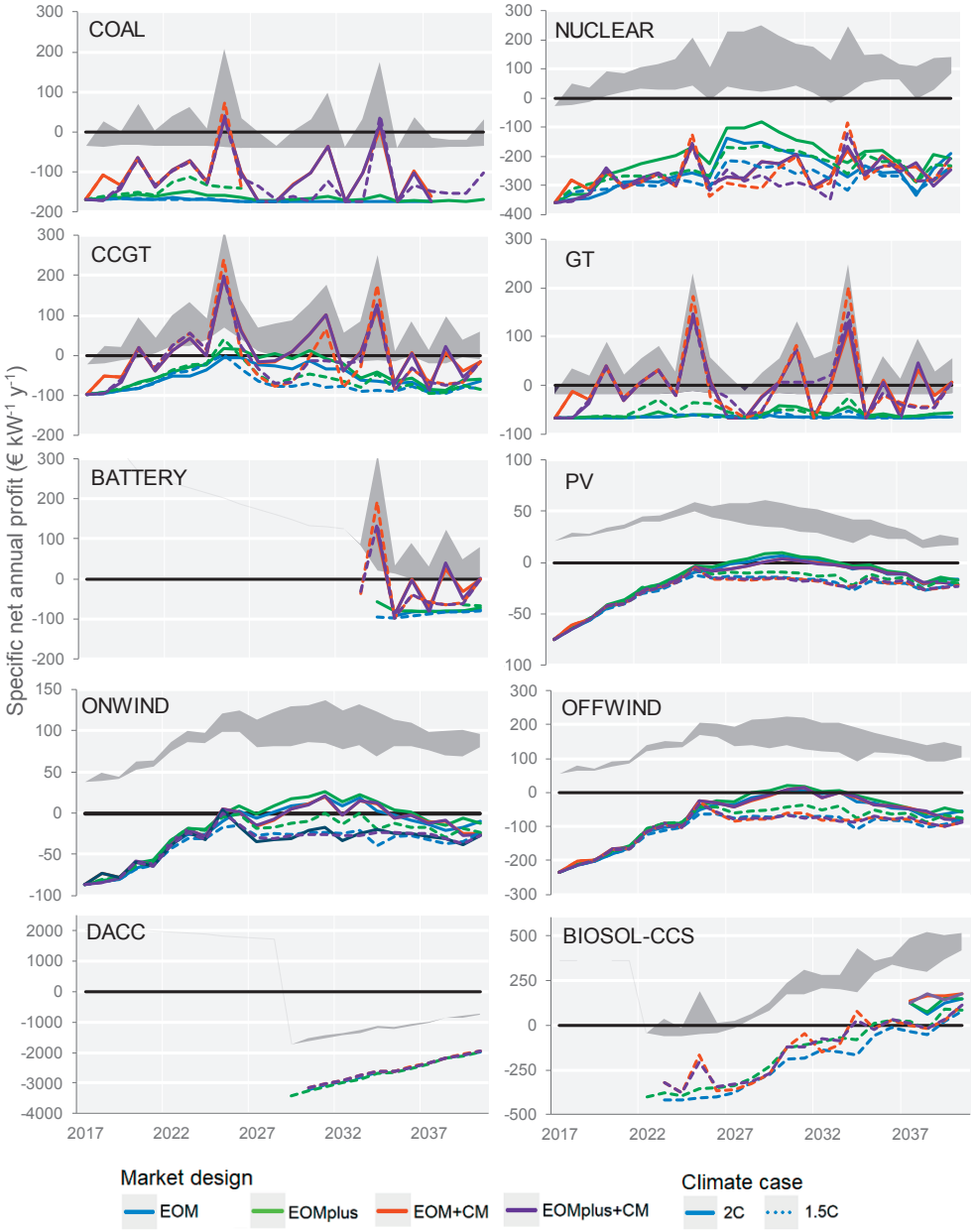

Figure 5-13 | Specific net annual profit per market scenario for selected technologies based on long-term simulations from 2017 to 2040, accounting for all revenues, variable and fixed costs, including annualised CAPEX. The darker shaded grey area indicates the range of specific profitability across the scenarios excluding annualised CAPEX.

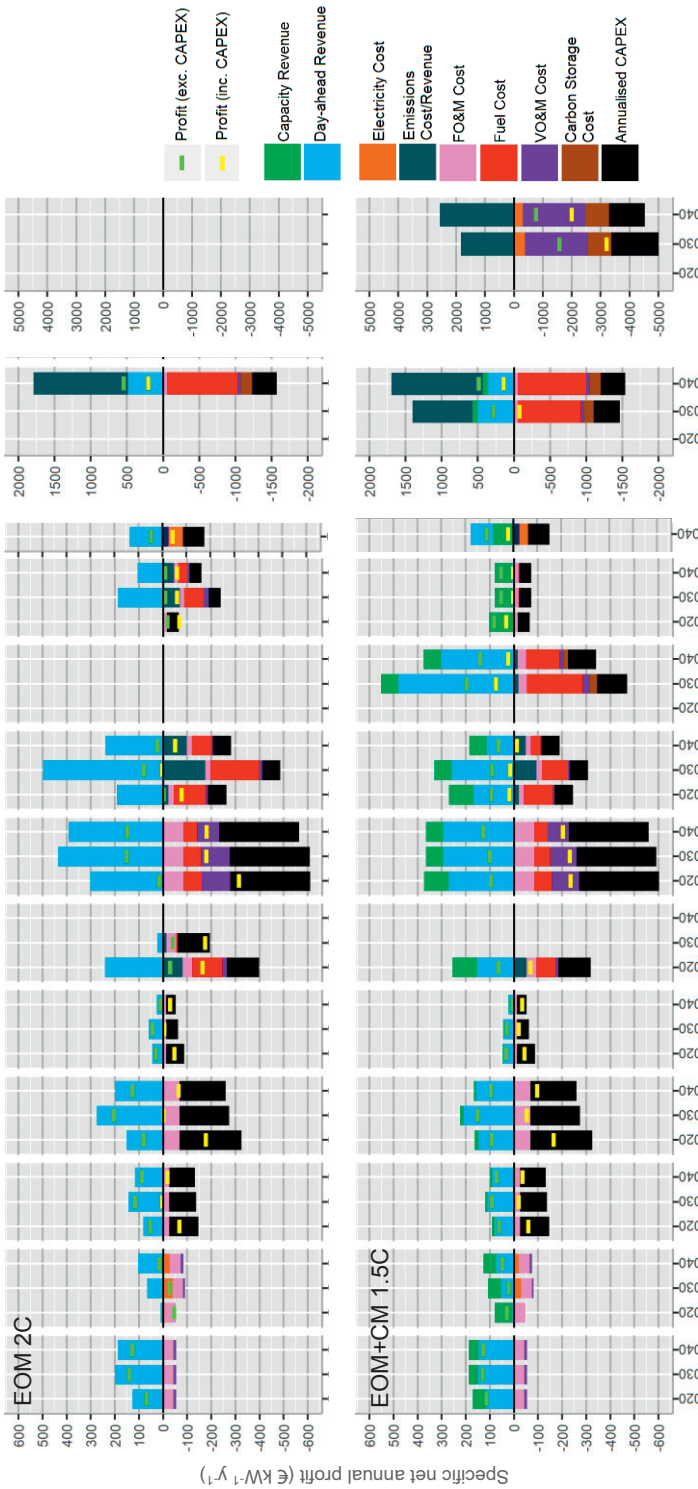

Figure 5-14 | Specific revenues, costs and profitability per technology aggregated across CWE for the *EOM 2C and EOM+CM 1.5C* scenarios based on short-term UCED simulations. Specific costs and revenues are depicted by the bars, with revenues given as positive and costs as negative. Specific profit is shown by the (—) symbols both excluding (green) and including (yellow) annualised CAPEX. Note the different vertical axis scales for the NETs. Annualised CAPEX is shown for new-build plants, while retrofits will be cheaper. Hydro investment costs are not shown as these vary considerably from one location to another. Electricity cost includes the costs for battery charging, pumping energy for hydro plants, and electricity demand for DAC.

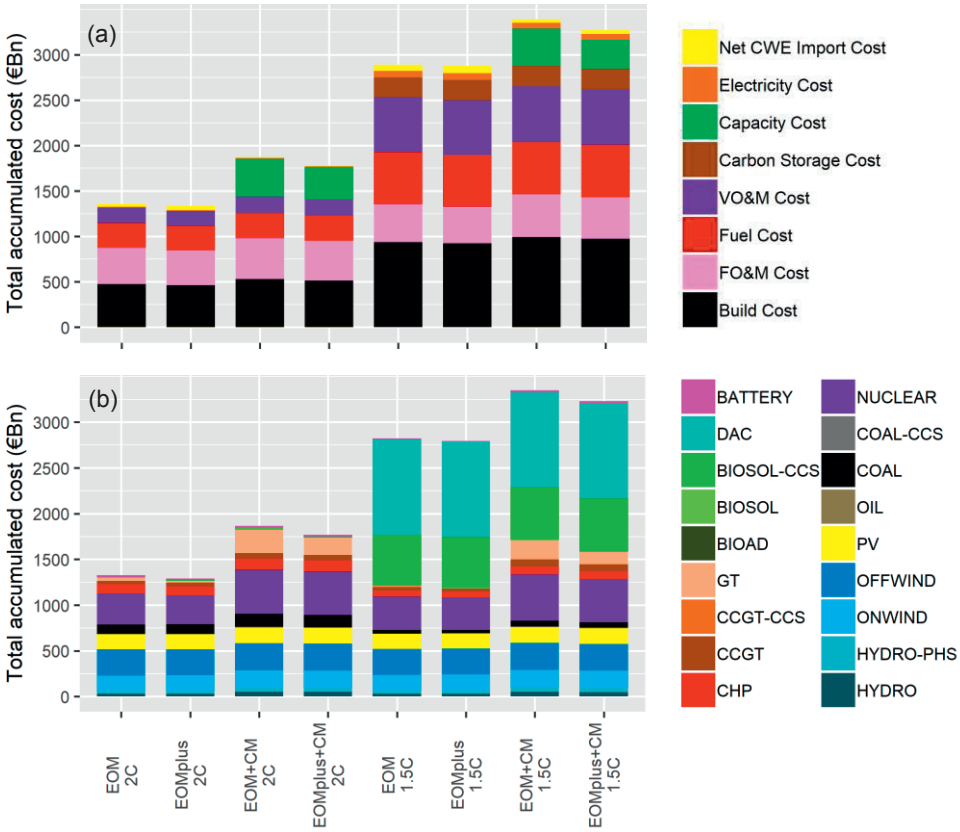

Figure 5-15 | Total accumulated costs (a) per cost type and **(b)** per technology for the period 2017-2040 for each scenario. Total costs for load shedding (approx. 4 €bn), generators start-ups (7 €bn), and unserved energy (less than 1 €bn) are relatively small and not shown. Capacity Cost is the total cost for capacity payments which, while a revenue for generators, represents a cost to society. Electricity Cost includes the costs for battery charging, pumping energy for hydro plants, and electricity demand for DAC. Net CWE import cost is the net cost of imports from countries neighbouring CWE. Costs for transmission investments and emissions are not included.

5.3.7 Sensitivity Analysis

An overview and rationale for the runs performed is shown in Table 5-5. Most runs use only the capacity expansion algorithm to examine the impact on the technologies deployed in the portfolios, rather than performing full UCED simulations. In most sensitivity runs, the minimum vRES capacity still increases exogenously per year as in the base runs. However, unlike in the base runs, the model is free to invest in more vRES capacity in all sensitivity runs[31]. The sensitivities are run based on the *EOM* market design for both the *2C* and *1.5C* climate cases, except for the *Tighter capacity margin* sensitivity which is run for the *EOM+CM* design.

Figure 5-16 shows the final 2040 generation portfolios and total accumulated costs for each sensitivity run. Most sensitivity runs show only minor impacts on the portfolios developments and long-term system costs, though there are some notable exceptions:

- when vRES capacity is fully optimised in the *optimised vRES* runs, far less vRES capacity is installed, and total costs fall by approximately 20% and 7% compared with the reference *EOM 2C* and *1.5C* cases respectively. Lower costs are achieved by deploying less vRES, fewer batteries, keeping more existing nuclear capacity online, and installing more NGCC-CCS and BECCS capacity (*1.5C* only);
- when the model is given even more freedom in the *free portfolio optimisation*, costs are reduced even further compared with the reference cases (-25% for *2C*, -9% for *1.5C*). This is achieved by keeping existing German and Belgian nuclear plants online, deploying less vRES, and installing more BECCS capacity (*1.5C* only);
- relaxing the upper limit on vRES deployment has no effect, as no sensitivity run results in more vRES capacity installed in 2040 than in the base runs. This observation, and the first two points above suggest that electricity for DAC is more cost-effectively supplied by baseload generators such as BECCS and nuclear than vRES, as capital-intensive DAC needs high capacity factors to maximise its effectiveness;
- *increasing the supply of biomass* has no impact on the *2C* case as the biomass constraint is not binding, but reduces total costs by 25% in the *1.5C* case as more BECCS can be deployed instead of DAC. However, biomass demand increases to 9.5 EJ y^{-1} in 2040, or three times the assumed CWE solid biomass potential; and
- *excluding BECCS* from the portfolio (e.g. due to public or political opposition) leads to 20% higher costs in the *1.5C* case due to higher DAC deployment required.

5.4 Discussion

5.4.1 Implications for vRES

Our results suggest that, assuming vRES investment costs continue to fall and the carbon price continues to rise, the profitability of vRES should improve – at least in the medium term. However, subsidies may still be required to cover investment costs. When subsidies are necessary, they should minimise electricity market distortions, and ensure vRES are exposed to market price signals (Hu et al., 2018). For example, feed-in premiums may be preferable to feed-in tariffs as the former expose vRES to market price signals. Others argue that in the long term, capacity-based subsidies for vRES may be preferable to energy-based payments, as they cause fewer market distortions (Hu et al., 2018)[32]. However, irrespective of the support mechanism, continued subsidy-driven vRES deployment is likely to put downward pressure on the carbon price, undermining its ability to act as a price signal for investments in low-carbon technologies (including NETs), and potentially locking in a need for continued subsidisation.

Table 5-5 | Overview of the sensitivity runs performed

Sensitivity run	Description	Motivation
Higher fossil fuel prices	Fossil fuel prices increase over take based on *450* Scenario from the IEA's WEO 2016 (IEA, 2016d). The gas price rises 50% to 8 € GJ $^{-1}$ by 2040, while coal falls nearly 50% to 1.4 € GJ $^{-1}$.	Investigate the impact of higher fuel price developments
Higher demand	Assume that electricity demand per CWE country increases with a year-on-year growth rate of 1.3% (Eurelectric, 2018), resulting in a total CWE demand of 1576 TWh in 2040 [a].	Many scenarios assume increased demand from electrification is offset by efficiency measures, which may not materialise. Also, electrification of industry, heating and transport may be stronger than assumed.
Higher battery cost	Battery costs remain at their base 2017 level, assuming significant cost reductions do not take place.	Investigate impact of less favourable battery cost developments.
Higher biomass price	Instead of a fixed biomass price of 8 € GJ $^{-1}$, the biomass price increases over time reaching 12 € GJ $^{-1}$ in 2040 (i.e. +50% vs 2017).	Investigate the impact of increased competition for biomass putting upward pressure on prices.
Blue hydrogen	Assume hydrogen is available at a cost of 13 € GJ $^{-1}$, the minimum required price for blue hydrogen to be profitable at the base natural gas price (5.9 € GJ $^{-1}$) (M. Mulder et al., 2019)	Determine if including blue hydrogen could play a role in the power system
No retrofits	Exclude the option to retrofit coal (and biomass) plants for BECCS, or natural gas plants with CCS	Determine the potential cost impact of retrofitting existing coal, natural gas and biomass plants
Lower/higher WACC	A lower WACC of 4% is assumed, closer to the social discount rate (EC, 2014b). A higher rate of 12% is also assumed.	Investigate the impact of different discount rates on the analysis.
No biomass limit	The constraint on CWE biomass potential of 3 EJ y^{-1} is removed. *Note: the biomass price remains the same.*	Test the impact of allowing additional biomass supply imported from outside CWE or even outside Europe.
No BECCS	Assume no BECCS plants can be built.	Investigate the impact of political opposition to BECCS.
CCS only with DACC	Assume that CCS can only be used for DAC, not with fossil fuels or biomass.	Investigate the impact of political opposition to CCS, which is only used as a last resort option for DAC.
Optimised vRES	Instead of fixing the minimum (and maximum) annual deployment of vRES exogenously, the model is completely free to optimise vRES from the 2017 starting level.	Determine the consequences of policy-driven vRES growth on the cost-optimum deployment of other portfolio technologies.
Full portfolio optimisation	Similar to the *Optimised vRES* run, with the addition that the model is fully free to retire or invest in any technologies with no restrictions. *This sensitivity includes higher (12%) and lower (4%) discount rate variants.*	Determine the unconstrained least-cost generation portfolio development.
Tighter capacity margin (EOM+CM)	Instead of maintaining capacity margins at their 2017 levels, the CM is set to match the yearly margins from the EOM scenarios.	Maintaining margins at 2017 levels could be maintaining overcapacity in the system.
Transmission outages included (UCED only)	Transmission lines between countries are modelled assuming a 10% outage rate based on reported availabilities (ENTSO-E, 2018d).	Investigate the impact of transmission outages on the solution.

[a] *Based on 'Scenario 2' from Eurelectric's Decarbonisation Pathways study (Eurelectric, 2018). This scenario sees electrification rates (share of final consumption) for transport, buildings and industry in the EU rise from 1% to 43%, 34% to 54% and 33 to 44% between 2015 and 2050 respectively, with the resulting economy-wide electrification rate increasing from 22% in 2015 to 48% in 2050. The electricity demand in 2040 is 26% higher than in 2017.*

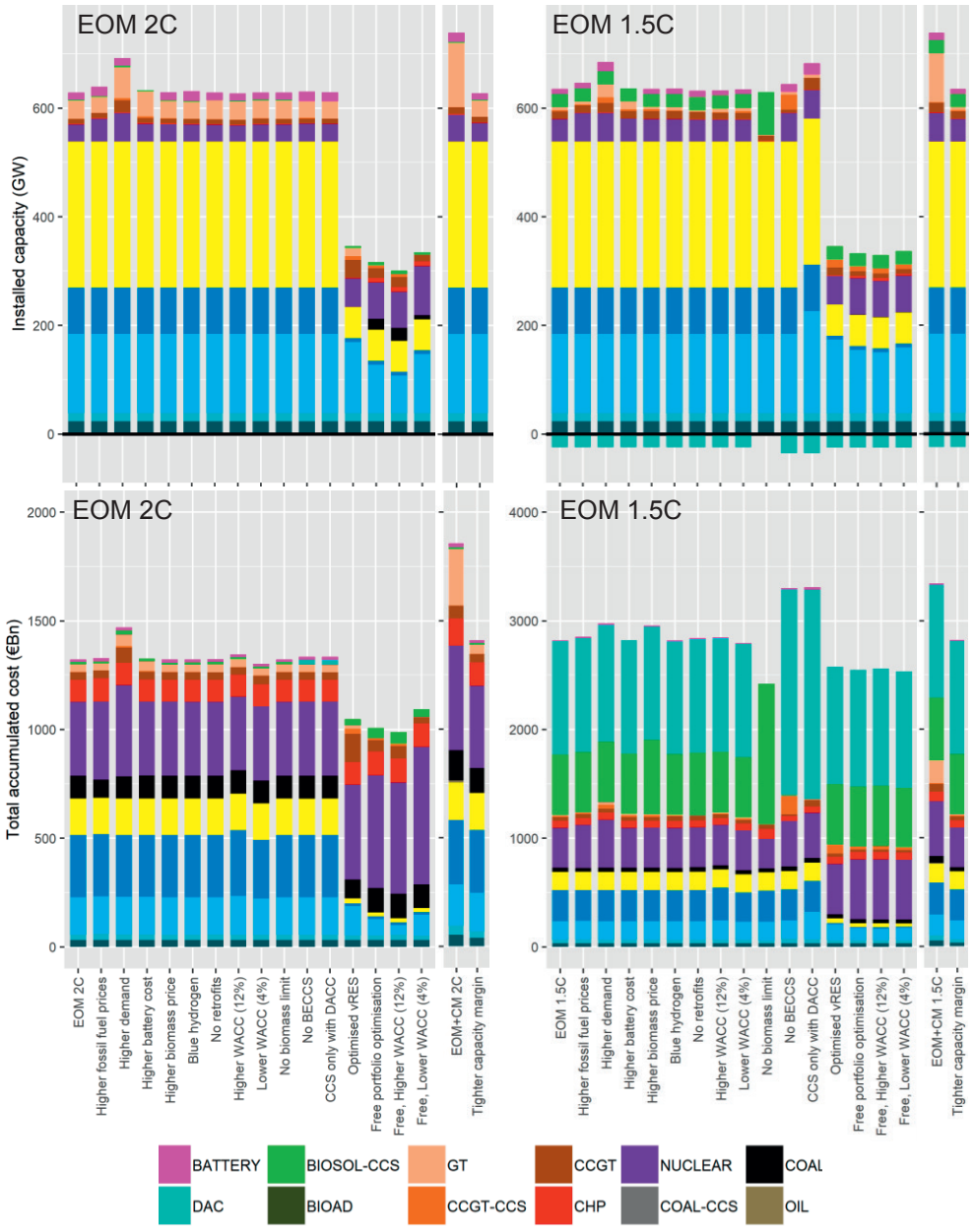

Figure 5-16 | Installed capacity per technology in 2040 (upper plots), and total accumulated costs for the period 2017-2040 per technology (lower plots) for each sensitivity run. The results of the original EOM(+CM) 2C and EOM(+CM) 1.5C base runs are also shown for reference. Note the different vertical axis scales for the *2C* and *1.5C* cases in the total cost plots.

Once vRES generates up to 60% of electricity across CWE in 2040, our scenarios show that purely SRMC-based bidding could lead to up to 1500 hours a year with electricity prices near zero, with a negative impact on generator profitability. However, these sustained periods with zero prices may not eventuate. For example, in periods when vRES generation is forecast to be very high (approaching 100% of demand) and prices would approach zero, vRES could essentially operate as a kind of distributed monopoly, and offer their electricity at a higher price more reflective of their LRMC. Secondly, significant periods with very low electricity prices may incentivise additional demand in the long term, putting upward pressure on prices (Ecorys, 2017).

5.4.2 Implications for NETs

NETs may have an important role to play to achieve a least-cost decarbonisation pathway, but they will also have several effects on the electricity market. For example, BECCS (retrofits) could lower the cost of decarbonisation by utilising existing coal infrastructure and reducing the need for additional GT capacity, but may also put downward pressure on electricity prices. DAC also has several impacts on market operation. At a carbon price of 120 € t^{-1}, DAC will operate whenever the electricity price is below approximately 135 € MWh^{-1}, leading to additional baseload electricity demand[33]. As DAC would be unprofitable at higher electricity prices, it would not operate during scarcity periods, and would not increase peak demand.

We find that BECCS could be profitable from the mid-2030s onwards, but only under the assumption that plants receive revenue for the negative emissions they deliver. Thus, the incentive for carbon capture and utilisation provided by the EU ETS – avoiding the need to surrender CO_2 allowances – is unlikely to be sufficient to incentivise development of NETs[34]. One possible method to help close the revenue gap for NETs would be to allow them to generate emission allowances. This mechanism would have the advantages of being market based, following the 'polluter pays' principle, and incentivising cost reductions in NETs. However, such a mechanism would need good governance systems to ensure that negative emissions were achieved sustainably, and require the quantity of annual centrally-auctioned certificates to be reduced based on the negative emissions achieved by NETs to prevent oversupply.

While such a mechanism could underpin the business case of BECCS, DAC would still be unprofitable in all scenarios – even when revenues from negative emissions are included. In order to increase carbon prices to the level needed to stimulate DAC by 2030 (~250 € t^{-1}), the volume of emission allowances auctioned annually would need to be rapidly reduced[35], or a carbon price floor could be implemented to top-up the ETS price (Newbery et al., 2019). By the time DAC is deployed, it would predominantly be used to generate carbon allowances to sell to non-energy sectors, as residual power sector emissions are close to zero. Our proposed mechanism would see some of the costs for DAC born by these sectors, but not all. Thus, if

DAC is to be deployed at large scale, policymakers would need to decide how society should pay for it in the most equitable way.

5.4.3 Caveats

Our results should be seen in the context of the scope limitations and uncertainties, as discussed below.

The investments in our study are determined by a model with perfect foresight finding least-cost pathways under given emission constraints. However, real-world energy transitions do not necessarily follow the least-cost pathway due to government interventions to achieve other policy goals, externalities not accounted for in investor costs, myopic investors, and imperfect cost assumptions (Trutnevyte, 2016). Instead, it has been argued that transitions follow the most 'investable' path (Gross et al., 2010; Trutnevyte, 2016). Some try to account for real investor behaviour by considering 'near-optimal' solutions (Trutnevyte, 2016), or using alternative models such as agent-based (Kraan et al., 2019) or equilibrium competition models (de Maere D'aertrycke et al., 2018; Gurkan et al., 2013). However, our focus is to understand whether different market designs would create business cases for investment in generation facilities. In this case, we consider cost minimisation a reasonable approach given the key aims of liberalised markets to achieve reliable supply of electricity within environmental limits at minimum costs. Thus, we evaluate the market designs versus the critical part of the investor behaviour that they need at minimum a viable business case before they invest. Given our results showing hardly any technology is profitable in the long-term, our finding is that even if the behaviour of real investors had been included, very few investments would have been made in any scenario. As a consequence, governments would likely need to intervene and tweak markets to create an investable path towards low-carbon electricity portfolios. This can hardly be considered a truly liberalised market.

This study solely addresses the direct cost of electricity generation and did not include indirect costs such as storage of nuclear waste, costs of negative environmental externalities, or decommissioning costs. We also do not consider the increasing cost (or environmental impacts) of biomass supply, CO_2 storage, or vRES with increasing use or deployment. Such considerations should also be taken into account when designing energy policies.

Other EOM and CRM designs have been proposed which we have not evaluated. For example, the ERCOT market in Texas has implemented a price 'adder', which is administratively added on top of the real-time electricity price during times of scarcity (Potomac Economics, 2018)[36]. Strategic reserves, capacity obligations, and reliability options are additional CRM designs which have been implemented in other countries, but were not evaluated in this study. Nevertheless, efficient coordination of the power system relies on effective short-term price signals which reflect the value of electricity at each moment in time, which are not delivered by a CRM.

Our study is limited to the day-ahead and capacity markets. While the requirements for FCR are included, we do not explicitly model frequency restoration reserves (FRR). However, even under the conservative assumption that FRR requirements rise linearly with vRES penetration (which is unlikely (Brouwer et al., 2014)), the modelled portfolios should be able to account for this[37]. Generators may also be able to garner additional revenues from ancillary services, intraday and balancing markets (Pollitt & Chyong, 2018). However, while balancing markets are growing (Tennet, 2018), their monetary value is expected to remain less than 4% of the day-ahead markets – at least up to a vRES penetration of around 30% (Ortner & Totschnig, 2019). Nevertheless, in the long term, intraday and balancing markets – which better reflect the instantaneous value of electricity – could grow in importance as a revenue source for providers of flexibility and firm capacity.

We assume the power sector must deliver all the negative emissions necessary to meet the 2 ºC and 1.5 ºC carbon budgets, while in fact BECCS may be cheaper to apply in other sectors (e.g. transport) (van Vliet et al., 2011). To avoid the high costs of DAC, policymakers could consider exploiting other potentially lower cost NETs first, such as afforestation (Smith et al., 2017). However, the IPCC carbon budgets consistent with 1.5 ºC warming already assume negative emissions from agriculture, forestry and land use of 1-11 Gt CO_2 y^{-1} globally by 2040, the upper limit of which exceeds the estimated potential of 3.6 Gt CO_2 y^{-1} [38]. By considering both a net-zero and a strongly negative emission scenario, we show the consequences of relying either marginally or strongly on the electricity sector to offset emissions from other sectors. Moreover, investing earlier in NETs in the power sector may also be a prudent insurance policy against climate overshoot as a result of delayed decarbonisation in other sectors, and spreading the cost of negative emissions over a longer period may be more socially equitable (Obersteiner et al., 2018).

Despite the growth in vRES, the need to deliver negative emissions means that our *1.5C* portfolios rely significantly on CCS technology to deploy BECCS, CCGT-CCS, and DAC. As a result, the amount of carbon stored annually in CWE approaches 1 Gt y^{-1} in 2040 in the *1.5C* cases, with the total cumulative amount of CO_2 stored reaching 8 Gt by 2040 (compared with only 70 Mt in the *2C* cases). While significant, this is below the total estimated CWE storage capacity of 28 Gt, and far below total European estimates of 97 to 116 Gt (EASAC, 2013; EU GeoCapacity Project, 2009). Also, we assume fixed CO_2 transport and storage costs of 15 € t^{--1} CO_2 (Zero Emissions Platform, 2011), which might not be realistic as cheaper sites are depleted and more costly storage sites must be used. However, even in the case that the cheapest offshore storage sites in CWE are depleted, estimated costs to transport CO_2 from CWE to large storage sites in the North Sea are comparable with the value assumed in this study[39].

Price developments are inherently uncertain, and CWE prices will depend not only on fuel prices, the carbon price and portfolio developments inside CWE, but also developments in

other sectors and neighbouring countries. For example, our scenarios still retain some fossil (gas) capacity without CCS in 2040 which, due to the high carbon price, leads to several hundred hours with prices above 100 € MWh^{-1}. However, if fossil capacity in CWE and in neighbouring countries were also equipped with CCS or converted to CO_2-free energy carriers, these high prices may not materialise, with a further adverse effect on generator profitability.

We assume the investment costs for PV, onshore and offshore wind fall by 60%, 14% and 34% respectively between 2017 and 2040, in line with the most optimistic RES deployment scenario from (Tsiropoulos et al., 2018). Notwithstanding these reductions, none can recover their annualised CAPEX in 2040. However, we only consider aggregated national capacity factors for vRES, and plants installed at locations with more favourable weather conditions will be more profitable. Generator costs are uncertain and CAPEX assumptions strongly affect their profitability. However, PV, onshore and offshore wind CAPEX would have to fall by a further 50% (to ~200 € kW^{-1}), 20% (to ~900 € kW^{-1}), and 40% (to ~1300 € kW^{-1}) respectively from the assumed 2040 values for them to be able to recover their investment costs from day-ahead market revenues alone. While possible, such reductions would be contingent on the most optimistic learning rates (Tsiropoulos et al., 2018)[40].

The increasing carbon price assumed in our study puts upward pressure on electricity market prices, an effect seen in other studies (Kraan et al., 2018; Tennet, 2019). This improves the profitability of vRES, baseload and mid-merit generators. However, market factors which put downward pressure on the carbon price such as subsidy-driven vRES deployment, or weaker economic conditions will also put downward pressure on electricity prices, reducing the profitability of generators and NETs. Thus, policy changes such as redesigning vRES subsidies, or more rapid reductions in the volume of allowances auctioned may be necessary to drive the carbon price to the level required for timely decarbonisation.

5.5 Conclusions and policy recommendations

In this study, we evaluate least-cost pathways to decarbonise the Central Western Europe (CWE) power system until 2040 under the assumption of an increasing share of variable renewable energy sources (vRES), for four different electricity market designs: the current energy-only market, a reformed energy-only market, both also with the addition of a capacity market. Each design is modelled for one decarbonisation pathway targeting net-zero emissions by 2040 consistent with a 2 ºC warming limit, and another targeting -850 Mt CO_2 y^{-1} net-negative emissions consistent, with a 1.5 ºC warming limit. Our main findings are:

- bioelectricity with carbon capture and storage (BECCS) is a cost-effective way of rapidly decarbonising the power sector, especially when aiming to limit warming to 1.5 ºC by mid-century. However, it may also put downward pressure on electricity prices;

- assuming a maximum biomass supply of ~3 EJ y^{-1}, the CWE power sector could offset up to 250 Mt CO_2 y^{-1} from other sectors using BECCS. Offsetting more than this leads to significantly higher costs due to the need for direct air carbon capture (DAC), and policymakers should consider exploiting cheaper negative emission technologies (NETs) where possible to reduce the need for DAC;
- if DAC is deployed, baseload generators such as BECCS and nuclear appear to be more cost-effective options for supplying electricity for DAC than vRES;
- keeping existing nuclear capacity online should help maintain security of supply, reduce carbon emissions, and lower electricity prices;
- deploying high levels of vRES (up to 70% penetration based on energy) may result in up to 1500 hours with an electricity price of zero by 2040, undermining the effectiveness of a carbon price as an investment signal for other low-carbon and NETs; and
- policies relying primarily on vRES for decarbonisation could increase the cost of the transition by 10% to 25% (depending on the level of climate ambition) compared to a more diversified portfolio containing vRES, nuclear, natural gas (with carbon capture and storage) and BECCS plants.

In terms of electricity market design and generator profitability, we find that:

- none of the market designs modelled allow all technologies to recover their investment costs in the long term in either decarbonisation scenario;
- while capacity markets can improve the profitability of mid-merit and peaking gas plants, they can also undermine the profitability of baseload and vRES generators if they result in oversupply and depress electricity prices. Thus, a capacity market is not necessarily a silver bullet for addressing capacity adequacy concerns;
- day-ahead market revenues of existing baseload and mid-merit generators may improve in the medium term (2030) thanks to higher infra-marginal rents induced by the effect of a higher carbon price on peak generators; however, this effect may be dwarfed in the long term by the downward pressure of vRES on market prices; and
- adding a mechanism in the European emissions trading scheme to remunerate NETs for negative emissions could help make BECCS profitable from carbon and electricity market revenues alone by the mid-2030s. However, DAC, if deployed at large scale, would likely still need government support.

Further research is needed to quantify to what extent intraday and balancing market revenues could complement day-ahead revenues for flexible generators, identify policy instruments to support vRES without reducing the effectiveness of the carbon price, and how large-scale investments in NETs could be supported.

Footnotes to Chapter 5

[1] For example, day-ahead prices in Germany and Sweden in 2015 were nearly 50% lower than in 2011 (Bublitz et al., 2017; Hirth, 2018). However, aside from vRES, generation overcapacity, lower fuel and carbon prices perhaps had an even more significant effect on prices (Bublitz et al., 2017; EC, 2016a; Hirth, 2018).

[2] VRES represented 15% of total EU28 generation in 2017 (Eurostat, 2019d). The Joint Research Centre's EU Reference Scenario 2016 considers 35% for the EU28 by 2050 (EC, 2016b), while the European Commission Energy Roadmap 2050 considers between 32%-65% (EC, 2011d). Meanwhile, ENTSO-E scenarios consider vRES shares between 31%-39% already in 2030, rising to 45-58% by 2040 (ENTSO-E & ENTSO-G, 2018). EU Commission scenarios consider up to 70% by 2050(EC, 2018a).

[3] As of 2017, twelve EU countries operated EOMs, while fifteen had implemented CRMs. A capacity market was in place in the UK; a capacity payment in Portugal, Spain, Ireland, Italy and Greece; a strategic reserve in Belgium, Germany, Poland, Sweden, Finland, Latvia, and Lithuania; a reliability obligation in France; and a capacity tender in Bulgaria. The remaining EU countries, Switzerland and Norway operate EOMs (ACER & CEER, 2018). For a detailed explanation of CRM designs, the reader is directed to significant literature on this topic e.g. (Bublitz et al., 2018; Cramton et al., 2013; EC, 2015, 2016c).

[4] Based on ENTSO-E's 2018/2019 system adequacy outlook (ENTSO-E, 2018g), there is no clear correlation between system adequacy concerns in those countries with CRMs and those without (including Denmark, which has the highest vRES penetration of all EU countries).

[5] Recent data shows the German average annual spot price rose 40% between 2015 and 2018, restoring it to a similar level as in 2011 (ENTSO-E, 2018b).

[6] 'Failures' refer to deviations from the assumptions underlying an ideal theoretical market such as perfect competition (e.g. all firms are price-taking, no barriers to entry or exit, an inelastic demand side), or distortions which prevent EOMs from working effectively such as (e.g. market price caps, out-of-market interventions by transmissions system operators (TSOs), price-inelastic demand) price caps, which lead to the so-called "missing money" problem (Biggar & Hesamzadeh, 2014; Lin & Magnago, 2017). However, examining historical day-ahead market prices in France, Germany, the Netherlands and Belgium for the years 2015-2018 reveals no periods when the price actually reaches the cap (ENTSO-E, 2018b). This may be due to TSOs making out-of-market interventions before scarcity events arise, implicit caps set by other markets, the presence of existing CRMs, or cautious market players restraining bids for fear of being accused of exerting market power (EC, 2016a).

[7] PLEXOS is developed by Energy Exemplar (https://energyexemplar.com/)

[8] For neighbouring countries, a single generator per type is defined with maximum capacity based on national statistics, with the portfolio following the deployment in ENTSO-E's TYNDP 2018 *Best Estimate* scenarios for the years 2020 and 2025, *Distributed Generation* scenario for 2030 and *Global Climate Agreement* scenario for 2040 (ENTSO-E, 2018f). These scenarios do not provide any information on the split between GTs and CCGTs in natural gas capacity, nor the share of capacity equipped with CCS in neighbouring countries. Thus, we assume a split of 30/70 split between GT/CCGT capacity based on the split in CWE, and do not consider CCS in neighbouring countries.

[9] The future direction of French nuclear policy is unclear. After attempting to legislate in 2014 to limit nuclear capacity to 63 GW and 50% of electricity supply by 2025 with the *Energy Transition for Green Growth* bill, this was met with resistance in the French Senate, and ultimately the decision was delayed until after 2017. In November 2018, a draft of the new policy delayed the target year for reducing the share of nuclear to 50% until 2035 with a plan to close 14 reactors by 2035, but with the option to build new reactors still available (World Nuclear Association, 2018). Given this policy uncertainty, and that even planned closures occur much later than in Germany or Belgium and may still be subject to debate, in this study we impose no caps or forced retirements for nuclear power in France.

[10] Demand profiles for 2017 are taken from historical data (ENTSO-E, 2018b), while demand profiles for the years 2020, 2025, 2030 and 2040 are taken from the *Best Estimate 2020 and 2025*, *Distributed Generation 2030* and *Global Climate Action 2040* scenarios. Demand profiles for the intervening years are interpolated on an hourly basis between the fixed scenario years so that the hourly demand profile also changes from 2017 to 2040. The Global Climate Action scenario is the most ambitious of all the TYNDP scenarios in terms of vRES growth. While exogenously specifying vRES capacity means the resulting portfolios are not necessarily least-cost, this is the policy direction many member states are pursuing.

[11] This value reflects the historical WACC of European power companies in the range of 6% to 10% (Donovan, 2015; Eurelectric, 2013b). At this level, the WACC is higher than the 4% financial discount rate or social discount rate of 3% to 5% recommended by (EC, 2014b). However, in the sensitivity analysis we find that the discount rate does not have a significant impact on the results when so much vRES capacity is forced in exogenously.

[12] If annual deployments are not limited, the model delays investments in new technologies until the end of the simulation horizon once costs have fallen, leading to very high deployment in a single year. Restricting the deployment rate

smooths investments over a longer period, accounting for higher costs in early years. While actual deployment rates are likely to follow a more exponential growth pattern, implementing such complex constraints was not possible in PLEXOS.

[13] Retrofitting with CCS is not considered for CHP plants as these will have less waste heat available for the capture solvent regeneration, and are unlikely to have sufficient full load hours to justify investment in CCS (IEA, 2016c).

[14] Two different carbon prices are used in the model: the shadow price, and the accounting price. The *shadow* price is the value of the dual variable associated with the carbon emissions constraint applied in the capacity expansion algorithm that is required to meet the decarbonisation trajectory. It is a model output which has a value of zero when non-binding, and non-zero value when binding. By contrast, the *accounting* price is the assumed economic value of carbon used in the profitability calculations (Section 5.3.5), specified exogenously to follow the IEA's 450 scenario. In the capacity expansion algorithm, we only implement a carbon constraint, as implementing both a carbon constraint and exogenous price may lead to methodological inconsistencies. However, when performing ex-post calculations on generator costs, revenues and profitability (Section 5.3.5), we use the emission accounting price. As a result of this, the accounting price taken from the 450 scenario is not included in the capacity expansion objective function, and does not affect the development of the generation portfolio. However, in the UCED runs, we incorporate the accounting carbon price in the objective function, so that the exogenous price of carbon is accounted for correctly in the dispatch decisions. The differences between the accounting and shadow carbon price are discussed in Section 5.3.2.

[15] For simplicity, we do not include the existing CRMs operating in Germany, French or Belgium. Instead, all new market design scenarios are implemented from the year 2018 onwards, from which point new investments or retirements can be made.

[16] Previous studies (e.g. (Bhagwat et al., 2017; Bucksteeg et al., 2017; Höschle et al., 2018; Mastropietro et al., 2015; Meyer & Gore, 2015; Västermark et al., 2015)) show that asymmetric CRMs between neighbouring countries can lead to perverse outcomes.

[17] A higher VoLL of 100,000 € MWh^{-1} is used in the capacity expansion module as (i) CWE consumers are accustomed to higher reliability levels than implied by a VoLL of 10,600 € MWh^{-1}, (ii) the vast majority of outages are due to faults in the distribution network which is not modelled, and (iii) the capacity expansion module uses a coarser temporal resolution than the UCED simulations. Further explanations are provided in Appendix F.

[18] Curtailable load is accounted for in the capacity margin but is remunerated based on the amount of energy curtailed and does not receive capacity revenues. Thus, we assume that the capacity costs for load shedding are small in comparison to the energy costs.

[19] The global budgets from 2011 to 2100 for the 2C and 1.5C scenarios are 1000 Gt CO_2 and 400 Gt CO_2 respectively. From these total global budgets, assumed budgets for non-OECD countries, cement production, and already-emitted carbon are subtracted based on Anderson & Broderick (Anderson & Broderick, 2017), with the remaining OECD budgets disaggregated to individual countries based on population. The CWE budgets assume net-zero emissions in the manufacturing, transport and other energy-related sectors by 2050, and that the power sector must deliver all negative emissions required to meet the total energy-related emission target.

[20] The capacity expansion is run with build decisions linearized so that the shadow price on the capacity margin constraint yields a reliable value for the capacity price.

[21] We run the UCED at hourly resolution with a time horizon of one week, plus a one-day look-ahead. In order to keep the solution time reasonable, we run the UCED simulations with linear relaxation of the unit commitment variables. As a result, minimum stable level, minimum up time and minimum down time constraints are not included. However, literature indicates that ramping constraints have a more significant impact on dispatch and total system costs than the inclusion of binary unit commitment variables (Schwele et al., 2019). Moreover, minimum up and down times which also characterise limitations in the flexibility of power plants are (in many cases) not hard limits, but economic ones (Panos & Lehtilä, 2016). As start-up costs are included in the optimisation, this avoids frequent unit start-ups and shutdowns, which has a similar effect as minimum up and down time constraints.

[22] As stated in Section 5.1 market design objectives are varied, and a wider definition accounting for more environmental criteria could be 'clean' or 'sustainable'. However, in this study, we restrict our environmental criteria to consider only carbon emissions, and do not consider other factors such as particulate emissions or water use.

[23] Based on ENTSO-E data (ENTSO-E, 2018g), approximately 32 GW of thermal generation capacity retired from the European power system in the years 2017 and 2018, of which most was coal (17.4 GW), other thermal fossil (9.1 GW) and nuclear (3 GW) plants, while retired gas capacity (2.3 GW) was offset by new investments (2.9 GW). These values are lower than observed in the model results for the year 2018, however the ENTSO-E values do not include plant mothballing, or the fact that in reality some plants may stay online operating a loss, while the model has perfect foresight and will retire plants at the earliest possible opportunity if it is cost-effective to do so.

[24] Some existing plants are still online in 2017 even though they exceed their assumed nominal lifetime. This may be due to inaccuracies in the database, life-extending refurbishments which have been performed, or plants simply lasting

longer than expected. However, to maintain consistent assumptions within the study, we assume these old plants must retire by 2020.

[25] The majority of BECCS capacity (17 GW) is achieved through coal retrofits, the rest is new BECCS plants.

[26] In the base runs we do not consider transmission outages. However, when a transmission outage rate of 10% is assumed in the sensitivity analysis (Appendix K), unserved energy up to 60 GWh is observed in Belgium in the year 2030 in the EOM-based scenarios, while none is observed in the scenarios with a CM. Still, even in this more extreme case, less than 0.07% of Belgian demand, or 0.005% of CWE demand is unserved.

[27] The actual CWE load-weighted price in 2017 was 40 € MWh^{-1}. Modelled 2017 day-ahead prices are slightly lower than those seen in reality. The largest discrepancies are seen in France, most likely due to significant nuclear outages in 2017. Accounting for these outages brings modelled prices closer to reality, however they are not included in the base model. See Appendix I for the model validation results.

[28] Determining the cost-effective volume of capacity is always a challenge with CRMs. We test the impact of maintaining tighter capacity margins in the sensitivity analysis (Appendix K).

[29] LRMC is equal to the variable costs plus fixed costs, including annualised CAPEX

[30] Profitability per technology is calculated by aggregating costs and revenues for all plants across the whole of CWE.

[31] The exogenous vRES deployment limits the ability of the model to fully optimise costs in the base runs. There is no minimum vRES deployment enforced in the *Optimised vRES* and *Full portfolio optimisation* sensitivity runs. Upper limits on total vRES deployment potential per technology in CWE are taken as 1300 GW and 540 GW for onshore and offshore wind respectively from (Dalla Longa et al., 2018), and 1000 GW for PV from (Zappa & van den Broek, 2018).

[32] References (Finon & Roques, 2013) and (Iychettira et al., 2017) provide a detailed overview of the different support instruments available for vRES.

[33] For economic operation, DAC utilisation should be maximised throughout the year, and will operate whenever its SRMC – comprised of VOM costs, electricity costs, and revenues from negative carbon emissions – is negative. However, in the UCED model runs, we force DAC to operate with a minimum capacity factor of 90% to ensure that annual emissions meet the target in the *1.5C* scenarios, and that the additional electricity demand is accounted for.

[34] Recital (14) of the amendments to the EU ETS Directive (European Parliament, 2018b) states that "*The main long-term incentive arising from Directive 2003/87/EC for the capture and storage of CO_2 ('CCS'), for new renewable energy technologies and for breakthrough innovation in low-carbon technologies and processes, including environmentally safe carbon capture and utilisation ('CCU'), is the carbon price signal it creates and the fact that allowances will not need to be surrendered for CO_2 emissions which are avoided or permanently stored.*" Other elements of the EU ETS may also constitute further barriers to NETs and would need to be addressed. For example, "*Projects involving CCU shall deliver a net reduction in emissions and ensure avoidance or permanent storage of CO_2*"

[35] Most likely this would be far more quickly than the 2.2% annual reduction that will commence from 2021 (Honegger & Reiner, 2018).

[36] The purpose of the adder is to try to incorporate the value of short-term operating reserves into the electricity price, whilst retaining an EOM design. It is based on an operating reserve demand curve originally proposed by Hogan (Hogan, 2013), and is a function of the loss of load probability and VoLL.

[37] The total contracted volume of FRR (aFRR+mFRR) in CWE in 2017 was almost 7 GW (900 MW in Belgium, 3000 MW in Germany, 1000 MW in the Netherlands, and 2000 MW in France) (Brinkel, 2018; Elia, 2019a; RTE, 2019). With a vRES penetration (energy basis) of 17% in 2017 and ~70% in the *EOM 2C* scenario in 2040, a proportional increase in FRR requirements would translate to a need of around 30 GW, which is less than the 85 GW of flexible generation capacity available in 2040. The other scenarios have even more flexible capacity provided by a CM, demand response or BECCS.

[38] In their budgets, Anderson & Broderick (Anderson & Broderick, 2017) assume that emissions from deforestation are matched by additional carbon sequestration through land use, land use change and forestry activities until 2100. In some IPCC scenarios limiting warming to 1.5 ºC, even the estimated global BECCS potential of 5 Gt $CO_2 y^{-1}$ is exceeded (IPCC, 2018).

[39] The cost of transporting and storing up to 120 Mt CO_2 y^{-1} from the Netherlands, Belgium and Germany in the Utsira formation – a saline aquifer located some 800 km offshore from the Dutch coastline in Norwegian waters with a storage capacity of 42 Gt CO_2 – is estimated to be in the range of 8.5 to 16 $€_{2007}$ t^{-1} (10 to 20 $€_{2017}$ t^{-1}, accounting for 2% annual inflation)(van den Broek et al., 2010). See (EASAC, 2013) for a more detailed overview of CO_2 transport and storage costs for different distances and storage sites.

[40] The base learning rates assumed in (Tsiropoulos et al., 2018) are 20% for PV, 5% for onshore wind and 11% (2020) falling to 5% (2040) for offshore wind, while the optimistic learning rates are 23%, 10% and 20% (2020) falling to 10% (2040) respectively.

Summary, conclusions and discussion

6

6.1 Research context and aims of thesis

After decades of delay, missed opportunities and accumulated greenhouse gas (GHG) emissions in the atmosphere, the actions required to address climate change are becoming increasingly urgent and severe. Recent analysis from the Intergovernmental Panel on Climate Change (IPCC) shows that in order to have a good (67%) chance of limiting global warming to 1.5 ºC by the end of the century as set out in the Paris Agreement, mankind should emit no more than 420 Gt CO_2 (net) from 2018 onwards (Rogelj et al., 2018)[1]. If global emissions remain at 2018 levels of approximately 37 Gt CO_2 y^{-1}, this budget will be exceeded sometime around the year 2030. This sobering fact has led many local, state and federal governments to declare a climate emergency (Aidt, 2019).

With total CO_2 emissions of 13 Gt in 2018 (38% of total energy-related CO_2 emissions), the electric power sector is currently the largest source of GHG emissions globally (IEA, 2019). Given the extent of its emissions, its ability to indirectly decarbonise other sectors, and close links with bioenergy with carbon capture and storage (BECCS) and direct air carbon capture (DAC) – two negative emission technologies (NETs) which could play a vital role in limiting global warming to 1.5°C – decarbonising the power sector is a key priority in the fight against climate change.

The European Union (EU) has long been a global leader in taking action against climate change and deploying renewable energy sources (RES). In the ten years from 2008 to 2018, the installed wind capacity in the EU tripled from 60 to 180 GW, and solar photovoltaic (PV) capacity increased more than tenfold from 10 to 115 GW over the same period (EurObserv'ER, 2018, 2019; Eurostat, 2017b; SolarPower Europe, 2019). Largely thanks to this growth in RES and falling generation from coal, GHG emissions from public electricity (and heat) generation in the EU fell by 24% between 2008 and 2017 to approximately 1 Gt y^{-1} (Eurostat, 2019a). However, this still represents 25% of total EU GHG emissions, and more must be done to decarbonise to the ambitious levels targeted in the Paris Agreement. Thankfully, the recent (November 2019) resolution of the European Parliament to declare a climate emergency shows Europe's commitment to reducing emissions even further (European Parliament, 2019).

While Europe's electricity sector must decarbonise, it is not clear how this should be done as there are three broad strategies which could be followed. Firstly, studies have shown that cost-effective low-carbon generation portfolios can be constructed from a mix of RES, nuclear, and fossil generation with carbon capture and storage (CCS) (Jenkins et al., 2018; Sepulveda et al., 2018). By committing to a target of net-zero emissions by 2050 and deploying a mix of RES, nuclear and potentially CCS, the UK is following such as a *technology-diverse approach* (UK Government, 2019). A second strategy, currently being followed by countries such as Denmark and Sweden, is to aim for a power system based almost *exclusively on RES* (KEFM, 2018; Swedish Ministry of the Environment and Energy, 2019). Germany, which has set a minimum

target of 80% RES electricity by 2050, is following a similar high-RES strategy (BMWi, 2018). A third strategy would be *deployment of NETs* to offset emissions from continued fossil fuel use in the electricity or in other sectors, though this strategy is not currently being followed by any country. Whichever strategy is implemented, the European electricity sector will likely face three major challenges over the coming decades, making the overarching objective of a modern electric power industry – to supply *clean* electricity *reliably* to consumers at the *lowest possible cost* – more difficult to achieve.

Firstly, the **growing penetration of variable renewable energy sources** like solar PV and wind is raising concerns about the reliability of the power system. For decarbonisation strategies targeting high levels of RES this will be a challenge. However, given the falling costs of wind and PV, many technology-diverse portfolios may also rely heavily on these two technologies. Secondly, decarbonisation ambitions are becoming increasingly stringent over time, and even net-zero power sector emissions by 2050 may not be enough to meet climate goals**.** Thus, deployment of NETs may become unavoidable, and it is unclear what the **impacts of large-scale deployment of NETs** on the European electricity sector could be. Lastly, there are concerns whether Europe's liberalised **electricity market design** will be able to incentivise sufficient investment in low-carbon generation capacity to meet climate goals while ensuring security of supply.

In light of these challenges, the main research question driving this thesis is:

What are the consequences of pursuing different strategies in the European power sector for reliability, achievement of climate objectives, and economic viability?

In addressing this broader question, this thesis focusses in more detail on the following sub-questions (SQ):

1. To what extent can the mix and spatial distribution of solar PV and wind be used to help integrate them into the power system?

2. What are the potential consequences of aiming for a 100% renewable power system?

3. What are the potential consequences of relying on BECCS and DAC in the power sector to meet a 1.5 ^{o}C warming target?

4. What elements should be present in future market designs to address the energy trilemma?

These research questions are addressed in four core chapters (see Table 1-2, reproduced below).

Table 1-2 | Correspondence between the chapters and research questions of this thesis

Chapter	Topic	Research question			
		SQ1	SQ2	SQ3	SQ4
2	Consequences of the mix and spatial distribution of wind and solar PV for residual demand	X	X		
3	Consequences of high vRES penetration in European electricity sector for intraday and balancing markets		X		X
4	Consequences of a 100% renewable power system	X	X		
5	Consequences of aiming for a 1.5 ºC target with BECCS and DAC under different market designs			X	X

The remainder of this chapter is structured as follows. Section 6.2 gives a brief summary of each core chapter. Section 6.3 draws on the findings of all four core chapters to address the research questions outlined above. Section 6.4 discusses the finding of this thesis in the context of the broader energy and climate debate, and provides a reflection on the research scope the methods used. Section 6.5 provides some recommendations for future research, and Section 6.6 concludes the thesis with several key recommendations for policymakers.

6.2 Chapter summary

Chapter 2 examines to what extent the mix and spatial deployment of vRES capacity across Europe could be used as a strategy to facilitate its integration into the power system by taking advantage of different weather patterns across the continent. The approach taken is to optimise the mix and spatial distribution of solar PV and wind (onshore and offshore) across Europe in such a way as to make the hourly total aggregated vRES generation profile throughout the year match the profile of total aggregated electricity demand as closely as possible. This is achieved by combining a high-resolution spatial grid (approximately 50 km x 50 km) with data on suitable land areas for vRES deployment, together with a long-term dataset of wind speed and solar radiation. The quantity of installed wind and solar PV in each grid cell is varied until the total absolute residual demand (i.e. unmet demand plus vRES curtailment) is minimised. This optimisation is performed for 36 years of weather data to examine how consistently the method distributes vRES capacity given interannual weather variability. The optimisation is also performed with different vRES penetration rates, electricity demand profiles, PV panel orientations, and allowable water depths for offshore wind to examine how the spatial optimisation is affected by these factors. To establish the maximum possible benefits of this approach, the method does not account for transmission limitations or losses (also known as the 'copper-plate' assumption), does not account for storage, nor costs. The approach is compared with a vRES spatial distribution based on maximising capacity factors.

Spatially optimising vRES to minimise residual demand results in a vRES penetration rate of 82% (energy basis), with a capacity mix of approximately 75% wind and 25% solar PV. However, dispatchable firm capacity representing up to 75% of peak demand would still be required to ensure long-term system adequacy. Compared with the traditional approach of installing vRES in locations with the highest capacity factors, optimising vRES capacity to minimise residual demand reduces total absolute residual demand by 29%, and peak residual demand (i.e. backup capacity requirements) by merely 2.6%. Thus, even in this optimal case of a copper-plate Europe, optimising the spatial distribution of vRES could play only a minor role in reducing residual demand. The greatest benefits of spatial vRES optimisation are found when water depth constraints are relaxed, and offshore wind capacity can be built in very deep waters far from shore; this reduces total residual demand by 53% and peak residual demand by 16% compared with a capacity factor-based distribution. Increasing use of heat pumps (HPs) and electricity vehicles (EVs) also effects the optimum distribution of vRES, assuming no demand-side flexibility in HP use and EV charging. For example, installing PV capacity at the eastern and western extremes of Europe could lead to more generation in the morning and evening, which may be beneficial for meeting future demand from EVs, while PV in northern Europe could extend the window of PV generation in summer by taking advantage of longer days. However, it is unlikely that such approaches would be cost-effective.

Chapter 3 explores how higher vRES forecast errors brought about by rising vRES penetration in Europe could affect intraday and balancing market volumes, and to what extent these errors could be resolved by trading between vRES generators in the case of no cross-border trading, and a copper-plate Europe. This is done by developing a new method for creating synthetic day-ahead forecasts for electricity demand and vRES generation with error distributions which are consistent with historical forecasts. The method is demonstrated by applying it in simulations of a future European power system in which the penetration of vRES rises from 15% in 2017 to 50% in 2040. The proposed method incorporates a generalised autoregressive conditional heteroscedasticity (AR-GARCH) model to account for the daily volatility observed in historical forecast errors, and a dependence on real-time generation (or load) level to account for hourly volatility. Intraday forecasts are based on persistence. Other factors which contribute to intraday trading and imbalance volumes such as forced outages, strategic deviations and schedule leaps are not considered.

Based on the simulation results, it is found that potential intraday market volumes increase by 60 TWh y^{-1} (+160%) between 2017 and 2040 as a result of additional day-ahead forecast errors. Intraday trading both within and between countries could allow between 40% (without cross-border trading) and 75% (copper plate) of day-ahead forecast errors to be resolved by vRES, reducing the need for dispatchable energy. In the absence of intraday trading, these errors would need to be resolved by transmission system operators (TSOs) on balancing markets, highlighting the role liquid intraday markets can play in supporting the integration of vRES in Europe. Regarding balancing markets, we find that full implementation of imbalance netting

and a common Europe-wide reserve could reduce balancing energy and capacity requirements for vRES integration by 19% and 32% respectively in 2040 compared with country-specific reserves and no imbalance netting.

Chapter 4 aims to test whether a 100% renewable power system could be feasible in Europe by 2050. Several scenarios for a fully renewable European power system are evaluated based on their reliability, cost, and whether the requisite deployment of RES could take place by 2050. This analysis is based on power system simulations performed at hourly resolution using the PLEXOS power market modelling framework. Flexibility limitations of dispatchable plants, cross-border transmission and operating reserves are modelled explicitly. All major forms of RES are included such as solar PV, onshore and offshore wind, bioelectricity, geothermal, concentrating solar power (CSP), and hydro power. In most scenarios, the deployment of geothermal and CSP is taken exogenously based on scenarios from the literature. Seasonal storage (e.g. with hydrogen) is not included. The model incorporates the high spatial- and temporal-resolution weather data developed in Chapter 2 directly in the optimisation, so that land and sea availability for vRES is accounted for explicitly, vRES generation profiles are consistent with their spatial deployment, and the cost of vRES deployment depends on the weather resource and proximity to load at each location. From a long-term weather dataset (1979 to 2015), the year 2010 is chosen for the model runs, as this is the most challenging year observed in the dataset. The geographic scope of the study is the EU28 countries, Norway and Switzerland. RES deployment (including biomass) is limited to resources from only these countries, including their territorial waters up to 50 m deep. Electricity demand is assumed to increase by 1300 TWh (40%) between 2015 and 2050 due to additional demand for HPs and EVs, based on literature estimates. Six scenarios for a 100% RES European power system are modelled to explore the impact of uncertainties in future demand and technology development, and one further scenario in which other non-RES low-carbon technologies are included, so that the costs of a 100% RES system can be compared with a more technology-diverse portfolio.

The results from Chapter 4 suggest that a 100% RES European power system could operate with the same level of reliability as the current power system, even when relying only on domestic European RES in the most challenging weather year. However, realising such a system by 2050 would be contingent on many developments. For example, generation capacity would need to expand to at least 1.8 TW, compared with ~1 TW installed in 2015. This increase (80%) is much higher than the 40% increase in demand, and requirements increase even further if portfolios must rely on higher shares of vRES, if total demand grows more strongly 40% (e.g. to produce hydrogen via electrolysis), or if peak demand increases significantly. Cross-border transmission capacity would need to increase by around 140 GW from the 60 GW installed today, as would the utilisation of bioenergy for power generation, reaching at least 8.5 EJ y^{-1} (compared with 1.9 EJ y^{-1} in 2015). While the annual wind and PV deployment levels required to realise a 100% RES system by 2050 have been achieved

historically, deployment of dispatchable RES sources such as bioenergy and CSP would need to be scaled up significantly from current levels. In terms of costs, a 100% RES power system in 2050 would be approximately 30% more expensive than a more technology-diverse system which includes nuclear power and CCS (or conversely, a technology-diverse system would be 22% cheaper than a 100% RES system), even when wind and PV are placed in the optimal locations. Moreover, the costs of 100% RES systems increase relatively more with higher demand as the best RES sites become exploited and less favourable locations must be used.

Chapter 5 explores the interactions between different decarbonisation trajectories and market designs on the power system by using the PLEXOS modelling framework to study the evolution of the Central Western Europe (CWE) power system between 2017 and 2040. Two decarbonisation scenarios are considered for 2040: one targets net-zero emissions consistent with a 2 ºC warming limit, while the other targets -850 Mt CO_2 y^{-1} net-negative emissions, consistent with the more ambitious 1.5 ºC warming limit set out in the Paris Agreement. These two decarbonisation scenarios are modelled for four archetypal electricity market design scenarios: (i) the current energy-only market (EOM) with price caps and (largely) price-insensitive demand side, (ii) a reformed EOM with price caps removed and price-responsive demand, (iii) the current EOM with the addition of a capacity market, and (iv) the reformed EOM with the addition of a capacity market. These scenarios are used to determine how electricity generation portfolios should develop over time to supply electricity reliably to consumers at the lowest cost (given the exogenous vRES increase), to what extent these least-cost portfolios can be supported by market revenues, and how the deployment of negative emission technologies could affect the electricity market. In all scenarios, it is assumed that the installed capacity of vRES in CWE increases over time from 133 GW in 2017 to 500 GW in 2040, and the CO_2 price increases from 17 € t^{-1} in 2017 to 120 € t^{-1} by 2040.

In terms of portfolio developments, the results show that BECCS is a cost-effective way of rapidly decarbonising the power sector and, assuming a maximum biomass supply of 3 EJ y^{-1}, the CWE power sector could offset up to 250 Mt CO_2 y^{-1} from other sectors using BECCS. Offsetting more than this increases costs significantly due to the need for DAC. No new nuclear capacity is built in any scenario; however, keeping existing nuclear capacity can be a cost-effective way of maintaining security of supply, reducing carbon emissions, and keeping electricity prices low for consumers. While this study assumes policy-driven large-scale vRES deployment, sensitivity analysis shows that a strategy relying primarily on vRES could increase the cost of decarbonisation by 10% to 25% (depending on the warming target) compared to a more diversified portfolio containing vRES, nuclear, natural gas (with CCS) and BECCS plants.

In terms of market developments, market revenues for existing baseload and mid-merit generators may improve in the medium term (~2030). This is due to higher infra-marginal rents induced by the effect of a higher carbon price on peaking fossil generators, resulting in average day-ahead prices in the range of 50 to 80 € MWh^{-1} in 2030 (depending on the

scenario), compared with 35 € MWh^{-1} in 2017. However, this effect is offset in the long term by the downward pressure exerted by vRES and BECCS on market prices, which fall to between 42 and 55 € MWh^{-1} by 2040. The downward pressure from vRES is due to the merit order effect, while the downward pressure from BECCS stems from the assumption that NETs are remunerated for their negative emissions at the CO_2 price, which allows BECCS to offer electricity at low (or even negative) prices. As a result, the combined impact of high vRES deployment (up to 70% penetration based on energy in CWE) and BECCS deployment may lead to up to 1500 hours with a day-ahead electricity price of zero by 2040, undermining the effectiveness of a carbon price as an investment signal for other low-carbon and NETs. Ultimately, most generation technologies fail to recover their investment costs in the long term in any modelled market design scenario. While capacity markets can improve the profitability of mid-merit and peaking gas plants, they can also undermine the profitability of baseload and vRES generators if they result in generation oversupply and depress electricity prices. Furthermore, volatile capacity prices may not guarantee the stable long-term investment environment called for by investors. Adding a mechanism in the EU Emissions Trading Scheme (ETS) to remunerate NETs for negative emissions could help make BECCS profitable from carbon and electricity market revenues by the mid-2030s. However, even with such a mechanism, the high cost of DAC means it would likely still need government support to see large-scale deployment.

6.3 Main findings and conclusions

The key findings regarding the main research questions of this thesis are discussed in the following sections.

6.3.1 To what extent can the mix and geographic distribution of solar PV and wind be used to help integrate them into the power system?

Optimising the spatial distribution of vRES is unlikely to be an effective strategy for reducing backup capacity requirements. Chapter 2 shows that even in the optimistic case of a copper-plate Europe, optimising the distribution of vRES to minimise residual demand could reduce peak residual demand by only 2% compared with a distribution based on the highest capacity factors. Investors are unlikely to accept the economic penalty of exploiting sites with fewer operating hours for a marginal benefit to the system, and it would not be cost-effective for governments to support them in doing so. Instead, other strategies for dealing with peak demand hours, such as demand-side response, are likely to be more cost-effective.

The mix of vRES technologies has a significant impact on how easy they are to integrate, with a higher share of wind being more favourable. Considering only the match with load and excluding costs, storage, and transmission limitations, the optimum deployment of vRES in Europe would be an energy penetration of 82% net (89% gross, including curtailment), with a capacity mix of approximately 25% solar PV and 75% wind. Of the total wind capacity, 65% is offshore. Based on the results presented in Chapter 2, these shares lead to the lowest total (positive and negative) residual demand across the year with 8% of vRES generation curtailed, and 18% of demand unmet. The optimum share of wind is higher as wind has a more stable generation pattern than solar PV, allowing it to supply an average of 250 GW baseload power throughout the year (see Figure 2-10). With these shares, total wind generation would be almost sufficient to cover demand in winter months (provided enough daily and weekly storage was available), while some unserved demand would remain during summer.

However, the optimal mix and spatial distribution of vRES depend more strongly on the investment costs of vRES and transmission lines. The optimisation algorithm used in Chapter 2 to minimise residual demand results in a vRES penetration of 82% (net), with a portfolio dominated by offshore wind due to its favourable generation profile. However, this algorithm considers only the match between aggregated load and generation, excluding the costs of vRES, transmission, and the residual generation portfolio. When these factors are included in Chapter 3, the optimal mix and distribution of vRES changes markedly. With a fully optimised portfolio (i.e. the *Free RES* scenario), the optimal penetration of vRES is found to be approximately 50%, with a capacity mix of one-third wind to two-thirds solar PV. The main reason for this is the high cost of offshore wind, making an offshore wind-dominated portfolio

less attractive, despite its more favourable generation profile. Including the costs of vRES and transmission in Chapter 3 also results in vRES deployment shifting to sites with higher capacity factors and sites located closer to load centres, giving a more even distribution of vRES capacity across Europe. This shows that the investment costs of vRES and transmission lines outweigh any potential benefits of spatial optimisation.

For supplying bulk energy generation, wind benefits more from geographic diversity than solar PV. As shown in Chapter 2, the reason for this is that at an hourly time scale, the correlation between wind generation at different sites falls with increasing distance much quicker than for solar PV (see Figure 2-19). For example, at a distance of 50 km, the median correlation coefficient between time series of hourly generation from wind and PV are both above 0.9. At 500 km however, the correlation falls to 0.3 for wind, but remains at 0.9 for solar PV.

6.3.2 What are the potential consequences of aiming for a 100% renewable power system?

The findings from Chapter 4 suggest that a European power system based on 100% RES could be realised by 2050 and operate with the same level of reliability as today's power system, even in a very challenging weather year for solar PV and wind generation. However, this strategy would be contingent on many developments over the coming years:

- **Generation capacity would need to increase considerably, potentially to at least 1.8 TW** compared with the 1 TW installed in 2015. This represents an increase of 80%, compared with an assumed electricity demand increase between 2015 and 2050 of 40% (1300 TWh) due to HPs and EVs. Generation capacity requirements increase even further if portfolios must rely on higher shares of vRES, if total demand grows even more strongly than the assumed base level of 40% (e.g. to produce hydrogen via electrolysis), or if peak demand increases significantly.

- **Cross-border transmission capacity would need to increase, potentially by a further 140 GW** compared with the 60 GW installed in 2015. Transmission requirements will be higher for 100% RES portfolios relying on significant CSP capacity deployed in southern Europe, for higher demand levels, and for peakier demand profiles. With more cross-border transmission, European countries would become more reliant on their neighbours for their security of supply, and on the reliability of the transmission network.

- **Deployment of firm, dispatchable renewable capacity of at least 18 GW y^{-1}** to supply electricity during periods of low-vRES generation and meet peak demand reliably. In a 100% RES system, this must come from CSP, bioenergy (solid biomass and biogas), geothermal, hydro, or storage. Given current deployment rates for these

technologies are below 1 GW y^{-1}, this presents a major hurdle to realising a 100% RES power system by 2050.

- **Total wind and solar deployment would need to average 7.5 GW y^{-1} and 15 GW y^{-1} respectively every year until 2050**. Such deployment levels have been achieved in the EU before in individual years, but not sustained.

- **Large-scale mobilisation of Europe's bioenergy resources would be required in the range of 8.5 to 13 EJ y^{-1}** compared with 1.9 EJ y^{-1} used in 2015. Bioenergy would be used to supply baseload generation during winter, and night-time demand in summer, while biogas would be needed to meet demand during peak periods. Deploying 8.5 EJ y^{-1} would mean utilising around 85% of the ~10 EJ y^{-1} of suitable biomass potential for energy (based on literature estimates).

A 100% RES power system may be more expensive than a more technology-diverse system including other low-carbon (but non-RES) technologies such as nuclear power or CCS. This is shown in Chapter 4, where a scenario in which nuclear and CCS technologies are allowed leads to total annualised costs in 2050 that are 22% lower than the least-cost 100% RES scenario. These lower costs are achieved due to deployment of nuclear and natural gas capacity as well as BECCS, which offsets the CO_2 emissions from natural gas. Transmission investments are also significantly lower than in the 100% RES scenarios. The benefits of a more diverse generation portfolio are also shown in the sensitivity analysis from Chapter 5 where compared with the base runs, which include an exogenous 3-fold increase in vRES capacity, the runs with optimised vRES capacity result in far less vRES deployment, and 7% to 20% lower system costs (depending on the climate target). Lower costs are achieved by deploying less offshore wind and PV capacity, keeping more existing nuclear capacity online, and installing some natural gas with CCS and BECCS capacity.

Demand-side measures would play a major role in improving the feasibility of a 100% RES power system. Assuming complete electrification of passenger vehicles and significant uptake of electric heating by 2050, literature sources estimate that HPs and EVs could increase electricity demand in Europe (currently 3100 TWh y^{-1}) by up to 1300 TWh y^{-1}. Chapter 4 shows that if this additional demand is inflexible, peak demand could increase significantly, increasing the amount of generation capacity (particularly peaking biogas) required. Thus, EVs and HPs should be deployed with technologies allowing demand flexibility (e.g. smart charging, energy management systems) to minimise the impact on peak demand.

The cost of a 100% RES power system increases relatively more with higher demand. In Chapter 4, a 36% increase in demand for a 100% RES system leads to a 50% increase in total costs. This is mainly due to depletion of the most favourable locations for vRES, the need to exploit costlier biomass resources, and higher generation capacity required to meet peak

demand. As a result, the cost of a 100% RES decarbonisation strategy is more sensitive to demand levels than a more diverse strategy which includes non-RES technologies.

Reserve (balancing) capacity and energy requirements will likely be higher for a 100% RES power system. The results from Chapter 3 show that increasing vRES penetration from 15% to 50% could increase balancing energy requirements across Europe by ~130% and capacity requirements by ~100%, depending on the extent of imbalance netting and reserve sharing. Moreover, Chapter 4 shows that in a 100% RES European power system, balancing requirements would vary considerably throughout the day, with especially high reserves required during periods when vRES supply approaches 100% of demand.

RES have an important role in strategies to deliver net-zero power sector emissions, but even a 100% RES portfolio may need the flexibility provided by NETs to meet a 1.5 ºC warming target. All the 100% RES scenarios modelled in Chapter 4 would achieve net-zero (direct) GHG emissions from the European power sector by 2050[2]. However, as shown by the most recent IPCC scenarios (see Figure 1-1), negative emissions may already be necessary in the 2030s to be consistent with a 1.5 ºC warming target. Most of the 100% RES portfolios modelled in Chapter 4 contain significant bioelectricity capacity which could be retrofitted with CCS to deliver negative emissions at relatively low cost. However, 100% RES portfolios relying on very high vRES penetrations (with storage) would not have this flexibility and would need to deploy additional BECCS and/or DAC capacity at higher cost.

6.3.3 What are the potential consequences of relying on BECCS and DAC in the power sector to meet a 1.5 ºC warming target?

Even with large-scale vRES uptake, early BECCS deployment may be a cost-effective strategy for meeting a 1.5 ºC target. Chapter 5 shows that the least-cost pathways consistent with a 2 ºC warming limit by 2040 lead to a small amount (2 GW) of BECCS deployment in CWE in the late 2030s. However, in the 1.5 ºC scenarios, BECCS is deployed already in the early 2020s by converting existing coal plants to use biomass and retrofitting them with CCS. By 2040, approximately 25 GW of BECCS is installed in CWE, delivering -250 Mt CO_2 y^{-1} negative emissions. If BECCS is not deployed, the sensitivity analysis performed in Chapter 5 shows that the total cost of meeting the 1.5 ºC target could increase by 20% compared to the case where BECCS is deployed due to the need for more costly DAC. Similarly, allowing for higher BECCS deployment than in the base case could reduce the costs of meeting a 1.5 ºC target by reducing the deployment of DAC.

Large-scale deployment of BECCS will be contingent on significant sustainable biomass supply chains to deliver real climate benefits. As shown in Chapter 5, CWE could deliver 250 Mt CO_2 y^{-1} negative emissions in the year 2040 by using ~3 EJ y^{-1} of biomass. Scaling this value up based on the total estimated suitable European bioenergy potential of ~10 EJ y^{-1} (excluding log wood, sugar, starch and oil crops, which are set aside for residential heating

and biofuels, see Chapter 4) suggests that up to 800 Mt CO_2 y^{-1} negative emissions could be achieved by 2040 across Europe from BECCS. However, these negative emissions should only be realised if the biomass can be sourced sustainably, without causing deleterious effects to soil quality and biodiversity, and without incurring a carbon debt so long that the use of biomass becomes futile (or even detrimental) on timescales relevant for climate policy (see section 6.4.1 for further discussion on biomass).

Deployment of BECCS could lead to more baseload electricity production, reducing the need for nuclear and vRES, and may also put downward pressure on electricity prices. BECCS is most cost-effective when operated with high capacity factors as this leads to more negative emissions. As a result, Chapter 5 shows that BECCS also leads to baseload electricity production in CWE of up to 15 TWh y^{-1} (1% of electricity demand) by 2040 in the 2 ºC scenarios, and ~190 TWh y^{-1} (15% of electricity demand) in the 1.5 ºC scenarios. This baseload production displaces some nuclear generation in cost-optimal portfolios. Moreover, assuming that NETs are remunerated for their negative emissions, and that the carbon price is high enough, baseload generation from BECCS could lead to vRES curtailment. This phenomenon is similar to what already occurs with combined heat and power (CHP) plants which, due to their heat revenues or 'must-run' status, can offer their electricity at a very low price and are preferentially dispatched over other sources. For the same reason, large-scale BECCS deployment may put downward pressure on electricity prices.

Baseload electricity demand would increase significantly due to DAC. The supply of biomass may be insufficient to achieve all the negative emissions required for a 1.5 ºC scenario with BECCS. In this case, Chapter 5 suggests that up to 25 GW (input electricity) of DAC may be required in CWE by 2040, requiring some 200 TWh y^{-1} of additional electricity. Due to DAC's high capital cost, cost-effective operation means it should run as much as possible. Thus, the additional demand imposed on the system would be for baseload electricity which, as shown by the optimised portfolios in Chapter 5, may be more cost-effectively supplied by baseload technologies such as BECCS or existing nuclear capacity.

Mechanisms are needed to remunerate NETs for the negative emissions they sequester. The analysis performed in Chapter 5 assumes that NETs are paid for the negative emissions they generate. This could be achieved by, for example, a direct government subsidy to NETs similar to a feed-in-tariff or – as proposed in Chapter 5 – a mechanism could be added to the EU ETS allowing NETs to generate emission allowances. NET plants could sell these allowances to emitters, and the volume of centrally offered allowances reduced accordingly to prevent an oversupply. Chapter 5 suggests that if the CO_2 price reaches levels around 120 € t^{-1} by 2040, BECCS could become profitable from these carbon and electricity revenues alone without further government subsidies. However, even at these prices, DAC would not be profitable based on assumed cost estimates (~13000 € kW^{-1} (input) for DAC in 2040 vs. ~3800 € kW^{-1} for BECCS) and additional government support would be required.

6.3.4 What elements should be present in future market designs to address the energy trilemma?

Liquid intraday markets with cross-border trading will help integrate vRES, reduce the need for dispatchable energy, and reduce balancing requirements for TSOs. European intraday markets are currently growing, and simulations performed in Chapter 3 suggest that this growth will continue with increasing vRES penetration. Assuming vRES penetration in Europe increases from 15% to 50% between 2017 and 2040, and forecast accuracy remains the same as the best available forecasts today, intraday trading volumes could increase by some 60 TWh y^{-1} (~160%) by 2040 as a result of the additional day-ahead forecast errors. However, depending on the amount of cross-border transmission capacity available, between 40% (without cross-border trading) and 75% (copper-plate Europe) of day-ahead forecast errors could be resolved by trading between vRES, reducing the need for dispatchable energy. In the absence of liquid intraday markets, these errors would need to be resolved by TSOs on balancing markets, adding to costs for consumers.

Imbalance netting and coordinated procurement of reserves will reduce the need and costs for balancing. Simulations performed in Chapter 3 suggest that up until a vRES penetration of ~25%, balancing requirements may remain relatively stable at current levels, as the imbalances caused by load forecast errors are larger than the imbalances caused by vRES. However, increasing vRES penetration beyond this level leads to increasing requirements for balancing energy and capacity and once vRES penetration reaches ~50% (around 2040 in the simulated scenario), imbalances could increase by ~130% and balancing capacity requirements by ~110% compared with 2017, in the case of no imbalance netting and a separate reserve per country. However, implementing imbalance netting and a common reserve across Europe could reduce these balancing energy and capacity requirements by 19% and 32% respectively.

Reformed EOMs without price caps and with price-responsive demand will help deliver system reliability, lower system costs, and efficient electricity pricing. Chapters 4 that 5 show that demand-side flexibility in the form of load shifting and shedding can be a cost-effective way of maintaining a reliable power system by reducing the need for peak generation capacity and avoiding the need for carbon-intensive peak generation from natural gas. For example, in Chapter 5, load shedding reduces total system costs by ~1% (in the case of EOM) to 5% (with CRM) mainly by reducing investments in gas turbines, and almost eliminates unserved energy in the EOM case. Moreover, the removal of price caps and fostering a price-responsive demand side will allow electricity markets to better reflect the value of electricity at each moment in time and reward market parties accordingly[3]. For example, in Chapter 5, demand-side bids in reformed EOMs become price setting up to 250 hours per year, leading to higher prices and generator revenues in these hours. However, a price-responsive demand

side will be contingent on developments with both large consumers (e.g. industry), as well as retailers (see section 6.4.1 for further discussion).

Capacity remuneration mechanisms (CRMs) may not guarantee enough investment in firm capacity to guarantee security of supply. Chapter 5 shows that even in the presence of a capacity market, not all firm generators are able to recover their long-run marginal costs. Even vRES generators fail to recover their investment costs in most cases. While capacity markets deliver additional revenues to mid-merit and peaking plants, leading to profitability in certain years, long-term profitability is not guaranteed. Moreover, they can undermine the profitability of baseload and vRES generators if they result in oversupply and depress electricity prices. Moreover, the volatile capacity prices seen with an average of 70 € MW^{-1}, (but a range of 0 € MW^{-1} to 250 € MW^{-1}) would not provide the stable revenues needed for investors to guarantee investment and security of supply.

6.3.5 What are the consequences of pursuing different strategies in the European power sector for reliability, achievement of climate objectives, and economic viability?

Based on the findings of this thesis and the detailed answers to the sub-questions provided in sections 6.3.1 to 6.3.4, the main research question is answered succinctly as follows:

A strategy aiming for a **technology-diverse** generation portfolio would:

- be just as reliable as the current power system,
- deliver net-zero or even net-negative CO_2 emissions (depending on NET deployment),
- cost less than a 100% RES or heavily NET-dominated strategy,
- require development of CCS for deployment with natural gas and biomass,
- benefit from keeping existing coal plants online so they can be converted to biomass and retrofit for CCS,
- benefit from keeping existing nuclear capacity online and potentially building new capacity, and
- require market reforms to remunerate NETs for the negative emissions they sequester (if NETs are deployed).

A strategy aiming for a power system **based on 100% RES** would:

- be just as reliable as the current power system, providing enough firm capacity is available,
- deliver net-zero GHG emissions,
- suffer from climate lock-in if net-negative power sector emissions are required which, in the absence of CCS, could not be achieved with 100% RES,

- be costlier than a more diverse portfolio containing other low-carbon technologies (e.g. nuclear, CCS, NETs),
- require large-scale transmission investments across Europe,
- entail significant dependence on biomass, in the absence of cost-effective seasonal storage, and
- require significant land and sea area for vRES deployment.

A strategy relying on **large-scale deployment of NETs** in the power sector would:

- deliver significant negative carbon emissions, capable of offsetting emissions in other sectors or countries,
- lead to very high costs, depending on the eventual cost of DAC and the capacity deployed,
- require development of CCS for deployment with BECCS and DAC,
- entail significant exploitation of biomass for BECCS,
- require market reforms to remunerate NETs for the negative emissions they sequester, and
- require significant storage of CO_2.

All three strategies would:

- benefit from market reforms to eliminate market price caps (including implicit ones) and develop more price-responsive demand,
- benefit from liquid intraday markets to support the integration of vRES, reduce balancing requirements and total costs,
- benefit from European market integration so that generation capacity can be shared between countries, reducing balancing requirements and total costs, and
- need public acceptance for the various technologies employed and market reforms implemented.

Considering the consequences of all three decarbonisation strategies, following a more **technology-diverse** strategy would appear to offer the best chance of supplying electricity to European consumers at the lowest possible cost, in a way that is consistent with the climate ambitions as set out in the Paris Agreement.

6.4 Discussion

This section discusses the findings and implications of this thesis in the context of broader debates on energy and climate policy (section 6.4.1), provides a reflection on some of the most important scope limitations (section 6.4.2), and gives an overview of the main methodological contributions and their potential applications (section 6.4.3).

6.4.1 Wider implications

This thesis has raised several issues which, while not addressed directly, are worth further discussion as they have implications for the wider debate on energy and climate policy.

VoLL and reliability: the political cost of lost load. Currently, TSOs are tasked with ensuring security of supply according to a certain reliability standard, defined using metrics such as loss of load expectation (LoLE), with a typical value being in the range of 3-8 hours per year (ENTSO-E, 2018c). The value of these metrics is often based on a uniform value of lost load (VoLL) for all consumers, which is used in system planning. However, as shown by historical data on outages experienced in Europe and ENTSO-E's system adequacy analysis (CEER, 2018; ENTSO-E, 2018c), the majority of European consumers currently enjoy much higher reliability levels than the reported reliability standards[4]. This suggests that TSOs treat reliability standards more as upper limits (in the case of LoLE) than targets. One reason for this may be that the real VoLL used by TSOs includes an implicit mark-up: the *political cost of lost load,* which is factored in to avoid the public backlash that would be felt in the event of serious supply interruptions. However, this additional reliability requirement may result in surplus generation and reserve capacity, the costs of which – in the case of a CRM – get passed down to consumers in the form of grid tariffs. As shown in Chapters 3 and 5, the increasing penetration of vRES is likely to increase the amount of capacity reserves required. This will make maintaining an over-reliable system more costly in the future for TSOs and ultimately, consumers. Thus, to make the energy transition as cost-effective as possible, reforms are needed to allow markets to determine the cost-optimal level of power system reliability.

To this end, a key reform would be encouraging a more price-responsive demand side. For large consumers, this would mean placing price-volume bids for load on electric power exchanges, in preference to forming bilateral contracts for emergency load shedding with TSOs which take place outside the market. For smaller commercial consumers and households, large-scale deployment of smart meters could enable price-responsive demand in different ways, based on new contract types offered by electricity retailers. For example, customers that are willing to expose themselves to market prices could opt for contracts in which they pay for electricity based on real-time market prices, giving them the flexibility to consume more during periods with low prices and avoid periods with high prices. Customers who do not want the hassle or risk of dynamic pricing could choose for a fixed tariff, while nominating an

electricity price at which they would be willing to have their supply interrupted (Biggar & Hesamzadeh, 2014, p. 131). Retail companies could then aggregate these price preferences, effectively customer differentiated VoLL values, into their market bids[5]. Concerns about equitable access to electricity could be addressed by establishing appropriate safeguards for low-income households[6]. By reforming demand-side measures, the political cost of lost load should fall as consumers would determine how much they value reliability, not politicians. With smart meter penetration expected to reach 80% across the EU by 2020, these reforms could foreseeably be made over the next few years (EC, 2014a).

The need for sustainable bioenergy. In Chapter 4, bioenergy is used in a net-zero emission 100% RES power system (in the absence of cost-effective hydrogen, limited CSP and geothermal capacity) to provide firm and dispatchable capacity to balance fluctuations in vRES output, and baseload generation in winter. In Chapter 5, bioenergy again plays a major role in achieving a more ambitious net-negative emission target by enabling BECCS. However, bioenergy should only be exploited for energy purposes if the carbon payback period is short enough to have a meaningful climate impact[7], the use of biomass is consistent with broader sustainability concerns, and does not lead to deleterious effects on e.g. soil quality, biodiversity, or water stress (Creutzig et al., 2015). Many of these impacts are restricted to certain locales, thus, both the positive and negative impacts of bioenergy are very case specific (Fajardy & Mac Dowell, 2017; Jonker et al., 2014). Due to the above concerns, some groups oppose the use of biomass for BECCS (e.g. (EASAC, 2018; Fern, 2018; Norton et al., 2019)). However, scenarios from the IPCC show that the total use of bioenergy can be as high or even higher when BECCS is excluded compared to when it is included, due to its potential for replacing fossil fuels across sectors (Allen et al., 2018). Thus, to allay sustainability concerns, the sustainability of BECCS (and bioenergy in general) can be improved by maximising the conversion efficiency to electricity, limiting the impacts of direct and indirect land-use change, preferencing certain biomass types (e.g. residues, high-yield, low-moisture crops) over others, employing low-carbon electricity and organic fertilisers in the biomass production, minimising the transport of biomass, prioritising sea over road transport, and employing alternative biomass upgrading processes such as natural drying or torrefaction (Creutzig et al., 2015; Fajardy & Mac Dowell, 2017; Jonker et al., 2014).

While the use of bioenergy could be avoided in a net-zero emission 100% RES system with large-scale seasonal storage using hydrogen, this is likely to be costly (see section 6.4.2). In scenarios requiring net-negative emissions from the power sector, avoiding bioenergy may be even costlier as the only alternative is DAC (as shown in Chapter 5). Although there are a variety of other potentially cheaper NETs which could be deployed outside the power sector (see section 1.1), these also have their drawbacks. For example, compared with afforestation, the underground may be a safer place to store carbon long-term, as forests are vulnerable to wildfires, the risk of which increases as the climate warms (Settele et al., 2014). Furthermore,

negative emissions would need to be measurable and verifiable to be used in global carbon accounting procedures, which may be easier with centralised point sinks such as BECCS and DAC than with decentralised options like biochar production.

The role of CCS in reaching 1.5°C. One could argue that the cost reductions achieved in RES technologies over recent years mean that CCS is no longer needed in the power sector, and that CCS deployment should be restricted to other sectors such as industry, where fewer cost-effective low-carbon technologies are available. With respect to the use of CCS with fossil fuels in the European countries considered in this thesis, the least-cost generation portfolios resulting from Chapters 4 and 5 would seem to *partly* support this argument. For example, under base case cost assumptions, no coal plants with CCS are present in the least-cost portfolios in either Chapter 4 and Chapter 5. This is partly due to costs, but also because the expected CO_2 capture rate from CCS plants (~90%) means that the residual CO_2 emissions from coal plants, even when equipped with CCS, are still too high when aiming for deep decarbonisation. This finding is supported by others (Budinis et al., 2018). Meanwhile, some natural gas plants with CCS, which have lower residual emissions than coal CCS plants, are installed in Chapter 5 to provide flexible low-carbon capacity. It has been shown that cost-effective deployment of CCS with natural gas is more sensitive to the CO_2 capture rate than with coal (*ibid.*), and technology developments allowing for higher CO_2 capture rates, such as the Allam cycle (up to 98%), mean that natural gas with CCS could still have a role to play in the electricity sector (Mitchell et al., 2019). However, even if the policy decision is made not to deploy CCS with fossil fuels for electricity production, relying on the power sector to meet a 1.5 ºC target would necessitate deployment of CCS, as this technology underpins both BECCS and DAC[8].

The need for NETs in Europe. Some have criticised NETs as a way for governments to reduce the political and economic challenges of taking climate action today, while making us reliant on technological advances and large-scale NET deployment in the future (Anderson & Peters, 2016). Arguments given against NETs are that (i) deep decarbonisation can be achieved in the near term without NETs by energy efficiency improvements, shifts towards low carbon behaviours, and deployment of RES, (ii) relying on NETs is risky as they have not been deployed at large scale, (iii) by applying discounting, integrated assessment models (IAMs) assume that the future costs of NETs are lower than the cost of decarbonising now, while deploying NETs in future decades will shift the financial burden of climate mitigation to future generations, and (iv) with respect to BECCS, questions remain about its potential impacts on land use, biodiversity, competing demands for biomass from other sectors, and real carbon neutrality/negativity (Anderson & Peters, 2016). However, rather than arguing against NETs, many of the concerns above strengthen the argument for more rapid deployment of NETs. For example, more rapid deployment of NETs will help demonstrate their technical feasibility and reduce uncertainty in their large-scale deployment, leading to faster cost reductions, spread the cost of negative emissions more equitably across generations, hedge against the

risks of delayed decarbonisation in other sectors/countries, and increase the chances of limiting warming to 1.5 ºC (Detz & van der Zwaan, 2019). In any case, relying less on (or even avoiding) NETs means emission reductions will need to be achieved sooner and more steeply, potentially at the upper limit of the mitigation ranges considered by the IPCC (see Figure 1-1) (van Vuuren et al., 2017). While some IAMs show that cost-optimal net-zero emissions (and hence negative emissions) may be achieved earlier in regions like India or China before the EU, or in regions with a large biomass and/or high CCS potential, it is questionable whether these countries will take the lead in deploying NETs given their current emission trajectories and track record of slow action (EC, 2018a; van Soest et al., 2018). In contrast, the EU has been a global leader in combatting climate change for decades and may need to assume this role once again in the deployment of NETs.

Public acceptance for a cost-effective energy transition. All decarbonisation strategies discussed in this thesis include elements which may face public opposition. For example, solar and wind require significantly more area than conventional thermal power plants to generate the same amount of electricity and in the *Base* 100% RES scenario in Chapter 4, the assumed land area available for onshore wind and ground-based PV in many countries (e.g. Germany, France, the Netherlands, Denmark, UK) is almost completely exploited[9]. Chapter 4 also shows that a 100% RES power system would be contingent on significant transmission investment across Europe. As a consequence, the well-known "not in my backyard" (NIMBY) phenomenon could result in public opposition to the large-scale vRES deployment and transmission investments required for a 100% RES scenario (Komendantova & Battaglini, 2016). Some also oppose the use of biomass for power generation, as previously discussed. Aside from RES, investments in nuclear or CCS plants as part of a more technology-diverse strategy may also face public opposition in some countries (Lipponen et al., 2017). Public opposition can be addressed with engineering solutions, but this will increase the cost of the energy transition. For example, opposition to onshore wind can be addressed by deploying more offshore wind instead; however, the average levelized cost of electricity (LCOE) for offshore wind in Europe is currently twice as high as for onshore wind (120 € MWh^{-1} vs. 65 € MWh^{-1} (IRENA, 2018)) and, in terms of capital costs, is projected to remain so for the foreseeable future (Tsiropoulos et al., 2018). Storing CO_2 offshore instead of onshore could also reduce opposition to CCS, but this is twice as costly (Zero Emissions Platform, 2011). Opposition to new overhead transmission lines can be avoided by installing cables underground, but this can increase the cost by up to tenfold (Parsons Brinckerhoff, 2012), which will ultimately be passed on to consumers via grid fees.

Until now, the level of power system reliability has been considered a (quasi-)public good as individual consumers could not choose their level of reliability, grid operators could not disconnect individual households, and investments in generation capacity increase reliability for all consumers (EC, 2016a; Müsgens et al., 2014). However, smart meter technology and price-responsive demand could make this principle worth revisiting, even though it may be

met with some public resistance. For these reasons, a broader public debate is necessary to encourage public participation in the energy transition, inform the public about the trade-offs of using different technologies and following different decarbonisation strategies, gain a political mandate for making the necessary market reforms, and agreement on how the benefits, costs and risks of limiting climate change to 1.5°C can be fairly distributed.

The evolution of European electricity market design. Market design is a gargantuan topic encompassing (but not limited to) the design of futures, day-ahead, intraday and balancing markets, capacity markets, the allocation and pricing of cross-border transmission capacity, congestion management, and bidding zone design. Each is a complex topic on its own and this thesis does not consider them all. Thus, it is not within the scope of this thesis to conclude which market design is the best. Nevertheless, the findings from Chapters 3 and 5 do allow some conclusions to be drawn on certain *elements* of market design (see section 6.3.4), namely that (i) reforming EOMs to remove price caps and encourage price-responsive demand can deliver benefits for system reliability and cost, (ii) liquid intraday markets will help integrate vRES and reduce balancing costs, (iii) imbalance netting and coordinated procurement of reserves will reduce the need and costs of balancing, and (iv) CRMs do not necessarily guarantee generator revenues and security of supply. These findings are discussed in more detail below.

Regarding point (i), this is in agreement with basic market principles that short-term prices should be at the point where the marginal utility of consumption and marginal cost of production intersect as this maximises overall welfare and optimal allocation of resources (Bublitz et al., 2018), price caps should be removed as they distort the market by preventing prices rising to levels needed for incentivising long-term investment, and price-elastic demand prevents suppliers exercising market power (Biggar & Hesamzadeh, 2014, p. 16,130,305).

Regarding point (ii), the growing importance of intraday markets has been observed in a recent review of European intraday market design (Ehrenmann et al., 2019). The authors note that while the day-ahead market was originally considered as the short-term "spot" market, and intraday and balancing markets used mostly for adjustments, in the future the intraday market should be considered the new "spot" market, and the day-ahead market should be regarded as another forward market. Both points (ii) and (iii) are consistent with the trend towards European market integration that many studies show can reduce costs and increase security of supply (Newbery et al., 2016; Ortner & Totschnig, 2019; Ringler et al., 2017; Schlachtberger et al., 2017). Several projects are underway to further integrate intraday (e.g. XBID) and balancing markets (e.g. IGCC, PICASSO, MARI and TERRE) over the coming years (ENTSO-E, 2019a; Gomez et al., 2019). The benefits of market integration will increase as the share of vRES increases thanks to geographical diversity, but realising these benefits will be contingent on large-scale transmission investments, better management and pricing of

transmission capacity, and acceptance on the part of national governments to become more dependent on their neighbours for their security of supply.

Regarding point (iv), the debate between EOMs and CRMs has been ongoing for many years, with no clear resolution (see Chapter 5.1). While the findings of this thesis support the case for reforming EOMs and go against the need for CRMs, they in no way demonstrate that EOMs triumph over CRMs, as Chapter 5 evaluates only one type of CRM (a capacity market), while there are a variety of other CRMs designs which may be less distortive, and ultimately none of the market designs modelled in Chapter 5 (which considers both EOMs and CRMs) enable all dispatchable and vRES technologies to recover their investment costs. This raises the question of how investments in the power system needed to reach a 1.5°C warming limit will be made.

Despite the failure of both EOMs and CRMs to deliver economically feasible systems in Chapter 5, there are several reasons why it may be too early to give up on EOMs just yet, and why implementation of CRMs should be avoided. Firstly, there is still considerable scope for reforming EOMs (e.g. removing price caps, price-responsive demand), the benefits of which have already been discussed. Secondly, now that vRES have largely achieved cost parity with conventional generation sources, several reforms are likely to be implemented to address the distorting impact of feed-in-tariffs and expose vRES to market signals (Henriot & Glachant, 2013; Hu et al., 2018). Thirdly, price hedging with bilateral contracts could play an important role in reducing investment risks for generators and serve as a long-term price floor on day-ahead markets. For example, if energy suppliers are unable to earn profits on day-ahead markets due to low average prices, they may instead decide to sell more of their electricity via long-term contracts such as purchase power agreements (PPAs), which would be agreed at prices reflective of their long-run costs. If this trend continued, the supply of electricity on day-ahead markets would fall, putting upward pressure on market prices until an equilibrium was found between average PPA prices and market prices. Lastly, implementation of CRMs can undermine the performance of existing EOMs (especially in neighbouring countries without CRMs) (Bucksteeg et al., 2017; Henriot & Glachant, 2013), potentially locking in a (perceived) structural dependence on CRMs in the long term.

6.4.2 Scope limitations

Due to research constraints, several relevant aspects are beyond the scope of this thesis. A justification and discussion of these topics is provided below.

The use of **electrolysis to produce (green) hydrogen for seasonal storage** and other power-to-gas technologies are not considered in this thesis, for several reasons. Currently, most hydrogen is produced from natural gas via steam methane reforming (SMR), resulting in CO_2 emissions (also called *grey* hydrogen). If this CO_2 is captured and stored, it is known as *blue* hydrogen (M. Mulder et al., 2019). The potential role of blue hydrogen for the power sector is considered in the sensitivity analysis in Chapter 5 by giving natural gas plants the option of

using hydrogen without any additional capital investment at a cost of 13 € GJ^{-1}, the estimated minimum price for blue hydrogen to be profitably produced at the assumed natural gas price (5.9 € GJ^{-1}) in the Netherlands (M. Mulder et al., 2019)[10]. Even in this optimistic case, no blue hydrogen is deployed by the model in a net-zero emission 2°C warming scenario, and only a small amount (50 PJ y^{-1}) is used in a more ambitious 1.5°C warming scenario from ~2030 onwards, generating an average of 9 TWh y^{-1}. These results suggest that blue hydrogen would only have a minor role in a low-carbon electricity sector, though it may feature more strongly in other sectors.

Turning to green hydrogen, some argue that it has an important role to play in low-carbon power systems relying on large shares of vRES, as electrolysis can be used to generate hydrogen from surplus cheap electricity from vRES (which would otherwise be curtailed) and store it for later use. However, there are several economic and practical reasons to doubt this. The economics of green hydrogen depends on several key factors, including (i) electrolyser cost and efficiency, (ii) hydrogen storage cost and efficiency, (iii) the cost and efficiency of converting hydrogen back to electricity, (iv) low electricity prices, and (v) high operating hours (van Leeuwen & Mulder, 2018).

Points (i)-(iii) above depend on future technology developments. The average investment costs of alkaline and proton exchange membrane (PEM) electrolysers in 2015 were approximately 1250 € kW_{el}^{-1} and 2100 € kW_{el}^{-1} respectively (Gambhir et al., 2017). By 2030, these are projected to fall to 550 € kW_{el}^{-1} and 600 € kW_{el}^{-1} with additional research and development and production scale-up (*ibid.*). However, the uncertainty in these future cost estimates is considerable (Saba et al., 2018). The efficiency of electrolysis is currently 61%-64%, and could rise to 75% by 2050 (Gorre et al., 2019). The conversion efficiency from hydrogen back to electricity depends on the technology, but lies between 40% and 70% (Pilavachi et al., 2009). Thus, even in the best case (and excluding any losses during storage) the roundtrip losses for producing and using green hydrogen in the power sector are around 50%[11]. Given that the land (and sea) requirements and costs of a 100% RES power system increase with vRES deployment (see Chapter 4), supplying bulk (i.e. baseload and load-following) electricity using vRES and hydrogen with seasonal storage would be challenging and costly. For example, trying to replace the 700 TWh y^{-1} of solid biomass generation in the 100% RES scenarios in Chapter 4 with vRES and hydrogen seasonal storage would require 1400 TWh of vRES generation. With most of the best locations on land for onshore wind and PV in central Europe already exploited, additional vRES capacity would need to come from more costly offshore wind, or onshore wind and utility PV in northern, southern or eastern Europe, further increasing transmission requirements.

Regarding points (iv) and (v), there are several reasons why many hours with low electricity prices (and hence economic operating hours for electrolyser) may not materialise. Firstly, large-scale cross-border transmission expansion will allow surplus vRES generation from one

country to meet demand in another, leading to price convergence[12]. Secondly, an increasing carbon price will put upward pressure on electricity prices (see Chapter 5). Thirdly, demand is likely to increase in future not only from EVs and HP, but also from supply-demand economics and substitution of other more costly energy sources for low-cost electricity. With few hours with low electricity prices, electrolysers would only be able to achieve a limited number of operating hours, while studies show that high electrolyser utilisation is necessary to make green hydrogen economically feasible (van Leeuwen & Mulder, 2018)[13].

Aside from green hydrogen for seasonal storage, industries seeking to decarbonise with hydrogen will demand a continuous, rather than intermittent supply. This will be difficult and more costly to deliver with green hydrogen from vRES for the reasons already explained above, and blue hydrogen may be a better option (van Cappellen et al., 2018). Moreover, studies have shown that additional demand for hydrogen changes the optimal mix of electricity generation technologies, with the share of baseload capacity increasing (Green et al., 2011).

Given the findings of this thesis that blue hydrogen has only a minor role in a least-cost decarbonisation pathway for the power system, and green hydrogen is expected to be even costlier than blue hydrogen for the foreseeable future[14], it does not seem likely that green hydrogen will be a cost-effective option for large-scale seasonal storage in a decarbonised power system either in the period until 2040/2050. This finding has been supported by other studies e.g. (van Zuijlen et al., 2019). For these reasons, including green hydrogen is unlikely to change the main conclusions of this thesis. However, given uncertainties around future cost developments, further research is required on the potential role of cost-effective green hydrogen in the power sector.

The representation of the **physical electricity network is simplified** throughout this thesis. For example, in Chapters 2 and 3, the European continent is treated as a copper plate. In Chapters 4 and 5, transmission between countries is treated in more detail based on net transfer capacities, while transmission within countries is again modelled as copper-plate. These simplifications mean that transmission investments are likely to have been underestimated, and unscheduled physical 'loop' flows, which reduce the cross-border capacity available for commercial flows, are not considered (Hagspiel et al., 2014). This could be addressed by using more detailed grid models (e.g. flow-based market coupling) in the transmission calculations (van den Bergh et al., 2016), but was beyond the scope of this thesis. In addition, this thesis does not consider the distribution network, where increasing vRES (mainly rooftop PV), EV and HP penetration will potentially have the greatest effects. For example, some studies show distribution grid investments may be even higher than transmission investments in a power system with large shares of vRES (DNV GL, 2014). However, significant distribution investments may ultimately be required even without vRES to accommodate the rollout of HPs and EVs. In any case, accounting for the simplifications applied to both transmission and distribution modelling in this thesis by using more detailed

models would have the greatest impact on strategies targeting high RES deployment, as the total costs for transmission and distribution grid reinforcements to supply energy and ensure reliability (or alternatively, the additional costs for redispatch, vRES curtailment and unserved energy) would increase more than in more diversified or high-NET portfolios. Thus, even using more detailed grid models, the key conclusions of this thesis are unlikely to change.

Power system stability, the process of maintaining system frequency and voltages at target levels, is not addressed in this thesis[15]. However, it is known that maintaining system frequency at target levels may become more challenging in decarbonised power systems with large shares of asynchronous vRES generators which, unlike synchronous generators (e.g. steam and gas turbines), provide no inertia to the system to slow frequency changes after the sudden disconnection of a large generator, load, or transmission line (Dreidy et al., 2017; IRENA, 2017). Most of the 100% RES portfolios modelled in Chapter 4 contain significant bioelectricity and CSP capacity which (if online) could provide inertia. However, during periods of very high non-synchronous vRES generation (e.g. a sunny windy day) and in portfolios relying on very high shares of vRES, a lack of inertia could threaten power system stability (IRENA, 2017). In such cases, TSOs may need to intervene in the market to keep synchronous generators online, or deploy other technologies to provide synthetic inertia including synchronous condensers, flywheels, HVDC interconnectors, and fast-responding batteries (Rezkalla et al., 2018). Maintaining bus voltages at target levels may also become more challenging with increasing vRES penetration, especially in locations which are poorly connected to the rest of the grid. However, analysis of system frequency and voltages requires detailed grid models and power flow calculations, which as stated previously, are beyond the scope of this thesis. In any case, the investments required for voltage control are reportedly small in comparison to what is needed for power generation (IRENA, 2017), and some modern vRES generators also have the ability to provide frequency and voltage support for grid operators (Brown et al., 2018).

Lastly, the investment module of the cost-optimisation model used to make investments in Chapters 4 and 5 (i) assumes **perfect foresight** of the entire modelled horizon, and (ii) makes **temporal simplifications** (e.g. generator ramping constraints are ignored) which, while dealt with appropriately in the short-term unit commitment and economic dispatch (UCED) simulations, are not fed back to the investment module. These aspects have several potential consequences. Firstly, perfect foresight models follow the least-cost pathway according to assumed cost developments, while real-world myopic investors do not necessarily follow the least-cost pathway, leading to potentially higher costs. However, cost minimisation can be a useful tool for policymakers in deciding which policies and regulations to implement, in order to steer myopic investors towards desired outcomes with appropriate market signals. Nevertheless, future cost developments are inherently uncertain, and deviations from the assumed developments may lead to potentially lower or higher cost pathways in reality. However, exploring the impacts of myopic investment decisions was beyond the scope of this study, and the sensitivity analysis performed in Chapters 4 and 5 showed that the main

conclusions were largely unaffected by different cost assumptions in the ranges considered. Secondly, temporal simplifications in the investment module could mean that insufficient flexible generation capacity may be present in the optimised generation portfolios. This would lead to unserved energy in the short-term UCED results and represent either (i) an underestimate of the amount and cost of flexible capacity required, or (ii) an underestimate of the costs of lost load. This potential issue is addressed in Chapter 4 by allowing for a small overcapacity in the investment module. Even if this approach means slightly more capacity is installed than required, this capacity is likely to come from relatively low-cost capacity sources, (e.g. gas turbines) which ultimately contribute a relatively minor amount to total costs.

6.4.3 Methodological contributions

While addressing the central content-based research questions, this thesis also resulted in the development of several new methods and modelling tips:

- A new algorithm to distribute solar PV and wind capacity across a spatial grid according to different optimisation objectives (e.g. minimum residual demand, maximum capacity factor), while incorporating a variety of spatial and technological constraints (Chapter 2). This can be used by power system modellers to generate distributions of solar PV and wind capacity for modelling studies.

- The detailed spatial optimisation of vRES capacity was included in a power system capacity expansion model at the European scale for (to the author's knowledge) the first time, allowing for more insights on how system costs and land/sea use increase with vRES penetration (Chapter 4).

- A new method for synthesising day-ahead forecasts for load and vRES generation based on historical forecast errors (Chapter 3). This method can be used by power system modellers and TSOs for power system planning studies to determine potential balancing requirements, based on different projections of future load and vRES deployment.

- Modelling power systems for many weather years at high temporal resolution with limited computational resources can be made easier with various techniques. For example, parallelising simulations of non-dependent weather years across multiple cores can reduce the required simulation time by up to 75% (used in Chapter 2). Using less memory-consuming variable types (e.g. half precision 16-bit floating point numbers instead of full precision 64-bit) combined with appropriate numerical scaling can reduce memory use considerably, making intractable simulations tractable (used in Chapter 3).

- Modelling DAC as a kind of pumped hydro storage in PLEXOS was found to be an effective method to account for its dynamics and costs in the power system (used in Chapter 5).

6.5 Recommendations for further research

This thesis has highlighted many topics requiring further research, some of which are given below:

- With competition for land likely to grow in the future not just for vRES deployment but also for agriculture, further research is needed to determine the **costs and climate impacts of using land for afforestation or dedicated rotating biomass crops for BECCS**.

- Further research is needed to **assess the potentials, environmental trade-offs and reduce the costs of all NETs** including afforestation, ocean carbon storage, and soil carbon sequestration, as relying on BECCS and DAC in the power sector to provide all negative emissions could be very costly. Moreover, research is needed to determine how society should pay for NETs in the most equitable way, and how negative emissions can be included in existing carbon market structures.

- Investigate **potential interactions and cost synergies between the electric power sector** and other sectors such as heat and transport (e.g. power to heat, vehicle-to-grid), including the provision of negative emissions.

- Further research is needed to better quantify the **cost-effective sustainable biomass supply potential** available (including potential imports) to use in a 100% RES power system or systems with large-scale BECCS deployment. Developing new governance systems for guaranteeing the sustainable use of biomass will also help alleviate public concerns.

- Better quantification of the impacts of **decarbonisation strategies which exclude bioenergy**, and the need for alternative options to supply seasonal generation such as hydrogen (with storage), geothermal, and natural gas with CCS.

- Explore the **impact of potentially game-changing technology breakthroughs** such as very cheap solar PV and battery storage, cheap hydrogen, small modular nuclear reactors, cost-effective CCS technologies achieving 100% carbon capture, and low-cost DAC.

- Quantify the requirements and costs of **maintaining power system stability** in power systems with very high shares of vRES.

- Explore potential developments in **trading behaviour and revenues between electricity markets at different time scales** (e.g. day-ahead, intraday, balancing) and bilateral contracts.

- **Faster algorithms are required for solving unit commitment and economic dispatch problems** in power system models which, when all flexibility and integer constraints are included, can become very time-consuming to perform. This renders probabilistic analysis of power systems impractical to undertake without significant simplifications. Alternatively, better ways of identifying which weather conditions are most challenging for power system operation would reduce the need for time-consuming simulations.

6.6 Recommendations for policymakers

- **A diverse generation portfolio made up of RES as well as other low-carbon technologies such as nuclear, CCS and NETs is likely to be the most cost-effective strategy for achieving a reliable, decarbonised European power sector in line with the climate ambitions set out in the Paris Agreement.** The most cost-effective strategy for individual countries will depend on their natural resources, geography, and existing portfolio of generation technologies.

- **Support development of NETs both in and outside the power sector** to reduce the uncertainties and costs of their deployment, with the expectation that they may be needed sooner rather than later. In the power sector, BECCS could be deployed relatively quickly and at a lower cost than building a new BECCS plant by first converting existing modern coal plants to biomass, then equipping them with CCS. However, DAC would be very costly, and deploying other cost-effective NETs outside the power sector would reduce the reliance on DAC (and BECCS).

- **Reform current EOMs to allow markets to determine the cost-optimal level of power system reliability.** Examples of such reforms are fostering price-responsive demand and allowing for high prices during times of scarcity by removing market price caps (including implicit ones). Refrain from implementing CRMs until their necessity has been demonstrated.

- **Continue to integrate electricity markets across Europe.** Increasing transmission capacity and coupling national markets will reduce costs to consumers, enhance reliability, facilitate the integration of vRES and accelerate decarbonisation.

- **Take measures to increase intraday market liquidity** by reducing entry barriers and integrating markets. This will support the integration of vRES and reduce balancing requirements.

- **Introduce a mechanism in the ETS to remunerate NETs for the negative emissions they produce.** This would contribute to but not fully underpin the economic operation of NETs, and further support will likely be necessary.

6.7 Samenvatting en conclusies

Na tientallen jaren vertraging, gemiste kansen en toegenomen broeikasgasconcentraties in de atmosfeer, zijn de vereiste acties om de klimaatverandering aan te pakken steeds urgenter en ernstiger. Een recente analyse van het Intergovernmental Panel on Climate Change (IPCC) laat zien dat om een goede (67%) kans te hebben om de opwarming van de aarde te beperken tot 1,5 ºC zoals vastgelegd in het Parijs-akkoord, de totale wereldwijde CO_2-uitstoot vanaf 2018 de 420 Gt CO_2 (netto) niet mag overschrijden (Rogelj et al., 2018). Als de uitstoot rond de 37 Gt CO_2 y^{-1} blijft, zoals in 2018, zal dit budget rond het jaar 2030 worden overschreden (Aidt, 2019).

Met een CO_2-uitstoot van 13 Gt in 2018 (38% van de totale CO_2-uitstoot voor de energieproductie) is de elektriciteitssector momenteel wereldwijd de grootste bron van broeikasgasemissies (IEA, 2019). De elektriciteitssector kan een cruciale rol spelen in het beperken van de opwarming van de aarde tot 1,5 °C dankzij de omvang van de uitstoot, de mogelijkheid om andere sectoren indirect koolstofvrij te maken, en connecties met 'bioenergy with carbon capture and storage' (BECCS) en 'direct air carbon capture' (DAC). Dit zijn twee negatieve emissietechnologieën (NET's) die zo worden genoemd omdat ze leiden tot een netto reductie van CO_2 uit de atmosfeer. Vanwege de bovenstaande redenen is het koolstofvrij maken van de energiesector een topprioriteit in de strijd tegen de klimaatverandering.

De Europese Unie (EU) is sinds lange tijd een wereldleider in het nemen van maatregelen tegen de klimaatverandering en het inzetten van hernieuwbare energiebronnen of 'renewable energy sources' (RES). In de tien jaar van 2008 tot 2018 is het geïnstalleerd windvermogen van windenergie in de EU verdrievoudigd van 60 naar 180 GW. Tegelijkertijd is het productievermogen van zonne-energie door fotovoltaïsche zonnepanelen (PV) meer dan vertienvoudigd van 10 naar 115 GW (EurObserv'ER, 2018, 2019; Eurostat, 2017b; SolarPower Europe, 2019). Dankzij deze groei in hernieuwbare energiebronnen en de dalende opwekking van steenkool, daalde de broeikasgasemissies van de opwekking van elektriciteit (en warmte) in de EU met 24% tussen 2008 en 2017 tot ongeveer 1 Gt y^{-1} (Eurostat, 2019a). Dit vertegenwoordigt echter nog steeds 25% van de totale uitstoot van broeikasgassen in de EU en meer actie is nodig om de ambitieuze klimaatdoelen in het Parijs-akkoord te bereiken. Gelukkig toont de recente (november 2019) motie van het Europees Parlement om een noodsituatie in het klimaat te verklaren, de inzet van Europa om de uitstoot nog verder te verminderen (European Parliament, 2019).

Hoewel het duidelijk is dat de Europese elektriciteitssector koolstofvrij moet worden, is het niet duidelijk hoe dit moet gebeuren, aangezien drie brede strategieën gevolgd kunnen worden. Ten eerste hebben studies aangetoond dat kosteneffectieve en koolstofvrije productieportfolio's kunnen worden opgebouwd uit een **diverse mix van technologieën** zoals hernieuwbare energie, nucleaire en fossiele productie met CO_2-afvang en -opslag of

'carbon capture and storage' (CCS) (Jenkins et al., 2018; Sepulveda et al., 2018). Door zich te houden aan een doelstelling van netto nul emissies tegen 2050 en een combinatie van RES, nucleaire en potentiële CCS te gebruiken volgt het Vereinigde Koningrijk een dergelijke technologie-diverse aanpak (UK Government, 2019). Een tweede strategie, die momenteel wordt gevolgd door landen als Denemarken en Zweden, is het streven naar een elektriciteitssysteem dat **vrijwel uitsluitend gebaseerd is op RES** (KEFM, 2018; Swedish Ministry of the Environment and Energy, 2019). Met een doelstelling van 80% RES-elektriciteit (minimum) tegen 2050 vastgesteld, volgt Duitsland ook een dergelijk overwegende hernieuwbare strategie (BMWi, 2018). Een derde strategie is het **grootschalig gebruik van NET's** om de uitstoot van het voortdurende gebruik van fossiele brandstoffen in de elektriciteit of andere sectoren te compenseren, maar momenteel geen enkel land deze strategie nastreeft. Ongeacht de gevolgde strategie wordt de Europese elektriciteitssector in de komende decennia waarschijnlijk geconfronteerd met drie grote uitdagingen. Deze uitdagingen maken de overkoepelende doelstelling van een moderne elektriciteitssector – het leveren van duurzame, betrouwbare elektriciteit tegen de goedkoopste prijs – moeilijker om te bereiken.

Ten eerste roept de **toenemende capaciteit van niet stuurbare hernieuwbare energiebronnen** of 'variable renewable energy sources' (vRES) zoals zon-PV en wind zorgen op over de betrouwbaarheid van het elektriciteitssysteem. Voor koolstofvrije strategieën die gericht zijn op de grootschalige inzet van RES, zal dit een uitdaging zijn. Gezien de dalende kosten van wind en PV is de rol van vRES in technologiediverse portfolio's met minimale maatschappelijke kosten waarschijnlijk ook groot. Daarmee zullen ook deze portfolio's uitdagingen voor de betrouwbaarheid kennen. Ten tweede zien we dat de voorwaarden voor het koolstofvrijmaken van de elektriciteitssector in de loop van de tijd steeds strenger worden, en netto-nul emissies tegen 2050 misschien niet voldoende zijn om de klimaatdoelstellingen te halen. De inzet van NET's wordt dus misschien onvermijdelijk, en **het is onduidelijk wat de effecten van de grootschalige inzet van NET's op de Europese elektriciteitssector kunnen zijn.** Ten slotte zijn er zorgen of een geliberaliseerde Europese elektriciteitsmarkt voldoende prikkels creëert om investeringen in koolstofarme opwekkingscapaciteit te stimuleren, klimaatdoelstellingen te bereiken, en tegelijkertijd de leveringszekerheid te waarborgen.

Hoofdstuk 2 onderzoekt hoeverre de ruimtelijke inzet van wind- en zon-PV vermogen in Europa kan gebruikt worden om de geaggregeerde elektriciteitsvraag- en vRES-opwekkingsprofielen beter op elkaar te laten aansluiten. Daardoor kunnen wind- end zonne-energie mogelijk beter geïntegreerd worden in het Europese elektriciteitssysteem. Een algoritme is ontwikkeld om de hoeveelheid en verdeling van zon-PV en wind vermogen over Europa te optimaliseren door het gebruik van een gedetailleerd (50 km x 50 km) ruimtelijk raster verbonden met data over het landgebruik en weeromstandigheden zoals windsnelheid en zoninstraling. Het algoritme wordt uitgevoerd met 36 klimaatjaren om rekening te houden

met variabele weersomstandigheden. De inzet van wind- en zon-PV vermogen is begrenst zodat ze alleen in geschikte gebieden kan worden geïnstalleerd.

Hoofdstuk 3 kijkt naar de rol dat de intraday en balanceringsmarkt kunnen spelen in een zeer hernieuwbaar Europees elektriciteitssysteem met toenemend wind- en zon-PV vermogen. Dit wordt onderzocht door het ontwikkelen van een nieuwe methode voor het maken van gemodelleerde day-ahead voorspellingen voor elektriciteitsvraag en productie uit wind- en zon-PV, met foutverdelingen die consistent zijn met historische voorspellingen. Deze methode wordt vervolgens gedemonstreerd door simulaties uit te voeren voor het Europese elektriciteitssysteem waarbij de penetratie (het aandeel in de totale elektriciteitsproductie) van wind- end zon-PV toeneemt van 15% in 2017 tot 50% in 2040.

Hoofdstuk 4, getiteld "Is een 100% hernieuwbaar Europees elektriciteitssysteem haalbaar tegen 2050?" onderzoekt deze vraag door het modeleren van verschillende scenario's voor een volledig hernieuwbaar Europees elektriciteitssysteem in 2050. Dit hoofdstuk test of deze 100% RES portfolio's even betrouwbaar kunnen zijn als het huidige elektriciteitssysteem, berekent de totale kosten daarvan, en kijkt of de noodzakelijke inzet van RES-technologieën tegen het jaar 2050 haalbaar is. Deze analyse is gebaseerd op gedetailleerd marktsimulaties uitgevoerd met het PLEXOS marktmodel.

Hoofdstuk 5 overweegt twee scenario's voor een toekomstig koolstofarm elektriciteitssysteem in Centraal-West-Europa (CWE). Het ene is gericht op netto-nul CO_2-emissies van het elektriciteitssysteem in 2040, consistent met het beperken van de opwarming van de aarde tot 2 °C. Het andere is gericht op het ambitieuzere doel om de klimaatopwarming beperkt te houden tot 1,5 °C door het grootschalig gebruik van negatieve emissies. Aan de hand van het PLEXOS model worden in dit hoofdstuk drie hoofdvragen onderzocht: (i) hoe elektriciteitsopwekkingsportfolio's zich zouden moeten ontwikkelen om betrouwbare elektriciteit te leveren aan consumenten tegen de laagste kosten, (ii) hoeverre deze goedkoopste portfolio's ondersteund kunnen worden door marktinkomsten onder verschillende archetypische marktontwerpen, en (iii) hoe NET's de elektriciteitsmarkt kunnen beïnvloeden.

Op basis van de inzichten in de kernhoofdstukken vat hoofdstuk 6 de belangrijkste bevindingen van dit proefschrift samen, bespreekt deze bevindingen in de context van het bredere energie- en klimaatdebat, en biedt enkele belangrijke aanbevelingen voor beleidsmakers en voor verder onderzoek.

In het licht van deze uitdagingen is de kernonderzoeksvraag in dit proefschrift:

Wat zijn de gevolgen van verschillende strategieën in het Europees elektriciteitssysteem voor leveringszekerheid, het behalen van klimaatdoelstellingen, en economische levensvatbaarheid?

Bij het behandelen van deze bredere vraag richt dit proefschrift zich meer in detail op de volgende deelvragen:

1. In hoeverre kunnen de mix en ruimtelijke verdeling van zon-PV en wind vermogen gebruikt worden om ze te integreren in het elektriciteitssysteem?
2. Wat zijn de mogelijke gevolgen van het streven naar een 100% hernieuwbaar elektriciteitssysteem?
3. Wat zijn de mogelijke gevolgen van het vertrouwen op BECCS en DAC in het elektriciteitssysteem om de klimaatopwarming beperkt te houden tot van 1,5 °C?
4. Welke elementen moeten aanwezig zijn in toekomstige marktontwerpen om het energietrilemma (een betrouwbaar, betaalbaar, en koolstofarm elektriciteitssysteem) aan te pakken?

Deze onderzoeksvragen zijn behandeld in vier hoofdstukken (zie tabel 1-2).

Tabel 1-2 | Correspondentie tussen de hoofdstukken en onderzoeksvragen van dit proefschrift

Hoofdstuk	Onderwerp	Deelvragen			
		SQ1	SQ2	SQ3	SQ4
2	Gevolgen van de mix en ruimtelijke verdeling van wind- en zon-PV energie voor de resterende vraag	X	X		
3	Gevolgen van hoge vRES-penetratie in het Europese elektriciteitssysteem voor de intraday- en balanceringsmarkten		X		X
4	Gevolgen van een 100% hernieuwbaar elektriciteitssysteem	X	X		
5	Gevolgen van de klimaatopwarming beperkt te houden tot 1,5 °C met BECCS en DAC onder verschillende marktontwerpen			X	X

De belangrijkste bevindingen en conclusies van dit proefschrift zijn hieronder per deelvraag gepresenteerd.

SQ1: In hoeverre kunnen de mix en ruimtelijke verdeling van zon-PV en wind vermogen gebruikt worden om ze te integreren in het elektriciteitssysteem?

- **Het optimaliseren van de ruimtelijke distributie van vRES is waarschijnlijk geen effectieve strategie voor het verminderen van de benodigde back-up vermogen.** Hoofdstuk 2 laat zien dat, zelfs in het optimistische geval van ongelimiteerde transmissie binnen Europa, het optimaliseren van de distributie van vRES om de resterende vraag te minimaliseren de piek van de resterende vraag met slechts 2% vermindert, in vergelijking met een verdeling op basis van de hoogste

capaciteitsfactoren. Andere strategieën voor het omgaan met piekvraaguren zoals vraagrespons zijn waarschijnlijk kosteneffectiever.

- **De mix van vRES- technologieën heeft een grote invloed op hoe eenvoudig ze kunnen worden geïntegreerd, waarbij een groter aandeel wind gunstiger is.** Alleen rekening houdend met de belasting, en exclusief kosten, opslag en transmissiebeperkingen, zou de optimale inzet van vRES in Europa een energiepenetratie zijn van 82% netto (89% bruto), met een capaciteitsmix van ongeveer 25% zonne-energie PV en 75% wind. Van het totale windvermogen is 65% offshore. Op basis van de resultaten uit hoofdstuk 2, leiden deze aandelen tot de laagste jaarlijkse totale (positieve en negatieve) restvraag met 8% van de wind- en zonopwekking ingekort en 18% van de vraag onvervuld.

- **De optimale mix en ruimtelijke verdeling van vRES hangen echter sterker af van de investeringskosten van vRES en het transmissienet.** Het optimalisatiealgoritme dat in hoofdstuk 2 wordt gebruikt om de resterende vraag te minimaliseren, resulteert in een vRES-penetratie van 82% (netto), met een portfolio gedomineerd door offshore wind vanwege zijn gunstiger opwekprofiel. Dit algoritme houdt echter alleen rekening met de match tussen geaggregeerde belasting en generatie, exclusief de kosten van vRES, transportcapaciteit en het portfolio voor resterende opwek. Wanneer deze factoren in hoofdstuk 3 opgenomen zijn, daalt de optimale vRESpenetratie tot ongeveer 50%, met een capaciteitsmix van een derde wind tot twee derde zon-PV. Het opnemen van de kosten van vRES en transportcapaciteit in hoofdstuk 3 resulteert ook in een verschuiving van vRES-implementatie naar locaties met hogere capaciteitsfactoren, en naar locaties die dichter bij vraagcentra liggen, waardoor een gelijkmatigere verdeling van vRES- capaciteit over Europa wordt verkregen.

SQ2: Wat zijn de mogelijke gevolgen van het streven naar een 100% hernieuwbaar elektriciteitssysteem?

- **De bevindingen uit hoofdstuk 4 laten zien dat een Europees elektriciteitssysteem op basis van 100% RES tegen 2050 kan worden gerealiseerd met hetzelfde betrouwbaarheidsniveau als het huidig systeem**. Maar, bij afwezigheid van grootschalige seizoensopslag (bijv. met waterstof), word deze strategie in de komende jaren van veel ontwikkelingen afhankelijk:

  - **De totale opwekkingscapaciteit zou aanzienlijk moeten toenemen, mogelijk tot ten minste 1,8 TW in vergelijking met de 1 TW geïnstalleerd in 2015**. Dit vertegenwoordigt een toename van 80%, vergeleken met een veronderstelde toename van de elektriciteitsvraag tussen 2015 en 2050 met 40% (1300 TWh) vanwege warmtepompen (heat pumps, HP's) en elektrische auto's (electric vehicles, EV's).

- **De landgrensoverschrijdende transportcapaciteit moet toenemen, mogelijk met 140 GW tegen 2050** in vergelijking met de huidige (2015) capaciteit van 60 GW. Met meer grensoverschrijdende transportcapaciteit worden Europese landen afhankelijker op hun buurlanden voor de leveringszekerheid.

- **De jaarlijkse groei van wind- en zon-PV capaciteit moet respectievelijk tot 7,5 GW y^{-1} en 15 GW y^{-1} bedragen tegen 2050. Tegelijkertijd moet de groei van stuurbare duurzame opwekkingscapaciteit ten minste 18 GW y^{-1} zijn tot 2050** om elektriciteit te leveren tijdens perioden van lage vRES-opwekking en piekvraag momenten. In een 100% hernieuwbaar systeem moet dit afkomstig zijn van concentrated solar power (CSP), bio-energie (vaste biomassa en biogas), geothermie, waterkracht of opslag. Gezien de huidige implementatiesnelheden voor deze technologieën lager dan enkele GW y^{-1} zijn, vormt dit een belangrijke hindernis voor het realiseren van een 100% hernieuwbaar elektriciteitssysteem tegen 2050.

- **Grootschalige mobilisatie van Europa's bio-energiebronnen van 8,5 tot 13 EJ y^{-1}** in vergelijking met een 2015 gebruikt tot 1,9 EJ y^{-1}.

- **Een 100% hernieuwbaar elektriciteitssysteem zal duurder zijn dan een meer technologiedivers systeem inclusief andere koolstofarme (maar niet hernieuwbare) technologieën zoals kernenergie of CCS.** Dit wordt aangetoond in hoofdstuk 4 waar een scenario waarin nucleaire en CCS-technologieën zijn toegestaan, leidt tot totale jaarlijkse kosten in 2050 die 22% lager zijn dan het goedkoopst 100% hernieuwbaar scenario. Bovendien nemen de kosten van een 100% hernieuwbaar elektriciteitssysteem relatief meer toe met een hogere vraag door de uitputting van de meest gunstige inzetlocaties voor zond en wind, en de noodzaak om duurdere biomassabronnen te gebruiken.

- **De vraagrespons zal een belangrijke rol hebben om de haalbaarheid van een 100% hernieuwbaar elektriciteitssysteem te faciliteren.** Een flexibele vraag zal belangrijk zijn om het toenemende aantal van HP's en EV's in 2050 te integreren en de benodigde stuurbare productiecapaciteit zo laag mogelijk te houden.

- **Hernieuwbaar energiebronnen kunnen en doel van netto-nul emissies in de energiesector leveren, maar zelfs een 100% hernieuwbaar systeem kan NET's nodig hebben om de klimaatopwarming beperkt te houden tot 1,5 °C.** Alle de 100% hernieuwbare gemodelleerde portfolio's in hoofdstuk 4 kunnen netto-nul CO_2-emissies bereiken tegen 2050. Echter volgens de meest recente IPCC-scenario's

(zie figuur 1-1) kunnen negatieve emissies al nodig zijn tussen 2030 en 2040 om de klimaatopwarming beperkt te houden tot 1,5 °C.

SQ3: Wat zijn de mogelijke gevolgen van het vertrouwen alleen op BECCS en DAC in het elektriciteitssysteem om de klimaatopwarming beperkt te houden tot van 1,5 °C?

- **Zelfs met grootschalige inzet van wind- en zonenergie, kan vroegere inzet van BECCS een kosteneffectieve strategie zijn om de klimaatopwarming beperkt te houden tot 1,5 °C.** Hoofdstuk 5 laat zien dat in de goedkoopste scenario's die consistent zijn met een opwarmgrens van 2 ºC er vanaf 2030 sprake is van circa 2 GW BECCS capaciteit in CWE. In ambitieuzere 1,5 ºC scenario's wordt BECCS echter al in het begin van de jaren '20 ingezet door bestaande kolencentrales die dan biomassa verstoken te combineren met CCS. Tegen 2040 is ongeveer 25 GW BECCS geïnstalleerd in CWE die -250 Mt CO_2 y^{-1} negatieve emissies leveren. Deze grootschalige inzet van BECCS is afhankelijk van significante (~3 EJ y^{-1}) duurzame biomassa om echte klimaatvoordelen op te leveren. Dit betekent dat het gebruik van biomassa zo weinig mogelijk schadelijke effecten heeft op de bodemkwaliteit en de biodiversiteit, en zonder een zo lange koolstofschuld te veroorzaken dat het gebruik van biomassa zinloos wordt op op een tijdschaal die relevant is voor het klimaatbeleid.

- **BECCS kan tot meer basislastproductie, minder behoefte aan andere energiebronnen, en neerwaartse druk op de elektriciteitsprijs leiden.** BECCS is het meest kosteneffectief wanneer het wordt gebruikt met een hoge bedrijfstijd. Hoofdstuk 5 laat zien dat BECCS tot 15 TWh y^{-1} (1% van de elektriciteitsvraag) in CWE genereert tegen 2040 in de 2 ºC scenario's, en circa 190 TWh y^{-1} (15% van de elektriciteitsvraag) in de 1,5 ºC scenario's. Deze BECCS-capaciteit verplaatst een deel van de opwekkingscapaciteit voor het verzekeren van de basislast (e.g. nucleaire vermogen) in kostenoptimale portfolio's. Als BECCS-eenheden geld krijgen voor zijn negatieve emissies, en de CO_2-prijs hoog genoeg is, kan grootschalige inzet van BECCS neerwaartse druk op de elektriciteitsprijzen opvoeren en generatie van wind- en zonenergie ook verplaatsen.

- **Basislastvraag zou aanzienlijk toenemen als gevolg van DAC.** In tegenstelling tot BECCS, dat elektriciteit opwekt, verbruikt DAC elektriciteit. Vanwege de hoge kapitaalkosten heeft DAC zoveel mogelijk draaiuren nodig om kosteneffectief te zijn. Dit betekent dat de extra elektriciteitsvraag die aan het systeem wordt opgelegd door DAC, basislastvraag is. In plaats van zonne- en windenergie, word dit basislast elektriciteitsvraag goedkoper geleverd door basislastproductie technologieën zoals BECCS of (bestaande) nucleaire capaciteit.

- **Mechanismen zijn nodig om NET's te vergoeden voor de productie van negatieve emissies.** De analyse in hoofdstuk 5 neemt aan dat NET's geld verdienen voor de geleverde negatieve emissies. Dit kan uitgevoerd worden door een directe overheidssubsidie aan NET's, of een nieuw mechanisme toe te voegen aan het Europees systeem voor emissiehandel waardoor NET's uitstootrechten kunnen genereren en verkopen. Zonder de ondersteuning van een dergelijk mechanisme, blijft de inzet van NET's onwaarschijnlijk.

SQ4: Welke elementen moeten aanwezig zijn in toekomstige marktontwerpen om het energietrilemma aan te pakken?

- **Liquide intradaymarkten en grensoverschrijdende handel zorgen voor het integreren van vRES, het verminderen van de behoefte aan stuurbare opwekkingscapaciteit en het verminderen van balanceringskosten voor transmissienetbeheerders.** De Europese intradaymarkten zijn aan het groeien. Simulaties uitgevoerd in hoofdstuk 3 suggereren dat deze groei zal doorgaan met een toenemende penetratie van zonne- en windenergie. Als de penetratie van vRES in Europa tussen 2017 en 2040 van 15% tot 50% toeneemt, terwijl de nauwkeurigheid van day-ahead voorspellingen gelijk blijft aan de huidige nauwkeurigheid, stijgen de handelsvolumes op intradaymarkten tegen 2040 met ongeveer 60 TWh y^{-1} (~160%). Afhankelijk van de hoeveelheid beschikbare grensoverschrijdende transportcapaciteit kan echter tussen 40% (zonder grensoverschrijdende handel) en 75% (ongelimiteerde transmissie binnen Europa) van de day-ahead voorspellingsfouten opgelost worden door handel op intradaymarkten. Zonder liquide handel moeten deze voorspellingsfouten opgelost worden door transmissienetbeheerders op balanceringsmarkten.

- **Onbalansnetting en de gemeenschappelijke inkoop van reserves kunnen de behoefte aan en kosten voor balancering verminderen.** Simulaties uitgevoerd in hoofdstuk 3 suggereren dat balanceringseisen op het huidige niveau blijven, totdat het aandeel van zon-PV en windenergie circa 25% van totale elektriciteitsproductie overtreft. Een hoger aandeel van zon-PV en windenergie leidt echter tot toenemende balanceringseisen. Met 50% zonne- en windenergie (rond het jaar 2040 in het gesimuleerde scenario), kunnen onbalansvolumen toenemen met circa 130% en de behoefte aan balanceringscapaciteit toenemen met 110% (in vergelijking met 2017), in geval van geen onbalansverrekening en een afzonderlijke reserve per land. Met onbalansnetting en een gemeenschappelijke reserve, dalen die balanceringsenergie- en capaciteitseisen echter met respectievelijk 19% en 32%.

- **Aangepaste 'energy-only' markten (EOM's) met prijsgevoelige vraag en zonder prijslimieten helpen bij het waarborgen van leveringszekerheid, lagere systeemkosten en efficiënte elektriciteitsprijzen.** Hoofdstukken 4 en 5 laten zien

dat een flexibele en prijsgevoelige vraag een belangrijke rol kan spelen in de ondersteuning van een kosteneffectief en betrouwbaar elektriciteitssysteem. Dit komt door minder behoefte aan piekproductiecapaciteit, en de mogelijkheid om vraag te verschuiven of af te schakelen tijdens momenten van schaarste.

- **Capaciteitsmechanismen geven mogelijk onvoldoende prikkels voor marktpartijen om in regelbare capaciteit te investeren.** Hoofdstuk 5 laat zien dat zelfs in de aanwezigheid van een capaciteitsmarkt maar enkele technologieën hun investeringskosten op de lange termijn kunnen terugverdienen. Zelfs zon-PV-panelen en windturbines verdienen hun investeringskosten in de meeste gevallen niet terug. Terwijl capaciteitsmarkten extra inkomsten leveren aan mid-merit en piekeenheden (en tot winstgevendheid in bepaalde jaren leiden) is winstgevendheid op de lange termijn niet gegarandeerd. Bovendien leveren volatiele capaciteitsprijzen (gemiddelde waarde van 70 € MW^{-1} maar met een bereik van 0 € MW^{-1} tot 250 € MW^{-1}) niet de stabiele inkomsten op die marktpartijen nodig hebben om te investeren.

Op basis van de bevindingen in dit proefschrift en de gedetailleerde antwoorden op de deelvragen, wordt de **kernonderzoeksvraag** bondig beantwoord:

Een strategie gericht op een **technologiedivers** opwekportfolio zou:

- net zo betrouwbaar zijn als het huidige systeem;
- netto-nul of zelfs netto-negatieve CO_2-emissies kunnen leveren (afhankelijk van de inzet van NET's);
- minder kosten dan een 100% RES of NET-gedomineerde strategie;
- de ontwikkeling van CCS voor inzet met aardgas en biomassa vereisen,
- van het in bedrijf houden van bestaande kolencentrales profiteren, zodat deze met biomassa gestookt en naar omgezet CCS kunnen worden;
- van het doordraaien van bestaande kerncentrales profiteren, met daarnaast de mogelijkheid om nieuwe nucleaire capaciteit te bouwen; en
- markthervormingen nodig hebben om NET's te vergoeden voor negatieve emissies (indien NET's ingezet zouden worden).

Een strategie gericht op een elektriciteitssysteem op **basis van 100% RES** zou:

- net zo betrouwbaar zijn als het huidige systeem, mits voldoende stuurbare capaciteit beschikbaar is;
- netto-nul CO_2-emissies leveren;
- last hebben van 'climate lock-in', in het geval dat netto-negatieve CO_2-emissies van de elektriciteitssector vereist zijn (die zonder CCS niet met 100% RES elektriciteitssector bereikt kunnen worden);
- duurder zijn dan een meer divers portfolio met andere koolstofarme technologieën (bijv. nucleair, CCS, NET's);

- grootschalige investeringen in het Europese transportnet vereisen;
- aanzienlijk afhankelijk zijn van biomassa, bij afwezigheid van kosteneffectieve seizoensopslag; en
- een groot land- en zeegebied vereisen voor de inzet van zon- en windcapaciteit.

Een strategie gericht op **grootschalige inzet van NET's** in het elektriciteitssysteem zou:

- veel negatieve koolstofemissies opleveren die de uitstoot van CO_2 in andere sectoren of landen kunnen compenseren;
- tot zeer hoge kosten leiden, afhankelijk van de hoeveelheid en kosten van ingezette DAC;
- de (verdere) ontwikkeling van CCS vereisen om de inzet van BECCS en DAC mogelijk te maken;
- aanzienlijk afhankelijk zijn van biomassa voor BECCS;
- markthervormingen nodig hebben om NET's te vergoeden voor negatieve emissies; en
- aanzienlijke opslag van CO_2 vereisen.

Alle drie de strategieën zouden:

- van markthervormingen profiteren die marktprijsplafonds (ook impliciete) elimineren en een prijsgevoeligere vraag ontwikkelen;
- van liquide intradaymarkten profiteren om de integratie van vRES te ondersteunen, balanceringseisen en balanceringskosten te verminderen;
- van de Europese marktintegratie profiteren zodat productiecapaciteit tussen landen gedeeld kan worden, waardoor balanceringseisen en totale kosten worden verminderd; en
- afhankelijk zijn van de maatschappelijke aanvaarding van de doorgevoerde technologieën en markthervormingen.

Gezien de gevolgen van alle drie de strategieën, lijkt het erop dat een meer **technologiediverse** strategie de beste kans heeft om elektriciteit te leveren aan Europese consumenten tegen de laagst mogelijke kosten en op een manier die consistent is met de ambitieuze klimaatdoelen in het Parijs-akkoord.

Footnotes to Chapter 6

[1] The likelihood is actually the percentile of the transient climate response to cumulative emissions of carbon, assessed by the IPCC Fifth Assessment Report to fall likely between 0.8–2.5°C/1000 PgC, considering a normal probability distribution (Rogelj et al., 2018).

[2] Aside from direct emissions, all generation technologies also result in indirect GHG emissions including supply-chain emissions from biomass production, or emissions from the production of PV panels. Preliminary calculations performed as part of Chapter 4 (see Appendix C) show that these indirect emissions could exceed 200 Mt CO_2 y^{-1} for a 100% RES European power system which would also need to be offset.

[3] Prices rarely (if ever) reach the level of the price cap in Europe's day-ahead markets. However, this may be due to *implicit* price caps present in the market. For example, if imbalance prices are too low, energy retailers will prefer to pay the imbalance price penalty rather than paying a higher price in the day-ahead market (EC, 2016a). Also, emergency interventions by TSOs in times of scarcity such as voltage reductions and emergency load shedding can suppress price signals (*ibid*.). Thus, these implicit price caps must also be removed as part of EOM reform.

[4] For example, in 2016, 9 countries (out of 28) experienced less than one hour of average total supply interruption (including mechanical failures in distribution and transmission networks, thus not just capacity shortfalls), 11 countries experienced fewer than two hours, and 7 countries experienced fewer than four hours (CEER, 2018).

[5] Thus, the term *price-responsive* is used to mean not only that customers adjust their demand in response to real-time prices, but also that demand is *price-proactive*. In fact, it would likely be more efficient to account for consumer price preferences earlier in the scheduling process (e.g. in the day-ahead market) rather than at real time in balancing markets, as this would give markets more time to find cheaper dispatch solutions which already account for consumer price preferences, rather than drawing on load resources in real-time at potentially higher cost.

[6] In most European countries, the energy cost represents less than 30% of the final electricity bill paid by retail customers. The majority comes from taxes and levies (40% on average, but up to 70% in Denmark) and fixed grid charges (typically 30%) (EC, 2019a). Thus, dynamic electricity pricing may only have a small effect on final electricity bills, and governments could support low-income earners with tax rebates.

[7] The carbon pay-back period is the period between initial harvest and the point in time were the overall carbon balance equals the carbon storage before initial harvest, taking into account carbon debt and avoided emissions from fossil fuels (Jonker et al., 2014).

[8] CCS technology also underpins blue hydrogen. This thesis considers that neither blue nor green hydrogen are likely to be cost-effective technologies for the power sector (see section 6.4.2). However, if the political decision is made to follow a hydrogen pathway in the power sector anyway, or if blue hydrogen is developed for industry, CCS would also be a necessary technology to kick-start the hydrogen economy (van Cappellen et al., 2018)

[9] Just giving some Dutch examples, the capacity density of the Magnum natural gas combined cycle plant is approximately 9000 MW km^{-2}, compared with ~9 MW km^{-2} for the Gemini offshore wind park, ~50 MW km^{-2} for the Noordoostpolder onshore wind park, and ~100 MW km^{-2} for the Delftzijl solar PV park.

[10] This cost is similar to other estimates from literature e.g. (van Cappellen et al., 2018) (Bruce et al., 2018).

[11] This means that for every MWh of electricity produced with vRES (or avoided curtailment) used for green hydrogen production and seasonal storage, only 0.5 MWh of electricity can be returned to the grid.

[12] 50 GW of cross-border transmission is already expected to come online in CWE and between neighbouring countries by 2040. The reduction in curtailment with transmission is evident from this thesis. In Chapter 3, curtailment in Europe with 50% vRES penetration falls from 200 TWh y^{-1} without transmission to 40 TWh y^{-1} in a copper-plate scenario. In Chapter 4, there is no vRES curtailment due to large-scale transmission (as well as extensive use of biomass and CSP). In Chapter 5, vRES curtailment in CWE reaches only 50 TWh in 2040 (4% of demand) even with 80% vRES penetration.

[13] Electrolysis plants could also conclude PPAs with solar PV and wind generators. However, the price would have to account not only for the LCOE, but also for the fact that solar and wind providers would need to buy electricity from the market when not producing themselves.

[14] CSIRO give blue hydrogen cost estimates for Australia of 11.9 to 14.5 € GJ^{-1} with base case (2018) assumptions, and 9.9 to 12.1 € GJ^{-1} with best case assumptions (i.e. lower CAPEX, higher operating hours, higher efficiency, economies of scale) (Bruce et al., 2018). For comparison, their green hydrogen cost estimates are 25.1 to 30.7 € GJ^{-1} (base case) and 13.1 to 16.3 € GJ^{-1} (best case) for alkaline electrolysis, and 31.9 to 39 € GJ^{-1} (base case) and 12 to 14.6 € GJ^{-1} (best case) for PEM electrolysis.

[15] Power system stability concerns several aspects of power system operation, typically classified as *rotor angle* stability, *frequency* stability, and *voltage* stability (Kundur, 2012). Rotor angle stability is the ability of the synchronous machines in the power system to remain in synchronism during normal operation and in response to a disturbance. Frequency stability is the ability of the power system to maintain system frequency within acceptable limits after a disturbance, and voltage stability is the ability of the power system to maintain voltages at acceptable levels at all buses under nominal conditions and in response to disturbances.

References

R

3TIER. (2010). *Development of Regional Wind Resource and Wind Plant Output Datasets. Subcontract Report NREL/SR-550-47676*. Golden, Colerado: National Renewable Energy Laboratory. Retrieved from https://www.nrel.gov/docs/fy10osti/47676.pdf

4C Offshore. (2016). Global Offshore Wind Farms Database. Retrieved 29 November 2016, from http://www.4coffshore.com/offshorewind/

Aalborg University. (2017). Mesap PlaNet. Retrieved 25 April 2017, from http://www.energyplan.eu/othertools/national/mesap-planet/

Abdelhaq, A. S. M. (2012). *Potential in Systematically Placing a High Capacity of PV and Wind Sources in Germany*. (MSc Thesis, Cairo University & University of Kassel). Retrieved from https://www.uni-kassel.de/eecs/fileadmin/datas/fb16/remena/theses/batch2/MasterThesis_Arabi_Abdelhaq.pdf

ACER. (2015). *Report on unit investment cost indicators and corresponding reference values for electricity and gas infrastructure (Electricity infrastructure, Version 1.1)*. Agency for the Cooperation of Energy Regulators. Retrieved from http://www.acer.europa.eu/Official_documents/Acts_of_the_Agency/Publication/UIC Report - Electricity infrastructure.pdf

ACER, & CEER. (2018). *ACER/CEER Annual Report on the Results of Monitoring the Internal Electricity and Natural Gas Markets in 2017: Electricity Wholesale Markets Volume*. Agency for the Cooperation of Energy Regulators, Council of European Energy Regulators. Retrieved from https://acer.europa.eu/Official_documents/Acts_of_the_Agency/Publication/MMR 2017 - ELECTRICITY.pdf

ACER, & CEER. (2019). *ACER/CEER Annual Report on the Results of Monitoring the Internal Electricity and Natural Gas Markets in 2018: Electricity wholesale markets volume*. Brussels: Agency for the Cooperation of Energy Regulators, Council of European Energy Regulators. Retrieved from https://www.acer.europa.eu/Official_documents/Acts_of_the_Agency/Publication/ACER Market Monitoring Report 2018 - Electricity Wholesale Markets Volume.pdf

ACIL Allen Consulting. (2014). *Report to Australian Energy Market Operator: Fuel and Technology Cost Review*. ACIL Allen Consulting. Retrieved from http://www.aemo.com.au/Electricity/Planning/Related-Information/Planning-Assumptions

ADEME. (2015). *Vers un mix électrique 100% renouvelable en 2050*. Angers: ADEME. Retrieved from https://www.actu-environnement.com/media/pdf/rapport100pourcentsENR_comite.pdf

AEBIOM. (2009). *A Biogas Road Map for Europe*. Brussels: European Biomass Association. Retrieved from https://www.4biomass.eu/document/news/AEBIOM_Biogas_Roadmap.pdf

AECOM Australia. (2016). *Co-location Investigation: A study into the potential for co-locating wind and solar farms in Australia*. Sydney: AECOM Australia. Retrieved from http://www.aecom.com/au/wp-content/uploads/2016/03/Wind-solar-Co-location-Study-Final.pdf

AEMO. (2017). National Transmission Network Development Plan (NTNDP) database. Retrieved 14 September 2017, from http://www.aemo.com.au/Electricity/National-Electricity-Market-NEM/Planning-and-forecasting/National-Transmission-Network-Development-Plan/NTNDP-database

Aidt, M. (2019). Climate Emergency Declaration - Call to declare a climate emergency. Retrieved 8 October 2019, from https://climateemergencydeclaration.org/

Aigner, T., Jaehnert, S., Doorman, G. L., & Gjengedal, T. (2012). The effect of large-scale wind power on system balancing in Northern Europe. *IEEE Transactions on Sustainable Energy*, *3*(4), 751–759. doi:10.1109/TSTE.2012.2203157

Alakoski, E., Jämsén, M., Agar, D., Tampio, E., & Wihersaari, M. (2016). From wood pellets to wood chips, risks of degradation and emissions from the storage of woody biomass - A short review. *Renewable and Sustainable Energy Reviews*, *54*, 376–383. doi:10.1016/j.rser.2015.10.021

Alam, M. J. E., Muttaqi, K. M., & Sutanto, D. (2013). Mitigation of Rooftop Solar PV Impacts and Evening Peak Support by Managing Available Capacity of Distributed Energy Storage Systems. *IEEE Transactions on Power Systems*, *28*(4), 3874–3884. doi:10.1109/TPWRS.2013.2259269

Albadi, M. H., & El-Saadany, E. F. (2010). Overview of wind power intermittency impacts on power systems. *Electric Power Systems Research*, *80*(6), 627–632. doi:10.1016/j.epsr.2009.10.035

Allen, M., Babiker, M., Chen, Y., de Coninck, H., Connors, S., van Diemen, R., … Zickfeld, K. (2018). Summary for Policymakers. In *Global Warming of 1.5°C. An IPCC Special Report on the impacts of global warming of 1.5°C above pre-industrial levels and related global greenhouse gas emission pathways, in the context of strengthening the global response to the threat of climate change,*. WMO, UNEP. Retrieved from http://report.ipcc.ch/sr15/pdf/sr15_spm_final.pdf

Alliss, R., Link, R., Apling, D., Mason, M., & Kiley, H. (2011). *Introducing the Renewable Energy Network Optimization Tool (ReNOT): Part I*. In *Second Conference on Weather, Climate, and the New Energy Economy, January 22-27 2011*. Seattle. Retrieved from https://ams.confex.com/ams/91Annual/webprogram/Paper178275.html

Amelin, M. (2009). Comparison of capacity credit calculation methods for conventional power plants and wind power. *IEEE Transactions on Power Systems*, *24*(2), 685–691. doi:10.1109/TPWRS.2009.2016493

Anderson, K., & Broderick, J. (2017). *Natural gas and climate change*. Retrieved from https://www.foeeurope.org/sites/default/files/extractive_industries/2017/natural_gas_and_climate_change_anderson_broderick_october2017.pdf

Anderson, K., & Peters, G. (2016). The trouble with negative emissions. *Science*, *354*(6309), 182–183. doi:10.1126/science.aah4567

Ardelean, M., & Minnebo, P. (2015). *HVDC Submarine Power Cables in the World. EUR 27527 EN*. Luxembourg: European Commission Joint Research Centre. https://doi.org/10.2790/023689

Argus. (2018). *Argus Biomass Markets: Weekly biomass markets news and analysis. Issue 18-5 | Wednesday 31 January 2018*. Retrieved from http://www.argusmedia.com/~/media/Files/PDFs/Samples/Argus-Biomass.pdf?la=en

Arrhenius, S. (1896). On the influence of carbonic acid in the air upon the temperature of the ground. *Philosophical Magazine and Journal of Science Series*, *41*(5), 237–276.

AWS TrueWind LLC. (2005). *An Analysis of the Impacts of Large-Scale Wind Generation on the Ontario Electricity System*. Albany: Canadian Wind Energy Association. Retrieved from http://www.ontla.on.ca/library/repository/mon/15000/267559.pdf

Barthelmie, R. J., Grisogono, B., & Pryor, S. C. (1996). Observations and simulations of diurnal cycles of near-surface wind speeds over land and sea. *Journal of Geophysical Research*, *101*(D16), 21327–21377.

Barton, J., Huang, S., Infield, D., Leach, M., Ogunkunle, D., Torriti, J., & Thomson, M. (2013). The evolution of electricity demand and the role for demand side participation, in buildings and transport. *Energy Policy*, *52*, 85–102. doi:10.1016/j.enpol.2012.08.040

Bassi, S., Boyd, R., Buckle, S., Fennell, P., Mac Dowell, N., Makuch, Z., & Staffell, I. (2015). *Bridging the gap: improving the economic and policy framework for carbon capture and storage in the European Union*. London: Centre for Climate Change Economics and Policy, Grantham Research Institute on Climate Change and the Environment, Grantham Institute for Climate Change. Retrieved from http://www.lse.ac.uk/GranthamInstitute/publication/bridging-the-gap-improving-the-economic-and-policy-framework-for-carbon-capture-and-storage-in-the-european-union/

Batel, S., Devine-Wright, P., & Tangeland, T. (2013). Social acceptance of low carbon energy and associated infrastructures: A critical discussion. *Energy Policy*, *58*, 1–5. doi:10.1016/j.enpol.2013.03.018

Bauer, F., Hulteberg, C., Persson, T., & Tamm, D. (2013). *Biogas upgrading – Review of commercial technologies*. Malmo: Swedish Gas Technology Centre. Retrieved from http://vav.griffel.net/filer/C_SGC2013-270.pdf

BBC. (2017, July 3). Hinkley Point: EDF adds £1.5bn to nuclear plant cost (3 July 2017). *BBC News*. Retrieved from http://www.bbc.com/news/business-40479053

Becker, S., Frew, B. A., Andresen, G. B., Zeyer, T., Schramm, S., Greiner, M., & Jacobson, M. Z. (2014). Features of a fully renewable US electricity system: Optimized mixes of wind and solar PV and transmission grid extensions. *Energy*, *72*, 443–458. doi:10.1016/j.energy.2014.05.067

Beranová, R., & Kyselý, J. (2013). Relationships between the North Atlantic Oscillation index and temperatures in Europe in global climate models. *Studia Geophysica et Geodaetica*, *57*(1), 138–153. doi:10.1007/s11200-012-0824-0

Bertsch, J., Growitsch, C., Lorenczik, S., & Nagl, S. (2012). *Flexibility options in European electricity markets in high RES-E scenarios*. Cologne: Institute of Energy Economics at the University of Cologne. Retrieved from http://www.ewi.uni-koeln.de/fileadmin/user_upload/Publikationen/Studien/Politik_und_Gesellschaft/2012/Flexibility_options_in_the_European_electricity_markets.pdf

Bhagwat, P. C., Richstein, J. C., Chappin, E. J. L., Iychettira, K. K., & De Vries, L. J. (2017). Cross-border effects of capacity mechanisms in interconnected power systems. *Utilities Policy*, *46*, 33–47. doi:10.1016/j.jup.2017.03.005

Biggar, D. R., & Hesamzadeh, M. R. (2014). *The Economics of Electricity Markets*. Chichester, UK: IEEE Press, John Wiley & Sons Ltd.

Billimoria, F., & Poudineh, R. (2018). *Decarbonized market design*. Oxford, United Kingdom: The Oxford Institute for Energy Studies. https://doi.org/10.26889/9781784671198

Black & Veatch. (2012). *Cost and Performance data for Power Generation Technologies*. Retrieved from https://www.bv.com/docs/reports-studies/nrel-cost-report.pdf

Bles, M., Afman, M., Benner, J., Blom, M., Croezen, H., Rooijers, F., & Schepers, B. (2011). *Nuclear energy : The difference between costs and prices*. CE Delft. Retrieved from http://assets.wnf.nl/downloads/report_nuclearenergy_wnf_nov2011.pdf

BMWi. (2018). *The energy of the future - Sixth Energy Transition Monitoring Report: Reporting year 2016*. Berlin: BMWi. Retrieved from https://www.bmwi.de/Redaktion/EN/Publikationen/Energie/sechster-monitoring-bericht-zur-energiewende-langfassung.pdf?__blob=publicationFile&v=6

Bobenhausen, W. (1994). *Simplified Design of HVAC Systems*. New York: John Wiley & Sons, Inc.

Boilley, A., & Wald, L. (2015). Comparison between meteorological re-analyses from ERA-Interim and MERRA and measurements of daily solar irradiation at surface. *Renewable Energy*, *75*, 135–143. doi:10.1016/j.renene.2014.09.042

Bojanowski, J. S., Vrieling, A., & Skidmore, A. K. (2014). A comparison of data sources for creating a long-term time series of daily gridded solar radiation for Europe. *Solar Energy*, *99*(January), 152–171. doi:10.1016/j.solener.2013.11.007

Bollerslev, T. (1986). Generalized autoregressive conditional heteroskedasticity. *Journal of Econometrics*, *31*, 302–327.

Boone, A. (2005). *Simulation of Short-term Wind Speed Forecast Errors using a Multi-variate ARMA(1,1) time-series model*. (MSc Thesis, KTH Royal Institute of Technology). Retrieved from http://citeseerx.ist.psu.edu/viewdoc/download;jsessionid=667802053765A31201B5A88FCA6DF78E?doi=10.1.1.65.6073&rep=rep1&type=pdf

Borne, O., Korte, K., Perez, Y., Petit, M., & Purkus, A. (2018). Barriers to entry in frequency-regulation services markets: Review of the status quo and options for improvements. *Renewable and Sustainable Energy Reviews*, *81*(July 2016), 605–614. doi:10.1016/j.rser.2017.08.052

Brijs, T., De Jonghe, C., Hobbs, B. F., & Belmans, R. (2017). Interactions between the design of short-term electricity markets in the CWE region and power system flexibility. *Applied Energy*, *195*, 36–51. doi:10.1016/j.apenergy.2017.03.026

Brinkel, N. (2018). *A balancing act: developments in Dutch and German balancing markets and the impact of variable renewable generation*. (Internship Report, Utrecht University). Retrieved from https://dspace.library.uu.nl/handle/1874/371107

Brinkerink, M., Deane, P., Collins, S., & Gallachóir, B. Ó. (2018). Developing a global interconnected power system model. *Global Energy Interconnection*, *1*(4), 330–343. doi:10.14171/j.2096-5117.gei.2018.03.004

British Oceanographic Data Centre. (2015). General Bathymetric Chart of the Oceans (GEBCO), 2014 Grid. Retrieved 26

May 2016, from http://www.gebco.net/data_and_products/gridded_bathymetry_data/

Brouwer, A. S., van den Broek, M., Özdemir, Ö., Koutstaal, P., & Faaij, A. (2016). Business case uncertainty of power plants in future energy systems with wind power. *Energy Policy*, *89*, 237–256. doi:10.1016/j.enpol.2015.11.022

Brouwer, A. S., Van Den Broek, M., Seebregts, A., & Faaij, A. (2014). Impacts of large-scale Intermittent Renewable Energy Sources on electricity systems, and how these can be modeled. *Renewable and Sustainable Energy Reviews*, *33*(MAY), 443–466. doi:10.1016/j.rser.2014.01.076

Brouwer, A. S., van den Broek, M., Seebregts, A., Faaij, A., Broek, M. van den, Seebregts, A., & Faaij, A. (2015). Operational flexibility and economics of power plants in future low-carbon power systems. *Applied Energy*, *156*, 107–128. doi:10.1016/j.apenergy.2015.06.065

Brouwer, A. S., Van den Broek, M., Zappa, W., Turkenburg, W. C. W. C., & Faaij, A. (2016). Least-cost options for integrating intermittent renewables in low-carbon power systems. *Applied Energy*, *161*, 48–74. doi:10.1016/j.apenergy.2015.09.090

Brown, T. W., Bischof-Niemz, T., Blok, K., Breyer, C., Lund, H., & Mathiesen, B. V. (2018). Response to 'Burden of proof: A comprehensive review of the feasibility of 100% renewable-electricity systems'. *Renewable and Sustainable Energy Reviews*, *92*, 834–847. doi:10.1016/j.rser.2018.04.113

Bruce, S., Temminghoff, M., Hayward, J., Schmidt, E., Munnings, C., Palfreyman, D., & Hartley, P. (2018). *National Hydrogen Roadmap*. AUstralia: CSIRO. Retrieved from https://www.csiro.au/en/Do-business/Futures/Reports/Hydrogen-Roadmap

Bruckner, T., Bashmakov, I. A., Mulugetta, Y., Chum, H., de la Vega Navarro, A., Edmonds, J., … Zhang, X. (2014). *Energy Systems*. (O. Edenhofer, R. Pichs-Madruga, Y. Sokona, E. Farahani, S. Kadner, K. Seyboth, … J. C. Minx, Eds.), *Climate Change 2014: Mitigation of Climate Change. Contribution of Working Group III to the Fifth Assessment Report of the Intergovernmental Panel on Climate Change*. Cambridge, United Kingdom and New York, NY, USA: Cambridge University Press. Retrieved from https://www.ipcc.ch/site/assets/uploads/2018/02/ipcc_wg3_ar5_chapter7.pdf

Bruninx, K., Orlic, D., Couckuyt, D., Grisey, N., Betraoui, B., Anderski, T., … Jankowski, R. (2015). *e-Highway 2050 Project: Deliverable 2.1 Data sets of scenarios for 2050*. Retrieved from http://www.e-highway2050.eu/fileadmin/documents/Results/D2_1_Data_sets_of_scenarios_for_2050_20072015.pdf

Bublitz, A., Keles, D., & Fichtner, W. (2017). An analysis of the decline of electricity spot prices in Europe: Who is to blame? *Energy Policy*, *107*(April), 323–336. doi:10.1016/j.enpol.2017.04.034

Bublitz, A., Keles, D., Zimmermann, F., Fraunholz, C., & Fichtner, W. (2018). *A survey on electricity market design: Insights from theory and real-world implementations of capacity remuneration mechanisms.Working Paper Series in Production and Energy, No. 27*. Karlsruhe: Karlsruhe Institute of Technology (KIT), Institute for Industrial Production (IIP). https://doi.org/http://dx.doi.org/10.5445/IR/1000080063

Bucksteeg, M., Spiecker, S., & Weber, C. (2017). *Impact of Coordinated Capacity Mechanisms on the European Power Market* (No. HEMF Working Paper No. 01/2017). Essen. Retrieved from http://hdl.handle.net/10419/162994

Budinis, S., Krevor, S., Dowell, N. Mac, Brandon, N., & Hawkes, A. (2018). An assessment of CCS costs, barriers and potential. *Energy Strategy Reviews*, *22*(May), 61–81. doi:10.1016/j.esr.2018.08.003

Budischak, C., Sewell, D., Thomson, H., MacH, L., Veron, D. E., & Kempton, W. (2013). Cost-minimized combinations of wind power, solar power and electrochemical storage, powering the grid up to 99.9% of the time. *Journal of Power Sources*, *225*, 60–74. doi:10.1016/j.jpowsour.2012.09.054

Bui, M., Fajardy, M., & Mac Dowell, N. (2017). Bio-Energy with CCS (BECCS) performance evaluation: Efficiency enhancement and emissions reduction. *Applied Energy*, *195*, 289–302. doi:10.1016/j.apenergy.2017.03.063

Bundesamt für Energie. (2017). Hydropower: Statistics of hydroelectric installations in Switzerland. Retrieved 31 July 2017, from http://www.bfe.admin.ch/themen/00490/00491/index.html?lang=en#

Bundesamt für kerntechnische Entsorgungssicherheit. (2018). Atomgesetz. Retrieved 18 August 2018, from https://www.bfe.bund.de/SharedDocs/Downloads/BfE/DE/rsh/1a-atomrecht/1A-3-AtG.html

Bundesnetzagentur. (2018). Power plant list. Retrieved 20 August 2018, from https://www.bundesnetzagentur.de/EN/Areas/Energy/Companies/SecurityOfSupply/GeneratingCapacity/PowerPlantList/PubliPowerPlantList_node.html

Buongiorno, J., Jurewicz, J., Golay, M., & Todreas, N. (2016). The Offshore Floating Nuclear Plant Concept. *Nuclear Technology*, *194*(1), 1–14. doi:10.13182/NT15-49

Bussar, C., Stöcker, P., Cai, Z., Moraes, L., Magnor, D., Wiernes, P., … Sauer, D. U. (2016). Large-scale integration of renewable energies and impact on storage demand in a European renewable power system of 2050-Sensitivity study. *Journal of Energy Storage*, *6*, 1–10. doi:10.1016/j.est.2016.02.004

Carrington, D. (2015, November 25). UK cancels pioneering £1bn carbon capture and storage competition. *The Guardian*. Retrieved from https://www.theguardian.com/environment/2015/nov/25/uk-cancels-pioneering-1bn-carbon-capture-and-storage-competition

Cassola, F., Burlando, M., Antonelli, M., & Ratto, C. F. (2008). Optimization of the regional spatial distribution of wind power plants to minimize the variability of wind energy input into power supply systems. *Journal of Applied Meteorology and Climatology*, *47*(12), 3099–3116. doi:10.1175/2008JAMC1886.1

CEER. (2017). *CEER Report on Power Losses*. Brussels: Council of European Energy Regulators. Retrieved from https://www.ceer.eu/documents/104400/-/-/09ecee88-e877-3305-6767-e75404637087

CEER. (2018). *CEER Benchmarking Report 6.1 on the Continuity of Electricity and Gas Supply*. Council of European Energy Regulators. Retrieved from https://www.ceer.eu/documents/104400/-/-/963153e6-2f42-78eb-22a4-06f1552dd34c

Chaves-Ávila, J. P., & Fernandes, C. (2015). The Spanish intraday market design: A successful solution to balance renewable generation? *Renewable Energy*, *74*, 422–432. doi:10.1016/j.renene.2014.08.017

Chen, J., & Rabiti, C. (2017). Synthetic wind speed scenarios generation for probabilistic analysis of hybrid energy systems. *Energy*, *120*, 507–517. doi:10.1016/j.energy.2016.11.103

Chen, W. H., Peng, J., & Bi, X. T. (2015). A state-of-the-art review of biomass torrefaction, densification and applications. *Renewable and Sustainable Energy Reviews*, *44*, 847–866. doi:10.1016/j.rser.2014.12.039

Child, M., Kemfert, C., Bogdanov, D., & Breyer, C. (2019). Flexible electricity generation, grid exchange and storage for the transition to a 100% renewable energy system in Europe. *Renewable Energy*, *139*, 80–101. doi:10.1016/j.renene.2019.02.077

Clack, C. T. M., Xie, Y., & Macdonald, A. E. (2014). Linear programming techniques for developing an optimal electrical system including high-voltage direct-current transmission and storage. *International Journal of Electrical Power and Energy Systems*, *68*, 103–114. doi:10.1016/j.ijepes.2014.12.049

Claus, S., de Hauwere, N., Vanhoorne, B., Souza Dias, F., Oset Garcia, P., Hernandez, F., & Mees, J. (2016). Exclusive Economic Zones Boundaries (EEZ) v8 - Marine Regions Database. Retrieved 10 May 2016, from http://www.marineregions.org/downloads.php

Clean Energy Wire. (2019). German commission proposes coal exit by 2038. Retrieved 20 March 2019, from https://www.cleanenergywire.org/factsheets/german-commission-proposes-coal-exit-2038

Climate Analytics. (2016). *Implications of the Paris Agreement for Coal Use in the Power Sector*. Berlin. Retrieved from http://climateanalytics.org/files/climateanalytics-coalreport_nov2016_1.pdf

Clò, S., Cataldi, A., & Zoppoli, P. (2015). The merit-order effect in the Italian power market: The impact of solar and wind generation on national wholesale electricity prices. *Energy Policy*, *77*, 79–88. doi:10.1016/j.enpol.2014.11.038

Cohen, J. J., Reichl, J., & Schmidthaler, M. (2014). Re-focussing research efforts on the public acceptance of energy infrastructure: A critical review. *Energy*, *76*, 4–9. doi:10.1016/j.energy.2013.12.056

Colombo, E. (2014). *Feasibility Study of Deep Water Power Cable Systems. Medgrid Project*. Paris: Medgrid Project. Retrieved from http://www.medreg-regulators.org/Portals/45/external_partner/medgrid/COLOMBO_Feasibilty_cable_2500m_V1.pdf

Commin, A. N., French, A. S., Marasco, M., Loxton, J., Gibb, S. W., & McClatchey, J. (2017). The influence of the North Atlantic Oscillation on diverse renewable generation in Scotland. *Applied Energy*, *205*(4), 855–867. doi:10.1016/j.apenergy.2017.08.126

Connolly, D., Lund, H., & Mathiesen, B. V. (2016). Smart Energy Europe: The technical and economic impact of one potential 100% renewable energy scenario for the European Union. *Renewable and Sustainable Energy Reviews*, *60*, 1634–1653. doi:10.1016/j.rser.2016.02.025

Connolly, D., Lund, H., Mathiesen, B. V., & Leahy, M. (2011). The first step towards a 100% renewable energy-system for Ireland. *Applied Energy*, *88*(2), 502–507. doi:10.1016/j.apenergy.2010.03.006

Couckuyt, D., Orlic, D., Bruninx, K., Zani, A., Leger, A.-C., & Grisey, N. (2015). *e-Highway 2050 Project: Deliverable 2.3 System simulations analysis and overlay-grid development*. Retrieved from http://cordis.europa.eu/project/rcn/106279_en.html

Cramton, P., & Ockenfels, A. (2012). Economics and Design of Capacity Markets for the Power Sector. *Zeitschrift Für Energiewirtschaft*, *36*(2), 113–134. doi:10.1007/s12398-012-0084-2

Cramton, P., Ockenfels, A., & Stoft, S. (2013). Capacity Market Fundamentals. *Economics of Energy & Environmental Policy*, *2*(2), 27–46. doi:10.5547/2160-5890.2.2.2

Creutzig, F., Ravindranath, N. H., Berndes, G., Bolwig, S., Bright, R., Cherubini, F., … Masera, O. (2015). Bioenergy and climate change mitigation: An assessment. *GCB Bioenergy*, *7*(5), 916–944. doi:10.1111/gcbb.12205

Cuff, M. (2016, January 12). Vattenfall starts work on UK hybrid wind and solar farm | Environment | The Guardian. *The Guardian*. Retrieved from https://www.theguardian.com/environment/2016/jan/12/vattenfall-starts-work-on-uk-hybrid-wind-and-solar-farm

D'haeseleer, W. (2013). *Synthesis on the Economics of Nuclear Energy*. Leuven: University of Leuven. Retrieved from https://www.mech.kuleuven.be/en/tme/research/energy_environment/Pdf/wpen2013-14.pdf

Daggash, H. A., Heuberger, C. F., & Mac Dowell, N. (2019). The role and value of negative emissions technologies in decarbonising the UK energy system. *International Journal of Greenhouse Gas Control*, *81*(July 2018), 181–198. doi:10.1016/j.ijggc.2018.12.019

Dai, H., Herran, D. S., Fujimori, S., & Masui, T. (2016). Key factors affecting long-term penetration of global onshore wind energy integrating top-down and bottom-up approaches. *Renewable Energy*, *85*, 19–30. doi:10.1016/j.renene.2015.05.060

Dalla Longa, F., Kober, T., Badger, J., Volker, P., Hoyer-Klick, C., Hidalgo, I., … Zucker, A. (2018). *Wind potentials for EU and neighbouring countries: Input datasets for the JRC-EU-TIMES Model, EUR 29083 EN*. Luxembourg. https://doi.org/10.2760/041705

Dallinger, B., Auer, H., & Lettner, G. (2018). Impact of harmonised common balancing capacity procurement in selected Central European electricity balancing markets. *Applied Energy*, *222*(March), 351–368. doi:10.1016/j.apenergy.2018.03.120

Davis, C., Chmieliauskas, A., Dijkema, G., & Nikolic, I. (2015). Enipedia: Power Plant Database. Retrieved 31 July 2017, from http://enipedia.tudelft.nl/wiki/Main_Page

de Maere D'aertrycke, G., Ehrenmann, A., Ralph, D., & Smeers, Y. (2018). Risk trading in capacity equilibrium models. On *EPRG Working Paper 1720, Cambridge Working Paper in Economics 1757* (EPRG Working Paper 1720, Cambridge Working Paper in Economics 1757). https://doi.org/10.17863/CAM.17552

de Mello, P. E., Lu, N., & Makarov, Y. (2011). An optimized autoregressive forecast error generator for wind and load uncertainty study. *Wind Energy*, *14*(8), 967–976. doi:10.1002/we.460

de Vos, K., Stevens, N., Devolder, O., Papavasiliou, A., Hebb, B., & Matthys-Donnadieu, J. (2019). Dynamic dimensioning approach for operating reserves: Proof of concept in Belgium. *Energy Policy*, *124*(October 2018), 272–285. doi:10.1016/j.enpol.2018.09.031

Deane, J. P., Drayton, G., & Ó Gallachóir, B. P. (2014). The impact of sub-hourly modelling in power systems with

significant levels of renewable generation. *Applied Energy*, *113*, 152–158. doi:10.1016/j.apenergy.2013.07.027

Deane, J. P., Gracceva, F., Chiodi, A., Gargiulo, M., & Gallachóir, B. P. Ó. (2015). Assessing power system security. A framework and a multi model approach. *International Journal of Electrical Power & Energy Systems*, *73*, 283–297. doi:10.1016/j.ijepes.2015.04.020

Dee, D. P., Uppala, S. M., Simmons, A. J., Berrisford, P., Poli, P., Kobayashi, S., … Vitart, F. (2011). The ERA-Interim reanalysis: Configuration and performance of the data assimilation system. *Quarterly Journal of the Royal Meteorological Society*, *137*(656), 553–597. doi:10.1002/qj.828

Dees, M., Elbersen, B., Fitzgerald, J., Vis, M., Anttila, P., Forsell, N., … Diepen, K. (2017). *A spatial data base on sustainable biomass cost-supply of lignocellulosic biomass in Europe - methods & data sources. Project Report S2BIOM.* Retrieved from http://www.s2biom.eu/images/Publications/D1.6_S2Biom_Spatial_data_methods_data_sources_Final_Final.pdf

Delbeke, J. (2019). Have 25 years of EU climate policy delivered? In J. Delbeke & P. Vis (Eds.), *Towards a climate-neutral Europe: Curbing the trend* (1st ed.). London: Routledge.

Deloitte. (2015). *European energy market reform. Country profile: France*. Retrieved from https://www2.deloitte.com/content/dam/Deloitte/fr/Documents/energie-et-ressources/Publications/deloitte_FR_Energy-market-reform-in Europe_mars-2015.pdf

Deng, Y., Haigh, M., Pouwels, W., Ramaekers, L., Brandsma, R., Schimschar, S., … de Jager, D. (2015). Quantifying a realistic, worldwide wind and solar electricity supply. *Global Environmental Change*, *31*, 239–252. doi:10.1016/j.gloenvcha.2015.01.005

Dent, C. J., Keane, A., & Bialek, J. W. (2010). Simplified methods for renewable generation capacity credit calculation: A critical review. *IEEE PES General Meeting*, 1–8. doi:10.1109/PES.2010.5589606

Detz, R. J., & van der Zwaan, B. (2019). Transitioning towards negative CO2 emissions. *Energy Policy*, *133*(July), 110938. doi:10.1016/j.enpol.2019.110938

Díaz-González, F., Hau, M., Sumper, A., & Gomis-Bellmunt, O. (2014). Participation of wind power plants in system frequency control: Review of grid code requirements and control methods. *Renewable and Sustainable Energy Reviews*, *34*, 551–564. doi:10.1016/j.rser.2014.03.040

Dierauf, T., Growitz, A., Kurtz, S., Cruz, J. L. B., Riley, E., & Hansen, C. (2013). *Weather-Corrected Performance Ratio. NREL Technical Report NREL/TP-5200-57991*. Golden: National Renewable Energy Laboratory. Retrieved from http://www.nrel.gov/docs/fy14osti/60204.pdf

Dixon, J., Member, S., Morán, L., Rodríguez, J., Member, S., & Domke, R. (2005). Reactive Power Compensation Technologies : State-of-the-Art Review, *93*(12).

DNV GL. (2014). *Integration of Renewable Energy in Europe*. Bonn: DNV GL. Retrieved from https://ec.europa.eu/energy/sites/ener/files/documents/201406_report_renewables_integration_europe.pdf

Donovan, C. W. (2015). *Renewable Energy Finance*. (C. W. Donovan, Ed.), *Renewable Energy Finance - Powering the Future*. IMPERIAL COLLEGE PRESS. doi:10.1142/p1030

Doorman, G. L., & van Der Veen, R. (2013). An analysis of design options for markets for cross-border balancing of electricity. *Utilities Policy*, *27*(January 2011), 39–48. doi:10.1016/j.jup.2013.09.004

Doquet, M., Fourment, C., & Roudergues, J. (2011). *Generation & transmission adequacy of large interconnected power systems: A contribution to the renewal of Monte-Carlo approaches*. In *2011 IEEE Trondheim PowerTech* (pp. 1–6). Trondheim: IEEE. doi:10.1109/PTC.2011.6019444

Doukas, H., Karakosta, C., Flamos, A., & Psarras, J. (2011). Electric power transmission: An overview of associated burdens. *International Journal of Energy Research*, *35*(11), 979–988. doi:10.1002/er.1745

Drake, B., & Hubacek, K. (2007). What to expect from a greater geographic dispersion of wind farms?-A risk portfolio approach. *Energy Policy*, *35*(8), 3999–4008. doi:10.1016/j.enpol.2007.01.026

Drax. (2018). Drax moves closer to coal-free future with unit four conversion. Retrieved 6 September 2018, from https://www.drax.com/press_release/drax-moves-closer-coal-free-future-unit-four-conversion/

Dreidy, M., Mokhlis, H., & Mekhilef, S. (2017). Inertia response and frequency control techniques for renewable energy sources: A review. *Renewable and Sustainable Energy Reviews*, *69*(July 2016), 144–155. doi:10.1016/j.rser.2016.11.170

Duffie, J. A., & Beckman, W. A. (2013). *Solar Engineering of Thermal Processes* (4th ed.). New Jersey: Wiley.

E3MLab. (2016). *PRIMES model version 6 (2016-2017): Detailed model description*. E3MLab, National Technical University of Athens. Retrieved from http://www.e3mlab.ntua.gr/e3mlab/PRIMES Manual/The PRIMES MODEL 2016-7.pdfItemid=80&lang=en

EASAC. (2013). *Carbon Capture and Storage in Europe. EASAC policy report 20*. Retrieved from https://www.easac.eu/fileadmin/Reports/Easac_13_CCS_Web_Complete.pdf

EASAC. (2018). *Negative emission technologies: What role in meeting Paris Agreement targets? EASAC Policy Report*. Halle: European Academies Science Advisory Council. Retrieved from https://easac.eu/fileadmin/PDF_s/reports_statements/Negative_Carbon/EASAC_Report_on_Negative_Emission_Technologies.pdf

EC. (n.d.). Energy Union and Climate | European Commission. Retrieved 22 February 2017, from https://ec.europa.eu/commission/priorities/energy-union-and-climate_en

EC. (2011a). *A Roadmap for moving to a competitive low carbon economy in 2050. COM(2011) 885*. Brussels: European Commission. https://doi.org/10.1002/jsc.572

EC. (2011b). *Commission Staff Working Paper: Impact Assessment accompanying the document Roadmap 2050*. Brussels: European Commission. Retrieved from https://ec.europa.eu/energy/sites/ener/files/documents/roadmap2050_ia_20120430_en_0.pdf

EC. (2011c). *Energy Roadmap 2050. COM(2011) 885*. Brussels: European Commission. Retrieved from https://ec.europa.eu/energy/en/topics/energy-strategy-and-energy-union/2050-energy-strategy

EC. (2011d). *Energy Roadmap 2050 Impact Assessment, Part 2/2: Accompanying the Document Energy Roadmap 2050. SEC(2011) 1565*. Brussels: European Commission. Retrieved from http://ec.europa.eu/energy/energy2020/roadmap/index_en.htm

EC. (2014a). *Benchmarking smart metering deployment in the EU-27 with a focus on electricity*. Brussels: European Commission. Retrieved from https://ses.jrc.ec.europa.eu/publications/reports/benchmarking-smart-metering-deployment-eu-27-focus-electricity

EC. (2014b). *Guide to Cost-benefit Analysis of Investment Projects: Economic appraisal tool for Cohesion Policy 2014-2020*. Brussels: European Commission. https://doi.org/10.2776/97516

EC. (2014c). *Identification of Appropriate Generation and System Adequacy Standards for the Internal Electricity Market*. Luxembourg: European Commission. https://doi.org/10.2832/089498

EC. (2014d). *Progress towards completing the Internal Energy Market. COM(2014) 634 final*. Brussels: European Commission. Retrieved from https://ec.europa.eu/energy/sites/ener/files/documents/2014_iem_communication_1.pdf

EC. (2015). *Launching the public consultation process on a new energy market design. SWD(2015) 142 final*. Brussels: European Commission. Retrieved from http://eur-lex.europa.eu/legal-content/EN/TXT/PDF/?uri=CELEX:52015DC0340&from=EN

EC. (2016a). *Commission staff working document accompanying the document 'Final Report of the Sector Inquiry on Capacity Mechanisms'. SWD(2016) 385*. Brussels: European Commission. Retrieved from http://ec.europa.eu/competition/sectors/energy/capacity_mechanism_swd_en.pdf

EC. (2016b). Energy modelling: EU Reference Scenario 2016. Retrieved 22 February 2017, from https://ec.europa.eu/energy/en/data-analysis/energy-modelling

EC. (2016c). *Final Report of the Sector Inquiry on Capacity Mechanisms*. Brussels: European Commission. Retrieved from http://ec.europa.eu/competition/sectors/energy/capacity_mechanisms_final_report_en.pdf

EC. (2017a). Commission regulation (EU) 2017/1485 of 2 August 2017 establishing a guideline on electricity transmission system operation. *Official Journal of the European Union*. Retrieved from http://eur-lex.europa.eu/legal-content/EN/TXT/PDF/?uri=CELEX:32017R1485&from=EN

EC. (2017b). Commission regulation (EU) 2017/2195 of 23 November 2017 establishing a guideline on electricity balancing. *Official Journal of the European Union*. Retrieved from https://eur-lex.europa.eu/legal-content/EN/TXT/?uri=uriserv:OJ.L_.2017.312.01.0006.01.ENG&toc=OJ:L:2017:312:TOC#d1e2376-6-1

EC. (2018a). *In-depth analysis in support of the Commission Communication COM (2018) 773 A Clean Planet for all: A European long-term strategic vision for a prosperous, modern, competitive and climate neutral economy*. Brussels: European Commission. Retrieved from https://ec.europa.eu/knowledge4policy/publication/communication-com2018773-clean-planet-all-european-strategic-long-term-vision-prosperous_en

EC. (2018b). *Quarterly report on European Gas Markets: Market Observatory for Energy* (Vol. 10). Brussels: European Commission. Retrieved from https://ec.europa.eu/energy/sites/ener/files/documents/quarterly_report_on_european_gas_markets_q4_2017_final_20180323.pdf

EC. (2019a). *Energy prices and costs in Europe*. Brussels: European Commission. Retrieved from https://www.enerdata.net/about-us/company-news/energy-prices-and-costs-in-europe.pdf

EC. (2019b). *Quarterly report on European electricity markets (Q2 2019)* (Vol. 12). Brussels: European Commission. Retrieved from https://ec.europa.eu/energy/sites/ener/files/quarterly_report_on_european_electricity_markets_q1_2019_final.pdf

EC. (2020). EU Emissions Trading System (EU ETS): Market Stability Reserve. Retrieved 10 March 2020, from https://ec.europa.eu/clima/policies/ets/reform_en

ECF. (2010a). *Roadmap 2050: a practical guide to a prosperous, low-carbon Europe. Policy Recommendations*. Brussels: European Climate Foundation. Retrieved from http://www.roadmap2050.eu/project/roadmap-2050

ECF. (2010b). *Roadmap 2050: a practical guide to a prosperous, low-carbon Europe. Technical Analysis*. Brussels. Retrieved from http://www.roadmap2050.eu/project/roadmap-2050

ECMWF. (n.d.). Reanalysis datasets: ERA-Interim. Retrieved 26 May 2016, from http://www.ecmwf.int/en/research/climate-reanalysis/era-interim

ECN. (2016). *Eindadvies basisbedragen SDE+ 2017*. (S. M. Lensink & J. W. Cleijne, Eds.). Petten: Energy Research Centre of the Netherlands. Retrieved from https://www.ecn.nl/publicaties/ECN-E--16-040

ECN. (2017). *Final advice on base rates SDE+ 2017*. (S. Lensink & J. Cleijne, Eds.). Petten: Energy Research Centre of the Netherlands. Retrieved from https://www.ecn.nl/collaboration/sde/sde-2017/

Economic Consulting Associates. (2015). *European Electricity Forward Markets and Hedging Products – State of Play and Elements for Monitoring Final Report*. London. Retrieved from http://www.acer.europa.eu/en/electricity/market monitoring/documents_public/eca report on european electricity forward markets.pdf

Ecorys. (2017). *Investments in a renewables-only market*. Rotterdam: Ecorys. Retrieved from http://www.ecorys.nl/news/ecorys-onderzoekt-marktmodel-een-volledig-duurzame-elektriciteitsmarkt

EDF. (2018). *Le parc nucleaire en exploitation en France: exploitation, maintenance et grand carénage. Atelier « filière nucléaire » Le 11 janvier 2018*. Retrieved from https://ppe.debatpublic.fr/sites/debat.ppe/files/documents/edf_presentation-_parc_en_exploitation.pdf

EDF. (2019). List of Outages | EDF France. Retrieved 24 June 2019, from https://www.edf.fr/en/the-edf-group/who-we-are/activities/optimisation-and-trading/list-of-outages-and-messages/list-of-outages

EEA. (2009). *Europe's onshore and offshore wind energy potential. Technical report No 6/2009*. Copenhagen. https://doi.org/10.2800/11373

EEA. (2016a). CORINE Land Cover Inventory 2012 (CLC 2012) — Copernicus Land Monitoring Services. Retrieved 10 May 2016, from http://land.copernicus.eu/pan-european/corine-land-cover/clc-2012/view

EEA. (2016b). Nationally designated areas (CDDA). Retrieved 10 May 2016, from http://www.eea.europa.eu/data-and-maps/data/nationally-designated-areas-national-cdda-10#tab-gis-data

EEA. (2016c). Overview of electricity production and use in Europe. Retrieved 20 July 2017, from https://www.eea.europa.eu/data-and-maps/indicators/overview-of-the-electricity-production-2/assessment

EEA. (2019). The EU Emissions Trading System in 2019: trends and projections. Retrieved 7 March 2020, from https://www.eea.europa.eu/themes/climate/trends-and-projections-in-europe/trends-and-projections-in-europe-2019/the-eu-emissions-trading-system

Ehrenmann, A., Henneaux, P., Bruce, J., & Schumacher, L. (2019). *The future electricity intraday market design*. Luxembourg: Publications Office of the European Union,. https://doi.org/10.2833/004191

Ela, E., Milligan, M., & Kirby, B. (2011). *Operating Reserves and Variable Generation*. *Technical Report NREL/TP-5500-51978*. Golden: National Renewable Energy Laboratory. https://doi.org/10.2172/1023095

Elia. (2018). Generating facilities. Retrieved 20 August 2018, from http://www.elia.be/en/grid-data/power-generation/generating-facilities

Elia. (2019a). Balancing: Capacity - Auction results. Retrieved 13 October 2019, from https://www.elia.be/en/grid-data/balancing/capacity-auction-results

Elia. (2019b). Elia: Transparency on Grid Data. Retrieved 19 September 2019, from https://www.elia.be/en/grid-data/

Elliston, B., MacGill, I., & Diesendorf, M. (2014). Comparing least cost scenarios for 100% renewable electricity with low emission fossil fuel scenarios in the Australian National Electricity Market. *Renewable Energy*, *66*. doi:10.1016/j.renene.2013.12.010

Energy Exemplar. (2015). *PLEXOS 7.2 Guide*. Energy Exemplar. Retrieved from https://energyexemplar.com/

Energy Numbers. (2016). UK offshore wind capacity factors. Retrieved 30 August 2016, from http://energynumbers.info/uk-offshore-wind-capacity-factors

Engle, R. F. (1982). Autoregressive Conditional Heteroscedasticity with Estimates of the Variance of United Kingdom Inflation. *Econometrica*, *50*(4), 987. doi:10.2307/1912773

Ensslin, C., Milligan, M., Holttinen, H., O'Malley, M., & Keane, A. (2008). *Current methods to calculate capacity credit of wind power, IEA collaboration*. In *2008 IEEE Power and Energy Society General Meeting - Conversion and Delivery of Electrical Energy in the 21st Century* (Vol. 1, pp. 1–3). Pittsburgh: IEEE. doi:10.1109/PES.2008.4596006

ENTSO-E. (2012). *Scenario outlook and adequacy forecast 2011-2025*. Brussels: European Network of Transmission System Operators for Electricity. Retrieved from https://www.entsoe.eu/fileadmin/user_upload/_library/SDC/SOAF/ENTSOE_SO_AF_2011-2025.pdf

ENTSO-E. (2015a). *Statistical Factsheet 2015*. Brussels: European Network of Transmission System Operators for Electricity. Retrieved from https://www.entsoe.eu/Documents/Publications/Statistics/Factsheet/entsoe_sfs2015_web.pdf

ENTSO-E. (2015b). *TYNDP 2016 Scenario Development Report - for public consultation*. Brussels: European Network of Transmission System Operators for Electricity. Retrieved from https://www.entsoe.eu/Documents/TYNDP documents/TYNDP 2016/150521_TYNDP2016_Scenario_Development_Report_for_consultationv2.pdf

ENTSO-E. (2016a). Hourly load values for all countries for a specific month (in MW). Retrieved 26 May 2016, from https://www.entsoe.eu/db-query/consumption/mhlv-all-countries-for-a-specific-month

ENTSO-E. (2016b). *Mid-Term Adequacy Forecast: Edition 2016*. Brussels: European Network of Transmission System

Operators for Electricity. Retrieved from https://www.entsoe.eu/Documents/SDC documents/MAF/ENSTOE_MAF_2016.pdf

ENTSO-E. (2016c). *Ten-Year Network Development Plan 2016 Edition: Executive Report*. Brussels: European Network of Transmission System Operators for Electricity. Retrieved from http://tyndp.entsoe.eu/

ENTSO-E. (2016d). Ten Year Network Development Plan 2016. Retrieved 16 August 2017, from http://tyndp.entsoe.eu/

ENTSO-E. (2017a). *2017/2018 winter outlook, summer review 2017*. Brussels: European Network of Transmission System Operators for Electricity. Retrieved from https://www.entsoe.eu/Documents/Publications/SDC/Winter_Outlook_2017-18.pdf

ENTSO-E. (2017b). ENTSO-E Transparency Platform. Retrieved 28 August 2015, from https://transparency.entsoe.eu/

ENTSO-E. (2017c). *Explanatory document for the Nordic synchronous area proposal for ramping restrictions for active power output in accordance with Article 137 (3) and (4) of the Commission Regulation (EU) 2017 / 1485 of 2 August 2017 establishing a guideline on elec*. European Network of Transmission System Operators for Electricity. Retrieved from https://consultations.entsoe.eu/markets/nordic-tsos-proposals-for-frr-and-frce-and-frequen/supporting_documents/8. Explanatory document for ramping restrictions for active power output.pdf

ENTSO-E. (2017d). *Mid-term Adequacy Forecast: 2017 edition*. European Network of Transmission System Operators for Electricity. Retrieved from https://www.entsoe.eu/outlooks/maf/Pages/default.aspx

ENTSO-E. (2018a). *An overview of the european balancing market and electricity balancing guideline*. European Network of Transmission System Operators for Electricity. Retrieved from https://docstore.entsoe.eu/Documents/Network codes documents/NC EB/entso-e_balancing_in _europe_report_Nov2018_web.pdf

ENTSO-E. (2018b). ENTSO-E Transparency Platform. Retrieved 13 June 2018, from https://transparency.entsoe.eu/

ENTSO-E. (2018c). *Mid-term Adequacy Forecast 2018: Appendix 1: Methodology and Detailed Results*. Brussels: European Network of Transmission System Operators for Electricity. Retrieved from https://www.entsoe.eu/outlooks/maf/Pages/default.aspx

ENTSO-E. (2018d). *Nordic and Baltic HVDC Utilisation and Unavailability Statistics 2017*. Brussels: European Network of Transmission System Operators for Electricity. Retrieved from https://docstore.entsoe.eu/Documents/Publications/SOC/Nordic/Nordic-and-Blatic-HVDC-Disturbance-Statistics-2017.pdf

ENTSO-E. (2018e). *Statistical Factsheet 2017. Entso-E*. European Network of Transmission System Operators for Electricity. Retrieved from https://docstore.entsoe.eu/Documents/Publications/Statistics/Factsheet/entsoe_sfs_2017.pdf

ENTSO-E. (2018f). TYNDP 2018: Maps & Data. Retrieved 8 August 2018, from https://tyndp.entsoe.eu/maps-data/

ENTSO-E. (2018g). *Winter Outlook 2018/2019, Summer Review 2018*. European Network of Transmission System Operators for Electricity. Retrieved from https://docstore.entsoe.eu/Documents/SDC documents/Winter Outlook 2018-2019_Report(final).pdf

ENTSO-E. (2019a). Electricity Balancing. Retrieved 31 December 2019, from https://www.entsoe.eu/network_codes/eb/

ENTSO-E. (2019b). Power Statistics. Retrieved 8 November 2019, from https://www.entsoe.eu/data/power-stats/

ENTSO-E. (2019c). Statistics and Data. Retrieved 23 November 2019, from https://www.entsoe.eu/publications/statistics-and-data/#statistical-factsheet

ENTSO-E, & ENTSO-G. (2018). *TYNDP 2018: Scenario Report, Main Report*. Brussels: European Network of Transmission System Operators for Electricity. Retrieved from https://www.entsoe.eu/Documents/TYNDP documents/TYNDP2018/Scenario_Report_2018_Final.pdf?Web=1

EPA. (2018). National Electric Energy Data System (NEEDS) v6. Retrieved 5 May 2018, from https://www.epa.gov/airmarkets/national-electric-energy-data-system-needs-v6

EPEX. (2018a). Day-ahead auction in The Netherlands and Belgium. Retrieved 13 September 2018, from http://www.epexspot.com/en/product-info/auction/the_netherlands

EPEX. (2018b). *Trading on EPEX SPOT 2018*. Paris. Retrieved from https://www.epexspot.com/document/38579/Epex_TradingBrochure_180129_Web.pdf

EPEX. (2019a). *EPEX Spot Operational Rules - 18 September 2019*. Retrieved from http://www.epexspot.com/en/extras/download-center

EPEX. (2019b). EPEX SPOT SE: Annual Reports. Retrieved 23 November 2019, from https://www.epexspot.com/en/extras/download-center/annual_reports

Erbs, D. G., Klein, S. A., & Duffie, J. A. (1982). Estimation of the diffuse radiation fraction for hourly, daily and monthly-average global radiation. *Solar Energy*, *28*(4), 293–302. doi:10.1016/0038-092X(82)90302-4

EREC. (2010). *RE-thinking 2050: a 100% renewable energy vision for the European Union*. Brussels: EREC. Retrieved from https://www2.warwick.ac.uk/fac/soc/pais/research/researchcentres/csgr/green/foresight/energyenvironment/2010_erec_rethinkhing_2050.pdf

EREC, & Greenpeace. (2009). *Renewables 24/7 Infrastructure Needed to Save the Climate*. Greenpeace International. Retrieved from http://www.greenpeace.org/international/en/publications/reports/renewables-24-7/

Ernst, B., Schreier, U., Berster, F., Pease, J., Scholz, C., Erbring, H., … Malarov, Y. (2010). *Large-Scale Wind and Solar Integration in Germany*. Richland, Washington: Pacific Northwest National Laboratory. Retrieved from https://www.pnnl.gov/main/publications/external/technical_reports/PNNL-19225.pdf

Eroğlu, Y., & Seçkiner, S. U. (2013). Wind farm layout optimization using particle filtering approach. *Renewable Energy*, *58*, 95–107. doi:10.1016/j.renene.2013.02.019

ESRI. (2016). Basiskaarten | ArcGIS Content | Esri Nederland. Retrieved 25 April 2016, from http://www.esri.nl/producten/content/content/basiskaarten

ETI. (2015). *Offshore Wind Floating Wind Technology*. Loughborough: Energy Technologies Institute. Retrieved from https://s3-eu-west-1.amazonaws.com/assets.eti.co.uk/legacyUploads/2015/10/3505-Floating-Wind-Insights-Midres-AW.pdf

EU GeoCapacity Project. (2009). *EU GeoCapacity Project - Assessing European Capacity for Geological Storage of Carbon Dioxide: Publishable Final Activity Report*. Retrieved from https://ec.europa.eu/clima/sites/clima/files/docs/0028/geocapacity_en.pdf

Eurelectric. (2009). *Power Choices: Pathways to Carbon-Neutral Electricity in Europe by 2050*. Brussels: Eurelectric. Retrieved from http://www.eurelectric.org/media/45274/power__choices_finalcorrection_page70_feb2011-2010-402-0001-01-e.pdf

Eurelectric. (2013a). *Power Distribution in Europe Facts & Figures. D/2013/12.105/46*. Brussels. Retrieved from https://www3.eurelectric.org/media/113155/dso_report-web_final-2013-030-0764-01-e.pdf

Eurelectric. (2013b). *The financial situation of the Electricity Industry – Economic and financial update*. Brussels. Retrieved from http://www.elecpor.pt/pdf/12_06_2013_EURELECTRIC_fg_fe_paper__final.pdf

Eurelectric. (2018). *Decarbonisation pathways: Full study results*. Brussels. Retrieved from https://cdn.eurelectric.org/media/3558/decarbonisation-pathways-all-slideslinks-29112018-h-4484BB0C.pdf

EurObserv'ER. (2017). All Photovoltaic Barometers 2010 - 2017. Retrieved 5 October 2017, from https://www.eurobserv-er.org/category/all-photovoltaic-barometers/

EurObserv'ER. (2018). *Photovoltaic Barometer 2018*. Retrieved from https://www.eurobserv-er.org/pdf/photovoltaic-barometer-2018-en/

EurObserv'ER. (2019). *Wind Energy Barometer 2019*. Retrieved from https://www.eurobserv-er.org/wind-energy-barometer-2019/

Europe Beyond Coal. (2017). Overview: National coal phase-out announcements in Europe, Coal phase-out status December 2017. Retrieved 18 August 2018, from https://beyond-coal.eu/wp-content/uploads/2017/12/National-phase-out-overview-171219.pdf

European Parliament. (2001). Directive 2001/77/EC of the European Parliament and of the Council of 27 September 2001 on the promotion of electricity produced from renewable energy sources in the internal electricity market. *Official Journal of European Communities*, *L283*, 33–40.

European Parliament. (2009). Directive 2009/28/EC of the European Parliament and of the Council of 23 April 2009 on the promotion of the use of energy from renewable sources and amending and subsequently repealing Directives 2001/77/EC and 2003/30/EC. *Official Journal of the European Union*, *L140*, 16–62. doi:10.3000/17252555.L_2009.140.eng

European Parliament. (2018a). Directive (EU) 2018/2001 of the European Parliament and of the Council of 11 December 2018 on the promotion of the use of energy from renewable sources (recast). *Official Journal of the European Union*, *L328*, 82–208. Retrieved from https://eur-lex.europa.eu/legal-content/EN/TXT/PDF/?uri=CELEX:32018L2001&from=EN

European Parliament. (2018b). Directive (EU) 2018/410 of the European Parliament and of the Council of 14 March 2018 amending Directive 2003/87/EC to enhance cost-effective emission reductions and low-carbon investments, and Decision (EU) 2015/1814. *Official Journal of the European Union*, *L76*, 3–27. Retrieved from https://eur-lex.europa.eu/legal-content/EN/TXT/PDF/?uri=CELEX:32018L0410&from=DE

European Parliament. (2019). The European Parliament declares climate emergency. Retrieved 7 December 2019, from https://www.europarl.europa.eu/news/en/press-room/20191121IPR67110/the-european-parliament-declares-climate-emergency

Eurostat. (2014). Administrative Units / Statistical Units - Countries. Retrieved 10 May 2016, from http://ec.europa.eu/eurostat/web/gisco/geodata/reference-data/administrative-units-statistical-units

Eurostat. (2016). Stock of vehicles at regional level. Retrieved 16 December 2016, from http://ec.europa.eu/eurostat/statistics-explained/index.php/Stock_of_vehicles_at_regional_level

Eurostat. (2017a). Energy balances (2017 Edition). Retrieved 4 October 2017, from http://ec.europa.eu/eurostat/web/energy/data/energy-balances

Eurostat. (2017b). Energy Statistics - Infrastructure - electricity - annual data (nrg_113a). Retrieved 31 July 2017, from http://ec.europa.eu/eurostat/web/energy/data/database

Eurostat. (2017c). Supply, transformation and consumption of electricity - annual data (nrg_105a). Retrieved 4 May 2017, from http://ec.europa.eu/eurostat/web/energy/data/database

Eurostat. (2019a). Eurostat - Greenhouse gas emissions by source sector (env_air_gge). Retrieved 8 November 2019, from http://appsso.eurostat.ec.europa.eu/nui/show.do?lang=en&dataset=env_air_gge

Eurostat. (2019b). Infrastructure - electricity - annual data (nrg_113a). Retrieved 8 November 2019, from http://appsso.eurostat.ec.europa.eu/nui/show.do?dataset=nrg_113a&lang=en

Eurostat. (2019c). Supply, transformation and consumption of electricity - annual data (nrg_105a). Retrieved 8 November 2019, from https://appsso.eurostat.ec.europa.eu/nui/show.do?dataset=nrg_105a&lang=en

Eurostat. (2019d). Supply of electricity - monthly data (nrg_105m). Retrieved 23 January 2019, from http://appsso.eurostat.ec.europa.eu/nui/show.do?dataset=nrg_105m&lang=en

EWEA. (2009). *TradeWind Project: Integrating Wind- Developing Europe's power market for the large-scale integration of wind power*. Brussels: European Wind Energy Association. Retrieved from https://backend.orbit.dtu.dk/ws/portalfiles/portal/195981748/Fulltext.pdf

EWEA. (2013). *Deep Water: The next step for offshore wind energy*. Brussels: European Wind Energy Association. Retrieved from http://www.ewea.org/fileadmin/files/library/publications/reports/Deep_Water.pdf

EWEA. (2016). *Wind in power - 2015 European statistics*. Retrieved from

http://www.ewea.org/fileadmin/ewea_documents/documents/publications/statistics/Stats_2011.pdf

Fachagentur Windenergie an Land. (2016). *Ausbausituation der Windenergie an Land im Jahr 2015*. Berlin. Retrieved from http://www.fachagentur-windenergie.de/aktuell/detail/ausbausituation-der-windenergie-an-land-im-jahr-2015.html

Fajardy, M., & Mac Dowell, N. (2017). Can BECCS deliver sustainable and resource efficient negative emissions? *Energy and Environmental Science*, *10*(6), 1389–1426. doi:10.1039/c7ee00465f

Fajardy, M., & Mac Dowell, N. (2018). The energy return on investment of BECCS: Is BECCS a threat to energy security? *Energy and Environmental Science*, *11*(6), 1581–1594. doi:10.1039/c7ee03610h

Farahmand, H., Aigner, T., Doorman, G. L., Korpås, M., & Huertas-Hernando, D. (2012). Balancing market integration in the northern European continent: A 2030 case study. *IEEE Transactions on Sustainable Energy*, *3*(4), 918–930. doi:10.1109/TSTE.2012.2201185

Farahmand, H., & Doorman, G. L. (2012). Balancing market integration in the Northern European continent. *Applied Energy*, *96*(4), 316–326. doi:10.1016/j.apenergy.2011.11.041

Fern. (2018). *Six problems with BECCS*. Brussels: Fern. Retrieved from https://www.fern.org/fileadmin/uploads/fern/Documents/Fern BECCS briefing_0.pdf

Fichter, T. (2012). *The Joint German-Jordanian Workshop 2012 Amman February 27th – 29th: Optimized integration of CSP plants into Jordan's power plant portfolio*. DLR. Retrieved from http://elib.dlr.de/75168/1/Amman_2012_Fichter_with_backup.pdf

Finon, D., & Roques, F. (2013). European Electricity Market Reforms : The " Visible Hand " of Public Coordination. *Economics of Energy & Environmental Policy*, *2*(2), 107–124.

Foley, A. M., Leahy, P. G., Marvuglia, A., & McKeogh, E. J. (2012). Current methods and advances in forecasting of wind power generation. *Renewable Energy*, *37*(1), 1–8. doi:10.1016/j.renene.2011.05.033

Forewind. (2016). Forewind - Dogger Bank Teesside A & B. Retrieved 29 November 2016, from http://www.forewind.co.uk/projects/dogger-bank-teesside-a-b.html

Frank, S., & Rebennack, S. (2016). An introduction to optimal power flow: Theory, formulation, and examples. *IIE Transactions*, *48*(12), 1172–1197. doi:10.1080/0740817X.2016.1189626

Fraunhofer ISE. (2016). *Photovoltaics Report*. Freiburg: Fraunhofer ISE. Retrieved from https://www.ise.fraunhofer.de/de/downloads/pdf-files/aktuelles/photovoltaics-report-in-englischer-sprache.pdf

Fraunhofer IWES. (2016). Wind Monitor. Retrieved 24 August 2016, from http://windmonitor.iwes.fraunhofer.de/windmonitor_en/index.html

Freeman, J., Whitmore, J., Kaffine, L., Blair, N., & Dobos, A. P. (2013). *System Advisor Model: Flat Plate Photovoltaic Performance Modeling Validation Report*. Golden: National Renewable Energy Laboratory (NREL). Retrieved from http://www.nrel.gov/docs/fy14osti/60204.pdf

Fuss, S., Lamb, W. F., Callaghan, M. W., Hilaire, J., Creutzig, F., Amann, T., … Khanna, T. (2018). Negative emissions - Part 2: Costs, potentials and side effects. *Environmental Research Letters*, *13*(6), 063002. doi:10.1088/1748-9326/aabf9f

Gambhir, A., Few, S., Nelson, J., Hawkes, A., Schmidt, O., & Staffell, I. (2017). Future cost and performance of water electrolysis: An expert elicitation study. *International Journal of Hydrogen Energy*, *42*(52), 30470–30492. doi:10.1016/j.ijhydene.2017.10.045

Gebrekiros, Y., Doorman, G., Jaehnert, S., & Farahmand, H. (2015). Reserve procurement and transmission capacity reservation in the Northern European power market. *International Journal of Electrical Power and Energy Systems*, *67*, 546–559. doi:10.1016/j.ijepes.2014.12.042

Gerbaulet, C., von Hirschhausen, C., Kemfert, C., Lorenz, C., & Oei, P. Y. (2019). European electricity sector decarbonization under different levels of foresight. *Renewable Energy*, *141*, 973–987.

doi:10.1016/j.renene.2019.02.099

Gernaat, D. E. H. J. (2019). *The role of renewable energy in long-term energy and climate scenarios*. (PhD Thesis, Utrecht University). Retrieved from https://dspace.library.uu.nl/handle/1874/381146

Geth, F., Brijs, T., Kathan, J., Driesen, J., & Belmans, R. (2015). An overview of large-scale stationary electricity storage plants in Europe: Current status and new developments. *Renewable and Sustainable Energy Reviews*, *52*, 1212–1227. doi:10.1016/j.rser.2015.07.145

Gianfreda, A., Parisio, L., & Pelagatti, M. (2018). A review of balancing costs in Italy before and after RES introduction. *Renewable and Sustainable Energy Reviews*, *91*(November 2017), 549–563. doi:10.1016/j.rser.2018.04.009

Gibbins, J., Chalmers, H., Lucquiaud, M., McGlashan, N., Li, J., & Liang, X. (2011). *Retrofitting CO2 Capture to Existing Power Plants*. IEAGHG. Retrieved from http://www.ieaghg.org/docs/General_Docs/Reports/2011-02.pdf

Gils, H. C. (2014). Assessment of the theoretical demand response potential in Europe. *Energy*, *67*, 1–18. doi:10.1016/j.energy.2014.02.019

Gils, H. C., Scholz, Y., Pregger, T., de Tena, D. L., & Heide, D. (2017). Integrated modelling of variable renewable energy-based power supply in Europe. *Energy*, *123*. doi:http://dx.doi.org/10.1016/j.energy.2017.01.115

Global CCS Institute. (2018). *The Global Status of CCS: 2018*. Melbourne, Australia. Retrieved from www.globalccsinstitute.com

Global Energy Observatory. (n.d.). Retrieved 31 July 2017, from http://globalenergyobservatory.org/

GME. (2017). *Annual Report 2017*. Rome. Retrieved from http://www.mercatoelettrico.org/En/MenuBiblioteca/documenti/20180801RelazioneAnnuale2017_En.pdf

GME. (2019a). GME's info - Library - annual reports. Retrieved 22 December 2019, from https://www.mercatoelettrico.org/en/GME/Biblioteca/RapportiAnnuali.aspx

GME. (2019b). Statistics - summary data - MPE-MGP. Retrieved 23 November 2019, from https://www.mercatoelettrico.org/En/Statistiche/ME/DatiSintesi.aspx

Gomez, T., Herrero, I., Rodilla, P., Escobar, R., Lanza, S., de la Fuente, I., … Junco, P. (2019). European Union Electricity Markets: Current Practice and Future View. *IEEE Power and Energy Magazine*, *17*(1), 20–31. doi:10.1109/MPE.2018.2871739

Gonzalez Aparicio, I., & Zucker, A. (2015). *Meteorological data for RES-E integration studies*. Petten: European Commission Joint Research Centre. https://doi.org/10.2790/349276

Gorre, J., Ortloff, F., & van Leeuwen, C. (2019). Production costs for synthetic methane in 2030 and 2050 of an optimized Power-to-Gas plant with intermediate hydrogen storage. *Applied Energy*, *253*(April), 113594. doi:10.1016/j.apenergy.2019.113594

Graabak, I., & Korpås, M. (2016). Balancing of Variable Wind and Solar Production in Continental Europe with Nordic Hydropower - A Review of Simulation Studies. *Energy Procedia*, *87*(1876), 91–99. doi:10.1016/j.egypro.2015.12.362

Graabak, I., Korpas, M., & Belsnes, M. (2017). Balancing needs and measures in the future West Central European power system with large shares of wind and solar resources. *International Conference on the European Energy Market, EEM*. doi:10.1109/EEM.2017.7981934

Grams, C. M., Beerli, R., Pfenninger, S., Staffell, I., & Wernli, H. (2017). Balancing Europe's wind-power output through spatial deployment informed by weather regimes. *Nature Climate Change*, *7*(8), 557–562. doi:10.1038/NCLIMATE3338

Green, R., Hu, H., & Vasilakos, N. (2011). Turning the wind into hydrogen: The long-run impact on electricity prices and generating capacity. *Energy Policy*, *39*(7), 3992–3998. doi:10.1016/j.enpol.2010.11.007

Greve, Z. D. E., Daniels, C., & Lobry, J. (2014). *A Review of Time Series Models for the Long Term Modeling of Wind*

Speed in Distribution Network Planning. In *CIRED Workshop, 11-12 June 2014, Rome*. CIRED. Retrieved from http://www.cired.net/publications/workshop2014/papers/CIRED2014WS_0363_final.pdf

Gross, R., Blyth, W., & Heptonstall, P. (2010). Risks, revenues and investment in electricity generation: Why policy needs to look beyond costs. *Energy Economics*, *32*(4), 796–804. doi:10.1016/j.eneco.2009.09.017

Grossmann, W. D., Grossmann, I., & Steininger, K. W. (2013). Distributed solar electricity generation across large geographic areas, Part I: A method to optimize site selection, generation and storage. *Renewable and Sustainable Energy Reviews*, *25*, 831–843. doi:10.1016/j.rser.2012.08.018

Grossmann, W. D., Grossmann, I., & Steininger, K. W. (2014). Solar electricity generation across large geographic areas, Part II: A Pan-American energy system based on solar. *Renewable and Sustainable Energy Reviews*, *32*, 983–993. doi:10.1016/j.rser.2014.01.003

Guerrero-Lemus, R., & Martínez-Duart, J. M. (2013). *Renewable Energies and CO2*. London: Springer London. doi:10.1007/978-1-4471-4385-7

Gurkan, G., Ozdemir, O., & Smeers, Y. (2013). *Generation Capacity Investments in Electricity Markets: Perfect Competition* (No. 2013–045). *CentER Discussion Paper Series*. Tilburg. https://doi.org/10.2139/ssrn.2314862

Gurobi Optimization. (2016). Gurobi Optimizer Reference Manual. Retrieved from http://www.gurobi.com

Gürtler, M., & Paulsen, T. (2018). The effect of wind and solar power forecasts on day-ahead and intraday electricity prices in Germany. *Energy Economics*, *75*, 150–162. doi:10.1016/j.eneco.2018.07.006

GWEC. (2017). *Global Wind Reports 2006 - 2016*. Global Wind Energy Council. Retrieved from http://gwec.net/publications/global-wind-report-2/

GWEC, SolarPower Europe, & Greenpeace. (2015). *Energy [R]evolution: 100% renewable energy for all. 5th edition*. Brussels. Retrieved from http://www.greenpeace.org/international/en/campaigns/climate-change/energyrevolution/

Haas, M. (2004). A New Approach to Markov-Switching GARCH Models. *Journal of Financial Econometrics*, *2*(4), 493–530. doi:10.1093/jjfinec/nbh020

Hagspiel, S., Jägemann, C., Lindenberger, D., Brown, T., Cherevatskiy, S., & Tröster, E. (2014). Cost-optimal power system extension under flow-based market coupling. *Energy*, *66*, 654–666. doi:10.1016/j.energy.2014.01.025

Hahn, H., Ganagin, W., Hartmann, K., & Wachendorf, M. (2014). Cost analysis of concepts for a demand oriented biogas supply for flexible power generation. *Bioresource Technology*, *170*, 211–220. doi:10.1016/j.biortech.2014.07.085

Hahn, H., Krautkremer, B., Hartmann, K., & Wachendorf, M. (2014). Review of concepts for a demand-driven biogas supply for flexible power generation. *Renewable and Sustainable Energy Reviews*, *29*, 383–393. doi:10.1016/j.rser.2013.08.085

Haller, M., Ludig, S., & Bauer, N. (2012). Decarbonization scenarios for the EU and MENA power system: Considering spatial distribution and short term dynamics of renewable generation. *Energy Policy*, *47*, 282–290. doi:10.1016/j.enpol.2012.04.069

Hansen, A. C., & Thorn, P. (2013). *PV potential and potential PV rent in European regions. ENSPAC Research Papers on Transitions to a Green Economy 01/13*. Roskilde: The Department of Environmental, Social and Spatial Change ENSPAC, Roskilde University. Retrieved from http://www.reshaping-res-policy.eu/downloads/D10_Long-term-potentials-and-cost-of-RES.pdf

Hansen, B. (1994). Autoregressive Conditional Density Estimation. *International Economic Review*, *35*(3), 705–730.

Hartner, M., Ortner, A., Hiesl, A., & Haas, R. (2015). East to west - The optimal tilt angle and orientation of photovoltaic panels from an electricity system perspective. *Applied Energy*, *160*, 94–107. doi:10.1016/j.apenergy.2015.08.097

Healy, S., Graichen, V., Graichen, J., Nissen, C., Gores, S., & Siemons, A. (2019). *Trends and projections in the EU ETS in 2019: The EU Emissions Trading System in numbers*. Mol, Belgium: European Topic Centre on Climate change mitigation and energy. Retrieved from https://www.eionet.europa.eu/etcs/etc-cme/products/etc-cme-

reports/etc-cme-report-3-2019-trends-and-projections-in-the-eu-ets-in-2019/@@download/file/ETC_CME_Technical_Report_2019_3 final.pdf

Heard, B. P., Brook, B. W., Wigley, T. M. L., & Bradshaw, C. J. A. (2017). Burden of proof: A comprehensive review of the feasibility of 100% renewable-electricity systems. *Renewable and Sustainable Energy Reviews*, *76*(September 2016), 1122–1133. doi:10.1016/j.rser.2017.03.114

Heat Roadmap Europe. (2019). Heat Roadmap Europe 4 Energy models for 14 EU MSs. Retrieved 20 February 2019, from https://heatroadmap.eu/energy-models/

Heather, L., Mitchell, D., & Glevey, W. (2018). *Study on the value of lost load of electricity supply in Europe - ACER*. Cambridge Economic Policy Associates. Retrieved from https://acer.europa.eu/Events/Workshop-on-the-estimation-of-the-cost-of-disruption-of-gas-supply-CoDG-and-the-value-of-lost-load-in-power-supply-systems-VoLL-in-Europe/Documents/CEPAPresentation_VoLLWorkshop.pdf

Heide, D., Greiner, M., von Bremen, L., & Hoffmann, C. (2011). Reduced storage and balancing needs in a fully renewable European power system with excess wind and solar power generation. *Renewable Energy*, *36*(9), 2515–2523. doi:10.1016/j.renene.2011.02.009

Heide, D., von Bremen, L., Greiner, M., Hoffmann, C., Speckmann, M., & Bofinger, S. (2010). Seasonal optimal mix of wind and solar power in a future, highly renewable Europe. *Renewable Energy*, *35*(11), 2483–2489. doi:10.1016/j.renene.2010.03.012

Heller, R., Deng, Y., & Breevoort, P. Van. (2013). *Renewable energy: a 2030 scenario for the EU*. Utrecht: ECOFYS. Retrieved from https://www.ecofys.com/files/files/ecofys-2013-renewable-energy-2030-scenario-for-the-eu.pdf

Hengeveld, E. J., van Gemert, W. J. T., Bekkering, J., & Broekhuis, A. A. (2014). When does decentralized production of biogas and centralized upgrading and injection into the natural gas grid make sense? *Biomass and Bioenergy*, *67*, 363–371. doi:10.1016/j.biombioe.2014.05.017

Henriot, A., & Glachant, J. M. (2013). Melting-pots and salad bowls: The current debate on electricity market design for integration of intermittent RES. *Utilities Policy*, *27*, 57–64. doi:10.1016/j.jup.2013.09.001

Herre, L., Matusevičius, T., Olauson, J., & Söder, L. (2019). Exploring wind power prognosis data on Nord Pool: The case of Sweden and Denmark. *IET Renewable Power Generation*, *13*(5), 690–702. doi:10.1049/iet-rpg.2018.5086

Hirth, L. (2018). What caused the drop in European electricity prices? A factor decomposition analysis. *The Energy Journal*, *39*(1), 143–158. doi:10.5547/01956574.39.1.lhir

Hirth, L., & Ueckerdt, F. (2014). *Ten propositions on electricity market design: energy-only vs. capacity markets*. In *Sustainable Energy Policy and Strategies for Europe:14th IAEE European Conference, October 28-31, 2014*. Rome. Retrieved from https://www.iaee.org/en/publications/proceedingsabstractpdf.aspx?id=12385

Hirth, L., & Ziegenhagen, I. (2015). Balancing power and variable renewables: Three links. *Renewable and Sustainable Energy Reviews*, *50*, 1035–1051. doi:10.1016/j.rser.2015.04.180

Hodge, B., Lew, D., Milligan, M., Gómez-lázaro, E., Flynn, D., & Dobschinski, J. (2012). *Wind Power Forecasting Error Distributions*. In *The 11th Annual International Workshop on Large-Scale Integration of Wind Power into Power Systems as well as on Transmission Networks for Offshore Wind Power Plants Conference* (pp. 1–8).

Hoefnagels, R., Junginger, M., Panzer, C., Resch, G., & Held, A. (2011). *RE-Shaping Project. Deliverable 10 Report: Long Term Potentials and Costs of RES Part I- Potentials, Diffusion and Technological learning*. Retrieved from http://www.reshaping-res-policy.eu/downloads/D10_Long-term-potentials-and-cost-of-RES.pdf

Hoefnagels, R., Resch, G., Junginger, M., & Faaij, A. (2014). International and domestic uses of solid biofuels under different renewable energy support scenarios in the European Union. *Applied Energy*, *131*, 139–157. doi:10.1016/j.apenergy.2014.05.065

Hoegh-Guldberg, Jacob, O. D., Taylor, M., Bindi, M., Brown, S., Camilloni, I., … Zhou, G. (2018). Impacts of 1.5°C of Global Warming on Natural and Human Systems. In *Global Warming of 1.5°C. An IPCC Special Report on the impacts of global warming of 1.5°C above pre-industrial levels and related global greenhouse gas emission pathways, in the context of strengthening the global response to the threat of climate change*, (pp. 175–311). Cambridge,

United Kingdom and New York, NY, USA: Cambridge University Press. Retrieved from https://www.ipcc.ch/sr15

Hogan, W. W. (2013). Electricity Scarcity Pricing Through Operating Reserves. *Economics of Energy & Environmental Policy*, *2*(2). doi:10.5547/2160-5890.2.2.4

Hoicka, C. E., & Rowlands, I. H. (2011). Solar and wind resource complementarity: Advancing options for renewable electricity integration in Ontario, Canada. *Renewable Energy*, *36*(1), 97–107. doi:10.1016/j.renene.2010.06.004

Holttinen, H. (2004). *The impact of large scale wind power production on the Nordic electricity system*. (PhD thesis, Helsinki University of Technology,VTT), Espoo. Retrieved from https://www.vtt.fi/inf/pdf/publications/2004/P554.pdf

Honegger, M., & Reiner, D. (2018). The political economy of negative emissions technologies: consequences for international policy design. *Climate Policy*, *18*(3), 306–321. doi:10.1080/14693062.2017.1413322

Hoogwijk, M., de Vries, B., & Turkenburg, W. (2004). Assessment of the global and regional geographical, technical and economic potential of onshore wind energy. *Energy Economics*, *26*(5), 889–919. doi:10.1016/j.eneco.2004.04.016

Horsch, J., & Brown, T. (2017). *The role of spatial scale in joint optimisations of generation and transmission for European highly renewable scenarios*. In *International Conference on the European Energy Market, 6-9 June 2017, Dresden*. doi:10.1109/EEM.2017.7982024

Höschle, H., Le Cadre, H., & Belmans, R. (2018). Inefficiencies caused by non-harmonized capacity mechanisms in an interconnected electricity market. *Sustainable Energy, Grids and Networks*, *13*, 29–41. doi:10.1016/j.segan.2017.11.002

Hu, J., Harmsen, R., Crijns-Graus, W., Worrell, E., & van den Broek, M. (2018). Identifying barriers to large-scale integration of variable renewable electricity into the electricity market: A literature review of market design. *Renewable and Sustainable Energy Reviews*, *81*(September 2016), 2181–2195. doi:10.1016/j.rser.2017.06.028

Huber, M., Dimkova, D., & Hamacher, T. (2014). Integration of wind and solar power in Europe: Assessment of flexibility requirements. *Energy*, *69*, 236–246. doi:10.1016/j.energy.2014.02.109

Huisman, R., & Kiliç, M. (2013). A history of European electricity day-ahead prices. *Applied Economics*, *45*(18), 2683–2693. doi:10.1080/00036846.2012.665601

Huld, T., Müller, R., & Gambardella, A. (2012). A new solar radiation database for estimating PV performance in Europe and Africa. *Solar Energy*, *86*(6), 1803–1815. doi:10.1016/j.solener.2012.03.006

Hyndman, R. J., & Athanasopoulos, G. (2018). *Forecasting: Principles and Practice* (2nd editio). Melbourne, Australia: OTexts. Retrieved from OTexts.com/fpp2

IEA-ETSAP, & IRENA. (2013). *Biomass Co-firing: Technology brief*. IEA-ETSAP, IRENA. Retrieved from https://www.irena.org/-/media/Files/IRENA/Agency/Publication/2015/IRENA-ETSAP-Tech-Brief-E21-Biomass-Co-firing.pdf

IEA. (2011). *Modelling the capacity credit of renewable energy sources*. Paris: OECD/IEA. Retrieved from https://www.iea.org/media/weowebsite/energymodel/Methodology_CapacityCredit.pdf

IEA. (2015). *World Energy Outlook 2015*. Paris: OECD/IEA.

IEA. (2016a). *Energy Technology Perspectives 2016*. Paris: OECD/IEA.

IEA. (2016b). *Next Generation Wind and Solar Power*. Paris: OECD/IEA. https://doi.org/10.1787/9789264258969-en

IEA. (2016c). *Ready for CCS retrofit: The potential for equipping China's existing coal fleet with carbon capture and storage*. Paris. Retrieved from https://www.iea.org/publications/insights/insightpublications/ReadyforCCSRetrofit.pdf

IEA. (2016d). *World Energy Outlook 2016*. Paris: OECD/IEA. https://doi.org/http://www.iea.org/publications/freepublications/publication/WEB_WorldEnergyOutlook2015Ex

ecutiveSummaryEnglishFinal.pdf

IEA. (2019). *Global energy & CO2 status report: The latest trends in energy and emissions in 2018*. Paris. https://doi.org/10.4324/9781315252056

Inflation.eu. (2017). Historic harmonised inflation Europe – HICP inflation Europe. Retrieved 13 October 2017, from http://www.inflation.eu/inflation-rates/europe/historic-inflation/hicp-inflation-europe.aspx

International Electrotechnical Commission. IEC 61400-1: Wind Turbine Generator (WTG) Classes (2005).

IPCC. (2010). *2006 IPCC Guidelines for National Greenhouse Gas Inventories. Volume 2: Energy. Chapter 2: Stationary Combustion.* Intergovernmental Panel on Climate Change. Retrieved from http://www.ipcc-nggip.iges.or.jp/public/2006gl/vol2.html

IPCC. (2014). *Climate Change 2014: Synthesis Report. Contribution of Working Groups I, II and III to the Fifth Assessment Report of the Intergovernmental Panel on Climate Change*. (R. Pachauri & L. Meyer, Eds.). Geneva: IPCC. https://doi.org/10.1017/CBO9781107415324

IPCC. (2018). *Global Warming of 1.5°C. An IPCC Special Report on the impacts of global warming of 1.5°C above pre-industrial levels and related global greenhouse gas emission pathways, in the context of strengthening the global response to the threat of climate change,*. (V. Masson-Delmotte, P. Zhai, H.-O. Pörtner, D. Roberts, J. Skea, P. Shukla, … T. Waterfield, Eds.).

IRENA. (2012). *Renewable Energy Technologies: Cost Analysis Series. Concentrating Solar Power. Volume 1: Power Sector, Issue 2/5*. Abu Dhabi: International Renewable Energy Agency. Retrieved from https://www.irena.org/documentdownloads/publications/re_technologies_cost_analysis-csp.pdf

IRENA. (2013). *Concentrating Solar Power: Technology Brief*. Abu Dhabi: International Renewable Energy Agency. Retrieved from https://www.irena.org/DocumentDownloads/Publications/IRENA-ETSAP Tech Brief E10 Concentrating Solar Power.pdf

IRENA. (2016). *The Power to Change: Solar and Wind Cost Reduction Potential to 2025*. Bonn: International Renewable Energy Agency. Retrieved from http://www.irena.org/DocumentDownloads/Publications/IRENA_Power_to_Change_2016.pdf

IRENA. (2017). *Planning for the Renewable Future: Long-term modelling and tools to expand variable renewable power in emerging economices*. Abu Dhabi: International Renewable Energy Agency. Retrieved from https://www.irena.org/publications/2017/Jan/Planning-for-the-renewable-future-Long-term-modelling-and-tools-to-expand-variable-renewable-power%0Ahttp://www.irena.org/DocumentDownloads/Publications/IRENA_Planning_for_the_Renewable_Future_2017.pdf

IRENA. (2018). *Renewable Power Generation Costs in 2018*. Abu Dhabi: International Renewable Energy Agency. Retrieved from https://www.irena.org/-/media/Files/IRENA/Agency/Publication/2019/May/IRENA_Renewable-Power-Generations-Costs-in-2018.pdf

IRENA. (2019). *Renewable capacity statistics 2019*. Abu Dhabi: International Renewable Energy Agency. Retrieved from https://www.irena.org/publications/2019/Mar/Renewable-Capacity-Statistics-2019

Iychettira, K. K., Hakvoort, R. A., & Linares, P. (2017). Towards a comprehensive policy for electricity from renewable energy: An approach for policy design. *Energy Policy*, *106*(August 2016), 169–182. doi:10.1016/j.enpol.2017.03.051

Jacobs, D., Couture, T., Zinaman, O., & Cochran, J. (2016). *Re-Transition - Transitioning To Policy Frameworks for Cost-Competitive Renewables*. Utrecht: IEA-RETD. Retrieved from http://iea-retd.org/wp-content/uploads/2016/03/IEA-RETD_RE-TRANSITION.pdf

Jacobson, M. Z., & Delucchi, M. A. (2018). 100% clean, renewable energy studies provide scientific solution that policymakers can rely on. *The Electricity Journal*, *31*(2), 78–80. doi:10.1016/j.tej.2017.11.011

Jacobson, M. Z., Delucchi, M. A., Bazouin, G., Bauer, Z. A. F., Heavey, C. C., Fisher, E., … Yeskoo, T. W. (2015). 100% clean and renewable wind, water, and sunlight (WWS) all-sector energy roadmaps for the 50 United States. *Energy*

Environ. Sci., *8*. doi:10.1039/C5EE01283J

Jacobson, M. Z., Delucchi, M. A., Cameron, M. A., & Frew, B. A. (2015). A Low-Cost Solution to the Grid Reliability Problem With 100% Penetration of Intermittent Wind, Water, and Solar for all Purposes. *Proceedings of the National Academy of Sciences*, 1–6. doi:10.1073/pnas.1510028112

Jägemann, C., Fürsch, M., Hagspiel, S., & Nagl, S. (2013). Decarbonizing Europe's power sector by 2050 - Analyzing the economic implications of alternative decarbonization pathways. *Energy Economics*, *40*, 622–636. doi:10.1016/j.eneco.2013.08.019

Jenkins, J. D., Zhou, Z., Ponciroli, R., Vilim, R. B., Ganda, F., de Sisternes, F., & Botterud, A. (2018). The benefits of nuclear flexibility in power system operations with renewable energy. *Applied Energy*, *222*(October 2017), 872–884. doi:10.1016/j.apenergy.2018.03.002

Jerez, S., Thais, F., Tobin, I., Wild, M., Colette, A., Yiou, P., & Vautard, R. (2015). The CLIMIX model: A tool to create and evaluate spatially-resolved scenarios of photovoltaic and wind power development. *Renewable and Sustainable Energy Reviews*, *42*, 1–15. doi:10.1016/j.rser.2014.09.041

Jerez, S., Tobin, I., Vautard, R., Montávez, J. P., López-Romero, J. M., Thais, F., … Wild, M. (2015). The impact of climate change on photovoltaic power generation in Europe. *Nature Communications*, *6*(November 2016), 10014. doi:10.1038/ncomms10014

Jerez, S., Trigo, R. M., Sarsa, A., Lorente-Plazas, R., Pozo-Vázquez, D., & Montávez, J. P. (2013). Spatio-temporal complementarity between solar and wind power in the Iberian Peninsula. *Energy Procedia*, *40*, 48–57. doi:10.1016/j.egypro.2013.08.007

Jerez, S., Trigo, R. M., Vicente-Serrano, S. M., Pozo-VáZquez, D., Lorente-Plazas, R., Lorenzo-Lacruz, J., … MontáVez, J. P. (2013). The impact of the north atlantic oscillation on renewable energy resources in Southwestern Europe. *Journal of Applied Meteorology and Climatology*, *52*(10), 2204–2225. doi:10.1175/JAMC-D-12-0257.1

Jia, Z., Wang, B., Song, S., & Fan, Y. (2014). Blue energy: Current technologies for sustainable power generation from water salinity gradient. *Renewable and Sustainable Energy Reviews*, *31*, 91–100. doi:10.1016/j.rser.2013.11.049

Jonker, J. G. G., Junginger, M., & Faaij, A. (2014). Carbon payback period and carbon offset parity point of wood pellet production in the South-eastern United States. *GCB Bioenergy*, *6*(4), 371–389. doi:10.1111/gcbb.12056

Joos, M., & Staffell, I. (2018). Short-term integration costs of variable renewable energy: Wind curtailment and balancing in Britain and Germany. *Renewable and Sustainable Energy Reviews*, *86*(January), 45–65. doi:10.1016/j.rser.2018.01.009

Jorgenson, J., Denholm, P., Mehos, M., & Turchi, C. (2013). *Estimating the Performance and Economic Value of Multiple Concentrating Solar Power Technologies in a Production Cost Model*. Golden, Colerado: National Renewable Energy Laboratory. Retrieved from https://www.nrel.gov/docs/fy14osti/58645.pdf

Joskow, P. L. (2008). Capacity payments in imperfect electricity markets: Need and design. *Utilities Policy*, *16*(3), 159–170. doi:10.1016/j.jup.2007.10.003

Jost, D., Speckmann, M., Sandau, F., & Schwinn, R. (2015). A new method for day-ahead sizing of control reserve in Germany under a 100% renewable energy sources scenario. *Electric Power Systems Research*, *119*, 485–491. doi:10.1016/j.epsr.2014.10.026

JRC. (2014). *ETRI 2014: Energy Technology Reference Indicator Projections for 2010-2050*. Petten: European Commission Joint Research Centre. https://doi.org/10.2790/057687

Kalogirou, S. A. (2009). *Solar Energy Engineering: Processes and Systems*. California: Academic Press.

Kampman, B., Leguijt, C., Scholten, T., Tallat-Kelpsaite, J., Brückmann, R., Maroulis, G., … Elbersen, B. (2016). *Optimal use of biogas from waste streams - An assessment of the potential of biogas from digestion in the EU beyond 2020*. European Commission. Retrieved from https://ec.europa.eu/energy/sites/ener/files/documents/ce_delft_3g84_biogas_beyond_2020_final_report.pdf

Kanellopoulos, K. (2018). *Scenario analysis of accelerated coal phase-out by 2030: A study on the European power*

system based on the EUCO27 scenario using the METIS model. EUR 29203 EN. Luxembourg: Publications Office of the European Union. https://doi.org/10.2760/751272

Kaunda, C. S., Kimambo, C. Z., & Nielsen, T. K. (2012). Hydropower in the Context of Sustainable Energy Supply: A Review of Technologies and Challenges. *ISRN Renewable Energy*, *2012*, 1–15. doi:10.5402/2012/730631

Keay, M. (2016). *Electricity markets are broken – can they be fixed? (OIES PAPER: EL 17)*. The Oxford Institute for Energy Studies. Retrieved from https://www.oxfordenergy.org/wpcms/wp-content/uploads/2016/02/Electricity-markets-are-broken-can-they-be-fixed-EL-17.pdf

KEFM. (2018). *Denmark's Draft Integrated National Energy and Climate Plan*. Retrieved from https://ens.dk/sites/ens.dk/files/EnergiKlimapolitik/denmarks_draft_integrated_energy_and_climate_plan.pdf

Keith, D. W., Holmes, G., St. Angelo, D., & Heidel, K. (2018). A Process for Capturing CO2 from the Atmosphere. *Joule*, *2*(8), 1573–1594. doi:10.1016/j.joule.2018.05.006

Kemna, R. (2014). *Average EU building heat load for HVAC equipment. Final Report*. Delft: Van Holsteijn en Kemna B.V. (VHK). Retrieved from https://ec.europa.eu/energy/sites/ener/files/documents/2014_final_report_eu_building_heat_demand.pdf

Khoshrou, A., Dorsman, A. B., & Pauwels, E. J. (2019). The evolution of electricity price on the German day-ahead market before and after the energy switch. *Renewable Energy*, *134*, 1–13. doi:10.1016/j.renene.2018.10.101

Kiesel, R., Paraschiv, F., & Sætherø, A. (2019). On the construction of hourly price forward curves for electricity prices. *Computational Management Science*, *16*(1–2), 345–369. doi:10.1007/s10287-018-0300-6

Killinger, S., Mainzer, K., McKenna, R., Kreifels, N., & Fichtner, W. (2015). A regional optimisation of renewable energy supply from wind and photovoltaics with respect to three key energy-political objectives. *Energy*, *84*, 563–574. doi:10.1016/j.energy.2015.03.050

Kim, S., & Kim, H. (2016). A new metric of absolute percentage error for intermittent demand forecasts. *International Journal of Forecasting*, *32*(3), 669–679. doi:10.1016/j.ijforecast.2015.12.003

Knorr, K., Zimmermann, B., Kirchner, D., Speckmann, M., Spieckermann, R., Widdel, M., … Ritter, P. (2014). *Kombikraftwerk 2 Final Report*. Retrieved from http://www.kombikraftwerk.de/fileadmin/Kombikraftwerk_2/English/Kombikraftwerk2_FinalReport.pdf

Koch, C., & Hirth, L. (2019). Short-term electricity trading for system balancing: An empirical analysis of the role of intraday trading in balancing Germany's electricity system. *Renewable and Sustainable Energy Reviews*, *113*(February), 109275. doi:10.1016/j.rser.2019.109275

Komendantova, N., & Battaglini, A. (2016). Beyond Decide-Announce-Defend (DAD) and Not-in-My-Backyard (NIMBY) models? Addressing the social and public acceptance of electric transmission lines in Germany. *Energy Research and Social Science*, *22*, 224–231. doi:10.1016/j.erss.2016.10.001

Kost, C., Hartmann, N., Senkpiel, C., Schlegl, T., Zampara, M., & Capros, P. (2015). *RESDEGREE Project: Towards an energy system in Europe based on renewables – Model based analysis of Greece and Germany by coupling a European wide demand and supply model (PRIMES) with a regional and temporal high resolution bottom-up investment and unit*. Retrieved from http://publica.fraunhofer.de/documents/N-435554.html

Kosztra, B., & Arnold, S. (2014). *Proposal for enhancement of CLC nomenclature guidelines*. European Environment Agency. Retrieved from http://land.copernicus.eu/user-corner/technical-library/CLC2006_Nomenclature_illustrated_guide_enhanced_final.pdf

Kougias, I., Szabó, S., Monforti-Ferrario, F., Huld, T., & Bódis, K. (2016). A methodology for optimization of the complementarity between small-hydropower plants and solar PV systems. *Renewable Energy*, *87*, 1023–1030. doi:10.1016/j.renene.2015.09.073

Kraan, O., Kramer, G. J., & Nikolic, I. (2018). Investment in the future electricity system - An agent-based modelling approach. *Energy*, *151*, 569–580. doi:10.1016/j.energy.2018.03.092

Kraan, O., Kramer, G. J., Nikolic, I., Chappin, E., & Koning, V. (2019). Why fully liberalised electricity markets will fail to

meet deep decarbonisation targets even with strong carbon pricing. *Energy Policy*, *131*, 99–110. doi:10.1016/j.enpol.2019.04.016

KU Leuven Energy Institute. (2015). *The current electricity market design in Europe. EI-FACT SHEET 2015-01.* Heverlee. Retrieved from https://set.kuleuven.be/ei/images/EI_factsheet8_eng.pdf/at_download/file

Kumler, A., Xie, Y., & Zhang, Y. (2018). *A New Approach for Short-Term Solar Radiation Forecasting Using the Estimation of Cloud Fraction and Cloud Albedo*. Golden, Colerado: National Renewable Energy Laboratory. https://doi.org/10.2172/1476449

Kundur, P. (2012). Power system stability. In L. Grigsby (Ed.), *Power system stability and control* (3rd ed.). Boca Raton, US: CRC Press.

Lacal-Arántegui, R., & Serrano González, J. (2015). *2014 JRC Wind Status Report*. Petten: European Commission Joint Research Centre. https://doi.org/10.2790/676580

Lassonde, S., Boucher, O., Breon, F., Jerez, S., Tobin, I., & Vautard, R. (2015). *Spatial optimization of an ideal renewable energy system as a response to intermittency*. In *3rd International Conference Energy & Meteorology 22-26 June 2015*. Boulder, Colorado USA.

Lassonde, S., Boucher, O., Breon, F., Tobin, I., & Vautard, R. (2016). *Spatial optimization of an ideal wind energy system as a response to the intermittency of renewable energies?* In *Geophysical Research Abstracts: EGU General Assembly 2016* (Vol. 18, p. 14241). Vienna.

Legifrance. Décret no 2016-1442 du 27 octobre 2016 relatif à la programmation pluriannuelle de l'énergie, Journal Officiel de la République Française § (2016). Retrieved from https://www.legifrance.gouv.fr/jo_pdf.do?id=JORFTEXT000033312688

Lévêque, F. (2013). *Estimating the costs of nuclear power: benchmarks and uncertainties. Working Paper 13-ME-01.* Paris, France: CERNA, MINES ParisTech. Retrieved from https://hal-mines-paristech.archives-ouvertes.fr/hal-00782190v2/document

Levin, T., & Botterud, A. (2015). Electricity market design for generator revenue sufficiency with increased variable generation. *Energy Policy*, *87*, 392–406. doi:10.1016/j.enpol.2015.09.012

Lew, D., Brinkman, G., Ibanez, E., Florita, A., Heaney, M., Hodge, B., … Venkataraman, S. (2013). *The Western Wind and Solar Integration Study Phase 2*. Golden: National Renewable Energy Laboratory. Retrieved from https://www.nrel.gov/docs/fy13osti/55588.pdf

Li, G., Wang, H., Zhang, S., Xin, J., & Liu, H. (2019). Recurrent neural networks based photovoltaic power forecasting approach. *Energies*, *12*(13), 1–17. doi:10.3390/en12132538

Lin, J., & Magnago, F. (2017). *Electricity Markets: Theories and applications*. New Jersey: John Wiley & Sons.

Lindø Offshore Renewables Centre (LORC). (n.d.). Offshore Wind Farms List – global database | LORC Knowledge. Retrieved 11 May 2016, from http://www.lorc.dk/offshore-wind-farms-map/list

Lipponen, J., McCulloch, S., Keeling, S., Stanley, T., Berghout, N., & Berly, T. (2017). The Politics of Large-scale CCS Deployment. *Energy Procedia*, *114*(November 2016), 7581–7595. doi:10.1016/j.egypro.2017.03.1890

Llorente García, I., Álvarez, J. L., & Blanco, D. (2011). Performance model for parabolic trough solar thermal power plants with thermal storage: Comparison to operating plant data. *Solar Energy*, *85*(10), 2443–2460. doi:10.1016/j.solener.2011.07.002

Lojowska, A., Kurowicka, D., Papaefthymiou, G., & van Der Sluis, L. (2010). Advantages of ARMA-GARCH wind speed time series modeling. *2010 IEEE 11th International Conference on Probabilistic Methods Applied to Power Systems, PMAPS 2010*, 83–88. doi:10.1109/PMAPS.2010.5528979

Lund, H., & Mathiesen, B. V. (2009). Energy system analysis of 100% renewable energy systems-The case of Denmark in years 2030 and 2050. *Energy*, *34*, 524–531. doi:10.1016/j.energy.2008.04.003

Lund, P. D., Lindgren, J., Mikkola, J., & Salpakari, J. (2015). Review of energy system flexibility measures to enable high

levels of variable renewable electricity. *Renewable and Sustainable Energy Reviews*, *45*, 785–807. doi:10.1016/j.rser.2015.01.057

MacDonald, A. E., Clack, C. T. M., Alexander, A., Dunbar, A., Wilczak, J., & Xie, Y. (2016). Future cost-competitive electricity systems and their impact on US CO2 emissions. *Nature Climate Change*, *6*(January), 4–7. doi:10.1038/nclimate2921

Macilwain, C. (2010). Supergrid. *Nature*, *468*(24), 624–625. Retrieved from http://www.nature.com.plymouth.idm.oclc.org/news/2010/101201/pdf/468624a.pdf

Madaeni, S. H., Sioshansi, R., & Denholm, P. (2011). *Capacity Value of Concentrating Solar Power Plants Capacity Value of Concentrating Solar Power Plants*. Golden: National Renewable Energy Laboratory. Retrieved from https://www.nrel.gov/docs/fy11osti/51253.pdf

Magagna, D. (2015). *2014 JRC Ocean Energy Status Report*. Petten: European Commission Joint Research Centre. https://doi.org/10.2790/866387

Magagna, D., & Uihlein, A. (2015). Ocean energy development in Europe: Current status and future perspectives. *International Journal of Marine Energy*, *11*, 84–104. doi:10.1016/j.ijome.2015.05.001

Mainzer, K., Fath, K., Mckenna, R., Stengel, J., Fichtner, W., & Schultmann, F. (2014). A high-resolution determination of the technical potential for residential-roof-mounted photovoltaic systems in Germany. *Solar Energy*, *105*, 715–731. doi:10.1016/j.solener.2014.04.015

Mamia, I., & Appelbaum, J. (2016). Shadow analysis of wind turbines for dual use of land for combined wind and solar photovoltaic power generation. *Renewable and Sustainable Energy Reviews*, *55*, 713–718. doi:10.1016/j.rser.2015.11.009

Manwell, J. F., McGowan, J. G., & Rogers, J. G. (2009). *Wind Energy Explained* (2nd ed.). Chichester: Wiley. doi:10.1017/CBO9781107415324.004

Marcu, A., Alberola, E., Caneill, J.-Y., Matteo Mazzoni, S., Schleicher, St., Vailles, C., … Cecchetti, F. (2019). *2019 State of the EU ETS Report*. ERCST, Wegener Center, ICIS, I4CE and Ecoact. Retrieved from https://www.i4ce.org/wp-core/wp-content/uploads/2019/05/2019-State-of-the-EU-ETS-Report.pdf

Markets Insider. (2020). CO2 European Emission Allowances History | Markets Insider. Retrieved 7 March 2020, from https://markets.businessinsider.com/commodities/historical-prices/co2-european-emission-allowances

Marshall, L. (2018). World's First Coal to Biomass Conversion Using Advanced Wood Pellets. *Power Engineering*. Retrieved from https://www.power-eng.com/articles/print/volume-122/issue-3/features/world-s-first-coal-to-biomass-conversion-using-advanced-wood-pellets.html

Mason, I. G., Page, S. C., & Williamson, A. G. (2010). A 100% renewable electricity generation system for New Zealand utilising hydro, wind, geothermal and biomass resources. *Energy Policy*, *38*(8), 3973–3984. doi:10.1016/j.enpol.2010.03.022

Mason, I. G., Page, S. C., & Williamson, A. G. (2013). Security of supply, energy spillage control and peaking options within a 100% renewable electricity system for New Zealand. *Energy Policy*, *60*. doi:10.1016/j.enpol.2013.05.032

Mastropietro, P., Rodilla, P., & Batlle, C. (2015). National capacity mechanisms in the European internal energy market: Opening the doors to neighbours. *Energy Policy*, *82*(1), 38–47. doi:10.1016/j.enpol.2015.03.004

Matek, B. (2015). *Geothermal Energy Association Issue Brief : Firm and Flexible Power Services Available from Geothermal Facilities*. Washington: Geothermal Energy Association. Retrieved from http://geo-energy.org/reports/2015/Firm and Flexible Power Services from Geothermal.pdf

Mathiesen, B. V., Lund, H., & Karlsson, K. (2011). 100% Renewable energy systems, climate mitigation and economic growth. *Applied Energy*, *88*(2), 488–501. doi:10.1016/j.apenergy.2010.03.001

McKenna, R., Hollnaicher, S., & Fichtner, W. (2014). Cost-potential curves for onshore wind energy: A high-resolution analysis for Germany. *Applied Energy*, *115*, 103–115. doi:10.1016/j.apenergy.2013.10.030

McKinsey. (2010). *Transformation of Europe's power system until 2050*. Dusseldorf: McKinsey. Retrieved from https://www.mckinsey.com/~/media/mckinsey/dotcom/client_service/epng/pdfs/transformation_of_europes_power_system.ashx

Mehleri, E. D., Zervas, P. L., Sarimveis, H., Palyvos, J. A., & Markatos, N. C. (2010). Determination of the optimal tilt angle and orientation for solar photovoltaic arrays. *Renewable Energy*, *35*(11), 2468–2475. doi:10.1016/j.renene.2010.03.006

Mehos, M., Turchi, C., Vidal, J., Wagner, M., Ma, Z., Ho, C., … Kruizenga, A. (2017). *Concentrating solar power Gen3 demonstration roadmap*. Golden: National Renewable Energy Laboratory. Retrieved from https://www.nrel.gov/docs/fy17osti/67464.pdf

Meibom, P., Barth, R., Hasche, B., Brand, H., Weber, C., & O'Malley, M. (2011). Stochastic Optimization Model to Study the Operational Impacts of High Wind Penetrations in Ireland. *IEEE Transactions on Power Systems*, *26*(3), 1367–1379. doi:10.1109/TPWRS.2010.2070848

Mennel, T., Ziegler, H., Ebert, M., Nybø, A., Oberrauch, F., & Hewicker, C. (2015). *The hydropower sector's contribution to a sustainable and prosperous Europe*. Bonn: DNV GL, KEMA Consulting GmbH. Retrieved from http://www.thehea.org/macro-economic-study-on-hydropower/

Mester, K. ., Christ, M., Degell, M., & Bunke, W. D. (2017). *Integrating Social Acceptance of Electricity Grid Expansion into Energy System Modeling: A Methodological Approach for Germany*. In V. Wohlgemuth, F. Fuchs-Kittowski, & J. Wittmann (Eds.), *Advances and New Trends in Environmental Informatics. Progress in IS*. (pp. 115–129). Springer. doi:10.1007/978-3-319-44711-7_10

Meyer, R., & Gore, O. (2015). Cross-border effects of capacity mechanisms: Do uncoordinated market design changes contradict the goals of the European market integration? *Energy Economics*, *51*, 9–20. doi:10.1016/j.eneco.2015.06.011

Miettinen, J., & Holttinen, H. (2019). Impacts of wind power forecast errors on the real-time balancing need: a Nordic case study. *IET Renewable Power Generation*, *13*(2), 227–233. doi:10.1049/iet-rpg.2018.5234

Mileva, A., Johnston, J., Nelson, J. H., & Kammen, D. M. (2016). Power system balancing for deep decarbonization of the electricity sector. *Applied Energy*, *162*, 1001–1009. doi:10.1016/j.apenergy.2015.10.180

Milligan, M., & Parsons, B. (1999). A comparison and case study of capacity credit algorithms for wind power plants. *Wind Engineering*, *23*(3), 159–166.

Mills, A., & Wiser, R. (2010). *Implications of Wide-Area Geographic Diversity for Short-Term Variability of Solar Power*. Berkeley: Lawrence Berkeley National Laboratory. Retrieved from http://eta-publications.lbl.gov/sites/default/files/report-lbnl-3884e.pdf

Mitchell, C., Avagyan, V., Chalmers, H., & Lucquiaud, M. (2019). An initial assessment of the value of Allam Cycle power plants with liquid oxygen storage in future GB electricity system. *International Journal of Greenhouse Gas Control*, *87*(March), 1–18. doi:10.1016/j.ijggc.2019.04.020

Möllersten, K., Yan, J., & Moreira, J. R. (2003). Potential market niches for biomass energy with CO2 capture and storage - Opportunities for energy supply with negative CO2 emissions. *Biomass and Bioenergy*, *25*(3), 273–285. doi:10.1016/S0961-9534(03)00013-8

Monforti, F., Huld, T., Bódis, K., Vitali, L., D'Isidoro, M., & Lacal-Arántegui, R. (2014). Assessing complementarity of wind and solar resources for energy production in Italy. A Monte Carlo approach. *Renewable Energy*, *63*, 576–586. doi:10.1016/j.renene.2013.10.028

Mooney, P. A., Mulligan, F. J., & Fealy, R. (2011). Comparison of ERA-40, ERA-Interim and NCEP/NCAR reanalysis data with observed surface air temperatures over Ireland. *International Journal of Climatology*, *31*(4), 545–557. doi:10.1002/joc.2098

Morbee, J., Driesen, J., De Vos, K., & Belmans, R. (2013). Impact of wind power on sizing and allocation of reserve requirements. *IET Renewable Power Generation*, *7*(1), 1–9. doi:10.1049/iet-rpg.2012.0085

Moreira, J. R., Romeiro, V., Fuss, S., Kraxner, F., & Pacca, S. A. (2016). BECCS potential in Brazil: Achieving negative

emissions in ethanol and electricity production based on sugar cane bagasse and other residues. *Applied Energy*, *179*, 55–63. doi:10.1016/j.apenergy.2016.06.044

Mulder, M., Perey, P., & Moraga, J. L. (2019). *Outlook for a Dutch hydrogen market: economic conditions and scenarios. CEER Policy Paper No. 5*. Retrieved from https://www.rug.nl/ceer/blog/ceer_policypaper_5_web.pdf

Mulder, T. (2015). *Capacity remuneration mechanisms in Europe: A quantitative impact assessment*. (MSc thesis, Utrecht University). Retrieved from https://dspace.library.uu.nl/bitstream/handle/1874/316937/Thesis FINAL.pdf

Munasinghe, M. (1979). *The Economics of Power System Reliability and Planning: Theory and Case Study*. Baltimore and London: The John Hopkins University Press. doi:10.2307/2580961

Muñoz, R., Meier, L., Diaz, I., & Jeison, D. (2015). A review on the state-of-the-art of physical/chemical and biological technologies for biogas upgrading. *Reviews in Environmental Science and Biotechnology*, *14*(4), 727–759. doi:10.1007/s11157-015-9379-1

Müsgens, F., Ockenfels, A., & Peek, M. (2014). Economics and design of balancing power markets in Germany. *International Journal of Electrical Power and Energy Systems*, *55*, 392–401. doi:10.1016/j.ijepes.2013.09.020

Myhr, A., Bjerkseter, C., Ågotnes, A., & Nygaard, T. A. (2014). Levelised cost of energy for offshore floating wind turbines in a life cycle perspective. *Renewable Energy*, *66*, 714–728. doi:10.1016/j.renene.2014.01.017

Nagata, M., Hirata, Y., Fujiwara, N., Tanaka, G., Suzuki, H., & Aihara, K. (2017). Smoothing effect for spatially distributed renewable resources and its impact on power grid robustness. *Chaos: An Interdisciplinary Journal of Nonlinear Science*, *27*(3), 033104. doi:10.1063/1.4977510

Naimo, A. (2014). A Novel Approach to Generate Synthetic Wind Data. *Procedia - Social and Behavioral Sciences*, *108*, 187–196. doi:10.1016/j.sbspro.2013.12.830

National Grid. (2017). *Duration-Limited Storage De-Rating Factor Assessment – Final Report*. National Grid. Retrieved from https://www.emrdeliverybody.com/Lists/Latest News/Attachments/150/Duration Limited Storage De-Rating Factor Assessment - Final.pdf

Netherlands Enterprise Agency. (2019). The Netherlands looks forward to second offshore wind farm without subsidy. Retrieved 25 April 2019, from https://english.rvo.nl/news/netherlands-looks-forward-second-offshore-wind-farm-without-subsidy

Newbery, D. M., Pollitt, M. G., Ritz, R. A., & Strielkowski, W. (2018). Market design for a high-renewables European electricity system. *Renewable and Sustainable Energy Reviews*, *91*, 695–707. doi:10.1016/j.rser.2018.04.025

Newbery, D. M., Reiner, D. M., & Ritz, R. A. (2019). The political economy of a carbon price floor for power generation. *Energy Journal*, *40*(1), 1–24. doi:10.5547/01956574.40.1.dnew

Newbery, D. M., Strbac, G., & Viehoff, I. (2016). The benefits of integrating European electricity markets. *Energy Policy*, *94*, 253–263. doi:10.1016/j.enpol.2016.03.047

Noothout, P., de Jager, D., Tesniere, L., van Rooijen, S., Karypidis, N., Bruckmann, R., … Resch, G. (2015). *The impact of risks in renewable investments and the role of smart policies*. Ecofys. Retrieved from https://www.ecofys.com/files/files/diacore-2016-impact-of-risk-in-res-investments.pdf

Nord Pool. (2017). *Annual Report 2017*. Retrieved from https://www.nordpoolgroup.com/globalassets/download-center/annual-report/annual-report-nord-pool_2017.pdf

Nord Pool. (2019). Annual report. Retrieved 23 November 2019, from https://www.nordpoolgroup.com/message-center-container/Annual-report/

Norgaard, P., & Holttinen, H. (2004). *A Multi-Turbine Power Curve Approach*. In *Nordic Wind Power Conference, March 1-2 2004*. Gothenburg.

Norton, M., Jones, M. B., Walloe, L., Wijkman, A., Schink, B., & Novo, F. (2019). Serious mismatches continue between science and policy in forest bioenergy, (May), 1–8. doi:10.1111/gcbb.12643

NREL. (2017). Concentrating Solar Power Projects: SolarPACES Project. Retrieved 30 September 2017, from https://www.nrel.gov/csp/solarpaces/

Obersteiner, M., Bednar, J., Wagner, F., Gasser, T., Ciais, P., Forsell, N., … Schmidt-Traub, G. (2018). How to spend a dwindling greenhouse gas budget. *Nature Climate Change*, *8*(1), 7–10. doi:10.1038/s41558-017-0045-1

Ocker, F., & Ehrhart, K. M. (2017). The "German Paradox" in the balancing power markets. *Renewable and Sustainable Energy Reviews*, *67*, 892–898. doi:10.1016/j.rser.2016.09.040

Olauson, J., Bladh, J., Lönnberg, J., & Bergkvist, M. (2016). A New Approach to Obtain Synthetic Wind Power Forecasts for Integration Studies. *Energies*, *9*(10), 800. doi:10.3390/en9100800

Olivier, J., & Peters, J. (2018). *Trends in global CO2 and total greenhouse gas emissions: 2018 report*. *PBL*. The Hague. Retrieved from https://www.pbl.nl/en/publications/trends-in-global-co2-and-total-greenhouse-gas-emissions-2018-report

Omie. (2017). *Price Report 2017*. Retrieved from http://m.omie.es/files/dipticoVIGENTEen.pdf

Omie. (2019a). Annual report. Retrieved 22 December 2019, from http://www.omel.es/en/home/publications/annual-report

Omie. (2019b). Interannual scope, daily market minimum, average and maximum price. Retrieved 23 November 2019, from http://m.omie.es/reports/index.php?m=yes&report_id=411

Ordnance Survey. (2016). Ordnance Survey: Britain's mapping agency. Retrieved 20 March 2016, from https://www.ordnancesurvey.co.uk/

Ordóñez, J., Jadraque, E., Alegre, J., & Mart??nez, G. (2010). Analysis of the photovoltaic solar energy capacity of residential rooftops in Andalusia (Spain). *Renewable and Sustainable Energy Reviews*, *14*(7), 2122–2130. doi:10.1016/j.rser.2010.01.001

Orita, S. (2013). *District Heating in Germany: 2013 Survey*. Frankfurt am Main: National District Heating Association. Retrieved from https://dbdh.dk/download/member_area/focus_groups/focus_group_germany/GERMANY.pdf

Ortner, A., & Totschnig, G. (2019). The future relevance of electricity balancing markets in Europe - A 2030 case study. *Energy Strategy Reviews*, *24*(January), 111–120. doi:10.1016/j.esr.2019.01.003

Panos, E., & Lehtilä, A. (2016). *Dispatching and unit commitment features in TIMES*. IEA-ETSAP. Retrieved from https://iea-etsap.org/docs/TIMES_Dispatching_Documentation.pdf

Papaefthymiou, G., & Dragoon, K. (2016). Towards 100% renewable energy systems: Uncapping power system flexibility. *Energy Policy*, *92*, 69–82. doi:10.1016/j.enpol.2016.01.025

Papaefthymiou, G., Grave, K., & Dragoon, K. (2014). *Flexibility options in electricity systems*. Berlin: Ecofys. Retrieved from https://www.ecofys.com/files/files/ecofys-eci-2014-flexibility-options-in-electricity-systems.pdf

Paraschiv, F., Erni, D., & Pietsch, R. (2014). The impact of renewable energies on EEX day-ahead electricity prices. *Energy Policy*, *73*, 196–210. doi:10.1016/j.enpol.2014.05.004

Parsons Brinckerhoff. (2012). *Electricity Transmission Costing Study*. Surrey: Parsons Brinckerhoff. Retrieved from https://www.atvinnuvegaraduneyti.is/media/fylgigogn-raflinur-i-jord/9-Transmission-report.pdf

Pasaoglu, G., Fiorello, D., Zani, L., Martino, A., Zubaryeva, A., & Thiel, C. (2013). *Projections for Electric Vehicle Load Profiles in Europe Based on Travel Survey Data Contact information*. Petten: European Commission Joint Research Centre. https://doi.org/10.2790/24108

Pegels, A., & Lütkenhorst, W. (2014). Is Germany's energy transition a case of successful green industrial policy? Contrasting wind and solar PV. *Energy Policy*, *74*(8225), 522–534. doi:10.1016/j.enpol.2014.06.031

Pereira, J., Ferreira, R. A., Adespa, I., & Martins, A. (2014). *Optimizing the Renewable Generation Mix in the Portuguese Power System based on Temporal and Spatial Diversity*. In *11th International Conference on the European Energy Market (EEM)*. Krakow: 28-30 May 2014: IEEE. doi:10.1109/EEM.2014.6861292

Perpiña Castillo, C., Batista e Silva, F., & Lavalle, C. (2016). An assessment of the regional potential for solar power generation in EU-28. *Energy Policy*, *88*, 86–99. doi:10.1016/j.enpol.2015.10.004

Persson, U., & Werner, S. (2015). *Stratego Project. Quantifying the Heating and Cooling Demand in Europe. WP 2. Background Report 4. Project No: IEE/13/650*. Halmstad: Stratego Project. Retrieved from http://heatroadmap.eu/resources/STRATEGO/STRATEGO WP2 - Background Reports - Combined.pdf

Petitet, M., Finon, D., & Janssen, T. (2017). Capacity adequacy in power markets facing energy transition: A comparison of scarcity pricing and capacity mechanism. *Energy Policy*, *103*(May 2016), 30–46. doi:10.1016/j.enpol.2016.12.032

Pfenninger, S., & Staffell, I. (2016). Long-term patterns of European PV output using 30 years of validated hourly reanalysis and satellite data. *Energy*, *114*. doi:10.1016/j.energy.2016.08.060

Pfluger, B., Sensfuß, F., Schubert, G., & Leisentritt, J. (2011). *Tangible ways towards climate protection in the European Union (EU Long-term scenarios 2050)*. Karlsruhe: Fraunhofer ISI. Retrieved from http://www.isi.fraunhofer.de/isi-media/docs/x/de/publikationen/Final_Report_EU-Long-term-scenarios-2050_FINAL.pdf

Philipsen, R., Morales-España, G., de Weerdt, M., & de Vries, L. (2019). Trading power instead of energy in day-ahead electricity markets. *Applied Energy*, *233–234*(November 2018), 802–815. doi:10.1016/j.apenergy.2018.09.205

Pikk, P., & Viiding, M. (2013). The dangers of marginal cost based electricity pricing. *Baltic Journal of Economics*, *13*(1), 49–62. doi:10.1080/1406099X.2013.10840525

Pilavachi, P. A., Stephanidis, S. D., Pappas, V. A., & Afgan, N. H. (2009). Multi-criteria evaluation of hydrogen and natural gas fuelled power plant technologies. *Applied Thermal Engineering*, *29*(11–12), 2228–2234. doi:10.1016/j.applthermaleng.2008.11.014

Plessmann, G., & Blechinger, P. (2017). How to meet EU GHG emission reduction targets? A model based decarbonization pathway for Europe's electricity supply system until 2050. *Energy Strategy Reviews*, *15*, 19–32. doi:10.1016/j.esr.2016.11.003

Polish Ministry of Economy. (2011). *Polish Nuclear Power Program*. Warsaw. Retrieved from http://www.ym.fi/download/noname/%7B115FC134-5AE7-41DF-A430-5B70624D9D00%7D/30841

Pollitt, M., & Chyong, C. K. (2018). *Europe's electricity market design - 2030 and beyond*. Brussels: Centre on Regulation in Europe. Retrieved from https://www.cerre.eu/sites/cerre/files/181206_CERRE_MarketDesign_FinalReport.pdf

Port of Rotterdam. (2017). ROAD project to be cancelled, CCS to continue. Retrieved 7 December 2019, from https://www.portofrotterdam.com/en/news-and-press-releases/road-project-to-be-cancelled-ccs-to-continue

Potomac Economics. (2018). *2017 State of the market report for the ERCOT electricity markets*. https://www.potomaceconomics.com/wp-content/uploads/2018/05/2017-State-of-the-Market-Report.pdf. Retrieved from https://www.potomaceconomics.com/wp-content/uploads/2018/05/2017-State-of-the-Market-Report.pdf

Poudineh, R., & Jamasb, T. (2012). Smart Grids and Energy Trilemma of Affordability, Reliability and Sustainability: The Inevitable Paradigm Shift in Power Sector. USAEE Working Paper No. 2111643. *SSRN Electronic Journal*. doi:10.2139/ssrn.2111643

Poudineh, R., & Peng, D. (2017). *Electricity market design for a decarbonised future*. Oxford, United Kingdom: Oxford Institute for Energy Studies. https://doi.org/10.26889/9781784670948

Pour, N., Webley, P. A., & Cook, P. J. (2018). Opportunities for application of BECCS in the Australian power sector. *Applied Energy*, *224*(April), 615–635. doi:10.1016/j.apenergy.2018.04.117

PwC, PIK, IIASA, & ECF. (2010). *100% renewable electricity: a roadmap to 2050 for Europe and North Africa*. London: PricewaterhouseCoopers LLP, Potsdam Institute for Climate Impact Research, International Institute for Applied Systems Analysis, European Climate Forum. Retrieved from http://www.pwc.co.uk/assets/pdf/100-percent-renewable-electricity.pdf

Rahbari, O., Vafaeipour, M., Fazelpour, F., Feidt, M., & Rosen, M. A. (2014). Towards realistic designs of wind farm

layouts: Application of a novel placement selector approach. *Energy Conversion and Management*, *81*, 242–254. doi:10.1016/j.enconman.2014.02.010

Rauner, S., Eichhorn, M., & Thrän, D. (2016). The spatial dimension of the power system: Investigating hot spots of Smart Renewable Power Provision. *Applied Energy*. doi:10.1016/j.apenergy.2016.07.031

Reichenberg, L., Johnsson, F., & Odenberger, M. (2014). Dampening variations in wind power generation—the effect of optimizing geographic location of generating sites. *Wind Energy*, *17*(April 2013), 1631–1643. doi:10.1002/we.1657

Reindl, D. T., Beckman, W. A., & Duffie, J. A. (1990). Evaluation of hourly tilted surface radiation models. *Solar Energy*, *45*(1), 9–17. doi:10.1016/0038-092X(90)90061-G

Rezkalla, M., Pertl, M., & Marinelli, M. (2018). Electric power system inertia: requirements, challenges and solutions. *Electrical Engineering*, *100*(4), 2677–2693. doi:10.1007/s00202-018-0739-z

Rienecker, M. M., Suarez, M. J., Gelaro, R., Todling, R., Bacmeister, J., Liu, E., … Woollen, J. (2011). MERRA: NASA's Modern-Era Retrospective Analysis for Research and Applications. *Journal of Climate*, *24*(14), 3624–3648. doi:10.1175/JCLI-D-11-00015.1

Riesz, J., & Milligan, M. (2015). Designing electricity markets for a high penetration of variable renewables. *Wiley Interdisciplinary Reviews: Energy and Environment*, *4*(3), 279–289. doi:10.1002/wene.137

Ringler, P., Keles, D., & Fichtner, W. (2017). How to benefit from a common European electricity market design. *Energy Policy*, *101*(May 2016), 629–643. doi:10.1016/j.enpol.2016.11.011

Rivas, R. A., Clausen, J., Hansen, K. S., & Jensen, L. E. (2009). Solving the Turbine Positioning Problem for Large Offshore Wind Farms by Simulated Annealing. *Wind Engineering*, *33*(3), 287–297. doi:10.1260/0309-524X.33.3.287

Röder, M., Whittaker, C., & Thornley, P. (2014). How certain are greenhouse gas reductions from bioenergy? Life cycle assessment and uncertainty analysis of wood pellet-to-electricity supply chains from forest residues. *Biomass and Bioenergy*, *79*, 50–63. doi:10.1016/j.biombioe.2015.03.030

Rodrigues, S., Restrepo, C., Kontos, E., Teixeira Pinto, R., & Bauer, P. (2015). Trends of offshore wind projects. *Renewable and Sustainable Energy Reviews*, *49*, 1114–1135. doi:10.1016/j.rser.2015.04.092

Rodríguez, R. a., Becker, S., Andresen, G. B., Heide, D., & Greiner, M. (2014). Transmission needs across a fully renewable European power system. *Renewable Energy*, *63*, 467–476. doi:10.1016/j.renene.2013.10.005

Rogelj, J., Shindell, D., Jiang, K., Fifita, S., Forster, P., Ginzburg, V., … Vilariño, M. V. (2018). Mitigation pathways compatible with 1.5°C in the context of sustainable development. In *Global warming of 1.5°C. An IPCC Special Report on the impacts of global warming of 1.5°C above pre-industrial lGlobal warming of 1.5°C. An IPCC Special Report on the impacts of global warming of 1.5°C above pre-industrial levels and related global greenh*. Cambridge, United Kingdom and New York, NY, USA: Cambridge University Press. Retrieved from https://www.ipcc.ch/sr15/

Rohlfs, W., & Madlener, R. (2010). *Cost Effectiveness of Carbon Capture-Ready Coal Power Plants with Delayed Retrofit. FCN Working Paper No. 8/2010.* Aachen,: Institute for Future Energy Consumer Needs and Behavior, RWTH Aachen University. Retrieved from https://www.fcn.eonerc.rwth-aachen.de/global/show_document.asp?id=aaaaaaaaaagvvdz

Roos, A., & Bolkesjø, T. F. (2018). Value of demand flexibility on spot and reserve electricity markets in future power system with increased shares of variable renewable energy. *Energy*, *144*, 207–217. doi:10.1016/j.energy.2017.11.146

RTE. (2018). Installed capacity of units above 1 MW, aggregated per production type. Retrieved 20 August 2018, from https://www.services-rte.com/en/view-data-published-by-rte/production-installed-capacity.html

RTE. (2019). Procured reserves. Retrieved 13 October 2019, from https://clients.rte-france.com/lang/an/visiteurs/vie/reserve_ajustement.jsp

Ruiz, P., Sgobbi, A., Nijs, W., Longa, F. D., & Kober, T. (2015). *The JRC-EU-TIMES model . Bioenergy potentials for EU and*

neighbouring countries. Petten: European Commission Joint Research Centre. https://doi.org/10.2790/39014

Saba, S. M., Müller, M., Robinius, M., & Stolten, D. (2018). The investment costs of electrolysis – A comparison of cost studies from the past 30 years. *International Journal of Hydrogen Energy*, *43*(3), 1209–1223. doi:10.1016/j.ijhydene.2017.11.115

Sanchez, D. L., Nelson, J. H., Johnston, J., Mileva, A., & Kammen, D. M. (2015). Biomass enables the transition to a carbon-negative power system across western North America. *Nature Climate Change*, *5*(February), 3–7. doi:10.1038/nclimate2488

Santos-Alamillos, F. J., Pozo-Vázquez, D., Ruiz-Arias, J. A., Lara-Fanego, V., & Tovar-Pescador, J. (2014). A methodology for evaluating the spatial variability of wind energy resources: Application to assess the potential contribution of wind energy to baseload power. *Renewable Energy*, *69*, 147–156. doi:10.1016/j.renene.2014.03.006

Santos-Alamillos, F. J., Pozo-Vázquez, D., Ruiz-Arias, J. A., Von Bremen, L., & Tovar-Pescador, J. (2015). Combining wind farms with concentrating solar plants to provide stable renewable power. *Renewable Energy*, *76*, 539–550. doi:10.1016/j.renene.2014.11.055

Scarlat, N., Martinov, M., & Dallemand, J. F. (2010). Assessment of the availability of agricultural crop residues in the European Union: Potential and limitations for bioenergy use. *Waste Management*, *30*(10), 1889–1897. doi:10.1016/j.wasman.2010.04.016

Schaber, K., Steinke, F., Mühlich, P., & Hamacher, T. (2012). Parametric study of variable renewable energy integration in Europe: Advantages and costs of transmission grid extensions. *Energy Policy*, *42*, 498–508. doi:10.1016/j.enpol.2011.12.016

Scharff, R., & Amelin, M. (2016). Trading behaviour on the continuous intraday market Elbas. *Energy Policy*, *88*, 544–557. doi:10.1016/j.enpol.2015.10.045

Schlachtberger, D. P., Brown, T., Schramm, S., & Greiner, M. (2017). The benefits of cooperation in a highly renewable European electricity network. *Energy*, *134*, 469–481. doi:10.1016/j.energy.2017.06.004

Schmid, E., & Knopf, B. (2015). Quantifying the long-term economic benefits of European electricity system integration. *Energy Policy*, *87*, 260–269. doi:10.1016/j.enpol.2015.09.026

Schmidt, O., Hawkes, A., Gambhir, A., & Staffell, I. (2017). The future cost of electrical energy storage based on experience rates. *Nature Energy*, *6*(July), 17110. doi:10.1038/nenergy.2017.110

Schneider, M., & Froggatt, A. (2018). *The World Nuclear Industry: Status Report 2018*. Paris, London: A Mycle Schneider Consulting Project. Retrieved from https://www.worldnuclearreport.org/IMG/pdf/20180902wnisr2018-hr.pdf

Scholten, D., & Bosman, R. (2016). The geopolitics of renewables; exploring the political implications of renewable energy systems. *Technological Forecasting and Social Change*, *103*, 273–283. doi:10.1016/j.techfore.2015.10.014

Schwele, A., Kazempour, J., & Pinson, P. (2019). Do unit commitment constraints affect generation expansion planning? A scalable stochastic model. *Energy Systems*. doi:10.1007/s12667-018-00321-z

Sepulveda, N. A., Jenkins, J. D., de Sisternes, F. J., & Lester, R. K. (2018). The Role of Firm Low-Carbon Electricity Resources in Deep Decarbonization of Power Generation. *Joule*, 1–18. doi:10.1016/j.joule.2018.08.006

Settele, J., Scholes, R., Betts, R. A., Bunn, S., Leadley, P., Nepstad, D., … Taboada, M. A. (2014). Terrestrial and Inland Water Systems. In C. B. Field, V. R. Barros, D. J. Dokken, K. J. Mach, M. D. Mastrandrea, T. Bilir, … L. L. White (Eds.), *Climate Change 2014 Impacts, Adaptation, and Vulnerability. Part A: Global and Sectoral Aspects. Contribution of Working Group II to the Fifth Assessment Report of the Intergovernmental Panel on Climate Change* (pp. 271–359). Cambridge, UK and New York, NY, USA: Cambridge University Press. doi:10.1017/CBO9781107415379.009

Shell. (2016). Stones | Shell Global. Retrieved 29 November 2016, from http://www.shell.com/about-us/major-projects/stones.html

Sheppard, K., Khrapov, S., Lipták, G., Capellini, R., esvhd, Hugle, … jbrockmendel. (2019, March 28). bashtage/arch: Release 4.8.1. doi:10.5281/ZENODO.2613877

Short, W., & Diakov, V. (2014). Matching Western US electricity consumption with wind and solar resources. *Wind Energy*, *16*(April 2013), 491–500. doi:10.1002/we.1513

Siemens AG. (n.d.). *Silyzer 300*. Retrieved from https://www.siemens.com/content/dam/webassetpool/mam/tag-siemens-com/smdb/corporate-core/sustainable_energy/hydrogensolutions/broschüren/ct-ree-18-047-db-silyzer-300-db-de-en-rz.pdf

Siemens AG. (2014). *Power Engineering Guide Edition 7.1*. Erlagen. Retrieved from http://dl.icdst.org/pdfs/files/e1805e090304a2d19c352fa18e52db47.pdf

Silva, J., Ribeiro, C., & Guedes, R. (2007). *Roughness length classification of Corine Land Cover Classes*. In *Proceedings of the European Wind Energy Conference* (Vol. 710). Milan. doi:10.1017/CBO9781107415324.004

SKM. (2012). *Calculating Target Availability Figures for HVDC Interconnectors*. Newcastle upon Tyne: Sinclair Knight Merz. Retrieved from https://www.ofgem.gov.uk/ofgem-publications/59247/skm-report-calculating-target-availability-figures-hvdc-interconnectors.pdf

Skovsgaard, L., & Jacobsen, H. K. (2017). Economies of scale in biogas production and the significance of flexible regulation. *Energy Policy*, *101*(November 2016), 77–89. doi:10.1016/j.enpol.2016.11.021

Śliż-Szkliniarz, B. (2012). *Energy Planning in Selected European Regions*. (PhD thesis, Karlsruher Institut für Technologie), Karlsruhe. Retrieved from https://publikationen.bibliothek.kit.edu/1000031312

Smith, P., Hamsik, M. R., Siikamäki, J. V., Gopalakrishna, T., Delgado, C., Houghton, R. A., … Silvius, M. (2017). Natural climate solutions. *Proceedings of the National Academy of Sciences*, *114*(44), 11645–11650. doi:10.1073/pnas.1710465114

SolarPower Europe. (2019). EU Solar Market Grows 36% in 2018. Retrieved 24 April 2019, from http://www.solarpowereurope.org/eu-solar-market-grows-36-in-2018/

Soria, R., Portugal-Pereira, J., Szklo, A., Milani, R., & Schaeffer, R. (2015). Hybrid concentrated solar power (CSP)-biomass plants in a semiarid region: A strategy for CSP deployment in Brazil. *Energy Policy*, *86*(March 2014), 57–72. doi:10.1016/j.enpol.2015.06.028

Staffell, I., & Pfenninger, S. (2016). Using bias-corrected reanalysis to simulate current and future wind power output. *Energy*, *114*. doi:10.1016/j.energy.2016.08.068

Statoil. (2015). Statoil to build the world's first floating wind farm: Hywind Scotland. Retrieved 13 May 2016, from http://www.statoil.com/en/NewsAndMedia/News/2015/Pages/03Nov_HywindScotland_news_page.aspx

Steinke, F., Wolfrum, P., & Hoffmann, C. (2013). Grid vs. storage in a 100% renewable Europe. *Renewable Energy*, *50*, 826–832. doi:10.1016/j.renene.2012.07.044

Steurer, R., & Hametner, M. (2013). Objectives and Indicators in Sustainable Development Strategies: Similarities and Variances across Europe. *Sustainable Development*, *21*(4), 224–241. doi:10.1002/sd.501

Strunz, S., Gawel, E., & Lehmann, P. (2014). On the alleged need to strictly europeanise the german energiewende. *Intereconomics*, *49*(5), 244–250. doi:10.1007/s10272-014-0507-x

Sugiyama, M. (2012). Climate change mitigation and electrification. *Energy Policy*, *44*, 464–468. doi:10.1016/j.enpol.2012.01.028

Sun, Q., Li, H., Yan, J., Liu, L., Yu, Z., & Yu, X. (2015). Selection of appropriate biogas upgrading technology-a review of biogas cleaning, upgrading and utilisation. *Renewable and Sustainable Energy Reviews*, *51*, 521–532. doi:10.1016/j.rser.2015.06.029

SunPower. (2014). X-Series Solar Panels. Retrieved 17 September 2016, from https://us.sunpower.com/sites/sunpower/files/media-library/data-sheets/ds-x21-series-335-345-residential-solar-panels-datasheet.pdf

SuperGrid Institute. (2017). Toward deeper submarine cable installations. Retrieved 2 October 2017, from http://www.supergrid-institute.com/en/toward-deeper-submarine-cable-installations

Šúri, M., Huld, T. A., Dunlop, E. D., & Ossenbrink, H. a. (2007). Potential of solar electricity generation in the European Union member states and candidate countries. *Solar Energy*, *81*(10), 1295–1305. doi:10.1016/j.solener.2006.12.007

Swedish Ministry of the Environment and Energy. (2019). *Sweden's draft integrated national energy and climate plan*. Retrieved from https://www.government.se/48ee21/contentassets/e731726022cd4e0b8ffa0f8229893115/swedens-draft-integrated-national-energy-and-climate-plan

Tennet. (2018). *Market review 2017: Electricity market insights*. Arnhem: Tennet. Retrieved from https://www.tennet.eu/fileadmin/user_upload/Company/Publications/Technical_Publications/Dutch/2017_TenneT_Market_Review.pdf

Tennet. (2019). *Annual Market Update 2018*. Arnhem: Tennet. Retrieved from https://www.tennet.eu/fileadmin/user_upload/Company/Publications/Technical_Publications/Dutch/Annual_Market_Update_2018_-_Final.pdf

Thomaidis, N. S., Santos-Alamillos, F. J., Pozo-Vázquez, D., & Usaola-García, J. (2015). Optimal management of wind and solar energy resources. *Computers & Operations Research*, *66*, 284–291. doi:10.1016/j.cor.2015.02.016

Thrän, D., Schaubach, K., Peetz, D., Junginger, M., Mai-Moulin, T., Schipfer, F., … Lamers, P. (2019). The dynamics of the global wood pellet markets and trade – key regions, developments and impact factors. *Biofuels, Bioproducts and Biorefining*, *13*(2), 267–280. doi:10.1002/bbb.1910

Tobin, I., Vautard, R., Balog, I., Bréon, F. M., Jerez, S., Ruti, P. M., … Yiou, P. (2015). Assessing climate change impacts on European wind energy from ENSEMBLES high-resolution climate projections. *Climatic Change*, *128*(1–2), 99–112. doi:10.1007/s10584-014-1291-0

TrinaSolar. (2016). The Tallmax Module. Retrieved 23 September 2016, from http://www.trinasolar.com/HtmlData/downloads/us/US_PD14_Datasheet.pdf

Troen, I., & Lundtang Petersen, E. (1989). *European wind atlas*. Roskilde: RisØ National Laboratory. Retrieved from http://orbit.dtu.dk/files/112135732/European_Wind_Atlas.pdf

Tröster, E., Kuwahata, R., & Ackermann, T. (2011). *European Grid Study 2030 / 2050*. Langen: Energynautics GmbH. Retrieved from http://www.greenpeace.org/eu-unit/Global/eu-unit/reports-briefings/2011 pubs/1/energynautics-grids-study.pdf

Trutnevyte, E. (2016). Does cost optimization approximate the real-world energy transition? *Energy*, *106*. doi:10.1016/j.energy.2016.03.038

Tsiropoulos, I., Tarvydas, D., & Zucker, A. (2018). *Cost development of low carbon energy technologies*. Luxembourg: Publications Office of the European Union. https://doi.org/10.2760/490059

Turner, S. D. O., Romero, D. A., Zhang, P. Y., Amon, C. H., & Chan, T. C. Y. (2014). A new mathematical programming approach to optimize wind farm layouts. *Renewable Energy*, *63*, 674–680. doi:10.1016/j.renene.2013.10.023

UCTE. (2004). UCTE Operation Handbook. Retrieved 24 May 2016, from https://www.entsoe.eu/publications/system-operations-reports/operation-handbook/Pages/default.aspx

UK Government. (2019). UK becomes first major economy to pass net zero emissions law. Retrieved 23 November 2019, from https://www.gov.uk/government/news/uk-becomes-first-major-economy-to-pass-net-zero-emissions-law

UNFCCC. (2017a). Greenhouse Gas Inventory Data. Retrieved 20 July 2017, from http://di.unfccc.int/detailed_data_by_party

UNFCCC. (2017b). The Paris Agreement. Retrieved 8 November 2017, from http://unfccc.int/paris_agreement/items/9485.php

UNFCCC. (2019). History of the Convention | UNFCCC. Retrieved 12 September 2019, from https://unfccc.int/process/the-convention/history-of-the-convention#eq-1

Urgenda. (2014). *Nederland 100% duurzame energie in 2030: het kan als je het wilt!* Urgenda. Retrieved from http://www.urgenda.nl/documents/Urgenda - Rapport Duurzame Energie in 2030 - v2 - 2017.pdf

Vaillancourt, K. (2014). *Electricity Transmission and Distribution. IEA ETSAP - Technology Brief E12*. IEA ETSAP. Retrieved from https://iea-etsap.org/E-TechDS/PDF/E12_el-t&d_KV_Apr2014_GSOK.pdf

van Cappellen, L., Croezen, H., & Rooijers, F. (2018). *Feasibility study into blue hydrogen*. Delft: CE Delft. Retrieved from https://www.cedelft.eu/en/publications/download/2585

van de Putte, J., & Short, R. (2011). *Battle of the Grids*. Amsterdam: Greenpeace. Retrieved from http://www.greenpeace.org/international/Global/international/publications/climate/2011/battle of the grids.pdf

van den Bergh, K., Boury, J., & Delarue, E. (2016). The Flow-Based Market Coupling in Central Western Europe: Concepts and definitions. *The Electricity Journal*, *29*(1), 24–29. doi:10.1016/j.tej.2015.12.004

van den Bergh, K., Bruninx, K., & Delarue, E. (2018). Cross-border reserve markets: network constraints in cross-border reserve procurement. *Energy Policy*, *113*(November 2017), 193–205. doi:10.1016/j.enpol.2017.10.053

van den Broek, M., Ramírez, A., Groenenberg, H., Neele, F., Viebahn, P., Turkenburg, W., & Faaij, A. (2010). Feasibility of storing CO2 in the Utsira formation as part of a long term Dutch CCS strategy: An evaluation based on a GIS/MARKAL toolbox. *International Journal of Greenhouse Gas Control*, *4*(2), 351–366. doi:10.1016/j.ijggc.2009.09.002

van Hertem, D., & Ghandhari, M. (2010). Multi-terminal VSC HVDC for the European supergrid: Obstacles. *Renewable and Sustainable Energy Reviews*, *14*(9), 3156–3163. doi:10.1016/j.rser.2010.07.068

van Leeuwen, C., & Mulder, M. (2018). Power-to-gas in electricity markets dominated by renewables. *Applied Energy*, *232*(October), 258–272. doi:10.1016/j.apenergy.2018.09.217

van Soest, H., den Elzen, M., Forsell, N., Esmeijer, K., & van Vuuren, D. (2018). *Global and Regional Greenhouse Gas Emissions Neutrality: Implications of 1.5 °C and 2 °C scenarios for reaching net zero greenhouse gas emissions*. The Hague: PBL Netherlands Environmental Assessment Agency. Retrieved from https://www.pbl.nl/sites/default/files/downloads/pbl-2018-global-and-regional-greenhouse-gas-emissions-neutrality_2934.pdf

van Vliet, O., van den Broek, M., Turkenburg, W., & Faaij, A. (2011). Combining hybrid cars and synthetic fuels with electricity generation and carbon capture and storage. *Energy Policy*, *39*(1), 248–268. doi:10.1016/j.enpol.2010.09.038

van Vuuren, D. P., Hof, A. F., van Sluisveld, M. A. E., & Riahi, K. (2017). Open discussion of negative emissions is urgently needed. *Nature Energy*, *2*(12), 902–904. doi:10.1038/s41560-017-0055-2

van Vuuren, D. P., Kok, M., Lucas, P. L., Prins, A. G., Alkemade, R., van den Berg, M., … Stehfest, E. (2015). Pathways to achieve a set of ambitious global sustainability objectives by 2050: Explorations using the IMAGE integrated assessment model. *Technological Forecasting and Social Change*, *98*, 303–323. doi:10.1016/j.techfore.2015.03.005

van Wees, J.-D., Boxem, T., Angelino, L., & Dumas, P. (2013). *A prospective study on the geothermal potential in the EU. Deliverable 2.5 of the GEOELEC project*. Brussels: TNO, EGEC. Retrieved from http://www.geoelec.eu/wp-content/uploads/2011/09/D-2.5-GEOELEC-prospective-study.pdf

van Zuijlen, B., Zappa, W., Turkenburg, W., van der Schrier, G., & van den Broek, M. (2018). *Assessment of the Role of CCS in the Provision of Long-Term Security of Power Supply and Deep CO2 Emission Reduction*. In *14th Greenhouse Gas Control Technologies Conference Melbourne 21-26 October 2018 (GHGT-14)*. Melbourne: SSRN.

van Zuijlen, B., Zappa, W., Turkenburg, W., van der Schrier, G., & van den Broek, M. (2019). Cost-optimal reliable power generation in a deep decarbonisation future. *Applied Energy*, *253*(July), 113587. doi:10.1016/j.apenergy.2019.113587

Vasilj, J., Sarajcev, P., & Jakus, D. (2016). Estimating future balancing power requirements in wind–PV power system. *Renewable Energy*, *99*, 369–378. doi:10.1016/j.renene.2016.06.063

Västermark, K., Hofmann, M., & Bergmann, E. (2015). *A European Energy-Only Market in 2030: Analysis report*. Oslo: Statnett. Retrieved from http://www.statnett.no/Documents/Nyheter_og_media/Nyhetsarkiv/2016/EOM-report_revised_april2016.pdf

Vattenfall. (2017). *Vattenfall Heat – Power Climate Smarter Living*. Retrieved from https://group.vattenfall.com/contentassets/da563d31cf814e8a901c3e6dd66c88b3/corporate/investors/investor_presentations/170508_heat_london_10may.pdf

Vázquez Hernández, C., Telsnig, T., & Villalba Pradas, A. (2017). *JRC Wind Energy Status Report 2016 Edition. EUR 28530 EN*. Petten: European Commission Joint Research Centre. https://doi.org/10.2760/332535

Veldman, E., Gibescu, M., Slootweg, H. J. G., & Kling, W. L. (2013). Scenario-based modelling of future residential electricity demands and assessing their impact on distribution grids. *Energy Policy*, *56*, 233–247. doi:10.1016/j.enpol.2012.12.078

VVA, Copenhagen Economics, Neon, & Deloitte. (2018). *Study on the quality of electricity market data of transmission system operators, electricity supply disruptions, and their impact on the European electricity markets*. Brussels: European Commission. Retrieved from https://ec.europa.eu/energy/sites/ener/files/documents/dg_ener_electricity_market_data_-_final_report_-_22032018.pdf

Wagner, F. (2014). Electricity by intermittent sources: An analysis based on the German situation 2012. *European Physical Journal Plus*, *129*, 1–18. doi:10.1140/epjp/i2014-14020-8

Ward, A. (2017, May 18). Nuclear plant nears completion after huge delays (May 18, 2017). *Financial Times*. Retrieved from https://www.ft.com/content/36bee56a-3a01-11e7-821a-6027b8a20f23

Weber, C., Meibom, P., Barth, R., & Brand, H. (2009). WILMAR: A Stochastic Programming Tool to Analyze the Large-Scale Integration of Wind Energy. In J. Kallrath, P. M. Pardalos, S. Rebennack, & M. Scheidt (Eds.), *Optimization in the energy industry* (pp. 437–460). Springer.

Welsch, M., Deane, P., Howells, M., O Gallachóir, B., Rogan, F., Bazilian, M., & Rogner, H. H. (2014). Incorporating flexibility requirements into long-term energy system models - A case study on high levels of renewable electricity penetration in Ireland. *Applied Energy*, *135*, 600–615. doi:10.1016/j.apenergy.2014.08.072

Werner, S. (2016). *European District Heating Price Series*. Retrieved from https://energiforskmedia.blob.core.windows.net/media/21926/european-district-heating-price-series-energiforskrapport-2016-316.pdf

Widén, J. (2011). Correlations between large-scale solar and wind power in a future scenario for Sweden. *IEEE Transactions on Sustainable Energy*, *2*(2), 177–184.

Widén, J., Carpman, N., Castellucci, V., Lingfors, D., Olauson, J., Remouit, F., … Waters, R. (2015). Variability assessment and forecasting of renewables: A review for solar, wind, wave and tidal resources. *Renewable and Sustainable Energy Reviews*, *44*, 356–375. doi:10.1016/j.rser.2014.12.019

Widiss, R., & Porter, K. (2014). *A Review of Variable Generation Forecasting in the West*. Golden, Colerado. Retrieved from https://www.nrel.gov/docs/fy14osti/61035.pdf

Wohland, J., Reyers, M., Weber, J., & Witthaut, D. (2017). More homogeneous wind conditions under strong climate change decrease the potential for inter-state balancing of electricity in Europe. *Earth System Dynamics*, *8*(4), 1047–1060. doi:10.5194/esd-8-1047-2017

World Nuclear Association. (2018). Nuclear Power in France. Retrieved 8 May 2019, from http://www.world-nuclear.org/information-library/country-profiles/countries-a-f/france.aspx

World Nuclear News. (2018). Belgium maintains nuclear phase-out policy. Retrieved from http://www.world-nuclear-news.org/NP-Belgium-maintains-nuclear-phase-out-policy-0404184.html

WWF. (2013). *The energy report: 100% Renewable Energy by 2050*. Gland: World Wild Fund for Nature. Retrieved from https://www.ecofys.com/files/files/ecofys-wwf-2011-the-energy-report.pdf

Wynn, G. (2018). *Power-Industry Transition, Here and Now Wind and Solar Won't Break the Grid: Nine Case Studies*. Retrieved from http://ieefa.org/wp-content/uploads/2018/02/Power-Industry-Transition-Here-and-Now_February-2018.pdf

Yan, R. F., Saha, T. K., Modi, N., Masood, N. A., & Mosadeghy, M. (2015). The combined effects of high penetration of wind and PV on power system frequency response. *Applied Energy*, *145*, 320–330. doi:10.1016/j.apenergy.2015.02.044

Yildiz, E., Dersch, J., Rau, C., Schmidt, N., & Heide, S. (2017). *CSPBankability Project Report: Draft for an Appendix D - Power Block to the SolarPACES Guideline for Bankable STE Yield Assessment*. Retrieved from http://www.dlr.de/sf/Portaldata/73/Resources/dokumente/linienfokusssyst/cspbank-solarpaces-guideline/CSPBankProjectReport_Draft_for_AppendixD_PowerBlock_170109.pdf

Zappa, W., Junginger, M., & van den Broek, M. (2019). Is a 100% renewable European power system feasible by 2050? *Applied Energy*, *233–234*(November 2018), 1027–1050. doi:10.1016/j.apenergy.2018.08.109

Zappa, W., & van den Broek, M. (2018). Analysing the potential of integrating wind and solar power in Europe using spatial optimisation under various scenarios. *Renewable and Sustainable Energy Reviews*, *94*(May), 1192–1216. doi:10.1016/j.rser.2018.05.071

Zero Emissions Platform. (2011). *The costs of CO2 capture, transport and storage: post-demonstration CCS in the EU*. Zero Emissions Platform. Retrieved from https://hub.globalccsinstitute.com/sites/default/files/publications/17011/costs-co2-capture-transport-and-storage.pdf

Zeyringer, M. (2017). *Temporal and spatial explicit modelling of renewable energy systems: modelling variable renewable energy systems to address climate change and universal electricity access*. (PhD thesis, Utrecht University).

Zeyringer, M., Price, J., Fais, B., Li, P. H., & Sharp, E. (2018). Designing low-carbon power systems for Great Britain in 2050 that are robust to the spatiotemporal and inter-annual variability of weather. *Nature Energy*, *3*(5), 395–403. doi:10.1038/s41560-018-0128-x

Zhang, H. L., Baeyens, J., Degrève, J., & Cacères, G. (2013). Concentrated solar power plants: Review and design methodology. *Renewable and Sustainable Energy Reviews*, *22*, 466–481. doi:10.1016/j.rser.2013.01.032

Zhang, J., Florita, A., Hodge, B. M., Lu, S., Hamann, H. F., Banunarayanan, V., & Brockway, A. M. (2015). A suite of metrics for assessing the performance of solar power forecasting. *Solar Energy*, *111*, 157–175. doi:10.1016/j.solener.2014.10.016

Zipp, A. (2017). The marketability of variable renewable energy in liberalized electricity markets – An empirical analysis. *Renewable Energy*, *113*, 1111–1121. doi:10.1016/j.renene.2017.06.072

Zountouridou, E. I., Kiokes, G. C., Chakalis, S., Georgilakis, P. S., & Hatziargyriou, N. D. (2015). Offshore floating wind parks in the deep waters of Mediterranean Sea. *Renewable and Sustainable Energy Reviews*, *51*, 433–448. doi:10.1016/j.rser.2015.06.027

Appendices

.

Appendix A Appendices to Chapter 2

Symbols

β	Plane tilt angle (°)
ρ	Surface albedo (-)
θ	Solar incidence angle (°)
ϕ	Solar zenith angle (°)
A	Left-hand-side constraint coefficient matrix; Anisotropy index (-)
B	Right-hand-side constraint value matrix;
c	Installed generation capacity (MW)
C	Vector containing values of c
CC	Capacity credit (%)
d	Electricity demand (MW, MWh h^{-1})
D	Wind turbine rotor diameter (m)
f	Capacity factor (-)
F	Matrix containing values of f (-)
g	Generation (MW, MWh h^{-1})
G	Irradiance (W m^{-2})
G_{sc}	Solar constant (1366.1 W m^{-2})
H	Wind turbine hub height (m)
k	Sky clearness index (-)
N	Day of the year
PR	Performance ratio (-)
r	Residual demand (MW, MWh h^{-1})
R	Total residual demand (MWh)
R_b	Geometric beam radiation tilt factor (-)
T	Temperature (°C); number of generation technologies

Subscripts

b	beam radiation component
c	country
CLC	Corine land cover class
d	diffuse radiation component
e	equality
g	global radiation
h	horizontal plane
i	vRES generation technology
ieq	inequality
LT	long-term
n	plane normal to the sun
o	extraterrestrial radiation
ST	short-term
t	time step, tilted plane
x	grid cell
y	year

Abbreviations

BEV	Battery electric vehicle
CCS	Carbon capture and storage
CDDA	Common Database on Designated Areas
CLC	Corine Land Cover
COP	Coefficient of performance
CSP	Concentrating solar power
CV	Coefficient of variation
ECF	European Climate Foundation
ECMWF	European Centre for Medium-Range Weather Forecasts
EEA	European Environment Agency
EEZ	Exclusive Economic Zone
ERA-I	European Reanalysis Interim Data
EU	European Union
EV	Electric vehicle
ENTSO-E	European Network of Transmission System Operators for Electricity
FLH	Full load operating hours
HDH	Heating degree hour
HP	Heat pump
IEC	International Electrotechnical Commission
IPCC	Intergovernmental Panel on Climate Change
JRC	Joint Research Centre
LLSQ	Linear least squares
OECD	Organisation for Economic Co-operation and Development
PHEV	Plugin hybrid electric vehicle
PSM	Power system model
PR	Performance ratio
PV	Photovoltaic
SSRD	Downward Surface Solar Radiation
STC	Standard test conditions
RES	Renewable energy source
vRES	Variable renewable energy source

A.1 Capacity factor profiles

Several steps are required to transform the wind speed and solar radiation data into generation and capacity factor profiles. These are explained in detail in the following sections.

Onshore & Offshore Wind

For determining wind farm production the most relevant data provided by the ERA-I dataset are the 3-hourly east-west (u) and north-south (v) surface (10 m) wind speed components which are used to calculate the effective horizontal wind speed (w) using Eq. (A-1).

$$w = \sqrt{u^2 + v^2} \tag{A-1}$$

To estimate wind farm generation profiles, wind turbine hub heights need to be assumed for both onshore and offshore wind. For onshore wind in Europe there is a clear trend towards installing taller towers for two main reasons i) wind speed increases more rapidly with height in high-surface roughness onshore locations than in offshore locations with smooth water surfaces, and ii) taller towers allow larger diameter rotors to be employed which can capture more energy at lower wind speeds (Fraunhofer IWES, 2016; Lacal-Arántegui & Serrano González, 2015). For example, the average rotor diameter of newly installed onshore wind turbines in Germany increased from 58 m in 2000 up to 109 m in 2016 (88%), while the mean hub height of new turbines increased from 71 m to 128 m (80%) over the same period (Fraunhofer IWES, 2016). Increases in offshore hub heights have been more modest rising from 64 m in 2000 to 89 m (40%) in 2013, with rotor diameter increasing from 75 m to 117 m (56%) over the same period. Ultimately the choice of wind turbine height, blade length and generator type is an economic decision based on trade-offs between faster wind speeds at higher elevations, greater blade swept area, foundation and structural costs, however a detailed optimisation of all these factors is beyond the scope of this study. Instead, different hub heights are assumed for onshore and offshore wind. For onshore wind sites a 150 m hub height is assumed (17% higher than the average for turbines installed in 2015) in the expectation that onshore hub heights will continue to increase as investment costs decrease over time, shifting the optimum towards higher hub heights[1]. For onshore coastal sites (*coastal* meaning grid cells containing both sea and land) a lower hub height of 100 m is assumed given that these locations tend to have higher wind speeds and high yields can be achieved even with lower hub heights (Fraunhofer IWES, 2016). For offshore wind sites a lower hub height of 100 m is assumed (12% higher than the 2013 average), in the expectation that offshore wind hub heights will not increase substantially as the economic penalties of increased foundation loads and tower cost will are more likely to outweigh any small energy gains from a much increased hub height, since the increase of wind speed with height is generally more pronounced in low-wind locations with high surface roughness (Lacal-Arántegui & Serrano González, 2015).

For both turbine types the horizontal wind speed at 10 m is extrapolated to hub height assuming a logarithmic vertical wind speed profile using Eq. (A-2) where w_{ref} is the horizontal wind speed (m s^{-1}) at known reference height H_{ref} (m), H is the height to which wind speed is extrapolated (m) and z_0 is the surface roughness length (m) (Manwell et al., 2009).

$$w = \frac{\ln\left(\frac{H}{z_0}\right)}{\ln\left(\frac{H_{ref}}{z_0}\right)} w_{ref} \quad \text{(A-2)}$$

In this study the roughness length for all onshore locations is assumed to be a constant value of 0.03 m, typical for natural grasslands and agricultural pastures (Troen & Lundtang Petersen, 1989). As onshore wind suitability is largely restricted to these land types, this is considered a reasonable simplification. For offshore locations a roughness length of 0.0001 m is assumed corresponding to open water (Silva et al., 2007; Troen & Lundtang Petersen, 1989). For each location the long-term mean wind speed at hub height is calculated from all available years of weather data and on this basis each onshore location is classified according to the IEC 61400 guidelines as either IEC class I (≥8.5 and <10 m s^{-1}), class II (≥7.5 and <8.5 m s^{-1}), class III (≥6 and <7.5 m s^{-1}) or class IV wind site (<6 m s^{-1}). Based on the wind class for each site, the hourly wind speeds are converted to wind turbine electric power output using power curves from three wind turbines with the same nominal output (3.3 MW) but designed for each of the three different wind classes (Class 1: Vestas V105-3.3MW Ia, Class II: Vestas V117-3.3MW IIa, Class III: Vestas V126-3.3MW IIIa. For locations with wind class 0 (higher than I), the IEC I curve is applied. For sites with class IV no equivalent power curve for a class IV turbine could be found and so the IEC III curve is applied. For offshore sites, the Vestas V164-8.0 IEC S turbine is applied. The multi-turbine method of Holttinen (Norgaard & Holttinen, 2004) is used to take into account spatial and temporal variations in wind speeds which occur across wind farms so that aggregated power curves better match wind farm generation profiles in reality. Using this approach, wind speeds at hub height for each location are first smoothed temporally using a moving-average based on a wind propagation time, calculated from the long-term average (36 year) hourly wind speed and a representative dimension based on the average ERA-I grid size. The single turbine power curves are subsequently convoluted using a normal distribution based on the long-term standard deviation in hourly wind speed for each location. After accounting for turbine wake losses (8%), electrical conversion (2%) and other losses (3%) in accordance with values taken from the literature (McKenna et al., 2014; Myhr et al., 2014; Rivas et al., 2009), the power output values for each site are converted to hourly capacity factors by dividing by the nominal turbine output. The effect of temperature and elevation on air density and subsequent effects on power output are not considered. The base onshore power curves and an example of a convoluted curve for an IEC I turbine shown in Figure A-1.

Table A-1 | IEC 61400-1 Wind Classes (International Electrotechnical Commission, 2005). Given the lack of sub-hourly data, we make no distinction between high and low turbulence wind sites.

Annual average wind speed at hub height (m s^{-1})	IEC Wind Class
10	I
8.5	II
7.5	III
6	IV

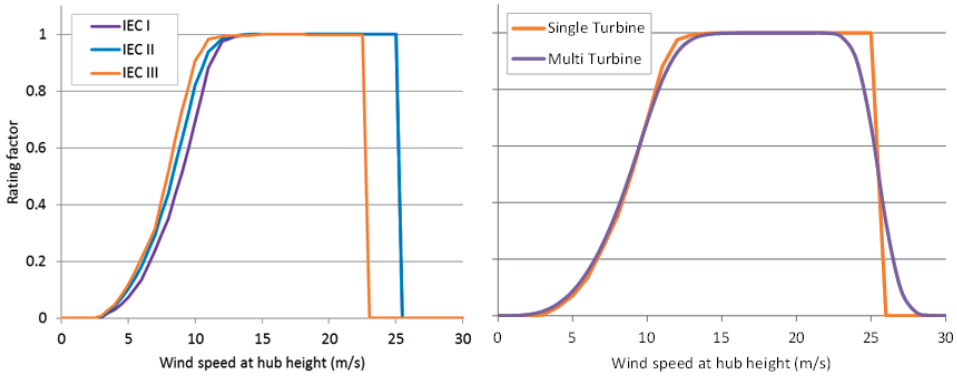

Figure A-1 | Wind turbine power curves applied. The left figure shows the raw single turbine power curves. The right figure shows the IEC I curve before and after convolution.

Rooftop and Utility PV

For determining PV production, the most relevant data provided by the ERA-I dataset is the accumulated SSRD flux forecast, which is the sum of the global (total of direct and diffuse) radiant energy (in J m^{-2}) passing through a square-metre of a flat horizontal plane since the start of the forecast period. Forecasts are available every three hours from 0:00 and 12:00. Thus the value reported for each 3-hour time step is the accumulated radiation[2]. As PV production is based on instantaneous irradiation (in W m^{-2}), to estimate hourly PV production and ultimately capacity factor profiles for an arbitrary inclined plane from the ERA-I accumulated SSRD data requires several intermediate steps:

- The 3-hour accumulated radiation from 0:00 and 12:00 is converted to the accumulated irradiation from the previous time step (J m^{-2})
- Total accumulated irradiation in each three-hour period is divided by the number of seconds in the period to determine the average irradiance in that period (W m^{-2})
- As average irradiance is best represented as an instantaneous value in the middle of a period and not at the end, the data is resampled to 30 minutes, shifted by 1.5 hours, and then resampled to hourly values using linear interpolation.
- The resulting global horizontal irradiance $G_{g,h}$ values are then split into their diffuse $G_{d,h}$ and beam (direct) $G_{b,h}$ components using the correlation of Erbs (Erbs et al., 1982) for the ratio of hourly diffuse radiation to the hourly global radiation ($G_{d,h}/G_{g,h}$) by first determining the extra-terrestrial horizontal irradiance in the normal $G_{o,n}$ and horizontal planes $G_{o,h}$, sky clearness index k_t (the ratio of the hourly global irradiance to the hourly extra-terrestrial irradiance) using Eq. (A-3)-(A-6) (Erbs et al., 1982; Kalogirou, 2009).

$$G_{o,n} = G_{sc}\left[1 + 0.033cos\left(\frac{360N}{365}\right)\right] \quad \text{(A-3)}$$

$$G_{o,h} = G_{o,n}\cos\,\phi \quad \text{(A-4)}$$

$$k = G_{g,h}/G_{o,h} \tag{A-5}$$

$$\begin{aligned}
\frac{G_{d,h}}{G_{g,h}} &= 1 - 0.09k && \text{for k} \leq 0.22 \\
\frac{G_{d,h}}{G_{g,h}} &= 0.9511 - 0.1604k + 4.388k^2 - 16.638k^3 \\
&\quad + 12.336k^4 && \text{for } 0.22 < \text{k} \leq 0.8 \\
\frac{G_{d,h}}{G_{g,h}} &= 0.165 && \text{for k} > 0.8
\end{aligned} \tag{A-6}$$

- Finally, the irradiance on the tilted surface of the PV panels is estimated using the tilted surface radiation model of Reindl (Reindl et al., 1990) as outlined below.

Many correlations for estimating global irradiance on tilted panels are available, varying mainly in their treatment of diffuse radiation. For a detailed overview of the topic reader is referred to any good textbook covering solar energy science and engineering (Duffie & Beckman, 2013; Kalogirou, 2009). Several studies have attempted to validate and compare these radiation models with experimental data (Freeman et al., 2013; Mehleri et al., 2010), however there is no consensus on which model performs best as performance varies depending on a number of factors including location and the split between direct and diffuse radiation. In this study, the model of Reindl et al (Reindl et al., 1990) is used as it not only accounts for diffuse isotropic and circumsolar radiation, but also horizontal brightening[3]. As in most diffuse models, ground reflected radiation is treated as isotropic. The Reindl equation is given by Eq. (A-7),

$$\begin{aligned}
G_{g,t} = \left(G_{b,h} + G_{d,h}A\right)R_b + G_{d,h}(1-A)\left(\frac{1+\cos\beta}{2}\right)\left(1 + \sqrt{\frac{G_{b,h}}{G_{b,h}+G_{d,h}}}\sin^3\left(\frac{\beta}{2}\right)\right) \\
+ \left(G_{b,h} + G_{d,h}\right)\rho\left(\frac{1-\cos\beta}{2}\right)
\end{aligned} \tag{A-7}$$

where $G_{g,t}$ is the global irradiance received on a tilted plane (W m^{-2}), $G_{b,h}$ and $G_{d,h}$ are the beam and diffuse radiation components in the horizontal plane respectively (W m^{-2}), R_b is a geometric beam radiation tilt factor equal to the ratio between the cosines of the incidence and zenith angles ($\cos\theta/\cos\phi$), A is an anisotropy index defined as the ratio between beam and extraterrestrial radiation received on a plane normal to the sun ($G_{b,n}/G_{o,n}$), and ρ is the surface albedo (reflectivity). The optimum surface azimuth and tilt angle (β) for PV panels is a topic in itself and depends on the optimum sought. To maximise annual yield in the Northern hemisphere, the generally accepted view is that PV panels should be installed facing true south (Hartner et al., 2015). However, installing panels east or west can be beneficial as PV production in the morning and afternoon can be increased, coinciding with demand and reducing residual load (Hartner et al., 2015). The optimum tilt angle for south-facing panels is reported to range from 30-45° across much of Europe (Hartner et al., 2015; Huld et al., 2012; Šúri et al., 2007). A typical rule of thumb is that panels are installed at a tilt angle equal to the latitude of the site, representing the average solar altitude angle and thus maximizing the direct radiation component, however shadowing from location terrain and surrounding buildings can reduce

direct irradiance making a flatter tilt angle more favourable in mountainous, built-up and high latitude locations (Mehleri et al., 2010; Šúri et al., 2007). Including shadowing from buildings and the landscape is beyond the scope of this study, thus given these uncertainties a single fixed rooftop tilt angle of 35° is used for all locations with all panels mounted true south. In the case of utility PV however where there is greater scope for the installation of tracking systems, two options are considered. The first is with panels oriented due South with a fixed tilt of 35° the same as rooftop PV, while the second includes full two-axis solar tracking. While tracking systems are more expensive than fixed systems, they can achieve higher yields and generate more power in morning and evening periods when demand is high.

Hourly generation profiles from rooftop and utility PV are estimated by combining technical data from two commercially available PV modules with the hourly tilted plain irradiance time series. To reflect a preference for higher efficiency PV modules on rooftops to compensate for space limitations a high-efficiency monocrystalline silicon module is selected for rooftop PV, and a lower-efficiency polycrystalline silicon module is used for utility PV (see Table A-2). Hourly AC output from the PV modules ($P_{AC,t}$) is calculated from Eq. (A-8) where P_{STC} is the nominal module output at standard test conditions (STC[4]) (W) and PR is a performance ratio which takes into account AC conversion and other electrical losses, dust and shading effects, for which a value of 0.9 is assumed in line with the literature (Dierauf et al., 2013; Fraunhofer ISE, 2016). The effect of cell operating temperature ($T_{cell,t}$) on module efficiency is included using the nominal operating cell temperature (T_{NOCT}) (44°C) and power temperature coefficients (δ) taken from the manufacturers data. The cell operating temperature is estimated using Eq. (A-9)-(A-10) where $T_{modback,,t}$ is the PV module back temperature (°C), w_t is the wind speed at 10 m height (m s^{-1}), T_t is the ambient temperature (°C), a and b are empirical convection and heat transfer coefficients, and ΔT_{cond} is a temperature drop due to conduction. The values of these last three parameters vary depending on the module materials and mounting configuration and can be found in (Dierauf et al., 2013).

$$P_{AC,t} = P_{STC}\left(\frac{G_{g,t}}{G_{STC}}\right)\left[1-\delta\left(T_{NOCT}-T_{cell,t}\right)\right]PR \quad \text{(A-8)}$$

$$T_{cell,t} = T_{modback,t}\left(\frac{G_{g,t}}{G_{STC}}\right)\Delta T_{cond} \quad \text{(A-9)}$$

$$T_{modback,t} = G_{g,t}exp^{(a+b*w_t)} + T_t \quad \text{(A-10)}$$

As with onshore and offshore wind, the hourly generation from rooftop and utility PV are converted to capacity factor profiles by dividing by the nominal module output P_{STC}.

Table A-2 | PV module technical specifications

Parameter	Rooftop PV	Utility PV
Manufacturer & model	Sunpower X21-345 (SunPower, 2014)	TrinaSolar TSM-PD14 (TrinaSolar, 2016)
Technology	Monocrystalline Silicon	Polycrystalline Silicon
Nominal power capacity at STC[a], P_{STC} (W)	345	325
Module efficiency (%)	21.5%	16.8%
Power temp coefficient, δ(% °C^{-1})	-0.3%	-0.41%
Module dimensions	1.046 m x 1.559 m (1.63 m^2)	1.956 m x 0.992 m (1.94 m^2)
Nominal power density at STC (W m^{-2})[b]	211	167

[a] Standard Test Conditions: 1000 W m^{-2} irradiance, air mass coefficient 1.5, temperature 25° C

[b] Calculated from module dimensions and nominal panel capacity

A.2 Maximum capacity constraints

Table A-4 lists the CLC classes deemed suitable for each technology, before applying any other limitations such as protected areas or water depths. Onshore wind is assumed to be only suitable for selected agricultural areas and grasslands where turbines could be installed without having a major effect on currently land use. Offshore wind can only be installed on open water in seas or oceans. For ground-based utility PV, we assume that this technology is only suitable in relatively sparse and unforested areas, while we assume rooftop PV can only be built on the roofs of residential and commercial buildings located in urban areas.

For onshore and offshore wind, the constraints on maximum capacity per technology i per grid cell x ($c_{i,x}^{max}$) are calculated using Eq. (A-11) where $A_{CLC,i,x}$ is the land area per suitable CLC class per grid cell (km^2), θ_i is the assumed land availability (%) and $\widehat{p_i}$ is a representative wind farm capacity density.

$$c_{i,x}^{max} = \left(\sum_{CLC} A_{CLC,i,x} \right) \theta_i \widehat{p_i} \qquad \text{(A-11)}$$

For onshore wind, we assume a land availability factor of 6% in line with (Bruninx et al., 2015; Deng et al., 2015), and for offshore wind we assume a uniform 20% availability irrespective of water depth or distance to shore. This is higher than values used for near-shore (< 10 km) sites but at the lower end of values used for sites further offshore (Bruninx et al., 2015; Deng et al., 2015). However, given that many of Europe's best wind sites are located in relatively shallow waters of the North and Baltic seas at sites greater than 10 km from shore (EEA, 2009), we believe a higher value is justified. A comparison of the land (and sea) availability factors found in the literature is given in Table A-3.

The values for $\widehat{p_i}$ vary between 4.2 MW km^{-2} and 6 MW km^{-2} depending on the IEC wind regime in that grid cell, and are based on the wind turbine technical data (rotor diameter and nominal power) assuming a typical wind farm turbine array spacing. Many studies have investigated the optimisation of wind farm turbine layouts with lower turbine spacing

increasing installed capacity density, at the cost of increased array losses due to aerodynamic wake effects between turbines (Eroğlu & Seçkiner, 2013; Rahbari et al., 2014; Turner et al., 2014). However such a detailed treatment is not possible in this study and a simplified approach assuming a regular turbine spacing of 10D x 5D (where D is rotor diameter) is used, with the literature reporting this should result in array losses below 10% (Manwell et al., 2009). Following this assumption, turbine capacity densities of 6, 4.8, 4.2 and 6 MW km^{-2} are calculated for the Vestas V105, V117, V126 onshore turbines and the V164 offshore turbine respectively. Comparing these values with the available literature, a 2009 NREL study of 161 onshore wind farms reported capacities densities ranging from 1.0 to 11.2 MW km^{-2} with an average of 3.0 ± 1.7 MW km^{-2} [8]. In a study published in the same year by the EEA investigating Europe's wind energy potential, capacity densities for onshore wind were given as 8 MW km^{-2} in 2005 and were not expected to change until 2030 (EEA, 2009). The values calculated in this study for the three onshore turbines thus lie within an acceptable range. For offshore wind, the EEA reported a typical capacity density of 10 MW km^{-2} in 2005, which was predicted to rise to 12 MW km^{-2} in 2020 and 15 MW km^{-2} in 2030 based on technology developments (EEA, 2009). Using publicly available data for 40 offshore wind farms installed around the world commissioned between 1991 and 2014 for which both installed capacity and farm area were available, 60% were found to have an installed capacity density between 6 and 10 MW km^{-2} with the mean and median offshore wind capacity density calculated as 8.3 and 7.6 MW km^{-2} respectively (Lindø Offshore Renewables Centre (LORC), n.d.). These values are higher than the 6 MW km^{-2} calculated for the Vestas V164, however for consistency with the turbine data the value of 6 MW km^{-2} is used.

For the two PV technologies a slightly different formulation is used for $c_{i,x}^{max}$ by including two additional parameters as shown in Eq. (A-12).

$$c_{i,x}^{max} = \left(\sum_{CLC} A_{CLC,i,x} b_{CLC} \right) \hat{s}_i \theta_i \hat{p}_i \qquad \text{(A-12)}$$

The first parameter b_{CLC} is the fraction of each suitable CLC class covered by buildings. This is used to provide a bottom-up assessment of the magnitude and geographic spread of rooftop PV potential in Europe by combining building footprint data with the CLC2012 dataset. We use ArcGIS to estimate the values of b_{CLC} for the UK and the Netherlands[5], finding that buildings cover up to 27% of land area in urban areas, and less than 1% in most agricultural areas (

Table A-5). The average values per class are in line with other values reported in the literature (A. C. Hansen & Thorn, 2013). We make the conservative assumption that only roofs in urban areas can be covered by PV and only include CLC codes 111, 112 and 121 as suitable for rooftop PV. We assume the average fractions of CLC classes covered by buildings in

Table A-5 apply for all countries in order to extrapolate total building footprint area in Europe. Note that for utility PV, the factor b_{CLC} is irrelevant and set to unity.

Table A-3 | Comparison of land and sea availability factors for PV and wind from literature

Technology	Land (sea) availability factor θ_i (%)					
	Deng et al. (Deng et al., 2015) (Low/Med/High)	Hoogwijk et al. (Hoogwijk et al., 2004)	Mainzer et al. (Mainzer et al., 2014)	Ordóñez et al. (Ordóñez et al., 2010)	Hoefnagels et al. (Hoefnagels et al., 2011)	e-Highway 2050 (Bruninx et al., 2015)
Onshore Wind	Agricultural, Desert Grassland, Barren land: 3%/6%/10%	Agricultural: 70% Grassland: 80% Forest: 10%	-	-	Agricultural: 10%-35% Grassland: 50% Forest: 10%	6%
Offshore Wind	0-10 km: 4%/5%/5% 10-50 km: 10%/30%/40% 50-200 km: 25%/60%/80%	-	-	-	-	3%[b]
Utility PV (ground-based)	Agricultural: 0.1%/0.5%/2% Grassland & Barren Land: 0.5%/1%/3%	-	-	-	Agricultural: 0.5%	Agricultural: 0.1% Other free land: 2%
Rooftop PV[a]	33%	-	Flat: 27% Pitched: 58%	Flat: 51-55% Pitched: 16-21%	50%	40%

[a] *Availability for rooftop PV is on the basis of roof area, not land area*

[b] *3% of the total area deemed suitable in an earlier study of approx. 750,000 km² (EEA, 2009) compared with 634,000 km² in this study. However the authors assumed a much higher capacity density (15 MW km⁻²) for offshore wind which partly compensates for this.*

The second additional parameter in Eq. (A-12) is $\hat{s}_i$, which in the case of rooftop PV is the specific roof area per square metre building footprint ($m^2\ m^{-2}$), or the panel to ground area ratio ($m^2\ m^{-2}$) in the case of utility PV. This factor accounts for the fact that not all roofs are flat for rooftop PV, and the inter-array spacing required for ground-based utility PV systems to avoid shading. In the case of rooftop PV, apartment and commercial buildings typically have flat roofs while detached and terraced houses typically have pitched roofs. In the simple case of a building with a pitched gable roof and rectangular footprint, the ratio of total roof area to building footprint can be simply calculated as the inverse of the cosine of the pitch angle. For a roof with 30° pitch, this results in approximately 1.19 m^2 of roof area per m^2 of building footprint. For a 45° pitch angle this increases to 1.41 $m^2\ m^{-2}$. In the absence of data on the prevalence of different roof types we assume a constant value of 1.22 $m^2\ m^{-2}$ for $\hat{s}_i$ for rooftop PV to be consistent with the assumed tilt angle of 35°. However, not all this roof area is available for PV installations due to area occupied by chimneys, ventilation systems, and non-optimally oriented roofs and so an availability factor of 30% is assumed for rooftop PV, in line with other studies (Mainzer et al., 2014; Śliż-Szkliniarz, 2012).

In the case of ground-based utility PV, we assume that only 1% of the total suitable land area is available for PV installations. The spacing between arrays of inclined panels on a flat surface is a trade-off between capacity density and shading between panels, with the latter depending on the installation azimuth angle and the solar altitude angle, which itself varies with location and the time of year. This study uses a simplified approach assuming that panels are mounted due south, and setting a minimum solar altitude angle equal to that of an intermediate latitude location (Berlin) on the winter solstice (December 21), which is 15°. Using trigonometry, this value yields a panel to ground area ratio $\hat{s}_i$ for utility PV of 0.366 m^2 m^{-2}. The capacity density for PV technologies is based on the nominal module power density at STC calculated from the manufacturer data (see Table A-2).

A breakdown of the final calculated available areas and maximum installed capacities by land class is shown in Table A-6, and Figure A-2 shows how this maximum capacity potential is distributed across Europe at the grid cell level.

Table A-4 | Assumed suitable CLC land classes for each technology. Tick signs indicate suitability, while cells in grey indicate no suitability for any vRES technology.

Main Class	1st Sub-Class	2nd Sub-Class	CLC Code	Suitability			
				Onshore Wind	Offshore Wind	Rooftop PV	Utility PV
Artificial surfaces	Urban fabric	Continuous urban fabric	111			✓	
		Discontinuous urban fabric	112			✓	
	Industrial, commercial and transport units	Industrial or commercial units	121			✓	
		Road and rail networks and associated land	122				
		Port areas	123				
		Airports	124				
	Mine, dump and construction sites	Mineral extraction sites	131				
		Dump sites	132				
		Construction sites	133				
	Artificial, non-agricultural vegetated areas	Green urban areas	141				
		Sport and leisure facilities	142				
	Arable land	Non-irrigated arable land	211	✓			✓
		Permanently irrigated land	212	✓			✓
		Rice fields	213				
	Permanent crops	Vineyards	221	✓			
		Fruit trees and berry plantations	222	✓			
		Olive groves	223	✓			
	Pastures	Pastures	231	✓			✓
	Heterogeneous agricultural areas	Annual crops associated with permanent crops	241	✓			
		Complex cultivation patterns	242	✓			
		Agricultural land with significant natural vegetation	243	✓			✓
		Agro-forestry areas	244				
Forest and semi natural areas	Forests	Broad-leaved forest	311				
		Coniferous forest	312				
		Mixed forest	313				
	Scrub and/or herbaceous vegetation associations	Natural grasslands	321	✓			
		Moors and heathland	322	✓			
		Sclerophyllous vegetation	323	✓			
		Transitional woodland-shrub	324				
	Open spaces with little or no vegetation	Beaches, dunes, sands	331				
		Bare rocks	332				
		Sparsely vegetated areas	333	✓			✓
		Burnt areas	334				
		Glaciers and perpetual snow	335				
Wetlands	Inland wetlands	Inland marshes	411				
		Peat bogs	412				
	Maritime wetlands	Salt marshes	421				
		Salines	422				
		Intertidal flats	423				
Water bodies	Inland waters	Water courses	511				
		Water bodies	512				
	Marine waters	Coastal lagoons	521				
		Estuaries	522				
		Sea and ocean	523		✓		

Table A-5 | Fraction of CLC 2012 classes covered by buildings for the UK and Netherlands

CLC code	Description	Fraction of CLC class covered by buildings (%)			Share of total building footprint area per country (%)	
		UK	NL	Avg	UK	NL
111	Continuous urban fabric	27.4%	- [a]	27.4%	2.9%	- [a]
112	Discontinuous urban fabric	12.6%	18.3%	15.4%	54.9%	47.6%
121	Industrial or commercial units	14.4%	21.7%	18.0%	8.6%	13.0%
123	Port areas	9.0%	11.9%	10.5%	0.4%	1.2%
211	Non-irrigated arable land	0.6%	2.0%	1.3%	13.7%	12.7%
231	Pastures	0.6%	1.2%	0.9%	13.9%	9.7%

[a] *The Netherlands did not contain any land designated under this class*

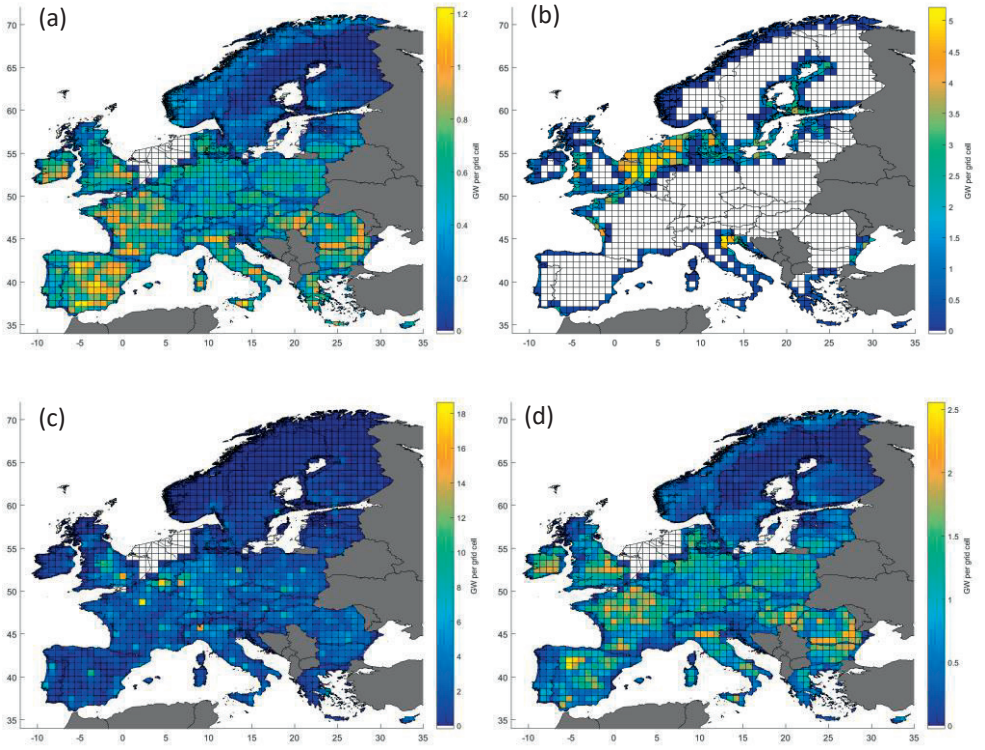

Figure A-2 | Maximum installable capacity per technology in GW per grid cell for the 50-m water depth grid for (a) onshore wind **(b)** offshore wind **(c)** rooftop PV and **(d)** utility PV. Note that the legend scale varies per technology.

Table A-6 | Calculated available area and maximum installed capacity by technology in the EU28 + NO + CH per CLC class.

Suitable CLC class description [a]	CLC Code	Total suitable area (km²)	Onshore wind		Offshore wind		Rooftop PV				Utility PV		
			Available land (km²)	Max capacity (GW)	Available sea (km²)	Max capacity (GW)	Building footprint area (km²)	Total roof area (km²)	Roof available (km²)	Max capacity [b] (GW)	Available land (km²)	Potential PV area (km²)	Max capacity [b] (GW)
Continuous urban fabric	111	5.25E+03	-	-	-	-	1440	1756	527	111	-	-	-
Discontinuous urban fabric	112	1.44E+05	-	-	-	-	22145	27017	8105	1715	-	-	-
Industrial or commercial units	121	2.59E+04	-	-	-	-	4663	5689	1707	361	-	-	-
Port areas	123	1.05E+03	-	-	-	-	-	-	-	-	-	-	-
Non-irrigated arable land	211	9.88E+05	59307	251	-	-	-	-	-	-	9885	3331	558
Permanently irrigated land	212	3.36E+04	2014	8	-	-	-	-	-	-	336	113	19
Vineyards	221	3.70E+04	2220	9	-	-	-	-	-	-	-	-	-
Fruit trees and berry plantations	222	2.69E+04	1612	7	-	-	-	-	-	-	-	-	-
Olive groves	223	4.38E+04	2625	11	-	-	-	-	-	-	-	-	-
Pastures	231	3.22E+05	19311	84	-	-	-	-	-	-	3218	1085	182
Annual crops associated with permanent crops	241	5.79E+03	347	1	-	-	-	-	-	-	-	-	-
Complex cultivation patterns	242	1.68E+05	10082	43	-	-	-	-	-	-	-	-	-
Land principally occupied by agriculture	243	1.61E+05	9685	41	-	-	-	-	-	-	1614	544	91
Natural grasslands	321	9.10E+04	5462	23	-	-	-	-	-	-	-	-	-
Moors and heathland	322	8.74E+04	5242	23	-	-	-	-	-	-	-	-	-
Sclerophyllous vegetation	323	7.72E+04	4632	20	-	-	-	-	-	-	-	-	-
Sparsely vegetated areas	333	7.96E+04	4775	21	-	-	-	-	-	-	796	268	45
Sea & Ocean [c]	523	6.34E+05	0	-	126810	754	-	-	-	-	-	-	-
Total			127315	543	126810	754	28248	34462	10339	2187	15849	5341	895

[a] Values only shown for CLC classes which are deemed suitable for at least one vRES generation technology.
[b] At STC
[c] Value given for the 50-m water depth grid. For the EEZ grid, total sea area increases to 4.97+06 km² and total maximum capacity increases to 5912 GW.

A.3 Demand profiles

The demand profiles are based on hourly electricity total load data available from ENTSO-E for 2015 for all EU28 countries as well as Norway and Switzerland (ENTSO-E, 2016a)[6]. These load values include grid losses, but exclude energy for pumped storage[7]. To investigate the impact of increased penetration of EVs and heat pumps in a future European power system and how these may affect the optimal geographic vRES capacity distribution, additional load profile variants are synthesised by adding additional demand (including grid losses) from EVs and HPs based on 2050 demand scenarios presented in ECF's Roadmap 2050 study (ECF, 2010b). Three variants are used: i) Base with EVs, ii) Base with HPs and iii) Base with EVs and HPs. To assess the impact of EVs an additional demand of 800 TWh (including grid losses) is added to the base 2015 demand of 3111 TWh. This is split between all countries based on the total number of vehicles in 2013, assuming that the share of vehicles will not change considerably in the future. The totals for each country are converted to hourly demand values using EV load profiles synthesised from a model developed by the JRC (Pasaoglu et al., 2013), incorporating driver behaviour data in six countries (UK,DE,FR,IT,ES,PL). Five types of electrical vehicles are considered based on their range and energy consumption: Small battery electric vehicles (BEVs), medium BEVs, large BEVs, medium plug in hybrid electric vehicles (PHEV) and large PHEVs. Batteries are assumed to recharge in 8 hours with normal recharging and 0.5 hours with fast recharging. The availability of recharging stations and willingness to charge is assumed the same as in the original study as shown in Table A-7.

Table A-7 | EV charging and fleet assumptions, based on JRC (Pasaoglu et al., 2013)**.**

Parking location	Charging station availability		Charging preferences	
	Normal	Fast	Period	Willingness to charge
Work	50%	0%	0:00 – 6:00	100%
Open air private	50%	5%	6:00 – 8:30	100%
Open air public	50%	5%	8:30 – 18:00	100%
Kerbside regulated	20%	2%	18:00 – 22:00	100%
Kerbside unregulated	20%	2%	22:00 – 0:00	100%
Private garage	50%	5%		
Public garage	50%	5%		

Vehicle type	EV Range (km)		Share of EV fleet (%)	
	JRC [c]	This study	JRC [c]	This study
Small BEV	80	100	10%	5%
Medium BEV	160	350[a]	25%	50%
Large BEV	200	500[b]	10%	25%
Medium PHEV	20	50	40%	15%
Large PHEV	40	100	15%	5%

[a] *Based on the range of the Tesla Model 3*
[b] *Based on the range of the Tesla Model X P90D*
[c] *Source: (Pasaoglu et al., 2013)*

Some modifications to the original fleet assumptions are made to reflect developments in the EV market. The base load profiles are built on the assumption that recharging is not time-constrained and occurs whenever a car is parked and a charging station is available (100% willingness to charge). This is a simplified 'worst case' approach which does not include the impact of smart charging which could help to smooth demand, however more detailed approaches are beyond the scope of this study. The countries which are missing EV charging profiles are assigned a charging profile from a country deemed most similar culturally or geographically. The normalised profiles for each country are shown in Figure A-3. The EV charging profiles are added to the base 2015 load data accounting for the correct day of the week and time zone differences.

To assess the impact HPs an additional final demand of 500 TWh (including grid losses) is added. This is disaggregated to each country based on current residential energy consumption for space heating. As the dynamics of heat for domestic hot water are much faster than the hourly resolution considered in this study demand patterns for showers etc. are not included. The resulting totals for each country are then distributed across the year in proportion to the number of heating degree hours (HDH) (Bobenhausen, 1994), calculated using the following formula where T is the ambient temperature (°C) and T_b is the threshold temperature below which heating is required to maintain a comfortable environment.

$$HDH = \begin{cases} 0 & \text{for } T \geq T_b \\ T_b - T & \text{for } T < T_b \end{cases} \quad \text{(A-13)}$$

To reflect that heating is mainly required when people are awake and buildings are occupied, different threshold temperatures are used throughout the day. From 6am until 10pm (local time), a minimum threshold temperature of 20°C is assumed for those hours when people are awake either at home, or at work. From 10pm until 6am (when households are asleep and commercial buildings are unoccupied) we assume that thermostat set temperatures are reduced in order to save energy, and a lower threshold temperature of 15°C is assumed. An urban area-weighted average of the HDH calculated for each country is used given that heat demand will occur mostly in urban areas. The disaggregated EV and HP demands are shown in addition to the base demand in Table A-8.

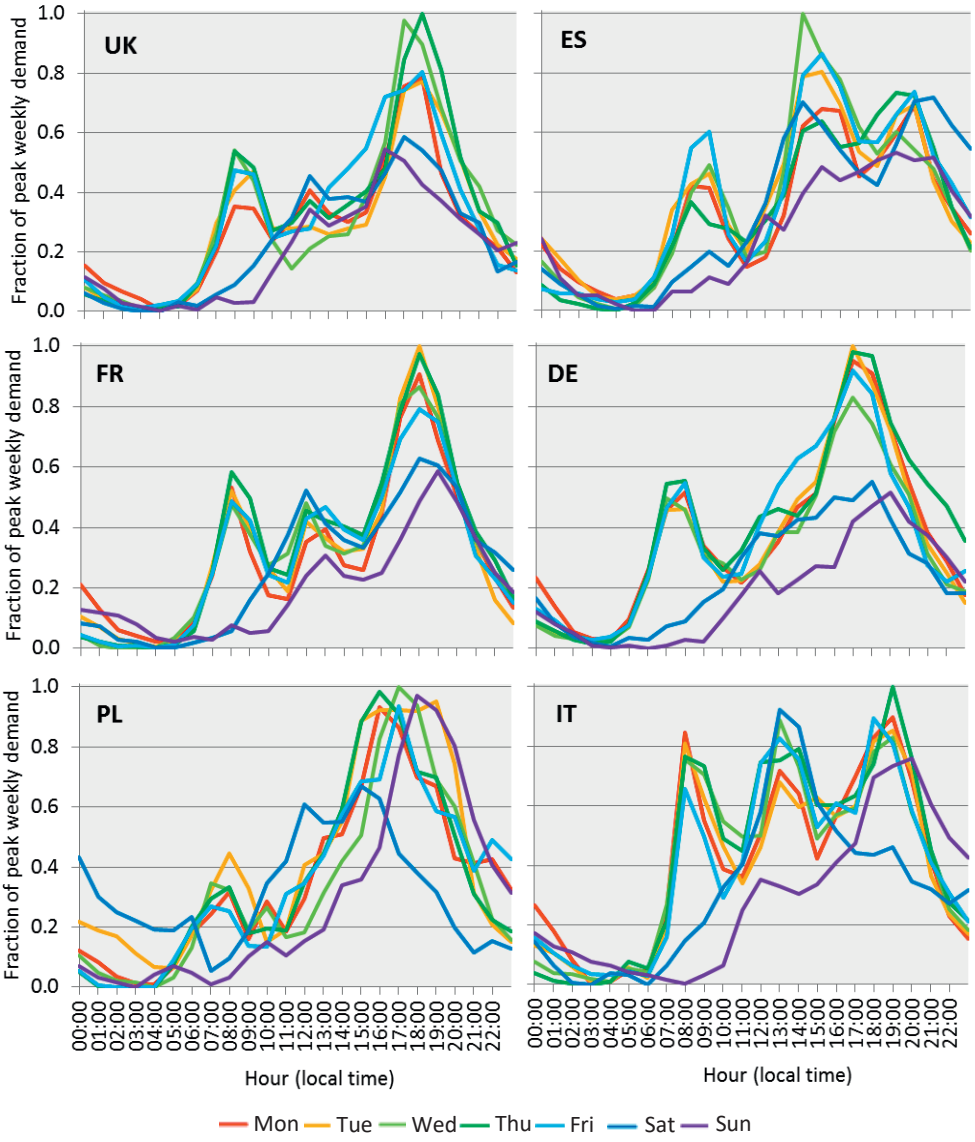

Figure A-3 | Assumed hourly EV charging profiles for each day of the week for **(UK)** the UK **(ES)** Spain **(FR)** France **(DE)** Germany **(PL)** Poland, and **(IT)** Italy.

Table A-8 | Base, EV and HP demand by country

Country	Base demand (TWh y^{-1})	Electric Vehicles		HP demand (TWh y^{-1})
		EV demand (TWh y^{-1})	EV Charging profile	
AT	69.6	14.7	DE	11.5
BE	85.2	17.4	FR	14.5
BG	38.6	9.2	PL	3.8
CH	62.1	13.7	DE	10.6
CY	4.4	1.5	ES	0.2
CZ	63.5	15.0	DE	10.8
DE	505.3	137.6	DE	102.8
DK	33.9	7.3	DE	10.0
EE	7.9	2.0	PL	1.5
EL	50.8	16.2	IT	8.5
ES	248.5	69.8	ES	19.2
FI	82.5	9.9	UK	9.8
FR	471.3	102.1	FR	71.4
HR	17.2	4.6	IT	2.6
HU	40.8	9.6	PL	9.1
IE	26.6	6.3	UK	5.0
IT	314.3	117.0	IT	47.4
LT	10.9	5.7	PL	2.6
LU	6.3	1.1	FR	0.8
LV	7.1	2.0	PL	2.4
MT	2.4	0.8	IT	0.0
NL	113.3	25.1	DE	17.5
NO	128.7	7.9	UK	9.7
PL	150.0	61.4	PL	34.6
PT	48.9	13.7	ES	1.4
RO	52.3	14.9	PL	9.8
SE	135.9	13.9	UK	10.9
SI	13.6	3.4	IT	1.9
SK	28.2	6.0	PL	3.5
UK	291.0	90.1	UK	66.1
Total	3111	800	-	500

A.4 Hourly changes in residual demand

While we do not consider generator flexibility limitations in this study, the hourly changes in residual demand for the optimised capacity distributions can give insights into the required flexibility and ramping potential of the dispatchable capacity in the generation portfolio. With this in mind, Figure A-4 shows a frequency plot of the hourly change in residual demand for the Scenario 1 (minimum residual demand) and Scenario 6 (maximum capacity factor) capacity distributions for weather year 2015. For comparison, the hourly changes in 2015 demand from ENTSO-E are also shown as representative of a power system with very low vRES penetration[8]. Figure A-4 shows that the distribution of hourly changes for Scenario 1 has more spread than the distribution of hourly changes in demand, but significant less spread than the distribution for Scenario 6. The minimum/maximum observed hourly changes for Scenario 1 are 71%/81% higher than those for the base demand profile, while for Scenario 6 they are 298%/210% higher than for base demand[9]. Thus, Figure A-4 suggests that going from a power system with 13% vRES penetration to 89% vRES penetration will lead to increased demands on flexible dispatchable capacity compared with the current power system, but not unmanageably so. Furthermore, the figure shows that a high vRES power system based on sites with maximum capacity (Scenario 6) is likely to be more unstable, and require more flexible dispatchable capacity, than a system in which capacity is sited to minimise residual demand (Scenario 1).

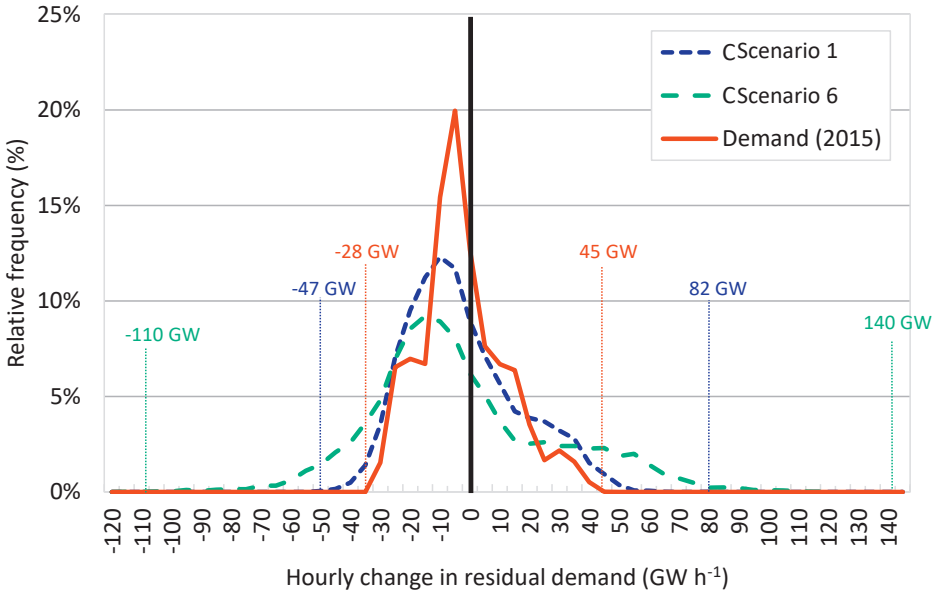

Figure A-4 | Frequency plot of the hourly change in residual demand based on weather year 2015 for Scenario 1 and Scenario 6. The hourly change in base 2015 demand from ENTSO-E is also shown for comparison. Hourly changes in demand are binned into 5 GW increments. The solid vertical black line indicates zero change. The minimum and maximum observed hourly changes for each scenario are also indicated.

Footnotes to Appendix A

[1] This is a conservative estimate as some current wind turbines already exceed this value, including a 3.3 MW wind turbine with a hub height of 164 m approved in Q1 2016 in Germany (Fachagentur Windenergie an Land, 2016).

[2] A note on terminology. *Irradiance* is the rate of radiant energy falling on a surface per unit area (W m^{-2}), whereas *irradiation* is the total incident radiation by a surface over a specific time interval (J m^{-2}). *Radiation* is a more general term, while *irradiation* refers specifically to a process by which an object is exposed to radiation. *Insolation* is another term for solar irradiation or radiation from the sun.

[3] Horizon brightening is the increase in diffuse radiation near the horizon due to a larger portion of the incident radiation scattering as it passes through a greater air mass at the horizon

[4] Standard Test Conditions (G_{STC}=1000 W m^{-2} irradiance, air mass 1.5, 25° C)

[5] These were the only two EU countries for which publicly available building footprint data could be found (ESRI, 2016; Ordnance Survey, 2016).

[6] No hourly demand profile was available for Malta which was instead estimated based on that of Cyprus, scaled down based on 2013 total power consumption from Eurostat.

[7] According to Commission Regulation No 543/2013

[8] Based on ENTSO-E data for the EU28 + NO + CH, the gross penetration of vRES in 2015 was approximately 13% (ENTSO-E, 2017b).

[9] These extremes could however be reduced using demand response.

Appendix B Appendices to Chapter 3

B.1 Fitted model parameters

The fitted model parameters presented in this Appendix are based on the selected load and vRES generation time series of historical day-ahead forecasts and real-time values from ENTSO-E for the years 2017 and 2018 (ENTSO-E, 2018b). The load, solar PV, onshore wind and offshore wind fits are based on the data for Spain, Germany, France and Denmark respectively.

- Table B-1 gives the fitted AR-GARCH model parameters for total daily deviation (Step 2),
- Table B-2 gives the fitted distribution parameters for devolatilised hourly errors (Step 5), and
- Table B-3 gives the means and standard deviations for the devolatilised hourly errors binned by generation (or load) level (Step 4).

Table B-1 | Fitted AR(a)-GARCH(p,q) model coefficients for total daily deviation load, solar PV, onshore and offshore wind

Parameter	Load	PV	Onshore wind	Offshore wind
AR(a)				
a	1	1	1	1
μ	0.1453	0.1418	0.4265	0.6552
ϕ_1	0.1417	0.1865	0.1569	0.2764
GARCH(p, q)				
p	1	1	1	1
q	1	1	1	1
ψ	0.7334	0.6220	0.0156	5.953
α_1	0.0703	0.0377	0.00355	0.0104
β_1	0 [a]	0.5287	0.995	0.6990

[a] *A value of zero for β_1 for load shows that, for this specific parameter, there is no significant autocorrelation in the daily error volatility from one day to the next Thus, in this special case, the GARCH(1,1) degenerates to an ARCH(1) model*

Table B-2 | Fitted distribution parameters for devolatilised hourly errors for load, solar PV, onshore and offshore wind

Parameter	Distribution	Location	Scale	Degrees of freedom
Load	t	0	1.4	4.204
Solar PV	Laplace	0	1.6	-
Onshore wind	Laplace	0	1.7	-
Offshore wind	Laplace	0	1.2	-

Table B-3 | Mean and standard deviation of devolatilised hourly errors for load, solar PV, onshore and offshore wind for the years 2017-2018, binned based on the normalised generation or load level

	Load		Solar PV		Onshore wind		Offshore wind	
Bin range (k)	μ_k	σ_k	μ_k	σ_k	μ_k	σ_k	μ_k	σ_k
[0.0,0.05]	*0.0%**	*0.1%**	-0.2%	1.4%	-0.1%	1.0%	-0.3%	0.9%
(0.05,0.1]	*0.0%**	*0.1%**	-0.5%	3.2%	-0.3%	1.3%	-0.2%	1.5%
(0.1,0.15]	*0.0%**	*0.1%**	-0.2%	3.8%	-0.2%	1.8%	-0.2%	2.0%
(0.15,0.2]	*0.0%**	*0.1%**	-0.2%	4.7%	0.2%	2.2%	-0.4%	2.5%
(0.2,0.25]	*0.0%**	*0.1%**	-0.3%	5.0%	0.7%	2.9%	-0.4%	3.0%
(0.25,0.3]	*0.0%**	*0.1%**	-0.4%	5.5%	1.6%	3.2%	-0.3%	3.1%
(0.3,0.35]	*0.0%**	*0.1%**	-0.2%	5.9%	1.8%	3.3%	-0.2%	3.4%
(0.35,0.4]	*0.0%**	*0.1%**	0.2%	6.2%	2.1%	3.3%	-0.1%	3.4%
(0.4,0.45]	1.8%	0.1%	0.7%	5.8%	2.6%	3.6%	-0.1%	3.3%
(0.45,0.5]	0.7%	2.3%	1.6%	5.1%	2.1%	4.1%	-0.3%	2.9%
(0.5,0.55]	0.2%	2.0%	2.2%	4.0%	1.5%	4.4%	-0.1%	3.2%
(0.55,0.6]	-0.1%	2.0%	2.1%	4.2%	1.5%	4.7%	-0.1%	3.1%
(0.6,0.65]	0.0%	2.2%	3.4%	3.9%	0.6%	4.4%	0.6%	3.1%
(0.65,0.7]	0.0%	2.5%	0.8%	3.9%	-0.5%	3.2%	1.3%	3.0%
(0.7,0.75]	0.1%	2.7%	*0.0%**	*3.9%**	-2.6%	2.5%	2.0%	3.2%
(0.75,0.8]	0.2%	2.8%	*0.0%**	*3.9%**	-2.8%	2.6%	2.1%	3.2%
(0.8,0.85]	0.1%	3.1%	*0.0%**	*3.9%**	*0.0%**	*2.6%**	2.1%	2.8%
(0.85,0.9]	-0.2%	3.3%	*0.0%**	*3.9%**	*0.0%**	*2.6%**	3.0%	2.1%
(0.9,0.95]	-0.8%	3.4%	*0.0%**	*3.9%**	*0.0%**	*2.6%**	3.2%	1.2%
(0.95,1.0]	-1.1%	2.8%	*0.0%**	*3.9%**	*0.0%**	*2.6%**	0.0%	1.2%

Note: Depending on the spread of the data, some bins contain fewer data points than others, which affects the reliability of the μ_k and σ_k values calculated for each bin. Depending on the spread of the data, some parameters may also contain empty bins, which could lead to errors if the method is applied to other countries in which real-time generation (or load) values exceed the fitted range of bins. These problems can be addressed by including more historical data when fitting the AR-GARCH model, or overriding the μ_k and σ_k values in less populated (or empty bins) with more representative values. In this study, we simply extrapolate σ_k values for empty bins based on the nearest populated bin, and set the value of the μ_k to zero (which is typically the average across all bins). As empty bins tend to occur at the upper and lower extremes of normalised generation (or load) which occur infrequently, the overall impact on the results is likely to be small.

B.2 Cross-correlation between day-ahead forecast errors in neighbouring countries, and between different parameters in the same country

The day-ahead forecast errors for each parameter (i.e. load, onshore wind, offshore wind, PV) between selected neighbouring countries were checked for correlation by determining the Pearson correlation coefficient, ρ, between the normalised error time series for the years 2017 and 2018 based on ENTSO-E data (ENTSO-E, 2018b). In addition, the forecast errors between parameters for the same country were also checked for cross-correlation. The results for the year 2018 are shown in Table B-4 to B-15 (2017 values are similar).

Comparing the cross-correlations for the same parameter between different countries, no strong positive or negative correlations (i.e. ρ >0.5 | ρ <-0.5) were found. The strongest correlation identified was a negative correlation between offshore wind forecast errors in the UK and NL with a value ρ = 0.34, which is relatively weak. Comparing the cross-correlations between parameters within a single country, a single moderate correlation was found (ρ = 0.58) between onshore and offshore wind forecast errors in the UK. However, this was not observed in the other countries.

Table B-4 | Calculated correlation coefficients between normalised load day-ahead forecast errors in neighbouring countries based on ENTSO-E data from 2018

	BE	DE	DK	ES	FR	IT	NL	UK
BE	1	-0.02	0.05	0.06	0.08	0.09	0.13	0.03
DE	-0.02	1	0.00	0.01	0.03	0.01	0.10	-0.08
DK	0.05	0.00	1	-0.02	-0.02	0.02	0.05	-0.05
ES	0.06	0.01	-0.02	1	0.02	0.07	-0.01	0.00
FR	0.08	0.03	-0.02	0.02	1	0.15	-0.06	0.00
IT	0.09	0.01	0.02	0.07	0.15	1	-0.01	-0.04
NL	0.13	0.10	0.05	-0.01	-0.06	-0.01	1	-0.04
UK	0.03	-0.08	-0.05	0.00	0.00	-0.04	-0.04	1

Table B-5 | Calculated correlation coefficients between normalised solar PV day-ahead forecast errors in neighbouring countries based on ENTSO-E data from 2018

	BE	DE	DK	ES	FR	IT	NL	UK
BE	1	0.18	0.01	0.00	0.02	0.02	-0.01	0.06
DE	0.18	1	0.04	0.02	0.01	0.04	-0.01	-0.05
DK	0.01	0.04	1	-0.01	0.02	-0.02	0.04	-0.02
ES	0.00	0.02	-0.01	1	-0.03	-0.06	0.00	0.06
FR	0.02	0.01	0.02	-0.03	1	0.26	0.03	0.22
IT	0.02	0.04	-0.02	-0.06	0.26	1	0.01	0.04
NL	-0.01	-0.01	0.04	0.00	0.03	0.01	1	0.00
UK	0.06	-0.05	-0.02	0.06	0.22	0.04	0.00	1

Table B-6 | Calculated correlation coefficients between normalised onshore wind day-ahead forecast errors in neighbouring countries based on ENTSO-E data from 2018

	BE	DE	DK	ES	FR	IT	NL	UK
BE	1	0.16	0.03	-0.04	0.15	-0.02	0.26	0.05
DE	0.16	1	0.09	0.02	0.09	0.02	-0.01	-0.07
DK	0.03	0.09	1	0.04	-0.01	0.01	-0.02	0.01
ES	-0.04	0.02	0.04	1	0.00	0.01	0.06	-0.01
FR	0.15	0.09	-0.01	0.00	1	0.03	-0.06	-0.02
IT	-0.02	0.02	0.01	0.01	0.03	1	0.00	-0.01
NL	0.26	-0.01	-0.02	0.06	-0.06	0.00	1	0.09
UK	0.05	-0.07	0.01	-0.01	-0.02	-0.01	0.09	1

Table B-7 | Calculated correlation coefficients between normalised offshore wind day-ahead forecast errors in neighbouring countries based on ENTSO-E data from 2018

	BE	DE	DK	NL	UK
BE	1	0.09	0.02	0.04	0.03
DE	0.09	1	0.14	0.25	-0.03
DK	0.02	0.14	1	0.09	-0.05
NL	0.04	0.25	0.09	1	-0.34
UK	0.03	-0.03	-0.05	-0.34	1

Table B-8 | Calculated correlation coefficients between normalised load, onshore wind, offshore wind and PV day-ahead forecast errors for Belgium in 2018

	Load	Onshore wind	Offshore wind	PV
Load	1	-0.08	0.06	0.07
Onshore wind	-0.08	1	0.18	-0.01
Offshore wind	0.06	0.18	1	-0.06
PV	0.07	-0.01	-0.06	1

Table B-9 | Calculated correlation coefficients between normalised load, onshore wind, offshore wind and PV day-ahead forecast errors for Germany in 2018

	Load	Onshore wind	Offshore wind	PV
Load	1	-0.05	0.17	0.05
Onshore wind	-0.05	1	0.15	-0.02
Offshore wind	0.17	0.15	1	0.03
PV	0.05	-0.02	0.03	1

Table B-10 | Calculated correlation coefficients between normalised load, onshore wind, offshore wind and PV day-ahead forecast errors for Denmark in 2018

	Load	Onshore wind	Offshore wind	PV
Load	1	-0.08	-0.03	0.08
Onshore wind	-0.08	1	0.27	0.00
Offshore wind	-0.03	0.27	1	-0.04
PV	0.08	0.00	-0.04	1

Table B-11 | Calculated correlation coefficients between normalised load, onshore wind, offshore wind and PV day-ahead forecast errors for the UK in 2018

	Load	Onshore wind	Offshore wind	PV
Load	1	-0.15	-0.04	-0.03
Onshore wind	-0.15	1	0.58	0.00
Offshore wind	-0.04	0.58	1	0.02
PV	-0.03	0.00	0.02	1

Table B-12 | Calculated correlation coefficients between normalised load, onshore wind, offshore wind and PV day-ahead forecast errors for Italy in 2018

	Load	Onshore wind	Offshore wind	PV
Load	1	0.00	-	-0.02
Onshore wind	0.00	1	-	-0.06
Offshore wind	-	-	-	-
PV	-0.02	-0.06	-	1

Table B-13 | Calculated correlation coefficients between normalised load, onshore wind, offshore wind and PV day-ahead forecast errors for France in 2018

	Load	Onshore wind	Offshore wind	PV
Load	1	0.01	-	0.00
Onshore wind	0.01	1	-	-0.03
Offshore wind	-	-	-	-
PV	0.00	-0.03	-	1

Table B-14 | Calculated correlation coefficients between normalised load, onshore wind, offshore wind and PV day-ahead forecast errors for Spain in 2018

	Load	Onshore wind	Offshore wind	PV
Load	1	0.03	-	0.10
Onshore wind	0.03	1	-	0.09
Offshore wind	-	-	-	-
PV	0.10	0.09	-	1

Table B-15 | Calculated correlation coefficients between normalised load, onshore wind, offshore wind and PV day-ahead forecast errors for the Netherlands in 2018

	Load	Onshore wind	Offshore wind	PV
Load	1	-0.02	-0.06	0.05
Onshore wind	-0.02	1	-0.19	0.01
Offshore wind	-0.06	-0.19	1	0.01
PV	0.05	0.01	0.01	1

B.3 Installed vRES capacity scenarios

Table B-16 shows the assumed deployment of vRES capacity in the simulations. Note that in some countries, the capacity may fall between 2030 and 2040. This is because the underlying assumptions differ between ENTSO-E scenarios. However, this combination of scenarios corresponds to the most ambitious level of vRES deployment from a Europe-wide perspective, despite some small discrepancies at the level of individual countries.

Table B-16 | Assumed installed vRES capacity per technology per country. The 2017 values are taken from EurObserv'ER (EurObserv'ER, 2018, 2019). The 2030 and 2040 capacities are taken from the *Distributed Generation 2030* and *Global Climate Agreement 2040* scenarios from ENTSO-E's TYNDP 2018 respectively (ENTSO-E & ENTSO-G, 2018).

	Solar PV			Onshore Wind			Onshore Wind			Total vRES		
Country	2017	2030	2040	2017	2030	2040	2017	2030	2040	2017	2030	2040
AT	1.2	7.8	5.6	2.8	5.0	5.5	2.8	5.0	5.5	4.1	12.8	11.1
BE	3.9	6.9	22.0	2.0	3.3	7.7	2.0	3.3	7.7	6.7	12.5	38.0
BG	0.1	4.2	2.5	0.7	1.3	1.5	0.7	1.3	1.5	0.8	5.5	4.0
CH	1.9	9.4	12.6	0.1	0.4	2.6	0.1	0.4	2.6	2.0	9.7	15.2
CZ	2.1	7.0	5.2	0.3	1.0	1.3	0.3	1.0	1.3	2.3	7.9	6.6
DE	42.4	94.6	141.0	50.2	58.5	81.6	50.2	58.5	81.6	98.0	167.7	256.1
DK	0.9	5.1	7.5	4.2	5.6	7.2	4.2	5.6	7.2	6.4	13.6	22.4
EE	0.0	0.9	1.0	0.3	1.5	1.6	0.3	1.5	1.6	0.3	2.4	2.9
EL	2.6	7.4	16.9	2.6	4.9	7.7	2.6	4.9	7.7	5.2	12.4	27.4
ES	4.4	47.2	77.0	22.9	31.0	47.6	22.9	31.0	47.6	27.4	78.2	128.0
FI	0.1	2.9	6.0	2.0	2.3	7.3	2.0	2.3	7.3	2.1	5.9	14.3
FR	8.0	41.5	60.0	13.6	36.3	49.1	13.6	36.3	49.1	21.6	84.8	129.1
HR	0.1	2.7	0.7	0.6	1.5	2.0	0.6	1.5	2.0	0.6	4.2	2.7
HU	0.4	6.2	4.0	0.3	1.0	2.0	0.3	1.0	2.0	0.7	7.2	6.0
IE	0.0	3.7	2.0	3.3	5.5	6.5	3.3	5.5	6.5	3.3	9.9	10.7
IT	19.7	46.4	58.3	9.7	15.6	17.8	9.7	15.6	17.8	29.4	62.6	87.5
LT	0.1	1.8	7.0	0.5	0.8	1.0	0.5	0.8	1.0	0.6	2.5	8.4
LV	0.0	0.9	0.0	0.1	0.3	0.8	0.1	0.3	0.8	0.1	1.4	1.3
NL	2.8	14.1	46.0	3.3	6.7	7.4	3.3	6.7	7.4	7.0	32.3	76.8
NO	0.0	3.0	3.0	0.9	3.3	10.0	0.9	3.3	10.0	0.9	6.3	13.4
PL	0.1	24.9	42.5	4.6	9.2	32.9	4.6	9.2	32.9	4.7	36.3	82.4
PT	0.6	6.6	17.6	5.3	5.6	10.0	5.3	5.6	10.0	5.9	12.2	30.2
RO	1.4	11.6	6.0	3.0	4.2	8.0	3.0	4.2	8.0	4.4	15.8	14.0
SE	0.2	5.4	6.7	6.5	10.8	17.4	6.5	10.8	17.4	7.0	16.4	25.4
SI	0.3	1.4	1.0	0.0	0.1	0.3	0.0	0.1	0.3	0.3	1.5	1.2
SK	0.5	3.6	1.5	0.0	0.3	0.3	0.0	0.3	0.3	0.5	3.8	1.9
UK	2.2	36.1	39.0	8.5	17.7	19.9	8.5	17.7	19.9	16.9	75.9	87.2

B.4 Cross-border trade and imbalance netting assumptions

In this study, transmission limitations within and between countries are not considered. Instead, simulations are performed for two cases: (i) no cross-border trading/imbalance netting, and (ii) unhindered cross-border trading/imbalance netting. The assumptions made in both these cases are outlined below:

- We do not consider intraday trading due to outages of power plants or transmission lines; thus, the volumes in this study are driven only by vRES and load forecast errors.
- As we only model load and vRES without other technologies in the portfolio (e.g. gas power plants, batteries, hydro), any load which cannot be met by vRES is assumed to be supplied by a 'residual' technology(s) in the system.
- We assume that all offers to sell or buy power on the intraday markets can be met by load (retailers), vRES suppliers, or from other market players with flexible generation or load assets (e.g. thermal plants, hydro, batteries) which we do not model. Thus, the total volume traded in an intraday period for a given country is the maximum of the stacked buy or sell offers (in MWh).
- We assume that all possible trades in vRES generation and load are made within national intraday markets first. This results in a net notional short or long position/imbalance for each country.
- In the case of no cross-border trading/imbalance netting:
    - The short/long positions per country are assumed to be met by residual technologies in the portfolio. In the case of a short system, this would most likely be a generation technology, or discharge from storage. In the case of long system, this could represent curtailment of vRES capacity, or charging of storage.
- When cross-border trading/imbalance netting is allowed:
    - The country positions/imbalances are first netted over the whole system, assuming no limitations on transmission capacity.
    - Any remaining imbalances are met by residual technologies as above. However, in this case, the amount of residual across the system is lower.

An example of the above approach is shown in Figure B-1. The top half of the figure shows intraday trading positions for three hypothetical countries in a single intraday trading period, before any cross-border trading has taken place. In Country A, expected production from solar PV based on an hour-ahead forecast is 100 MW lower than what was expected and sold on the day-ahead market; hence, they are expecting to be short at real time. Thus, the solar PV owner is seeking to buy 100 MW on the intraday market to balance their position. Meanwhile, more recent load forecasts from electricity retailers show that load is expected to be 200 MW higher than forecast the day before, and they are also seeking to buy electricity on the intraday market. However, hour-ahead forecasts for onshore and offshore wind producers suggest they will generate 50 and 75 MW more than their day-ahead positions respectively and – expecting to be long – are trying to sell this electricity on the intraday market. Thus, as a whole, the intraday market in Country A is 175 MW short. Across the border in Country B, onshore wind and PV producers are expecting to be short on their day-ahead position, while offshore wind

and retailers are expecting to be long, giving an expected overall long position of 75 MW. Country C is also expected to be long, but by a slightly lower amount of 50 MW.

In the case where no cross-border trading is allowed, a total of 175 MW of residual upwards capacity would be required for Country A, while a total of 125 MW of downwards residual capacity would be needed for Countries B and C.

In the case where cross-border trading is allowed, sellers located in Country B sell 75 MW of capacity to Country A. This would leave Country A still short 100 MW, Country B balanced, and Country C long 50 MW. Thus, 50 MW of capacity located in Country C is sold on Country A. Finally, the last remaining 50 MW of short capacity on the market is assumed to be provided by the residual portfolio. In this case, no negative residual capacity is required in the system, and the requirement for positive residual capacity is reduce to only 50 MW.

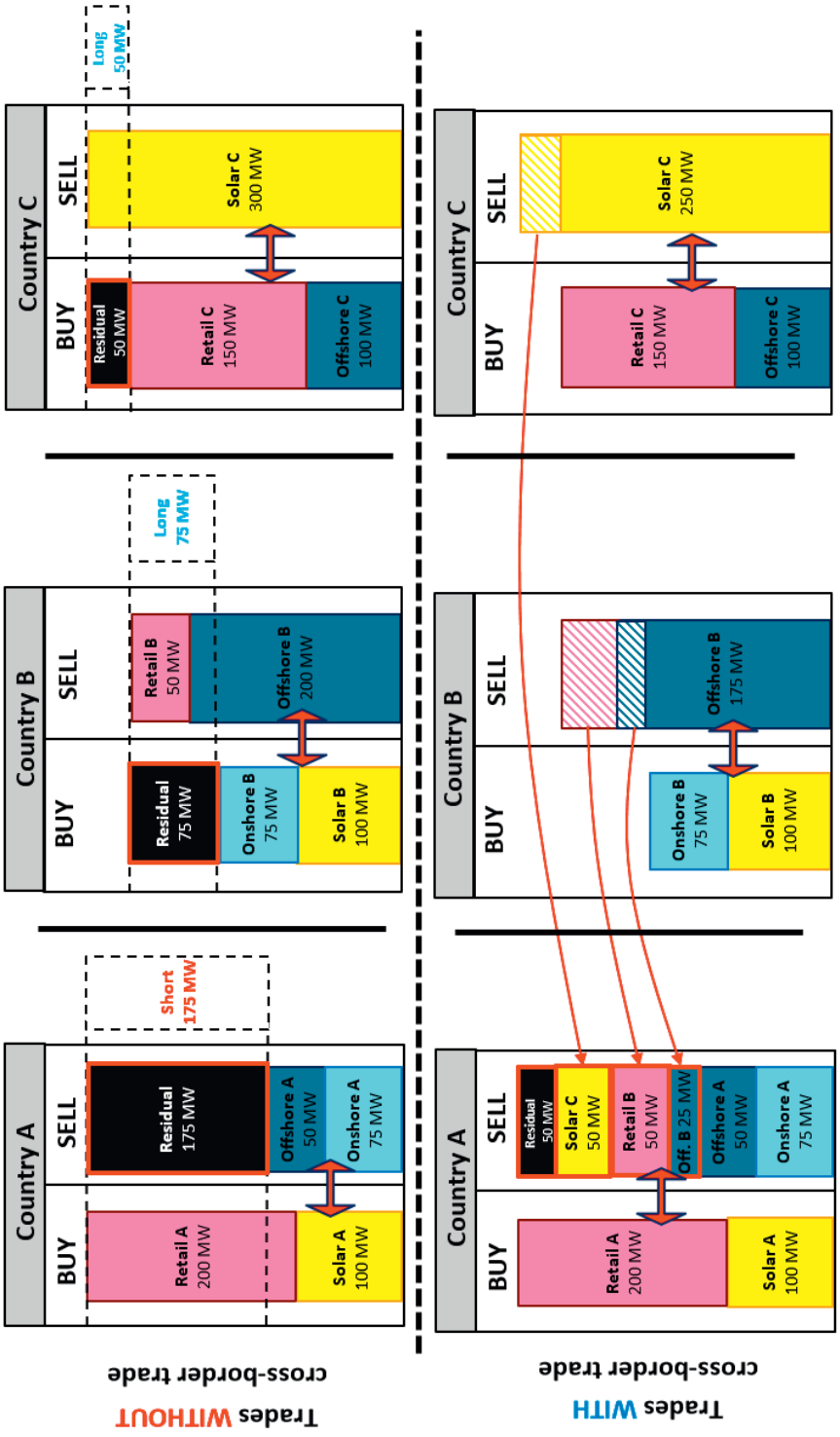

Figure B-1| Example of approach used to model intraday and balancing markets with and without cross-border trading/imbalance netting

Appendix C Appendices to Chapter 4

Abbreviations

AD	Anaerobic digestion
CCS	Carbon capture and storage
CLC	Corine Land Cover
COP	Coefficient of performance
CSP	Concentrating solar power
DNI	Direct normal irradiance
DSM	Demand-side management
ECF	European Climate Foundation
ECMWF	European Centre for Medium-Range Weather Forecasts
EEA	European Environment Agency
EEZ	Exclusive Economic Zone
ENTSO-E	European Network of Transmission System Operators for Electricity
ERA-Interim	European Reanalysis Interim Dataset
ETRI	Energy Technology Reference Indicators
EU	European Union
EV	Electric vehicle
FOM	Fixed operating and maintenance
GHG	Greenhouse gas
HDH	Heating degree hour
HP	Heat pump
HVAC	High voltage alternating current
HVDC	High-voltage direct current
IEC	International Electrotechnical Commission
ILUC	Indirect land use change
IPCC	Intergovernmental Panel on Climate Change
JRC	Joint Research Centre
LDC	Load duration curve
LoLP	Loss of Load Probability
LT	Long term
NAO	North-Atlantic oscillation
OCGT	Open-cycle gas turbine
PHS	Pumped hydro storage
PR	Performance ratio
PV	Photovoltaic
RES	Renewable energy source
RoR	Run-of-river hydro
STC	Standard test conditions
STO	Storage hydro
TYNDP	Ten-Year Network Development Plan
UCED	Unit commitment and economic dispatch
VOM	Variable operating and maintenance
vRES	Variable renewable energy source

C.1 Weather year selection

The mean annual wind speed and annual global horizontal radiation received are calculated for each year of ERA-Interim (Figure C-1). Each year is then given a rank from 1 to 37 (1 being highest) based on the magnitude of the wind speed or radiation received in that particular year, as a proxy for the total renewable resource which would be available. By multiplying the wind speed and radiation rankings together (giving wind and solar radiation equal weighting), we arrive at a metric indicating how 'good' or 'bad' each weather year is in terms of both resources. From this analysis, we identify 2010 as the 'worst' (most challenging) year of those considered (Wind ranking: 37, radiation ranking: 32), and 1990 as the best year (wind ranking 1, radiation ranking 5). This selection is validated by the fact that the 2010 European winter was strongly affected by a very negative North Atlantic Oscillation (NAO), which resulted in lower wind speeds and colder temperatures (Commin et al., 2017). Thus, we use weather year 2010 as the basis for the LT plan in our study. However, we note that at this aggregated level annual differences are quite small, with mean annual wind speed and radiation only 4% higher than the long-term (1979-2016) mean in the highest year, and 4% below the mean in the lowest year. A more detailed analysis including hourly ramps of residual load could reveal another year as more challenging, however the quantity and distribution of vRES capacity is not known until after the capacity expansion optimisation has been performed.

Note that we do not consider variations in rainfall as mean EU+NO hydro generation between 1990 and 2015 was 462 TWh y^{-1}, with a standard deviation of 38 TWh y^{-1}. The minimum generation was 394 TWh in 1991, however installed capacity was 28% lower at that time (Eurostat, 2017c). Thus, compared with total demand, potential wind and PV generation, interannual hydro variability is relatively small. To check the validity of the weather year selection method, we perform the LT Plan optimisation for the *Base* scenario for weather years 2000 to 2015. The resulting generation portfolios (Figure C-2) confirm 2010 as the most challenging year in this period, with 2091 GW of generation capacity installed, 139 GW (7%) more than in the best year for RES supply (2012). Looking at Figure C-1, performing the optimisation for additional weather years (pre-2000) is unlikely to change this conclusion.

C.2 Generator modelling

This section outlines how each of the generator technologies is modelled. For wind and PV, the approach used is largely the same as outlined in Appendix A for Chapter 2, with some modifications as outlined below.

Wind

Wind generation is estimated by combining wind speeds calculated from ERA-Interim (ECMWF, n.d.) with assumed wind farm parameters as outlined in Appendix A. However, as Chapter 4 considers transmission and costs (which Chapter 2 does not), some additional parameters are accounted for. The cost of onshore wind farms is affected by the distance from the notional country load centre, as explained in 4.2.2.2. For offshore wind farms, offshore wind farms located within 40 km from shore are typically connected by medium voltage alternating current (MVAC) (< 35 kV) or HVAC (130 – 150 kV), while sites more than 40 km

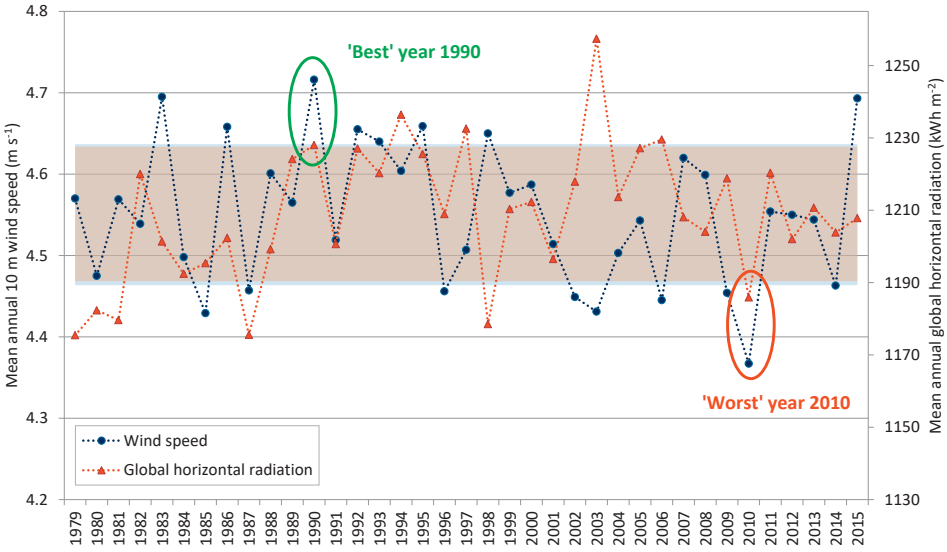

Figure C-1 | Plot of mean annual 10-m wind speed and mean global horizontal radiation received in the study area based on ERA-Interim for weather years 1979-2015. The coloured bands indicate the interannual variability as ±1σ from the long-term (1979-2016) mean wind speed (4.55 m^{-1}) and mean annual radiation (1209 kWh m^{-2}). The axes' scales are adjusted so that the variability bands for both parameters overlap.

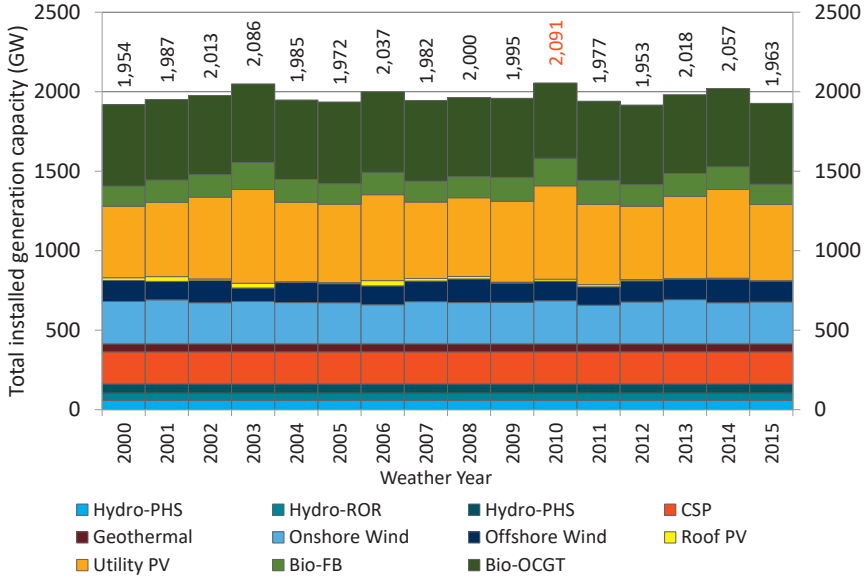

Figure C-2 | Optimised generation portfolio for the *Base* scenario, optimised for all weather years 2000 to 2015 from ERA-Interim. The total capacity installed in each year is shown above the graph, confirming 2010 as a particularly challenging weather year with 2091 GW required to meet demand, 139 GW (7%) more than in the best year (2012).

offshore are connected by HVDC (150 kV) technology in order to reduce losses (Vázquez Hernández et al., 2017). However, the economic choice between HVAC and HVDC is very project specific and depends on the size of the wind farm, distance from shore, local grid strength, and water depth. In this study, we follow a simpler approach by applying linear cost multipliers (F_{shore}, F_{depth}) taken from an earlier study (EEA, 2009) to the reference offshore wind investment cost ($C_{offWind,i}$) to account for the mean distance from shore ($\overline{W_i}$) and mean water depth ($\overline{D_i}$) for each location i (Eqs. (C-1)-(C-3)). This additional transmission capacity is not modelled explicitly as individual lines.

$$F_{depth,i} = \begin{cases} 1 & 0 < \overline{W_i} \leq 15 \\ 0.0125\overline{W_i} + 0.812 & 15 < \overline{W_i} \leq 50 \end{cases} \quad \text{(C-1)}$$

$$F_{shore,i} = \begin{cases} 1 & 0 < \overline{D_i} \leq 10 \\ 0.00285\overline{D_i} + 0.972 & 10 < \overline{D_i} \end{cases} \quad \text{(C-2)}$$

$$C_{offWind,i} = C_{offWind,ref} * F_{depth,i} * F_{shore,i} \quad \text{(C-3)}$$

PV

PV generation is estimated by combining solar radiation data from ERA-Interim (ECMWF, n.d.) with assumed solar PV modules as outlined in Appendix A. Given that determining optimum PV mounting angles is very site specific[1], we take a simple approach and assume a fixed PV tilt angle of 35°, with all panels mounted south.

CSP

We model CSP generators as solar tower (central receiver) plants equipped with full-tracking heliostats, using molten salt as a heat transfer fluid with 8 hour-storage capacity at nominal load. While currently more expensive than parabolic trough plants, we choose solar tower technology over other CSP technologies (e.g. parabolic trough or dish collectors, linear Fresnel reflectors) given its strong technical advantages (e.g. lower piping losses, higher operating temperature, hence higher efficiency and easier storage), better cost-reduction potential, and high prospective market share (H. L. Zhang et al., 2013)[2]. The solar field for each plant is sized assuming a solar multiple (SM) of 2.5 based on a design direct normal irradiance (DNI) of 800 W m^{-2}, and nominal power block steam cycle efficiency of 40% In these calculations, we also take into account fixed losses for the heliostat field (51%), with respect to incident DNI), receiver tower (1%), piping (1%), storage (injection/withdrawal) (1%), and plant parasitic losses (10%) (H. L. Zhang et al., 2013). Additional storage decay losses of 2% h^{-1} are assumed (Jorgenson et al., 2013).

DNI profiles for each location are also derived from the ERA-Interim dataset. At present, CSP plants require DNI levels of at least 2000 kWh m^{-2} y^{-1} to be economic (IRENA, 2012). However, future cost reductions will lower the minimum DNI for cost competitiveness. On this basis, we allocate CSP capacity to grid cells with average DNI levels of 1600 kWh m^{-2} y^{-1} or higher, located mainly in Spain (80%), Portugal (10%), Italy (8%), Greece (3%) and Cyprus (0.5%). The area required for CSP plants is accounted for assuming a typical capacity density of 25 MW km^{-2} based on plants currently in operation (IRENA, 2013; NREL, 2017).

Hydropower

Of the approximately 200 GW of hydro capacity currently installed in Europe[3], 31% is RoR, 48% is STO, and 21% is PHS (Mennel et al., 2015). RoR plants have little or no significant storage capacity, and power generation is driven by natural river flows. STO plants utilise the potential energy difference between an upper and a lower reservoir (or river) to generate electricity when prices are high. The upper reservoir receives natural stream flows and runoff from surrounding areas and, depending on the storage volume, can store water for weeks or months. PHS plants are similar to storage plants, but can pump water from a lower reservoir back into their upstream reservoir to be used again.

Total European hydro capacity is provided by thousands of individual plants, with capacity ranging from several megawatts to more than 1 GW. Accurately modelling hydro generation is very data intensive and requires information on the type of plant, the number and capacity of turbine/pumping units, as well as hydrological data of the reservoir inflows, and associated river networks. In this study, we take a simplified approach and aggregate hydro generation capacity per country according to the three plant categories (RoR, STO, PHS), based on data from ENTSO-E and Eurostat. First, the total required capacity per country is found by subtracting the capacity of the detailed individual plants from the total hydro capacity per country reported in Eurostat (Eurostat, 2017b). This total capacity is divided into the three hydro plants types based on a detailed plant list from ENTSOE, in order to reflect the proportions of RoR, STO and PHS in each country[4]. Assuming a typical size for each hydro plant type (RoR: 70 MW, STO: 100 MW, PHS: 400 MW) based on the same ENTSOE plant list, and average specific storage capacity per hydro plant calculated from an in-house hydro database (RoR: 60 MWh MW^{-1}, STO: 1608 MWh MW^{-1}, PHS: 113 MWh MW^{-1}), the number of lumped hydro plants to represent the total hydro capacity per country can be found. With these assumptions, the modelled shares of RoR, STO and PHS capacity in Europe are 26%, 47%, and 27% respectively, within the reported range (ENTSO-E, 2017b; Mennel et al., 2015). In the absence of inflow data, the lumped RoR and STO plants have their annual capacity factors capped at historical levels for each country based on Eurostat data. For lumped PHS plants, we assume that these are closed-loop pure PHS with no natural inflow, and set the tail storage volume equal to the head storage volume.

Flexibility constraints and part-load performance of thermal generators

Table C-1 shows the modelled flexibility constraints and start costs for each dispatchable generator type. The part-load efficiencies for all thermal generators are based on normalised profiles of Brouwer et al. (Brouwer et al., 2015), (Figure C-3). For those generators for which specific curves could not be found, the curve for a similar generator is assumed, namely: (i) the Gas-OCGT curve is applied to Bio-OCGTs as a similar technology, (ii) the Coal-PC curve is applied to Bio-FBs with and without CCS under the assumption that burning biomass does not affect part-load performance. CSP part-load performance is much like other thermal plants (see (Llorente García et al., 2011)). Unfortunately, due to model functionality issues, the part-load performance of CSP plants could not be included in PLEXOS, and instead a constant power block efficiency of 40% is used.

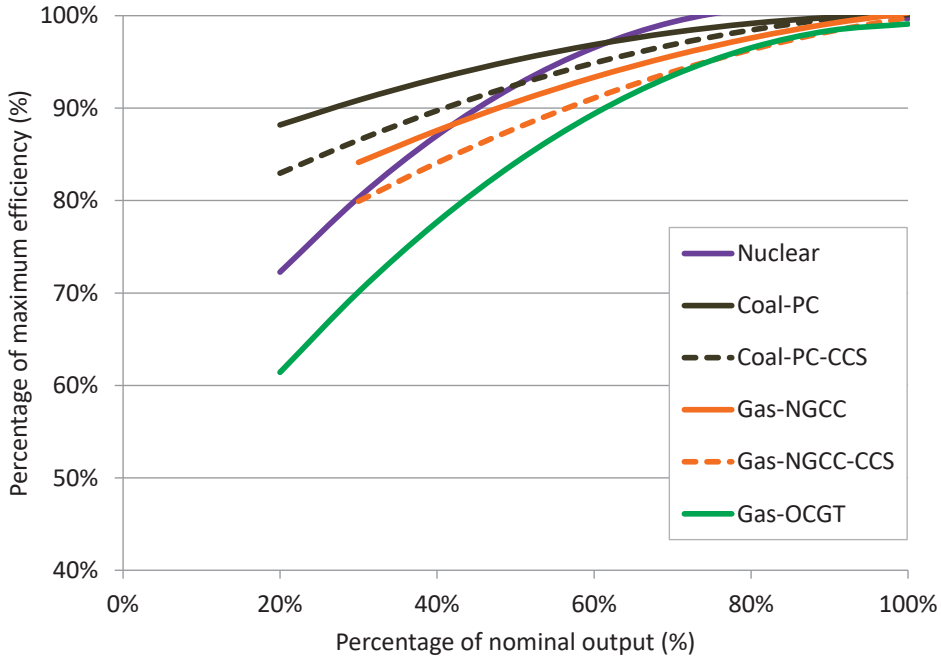

Figure C-3 | Assumed part-load performance of thermal generators, based on (Brouwer et al., 2015)

Table C-1 | Assumed generator flexibility parameters and start costs for dispatchable generators

Generator type	Min. stable level (%)*	Max. ramp rate (% min^{-1})*	Time since offline (h)			Start-up time (h)			Start-up cost (€ MW^{-1}) *[c]		
			Hot	Warm	Cold	Hot	Warm	Cold	Hot	Warm	Cold
Hydro (all)	-	50%	-	-	-	-	-	-	-	-	-
Bio-FB [b]	20%	6%	<8	<48	>48	2	4	8	39	46	75
Bio-OCGT [b]	20%	15%	<8	<48	>48	¼	¼	½	13	16	23
CSP	20%	6%	<2	<8	>24	¼	½	2	27	39	57
Geothermal	20%	4%	<8	<48	>48	1	2	3	27	39	57
Gas-OCGT [g]	20%	15%	<8	<48	>48	¼	¼	½	13	16	23
NGCC	25%	9%	<8	<48	>48	1	2	3	27	39	57
NGCC-CCS [a]	25%	9%	<8	<48	>48	1	2	3	27	39	57
Coal-PC	20%	6%	<8	<48	>48	2	4	8	39	46	75
Coal-PC-CCS	20%	6%	<8	<48	>48	2	4	8	39	46	75
Bio-FB-CCS [ab]	20%	6%	<8	<48	>48	2	4	8	39	46	75
Nuclear	20%	5%	<8	<48	>48	3	8	20	39	46	75
Source	[d]	[e]		[f]			[g]			[h]	

** In terms of installed capacity*

[a] CCS technology is assumed not affect flexibility compared with traditional plants (AEMO, 2017)

[b] Combustion of biomass is assumed not to affect flexibility parameters compared with fossil fuels

[c] No start costs could be found for CSP or geothermal. For CSP and geothermal, costs for NGCC assumed. For Bio-FB, start costs assumed same as Coal-PC pulverised coal plants, as start costs for plants using solid fuels appear more expensive than for gaseous fuels (Lew et al., 2013).

[d] Hydro: (ACIL Allen Consulting, 2014), CSP: (Yildiz et al., 2017), Rest: (Brouwer et al., 2015)

[e] CSP: (Fichter, 2012), Geothermal: (Matek, 2015), Hydro: (Black & Veatch, 2012), Rest: (Brouwer et al., 2015) (for 2030)

[f] CSP: (Yildiz et al., 2017). Rest: (Brouwer, Van den Broek, et al., 2016) (for 2030)

[g] CSP: (Yildiz et al., 2017), Geothermal: Assumed same as NGCC, Rest: (Brouwer et al., 2015) (for 2030)

[h] Geothermal, CSP: Assumed same as NGCC, Bio-FB: Assumed same as pulverised coal plant, Rest: (Brouwer et al., 2015) (for 2030)

C.3 Capacity credit of vRES generators

Various methods for estimating the capacity credit of vRES are reported in the literature, such as chronological reliability models and probabilistic methods, typically incorporating values for the LoLP (Amelin, 2009; Ensslin et al., 2008; IEA, 2011). These methods can be computationally intensive and are not easily integrated into the PLEXOS capacity expansion algorithm. In the case of wind power, several authors have shown that at low wind penetration, its capacity credit is close to the average production of wind power during periods of peak demand, but decreases as the penetration of wind increases due to deployment in less favourable sites (Holttinen, 2004; Milligan & Parsons, 1999).

In this study, we base our approach on the simplified approach of Milligan (Milligan & Parsons, 1999) to estimate the capacity credit of vRES as the average capacity factor observed during peak system demand hours, based on all available weather years (1979-2015). To demonstrate, we calculate the capacity factor for each vRES technology for each grid cell, for the top 0.01%, 0.1%, 1%, 5%, 10%, and 30% of the peak load hours[5]. For comparative purposes we do this not only for the Base 2015 load profile, but also for the actual load profiles from 2012-2015, as well as four future demand profile scenarios from ENTSO-E's TYNDP (Vision 1,2,3,4). The results are shown in Figure C-1, revealing that irrespective of the demand profile considered, the capacity credit of both PV technologies is essentially zero as the sun is almost never shining during hours of peak demand. Wind capacity credit is much more variable from site to site (e.g. some sites have a capacity credit above 80% while others have zero), and from year to year. Thus, rather than taking the average capacity factors averaged across all weather years from 1979 to 2015 as the capacity credit, we take the capacity factors from the year with the lowest average capacity factor during the peak 1% of demand hours[6].

To demonstrate, Figure C-2 shows the resulting distribution of wind capacity credit across all grid cells, based on the year with the lowest average capacity factor during the top 1% of demand hours. Onshore wind capacity credit ranges from 0% to 59% with a median of 12%, and offshore wind capacity credit ranges from 0% to 56%, with a median of 10%. PV receives a capacity credit of zero in essentially all grid cells.

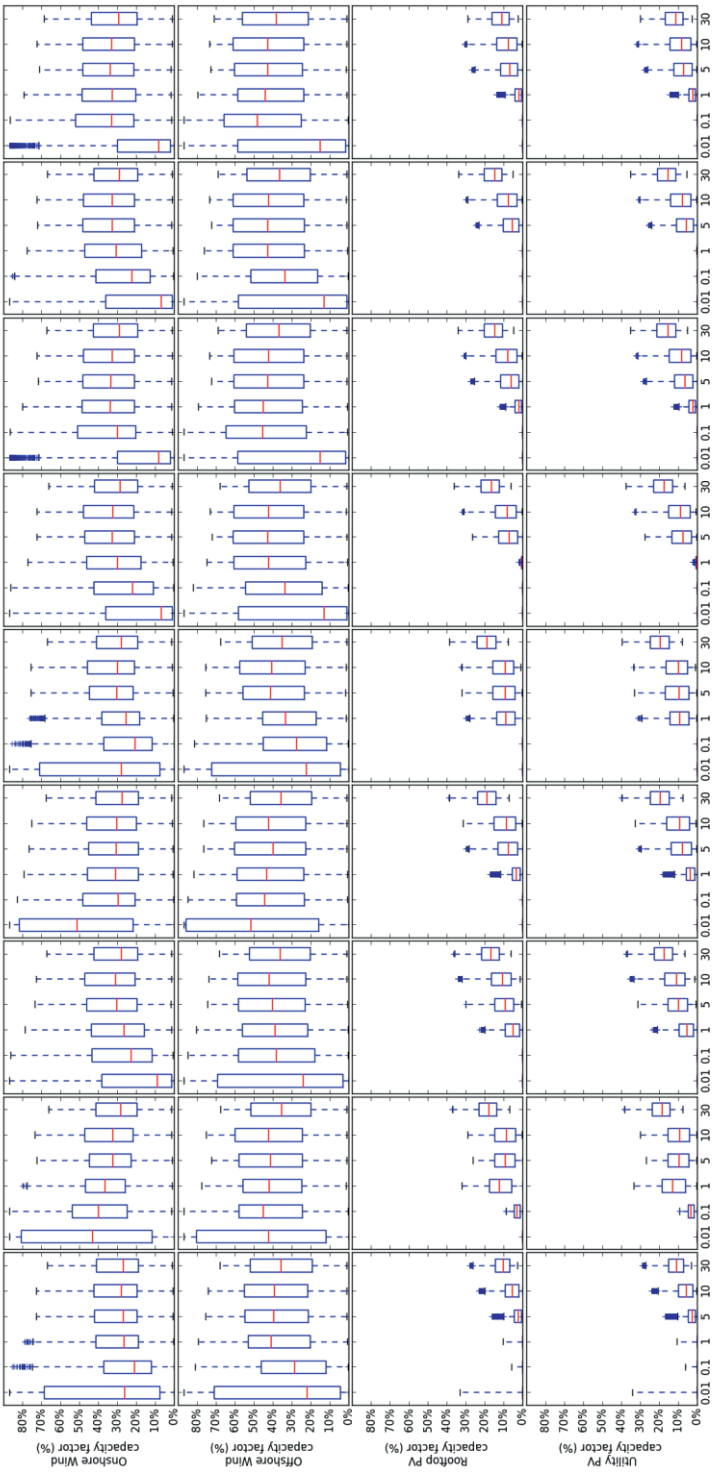

Figure C-4 | Average capacity factors for vRES technologies during the peak 0.01%, 0.1%, 1%, 5%, 10% and 30% demand hours of each year based on weather years 1979-2015, for different demand profiles: (a) Base (2015 historical demand, modified to account for HPs and EVs), **(b)-(e)** Actual 2012, 2013, 2014, 2015 demand from ENTSO-E (ENTSO-E, 2017b), and **(f)-(i)** Vision 1-4 Demand scenarios for 2030 from ENTSO-E's Ten Year Network Development Plan (ENTSO-E, 2016d). Values based on average capacity factor of all grid cells during peak Europe (total) demand hours, averaged across all weather years.

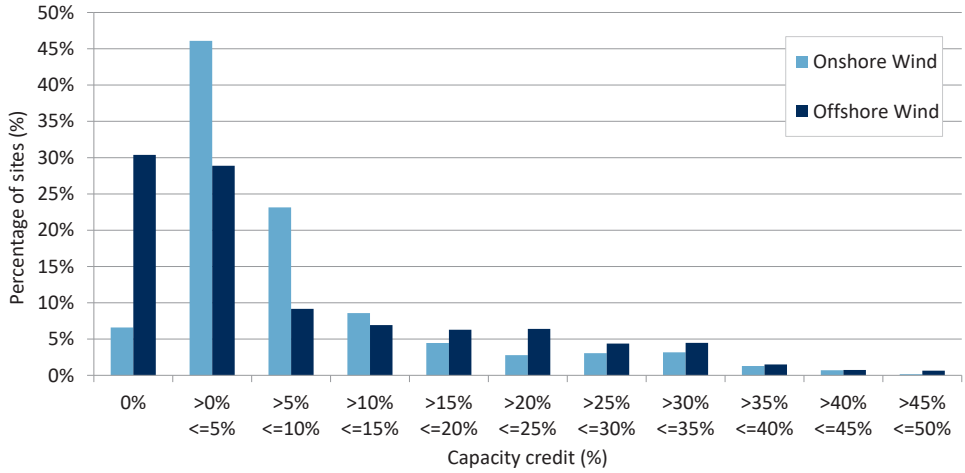

Figure C-5 | Distribution of capacity credit for onshore and offshore wind across all grid cells, using the Base demand profile. The capacity credit is taken as the year with lowest average capacity factor calculated during the top 1% of demand hours.

C.4 Demand response

Various studies have estimated the potential of DSM in Europe, given its ability to reduce peak demand, reduce network congestion, and provide balancing reserves. However, there are a wide range of values reported in the literature. In this study, we base the 2050 DSM potential on the work of Gils (Gils, 2014), as potentials are provided explicitly for each country. We aggregate the 30 different processes from Gils' original study into 11 groups of similar processes as shown in Table C-2, using the same grouping as Brouwer et al. (Brouwer, Van den Broek, et al., 2016). A total of 16 GW of load shedding and 82 GW of load shifting is included. Load shedding can be activated freely by the model if it is cost-effective to do so; however, load shifting availability is capped at 12.5% of the year for each process. Also, the potential of some shifting processes varies seasonally (e.g. no shifting potential from heating during summer or from air-conditioning during winter). Due to computational limitations, only demand shedding is included in the long-term capacity expansion algorithm. In the short-term UCED, both demand shedding and demand shifting are included.

Table C-2 | Assumed DSM potentials and costs by process

Sector	Process	Type	Max shift (h)	Technical Potential (GW)	Utilised Potential		FOM (€ kW^{-1} y^{-1})	VOM (€ kWh^{-1})
					Technical (%)	GW		
Industry	Electrolytic metal production	Shed	∞	1.5	90%	1.3	1.1	1072
Industry	Electric arc steel production	Shed	∞	5.7	90%	5.1	1.1	2144
Industry	Chloralkali process	Shed	∞	1.5	90%	1.5	1.1	107
Industry	Cement and other	Shed	∞	3.6	90%	3.2	17.1	750
Industry	Pulp and paper production	Shed	∞	5.8	90%	5.3	14.0	107
All	Shift 1 h load by 2 h	Shift (delay)	2	26.3	33-90%	12.3	3.2	0
All	Shift 2 h load by 2 h	Shift (delay)	2	7.5	33-90%	4.5	3.2	0
Tertiary & Residential	Air conditioning	Shift (advance)	2	5.1	33-90%	2.1	18.2	0
Tertiary & Residential	Space and water heating	Shift (advance)	12	154.4	33-90%	55.3	3.2	0
Residential	Washing machines, dryers, dishwashers	Shift (delay)	6	10.5	33%	3.5	107.2	0
Residential	Freezers & refrigerators	Shift (delay)	2	14.1	33%	4.7	46.1	0
Source			a	a	b		b,c	b,c

[a] *Source: (Gils, 2014)*
[b] *Source: (Bertsch et al., 2012)*
[c] *Source: (Brouwer, Van den Broek, et al., 2016)*

C.5 Installed capacity constraints per grid cell

The spatial grid and capacity constraints for wind and PV are the same as the approach used in Chapter 2 and explained in detail in Appendix A. Some modifications were made to account for CSP as explained below.

We assume that the suitable land types for CSP are the same as for utility PV. The availability for each Corine land class (CLC) and DNI cut-off point are adjusted until the assumed exogenous 200 GW of CSP capacity in the *Base* scenario can accommodated – with a preference for non-agricultural and non-vegetated land. The resulting land types used for CSP are 6% for non-irrigated arable land (CLC code 211), 3% of permanently irrigated land (CLC code 212), 5% of pastures (CLC code 231), 5% of agricultural land with significant natural vegetation (CLC code 243) and 50% of sparsely vegetated areas (CLC code 333). Ultimately, the 200 GW of CSP capacity can be accommodated with the assumed availability given and a DNI cut-off level of 1600 kWh m^{-2} y^{-1}. Thus, the availability for CSP is not taken as a hard constraint (as with PV or wind) but indicates the area which would need to be deployed in order to accommodate 200 GW of CSP.

C.6 Biomass fuel potentials and costs

Country-specific biomass potentials and cost scenarios for 2050 are taken from a study by the JRC (Ruiz et al., 2015). Of the 22 biomass commodities included in the original study, we exclude six due to a lack of data, or on the assumption that they will be used for another sector. The remaining 16 biomass types are aggregated into three categories (solid woody biomass[7], solid waste biomass, and biogas substrate) based on the form of the biomass, and its suitability for generating electricity with a particular technology. Three different levels of biomass supply are considered as shown in Table C-3, ranging from 6 EJ y^{-1} to 19 EJ y^{-1}. The medium scenario level of 10 EJ y^{-1} is used for all the base model runs. The supply potential for each scenario per country is shown in Table C-4.

We allow for the free trade and transport of solid woody biomass across Europe, assuming intra- and inter-country transport costs (Table C-5) taken from Hoefnagels et al. (Hoefnagels et al., 2014), which are added to the base feedstock costs (Table C-4). The costs in Table C-3 include the costs of biomass production, harvesting, transport, and pre-treatment (e.g. chipping, road-side storage) up-to the conversion gate in each country. While this is sufficient for the solid woody and waste biomass streams, the cost of producing useful biogas from substrates are not included and must be added.

Table C-3 | Biomass feedstocks, costs and potentials included for 2050 by fuel type, based on (Ruiz et al., 2015)**.**

Sector	Biomass category	Biomass type	Commodity	Assigned fuel category	Assigned technology	Feedstock cost range [d] (€2016 GJ^{-1})	Supply potential scenario for energy uses (PJ y^{-1}) [e]		
							Low	Medium	High
Agriculture	Energy Crops	Sugar, starch & oil crops	Sugar beet, rape seed, starchy crops, other oil crops			Not included [a]			
		Dedicated perennials-woody/ lignocellulosic biomass	Grassy crops	Solid woody biomass	Bio-FB	2.8-8.5	953	1525	2528
			Willow			7-14.4	313	286	445
			Poplar			9.5-19.3	76	78	154
		Energy maize/silage	Wet/silage			Not included [b]			
	Primary residues	Dry manure	Biogas	Biogas substrate	Bio-OCGT	3.2-7.6	625	1250	1873
		Liquid/wet manure							
	Secondary residues	Olive pits	Wood-like fuel	Solid woody biomass	Bio-FB	2.3-5.6	607	1025	2136
	Solid agricultural residues	Pruning and straw/stubble							
Forestry	Stemwood production	Stemwood logwood	Wood-like fuel			Not included [f]			
		Additionally harvestable stemwood	Wood-like fuel	Solid woody biomass	Bio-FB	2.6-9.4	2082	2392	2878
	Primary forestry residues	Logging residues	Wood-like fuel			1.4-6.5	489	1953	6038
		Landscape care	Wood-like fuel			2.2-3.3	71	283	708
	Secondary forestry residues	Woodchips, pellets, sawdust and black liquor	Woodchips			1.4-3.2	90	360	900
			Sawdust			1.4-2.3	32	129	321
			Black liquor			Not included [c]			
Waste	Primary residues	Biodegradable waste [g]	Solid fuel	Solid waste biomass	Bio-FB	6 [i]	437	730	914
	Tertiary residues	Other waste [h]	Biogas substrate	Biogas substrate	Bio-OCGT	6-6	30	53	69
Total							**5803**	**10063**	**18967**

Footnotes for Table C-3

[a] *Sugar, starch and oil crops (potential 2.3 – 2.6 EJ y^{-1}) are reserved for liquid biofuel production in the transport sector.*

[b] *No supply potential data available in the original study*

[c] *No supply potential data available in the original study, though only relevant for countries with significant pulp and paper industries (e.g. FI, SE, DE).*

[d] *Original costs in €2010 corrected to €2016 based on historical inflation rates. Includes the cost of biomass production, harvesting, transport, and pre-treatment up-to the conversion gate. The costs of converting the feedstock into useful energy (e.g. anaerobic digestion for biogas) are not included. The range given indicates the cost difference between the lowest-cost country and the highest-cost country for each fuel*

[e] *Supply scenarios are based on different levels of raw material demand, collection rates, recycling rates, and competing uses. For example, the Med scenario assumes 50% to 60% of primary forestry residues, secondary forestry residues, agricultural wastes and energy crops are used in other sectors.*

[f] *Stemwood logwood (241 – 334 PJ y^{-1}) assumed to be reserved for domestic heating.*

[g] *Includes municipal solid (bio) waste, roadside verge grass, vegetable waste, shells/husks*

[h] *Includes sewage sludge, paper and cardboard waste, dredging spoil*

[i] *The original study was unclear regarding the costs for biodegradable waste. Waste streams can have zero or even negative cost, if their producer must pay for disposal. However, some wastes are traded commodities, and for these the price can be significant (e.g. waste paper and cardboard, approximately 120 € t^{1} or 8 € GJ^{-1} (Ruiz et al., 2015)). Wastes cost per country varied considerably from 0 € GJ^{-1} to 128 € GJ^{-1}, which seems rather unreasonable. Thus, we assume a uniform cost of 6 € GJ^{-1} for biodegradable wastes, the same as other tertiary wastes.*

Before they can be used for electricity generation, biogas substrates from municipal and agricultural wastes must be converted to biogas using anaerobic digestion (AD). The raw biogas product, which typically contains 50 – 60% methane (CH_4), can then be either (i) combusted locally at the generation site (e.g. in a gas engine or gas turbine) to produce electricity which is used on site or fed into the grid, or (ii) further upgraded to biomethane (>98% CH_4), injected into the gas network, and combusted elsewhere for electricity production (Hahn, Krautkremer, et al., 2014). The AD process typically results in 5% energy loss due to internal process heating requirements (ECN, 2017), while the losses involved in biogas upgrading, depending on the technology, are minimal (Sun et al., 2015). Thus, assuming 95% efficiency for AD, we consider that 1 GJ substrate is equivalent to 0.95 GJ raw biogas, and 0.95 GJ biomethane.

The choice between generating electricity onsite or injecting into the gas grid is an economic one. Whether they produce electricity (and heat) or generate biomethane for grid injection, biogas plants are usually limited in size due as: i) increased transport costs for input substrates and AD residues which offset lower specific investment costs (AEBIOM, 2009), ii) limited availability of local substrate resources, iii) limited economies of scale for AD and upgrading plants, irrespective of the technology used (Bauer et al., 2013; Skovsgaard & Jacobsen, 2017), and iv) in agricultural settings biogas is often used for combined heat and power (CHP) rather than electricity-only production, for which there must be sufficient heat demand to warrant operating the CHP plant (Skovsgaard & Jacobsen, 2017). Several studies have estimated the cost of biogas production, upgrading and injection into the gas grid, depending on the technology used (e.g. (Bauer et al., 2013; Hahn, Krautkremer, et al., 2014; Hengeveld et al., 2014; Muñoz et al., 2015)). However, the different ways these costs are reported makes a consistent comparison difficult. In this study, we take the values from (Hengeveld et al., 2014) and assume an additional cost of 10.4 € GJ^{-1} substrate for the conversion of substrates to biogas by AD, and a further 3.2 € GJ^{-1} to upgrade the biogas to biomethane for injection into the gas grid so it can be used in other countries. In order to avoid infeasible solutions, we model biomass supply as a soft constraint by allowing the model to draw on additional biogas supply, at the significantly higher cost of 100 € GJ^{-1}.

Table C-4 | Biomass feedstock potentials considered for the low, medium and high availability scenarios in 2050. Based on (Ruiz et al., 2015).

Country	Solid woody biomass (PJ y^{-1}) (Low / Med / High)	Solid waste biomass (PJ y^{-1}) (Low / Med / High)	Biogas substrate (PJ y^{-1}) (Low / Med / High)	Total (PJ y^{-1}) (Low / Med / High)
AT	147 / 249 / 491	6 / 11 / 13	3 / 9 / 15	156 / 269 / 519
BE	33 / 67 / 140	29 / 54 / 68	22 / 58 / 92	83 / 179 / 300
BG	88 / 156 / 329	3 / 4 / 4	3 / 6 / 8	93 / 166 / 342
CH [b]	52 / 106 / 221	21 / 32 / 39	3 / 7 / 10	76 / 144 / 270
CY	1 / 1 / 4	2 / 3 / 3	3 / 5 / 6	6 / 9 / 12
CZ	118 / 221 / 431	3 / 4 / 5	35 / 43 / 51	156 / 268 / 486
DE	668 / 1075 / 2084	76 / 132 / 169	52 / 117 / 180	797 / 1324 / 2432
DK	29 / 60 / 129	20 / 29 / 33	32 / 44 / 56	80 / 132 / 218
EE	46 / 76 / 151	3 / 4 / 5	7 / 8 / 10	55 / 88 / 165
EL	41 / 68 / 187	2 / 3 / 4	4 / 8 / 13	46 / 80 / 204
ES	385 / 633 / 1436	23 / 38 / 47	76 / 112 / 147	484 / 783 / 1630
FI	248 / 432 / 871	10 / 17 / 22	4 / 8 / 12	262 / 457 / 905
FR	632 / 975 / 1894	66 / 114 / 145	56 / 258 / 461	754 / 1347 / 2500
GB [a]	138 / 214 / 354	16 / 22 / 25	67 / 153 / 238	221 / 389 / 617
HR	26 / 47 / 112	0 / 0 / 0	2 / 3 / 4	29 / 51 / 116
HU	147 / 261 / 526	7 / 12 / 15	55 / 64 / 73	209 / 337 / 614
IE	31 / 54 / 105	2 / 3 / 3	4 / 18 / 33	37 / 75 / 140
IT	235 / 441 / 977	26 / 43 / 53	55 / 116 / 177	316 / 600 / 1206
LT	60 / 106 / 201	1 / 2 / 2	15 / 17 / 19	76 / 125 / 222
LU	3 / 6 / 12	0 / 0 / 0	0 / 2 / 3	4 / 8 / 16
LV	77 / 145 / 300	1 / 1 / 1	6 / 9 / 11	84 / 155 / 312
NI [a]	9 / 13 / 22	1 / 1 / 2	4 / 9 / 15	14 / 24 / 38
NL	29 / 42 / 79	37 / 68 / 89	26 / 49 / 73	92 / 159 / 241
NO [b]	95 / 184 / 390	20 / 33 / 42	1 / 4 / 7	116 / 222 / 439
PL	430 / 740 / 1389	20 / 33 / 41	73 / 96 / 118	524 / 869 / 1548
PT	80 / 144 / 317	10 / 18 / 23	13 / 25 / 36	103 / 186 / 376
RO	388 / 663 / 1209	7 / 10 / 12	15 / 21 / 27	410 / 695 / 1248
SE	388 / 683 / 1407	23 / 35 / 42	7 / 20 / 33	418 / 737 / 1482
SI	39 / 72 / 151	1 / 1 / 1	1 / 2 / 2	41 / 74 / 155
SK	50 / 95 / 191	3 / 5 / 6	9 / 12 / 16	63 / 113 / 213
Total	4711 / 8031 / 16108	437 / 730 / 914	654 / 1302 / 1942	5803 / 10063 / 18964

[a] Original data reported for UK only. Split between GB and NI in proportion to land area

Table C-5 | Transport costs for solid woody biomass from country of origin (rows) to destination (columns) in € GJ^{-1} from (Hoefnagels et al., 2014)**.**
Note: As Norway and Switzerland were not included in the original study, the values for SE and AT are used respectively as proxies.

From / To	AT	BE	BG	CY	CZ	DE	DK	EE	EL	ES	FI	FR	UK	HR	HU	IE	IT	LT	LU	LV	NL	PL	PT	RO	SE	SI	SK
AT	1.3	7.1	7.3	8.7	3.7	6.0	9.9	10.8	7.9	10.4	11.5	9.4	10.4	2.7	3.1	10.4	6.2	8.5	6.7	10.3	7.0	6.1	10.2	7.3	10.6	2.3	3.2
BE	6.6	1.3	10.8	9.8	6.3	3.5	4.2	5.1	9.4	7.0	6.0	4.4	4.5	9.7	7.7	4.6	7.8	7.7	1.4	5.0	1.8	6.7	5.7	11.4	5.1	9.5	7.6
BG	7.0	10.6	0.9	6.6	8.9	11.0	12.4	13.3	4.9	9.9	14.2	11.6	12.3	6.9	6.0	11.4	7.8	12.0	11.8	13.1	10.8	9.9	10.0	3.6	13.3	7.7	6.7
CY	7.9	7.1	4.8	1.0	10.1	9.3	8.8	9.8	2.7	6.2	10.6	8.1	8.7	5.5	8.6	7.8	4.3	12.4	9.8	9.6	7.4	10.9	6.4	6.0	9.7	4.9	9.2
CZ	2.6	6.2	7.9	11.7	1.1	4.2	7.4	8.1	10.4	11.5	8.8	9.7	9.0	4.8	3.4	9.3	9.3	5.7	6.6	7.6	5.7	3.2	10.3	7.6	8.0	5.0	2.8
DE	4.4	3.4	9.6	11.0	4.0	1.3	5.9	6.9	10.4	8.9	7.6	6.7	6.6	7.3	5.5	6.7	8.0	8.0	3.5	6.8	3.1	5.6	7.7	9.6	6.7	6.9	5.2
DK	9.0	3.2	12.5	10.4	6.6	4.5	1.4	4.2	10.0	7.7	4.9	6.8	4.9	11.0	9.5	5.2	9.1	6.3	5.7	4.1	3.2	5.4	6.3	12.2	3.9	11.6	8.3
EE	11.0	5.6	14.9	12.9	9.1	7.1	5.6	1.0	12.5	10.1	5.1	9.2	7.3	13.0	11.3	7.6	11.5	4.0	8.0	2.1	5.6	7.0	8.8	13.2	5.3	14.0	10.1
EL	7.8	7.9	3.9	4.2	10.1	10.0	9.6	10.6	1.1	7.1	11.4	8.9	9.5	6.1	7.8	8.6	5.1	13.0	10.7	10.4	8.2	11.1	7.3	6.2	10.5	5.5	8.6
ES	11.1	6.1	10.5	8.6	11.1	8.3	7.8	8.8	8.2	1.2	9.6	7.4	7.7	10.1	12.2	6.8	7.2	11.0	8.4	8.6	6.2	10.1	4.3	11.8	8.6	9.4	12.1
FI	11.9	6.6	15.9	13.9	10.0	8.1	6.5	5.6	13.5	11.1	1.3	10.3	8.4	14.0	12.3	8.6	12.5	8.6	9.1	5.9	6.6	8.1	9.8	14.8	6.1	15.0	11.1
FR	9.8	5.5	11.8	10.3	10.2	7.3	7.9	8.9	9.9	7.3	9.7	1.3	8.0	10.5	11.1	7.5	7.7	11.2	5.3	8.8	5.8	10.2	7.7	12.8	8.8	9.8	11.0
UK	9.6	3.7	12.4	10.5	8.8	6.0	5.1	6.1	10.1	7.7	6.9	7.0	1.3	12.0	10.5	4.7	9.2	8.5	6.2	6.0	3.9	7.6	6.4	12.9	5.9	11.6	9.9
HR	3.8	9.2	6.4	7.3	6.0	8.6	11.5	12.2	6.6	9.6	13.0	10.5	11.6	1.0	3.6	11.1	5.9	10.2	9.5	11.8	9.3	7.6	9.7	6.9	12.2	2.0	4.3
HU	2.3	7.8	5.9	10.1	4.0	6.5	10.0	10.4	8.8	12.0	11.1	10.7	10.9	2.9	1.0	11.0	8.3	7.5	7.3	9.6	7.6	5.0	11.8	5.0	10.4	3.4	2.0
IE	11.9	5.9	13.7	11.8	11.2	8.3	7.5	8.5	11.3	9.1	9.4	8.6	6.9	13.4	12.9	1.3	10.6	11.0	8.6	8.4	6.1	10.1	7.7	14.6	8.4	12.8	12.3
IT	7.5	7.1	7.9	6.1	9.5	8.3	9.3	10.3	5.6	6.6	11.1	7.3	9.2	5.6	8.6	8.4	1.1	12.6	8.3	10.1	7.1	11.1	6.9	9.1	10.1	4.9	9.1
LT	7.8	5.9	12.0	13.1	6.2	6.7	5.9	3.7	12.7	10.4	6.3	9.5	7.7	9.9	7.7	8.0	11.7	1.0	8.3	1.5	5.9	3.7	9.1	9.9	5.9	10.3	6.5
LU	5.8	2.1	10.7	11.2	6.3	3.5	5.7	6.6	10.9	8.5	7.4	4.6	6.0	9.1	6.8	6.1	8.5	9.0	1.3	6.5	2.6	7.4	7.1	11.1	6.5	8.8	6.8
LV	9.0	5.3	12.9	12.5	7.5	6.8	5.3	3.3	12.1	9.8	5.4	8.9	7.1	11.1	9.0	7.3	11.2	1.9	7.7	1.0	5.3	5.1	8.5	11.2	5.1	11.6	7.7
NL	5.9	0.9	10.2	9.2	5.1	2.4	3.6	4.5	8.8	6.4	5.3	4.8	4.0	9.0	6.9	4.1	7.3	6.9	2.4	4.4	1.3	5.6	5.1	10.8	4.4	8.9	6.8
PL	4.9	5.7	9.3	12.5	3.1	4.6	5.6	5.9	11.8	10.1	6.6	9.2	7.4	7.0	4.9	7.7	10.8	3.7	7.2	5.2	5.4	1.0	8.8	7.6	5.9	7.4	3.7
PT	10.7	5.3	10.7	8.7	10.3	7.5	7.0	7.9	8.3	4.7	8.7	7.4	6.9	10.3	11.9	6.0	7.4	10.3	7.6	7.8	5.4	9.4	1.1	12.1	7.8	9.7	11.5
RO	5.6	10.4	3.8	8.6	7.0	9.2	11.9	12.2	7.4	12.0	12.9	12.5	12.9	6.1	4.0	12.8	9.5	8.8	10.4	10.9	10.3	6.8	12.2	1.0	12.2	7.0	4.6
SE	10.5	5.2	14.5	12.5	8.6	6.7	4.6	4.6	12.2	9.7	5.0	8.8	6.9	12.6	10.9	7.1	11.1	7.3	7.6	4.7	5.2	6.7	8.4	13.4	1.4	13.6	9.7
SI	3.0	9.2	6.8	7.1	5.1	7.8	11.7	12.5	6.5	9.3	13.2	10.0	11.8	1.1	3.5	10.9	5.1	9.8	8.7	11.9	9.0	7.3	9.5	7.4	12.4	1.2	4.1
SK	2.9	7.9	6.7	11.6	3.3	5.9	8.4	8.6	10.1	12.5	9.3	11.1	10.2	4.4	1.9	10.4	9.8	5.5	7.7	7.6	7.6	3.2	11.5	5.5	8.7	4.9	1.2

C.7 Demand assumptions

The *Base* demand profile is the same used in Chapter 2, and fully explained in Appendix A. Figure C-6 shows the total aggregated base demand profile for the EU28, Norway and Switzerland during (a) a typical winter week and (b) a typical summer week. For comparison the actual 2015 demand is also shown, the original TYNDP 2016 *Vision 4* demand profile, and the *Alternative Demand Profile* (Vision 4 demand profile scaled up to the Base 4409 TWh y^{-1}) variants included in this study. The *Base* profile is peakier than the Vision 4 profile, mainly due to the impact of EV charging. This is because the Vision 4 profile includes the effect of EV smart charging, which shifts some demand into the night.

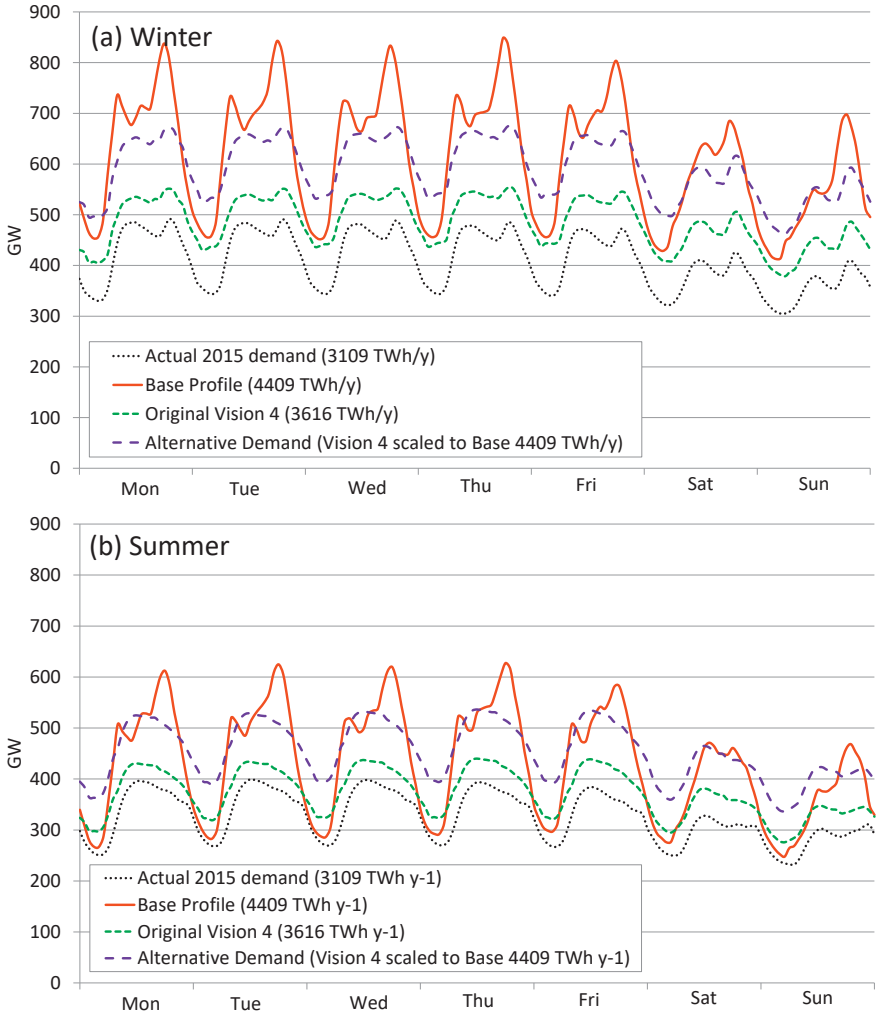

Figure C-6 | Comparison between the input demand profiles for a typical (a) winter and **(b)** summer week respectively. Demand is shown as the total for the EU28 plus Norway and Switzerland.

C.8 Transmission modelling

We use a 'centre-of-gravity' approach to model transmission flows between countries, with the urban area-weighted centres of each country serving as node terminals. Taking the existing net transfer capacity (NTC) in 2016 from ENTSO-E (ENTSO-E, 2017b) as a starting point (approximately 60 GW total capacity, some soon-to-be-commissioned lines are also included) which are included exogenously in all scenarios (see Table C-6), the model can build new transmission capacity if this reduces total system costs. Note that for simplicity, the transmission lines in Table C-6 are modelled as bi-directional with the same NTC value in both flow directions (i.e. $NTC_{CH\text{-}AT} = NTC_{AT\text{-}CH}$). The cost of transmission reinforcement is estimated by finding the shortest path distance between two country nodes, and calculating the total cost as the sum of the onshore and offshore components. We assume subsea high voltage direct current (HVDC) cables are used for underwater lines and high voltage alternating current (HVAC) for land-based lines[8]. For vRES technologies, we assume that generation capacity is located at the centroid of each grid cell and calculate the shortest transmission cost-path distance (across either land or sea) to the nominal load centre (Figure C-7). This additional transmission cost (in € MW^{-1}) is then added to the base investment cost, making capacity installed at more remote sites relatively more expensive. These notional 'reinforcement lines' are not modelled explicitly as part of the transmission network, and only serve to include the cost of bringing electricity from vRES sites to load centres.

Figure C-7 | Example of the 'centre of gravity' approach used to estimate grid reinforcement costs for wind and PV.

Table C-6 | Assumed reference transmission capacity (2016), reinforcement cost and losses for each transmission line (ENTSO-E, 2017b)

Line	Reference NTC[a] (MW)	Line length (km)			Reinforcement cost (2016 €000 MW^{-1})	Losses (%)
		Land (HVAC)	Subsea (HVDC)	Total		
CH-AT	1200	520	0	520	408	3.5%
CZ-AT	525	235	0	235	227	1.6%
DE-AT	4000	497	0	497	394	3.4%
DE-BE	0	369	0	369	313	2.5%
DE-CH	2000	443	0	443	360	3.0%
DE-CZ	867	431	0	431	352	2.9%
DK-DE	585	463	153	616	830	5.0%
EL-BG	250	576	0	576	445	3.9%
EL-CY	0	0	1138	1138	1914	5.3%
FI-EE	888	257	92	349	612	3.4%
FR-BE	1850	438	0	438	357	3.0%
FR-CH	3083	405	0	405	336	2.7%
FR-DE	1800	663	0	663	499	4.5%
FR-ES	450	945	0	945	680	6.4%
GB-BE	1000[b]	355	130	485	728	4.2%
GB-DK	1400[c]	328	579	907	1340	5.5%
GB-FR	1750	681	55	736	831	6.1%
HU-AT	300	358	0	358	305	2.4%
HU-HR	700	326	0	326	285	2.2%
IE-FR	0	662	513	1175	1460	7.6%
IE-GB	500	258	180	437	736	3.7%
IT-AT	85	616	0	616	470	4.2%
IT-CH	1656	556	0	556	432	3.8%
IT-EL	417	907	170	1077	1136	8.0%
IT-FR	943	885	0	885	641	6.0%
LU-BE	0	167	0	167	184	1.1%
LU-DE	1700	282	0	282	257	1.9%
LU-FR	0	393	0	393	328	2.7%
LV-EE	462	234	0	234	226	1.6%
LV-LT	829	187	0	187	197	1.3%

NI-GB	500	533	56	590	739	5.1%
NI-IE	1100	184	0	184	195	1.2%
NL-BE	946	151	0	151	174	1.0%
NL-DE	2258	336	0	336	292	2.3%
NL-DK	700	339	271	609	915	4.5%
NL-GB	975[d]	294	235	529	837	4.1%
NO-DE	1400[e]	676	580	1256	1563	7.9%
NO-DK	850	472	222	694	932	5.3%
NO-FI	100	2208	0	2208	1484	14.9%
NO-GB	1400[f]	534	693	1227	1631	7.3%
NO-NL	665	546	540	1086	1424	6.9%
PL-CZ	567	342	0	342	295	2.3%
PL-DE	2086	679	0	679	510	4.6%
PL-LT	500	497	0	497	394	3.4%
PT-ES	2954	492	0	492	391	3.3%
RO-BG	100	331	0	331	288	2.2%
RO-HU	300	480	0	480	383	3.2%
SE-DE	615	772	245	1017	1155	7.4%
SE-DK	1403	499	0	499	395	3.4%
SE-FI	2633	411	216	627	885	4.8%
SE-LT	0	430	401	830	1155	5.6%
SE-NO	2837	386	0	386	323	2.6%
SE-PL	275	674	225	899	1065	6.6%
SI-AT	950	181	0	181	192	1.2%
SI-HR	800	157	0	157	178	1.1%
SI-HU	0	367	0	367	311	2.5%
SI-IT	181	527	0	527	413	3.6%
SK-CZ	1200	296	0	296	266	2.0%
SK-HU	400	154	0	154	176	1.0%
SK-PL	458	340	0	340	294	2.3%

[a] *Taken from ENTSO-E (ENTSO-E, 2017b) unless otherwise stated*
[b] *Includes the 1 GW NEMO link (http://www.nemo-link.com/)*
[c] *Includes the 1.4 GW Viking link (http://viking-link.com/)*
[d] *Includes the 700 MW Cobra cable (http://www.cobracable.eu/)*
[e] *Includes the 1.4 GW NordLink cable (https://www.tennet.eu/our-grid/international-connections/nordlink/)*
[f] *Includes the 1.4 GW North Sea Link (http://northsealink.com/)*

C.9 Operating reserves

Operating reserves are required to balance out mismatches between demand and generation due to (i) demand forecast errors, (ii) vRES forecast errors, and (iii) unplanned generator outages. These reserves take the form of additional (non-dispatched) generation capacity which can be made available when required at short notice. The provision of these reserves results in additional costs; therefore, in a power system with a heavy reliance on vRES, it is important to ensure sufficient reserve capacity is available.

There is no standard method used to determine the required reserve size. In this study, we follow the approach of Brouwer et al. (Brouwer, Van den Broek, et al., 2016) by considering three types of reserves: (i) *spin-up*: fast-responding spinning (within 5 minutes) up-regulation reserves, based on 1h-ahead forecast errors of wind and PV generation, available for 15 minutes; (ii) *spin-down*: fast-responding spinning (within 5 minutes) down-regulation reserves, also based on 1h-ahead forecast errors of wind and PV generation, available for 15 minutes; and (iii) stand-up: slower-responding standing reserves (available within 60 minutes), based on day-ahead forecast errors of wind and PV generation, available for 15 minutes. In addition to the vRES forecast errors, we also account for demand forecast errors and unplanned generator outages in the spinning reserves (see Figure C-8).

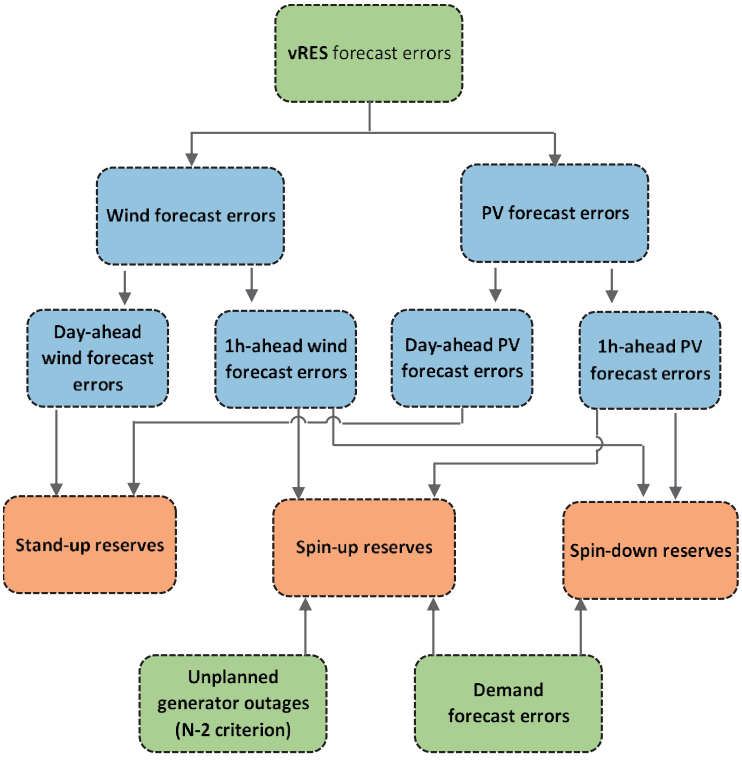

Figure C-8 | Reserve sizing approach

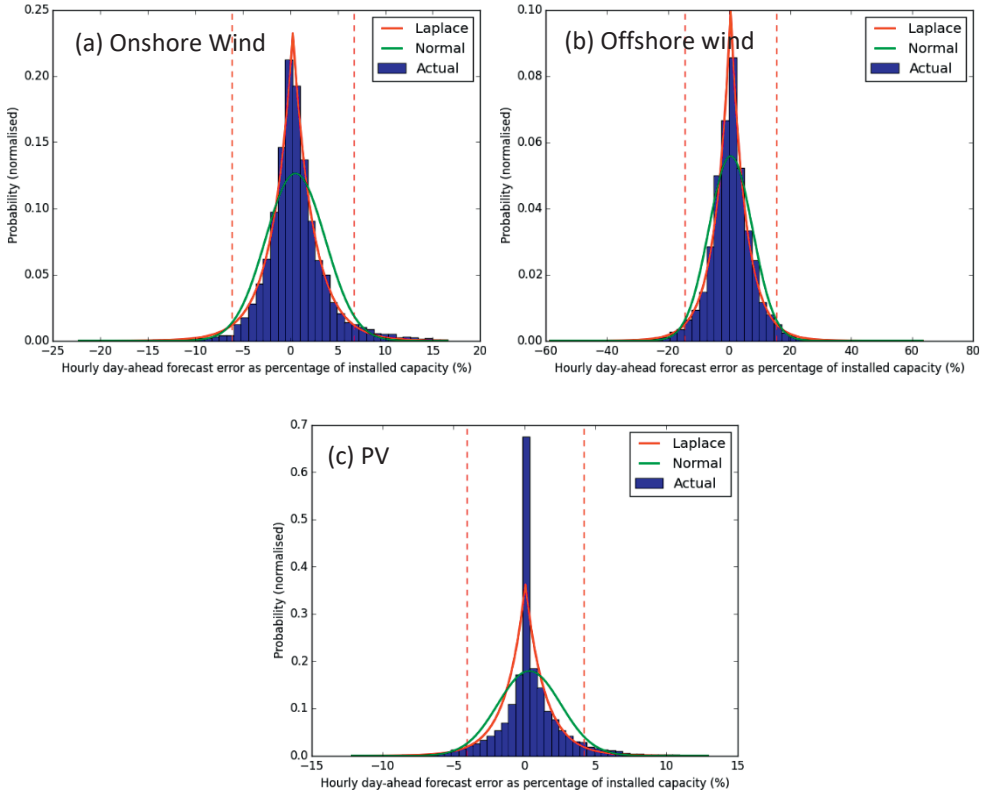

Figure C-9 | Probability density plots of hourly forecast errors from day-ahead predictions for (a) onshore wind (b) offshore wind and (c) PV in Germany for the year 2016, based on ENTSO-E data (ENTSO-E, 2017b)**.** Forecast errors are expressed as a percentage of total installed capacity (Onshore wind 41.4 GW, offshore wind 3.3 GW, PV 38.6 GW) using 50 bins. The original data at 15-min resolution is averaged to match the coarser hourly temporal resolution used in our study. Errors are fit to both the Normal and Laplace distributions, revealing the Laplace distribution as a better fit in agreement with Morbee (Morbee et al., 2013). The vertical red lines indicate 95% of all forecast errors based on the fitted Laplace distributions. Note that for PV, we exclude hours in which either predicted or actual PV generation is zero.

There are two main approaches to estimate vRES forecast errors: (1) determine typical errors for existing forecast methods, or (2) synthesise forecasts for each generation technology, and determine the errors. For the stand-up reserve requirement, we use the first approach and assume that the day-ahead vRES forecasts reported by ENTSO-E (ENTSO-E, 2017b) are representative of the best forecasting methods available. Calculating the day-ahead forecast errors for each hour of 2016 for Germany[9], we fit these data to Laplace distributions following the approach of Morbee et al. (Morbee et al., 2013) (see Figure C-9). These graphs show that as a share of installed capacity, day-ahead forecast errors for onshore wind are better than for offshore wind. Also, we see that the Laplace fit is poorer for PV than for wind, due mainly to the large number of hours with very low PV generation, and hence concomitantly small forecast areas. Rather than determining a fixed annual reserve size from these graphs which

would overestimate the required reserves, we use the dynamic reserve sizing method of Lew et al. (Lew et al., 2013) (also used by Brouwer et al. (Brouwer, Van den Broek, et al., 2016)) to estimate hourly reserves by binning vRES forecast errors into tranches, according to a limited number of variables. For each technology, we use eight three-hour bins for the period of the day (12am – 3am UTC … 9pm – 12pm UTC), and eight generation bins, giving a total of 64 tranches. Fitting the tranche errors to Laplace distributions, we calculate the forecast error in each tranche as a share of installed capacity (e.g. see Figure C-10 for an example). The standing reserves are then calculated by multiplying our vRES generation profiles by these typical day-ahead error tranches, assuming reserves must cover 95% of day-ahead forecast errors.

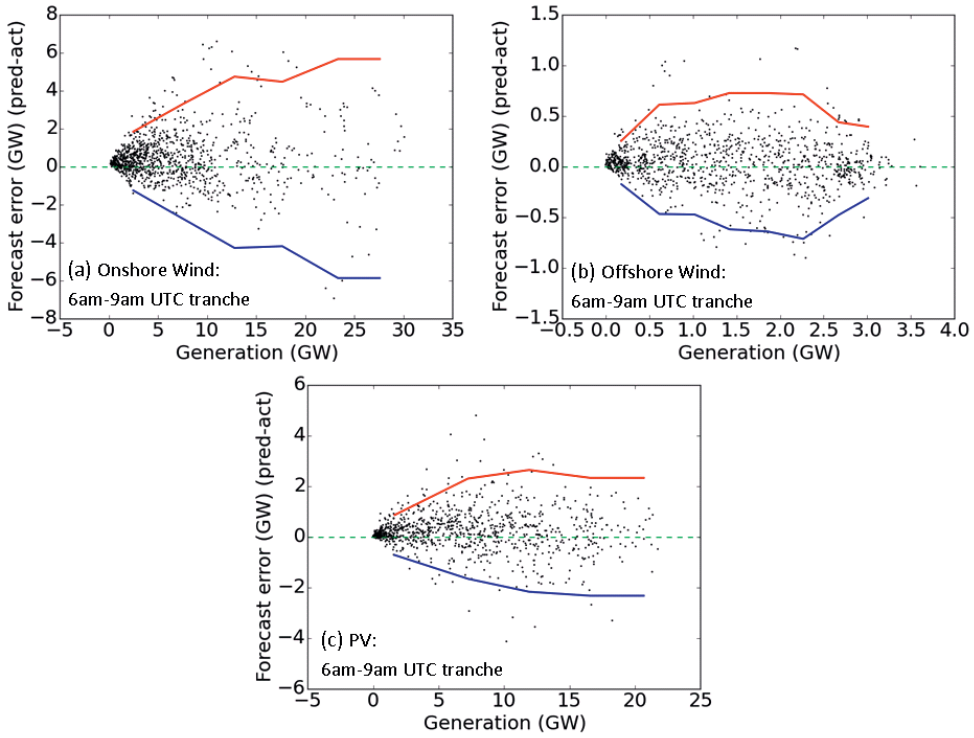

Figure C-10 | Calculated day-ahead vRES forecast errors as a function of actual generation for (a) onshore wind, **(b)** offshore wind, and **(c)** PV production for Germany in 2016 for the 6am – 9am time-of-day tranche. The red and blue lines indicate the 95% confidence limits for each generation level tranche, assuming the errors are Laplace distributed.

For spinning reserves, no publicly available historical hour-ahead vRES forecasts could be found to estimate typical hour-ahead forecast errors. Instead, we take the second approach and generate our own hour-ahead persistence forecasts from the 'actual' generation patterns to estimate wind and PV forecasts errors, again following the method of Lew et al. (Lew et al., 2013) and Brouwer et al. (Brouwer, Van den Broek, et al., 2016)[10]. However, as our persistence forecasts are likely to be less accurate than the advanced methods used by TSOs, slightly different variables and binning methods are used for PV and wind as explained below:

- For solar PV (both rooftop and utility), simple hour-ahead persistence forecasts often lead to significant positive forecast errors in the morning as the sun rises, and negative forecast errors in the evening as the sun sets (Lew et al., 2013); however, these diurnal generation patterns can be accurately predicted without the need for complex weather models by using solar position calculations, assuming clear-sky conditions. Thus, we improve the simple persistence forecast to account for the predictable diurnal pattern of PV by calculating the forecast generation F (MW) at a given hour t using the equation below (Lew et al., 2013), where P is the actual PV generation (MW), P_{CS} is the expected power generation under clear sky conditions (calculated using the same method for PV described in Appendix A but assuming a constant clear-sky value of 0.8 for k_t(Erbs et al., 1982)), and SPI is the solar power index – the ratio between actual generation and clear-sky generation ($SPI = P/P_{CS}$) which reflects the level of cloud cover. As future SPI is not known, we take the persistence of SPI ($SPI(t) = SPI(t-1)$)

$$F(t) = P(t-1) + SPI(t)[P_{CS}(t) - P_{CS}(t-1)] \quad \text{(C-4)}$$

  We use eight three-hour bins for the period of the day (12am – 3am UTC, 3am – 6am UTC … 9pm – 12pm UTC), and eight (equally spaced) generation level bins for in each period, giving a total of 64 tranches. By assuming the forecast errors in each tranche also follow a Laplace distribution (as we found for day-ahead errors), we determine upper and lower confidence limits which cover 95% of forecast errors. For tranches with fewer than 10 members and therefore difficult to fit to a reliable distribution, we maintain the upper and lower limits of the previous tranche.

- For onshore wind, we find that hourly persistence forecasts also lead to a diurnal bias, with positive forecast errors in the morning and negative forecast errors in the evening – most likely due to the effects of morning sea breezes and afternoon land breezes (see Figure C-11). While these biases could be accounted for with regression or improved forecast methods, this is beyond the scope of this paper and by using the same period-of-day and generation level bins as for PV, we account for the different spin-up and spin-down requirements throughout the day. For offshore wind, we find no diurnal bias in forecast errors, but maintain the same 64 tranches for time-of-day and generation level for consistency.

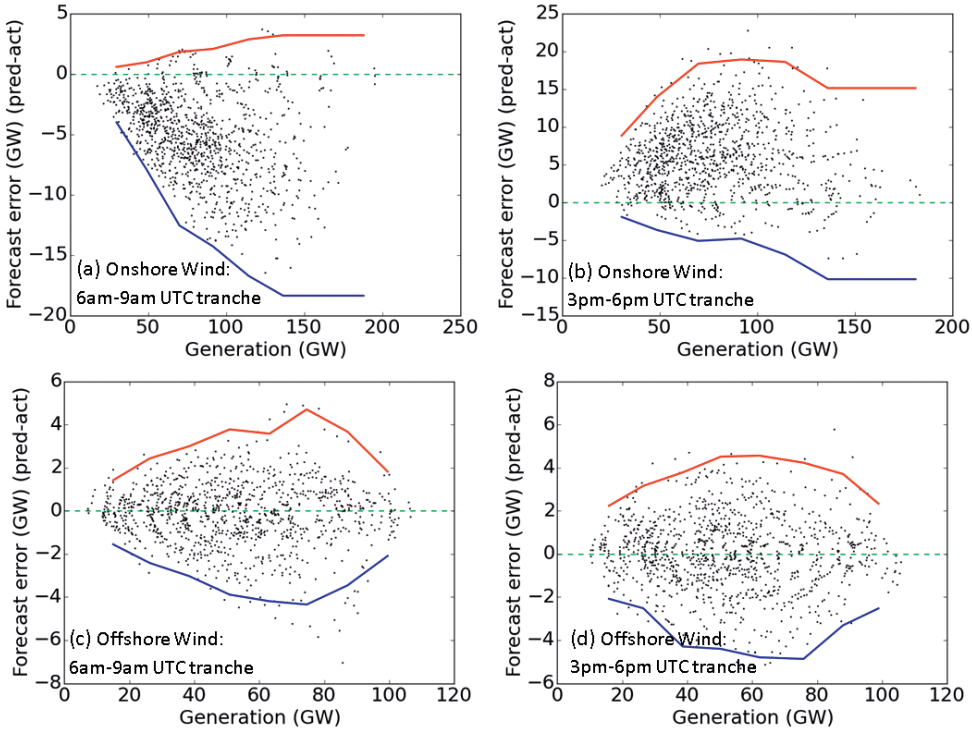

Figure C-11 | Hour-ahead forecast errors as a function of actual generation for the Base scenario capacity distribution for onshore (a,b) and offshore (c, d) wind, for a morning and evening period tranche. The actual generation and persistence forecasts are based on ERA-Interim weather year 2010. The spin-up and spin-down requirements are based on the upper and lower 95% confidence limits, shown in red and blue respectively.

Assuming that for short time steps individual forecast errors are uncorrelated, the combined spin-up reserve requirement is calculated as the geometric sum of the reserve requirements to cover wind forecast errors, PV forecast errors, load forecast errors, and a system wide N-2 generator contingency of 3 GW (Brouwer, Van den Broek, et al., 2016).

C.10 Indirect greenhouse gas emissions

Although all the 100% RES scenarios we model result in no direct GHG emissions, RES generation technologies can also result in indirect GHG emissions arising not from the generators themselves, but from upstream activities such as mining, and fuel transport. Performing rigorous environmental life-cycle analysis is beyond the scope of this study; however, we can make a rough estimate and comparison of the indirect GHG emissions of our 100% RES scenarios, using indirect emissions factors available from the JRC given in Table C-7 (JRC, 2014). The results are given in Figure C-12, showing that most 100% RES scenarios result in indirect emissions of approximately 250 Mt CO_{2eq} y^{-1}, a 100 Mt CO_{2eq} y^{-1} (71%) increase from the current indirect emissions of about 150 Mt CO_{2eq} y^{-1}. While this is a significant relative increase, it should be kept in mind that the 100% RES scenarios also result in a saving of

1100 Mt CO_{2eq} y^{-1} of direct GHG emissions compared with 1990 levels. Furthermore, this 100 Mt CO_{2eq} y^{-1} could be offset by replacing approximately 16 GW of the Bio-FB capacity with Bio-FB-CCS.

Biomass is the largest source of indirect emissions due to cultivation, harvesting and transport. Note that while emissions from indirect land use change (ILUC) are not considered above, they are unlikely to be significant as almost all the biomass used by the model derives from agricultural and forestry industry residues and wastes, not from dedicated energy crops which would displace existing forests. Furthermore, forested areas are completely excluded from the list of suitable locations for the deployment of vRES capacity.

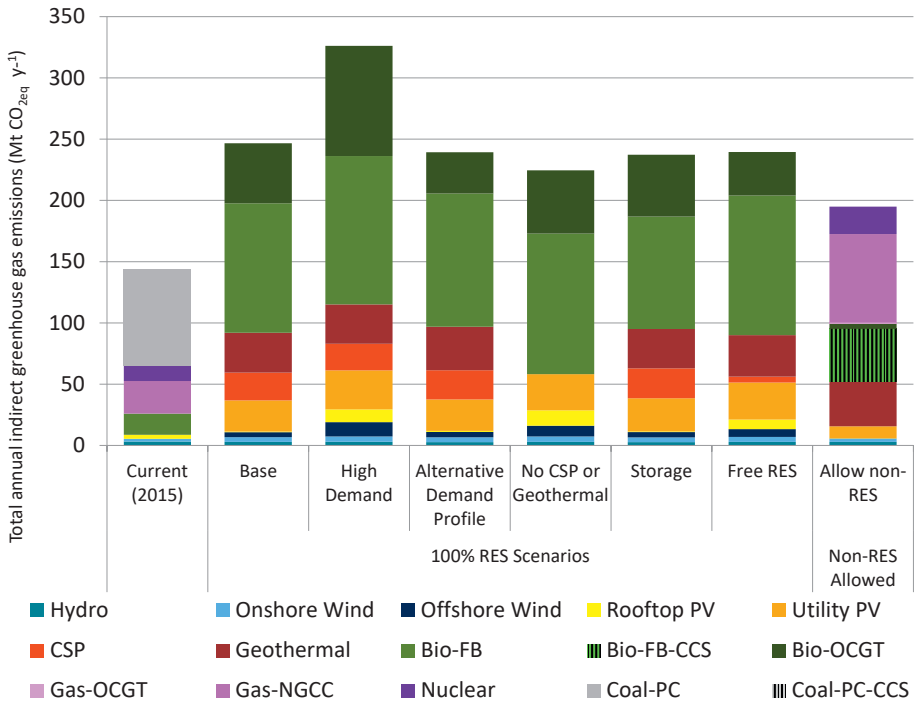

Figure C-12 | Estimated indirect GHG emissions from the 2050 power system scenarios from this study, based on calculated generation in the worst weather year 2020. Estimated emissions from the power system in 2015 are also shown as a comparison. Indirect GHG emission factors are taken from (JRC, 2014).

Table C-7 | Indirect GHG emission factors for electricity production (JRC, 2014)

Technology	Indirect greenhouse gas emissions (t CO_{2eq} GWh^{-1} generated)
Onshore Wind	7
Offshore Wind	11
Rooftop PV	32
Utility PV	38
CSP	35
Geothermal	92
Hydro (all)	6
Biomass (all) [a]	146
Gas-OCGT	100
Gas-NGCC	65
Gas-NGCC-CCS	77
Nuclear	15
Coal-PC	89
Coal-PC-CCS	115

[a] *No value is available for biogas in the raw data, thus we assume the same value as for Bio-FBs.*

Footnotes to Appendix C

[1] A general rule of thumb is that panels are installed at a tilt angle equal to the latitude of the site, representing the average solar altitude angle and thus maximizing the direct radiation component. However, shadowing from location terrain and surrounding buildings can reduce direct irradiance making a flatter tilt angle more favourable in mountainous, built-up and high latitude locations, thus the optimum angle is not always straightforward, or achievable (Mehleri et al., 2010; Šúri et al., 2007).

[2] As of 2017, solar tower technologies represent two-thirds of new CSP capacity that has been announced, is under development, or under construction (Mehos et al., 2017). Ultimately, either technology could be used in the modelling.

[3] This value includes Turkey

[4] A detailed list of generators per country is available from (ENTSO-E, 2017b) under *'Installed generation capacity per unit [14.1.B]'*. The list does not include all hydro plants, but the shares of RoR, STO and PHS capacity in the list are assumed to reflect reality.

[5] The unmet demand in the peak hour of residual demand (demand – vRES generation) dictates the required system capacity and would ideally be used for this calculation. However, before performing the capacity expansion optimisation it is not known where and how much solar PV and wind is installed, thus we use raw demand values as a proxy, as higher raw demand hours are more likely to be high residual demand hours. Given this uncertainty, and the fact that demand shedding and shifting can also impact the peak residual demand hour, we average over several peak load hours.

[6] Based on the total demand aggregated across all countries. For example, if the average wind capacity factor in one grid cell during the top 0.1% demand hours was 12% in 2004, 15% in 2005, and 9% in 2006, the wind capacity credit for that cell would be taken as 9%. This is a simplification as there is no guarantee that the hours of total peak demand will also be the hours with peak residual demand. However, the higher absolute demand makes this more likely. This approach also ensures that the reliability of vRES across all years it taken into account.

[7] Included in this category are grassy and agriculture fuels which are not strictly 'woody' (lignocellulosic), but we use this term loosely as 'wood-like' to distinguish between fuels which are solid and relatively clean, as opposed to waste-based solid fuels, and biogas substrates which may be in slurry or liquid form, contain significant impurities, and not suitable for direct combustion.

[8] This is a simplification as large countries (e.g. Germany) are also building HVDC lines to overcome internal grid constraints. Also, HVDC may also be chosen for long underground cables to reduce losses. However, without detailed data of the full transmission network infrastructure, this simplification is necessary.

[9] While forecast accuracy may vary for different countries, we take Germany as the country with the highest installed capacity of both wind and PV in Europe, and thus more likely to utilise the best forecasting methods available.

[10] The 'actual' generation patterns are formed by combining the optimised vRES capacity distribution from PLEXOS' capacity expansion algorithm with the capacity factor profiles built from ERA-Interim. As the distribution of vRES capacity is not known until the capacity expansion problem has been solved, reserves cannot be included in the capacity expansion problem, but they are included in the detailed hourly UCED calculations.

Appendix D Appendices to Chapter 5

Abbreviations

AD	Anaerobic digestion
BECCS	Bioelectricity with carbon capture and storage
CAPEX	Capital expenditure
CCS	Carbon capture and storage
CF	Capacity factor
CM	Capacity market
CWE	Central Western Europe
DAC	Direct air carbon capture
ENTSO-E	European Network of Transmission System Operators for Electricity
EDF	Electricity de France
EOM	Energy-only market
ETRI	Energy Technology Reference Indicators
EU	European Union
FCR	Frequency containment reserve
FOM	Fixed operating and maintenance
GT	Open-cycle gas turbine
HVAC	High-voltage alternating current
HVDC	High-voltage direct current
IPCC	Intergovernmental Panel on Climate Change
JRC	European Union Joint Research Centre
LoLE	Loss of load expectation
LoLP	Loss of load probability
OCC	Overnight capital cost
OECD	Organisation for Economic Co-operation and Development
PHS	Pumped hydro storage
PV	Photovoltaic
RES	Renewable energy source
RoR	Run-of-river hydro
SRMC	Short-run marginal cost
STO	Storage hydro
TCR	Total Capital Requirement
TSO	Transmission system operator
TYNDP	Ten-Year Network Development Plan
UCED	Unit commitment and economic dispatch
VOM	Variable operating and maintenance
VoLL	Value of lost load
vRES	Variable renewable energy source
WACC	Weighted average cost of capital

D.1 Installed vRES capacity scenarios

The exogenous increase in variable renewable energy source (vRES) capacity from 2017 to 2040 in the considered four countries is based on scenarios taken from ENTSO-E's Ten Year Network Development Plan (TYNDP) 2018 (ENTSO-E & ENTSO-G, 2018). Starting from the actual installed capacity in 2017, the 2025 capacity is taken from the *Best Estimate* scenario, the 2030 capacity taken from the *Distributed Generation* scenario, and 2040 capacity taken from the *Global Climate Action* scenario. As shown in Figure D-1, TYNDP18 provides a number of scenarios for 2030 and 2040, with different levels of vRES deployment. Only two scenario sets provide capacity for the years 2030 and 2040: the *Distributed Generation* and *Sustainable Transition* scenarios. However, the *Global Climate Action* scenario is more ambitious regarding the amount of vRES deployment by 2040, particularly regarding the offshore wind. For this reason, we chose to base vRES deployment by mixing the *Distributed Generation* scenario for 2030 and *Global Climate Action* scenario for 2040 to explore a high level of vRES penetration. The installed capacity in intermediate years it found by linear interpolation between the scenario years 2017, 2025, 2030 and 2040. As a result, total installed solar photovoltaic (PV) capacity increases by 217 GW (~410%), onshore wind by 83 GW (~130%) and offshore wind by 80 GW (~1400%) between 2017 and 2040.

D.2 Electricity demand

Like the vRES capacity, developments in electricity demand until 2040 are based on the ENTSO-E's TYNDP 2018. Starting from actual demand in 2017 of 1169 TWh, base electricity demand increases to 1256 TWh in 2040 based on the *Global Climate Action* scenario. Demand for the years 2020, 2025 and 2030 is taken from the *Best Estimate 2020*, *Best Estimate 2025* and *Distributed Generation 2030* scenarios[1]. Demand for all intermediate years is estimated by linear interpolation between the fixed scenario years. Note that this underlying demand does not include any contribution from charging batteries, pump load for pump storage hydro, additional demand for direct air carbon capture (DAC), or hydrogen production.

D.3 Transmission

Transmission capacity within Central Western Europe (CWE) and between neighbouring countries increases over time based on ENTSO-E's TYNDP2018 *Global Climate Agreement* scenario (ENTSO-E & ENTSO-G, 2018). Transmission capacities are increased in the year 2020, 2027, and 2035[2]. We also include transmission losses of 2% (CEER, 2017; ENTSO-E, 2017c). Transmission line outages are not included as forced outages are reportedly very rare, and all interconnectors are modelled as notional single (bi-directional) high voltage direct current (HVDC) lines (VVA et al., 2018), while in reality neighbouring countries are linked by several high voltage alternating current (HVAC) interconnectors with individual outages.

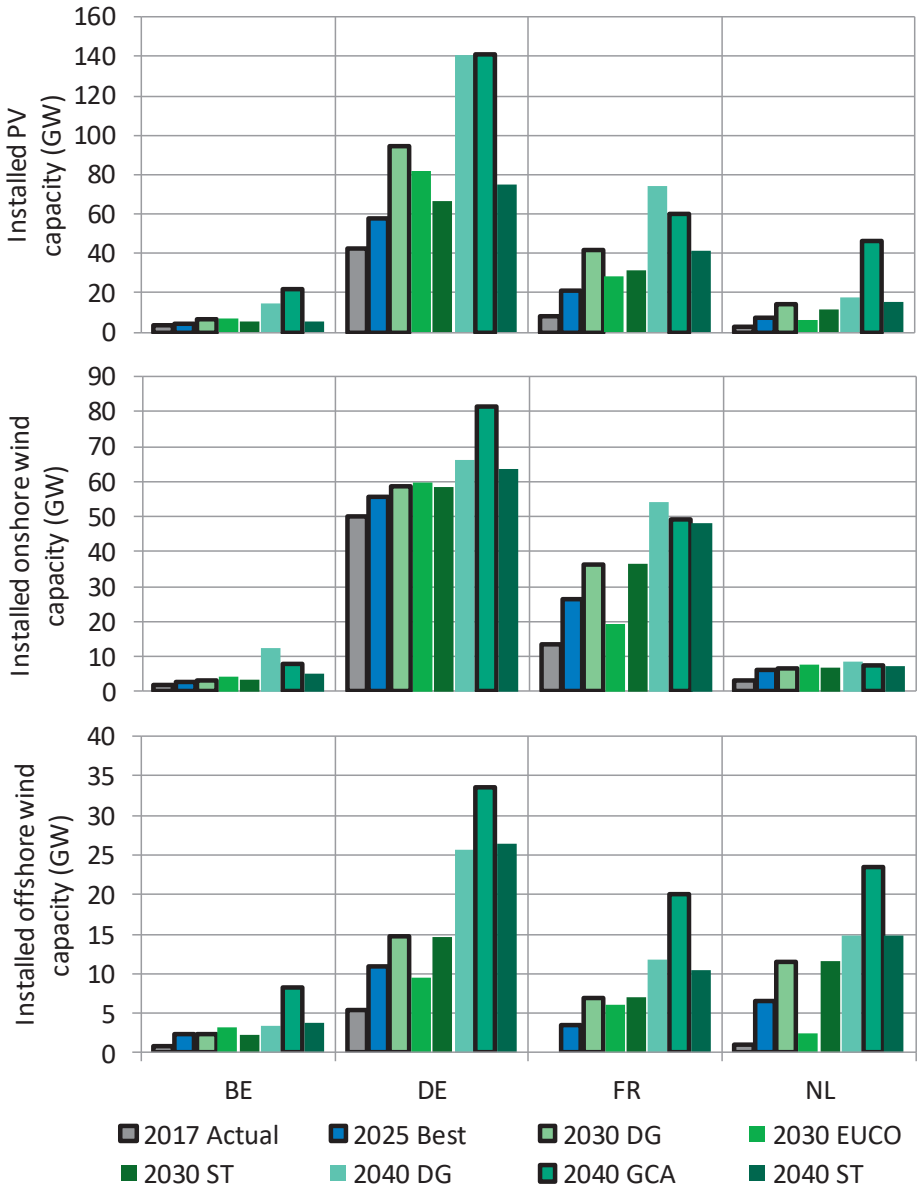

Figure D-1 | Installed capacities of PV, onshore wind and offshore wind in Belgium, Germany, France and the Netherlands for 2017, as well as several future scenarios from ENTSO-E's TYNDP 2018 (ENTSO-E & ENTSO-G, 2018)**.** The assumed deployment of PV and wind in the present study is based on the scenarios outlined in black, with intermediate years interpolated.

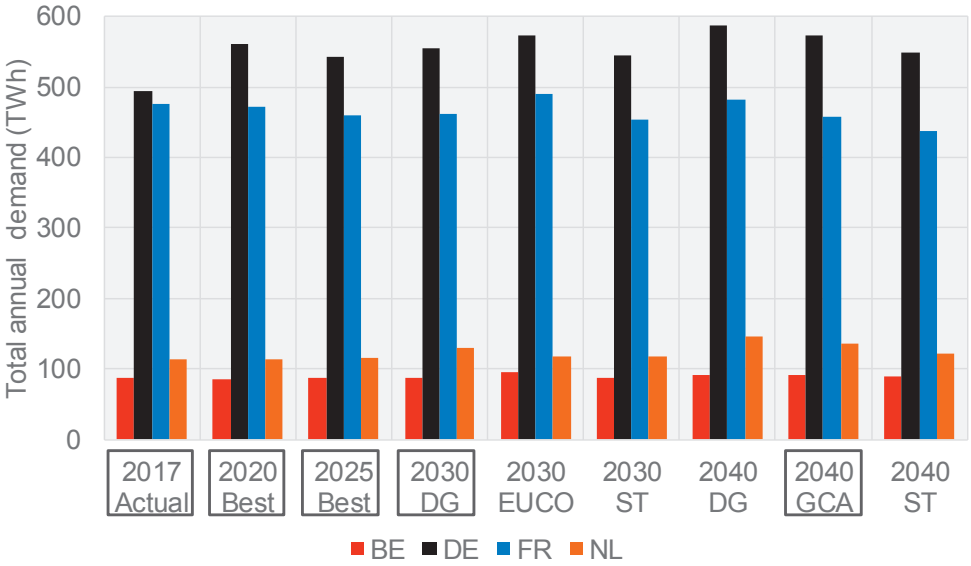

Figure D-2 | Current (2017) and future demand scenarios from ENTSO-E's TYNDP 2018 for Belgium, Germany, France and the Netherlands (ENTSO-E & ENTSO-G, 2018)**.** The scenarios highlighted with a black rectangle are used to construct the demand profiles in the present study, with linear interpolation used for intermediate years.

Table D-1 | Assumed development of transmission capacity in the forward (=>) and reverse (<=) directions (MW) (ENTSO-E & ENTSO-G, 2018)

	2017		2020		2027		2035	
Border	=>	<=	=>	<=	=>	<=	=>	<=
DE-AT	5000	5000	5000	5000	7500	7500	7500	7500
BE-DE	1000	1000	1000	1000	1000	1000	2000	2000
BE-FR	600	1850	1800	3300	2800	4300	4300	5800
BE-GB	0	0	1000	1000	1000	1000	2000	2000
BE-NL	950	950	2400	1400	3400	3400	4900	4900
DE-CH	800	4000	2700	4600	3300	5600	4100	6500
FR-CH	3150	1300	3150	1300	3700	1300	6200	3800
DE-CZ	1500	2100	1500	2100	2000	2600	2000	2600
DE-DK	2100	2380	2500	2765	4000	3985	4000	4000
FR-DE	1800	2300	1800	2300	4500	4500	4800	4800
DE-GB	0	0	0	0	1400	1400	1400	1400
DE-PL	500	2500	500	2500	2000	3000	4500	3000
DE-NL	4250	4250	4250	4250	5000	5000	5000	5000
DE-NO	0	0	1400	1400	1400	1400	1400	1400
DE-SE	615	615	615	615	1315	1300	2315	2315
NL-DK	0	0	700	700	700	700	700	700
FR-ES	2800	2600	2800	2600	5000	5000	9000	9000
FR-IT	3150	1160	4400	2310	4500	2360	5500	3360
FR-GB	2000	2000	2000	2000	6900	6900	5900	5900
NL-GB	1000	1000	1000	1000	1000	1000	2000	2000
NL-NO	700	700	700	700	700	700	1700	1700
AT-CZ	700	700	900	800	1000	1200	1000	1200
AT-CH	250	1200	1200	1200	1700	1700	1700	1700
AT-IT	300	100	405	235	1050	850	1605	1335
CZ-PL	600	800	600	800	600	600	600	800
GB-NO	0	0	0	0	2800	2800	2400	2400
DK-NO	0	0	1640	1640	1700	1640	2640	2640
DK-SE	1700	1300	1700	1300	1700	1300	2700	2300
DK-PL	0	0	0	0	0	0	500	500
NO-SE	3695	3995	3695	3995	3695	3995	4195	4495
PL-SE	600	600	600	600	600	600	1100	1100

D.4 Generator techno-economic and other parameters

Costs for new generation investments

Consistent cost data for all considered generators types is difficult to find in a single source. Table D-2 presents an overview of investment costs for conventional and low-carbon technologies from three different studies, showing the ranges and uncertainty in the data. Significant cost reductions are also expected for some technologies over time which should be taken into account. Based on a review of the literature, the sources and assumptions below are taken. The assumed OCC for all technologies over time is shown in Figure D-3.

- The OCCs for conventional thermal coal and gas plants without carbon capture and storage (CCS) as well as nuclear are taken from the European Commission Joint Research Centre (JRC)'s Energy Technology Reference Indicators (ETRI) 2014 (JRC, 2014). No cost reductions are assumed for these mature technologies. VOM and FOM costs are also taken from (JRC, 2014).
- The OCCs for vRES and low-carbon thermal technologies (e.g. coal and gas plants with carbon capture and storage (CCS), biogas and biomass plants) are taken from a more recent JRC publication by Tsiropoulos et al. for the years 2015, 2020, 2030 and 2040 (Tsiropoulos et al., 2018). These fall over time in line with the 'ProRES' scenario for the vRES technologies and 'Diversified' scenario for the other technologies. The OCC for other years is found by interpolation. VOM and FOM costs are taken from (JRC, 2014).
- The costs for batteries and electrolysers are taken from Child et al. (Child et al., 2019), which assume optimistic cost reductions of 80% and 50% respectively between 2017 and 2040.
- The costs for DAC are based on Keith et al. (Keith et al., 2018).
- The costs for bioenergy with CCS are derived from other assumptions, explained later.

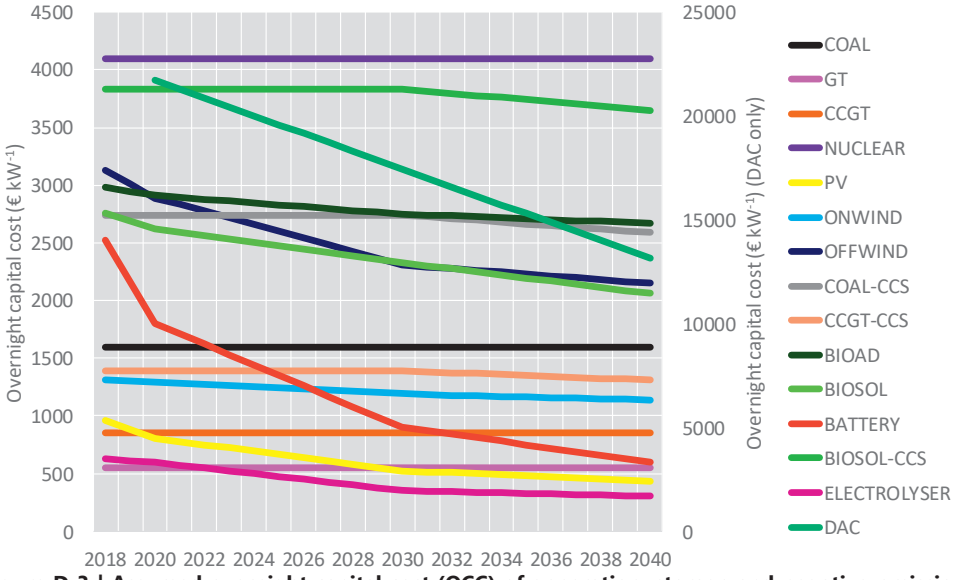

Figure D-3 | Assumed overnight capital cost (OCC) of generation, storage and negative-emission technologies over time. (excluding IDC). Costs for DAC are on the basis of electricity demand.

Table D-2 | Comparison of future overnight capital cost (OCC) estimates in € kW^{-1} for different power generation technologies

Generator category	Technology variant	Tsiropoulos et al. (2018)			IEA WEO 2016 (2016)			JRC ETRI 2014 (2014)		
		2020	2030	2040	2020	2030	2040	2020	2030	2040
Coal	PC, SC	-	-	-	1800-1800	1800-1800	1800-1800	1550-1700	1550-1700	1550-1700
	Lignite, SC	-	-	-				1700-2400	1700-2400	1700-2400
	PC, IGCC	-	-	-	2250-2250	2115-2115	2070-2070	2255-2850	2255-2850	2055-2850
	Lignite IGCC	-	-	-				2600-3250	2600-3250	2600-3250
Coal+ CCS	PC, SC, post-combustion	-	2630-2830	2400-2790	4590-4950	3600-4500	3150-4320	2340-3020	2210-2850	2210-2850
	PC SC, oxyfuel	-	2560-2810	2270-2750	4770-5130	3780-4680	3330-4500	2340-3060	2210-2890	2210-2890
	Lignite IGCC, pre-combustion	-	3570-4200	2900-4040	4905-5265	3825-4725	3375-4455	3820-4850	3820-4850	3820-4850
	PC, IGCC, pre-combustion	-	2350-2760	1900-2660				2600-3300	2550-3230	2550-3230
GT		-	-	-	450-450	450-450	450-450	400-650	400-650	400-650
CCGT		-	-	-	900-900	900-900	900-900	700-950	700-950	700-950
CCGT+CCS	Post-combustion	-	1320-1510	1190-1510	2565-2790	1980-2520	1710-2385	1250-1750	1250-1750	1250-1750
Nuclear	3rd generation LWR	-	-	-	5400-5400	4590-4590	4050-4050	3850-5800	3650-5450	3400-5050
Biomass	Grate furnace steam turbine	-	-	-	2115-2115	2070-2070	1980-2025	2250-3500	2020-3140	1820-2810
	FBB	-	-	-				1540-3170	1350-2780	1190-2440
	IGCC	-	-	-				1390-4380	1230-3640	1090-3260
	ORC	4200-4600	3950-4540	3720-4510				-	-	-
	AD	2770-3030	2600-3000	2450-2970	-	-	-	2080-5210	1700-4260	1530-3830
	MSW	-	-	-	6615-6615	6480-6525	6300-6390	4430-8020	4010-7260	3630-6560
BECCS	IGCC, pre-combustion	-	5160-5800	3680-5800	-	-	-	-	-	-
Solar PV	Utility (ground) , no tracking	650-920	390-870	310-780	918-936	720-774	630-702	650-900	520-720	470-650
	Residential (buildings) inclined	860-1230	520-1150	410-1050	1152-1152	918-972	810-882	950-1250	850-1120	810-1060
Wind onshore	Low capacity, low hub height	1670-1830	1430-1800	1310-1780	1602-1602	1530-1548	1494-1512	1100-2000	1000-1800	900-1700
	Med capacity, med hub height	1220-1330	1040-1320	960-1300						
	High capacity, high hub height	990-1080	840-1060	770-1050						
Wind offshore	Monopole, 30-60 km offshore	2390-3260	1550-3180	1350-3140	3465-3465	2655-2880	2295-2610	2580-4270	2280-3970	2080-3470
	Jacket, 30-60 km offshore	2460-3360	1600-3280	1390-3230						
Notes (general): •OCC does not include interest during construction (IDC) •Costs for CO_2 transport and storage included		•Costs in €$_{2015}$ kW^{-1} •Study considered several scenarios based on different learning and deployment rates. The range (min-max) is given here. •Utility PV >10 MW, residential PV <20 kW			•Costs in €$_{2015}$ kW^{-1} converted from USD$_{2015}$ assuming exchange rate of 1 USD= 0.9 € •Lower value in range is for the *450* scenario, upper for the *New Policies*			•Costs given in €$_{2013}$ kW^{-1} •Range given for low and high capex estimates •Utility PV >2 MW, residential PV < 100 kW		

Abbreviations: AD - Anaerobic digestion, CCGT – Combined cycle gas turbine, FBB – Fluidised bed boiler, IGCC – Integrated gasification combined cycle, LWR – Light water reactor, GT – Open cycle gas turbine,ORC – Organic Rankine cycle, PC – Pulverised steam coal, SC – Supercritical

Retrofits

In order to see how existing generation infrastructure could be utilised in a future low-carbon power system with high shares of vRES, two retrofit options are possible for both relatively new legacy generators (built between 1990 and 2016), and generators built by the model after 2017: (i) retrofitting with CCS (coal, CCGT and biomass generators only), and (ii) full conversion to 100% biomass (coal generators only). The possible retrofit pathways are shown in Figure D-4. In order to simplify the modelling, a generator can only undergo one retrofit step. For example, a coal generator cannot first be retrofit with CCS in one year, and then undergo biomass conversion in another year. However, it can undergo both conversion to biomass and retrofit to CCS in a single retrofit. These conversions/retrofits are one-way only and cannot be reversed.

Regarding CCS retrofits, the IEA notes that from an economic point of view, CCS retrofits for power plants are generally only profitable if the original plant has a net electrical efficiency higher than 40% (Rohlfs & Madlener, 2010). For this reason, we assume that only relatively modern coal and gas plants built after 1990 can be retrofit with CCS. Regarding conversion to biomass, we assume that coal plants can directly co-fire up to a maximum of 10% biomass fuel with no additional capital requirements. However, full conversion to biomass requires significant capital investment, as explained in the next section.

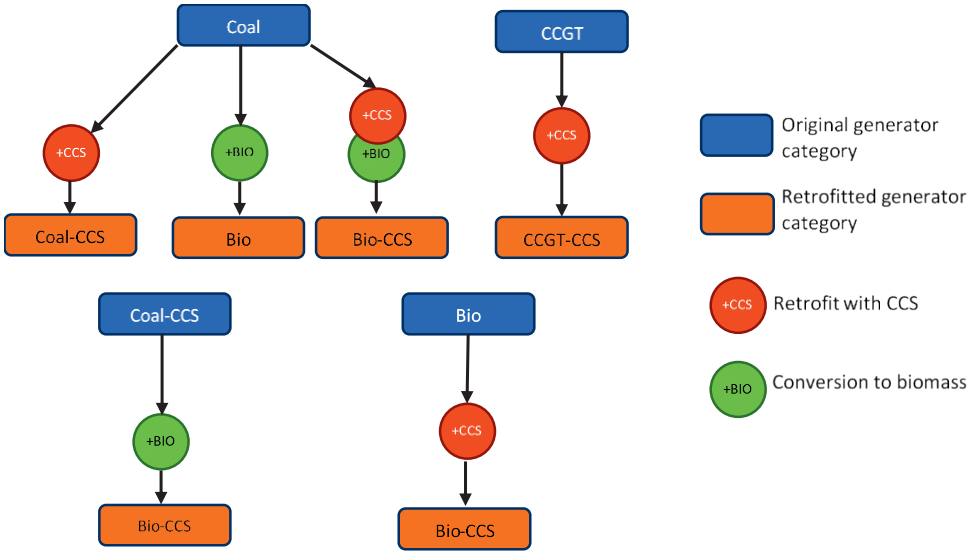

Figure D-4 | Allowable retrofit pathways for different generator types.

Cost of retrofits

The cost of retrofitting an existing gas or coal plant with CCS is assumed to be 60% the total capital requirement (TCR) of a newly-built plant with CCS based on (Gibbins et al., 2011). This investment level assumes that sufficient additional capacity is added during the retrofit that the total electric capacity of the plant remains the same after the retrofit, despite a fall in nominal efficiency.

A survey of the literature was performed on the cost of converting an existing coal-fired power plant to biomass (Table D-3). Some of these data were taken from general sources, while others were taken for actual conversions of specific individual plants. Due to the model complexities introduced by allowing both co-firing of biomass and one-way conversion of biomass, some simplifications were necessary as explained below:

- Coal plants (with and without CCS) can co-fire up to maximum 10% biomass fuel with no additional capital expenditure (CAPEX) requirements, and
- Coal plants can undergo a one-way conversion to 100% biomass at a cost of 700 € kW^{-1}. Once this conversion is complete, coal can no longer be used.

Table D-3 | Comparison of investment cost estimates for partial or full conversion of coal plants to solid biomass fuel

	Source				
Parameter	JRC (JRC, 2014)	IEA-ETSAP (IEA-ETSAP & IRENA, 2013)	ECN (ECN, 2016)	Ontario Power Generation (Marshall, 2018)	Drax (Drax, 2018)
Co-firing Investment cost (€ kWe^{-1})	160-(420)-960	220	30 - 350	~530	~390
Type of conversion	Co-firing	Co-firing	Co-firing (up to 20% biomass)	Full conversion (100% biomass)	Full conversion (100% biomass)
Nominal plant capacity (MW)	-	-	700-1100	205	3 x 660
Comments	*Max. share of biomass not specified*	*Max. share of biomass not specified*	*Based on calculations by ECN for the Dutch SDE+ subsidy rates in 2017.*	*Ontario Power Generation spent $170 million CAD (€110 million) to convert its 205 MW Atikokan coal plant to biomass*	*Drax spent £700 million (€780 million) to upgrade three of its 660 MW units and associated supply chain infrastructure to use biomass*

In order to allow for the retrofitting of existing coal, gas and biomass plants with CCS, and the conversion of coal plants to biomass, some deviations from literature cost values were necessary to ensure internal consistency within the model, based on the following principles:

- the TCR of a completely new gas/coal/biomass plant equipped with CCS should be lower than the total cost of building a new gas/coal/biomass plant and subsequently retrofitting it with CCS, and

- the TCR of a completely new Biomass-CCS plant should be:
  - lower than the cost of building a new coal plant, retrofitting it with CCS, and performing a full biomass conversion (~ 4650 € kW^{-1} in 2030),
  - lower than the cost of building a new Coal-CCS plant and performing a full biomass conversion (~4030 € kW^{-1} in 2030), and
  - lower than cost of building a new biomass plant and retrofitting it with CCS (~5500 € kW^{-1})[3].

As the reported cost of new Biomass-CCS plants in Tsiropoulos et al. (Tsiropoulos et al., 2018) for the Diversified scenario (~5380 € kW^{-1}) is higher than in the above retrofit pathway costs, the model could choose to add carbon negative capacity by installing new biomass or Coal-CCS capacity and retrofitting it all in the same year, rather than installing a purpose-built Biomass-CCS plant which seems illogical. To avoid this, the TCR for Biomass-CCS plants is set at a level (~ 3800 € kW^{-1} in 2030) which makes the TCR of a new plant slightly lower than the TCR of any of the retrofit pathways. The assumed cost for new Biomass-CCS plants is thus somewhat lower than reported by the above literature sources, though higher than that assumed in some other studies[4].

vRES Capacity Factors

Country- and technology-specific hourly capacity factors (CF) for wind and PV are taken from the Renewables Ninja dataset (Pfenninger & Staffell, 2016; Staffell & Pfenninger, 2016). For vRES generation in 2017 we use historical generation from ENTSO-E (ENTSO-E, 2018b) while for all subsequent years, a random weather year is selected from Renewables Ninja. The selected years used in the simulations are shown in Table D-4.

Table D-4 | Weather years selected for the simulated model years

Model year	Weather Year	Model year	Weather Year
2017	-	2029	2011
2018	2005	2030	2009
2019	2016	2031	2002
2020	1997	2032	2009
2021	2010	2033	1999
2022	2011	2034	2007
2023	1995	2035	2016
2024	1997	2036	1987
2025	2011	2037	2005
2026	1999	2038	2000
2027	1996	2039	2013
2028	2014	2040	2011

Several inconsistencies were found between the vRES generation and installed capacities (and resulting CFs) reported by ENTSO-E, industry bodies and national statics offices, and the CFs Renewables Ninja. Moreover, vRES CFs are likely to increase over time due to technology improvements and re-powering of old plants (JRC, 2014). As a result, some adaptations are made to the ENTSO-E generation data and vRES profiles from Renewables Ninja:

- Due to some significant differences (e.g. onshore wind in Belgium), the hourly 2017 generation values from ENTSO-E (used for 2017 only) are scaled so that the CFs match those calculated from EurObserver generation and capacity data (EurObserv'ER, 2018, 2019).
- Assuming that 2017 was a typical weather year in terms of solar and wind generation, the hourly CFs from Renewables Ninja are scaled so that the average long-term CFs match those calculated for EurObserver in 2017.[5]
- The very high offshore wind CF for France in the Renewables Ninja dataset (46%) was based on only 6 MW of turbine capacity, which is unlikely to be a representative value for the whole country once deployment levels increase. Thus, the CFs were scaled down to match the average of the other CWE countries (38.6%)
- After the above corrections were performed on the raw profiles, the CFs for PV and wind in future years were gradually increased over time based on projected CFs from (JRC, 2014).

The net result of these adaptations are that (i) the CFs and installed capacities in the reference year 2017 align with the generation reported by EurObserver, (ii) thanks to the use of the (corrected) Renewables Ninja profiles the CFs are country specific, and retain some natural interannual variability whilst being consistent with the EurObserver data, and (iii) CFs generally increase over time due to technology improvements (Table D-5) .

Firm capacity

The firm generation is relevant for determining the amount of capacity required to meet firm capacity constraints in the market designs with a capacity margin. Firm capacity varies depending on the generator type and in some cases the country, as explained below:

- The firm capacity of all thermal generators is set at 90%,
- The firm capacity of hydro is set based on the ENTSO-E Winter 2017 Outlook (ENTSO-E, 2017a) as follows:
    - For storage and run-of-river (ROR) hydro,
        - FR: 38% (Autumn/Summer), 74% (Winter/Spring), DE: 25% (all year)
    - For pumped storage.
        - BE: 100%, DE: 80%, FR: 27% (Autumn/Summer), 45% (Winter/Spring)
- The firm capacity of vRES varies with its penetration, and is estimated by calculating the average capacity factor during the top 5% of hours with the highest residual load, using the load scenarios and Renewables Ninja vRES profiles for the years 2017 to 2041 (Figure D-5).
- Batteries are assumed to be fully firm[6].

Table D-5 | Adjustments made to 2017 generation profiles from ENTSO-E and hourly capacity factor (CF) profiles from Renewables Ninja

Technology	Country	Reported 2017 generation (TWh)			Installed capacity in 2017 (GW) [b] (EurObserv'ER, 2018, 2019)	Calculated CF (%) in 2017 based on generation from...		Correction applied to ENTSO-E 2017 generation (%)relative)	Long-term [c] average CF from Renewables Ninja (%)	Correction applied to Renewables Ninja CFs (% absolute)	Increase in average CF between 2017 and 2040 (%)
		ENTSO-E (ENTSO-E, 2018b)	EurObserver (EurObserv'ER, 2018, 2019)	Difference (%)		ENTSO-E	EurObserver				
PV	BE	2.9	3.1	-9%	3.8	8.6%	9.3%	+9%	12.3%	-3.0%	+2%
	DE	35.9	39.9	-11%	42.4	9.7%	10.7%	+11%	12.4%	-1.7%	
	FR	8.9	8.6	3%	8.0	12.6%	12.2%	-3%	14.0%	-1.8%	
	NL	1.9	2.1	-12%	2.7	7.8%	8.7%	+12%	12.2%	-3.5%	
Onshore wind	BE	2.6 [a]	3.9	-46%	2.0	15.3%	22.4%	+46%	24.5%	-2.1%	+7%
	DE	85.3	88.0	-3%	50.2	19.4%	20.0%	+3%	19.4%	0.6%	
	FR	22.8	24.7	-8%	13.6	19.2%	20.8%	+8%	24.7%	-3.9%	
	NL	7.4	6.9	7%	3.3	25.3%	23.7%	-7%	24.4%	-0.7%	
Offshore wind	BE	2.8	2.6	4%	0.9	36.0%	34.4%	-4%	31.6%	2.8%	+6%
	DE	17.4	17.7	-1%	5.4	36.8%	37.3%	+1%	33.3%	4.0%	
	FR	0.0	0.0	0%	0.0	-	-	-	46.0%	-7.4%	
	NL	3.6	3.7	-2%	1.0	43%	44.1%	+2%	33.1%	11.0%	

[a] *The Belgian onshore wind data from ENTSO-E was clearly erroneous, and the data was taken from ELIA instead.*

[b] *EurObserver values were used instead of ENTSO-E reported values as these seem to agree better with national statistics.*

[c] *The average across all weather years available in the Renewables Ninja dataset (1980-2016 for wind, 1985-2016 for PV)*

Planned and forced outages

Generators are assumed to be offline 4% of the year due to planned outages, and 6% of the year due to unplanned/forced outages based on (VVA et al., 2018). The mean time to repair for forced outages is 9 hours, based on the same source.

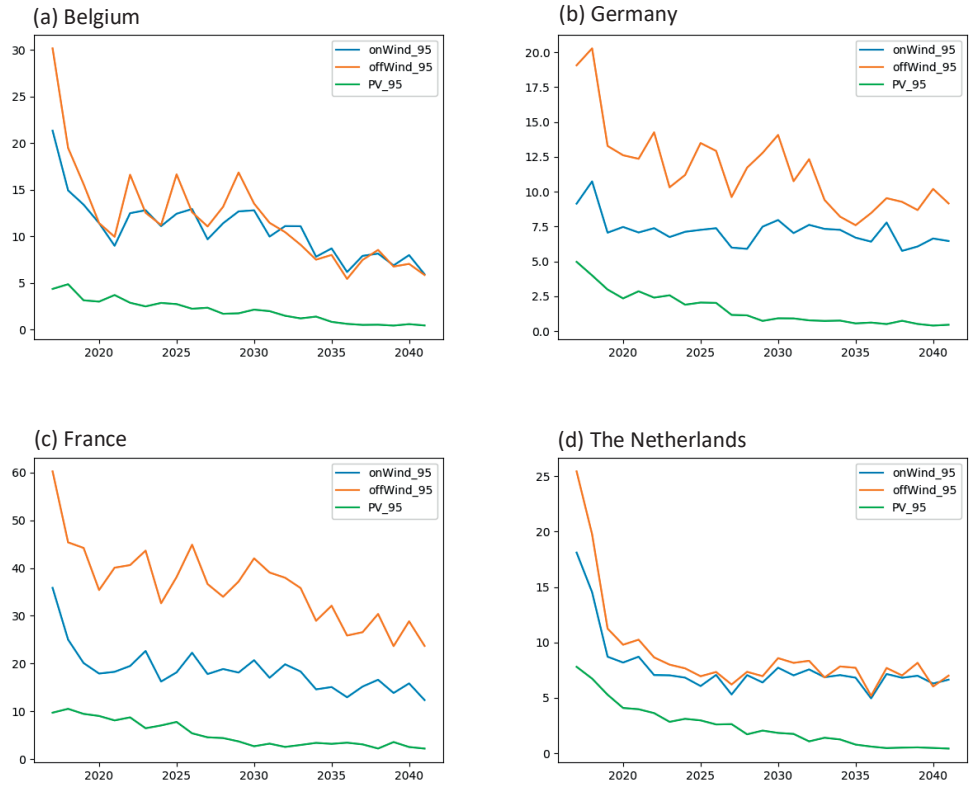

Figure D-5 | Estimated firm capacity (in %) of vRES technologies in the CWE countries, calculated based on the average capacity factor during the top 5% of hours per year with the highest residual demand, calculated using the ENTSO-E TYNDP18 demand profiles and vRES capacity factors from Renewables Ninja. The weather years used are the same randomly selected years used in the main study.

D.5 VoLL and load shedding

Several studies have attempted to determine the value of lost load (VoLL) for different consumer types in Europe. An overview is presented in a recent study by Cambridge Economic Policy Associates (CEPA) (Heather et al., 2018), which also made its own estimation of the VoLL of different consumer groups across the EU based on extensive surveys. They found that VoLL varies significantly between consumer groups and was highest for the residential and service sectors with values typically above 7000 € MWh^{-1} (see Figure D-6). Values for industrial consumers were typically lower ranging from 300 € MWh^{-1} up to 5000 € MWh^{-1}, though certain industrial sectors (e.g. construction) also yielded high values. However, there were also significant differences between countries, with the domestic VoLL ranging from some 7000 € MWh^{-1} in France up to 23000 € MWh^{-1} in the Netherlands.[7] These VoLL levels can be used to estimate the implied socially-acceptable level of system reliability by calculating the number of hours at which the cheapest provider of peak capacity (e.g. a GT) would need to run annually to break even. For example, in an ideal EOM, the market should result in generation capacity

being built up to the point where the marginal expected revenues of adding new generation capacity (i.e. $VoLL * LoLP * 8760$) become equal to the marginal costs of providing that capacity (Cramton et al., 2013). On an annualised per MW basis, this can be expressed as:

$$LoLE = \frac{CAPEX + FOM}{VoLL - SRMC} \quad \text{(D-1)}$$

where $VoLL$ is the value of lost load (€ MWh^{-1}), $LoLE$ is the loss of load expectation (h y^{-1}) - calculated as the product of the $VoLL$ (%) and number of hours in a year (8760), while $SRMC$, $CAPEX$ and FOM are the short-run marginal cost (€ MWh^{-1}), annualised investment cost (€ MW^{-1}) and fixed operating and maintenance costs of additional capacity respectively (€ MW^{-1}). Assuming this additional capacity is provided by GTs with cost parameters provided in Table 5-3, this yields LoLE values between 2.6 and 8.5 h y^{-1}, as shown in Table D-1. These levels are broadly consistent with the reliability standards used in practice by several member states of between 3 and 8 h y^{-1} (ENTSO-E, 2017d). In practice however, system reliability is considerably better than both the reliability standards and socially-acceptable level determined from the CEPA VoLL estimates, with consumers in most EU countries experiencing outages of less than one hour per year (Eurelectric, 2013a). This implies that consumers are actually accustomed to enjoying a higher level of reliability, and back-calculating the corresponding VoLL leads to much higher values than in the CEPA study. This could suggest that transmission system operators (TSOs) implicitly consider a higher VoLL in practical system planning for fear of the social outcry and political fallout associated with large-scale outages, and treat LoLE standards more as limits than targets.

For these reasons, in the PLEXOS capacity planning module, we assume a higher VoLL of 100,000 € MWh^{-1} to account for the fact that (i) consumers are accustomed to higher reliability levels than published LoLE targets which we assume must be maintained, and (ii) the vast majority of outages are due to faults in the distribution network (i.e. not transmission faults or insufficient generation capacity) which are not accounted for in our PLEXOS modelling (VVA et al., 2018), and (iii) the capacity expansion module uses load duration curves to approximate load and generation, which can miss periods of unserved energy. We take this VoLL as a uniform value across all countries and consumer types as, during scarcity events, it is not clear which consumers would be disconnected[8].

Furthermore, incorporating consumer- and region-specific VoLL values is not possible with the PLEXOS model, and using a weighted average VoLL across all consumer types would not be accurate. Instead, we model the VoLL and price sensitivity of industrial consumers by assuming that these consumers would be willing and capable of reducing their demand through voluntary load shedding at times of scarcity. In the hourly dispatch modelling (ST Schedule) however, we use a load-weighted average of the actual VoLL estimates from CEPA (10,600 € MWh^{-1}) to account for the costs of unserved consumer load as perceived by the load.

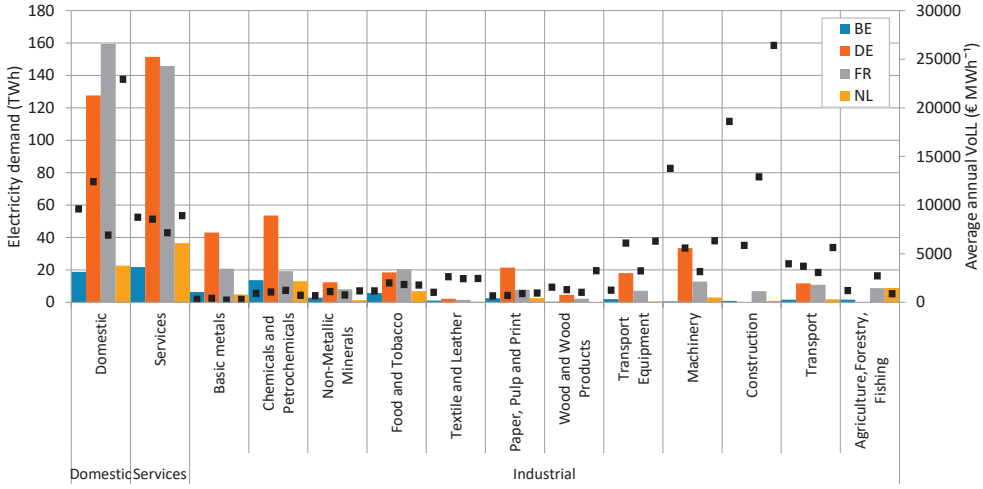

Figure D-6 | Electricity demand for 2016 and estimated average VoLL per sector for Belgium, Germany, France and the Netherlands. Demand data (bars) are taken from Eurostat (nrg_105a) (Eurostat, 2017c), while VoLL data are taken from CEPA (Heather et al., 2018).

Table D-1 | Comparison between reported loss of LoLE indices and VoLL estimates from various sources. Calculated assuming an open cycle gas turbine provides the additional capacity, using the assumptions from Table 5-3.

Country	Reported LoLE standard (ENTSO-E, 2017d) (h y^{-1})	Based on CEPA VoLL study (Heather et al., 2018)		Back-calculated from actual lost load (VVA et al., 2018)	
		Estimated VoLL [a] (€ MWh^{-1})	Implied LoLE (h y^{-1})	Average load disruption (h y^{-1}) [b]	Implied experienced VoLL (€ MWh^{-1})
BE	3	9600	7.5	No data	No data
DE	-	12400	5.8	0.48	149,000
FR	3	6900	10.5	1.45	49,500
NL	4	22300	3.22	0.52	138,000
Average [c]	-	10,600	-	-	-

[a] *Estimated based on average of all customer types (residential, commercial, industrial), from surveys*
[b] *Due to both planned and unplanned outages in period 2010-2014*
[c] *Load-weighted*

The load shedding potential per sector (in MW) per country is estimated by taking the electricity consumption per sector from 2016 (Eurostat, 2017c), calculating the average load assuming continuous operation, and assuming that 50% of this can be shed. This results in approximately 25 GW of interruptible load, or ~11% of total CWE peak demand[9].

With the lower VoLL values from industry accounted for with load shedding, we assume a higher ultimate VoLL of 10,600 € MWh^{-1} by weighting the country-specific VoLL for domestic consumers by the country-specific domestic demand.

Table D-2 | Industrial load shedding assumptions. Load shedding capacity is based on consumption data from Eurostat (Eurostat, 2017c), while load shed prices are based on average VoLL estimates from CEPA (Heather et al., 2018).

Industrial sector	Load shed capacity (GW)					Load shed price (€ MWh^{-1})
	BE	DE	FR	NL	Total CWE	
Basic metals	0.36	2.46	1.19	0.28	4.28	350
Chemicals and Petrochemicals	0.78	3.06	1.10	0.74	5.68	1030
Non-Metallic Minerals	0.16	0.70	0.46	0.07	1.40	950
Food and Tobacco	0.33	1.06	1.17	0.39	2.94	1810
Textile and Leather	0.06	0.13	0.09	0.02	0.30	220
Paper, Pulp and Print	0.15	1.22	0.45	0.14	1.96	770
Transport Equipment	0.12	1.03	0.41	0.04	1.59	5010
Machinery	0.03	1.91	0.73	0.17	2.85	5100
Wood and Wood Products	0.02	0.27	0.13	0.01	0.42	1290
Construction [a]	0.05	-	0.39	0.05	0.49	6000
Transport	0.09	0.67	0.62	0.11	1.49	3600
Agriculture, Forestry, Fishing	0.10	-	0.50	0.50	1.10	1750
Total	2.2	12.5	7.2	2.5	24.5	-

[a] *The reported VoLL for the construction sector varied considerably from 6000 € MWh^{-1} in Germany to 26000 € MWh^{-1} in the Netherlands. Even though no data on construction sector electricity consumption was available for Germany, it is likely to exceed the other countries due to the larger economy. Thus, we use a lower VoLL for this sector more in line with that of Germany.*

D.6 Reserve requirements

We account for spinning frequency containment reserve (FCR) requirements for the CWE countries by assuming a maximum risk of 3000 MW which must be procured across the whole Continental Europe (CE) interconnected system, based on current rules. The contribution from each country is based on its share of total CE generation in 2016. This gives 95 MW for Belgium, 721 MW for Germany, 128 MW for the Netherlands, and 618 MW for France. These amounts are kept the same from 2017 until 2040. Frequency restoration reserves (FRR) are not modelled.

Table D-3 | Calculated frequency containment reserve requirements

Country	Generation in 2016 (GWh) (ENTSO-E, 2018b)	Generation share 2016 (%)	Minimum FCR requirement (MW)
AT	68	2.5%	76
BE	**86**	**3.2%**	**95**
BG	45	1.7%	50
CH	64	2.4%	71
CZ	83	3.1%	93
DE	**649**	**24.0%**	**721**
DK	31	1.1%	34
EL	51	1.9%	57
ES	275	10.2%	305
FR	**556**	**20.6%**	**618**
HR	13	0.5%	14
HU	32	1.2%	35
IT	290	10.7%	322
LT	4	0.2%	5
LU	2	0.1%	2
NL	**115**	**4.3%**	**128**
PL	167	6.2%	185
PT	60	2.2%	67
RO	65	2.4%	72
SI	17	0.6%	18
SK	27	1.0%	30
Total CE	2,700	100%	3000

D.7 Carbon budgets and decarbonisation trajectories

Carbon budgets and decarbonisation trajectories for the CWE countries from 2017 onwards are determined as below, following the approach used in an earlier work (van Zuijlen et al., 2018).

- Remaining global total allowable carbon budgets from 2011 to 2100 for three climate scenarios are taken from the IPCC's 5th Assessment 2014 Synthesis report (IPCC, 2014):
    - **400 Gt CO_2** for a 66% chance of limiting global warming to 1.5 ºC i.e. the only scenario consistent with the Paris Agreement
    - **850 Gt CO_2** for a 33% chance of limiting global warming to 1.5 ºC, and
    - **1000 Gt CO_2** for a 66% chance of limiting global warming to 2 ºC

- From these values, assumed budgets for non-OECD countries, cement production, and already-emitted carbon are subtracted based on a study by Anderson & Broderick (Anderson & Broderick, 2017)[10]:
    - a total energy-related[11] emission budget for non-OECD countries of **560 Gt CO_2**, which assumes non-OECD emissions peak between 2020 and 2025, before falling by 95% (compared with 2015) by 2065.
    - a budget of **100 Gt CO_2** for the cement industry, which assumes 98% decarbonisation of cement production after 2060, and
    - a further **260 Gt CO_2** already emitted between 2011 and 2017 (Anderson & Broderick, 2017).

- The remaining total carbon budget for the energy-related sectors in the OECD countries is then allocated to the CWE countries based on population[12].

After performing these calculations, we find that the energy-related sectors in the CWE countries must sequester net emissions of between -71 Gt CO_2 to 11 Gt CO_2Gt CO_2 by the end of the century depending on the level of warming to be avoided, as shown in Table D-6. Assuming that the transformation of the energy-related sectors is completed by 2050, one can derive corresponding decarbonisation pathways for each climate scenario as shown in Figure D-7. Given that total energy-related carbon emissions in the CWE countries for 2016 was 1.3 Gt CO_2 (see Table D-7), this shows that achieving the ambitions of the Paris Agreement (or even remaining below 2 ºC) without the use of negative emission technologies or some other method of large-scale atmospheric carbon dioxide removal (e.g. afforestation) is practically unavoidable. While it might be considered optimistic to assume that the transformation occurs by 2050, delaying this beyond 2050 will mean that in order to meet the same carbon budget, more negative emissions will be required later in the century, increasing the risk of temperature overshoot.

Table D-6 | Calculation of estimated carbon budget (total Gt CO_2) for the period 2017-2100 for the CWE countries based on (Anderson & Broderick, 2017).

	Climate mitigation scenario		
	66% chance <1.5 ºC	33% chance < 1.5 ºC	66% chance < 2 ºC
Remaining global budget for 2011-2100 [a]	400	850	1000
- non-OECD energy-related emissions for 2011-2100 [b]	560	560	560
- emissions from cement and deforestation of 2011-2100 [b]	100	100	100
- Emissions already emitted between 2011-2016 [b]	260	260	260
= OECD energy-related carbon budget for 2017-2100	-520	-70	80
x CWE population as % of OECD population (%)	13.7%	13.7%	13.7%
= CWE energy-related carbon budget for 2017-2100 [c]	-71	-10	11

[a] *Based on IPCC 2014 Synthesis Report (IPCC, 2014). A more recent update suggests these values haven't changed significantly (Rogelj et al., 2018)*

[b] *Estimated by Anderson & Broderick (Anderson & Broderick, 2017)*

[c] *Downscaled from total OECD to CWE countries based on population in 2014*

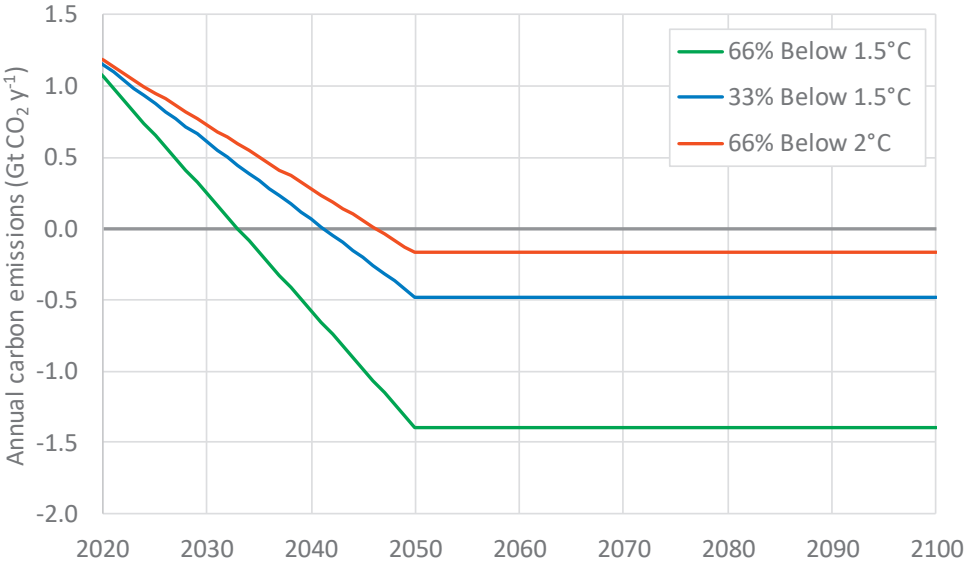

Figure D-7 | Assumed decarbonisation trajectories for the energy-related industries in the CWE countries under various climate scenarios

As shown in Table D-7, approximately 31% of energy-related emissions in CWE result from the production of electricity and heat. In order to derive a specific carbon budget for the public electricity and heat production sector[13], it is necessary to make some assumptions about how quickly total energy-related emissions falls, and how the other sub-sectors will decarbonise through till 2100. We assume that:

- as the technology options for generating negative emissions in other sub-sectors (e.g. transport, manufacturing) are limited, we assume that all negative emissions must be achieved in the electricity and heat production sector,
- for consistency with the assumed decarbonisation profile of total energy-related emissions, we assume that the other energy-related subsectors (i.e. non-electricity and heat) are fully decarbonised by the year 2050 with emissions falling linearly from 2017 to 2050, then remaining at zero thereafter,
- the required emissions from electricity and heat production are set at the level necessary to match the total energy-related carbon budgets in Figure D-7, accounting for the emissions in the other sectors.

The resulting sub-sectoral decarbonisation trajectories are shown in Figure D-8 for the three different climate scenarios, and the total budgets for electricity and heat production are shown in Table D-8. In order to be consistent with the Paris Agreement (i.e. 66% chance of keeping warming below 1.5 ºC), the CWE power sector must generate total negative emissions of approximately -87 Gt CO_2 over the period 2017-2100. This is lower (i.e. more negative) than the total energy-related budget of -71 Gt CO_2 as the power sector must compensate for the positive emissions in the other energy-related subsectors until they reach net-zero emissions in 2050. In this climate scenario, net power sector emissions turn net-negative by 2025, ultimately reaching -1.4 Gt CO_2 y^{-1} in 2050. Even in the less ambitious case of a 66% chance of remaining below 2 ºC warming, power sector emissions turn net negative by 2041, and reach -0.2 Gt CO_2 y^{-1}.

Table D-7 | Energy-related carbon emissions for the CWE countries in 2016 by sub-sector (Source: Eurostat/EEA [env_air_gge])

Sector/Subsector	Total emissions (Mt CO_2)
Energy	1,312
Fuel combustion - sectoral approach	1,306
Fuel combustion in energy industries	458
Fuel combustion in public electricity and heat production	402
Fuel combustion in petroleum refining	41
Fuel combustion in manufacture of solid fuels and other energy industries	15
Fuel combustion in manufacturing industries and construction	213
Fuel combustion in transport	352
Other fuel combustion sectors	280
Other fuel combustion sectors n.e.c.	1
Fuels - fugitive emissions	7
Transport and storage of CO_2	0

Table D-8 | Calculated carbon budget for public electricity and heat production in the CWE countries, as well as net emissions in 2030, 2040 and 2050 for various climate scenarios

		Climate mitigation scenario (% chance of remaining below)		
		66% <1.5 ºC	33% < 1.5 ºC	66%< 2 ºC
Total CWE public electricity and heat budget for 2017-2100 (Gt CO_2)		-87	-25	-5
Net emissions from public heat and electricity (Gt CO_2)				
	2030	-0.31	0.06	0.18
	2040	-0.85	-0.21	0.00
	2050	-1.40	-0.48	-0.17

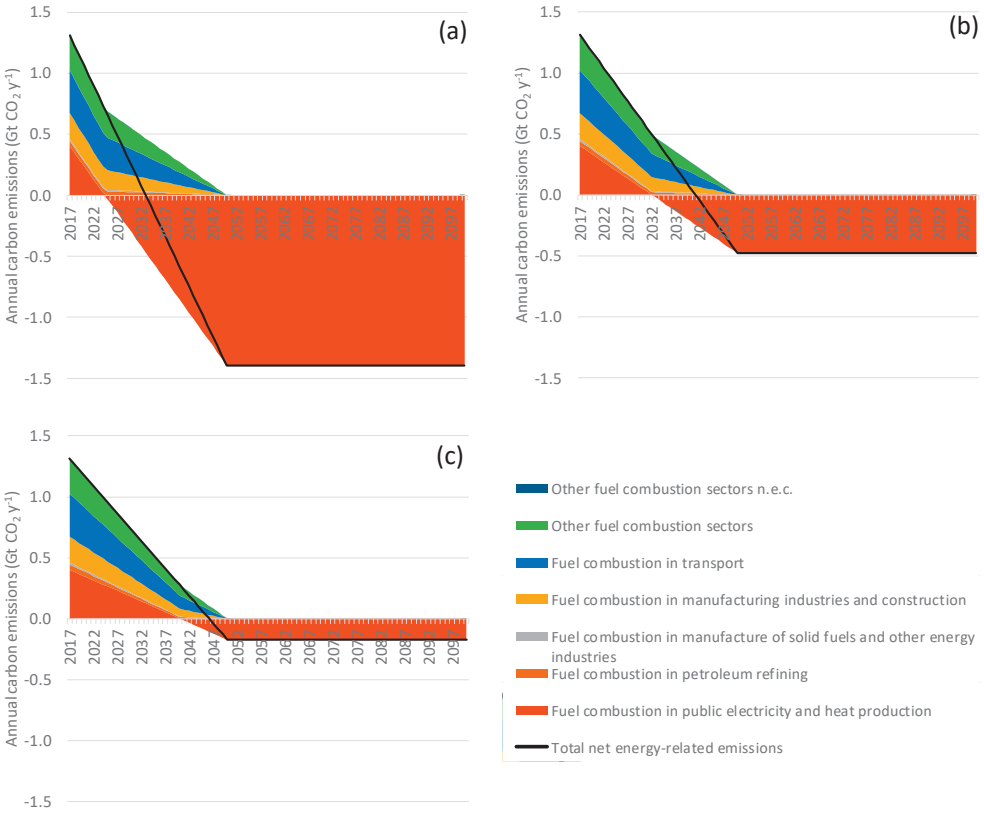

Figure D-8 | Sub-sectoral decarbonisation trajectories for energy-related industry emissions in the CWE countries consistent with (a) 66% chance of limiting global warming to 1.5 ºC, **(b)** 33% chance of limiting global warming to 1.5 ºC and (c) 66% chance of limiting global warming to 2 ºC.

Assuming complete decarbonisation of the non-power or heat-related energy sectors is clearly very ambitious, but if net-zero emissions from these sub-sectors is not achieved, or is delayed past 2050, this will increase the need for negative emissions later in the century. Assuming that the power sector must deliver all negative emissions may also not be very realistic, as other means of removing carbon dioxide from the atmosphere may be cheaper[14]. However, by including a *2C* scenario (66% chance to remain below 2 ºC) and a *1.5C* scenario (66% chance of limiting global warming to 2 ºC) in this study, we consider both lower and upper limits of what could be expected from the power sector in terms of negative emissions in the future.

D.8 Model validation

To validate the model used for this study, PLEXOS' ST Schedule module was run for the EOM scenario for the year 2017 and the resulting hourly prices compared with historical day-ahead price data from ENTSO-E (ENTSO-E, 2018b). Historical hourly prices are used for the neighbouring countries, as well as historical vRES and hydro generation, but the model must perform the UCED and generate the prices for the CWE countries. The results are given on the following pages with Figure D-9 showing box-and-whisker plots of the hourly day-ahead electricity price per country, Figure D-10 showing the monthly average electricity price, and Figure D-11 showing hourly price duration curves. Based on the results, we note that:

- The model gives hourly prices for most of the year (i.e. between the 25th and 75th percentiles) which accord reasonably well with historical data for Belgium, Germany and the Netherlands. The biggest discrepancy is seen in France, where model prices are significantly lower than average.

- The model is less good at reproducing low and high price extremes; typically underestimating high prices, and overestimating low prices. Also, the model results show no hours with negative prices, while in reality there were approximately 100 hours in which prices were negative in Germany.

- Monthly prices from the model generally follow the seasonal patterns from historical data, i.e. higher prices in winter and lower prices in summer. However, the model prices are typically higher than the actual prices in summer, and lower in winter.

There are several possible reasons for these discrepancies:

- Unlike the more liberalised German, Belgian and Dutch markets, France's electricity market is highly concentrated, and all of France's nuclear plants – which supply 75% of electricity demand – are owned and operated by Electricity de France (EDF), the vertically integrated state-owned utility (Deloitte, 2015; World Nuclear Association, 2018). With EDF having a market share of roughly 80%, the French power system could be seen as a regulated monopoly (Deloitte, 2015). In order to increase competition in the retail market, in 2010 the French government passed a law (the 'Regulated Access to Incumbent Nuclear Electricity', or ARENH) forcing EDF to make 25% of its nuclear electricity available to alternative suppliers on the market at a price set by the energy regulator (CRE) of 42 € MWh^{-1} nominally based on the cost of production (Deloitte, 2015), which acts as a

floor price for nuclear power in France. However, this price is considerably higher than the estimated SRMC of nuclear power of 11 € MWh^{-1} based on the costs found in the literature and used in this study[15]. This regulated price must therefore also ensure that the state-owned nuclear plants can recover investment, upgrade and life-extension costs: a possibility not open to players operating in a truly liberalised market. Given that market reforms are likely to increase competition in the future, the increasing penetration of vRES which could underbid nuclear, and our assumption of modelling ideal competitive markets, we do not take into account this floor price for French nuclear power. However, in order to bring the cost of nuclear generation somewhat closer to historical values, and account for the fact that older nuclear plants will have higher maintenance costs and will need new investments to prolong their lives, we increase the VOM of existing old nuclear plants (those built before 1990) by 13.6 € MWh^{-1} based on our estimated nuclear SRMC and costs reported in (EDF, 2018; Schneider & Froggatt, 2018).

- We do not include actual historical generator or transmission line outages. Discussions with experts highlighted that recent outages in French nuclear plants have been significant.

- Power plants are aggregated per category in our model, which results in a bid-supply curve with much coarser resolution than in reality.

- We assume fixed prices for gas and coal, while in reality these can vary throughout the year in response to the heating season (e.g. higher in winter, lower in summer)[16].

- We do not account for feed-in tariff support schemes which give an incentive for wind and PV generators to bid into the market at negative prices (hence the reason for not seeing negative prices in Germany), reducing prices overall.

- If a thermal generator would expect to shut down but need to turn on again several hours later, we do not include the option for them to bid at a negative price to remain online, if this option would be overall cheaper than incurring the resulting start-up costs.

- In reality hydro plants reservoir levels have a significant impact on the opportunity cost of hydro generation, and hence on the bids made by hydro plants (Pikk & Viiding, 2013; Riesz & Milligan, 2015). For example, low levels increase the opportunity cost of using water for power production leading to higher bids, while high levels reduce the opportunity cost and result in lower bids. However, implementing such detailed bidding strategies was beyond the scope of this study. Instead, hydro plants bid based on the shadow price of the water in the reservoir, which is only calculated monthly.

To try to reduce the difference between the actual and modelled prices, the 2017 validation run was performed again but including the historical French nuclear outages reported by EDF (EDF, 2019). Including these outages results in modelled French prices more in line with historical values (Figure I-4). However, as these outages may be particularly high due to life extensions and post-Fukushima safety related modification, we do not include these outages in the main model runs, and assume the same 90% availability as for all other generation technologies.

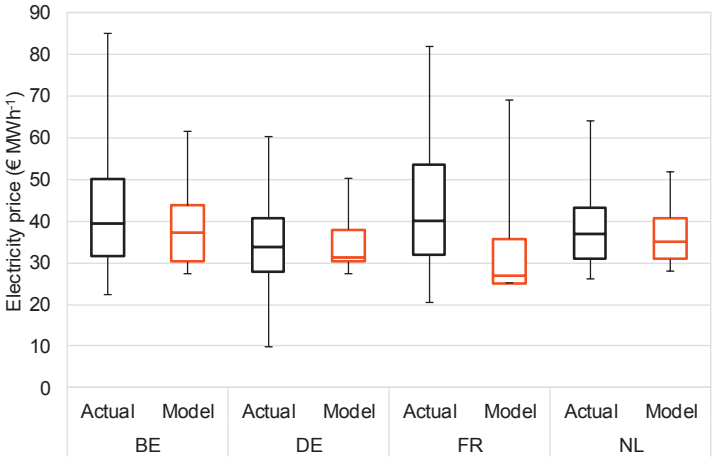

Figure D-9 | Box-and-whisker plot of the actual hourly day-ahead electricity price in 2017 for the CWE countries from ENTSO-E (black), and the prices calculated by the PLEXOS model (red). The boxes indicate the 25th (lower line), 50th/median (middle line), and 75th (upper line) percentile values. The lower and upper whiskers are drawn at the 5th and 95th percentile respectively. Outliers are not shown for clarity, but they can be seen in the price duration curves (Figure D-11).

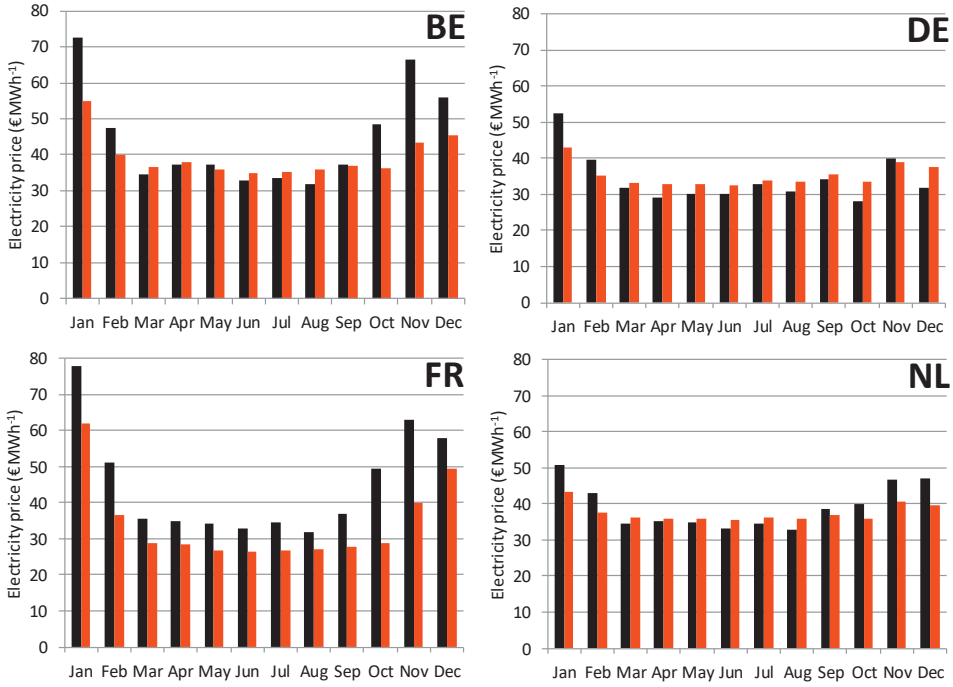

Figure D-10 | Comparison between the average monthly electricity price per region in 2017 based on historical data (black) and that calculated from the PLEXOS model (red)

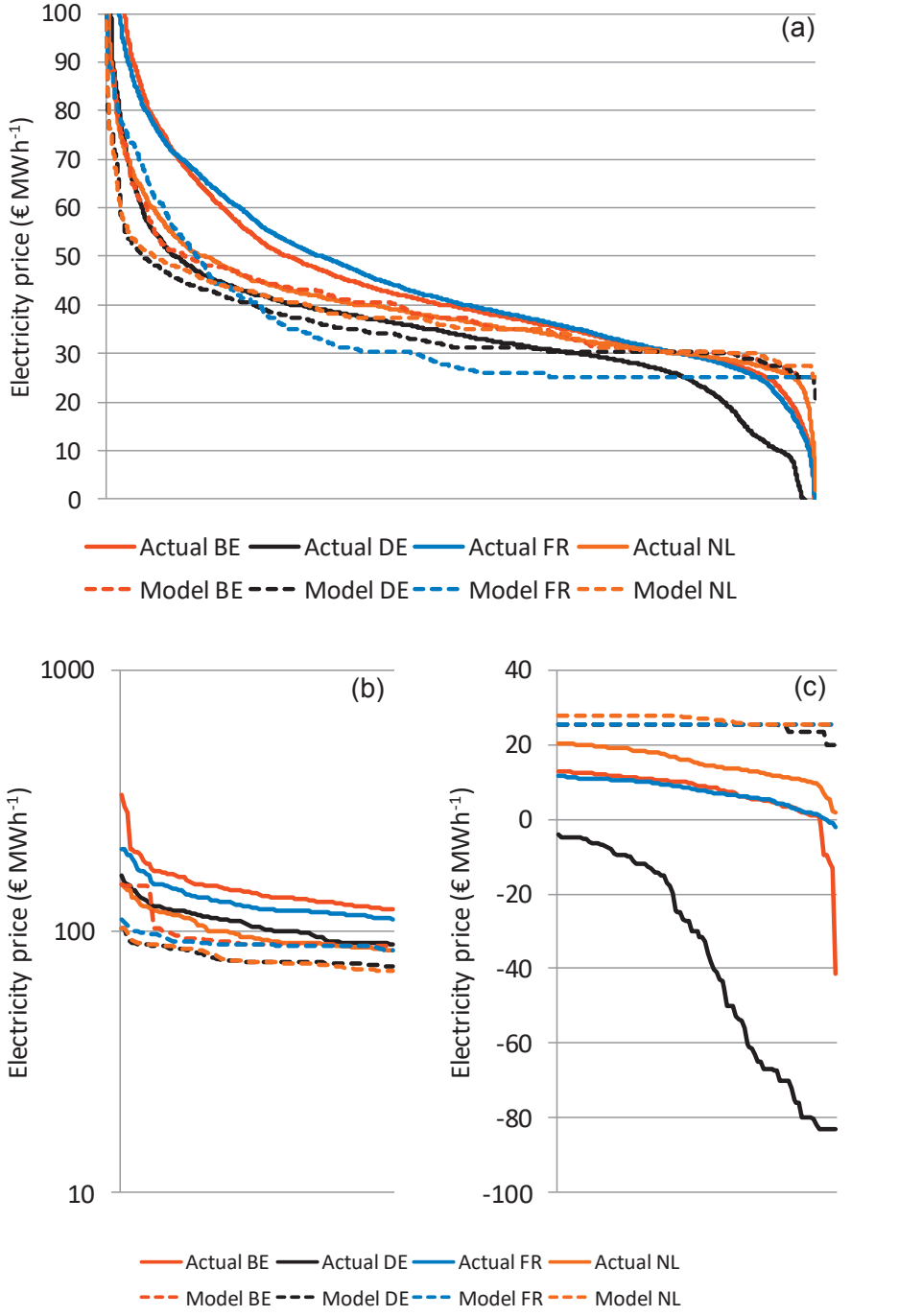

Figure D-11 | Day-ahead market price duration curves for the CWE countries based on historical data and model results for the year 2017 for the (a) whole year, **(b)** most expensive 100 hours and **(c)** least expensive 100 hours

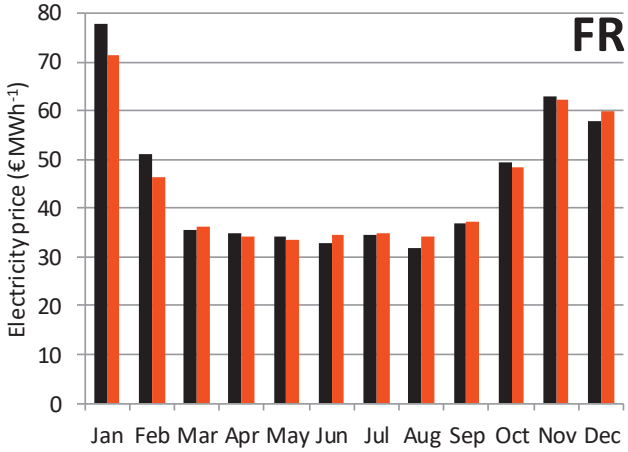

Figure D-12 | Comparison between the average monthly electricity price in France in 2017 based on historical data (black) and that calculated from the PLEXOS model (red), when historical nuclear plant outages are included.

D.9 Additional results

Addition model results are provided in the following tables and figures.

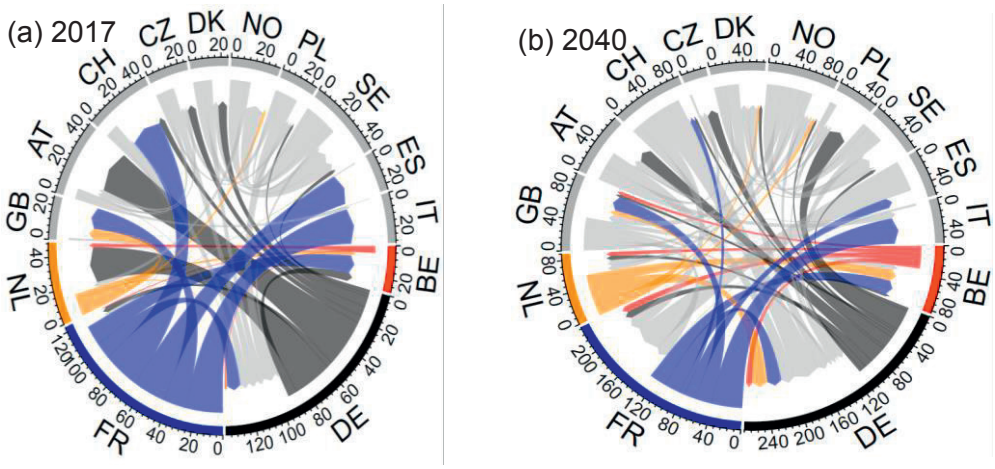

Figure D-13 | Transmission flows between countries from (a) the 2017 model validation run, and (b) the *EOM 2C* scenario in the year 2040 in TWh. Note the different scales as, while the two plots are the same size for convenience, total transmission flows are twice as high in 2040 as in 2017.

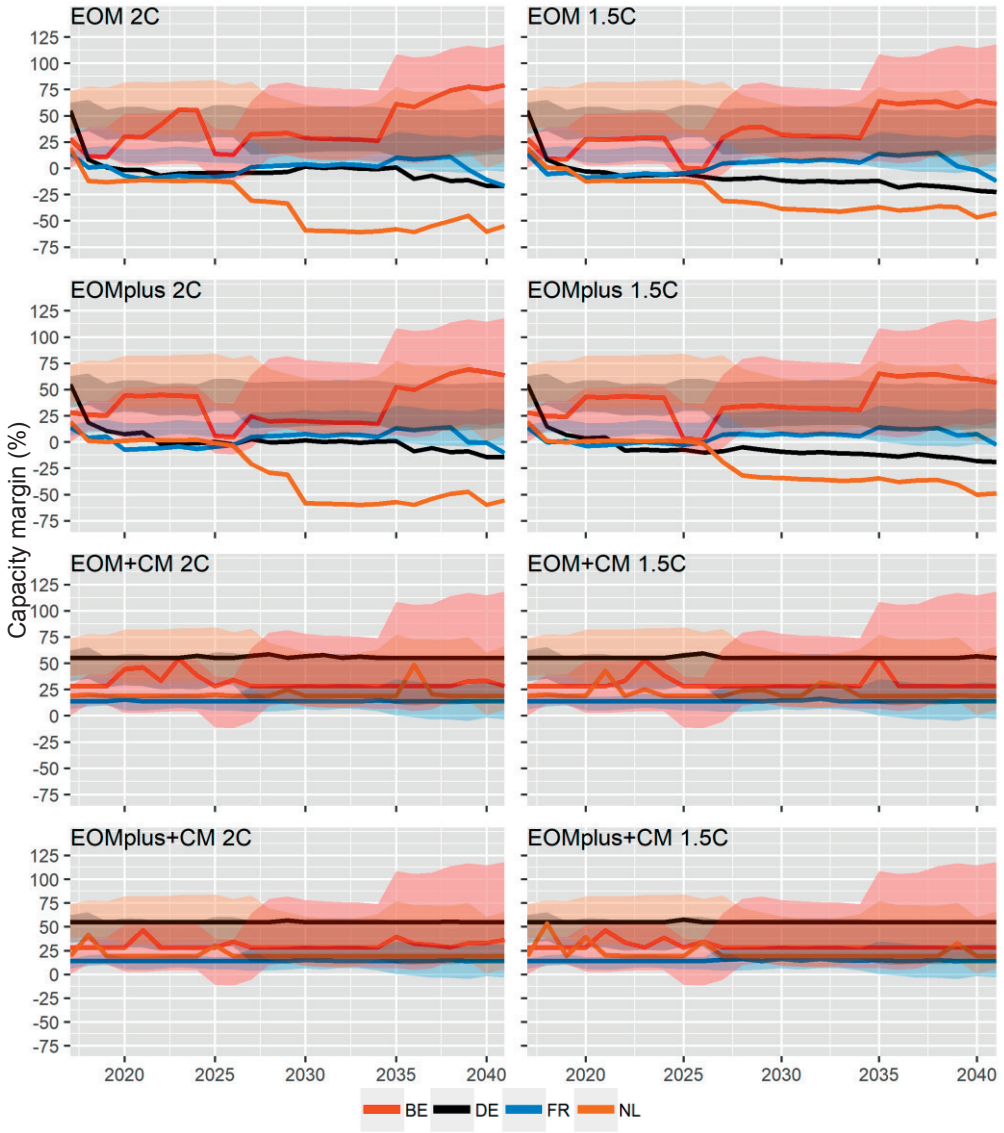

Figure D-14 | Capacity margins from 2017 to 2040 per country for each market design scenario. The solid lines show the margin at the time of the notional peak country load, while the shaded bands show the lower and upper limits of the capacity margin assuming no contribution from transmission and maximum contribution respectively. Transmission capacity with neighbouring non-CWE countries is also included. As PLEXOS reports the capacity margin at the time of the country peak load, accounting for simultaneous imports and exports, it may happen that at the time of peak load, a country may export more than it imports if this leads to a cheaper overall system dispatch, resulting in a negative margin.

Table D-9 | Total installed capacity for the CWE countries per scenario (GW)

		EOM 2C			EOMplus 2C			EOM+CM 2C			EOMplus+CM 2C		
	2017	2020	2030	2040	2020	2030	2040	2020	2030	2040	2020	2030	2040
OIL	19.3	1.0	0.0	0.0	0.0	0.0	0.0	9.0	0.0	0.0	9.0	0.0	0.0
COAL	47.6	37.8	11.7	0.0	37.4	11.7	0.0	47.6	11.7	0.0	47.6	11.7	0.0
COAL-CCS	0.0	0.0	0.0	0.0	0.0	0.0	0.0	0.0	0.0	0.0	0.0	0.0	0.0
CCGT	27.4	20.9	17.1	8.9	20.8	17.3	9.1	20.9	17.1	12.3	20.9	17.1	12.3
CCGT-CCS	0.0	0.0	0.0	0.0	0.0	0.0	0.0	0.0	0.0	0.0	0.0	0.0	0.0
GT	14.2	2.8	35.3	33.5	2.8	14.5	15.3	52.2	101.5	118.3	26.2	74.7	91.1
NUCLEAR	80.5	69.4	50.2	30.9	57.0	46.0	33.7	80.5	60.3	49.0	79.2	59.9	49.8
CHP	23.9	17.5	12.6	1.9	17.5	12.6	1.9	19.9	13.2	1.9	19.9	13.2	1.9
HYDRO	23.2	23.2	23.2	23.2	23.2	23.2	23.2	23.2	23.2	23.2	23.2	23.2	23.2
HYDRO-PHS	15.0	15.0	15.0	15.0	15.0	15.0	15.0	15.0	15.0	15.0	15.0	15.0	15.0
BIOAD	9.6	0.0	0.0	0.0	0.0	0.0	0.0	0.0	0.0	0.0	0.0	0.0	0.0
BIOSOL	0.0	0.0	0.0	0.0	0.0	0.0	0.0	0.0	0.0	0.0	0.0	0.0	0.0
ONWIND	69.0	77.2	104.8	145.7	77.2	104.8	145.7	77.2	104.8	145.7	77.2	104.8	145.7
OFFWIND	7.3	13.3	35.5	85.2	13.3	35.5	85.2	13.3	35.5	85.2	13.3	35.5	85.2
PV	57.0	69.8	157.0	269.0	69.8	157.0	269.0	69.8	157.0	269.0	69.8	157.0	269.0
BATTERY	0.0	0.0	0.0	13.0	0.0	0.0	13.0	0.0	0.0	16.9	0.0	0.0	16.1
BIOSOL-CCS	0.0	0.0	0.0	1.9	0.0	0.0	1.9	0.0	0.0	1.7	0.0	0.0	1.7
DAC	0.0	0.0	0.0	0.0	0.0	0.0	0.0	0.0	0.0	0.0	0.0	0.0	0.0
Total (ex. DAC)	394	348	462	628	334	438	613	429	539	738	401	512	711

		EOM 1.5C			EOMplus 1.5C			EOM+CM 1.5C			EOMplus+CM 1.5C		
	2017	2020	2030	2040	2020	2030	2040	2020	2030	2040	2020	2030	2040
OIL	19.3	0.0	0.0	0.0	0.0	0.0	0.0	9.0	0.0	0.0	9.0	0.0	0.0
COAL	47.6	32.9	0.0	0.0	25.2	0.0	0.0	47.6	0.0	0.0	46.4	0.0	0.0
COAL-CCS	0.0	0.0	0.0	0.0	0.0	0.0	0.0	0.0	0.0	0.0	0.0	0.0	0.0
CCGT	27.4	20.9	21.5	13.6	20.9	13.7	8.9	21.1	22.4	17.6	21.1	22.2	17.4
CCGT-CCS	0.0	0.0	2.0	2.0	0.0	0.3	0.3	0.0	0.8	0.8	0.0	0.9	0.9
GT	14.2	2.8	8.6	5.9	2.6	2.6	0.0	51.9	79.5	90.1	26.0	56.1	62.6
NUCLEAR	80.5	71.5	54.6	41.2	68.8	51.9	43.2	80.5	63.6	52.3	80.5	61.3	52.3
CHP	23.9	17.4	12.5	1.0	17.4	7.2	1.0	19.9	13.2	1.9	19.9	13.2	1.9
HYDRO	23.2	23.2	23.2	23.2	23.2	23.2	23.2	23.2	23.2	23.2	23.2	23.2	23.2
HYDRO-PHS	15.0	15.0	15.0	15.0	15.0	15.0	15.0	15.0	15.0	15.0	15.0	15.0	15.0
BIOAD	9.6	0.0	0.0	0.0	0.0	0.0	0.0	0.0	0.0	0.0	0.0	0.0	0.0
BIOSOL	0.0	0.0	0.0	0.0	0.0	0.0	0.0	0.0	0.0	0.0	0.0	0.0	0.0
ONWIND	69.0	77.2	104.8	145.7	77.2	104.8	145.7	77.2	104.8	145.7	77.2	104.8	145.7
OFFWIND	7.3	13.3	35.5	85.2	13.3	35.5	85.2	13.3	35.5	85.2	13.3	35.5	85.2
PV	57.0	69.8	157.0	269.0	69.8	157.0	269.0	69.8	157.0	269.0	69.8	157.0	269.0
BATTERY	0.0	0.0	0.0	8.8	0.0	0.0	4.0	0.0	0.0	13.5	0.0	0.0	13.8
BIOSOL-CCS	0.0	0.0	24.4	24.4	0.0	24.4	24.4	0.0	24.4	24.4	0.0	24.4	24.4
DAC	0.0	0.0	2.2	24.7	0.0	2.2	24.7	0.0	2.2	24.6	0.0	2.2	24.6
Total (ex. DAC)	394	344	459	635	333	436	620	429	539	739	401	514	711

Table D-10 | Installed capacity (GW) per country per scenario for the year 2040

	EOM 2C				EOMplus 2C				EOM+CM 2C				EOMplus+CM 2C			
	BE	DE	FR	NL	BE	DE	FR	NL	BE	DE	FR	NL	BE	DE	FR	NL
OIL	0.0	0.0	0.0	0.0	0.0	0.0	0.0	0.0	0.0	0.0	0.0	0.0	0.0	0.0	0.0	0.0
COAL	0.0	0.0	0.0	0.0	0.0	0.0	0.0	0.0	0.0	0.0	0.0	0.0	0.0	0.0	0.0	0.0
COAL-CCS	0.0	0.0	0.0	0.0	0.0	0.0	0.0	0.0	0.0	0.0	0.0	0.0	0.0	0.0	0.0	0.0
CCGT	0.8	1.4	0.0	6.7	1.1	1.4	0.0	6.7	0.8	1.4	3.4	6.7	0.8	1.4	3.4	6.7
CCGT-CCS	0.0	0.0	0.0	0.0	0.0	0.0	0.0	0.0	0.0	0.0	0.0	0.0	0.0	0.0	0.0	0.0
GT	4.4	26.5	0.0	2.6	0.2	15.1	0.0	0.0	11.5	87.9	7.3	11.6	8.8	73.4	1.7	7.2
NUCLEAR	0.0	0.0	30.9	0.0	0.0	0.0	33.7	0.0	0.0	0.0	49.0	0.0	0.0	0.0	49.8	0.0
CHP	0.1	0.9	0.9	0.0	0.1	0.9	0.9	0.0	0.1	0.9	0.9	0.0	0.1	0.9	0.9	0.0
HYDRO	0.0	4.7	18.6	0.0	0.0	4.7	18.6	0.0	0.0	4.7	18.6	0.0	0.0	4.7	18.6	0.0
HYDRO-PHS	1.3	8.7	5.0	0.0	1.3	8.7	5.0	0.0	1.3	8.7	5.0	0.0	1.3	8.7	5.0	0.0
ONWIND	7.7	81.5	49.1	7.4	7.7	81.5	49.1	7.4	7.7	81.5	49.1	7.4	7.7	81.5	49.1	7.4
OFFWIND	8.3	33.5	20.0	23.4	8.3	33.5	20.0	23.4	8.3	33.5	20.0	23.4	8.3	33.5	20.0	23.4
PV	22.0	141.0	60.0	46.0	22.0	141.0	60.0	46.0	22.0	141.0	60.0	46.0	22.0	141.0	60.0	46.0
BATTERY	4.0	5.0	0.0	4.0	4.0	5.0	0.0	4.0	4.6	6.0	1.3	5.0	4.1	6.0	1.0	5.0
BIOSOL-CCS	0.0	1.9	0.0	0.0	0.0	1.9	0.0	0.0	0.0	1.7	0.0	0.0	0.0	1.7	0.0	0.0
DAC	0.0	0.0	0.0	0.0	0.0	0.0	0.0	0.0	0.0	0.0	0.0	0.0	0.0	0.0	0.0	0.0
TOTAL (exc. DAC)	49	305	184	90	45	294	187	87	56	367	215	100	53	353	209	96
	EOM 1.5C				EOMplus 1.5C				EOM+CM 1.5C				EOMplus+CM 1.5C			
	BE	DE	FR	NL	BE	DE	FR	NL	BE	DE	FR	NL	BE	DE	FR	NL
OIL	0.0	0.0	0.0	0.0	0.0	0.0	0.0	0.0	0.0	0.0	0.0	0.0	0.0	0.0	0.0	0.0
COAL	0.0	0.0	0.0	0.0	0.0	0.0	0.0	0.0	0.0	0.0	0.0	0.0	0.0	0.0	0.0	0.0
COAL-CCS	0.0	0.0	0.0	0.0	0.0	0.0	0.0	0.0	0.0	0.0	0.0	0.0	0.0	0.0	0.0	0.0
CCGT	0.8	6.1	0.0	6.7	0.8	1.4	0.0	6.7	0.8	6.6	3.4	6.7	0.8	6.5	3.4	6.7
CCGT-CCS	0.0	0.2	0.0	1.7	0.0	0.2	0.0	0.1	0.0	0.2	0.0	0.6	0.0	0.2	0.0	0.7
GT	1.4	4.5	0.0	0.0	0.0	0.0	0.0	0.0	8.7	70.6	5.5	5.3	3.6	56.6	0.1	2.3
NUCLEAR	0.0	0.0	41.2	0.0	0.0	0.0	43.2	0.0	0.0	0.0	52.3	0.0	0.0	0.0	52.3	0.0
CHP	0.1	0.9	0.0	0.0	0.1	0.9	0.0	0.0	0.1	0.9	0.9	0.0	0.1	0.9	0.9	0.0
HYDRO	0.0	4.7	18.6	0.0	0.0	4.7	18.6	0.0	0.0	4.7	18.6	0.0	0.0	4.7	18.6	0.0
HYDRO-PHS	1.3	8.7	5.0	0.0	1.3	8.7	5.0	0.0	1.3	8.7	5.0	0.0	1.3	8.7	5.0	0.0
ONWIND	0.0	0.0	0.0	0.0	0.0	0.0	0.0	0.0	0.0	0.0	0.0	0.0	0.0	0.0	0.0	0.0
OFFWIND	0.0	0.0	0.0	0.0	0.0	0.0	0.0	0.0	0.0	0.0	0.0	0.0	0.0	0.0	0.0	0.0
PV	22.0	141.0	60.0	46.0	22.0	141.0	60.0	46.0	22.0	141.0	60.0	46.0	22.0	141.0	60.0	46.0
BATTERY	1.9	4.0	0.0	2.9	1.0	2.0	0.0	1.0	3.0	4.5	1.0	5.0	3.0	4.8	1.0	5.0
BIOSOL-CCS	3.4	15.2	0.0	5.8	2.6	16.0	0.0	5.8	5.9	12.7	0.0	5.8	5.9	12.7	0.0	5.8
DAC	0.7	6.0	10.2	7.8	0.0	7.1	11.2	6.4	3.0	3.5	10.9	7.3	3.0	3.5	10.9	7.3
TOTAL (exc. DAC)	47	300	194	94	44	290	196	90	58	365	216	100	53	351	210	97

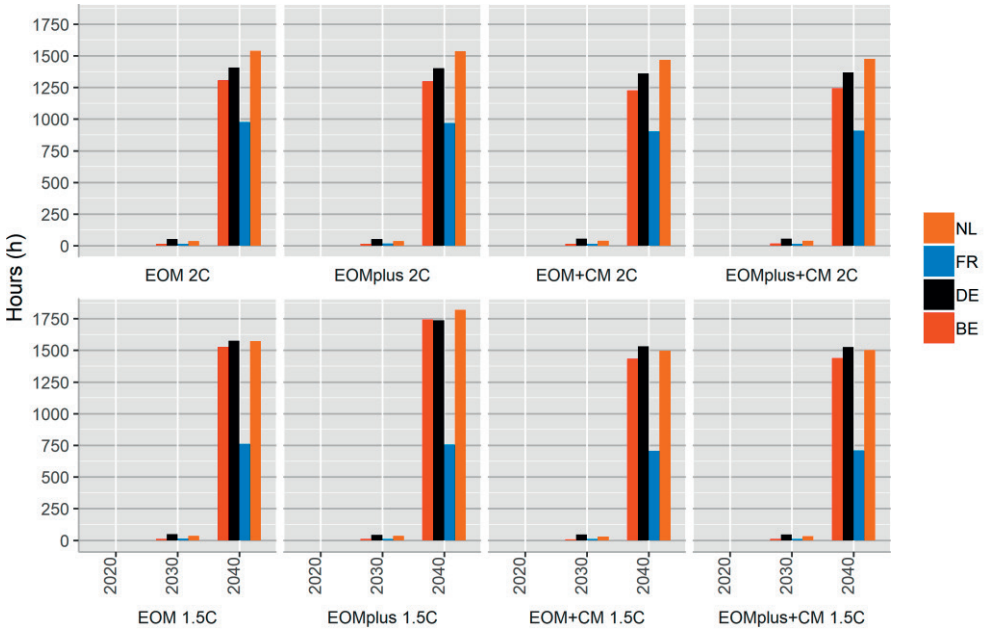

Figure D-15 | Number of hours per scenario with electricity price of zero based on hourly simulations of the years 2020, 2030 and 2040 for each market design scenario

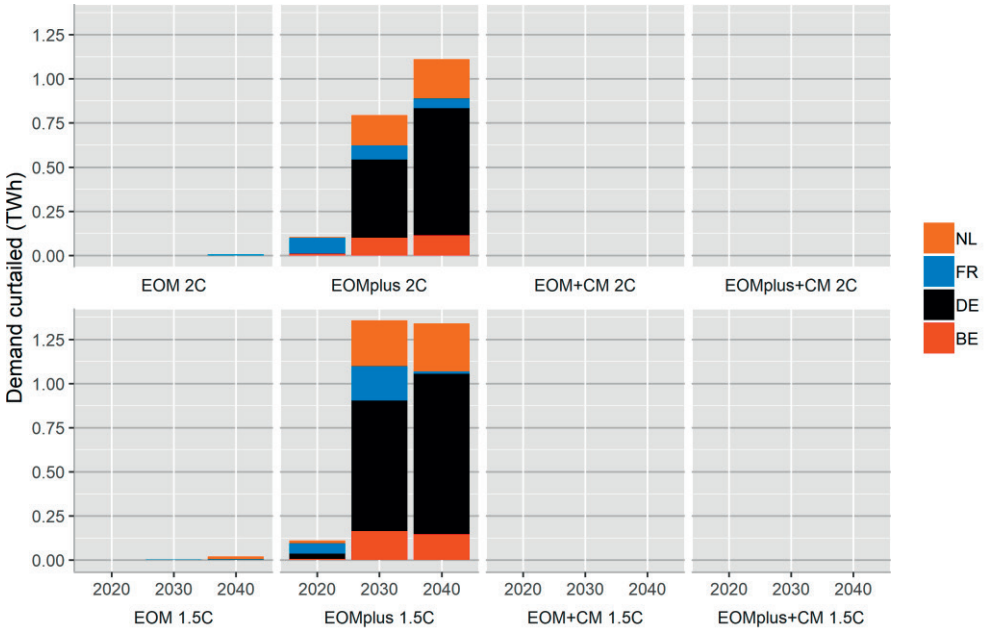

Figure D-16 | Demand curtailed based on hourly simulations for the years 2020, 2030 and 2040 for each market design scenario

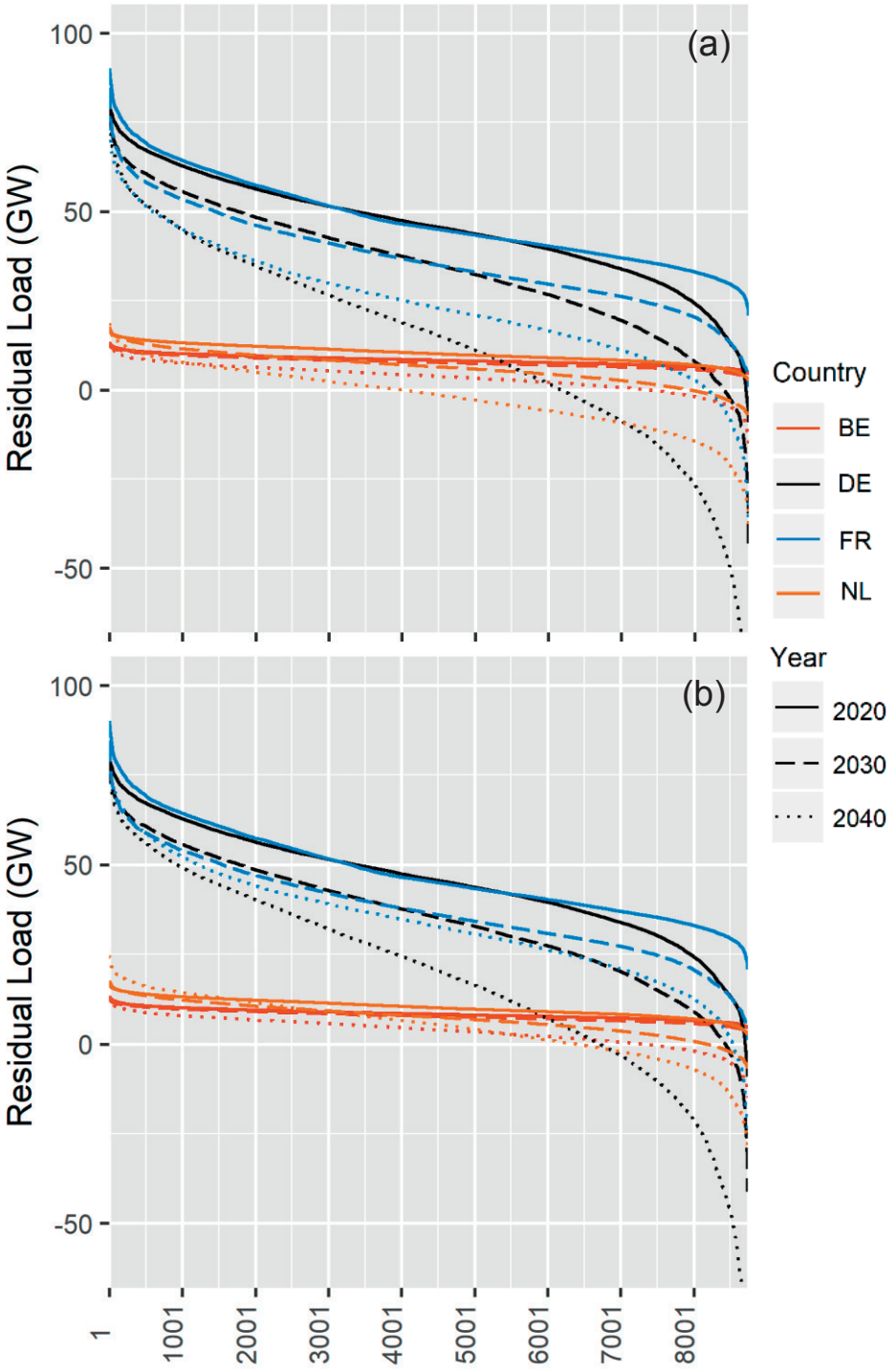

Figure D-17 | Residual load duration curves for the (a) *EOM 2C* scenario and (b) *EOM 1.5C* scenario.

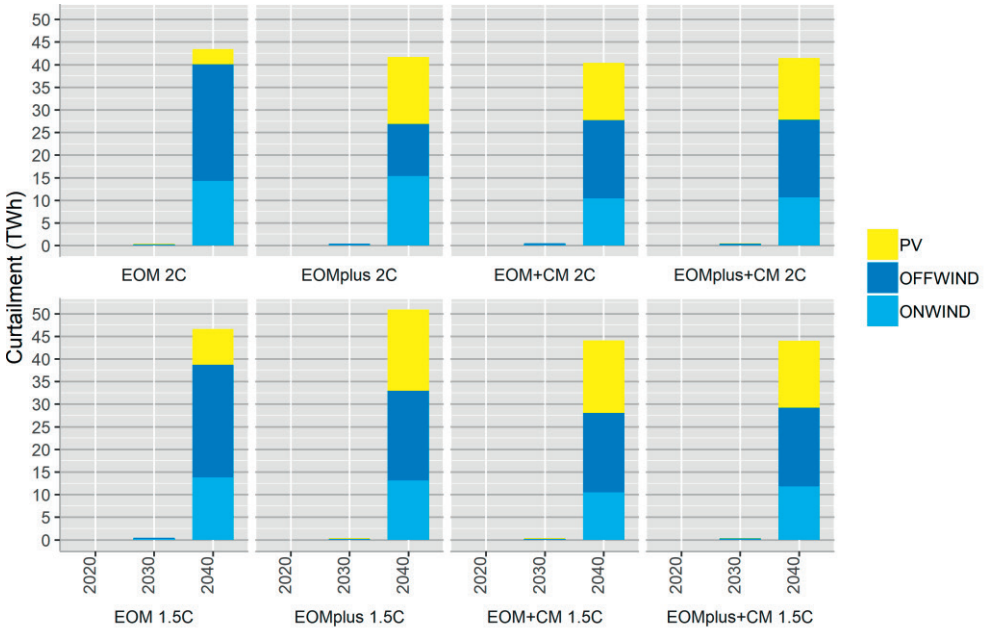

Figure D-18 | vRES curtailment in the years 2020, 2030, and 2040 per technology for each market design scenario.

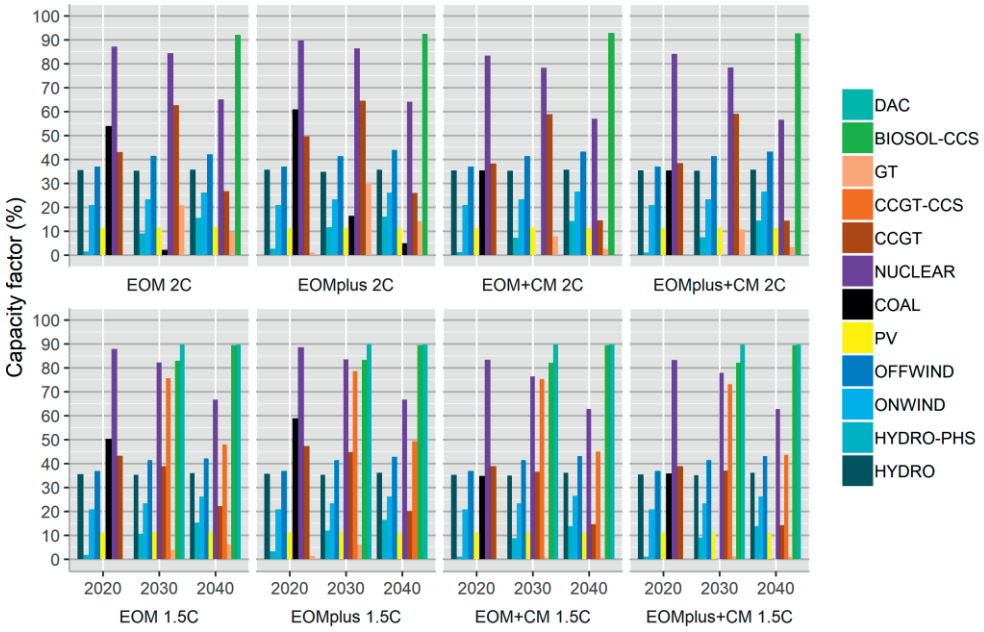

Figure D-19 | Capacity factors per technology for the years 2020, 2030 and 2040 for each scenario.

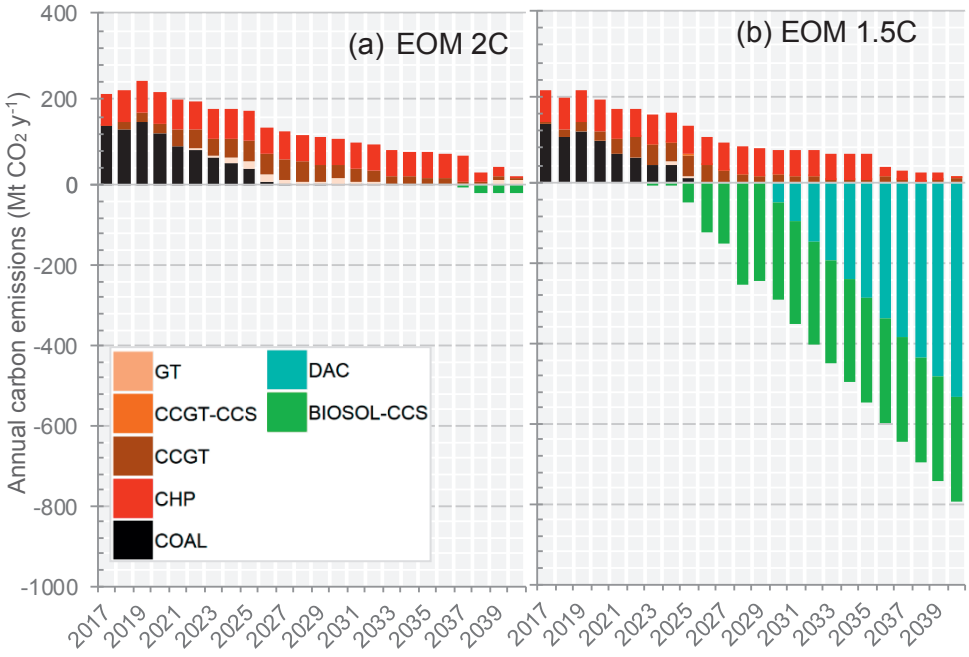

Figure D-20 | Carbon emissions over time per technology in the (a) *EOM 2C* and (b) *EOM 1.5C* scenarios.

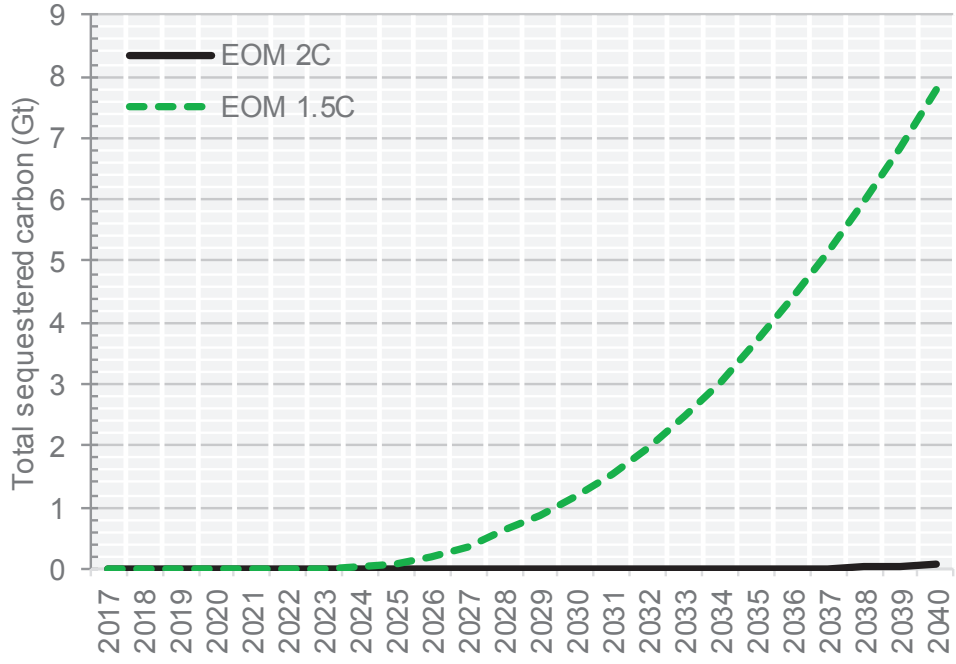

Figure D-21 | Total sequestered carbon emissions in the *EOM 2C* and *EOM 1.5C* scenarios. Total carbon storage capacity is estimated at around 28 Gt for CWE (EU GeoCapacity Project, 2009)**.**

D.10 Sensitivity analysis results

The following paragraphs give more details on the results of the sensitivity analysis.

In the *higher fossil fuel prices* sensitivity less new natural gas capacity is built, and the model keeps existing nuclear capacity online for longer in both the *2C* and *1.5C* cases. With higher gas and coal costs, total system costs also increase, though the effect is partly mitigated by the switch to nuclear.

With *higher demand*, the model satisfies the additional demand in the *2C* case by keeping 20 GW more nuclear capacity online, installing more new natural gas capacity, and nearly double the amount of BECCS as in the base run. The results are similar for the *1.5C* case except that CCGT-CCS plants are built instead of CCGTs, and double the amount of battery capacity. No significant additional DAC capacity is required.

With *higher battery costs*, batteries no longer appear in the 2040 portfolio in either climate case. Instead, the model builds more peaking GT capacity, which leads to slightly more BECCS capacity to offset the higher natural gas emissions.

In the *2C* case, a *higher biomass price* results in a slight shift towards more nuclear and gas (with CCS) capacity, with only a minimal impact on total cost. Even with a higher biomass price, the combination of nuclear, natural gas and BECCS remains the most cost-effective way of achieving zero-emissions, and no DAC is built[17]. In the *1.5C* case, BECCS is still cheaper than DAC at delivering negative emissions. With such deep decarbonisation required, BECCS capacity is still fully exploited, and the higher biomass price simply translates into higher cumulative costs.

Assuming a *higher or lower discount rate* (WACC) makes almost no impact on the 2040 portfolios in either the *2C* or *1.5C* cases. However, as expected, total costs are slightly higher in the *higher WACC* sensitivity and slightly lower in the *lower WACC* sensitivity.

When *no biomass limit* is enforced, there is no impact on the 2C case as the biomass constraint is not binding. However, in the 1.5C case, removing the limit biomass allows much greater deployment of BECCS (80 GW), which also avoids the need to install costlier DAC. With more baseload generation from BECCS and no additional electricity demand required for DAC, nuclear is completely phased out of the portfolio by 2039. Thanks largely to the avoidance of DAC, total costs are 25% lower than in the base 1.5C case. However, biomass use reaches 9.5 EJ in 2040, or three times the notional CWE solid biomass potential assumed in the base runs.

When *no BECCS* is allowed, the model can still achieve nearly net-zero emissions in the *2C* case by keeping some additional nuclear capacity online, and building some additional CCGT-CCS and battery capacity. In the *1.5C* case, the model again keeps more nuclear online, but also significantly expands CCGT-CCS capacity (27 GW) and even installs some solid biomass capacity without CCS (9 GW). However, in order to reach the deep carbon target without BECCS, the model has no choice but to invest in an additional 10 GW of DAC capacity compared with the base *EOM 1.5C* case, leading to 20% higher costs.

When *CCS is only allowed with DAC*, there are only minor portfolio changes in the 2C case as the near-zero target can be achieved by keeping more nuclear capacity online. However, in the 1.5C case, an additional 60 GW of onshore wind is built compared with the base runs, more (unabated) CCGT plants, more batteries, and more nuclear capacity remains online. However, as in the *no BECCS* sensitivity, the model is forced to invest in an additional 10 GW of DAC to meet the climate target, significantly increasing total costs.

In the *Blue hydrogen* sensitivity no blue hydrogen is used in the *2C* case, but in the *1.5C* case a relatively small amount (50 PJ y^{-1}) is used from 2029 onwards in gas plants, generating an average of 9 TWh y^{-1}. This use of hydrogen results in marginally lower system costs compared to the base *1.5C* case by reducing investments in NGCC-CCS plants.

Fully *optimising vRES capacity* (from the 2017 starting levels) results in much less vRES installed by 2040 than in the exogenous deployment. In the *2C* case, no additional offshore wind or PV capacity is built after 2017, though onshore wind deployment reaches 130 GW in 2040 - almost the level assumed in the base scenarios (145 GW). In place of vRES, more nuclear capacity is kept online, more CCGT and CCGT-CCS capacity is built, while the higher residual emissions are offset with more BECCS. With significantly less vRES capacity in the portfolio, no batteries are installed. As a result of these differences, total costs are nearly 20% lower when vRES capacity is optimised than in the base *EOM 2C* scenario. In the *1.5C* case, the same amount of onshore wind expansion occurs as in the 2C *optimised vRES* sensitivity, together with an additional 50 GW of PV deployment, though the installed capacity in 2040 (107 GW) is still lower than in the reference case (270 GW). The missing generation from vRES is replaced by more nuclear capacity (fewer retirements), and significantly higher deployment of CCGT-CCS. However, due to the demanding climate target and dominance of NETs in the portfolio, total costs in the *optimised vRES* sensitivity are only 7% lower than the reference *1.5C* case.

When the portfolio is *freely optimised* (from the 2017 starting levels), even less vRES capacity is installed in the *2C* case than in the *optimised vRES* sensitivity. Instead, a significant amount of existing coal (20 GW) and nuclear capacity (66 GW) is kept online until 2040, while some coal and gas capacity is converted to BECCS and CCGT-CCS to meet the emission target. In this case, costs are 24% lower than in the base *2C* run. If a lower discount rate of 4% is assumed, then instead of CCGT-CCS and BECCS, a significant amount (24 GW) of new nuclear capacity is built[18]. A higher discount rate leads to more coal and BECCS capacity. In the *1.5C* case, a lower discount rate doesn't result in nuclear being built, and the discount rate only makes minor changes to the portfolios and total costs due to the dominating effect of the NETs.

Compared with the *EOM+CM* reference case, the *tighter capacity margin* sensitivity results in far less GT capacity being built, and earlier retirements of existing nuclear capacity. Thanks to the lower capacity requirement and lower capacity prices (Figure D-22), total costs in the tighter capacity margin sensitivities fall by 24% in the *2C* case, and 16% in the *1.5C* case compared with EOM+CM reference case, but even these lower values are still higher than the EOM-only scenarios. For example, total costs in the *EOM+CM 2C* scenario with tighter capacity margin are 7% higher than in the EOM 2C scenario.

When *transmission line outages* are included in the UCED runs (Figure D-23), unserved energy increases in the *EOM*-based market designs compared to the core results with up to 60 GWh unserved in 2030 in the *EOMplus 2C* scenario. The most problematic region is Belgium as, after the nuclear phase out in 2025, the model doesn't replace the lost nuclear capacity with new domestic generation capacity, and instead relies on transmission capacity to maintain reliability. However, the coarser temporal resolution (monthly) used in the capacity expansion algorithm and exclusion of inter-temporal constraints (e.g. ramping rates, minimum up-down time) can mean that when the UCED simulations are performed at hourly resolution including these constraints, unserved energy can result. It is important to note that transmission lines are modelled as single bi-directional HVDC lines in this study and, when forced offline for maintenance, represent a significant capacity loss. However, in reality, neighbouring countries with land borders are typically connected by several HVAC lines. Thus, when one fails, the others should still be able to operate. Despite the increase in unserved energy compared with transmission outages compared with the base runs, even in 2030, unserved energy represents only 0.005% of total CWE annual demand.

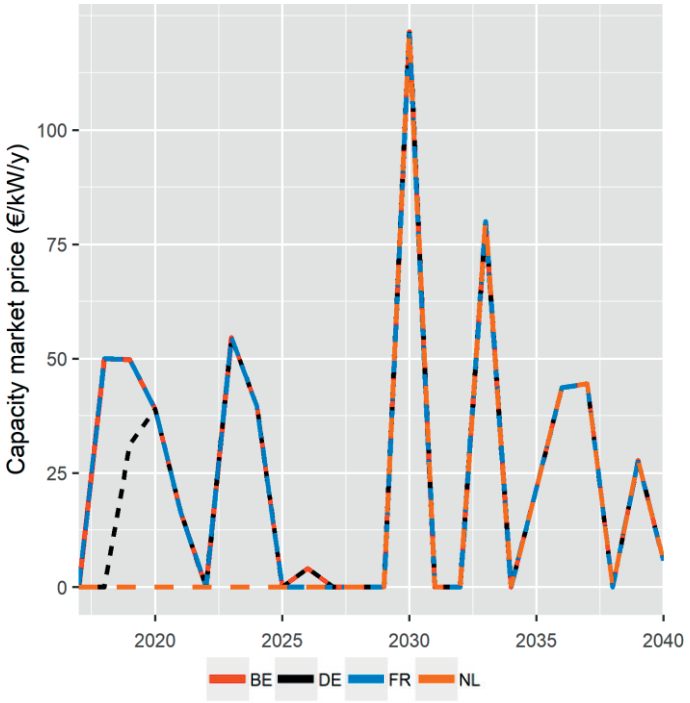

Figure D-22 | Capacity market prices in the EOM+CM 2C scenario with the tighter capacity margin sensitivity.

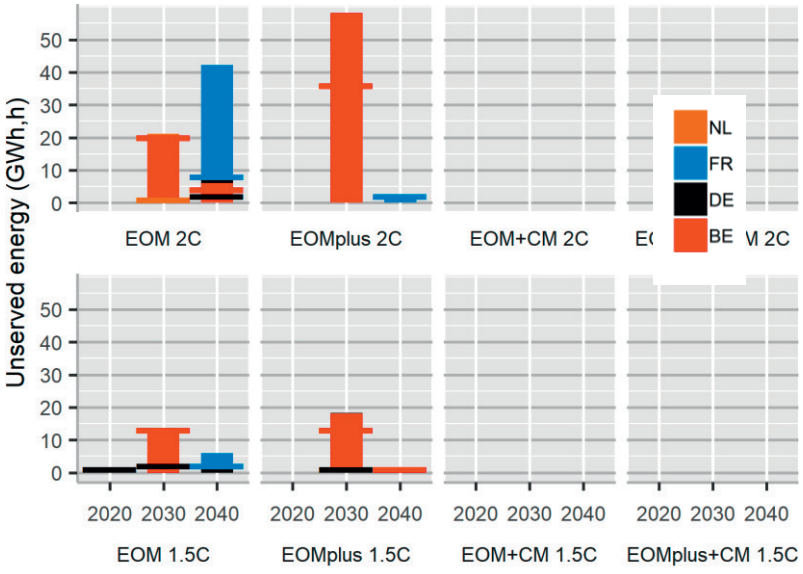

Figure D-23 | Unserved energy based on hourly simulations of the years 2020, 2030 and 2040 for each market design scenario when a transmission outage rate of 10% is assumed. The stacked bars show the volume (GWh) of unserved energy, while the horizontal bars indicate the number of hours in which unserved energy is observed.

Footnotes to Appendix D

[1] These scenarios were chosen to be consistent with the selected scenarios for vRES capacity deployment.

[2] The data supporting the TYNDP2018 only reports transmission capacity for these years 2020, 2027 and 2040. However, we bring forward the Global Climate Scenario capacities from 2040 to 2035 so that their impact is spread over more years.

[3] Assuming the cost of retrofitting a biomass plant with CCS is also ~60% the cost of a new Coal-CCS plant.

[4] For example, Daggash et al. (Daggash et al., 2019) assumed the cost of a Biomass-CCS plant to be equivalent to that of a Coal-CCS plant retrofitted for biomass conversion, arriving at a figure of 2721 £ kW^{-1} (~3000 € kW^{-1}), however this does not appear to include interest during construction.

[5] Renewables Ninja only contains CFs up until the year 2016, thus a direct comparison of 2017 CFs could not be made. We scale the Renewables Ninja factors to match the EurObserver ones (and not the other way around) as these match better with historical data from other sources. For example, the average lifetime CF of offshore wind farms is 39% in Germany, 38% in the UK, 42% in Denmark, and 37% in Belgium (Energy Numbers, 2016).

[6] Battery firm capacity depends on the size of the storage, and the manner in which it is deployed during shortage. Based on calculations performed for the UK capacity market an energy storage technology with 6 hours storage has a firm capacity exceeding 90% (National Grid, 2017). Thus, this limitation has limited impact.

[7] VoLL is difficult to estimate and values in the literature vary. For example, (VVA et al., 2018) report higher VoLL values for industrial and commercial consumers (20,000 to 30,000 € MWh^{-1}) than for households (5,000 to 10,000 € MWh^{-1}).

[8] Even taking into account these quantitative VoLL differences would raise serious equity and social questions. For example, if a higher VoLL was used for Dutch consumers than for French consumers, the model would choose to cut supply to French consumers before Dutch ones.

[9] This is a rather conservative estimate as interruptible load in US power systems is reported already 11% (Hirth & Ueckerdt, 2014).

[10] Anderson & Broderick assume that emissions from deforestation are matched by carbon sequestration through Land Use, Land Use Change and Forestry (LULUCF) activities across the century, and thus not included.

[11] 'Energy-related' sectors include fuel combustion for electricity and/or heat production by large utilities, industry, commerce and households, fuel combustion in the transport sector, as well as fugitive fuel emissions. See Table D-7 for further details.

[12] Other methods are also possible such as grandfathering (based on historical emissions) and gross domestic product.

[13] Given that statistics are only reported for public electricity production combined, we cannot easily separate out the emissions attributed to electricity and heat individually. By lumping heat and electricity together, we essentially assume that all district heat is produced via combined heat and power.

[14] For example, the production of renewable hydrogen or Fisher-Tropsch liquid fuels from gasified biomass results in a nearly pure stream of CO_2 which may be a cheaper way of deploying BECCS than in the power sector (van Vliet et al., 2011).

[15] This estimate largely agrees with (Lévêque, 2013) which report an estimated French nuclear SRMC of 6 € MWh^{-1} in 2013.

[16] See https://ycharts.com/indicators/europe_natural_gas_price

[17] By 2040, DAC is cost competitive with BECCS at a biomass price of 12.5 € GJ^{-1}

[18] Note, this is the only scenario in the whole study in which new nuclear capacity is built, showing that the higher capital cost and long construction time of nuclear inhibit new builds at the base 8% discount rate.

Appendix E Description of the PLEXOS modelling framework

Indices and sets

$g \in \mathcal{G}$	Generating units, running from 1 to $\mathcal{G}$, the total set of generation unit types
k	Run up/down interval
i	Dummy variable (e.g. to sum across each year i preceding year y
$t \in \mathcal{T}$	Dispatch intervals, running from 1 to $\mathcal{T}$, depending on phase and settings (e.g. 1 to 168, for an hourly ST Schedule simulation of one week)
$y \in \mathcal{Y}$	Years, running from 1 to $\mathcal{Y}$, the set of years in the (LT) planning horizon

Nomenclature

$BuildCost_g$	Overnight capital cost of generating unit g (€ MW^{-1})
$CapShort_y$	Capacity shortage in y (MW^{-1})
DF_y	Discounting factor applied in year y
FOM_i	Fixed operating and maintenance costs of generating unit g (€ MW^{-1})
$GenBuild_{g,y}$	Number of generating units g built in year y
$GenLoad_{g,t}$	Load of generating unit g in dispatch interval t (MWh)
$GenOn_{g,t}$	Binary variable indicating if generating unit g is online during interval t
$GenStart_{g,t}$	Binary variable indicating if generating unit g starts in interval t
$GenStop_{g,t}$	Binary variable indicating if generating unit g stops in interval t
$Load_t$	Load in dispatch interval t (MW)
$MaxCapacity_g$	Maximum power of generating unit g (MW)
$MaxUnitsBuilt_{g,y}$	Maximum number of generating unit g units built in year y
MDT_g	Minimum down time of generating unit g (h)
MSL_g	Minimum stable level of generating unit g (MW)
MUT_g	Minimum up time of generating unit g (h)
$NoLoadCost_{g,t}$	No-load cost of generating unit g in interval t (€ h^{-1})
$PeakLoad_y$	Peak electricity demand in y (MW)
$ResMargin_y$	Capacity reserve margin in y (MW)
$RampDown_g$	Maximum ramp-down rate for generator g (MW min^{-1})
$RampUp_g$	Maximum ramp-up rate for generator g (MW min^{-1})
$SRMC_g$	Short-run marginal cost of generating unit g (€ MWh^{-1})
$StartCost_{g,t}$	Start-up cost of generating unit g in interval t (€)
$Units_g$	Number of generating unit g units installed at start of simulation
$UnitsBuilt_{g,y}$	Number of generating unit g units built in year y
USE_t	Unserved energy in dispatch interval t (MW)
$VoLL$	Value of lost load (€ MWh^{-1})

PLEXOS is a power market modelling framework developed by Energy Exemplar (www.energyexemplar.com) based on mixed-integer linear programming (MILP). PLEXOS is not a single model, but rather a flexible modelling framework that enables the analyst to model the power system with varying level of detail, depending on their needs and data availability. Using the framework, models are built by adding power system *objects* (e.g. nodes, regions, transmission lines, generators, fuels, emissions, storages, reserves) and linking them together via so-called *memberships*. Model input data is assigned to the various objects as properties (e.g. Minimum up/down times for generators, load for a node, losses for a transmission line), which can be enabled or disabled as desired. When the model is run, the user can choose to output the mathematical problem in full, allowing for full transparency and inspection of the underlying equations. PLEXOS does not solve the resulting mathematical problem itself, but instead allows the user to specify one of several open-source (e.g. GLPK, SCIP) or commercial solvers (e.g. Gurobi, CPLEX, MOSEK).

PLEXOS is built around several simulation algorithms or *phases* which allow it perform capacity expansion and unit commitment and economic dispatch (UCED), while taking into account constraints which can apply over short (e.g. hourly) or long-term (e.g. multi-annual) horizons. The results are passed down from one simulation phase to the next (Figure E-1), as explained below.

- The **Long-term Plan (LT Plan)** phase is a capacity expansion/investment module with a time horizon of at least one year, but which can extend up to several decades. The LT Plan is run first for the whole simulation horizon to find the optimum build/retire decisions in generation and transmission infrastructure assuming perfect foresight. However, if a multi-year simulation horizon is too complex to solve, the LT Plan can be performed in several steps to reduce the size of the mathematical problem, in which case the model foresight reduces to the length of the simulated step size. The level of temporal detail is typically simplified in the LT Plan by approximating (hourly) load with load duration curves (LDC), or sampling techniques.

- After the LT Plan, the **Projected Assessment of System Adequacy (PASA)** phase can be run which has two main functions: (1) to compute system adequacy statistics such as loss of load probability (LoLP) using a convolution approach, and (2) to create discrete planned and forced maintenance (outage) events for the subsequent more detailed simulation phases. It does this by solving a quadratic programming problem to equalise capacity reserves across the full year.

- The **Medium-Term Schedule (MT Schedule)** phase is also run after the LT Plan. Its purpose is to manage constraints and commercial considerations that need to be addressed over time scales longer than a day or week. Examples are optimum hydro dam storage levels throughout the year, as well as annual fuel or emission constraints. The MT Schedule addresses these issues by decomposing long-term (e.g. yearly, monthly) constraints into short-term ones so that can be accounted for correctly at shorter time scales.

- The **Short-term Schedule (ST Schedule)** phase is a UCED algorithm which solves the UCED problem with full chronological detail, and can be run with a temporal resolution of one hour down to 5 minutes. The ST Schedule UCED simulation assumes that generators bid at their short-run marginal cost, under the assumption of perfectly competitive markets. In this case, the UCED approximates the result of a real-world market clearing process. This phase takes into account the inter-temporal flexibility constraints of generators which are not accounted for in the other phases. The ST Schedule can be run using either full integer programming, or with integer constraints relaxed.

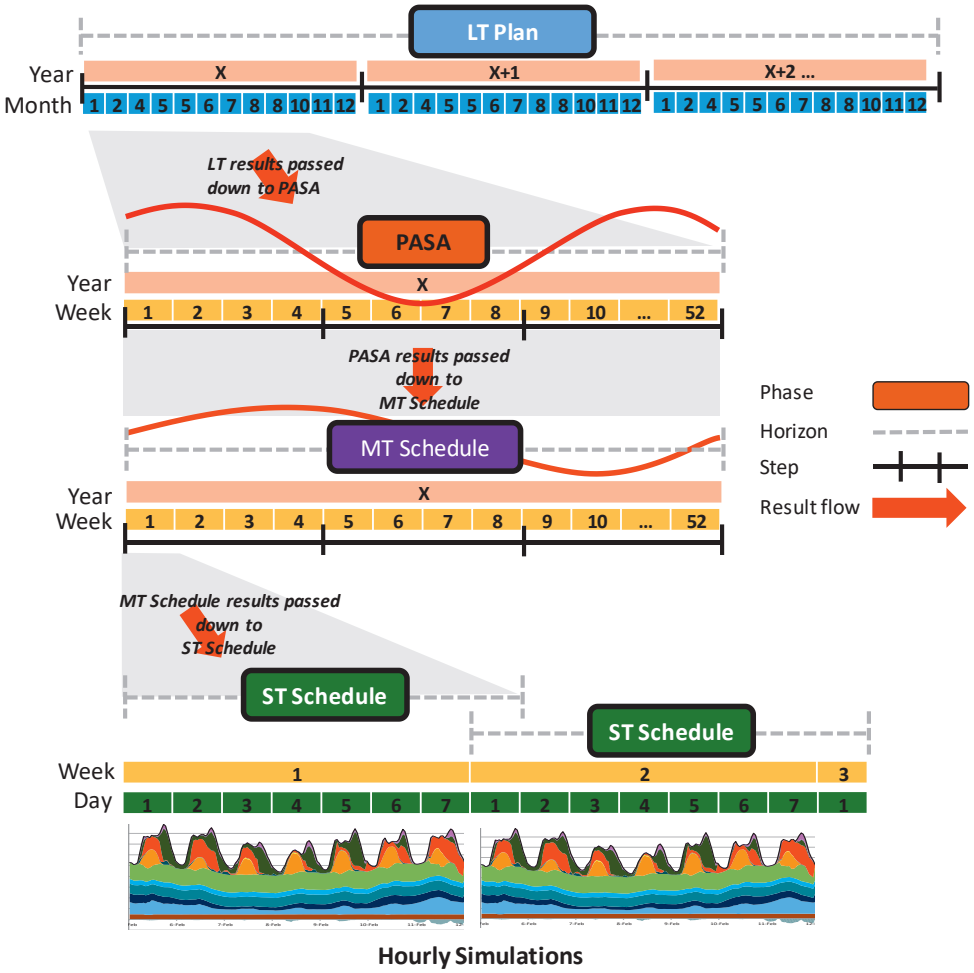

Figure E-1 | Schematic overview of the PLEXOS market model showing how results are passed between the different simulation phases.

The most important equations describing the PLEXOS mathematical formulation, similar to those employed in other power system models, are outlined below. These are taken directly from the PLEXOS documentation (Energy Exemplar, 2015) and published literature (Brinkerink et al., 2018; Deane et al., 2014). Note that this list of equations is only illustrative and not exhaustive, as the exact equations used will depend on the components modelled.

LT Plan formulation

The objective function of the LT Plan (excluding generator retirements and transmission investments) is to minimise the net present value of the total sum of investment costs, fixed operating and maintenance (FOM) costs, and variable generation costs across the whole power system, subject to various constraints on energy and unit builds (Energy Exemplar, 2015).

MINIMISE:

$$\begin{aligned}&\sum_{y}\sum_{g} DF_y\left(GenBuild_{g,y} \times BuildCost_g\right)\\&+\sum_{y} DF_y\left[FOM_g \times MaxCapacity_g\right.\\&\left.\times\left(Units_g+\sum_{i\le y} UnitsBuilt_{g,i}\right)\right]\\&+\sum_{t} DF_{t\in y} \times Load_t\\&\times\left[VoLL \times USE_t+\sum_{g}\left(SRMC_g \times GenLoad_{g,t}\right)\right]\end{aligned} \tag{E-1}$$

Subject to: Energy balance constraint

The total amount of generation in each dispatch period must be equal to the load less the unserved energy (Energy Exemplar, 2015).

$$\sum_{g} GenLoad_{g,t} = Load_t - USE_t \quad \forall\, t \tag{E-2}$$

Subject to: Feasible energy dispatch

The total generation from a certain generator type must be less than the total capacity of all installed units of that generator type (Energy Exemplar, 2015).

$$GenLoad_{g,t} \le MaxCapacity_g\left(Units_g+\sum_{i\le y} UnitsBuilt_{g,i}\right) \tag{E-3}$$

Subject to: Feasible unit builds

There may be constraints to the number of units of a certain generator type built each year (Energy Exemplar, 2015).

$$\sum_{i \leq y} UnitsBuilt_{g,i} \leq MaxUnitsBuilt_{g,y} \tag{E-4}$$

Subject to: Capacity margins

In its most basic form, the LT Plan will optimise investment decisions to meet the natural trade-off between unserved energy (priced at the VoLL) and investments. In this respect, it will make investments up to the point where the electricity price – the shadow price (dual variable) on the energy balance constraints – should compensate the last generator built for its investment and operating costs. However, it is also possible to implement a constraint on the capacity margin i.e. the margin of surplus generation capacity above the peak load (Energy Exemplar, 2015).

$$\sum_{g} MaxCapacity_g(Units_g + \sum_{i \leq y} UnitsBuilt_{g,i}) + CapShort_y \geq PeakLoad_y + ResMargin_y \quad \forall\, y \tag{E-5}$$

The preceding equations are only illustrative for a single region, and do not account for all factors such as outages, reserves, multiple regions, or cross-border transmission.

ST Schedule formulation

The objective function of the ST Schedule is to minimise the total generation costs in a modelled period, as well as the costs of unmet load, subject to various operational constraints (Brinkerink et al., 2018).

MINIMISE:

$$\sum_{t \in \mathcal{T}} \sum (StartCost_{g,t} \times GenStart_{g,t-1} + NoLoadCost_{g,t} \times GenOn_{g,t} + SRMC_g \times GenLoad_{g,t} + USE_t \times VoLL) \tag{E-6}$$

Subject to: Generator start and stop definitions

The operating state (online/offline) of a generation unit during a dispatch interval can only change if a stop or start has occurred (Deane et al., 2014).

$$GenOn_{g,t} - GenOn_{g,t-1} - GenStart_{g,t} + GenStop_{g,t} = 0 \;\forall\, g, \forall\, t \tag{E-7}$$

Subject to: Energy balance constraint

The ST Schedule is also subject to an energy balance constraint in each dispatch interval, the same as Eq. (E-2).

Subject to: Minimum stable level and ramping limits

Generators typically cannot operate below a minimum stable operating level (MSL), and are limited in how fast they can ramp up and down in production from one interval to another:

$$GenLoad_{g,t} - GenLoad_{g,t-1} \leq \left(60RampUp_g + MSL_g\right)GenOn_{g,t} - (MSL_g)GenOn_{g,t-1} \quad \text{(E-8)}$$

$$GenLoad_{g,t-1} - GenLoad_{g,t} \leq \left(60RampDown_g + MSL_g\right)GenOn_{g,t-1} - (MSL_g)GenOn_{g,t} \quad \text{(E-9)}$$

Subject to: Generator minimum up and down times

If a generator unit has a minimum up time (MUT) defined, it must be online if started in any dispatch interval looking back over the MUT (Deane et al., 2014).

$$GenOn_{g,t} - \sum_{k=t-MUT_g+1}^{t} GenStart_{g,k} \geq 0 \qquad \forall\, g, \forall\, t \qquad \text{(E-10)}$$

If a generator unit has a minimum down time (MDT) defined, it must be offline if shutdown in any dispatch interval looking back over the MDT (Deane et al., 2014).

$$GenOn_{g,t} - \sum_{k=t-MDT_g+1}^{t} GenStop_{g,k} \leq 1 \qquad \forall\, g, \forall\, t \qquad \text{(E-11)}$$

Acknowledgements

This thesis would not have been possible without the support of my colleagues, collaborators, friends and family. I can't thank everyone here, but certain people require a special mention.

My first thanks go to my co-promotor Machteld van den Broek, and my promotor Martin Junginger. Machteld, your support over the years has been invaluable. You guided me through the PhD not just from a technical perspective, but also as a mentor. You really care about and support your PhDs and do your best to find opportunities for them. I wish you every success in Groningen! Martin, you fundamentally enabled my PhD by securing my funding from several EU projects, without which my PhD journey may well have come to an end after only my first year. You trusted me to manage this work whilst giving me the freedom to pursue my own research interests, and I really valued your feedback on my ideas and papers.

Secondly, to my dear friends and officemates – Anna and Lotte. Doing a PhD can be a long and solitary process, but sharing this journey with you made every day enjoyable. From unbeatable birthday commemorations, inspiring verbs, or moral support during the most difficult times (e.g. model crashes), I don't think there has ever been – or is ever likely to be – a gezelliger office than ours!

Thirdly, I would like to thank my research associates and the true workhorses of this PhD: my two high-performance desktop PCs. Let the 22 MWh (by my calculations) of electricity we've used over the past five years not be in vain.

Next, my thanks go to my co-authors, colleagues and friends from Utrecht University I worked closely with. Anne Sjoerd, you were my first PLEXOS partner in crime, and introduced me to the world of PSM. Since then you've become a great friend and (together with Emily, William and Elanor) thanks for the dinners, games nights and motivational jogs. Bas, it was great working together the last couple of years. Thanks for your help with my Dutch summary, for enriching my vocabulary (Hè hè, nou nou, poe poe), and nice that we stay colleagues at TenneT. Thomas, for your help with the 2nd chapter. I really enjoyed our Python hackathons, and without you I think the PhD would have taken me another six months to finish! Wen, for all your work and help with the district heating article. Wim, for your feedback on the 3rd chapter, interesting email discussions, your passion and energy for the energy transition is inspiring. Gert Jan, for your advice, perspectives, and shared sense of humour. Robert, for your policy expertise and nice collaboration together with Alex. Ludo, for all the coffee breaks and delicious goodies you brought to the office. To my master students Alex, Diede, Diederik, Dies, Gilles, Maarten, and Tiemen – I enjoyed working with every one of you! Aisha, for all your help and on behalf of all the PhDs, MScs and BScs at UU, for going above and beyond the call of duty. To Siham, Fiona, Lisa and Ineke - for all your help making things run smoothly during my time at E&R. To the rest of my colleagues, thanks for the nice dinners, lunches, and

conversations: Ana, Anand, Andrea, Birka, Ernst, Christian, David, Floor, Gijs, Hu Jing, Ibti, Ioanna, Ioannis, Ivan (x2), Juraj, Lennard, Li, Lukas, Madeleine, Marc, Matteo, Nick, Nico, Ody, Oscar, Panos, Paul, Pita, Ric, Rojier, Sara, Steven, Thuy, Vincenz, Wina, Wilfried, and Wouter.

A big thank you to all the people from other research institutes and from industry for their insights, feedback on my work and/or various collaborations: Gerard, Ine, Maurice and Kate from KNMI; Andreas and Lukas from TU Wien, Paul from UCC, Arjan from Stedin, Frank (W.) and Frank (N.) from TenneT, and all the partners I worked with as part of the Flexifuel-SOFC and Flexifuel-CHX projects. Also, thanks to the folks at Energy Exemplar support for addressing my PLEXOS pickles.

To Asier, Belen (& Jordi), Blanca (& Jos), Carina, Davina, Elena, Jesus, Luca (& Sara), Rosalien (& Joeri), Sara, Tarek (& Betul), Vincent and Xavi – thanks for the great cycling and skiing trips, parties, bouldering, dancing, excellent wines and games nights that have kept me sane these last years!

Lastly, I would like to thank mum and dad – I couldn't ask for better parents. Growing up you always gave me every opportunity you possibly could, encouraged me to take risks, and supported me in all my (sometimes strange) decisions. Living on the other side of the world can be difficult, but to me you never feel very far away. Thanks also to Shona & Mike, grandma & grandad, and the rest of my family for looking after mum and dad while I'm swanning around in Europe.

William Zappa

Utrecht, March 2020

About the author

Born in Perth Western Australia (1986), William Zappa studied a Bachelor of Engineering (Chemical Engineering) at Curtin University of Technology, graduating in 2009 with 1st Class Honours. After completing his studies, he worked for several years as a chemical engineer at the Alcoa Pinjarra Alumina refinery, focussing on energy efficiency, environmental and product quality issues. In 2012 he was awarded an Erasmus Mundus scholarship and relocated to Europe to pursue a double master's degree in Sustainable Energy Technologies at Eindhoven University of Technology (the Netherlands) and Aalto University (Finland), graduating *cum laude* in 2014.

After completing his MSc, he returned to the Netherlands and joined the Copernicus Institute of Sustainable Development at Utrecht University as a junior researcher. In this role, he worked on several Dutch and EU projects on topics including the integration of variable renewable energy sources, and the development of small-scale heating and combined heat and power systems. In January 2020, William joined TenneT, the Dutch-German transmission system operator where he works on topics related to security of supply and electricity market design.

Publications

Peer-reviewed articles

Liu, W., Klip, D., Zappa, W., Jelles, S., Kramer, G. J., & van den Broek, M. (2019). The marginal-cost pricing for a competitive wholesale district heating market: A case study in the Netherlands. *Energy*, 189, 116367. doi:10.1016/j.energy.2019.116367

van Zuijlen, B., Zappa, W., Turkenburg, W., van der Schrier, G., & van den Broek, M. (2019). Cost-optimal reliable power generation in a deep decarbonisation future. *Applied Energy*, *253*, 113587. doi:10.1016/j.apenergy.2019.113587

Zappa, W., Junginger, M., & van den Broek, M. (2019). Is a 100% renewable European power system feasible by 2050? *Applied Energy*, *233–234*, 1027–1050. doi:10.1016/j.apenergy.2018.08.109

Zappa, W., & van den Broek, M. (2018). Analysing the potential of integrating wind and solar power in Europe using spatial optimisation under various scenarios. *Renewable and Sustainable Energy Reviews*, *94*, 1192–1216. doi:10.1016/j.rser.2018.05.071

Brouwer, A. S., Van den Broek, M., Zappa, W., Turkenburg, W. C. W. C., & Faaij, A. (2016). Least-cost options for integrating intermittent renewables in low-carbon power systems. *Applied Energy*, *161*, 48–74. doi:10.1016/j.apenergy.2015.09.090

Conferences

van Zuijlen, B., Zappa, W., Turkenburg, W., Van der Schrier, G., & van den Broek, M. (2018). Assessment of the Role of CCS in the Provision of Long-Term Security of Power Supply and Deep CO2 Emission Reduction. *Proceedings of the 14th Greenhouse Gas Control Technologies Conference Melbourne 21-26 October 2018 (GHGT-14)*. Melbourne: SSRN.

Zappa, W., Mulder, T., Junginger, M., & van den Broek, M. (2018). A Quantitative Evaluation of Capacity Remuneration Mechanisms in Europe. *Proceedings of the 15th International Conference on the European Energy Market (EEM)* (27-29 June 2018) Lodz: IEEE. doi:10.1109/EEM.2018.8469833

Götz, T., Saurat, M., Tholen, L., Adisorn, T., Obernberger, I., Brunner, T., … Zappa, W. (2017). Green on-site power generation : environmental considerations on small-scale biomass gasifier fuel-cell CHP systems for the residential sector. In P. Bertoldi (Ed.), *Proceedings of the 9th international conference on Energy Efficiency in Domestic Appliances and*

Lighting (EEDAL '17) : part 3 (pp. 909–921). Luxembourg: Publications Office of the European Union.

Brunner, T., Ramerstorfer, C., Obernberger, I., Kerschbaum, M., Aravind, P. V., Makkus, R., … Zappa, W. (2017). Development of a highly efficient micro-scale CHP system based on fuel-flexible gasification and a SOFC. *Proceedings of the 25th European Biomass Conference and Exhibition Proceedings*. doi:10.5071/25thEUBCE2017-2CV.3.5